

ASSESSMENT OF HYDRAULIC CONDUCTIVITY OF A FRACTURED CHALK AQUIFER USING BOREHOLE GEOPHYSICAL LOGGING

BY

Gerasimos P. Tselentis, B.Sc., M.Sc.

February 1983

A thesis submitted for the degree of Doctor of Philosophy of the University of London and for the Diploma of Membership of Imperial College

Engineering Geology Section
Department of Geology
Imperial College of Science
and Technology
London, SW7. 2BP

A B S T R A C T

This thesis is concerned with using geophysical well logs to assess the in situ hydraulic character of fractured Chalk aquifers: the thesis is divided into four PARTS.

In PART I the extent to which fluid and formation geophysical well logs can be used to estimate the hydraulic conductivity of the Chalk is examined. Special attention is given to the heat pulse flowmeter whose limits of usefulness are defined by theoretical and experimental investigation.

In PART II, an attempt is made to study the hydraulic behaviour of fractured Chalk from the flow characteristics of a number of fissure elements. Various associated topics are discussed such as the dependence of the hydraulic conductivity upon fissure contact area and the local hydraulic gradient. This is followed by a description of the progress made in correlating geophysical formation parameters, as measured by the geophysical logs, with the formation's hydraulic conductivity. The correlation is made by simulating the Chalk with a double porosity numerical model. Special attention is given to the effect that fissures have on certain geoelectric parameters. New formation parameters are presented that are very sensitive to fissure zones.

In PART III the construction details of a microcomputer based hardware and software package for the automatic evaluation of geophysical logs are presented. The package incorporates the findings described in PART II and enables the output from conventional geophysical logs used in the field, to be processed so as to give a quantitative measure of the geophysical parameters which characterize the formation, and in certain cases indicate zones with high hydraulic conductivity.

Finally the methods introduced in PARTS II and III are applied to a number of wells and the results obtained are analysed and discussed.

The Thesis is accompanied by an APPENDIX in which the details of certain technical aspects of the research are recorded.

ACKNOWLEDGEMENTS

The author wishes to thank his supervisor, Dr. M. de Freitas for the helpful suggestions and guidance, and whose consistent assistance and encouragement made this research possible.

In addition, the author wishes to express his gratitude to Prof. J. Dracopoulos of Athen's University, as he was the man who inspired the author's love to the Earth Sciences.

The assistance given by Dr. M. Fleet of the Water Research Centre who also supplied some of the data used in the present research, Mr. V. Robinson of Thames Water and Miss A. Robertson of the Institute of Geological Sciences is also acknowledged.

Special thanks to Mr. J. Ellis of the Southern Water Authority for his assistance during the field work and for his continuing interest in this research and to Dr. T. Bear, geophysical consultant for his help during the various stages of the research.

Thanks are also due to Southern Water Authority for supplying most of the data used in the present research and allowing the author to make use of its geophysical logging unit, to G. Stow & Co. Ltd., Drilling Contractors, for allowing the author to take part in the drilling of 8 wells, to Anglian Water Authority at Cambridge with the geophysical logging unit of which the author spent some time and to British Driver-Harris Co. Ltd. for supplying the wire for the heat pulse flowmeter experiment.

The author wishes also to thank the staff of the Engineering Geology, Mining and Mineral Technology and Electronics laboratories of the Royal School of Mines of Imperial College for their co-operation, especially Mr. T.

Rogers for his help during the experimental set up, and Mr. K. O'hara for his useful suggestions during the design of the heat pulse generator.

The help of Prof. P. Bradshaw of the Aeronautics Department, Prof. D. Spalding of the Department of Mechanical Engineering and Mr. E. Ejimuda, research student at Engineering Geology is also appreciated.

The Greek State Scholarship Foundations (I.K.Y.) is acknowledged for its generous financial support.

The author would also like to thank Miss E. Jenks for her kind co-operation in typing this thesis.

Finally, the author wishes to thank his fiancee, Chrissy, for her encouragement and support throughout the duration of the research.



Drilling for groundwater in the Chalk aquifer

NOMENCLATURE

A. Roman Letters

A	(i) cross section area of flow conduits
	(ii) certain constant
a	first temperature coefficient of resistance
a_{2i}	half opening of a fissure
B	a certain constant
b	spacing between two fissures
C	a certain constant, functional
Cp	specific heat at constant pressure
D	(i) diameter
	(ii) a certain constant
E	Young's modulus
E_d	diffusion potential
E_m	membrane potential
E_k	electrokinetic potential
F	(i) Faraday constant
	(ii) formation factor
	(iii) certain functional
F_o	initial formation factor
F_t	total formation factor
f	fissure index
$\vec{f}$	direction of hydraulic gradient
G	a certain functional
G_2	critical thermal gradient
g	(i) acceleration due to gravity
	(ii) geometric factor
H	thickness of formation
h	piezometric head
J_L	total area of fissure contact
k	(i) thermal conductivity
	(ii) hydraulic conductivity
k_e	equivalent hydraulic conductivity
k_T	hydraulic conductivity
$k_{d,m,t}$	constants related to S.P.

$\hat{k}$	(i) thermal diffusivity
	(ii) hydraulic permeability
$\hat{k}_f$	directional permability
$\hat{k}_{1,2,3}$	Principal permeabilities
$\hat{k}_{2j}$	permeability tensor
L	(i) total thickness of fissured formation
	(ii) distance between heated wire and sensor
	(iii) length of flow path
l	(i) distance between two fissure zones
	(ii) length of heated wire
m	cementation factor
m_o	initial cementation factor
N	Avogadro's number
Nu	Nusselt's number
n	(i) ion valence
	(ii) number of wires in the heated grid
	(iii) number of fissures in a fissure zone
P	fluid pressure
Pe	Peclet's number
Pr	Prandl's number
Q	(i) heat
	(ii) total water discharge
R	electrical resistivity
R_{16}	resistivity measured from 16-inches log
R_{64}	" " " 64-inches log
R_{eq}	equivalent resistivity
R_{tr}	transverse resistivity
R_l	longitudinal resistivity
R_a	apparent resistivity
R_f	formation resistivity
R_o	formation resistivity at 100% water saturation
R_m	mud resistivity
R_i	resistivity of invaded zone
R_e	Reynold's number
S	(i) area
	(ii) storativity
s	electrode spacing

T	(i) temperature
	(ii) tortuosity
	(iii) transmissivity
u	velocity
V	electrical potential
v	kinematic viscosity
x,y,z	cartessian coordinates

B. Greek Letters

β	volume coefficient of expansion of the water
δ	dimensionless variable
θ	polar coordinate denoting angle
ϑ	angle of contact
μ	dynamic viscosity
	dimensionless variable
ρ	density
σ	(i) electric conductivity
	(ii) surface tension
τ	dimensionless time
ϕ	porosity
ϕ_o	formation porosity
ϕ_f	fissure porosity

In all the symbols used in Chapter III:

index w means: wire
f " fluid
a " ambient

C O N T E N T S

	Page
ABSTRACT	(ii)
ACKNOWLEDGEMENTS	(iv)
NOMENCLATURE	(vii)
CONTENTS	(x)
LIST OF FIGURES	(xviii)
LIST OF TABLES	(xxvi)
LIST OF PLATES	(xxvii)
CHAPTER I INTRODUCTION	1
1.1 Scope of research	2
1.2 The importance of knowing the hydraulic conductivity of the Chalk	3
1.3 Current status on the study of the hydraulic conductivity of fissured aquifers	5
1.3.a. Introduction	5
1.3.b. Laboratory	5
1.3.c. Optical	7
1.3.d. Geophysical	8
1.3.e. Pumping tests	10
1.3.f. Packers	11
1.4 Outline of the Thesis	12
P A R T I	14
CHAPTER II THE USE OF PHYSICAL FLUID LOGS FOR EVALUATING THE HYDRAULIC PROPERTIES OF FISSURED AQUIFERS	16
2.1 Introduction	16
2.2 Properties of the fluid column as related to the hydraulic properties of the aquifer	16
2.3 The use of flow velocity measurements in wells and boreholes	21
2.4 The flow regime inside a well	22

Page

2.5 Methods of flow measurement 25
2.6 The relation of flow velocity measurements to the hydraulic conductivity of an aquifer 33
2.7 The use of flow temperature log 37
2.7.a The temperature regime inside a borehole 37
2.7.b Methods of temperature logging 40
2.7.c The relation of temperature measurements to the hydraulic conductivity of the aquifer 41
2.8 The use of fluid conductivity log 47
2.8.a The fluid conductivity regime inside a borehole 47
2.9 General conclusions 55

CHAPTER III THEORETICAL AND EXPERIMENTAL INVESTIGATION OF THE HEAT PULSE FLOWMETER 57
3.1 Introduction 57
3.2 Theoretical considerations 61
3.2.1 Formulation of the problem 61
3.2.2 Analytical solution 65
3.2.3 Mathematical modelling of the temperature field produced by a grid 69
3.3 Experimental considerations 73
3.3.1 Probe design 73
3.3.2 The electronic circuit 76
3.3.3 The calibration device 80
3.4 Discussion of the results 85
3.5 General conclusions 89

CHAPTER IV GEOPHYSICAL FORMATION LOGS USED IN THE WATER INDUSTRY 91
4.1 Introduction 91
4.2 Resistivity logs 92
4.2.a Instrumentation and theory 92

		Page
4.2.b	Volume of ground investigated by normal resistivity logs	99
4.2.c	Thin bed effects	101
4.3	The spontaneous potential log	103
4.4	The gamma ray log	105
4.5	The caliper log	107
4.6	Interpretation practice of formation resistivity logs in the Chalk	108
4.7	The relation of formation logging measurements to the hydraulic conductivity of an aquifer	113
4.7.a	Resistivity logs	114
4.7.b	Gamma ray logs	117
4.7.c	Spontaneous potential log	120
4.8	Other devices for formation logging	120
4.8.a	The lateral device	122
4.8.b	The gamma-gamma log	122
4.8.c	The neutron log	125
4.8.d	The sonic log	128
4.8.e	The focused devices	131
4.9	General conclusions	134
P A R T II		136
CHAPTER V	HYDRAULIC PROPERTIES OF THE CHALK	137
5.1	Introduction	137
5.2	Primary porosity and hydraulic conductivity	137
5.3	Secondary porosity and hydraulic conductivity	142
5.3.a	Secondary porosity and hydraulic conductivity	142
5.3.b	Fissure distribution	144
5.3.c	Vertical variation of hydrogeologic parameters	145
5.4	Flow mechanism through the Chalk	147
5.5	The fundamental equations of fissure flow	153

		Page
5.6	Review of some experimental results	156
5.7	Equivalent hydraulic conductivity of a set of parallel (horizontal) fissures	159
5.8	Inclined fissures	166
5.9	An algorithm for the fast calculation of the equivalent directional hydraulic conductivity of an inclined fissure zone	171
5.10	The dependence of the hydraulic conductivity of a fissure zone upon the pressure head distribution near the well	175
5.11	The dependence of the hydraulic conductivity of a fissure upon its contact area	180
5.12	Flow through a conduit bisecting a semi-permeable matrix	184
	5.12.a Mathematical formulation of the problem	184
	5.12.b Solution of the differential equations	186
5.13	General conclusions	191

CHAPTER VI SIMULATION OF CHALK CONDUCTIVITY BY A DOUBLE POROSITY MODEL AND EVALUATION OF IN-SITU HYDRAULIC CONDUCTIVITY FROM GEOPHYSICAL FORMATION LOGS 194

6.1	Introduction	194
6.2	Formation factor porosity relation	195
6.3	Theoretical investigation of the formation factor porosity relation	201
6.4	Typical forms of Archie's law for Chalk	203
6.5	Simulation of the Chalk aquifer by a double porosity model	204
	6.5.a Pore system description and analysis	206
	6.5.b Discussion of the results	213
6.6	Relation between the fissure index of Chalk and its hydraulic conductivity	222
6.7	Hydraulic conductivity vs. electric conductivity	227

Page

6.8 An investigation of the effect that fissures have upon some parameters measured from the geophysical formation resistivity logs 228
6.8.a Example of borehole No. 5 234
6.9 General conclusions 237

P A R T III 239

CHAPTER VII DESIGN OF A MICROCOMPUTER SYSTEM FOR THE AUTOMATIC EVALUATION OF THE LOGS 240
7.1 Introduction 240
7.2 Current status of the use of microcomputers in hydrogeophysical logging 241
7.3 Design of a microcomputer system - general requirements 242
7.3.a The hardware 243
7.3.b The software 244
7.4 The structure of a microcomputer 246
7.5 Organization of the information contained in the logs 247
7.6 Corrections 250
7.6.a Corrections for changes in the conductivity of the fluid column 253
7.7 Zonation of the logs 255
7.7.1 The program window 256
7.8 Evaluation of the formation parameters 261
7.9 Digital filtering of logs 267
7.10 Optimum operation of the software package 275
7.11 General conclusions 281

CHAPTER VIII MATHEMATICAL MODEL SIMULATION, USING A MICROCOMPUTER, OF THE RESPONSE OF AN ELECTRIC LOGGING TOOL 282
8.1 Introduction 282
8.2 General problem 283

		Page
8.3	Evaluation of the potential	286
8.4	Resistivity log simulation	288
8.5	Flow diagram of computer program	292
8.6	Range of validity of the algorithm	299
8.7	General conclusions	302
P A R T IV		303
CHAPTER IX CASE HISTORIES		304
9.1	Introduction	305
9.2	Borehole No. 1: Victoria Gardens North (Brighton Chalk Block)	306
9.3	Borehole No. 2: Findon (Brighton Chalk Block)	310
9.4	Borehole No. 3: Brick Kiln Farm (Chichester Chalk Block)	312
9.5	Borehole No. 4: Park Bottom Barn Arundel (Chichester Chalk Block)	314
9.6	Borehole No. 5: Kingstone Middle Rd. (Brighton Chalk Block)	316
9.7	Borehole No. 6: St. Peter's Church (Brighton Chalk Block)	318
9.8	Borehole No. 7: St. Catherines Hill, Winchester (Thames Chalk)	321
9.9	Borehole No. 8: Madehurst (Thames Chalk)	324
9.10	Borehole No.9: Ludgershall Sewage Works, Well 5 (Thames Chalk)	327
9.11	Borehole No. 10: Ludgershall Sewage Works, Well 3 (Thames Chalk)	327
9.12	Borehole No. 11: Adcote (Thames Chalk)	331
9.13	Borehole No. 12: Houndean Bottom (Brighton Chalk Block)	334
9.14	General conclusions	341

Page

CHAPTER X GENERAL CONCLUSIONS OF RESEARCH AND RECOMMENDATIONS 343

BIBLIOGRAPHY 351

APPENDICES 366

APPENDICES

A.1	Conversion factors	366
A.3.1	Physical properties of water at 10°C	368
A.3.2	Physical properties of Pt	368
A.3.3	Thermodynamic definitions	368
A.3.4	Proof of equation 3.32	369
A.3.5	Experimental results of heat pulse propagation experiment	376
A.3.6	Computer program used for the theoretical calculations	374
A.4.1	The hydrologger	378
A.5.1	Computer program for the evaluation of the directional hydraulic conductivity of a fissured formation	384
A.5.2	Drawings showing flow patterns	388
A.6.a	Program for generating Table A.6.1	396
A.7.1	Memory map of the microcomputer	423
A.7.2	Evaluation of the coefficients of equation 7.1 for a 150 mm diameter borehole	424
A.7.3	Curve fitting	426
A.7.e	Program "WINDOW"	436
A.7.5	Program "FILTER"	438
A.7.6	Program "CORRECT"	440
A.7.7	Program "FORM"	441
A.8.1	Computer program for log simulation	444
A.9.1	Information related to the examined boreholes	447
A.9.2	Output of program "FORM" for borehole No. 1	448
A.9.3	Analogue to digital and digital to analogue interface	458
A.9.4	Permanent storage of software in the micro-computer	460
A.9.5	Electronic circuit of the microcomputer	462
A.9.6	Tables containing the calculated geoelectric parameters of the examined boreholes	463

LIST OF FIGURES

No.	Title	Page
1.1	Outcrops of Chalk in England showing locations of recent groundwater schemes	4
1.2	Methods for estimating the hydraulic conductivity of aquifers	5
1.3	Slippage and turbulence in air permeability measurements (1.3.a), turbulence only (1.3.b)	7
1.4	Dependence of attenuation of light on specific gravity of the suspension, thickness h of the layer and wavelength of light	8
2.1	The possible ways by which the three basic sets of properties of the formation and fluid affect each other	17
2.2	Arrangements for a flow logging investigation	19
2.3	Datum points for hydrologger probes. T/C: temperature-conductivity, ΔT/C: differential temperature-conductivity	20
2.4	Critical temperature gradient for different borehole diameters	24
2.5	Convection cells representing water movement due to thermal instability	22
2.6	Subsequent dye fronts inside the tube representing the well, at the level of the fissure	28
2.7	Velocity components at a point inside a borehole	35
2.8	Temperature variations inside the borehole	39
2.9	Conductivity and temperature logs in both the ways up and down	43
2.10	Differential temperature log in both the ways up and down	45
2.11	Differential temperature and temperature logs	46
2.12	Resistivity, temperature and differential temperature logs	48
2.13	Compositional differences between interstitial water in the fissure zones	50

Page

2.14 Permeability values together with conductivity and flow logs (Price et al, 1980) 51

2.15 Radial view of the fissure at 29.3m below datum 52

2.16 Radial view of the fissure at 58.8m below datum 52

2.17 Conductivity profiles for 10 boreholes in the Brighton Chalk 54

2.18 Tide cycle log 55

3.1 Response of the sensor with conditions of different thermal diffusion and sensor wire inertia 60

3.2 The temperature field to be described, at Point A 60

3.3 Construction details of the heating grid used in the experiment 70

3.4 Temperature field at a point 10mm downstream from a heating grid consisting of 10 wires of 0.25mm diameter and heated up to 75°C 72

3.5 Temperature field at a point 15mm downstream from a heating grid consisting of 10 wires of 0.25mm diameter and heated up to 75°C 72

3.6 Typical sensors tested in the research. All lengths are in mm 75

3.7 Construction details of the probe containing the heating grid and the sensor 76

3.8 Electronic circuit of the pulse generator 77

3.9 Typical waveform produced by the pulse generator 78

3.10 Typical pulses of different periods and duration produced by the pulse generator 79

3.11 Sample of a recorded signal 85

3.12 Comparison between theoretical and experimental results for a 0.25mm Pt-wire and for separations 10mm (Fig. 3.12.a) and 15mm (Fig. 3.12.b) 86

3.13 Difference between theoretical and experimental results as a function of the fluid velocity 87

		Page
4.1	Typical resistivity logging arrangement	93
4.2	Departure curves for normal device - infinitely thick bed, no invasion (Courtesy Schlumberger Well Surveying Corp.)	98
4.3	Theoretical geometric factors for normal and lateral measuring systems in an infinite homogeneous medium (Lynch 1962)	100
4.4	Response of a normal device opposite beds of various thickness (Courtesy of Schlumberger Well Surveying Corp.)	102
4.5	Apparent resistivity indicated by a normal device for various bed thicknesses (Lynch 1962)	103
4.6	Schematic representation of the spontaneous potential (S.P.)	104
4.7	Range of radioactivity of some sedimentary rocks	106
4.8	Dynamic response of a natural gamma probe	107
4.9	Possible combinations between fluid and formation in a borehole with saline intrusion	112
4.10	Idealised 16-inches normal resistivity log for the Chalk	115
4.11	Normal resistivity logs showing thin bed reversal effects	116
4.12	Comparison of 16-inches resistivity log with results from packer tests	118
4.13	Part of the natural gamma log in a Chalk borehole	119
4.14	Part of the S.P. log indicating permeable zones	121
4.15	Lateral resistivity device	123
4.16	Response of a lateral device opposite beds of various thickness. (Courtesy of Schlumberger Well Surveying Corp.)	124
4.17	The equipment, principles, and interpretation of gamma-gamma logs (Keys et al 1971)	125
4.18	The equipment, principles, and interpretation of neutron logs (Keys et al 1971)	126

		Page
4.19	Methods of nuclear logging	127
4.20	Principles and equipment for making borehole adjusted acoustic velocity logs	129
4.21	Illustrative waveform of received signal showing compressional, shear, and fluid arrivals	130
4.22	Use of variable density log for identification of arrivals	131
4.23	Principles of the guard log	132
4.24	Principles of the laterolog and schematic comparison of current patterns from laterolog and normal device	133
5.1	Electron microscope photograph of a sample of Upper Chalk (Price et al 1976)	138
5.2	Envelopes of available pore-size distribution curves for the Upper and Middle Chalk (Price et al 1976)	139
5.3	Integranular permeability against effective porosity for 36 Chalk samples (Price et al 1976)	140
5.4	Typical time-drawdown response in a Chalk well	143
5.5	Histogram of the occurrence of major yielding fissures constructed from the results of geophysical logging. The presence of the casing prevented results to be obtained from all the boreholes for depths less than 30m and this is shown by the two smoothed distribution curves	145
5.6	Storativity and transmissivity against rest water level	146
5.7	Diagram of aquifer model	149
5.8	Fissure geometry of the Chalk	151
5.9	General flow in a fissure plane	155
5.10	Illustration of a fissure surface	158
5.11	Laws of resistance for flow in a joint (Louis 1969)	159
5.12	Set of equispaced fissures of the same opening	161
5.13	Set of non-equispaced fissures of different openings	161

		Page
5.14	Set of diagrams relating the equivalent hydraulic conductivity of a set of parallel fissures with the fissures opening and the fissure frequency	163
5.15	Coordinate reference for a set of inclined fissures	167
5.16	General case of a borehole intersecting sets of inclined fissures of different orientations	170
5.17	Logic diagram of the algorithm for the calculation of the equivalent hydraulic conductivity of an arbitrary fissure set	173
5.18	Pumping well intersecting a single fissure	176
5.19	Pressure distribution in the vicinity of a pumped well	177
5.20	Usual variation of the direction of the local hydraulic gradient during pumping	178
5.21	Direction equivalent hydraulic conductivity of a fissure zone K_{fe}, during pumping	179
5.22	Flow rate as a function of contact area	183
5.23	Fissure bisecting a semipermeable matrix	185
5.24	Fissure discharge as a function of the permeability ratio between matrix and formation	190
6.1	Formation factor vs. formation porosity for the Archie equation	197
6.2	Models illustrating the resistivity and equivalent resistivity of a porous block	201
6.3	Porosity as a function of tortuosity for constant values of formation factor and cementation factor (Willie et al 1950)	203
6.4	Typical forms of Archie's law for Chalk	205
6.5	Relation of permeability to formation resistivity factor for consolidated sandstone cores of the Gulf Coast (Archie 1952)	207
6.6	Permeability vs. formation factor (Jones et al 1951)	207
6.7	Double porosity system for the Chalk	208
6.8	Relation between the formation parameters of the double porosity model	214

		Page
6.9	Total cementation factor vs. fissure porosity	220
6.10	Chalk block with one fissure per unit length	222
6.11	Permeability vs. fissure index	224
6.12	Permeability vs. total porosity	225
6.13	Geoelectric model of fissured formation	229
6.14	Anisotropy index vs. fissure porosity	231
6.15	Transverse resistivity P_{tr}, longitudinal resistivity P_l and longitudinal conductivity σ_l vs. fissure porosity	232
6.16	Difference between transverse and longitudinal resistivities vs. depth	235
6.17	Difference between transverse and longitudinal resistivities vs. depth with regression line fitted through the data	236
7.1	Typical procedure for the automatic processing of geophysical logs	245
7.2	Example of log digitization with different sampling intervals	249
7.3	Arrangement used for the automatic processing of the logs	251
7.4	Typical zonation of a log	255
7.5	Logic diagram for the zonation algorithm	257
7.6	Examples of the zonation of a geophysical log by using program "WINDOW"	262
7.7	Diagram showing the manipulation of the data	266
7.8	Logic diagram of the algorithm which was designed for the manipulation of the data	268
7.9	Example of a 16-inches resistivity log filtered by 5-,10-,15-, and 20-term moving average filtering	271
7.10	Comparison between 20-term moving average filtered version of 16-inches resistivity log with the 64-inches resistivity log	272
7.11	Example of 5-,10-, and 15-term moving average filtering of a caliper log	273

		Page
7.12	(a) Three-term moving average, (b) Sheppard's five-term equation, (c) Spencer's twenty-one-term equation, (d) Spencer's and Sheppard's seven term equation	274
7.13	Example of a caliper log filtered by 21-term Spencer's filter and 7-term Spencer's and Sheppard's filter	276
7.14	Operation of the software package	277
7.15	Comparison between caliper and porosity logs	279
7.16	Difference between 64N and 16N vs. depth	280
8.1	Current source outside the thin bed	284
8.2	Current source inside the thin bed	285
8.3	Example of log simulation for the case that the tool spacing is larger than the bed's thickness	289
8.4	Example of log simulation for the case that the tool spacing is shorter than the bed's thickness	290
8.5	Examples of theoretical simulation of the normal resistivity logging process	293
8.6	Logic diagram of the algorithm which performs the normal resistivity logging process simulation	296
8.7	Range of validity	300
9.1	Geophysical and driller's logs of Borehole No. 1	307
9.2	Temperature, differential temperature and S.P. logs of Borehole No. 1	308
9.3	Values of longitudinal resistivity vs. depth for Borehole No. 1	309
9.4	Geophysical and driller's logs of Borehole No. 2	311
9.5	Geophysical and driller's logs of Borehole No. 3	313
9.6	Geophysical and driller's logs of Borehole No. 4	315
9.7	Geophysical and driller's logs of Borehole No. 5	317

		Page
9.8	Geophysical and driller's logs of Borehole No. 6	319
9.9	Temperature, differential temperature and S.P. logs of Borehole No. 6	320
9.10	Geophysical and driller's logs of Borehole No.7	322
9.11	Temperature, differential temperature and flow velocity logs for Borehole No. 7	323
9.12	Geophysical logs of Borehole No. 8	325
9.13	Temperature and differential temperature logs of Borehole No. 8	326
9.14	Geophysical logs of Boreholes No. 9 and No. 10	328
9.15	Temperature and differential temperature logs of Borehole No. 9	329
9.16	Temperature and differential temperature logs of Borehole No. 10	330
9.17	Geophysical logs of Borehole No. 11	332
9.18	Caliper and flow logs of Borehole No. 11	333
9.19	16N and 64N resistivity logs of Borehole No. 12	336
9.20	64N resistivity log of Borehole No. 12 reconstructed from the samples	336
9.21	T-L log of Borehole No. 12	339
9.22	Differential temperatures and caliper logs of Borehole No. 12	340

APPENDIX FIGURES

A.1	Hydrologer equipment layout	380
A.2	Equipotential and flow lines	389
A.3	Memory map of the microcomputer	423
A.4	Electronic circuit of ADA interface	439
A.5	Electronic circuit of EPROM programmer	460
A.6	EPROM extension socket	461
A.7	Electronic circuit of the microcomputer	462

LIST OF TABLES

No.	Title	Page
2.1	Methods of flow velocity measurements and their optimum range of operation	34
2.2	Information about the coastal boreholes used to study the variations of the water's electrical conductivity	53
3.1	Velocities studied by other authors	58
3.2	Thermodynamic parameters for different velocities	89
4.1	Typical groundwater conditions in a borehole with saline intrusion	113
5.1	Characteristic values for the porosity and intrinsic permeability of the Chalk	141
5.2	Elastic properties of Chalk	182
7.1	Manufacturer and price of instruments used	244
7.2	Sample output from program "WINDOW"	267
8.1	Values of functional F for different values of t and for resistivity ratio 2 or 0.5	288
9.1	Hand calculation of the T-L log	337

LIST OF PLATES

No.	Title	Page
Frontise	Drilling for groundwater in the Chalk aquifer	(vi)
1	Arrangement for geophysical well logging	15
2	Perspex model used to simulate fissure flow	26
3	Fissure flow clearly illustrated by dye	27
4	General layout of the experiment	82
5	The probe mounted just above the grid	83
6	The effect of the grid on flow	84
7	Caliper probe with the arms open	109
8	Well bedded Upper Chalk with vertical and horizontal fissures in a fresh face of Caistor St. Edmund Quarry, Norwich	150
9	Electric analogue arrangement used to study the effect that the contact area of fissure has upon its discharge	181
10	Adjusting the geophysical logging probe inside Borehole No.12	335
11	A view of the hydrologger, mounted at the back of a LAND ROVER	378

INTRODUCTION

In this introduction the scope of the research is explained and the relevance of it to general studies of Chalk hydrogeology introduced. The current status of studies of the hydraulic conductivity of fissured aquifers is then briefly reviewed. The introduction concludes with an outline of the Thesis and its various PARTS.

1.1 SCOPE OF RESEARCH

The main objective of this research is to examine the use of geophysical well logs for assessing the in situ hydraulic character of fractured Chalk aquifers.

In doing this it became necessary to:-

(i) study the methods of geophysical well logging, in particular those methods that are most appropriate to the assessment of fractures in consolidated rocks, both their location and their in-situ geological and hydrogeological character: this culminated in a detailed study of flow metering.

(2) study the hydraulic behaviour of fractures, singly and in combination, and under conditions of increasing effective stress brought about by a reduction in pressure head around a well and the increase of contact area that results in the plane of the fissure.

(3) study the behaviour of a double porosity model for an aquifer, consisting of pores and fractures, and the manner in which a geophysical log will respond to such a material.

To achieve these objectives microcomputer based hardware and software were developed and tested. Further the general conclusions coming from a study of these objectives were tested by analysing the geophysical well logs of real wells.

1.2 THE IMPORTANCE OF KNOWING THE HYDRAULIC CONDUCTIVITY OF THE CHALK

The Cretaceous limestone formation known as the Chalk forms one of the country's major aquifers and underlies a large area of lowland S.E. Britain (Fig. 1.1). It is predominantly a fine grained, massive white limestone with occasional significantly marly strata.

Reliable supplies of good potable water have for many years been obtained from the Chalk, which accounts for some 15 per cent of the national water supply and is a major source of supply for London and the S.E.

In England the licenced abstraction from the aquifer is currently $1.26.10^6$ m^3/day compared to a total water use of $2.24.10^6$ m^3/day, thus it accounts for about 56 per cent of the water supply. Further, in the catchments of Southern and Eastern England where Chalk is the bedrock, the groundwater component of total river discharge frequently exceeds 50 per cent, and may reach 90 per cent. (Foster et al 1974).

Since the hydraulic conductivity of an aquifer is a fundamental concept of its hydrogeological properties, its knowledge is useful in the selection of sites for the drilling of production wells associated with high yields.

Current interest centres on the possibility of augmenting low river flows by pumping from groundwater storage such as the Lamborne Scheme (Lloyd 1981) and the design of each river regulation schemes requires a more precise knowledge of aquifer hydrogeological properties than has been used previously.

This knowledge is also of relevance in predicting the movement of pollutants and in the design of deep excavations at and below ground level.

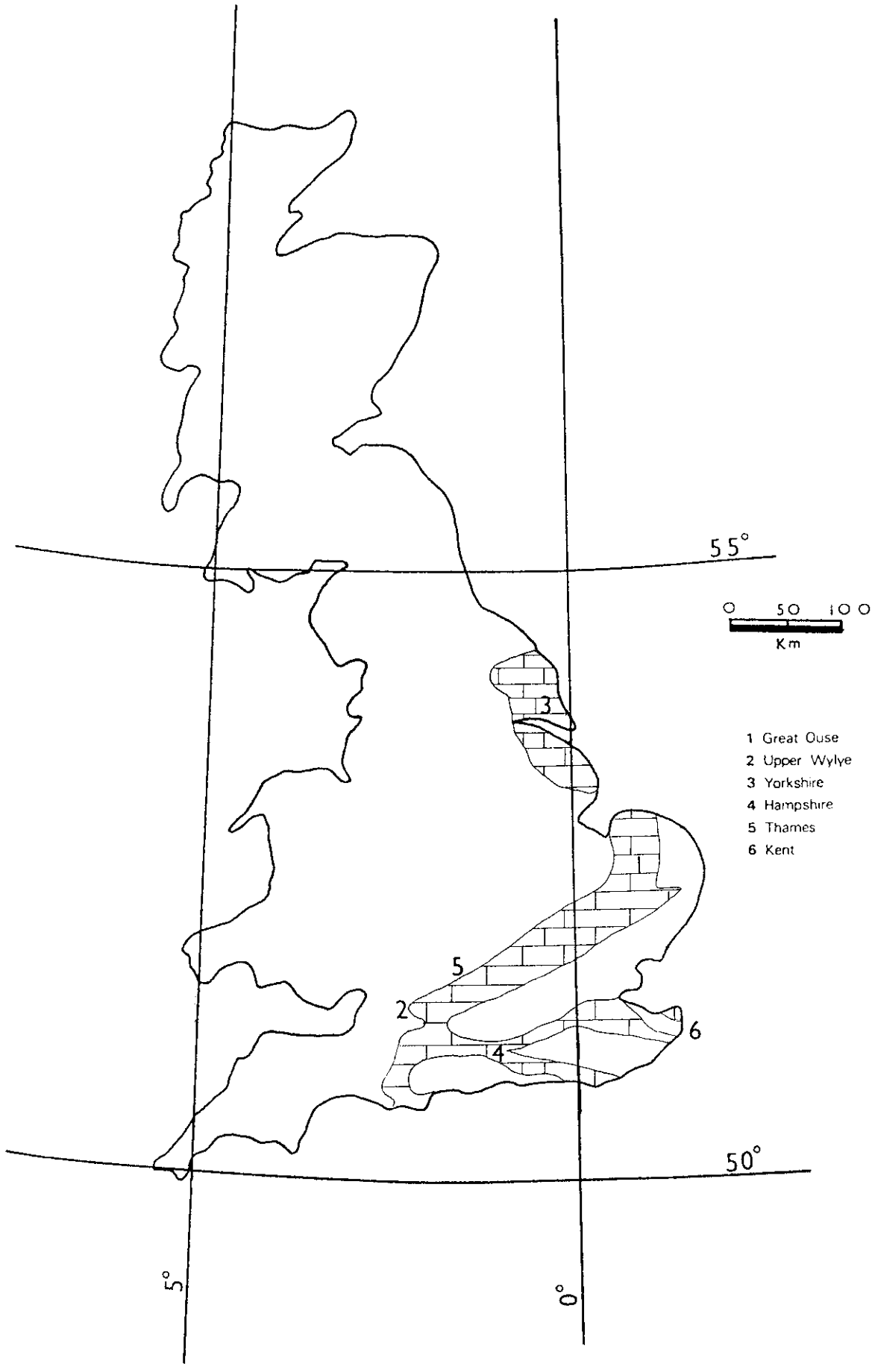


Fig. 1.1 Outcrop of Chalk in England showing locations of recent groundwater schemes

1.3 CURRENT STATUS ON THE STUDY OF THE HYRAULIC CONDUCTIVITY OF FISSURED AQUIFERS

1.3.a Introduction

This section presents the results of an attempt to summarize available methods used by the water industry for the study of the hydraulic conductivity of fissured aquifers, with specific reference to the Chalk types.

The accuracy of the (mean) hydraulic conductivity is influenced by the method of its determination and of the character of its distribution.

In general, fissure zones can be detected by direct and/or indirect examination (Parsons 1966) and the hydraulic conductivity can be estimated by four groups of methods which are: laboratory, optical, geophysical and hydrodynamic (Fig. 1.2).

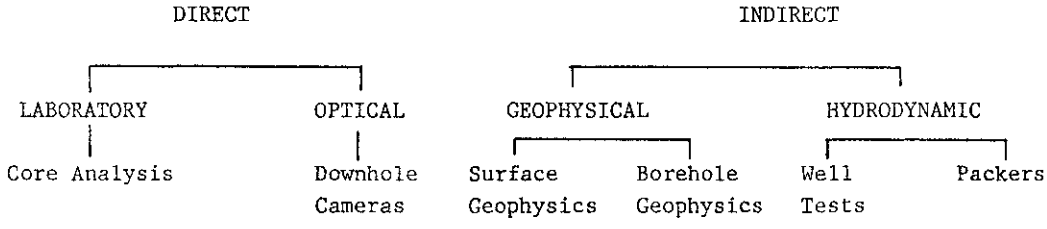


Fig. 1.2 Methods for estimating the hydraulic conductivity of aquifers

In the following the above methods are examined except for geophysical logging which is discussed in Chapters II and IV.

1.3.b Laboratory

It is customary to make use of Darcy's law and modifications of this law, together with laboratory data on formation core samples to predict the peformance of producing wells.

Such predictions are based on an assumption that fluid flow is laminar for the laboratory test. For the case of fissured aquifers the "pore space" is characterized by a wide variation in the size, shape, and distribution of pores including extensive planar 'pores' (i.e. fissures) having irregular surfaces. It is therefore apparent that conditions are much more favourable for turbulent flow.

The apparatus used for the flow tests on heterogeneous-type porosity core samples is well documented in the literature (Klinkenberg 1941; Stewart et al 1953). Investigations of the frequency and magnitude of turbulence and slippage* during these tests have shown that both slippage and turbulence affect the measured hydraulic conductivity (Fig. 1.3.a and 1.3.b). When the fissure system is responsible for almost all of the hydraulic conductivity of the core, it has been found (Stewart 1958) that slippage effects become too small to be measured. On the other hand, if the pore space consists of low permability intergranular matrix and a higher permeability fissure system (as in the case of Chalk), the effect of slippage becomes important.

In addition to this, even if laboratory methods gave a high enough accuracy, the smallness of the sample usually means the result is unrepresentative. Where the formation is sufficiently consolidated, cores can be taken but they will probably be fractured. On the other hand, in poorly cemented material, core loss will usually occur from friable zones, which are usually the most permeable; there is thus a danger that the results will be weighted towards the lower permeability values (Price, M. et al 1982). The obtained values are therefore characterized by a considerable variation which means that the micro-heterogeneity of the aquifer tends to be assessed by laboratory based studies rather than its megaconductive character.

---

* As a result of slippage, apparent permeabilities to gas are greater than the true value because there is no stationary layer of gas in contact with the walls of the flow channels. Gas slippage decreases with increasing static pressure and this has an effect to lower the apparent gas permeability.

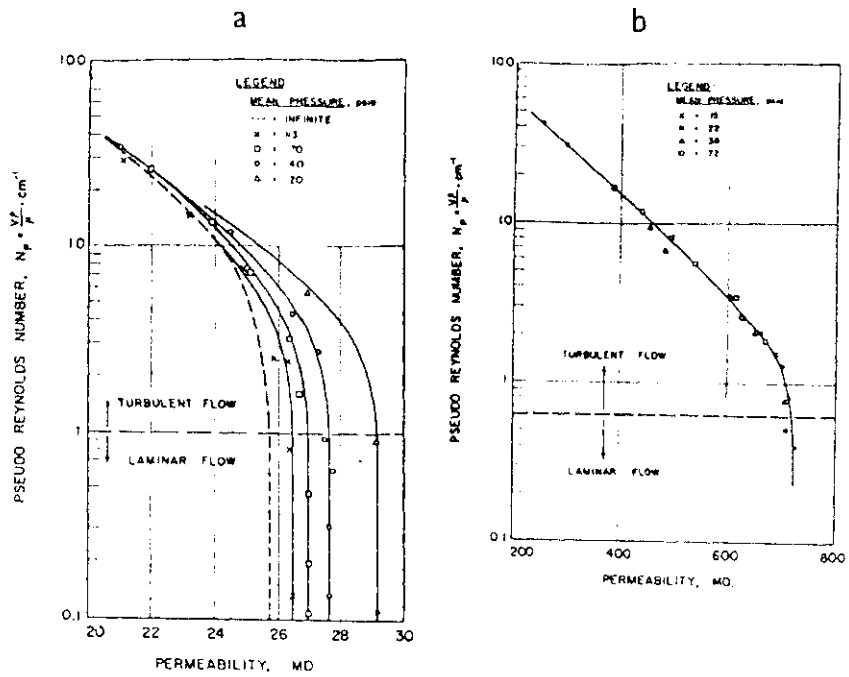


Fig. 1.3 Slippage and turbulence in air permeability measurements (1.3.a), turbulence only (1.3.b)

1.3.c Optical

Small diameter downhole cameras (Fons 1960) can be useful to obtain direct information regarding fissure distribution. Recently direct observation of fissures (Slater 1966; Tate et al 1970) has been undertaken using closed circuit underwater television equipment which includes facilities for viewing boreholes either axially or radially. By suspending a number of flow indicating streamers beneath the television camera, a general idea about the horizontal movement of the fluid column in the well can be achieved. Sometimes visible tracers can be injected which also permit a semiquantitative measurement of the flow.

All usual problems of photography like clean lens, clear water and focus depth are associated with this type of technique.

Since the bore-hole is filled with water, there will be between the wall of the well and the lens of the camera a layer of water which impairs visibility, according to its clay content.

Shcherbakova (1956) studied in detail the attenuation of a light beam by the clay suspension layers of various thickness. The following figure represents the value of transmittance T as a function of the thickness h of the layers of clay suspensions for various wavelengths.

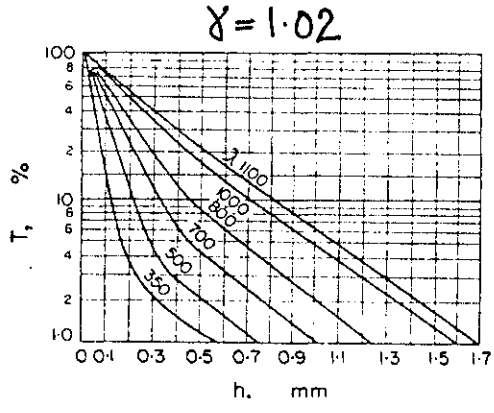


Fig. 1.4 Dependence of attenuation of light on specific gravity of the suspension, thickness h of the layer and wavelength λ of light

It can be seen that clay suspensions are indeed very turbid media and even in thin layers transmit very little light. For example from the above figure, one can see that even if the thickness of the layer of clay suspension is only some tenths of a millimetre the transmittance of the light is only about one percent.

1.3.d Geophysical

Of all the surface geophysical methods, the electrical resistivity method has been the most widely used in

groundwater investigations. The four-point method proposed by Wenner (1916) and Schlumberger brothers (1920) was developed for routine work in the following decades and has been brought to a very high standard today.

A number of excellent papers and reports have been published on the utilization of resistivity techniques in groundwater investigations and in recent years there has been a "boom" in modern computer techniques that allow an automatic inversion of vertical electric sounding data (Koefoed 1979).

Quite recently a few authors have attempted to correlate the resistivity of an aquifer to its hydraulic conductivity (Heigold et al 1980; Kosinski et al 1981; Kelly 1978; Griffiths 1976; Barker et al 1973) but they were concerned for granular aquifers only.

Results indicate that electrical resistivity determined from soundings can be used to predict aquifer hydraulic conductivities and different empirical relations between aquifer electrical resistivity and aquifer hydraulic conductivity were developed.

The fundamental relation between the above two parameters is their common dependence on tortuosity and porosity (Bear 1972).

Unfortunately for the case of fissured aquifers, no relevant work, according to the opinion of the author, exists up to now. The difficulty of establishing a relation between the electrical resistivity and the hydraulic conductivity of fissured aquifers is mainly due to the two main handicaps of electrical methods: the principle of equivalence and the principle of suppression.

Resistivity contrasts and "effective" relative thickness of fissure zones within the aquifer are too small to be

distinguishable (Keller and Frischknecht 1966). Flathe in a series of publications (1955, 1967, 1976) has examined the problem of recognizing an underground layer from a sounding graph with regard to its depth, thickness and resistivity and concluded that without a geological concept an interpretation of geoelectrical measurements is almost impossible if the number of layers concerned exceeds three and the accuracy of measured data is ±5%. Theoretically the fissure zone distribution can be calculated, but realistically, in most of the cases, it cannot be observed on the field curve.

1.3.e Pumping/tests

The hydrodynamic investigation of the aquifers by pumping, frequently followed by the recovery of the water level in the experimental well, constitutes an investigation technique indispensible to any kind of hydrogeological research.

In the last few decades the flow of groundwater towards pumped wells has received thorough mathematical treatment, thus it is not surprising that a wealth of literature dealing with the determination of hydraulic coinductivity from pumping tests has gradually become available.

Various methods are available for calculating hydraulic conductivities from well data and a useful compilation of the standard techniques, mainly applicable to granular deposits, has been produced by Kruseman and de Ridder (1970).

Inherent in the standard methods of analysis of pumping test data, are a great many assumptions and a detailed discussion on the deviations of the Chalk from these can be found in Ineson (1959a and 1959b). One of the main assumptions is that the aquifer is homogeneous, isotropic and of infinite areal extent.

In the case of the Chalk, its inhomogeneity and anisotropy have been clearly demonstrated by past workers, and it is well known that inflow into Chalk wells is commonly from only a few restricted horizons.

Regarding the interpretation and use of the results of pumping test analyses, the layered hydraulic structure of the Chalk is likely to cause borehole yields, and yield-drawdown characteristics to show marked variations with groundwater level. The importance of this was illustrated during the early stages of the Thames Groundwater Scheme, where the transmissivity of the unconfined Chalk aquifer was shown to decrease at a disproportionately high rate as water levels declined (Hardcastle 1978; Owen et al 1978). In the same area, Rushton et al (1976) used a numerical model with varying aquifer characteristics versus depth in order to match the drawdown predictions with those found in practice.

Under these circumstances, what is measured by a pumping test is a value for the "average" fluid hydraulic conductivity, but since Vandenberg (1977) has shown that the use of conventional formulae may be valid in the presence of lateral heterogeneity, but not vertical heterogeneity, it is often virtaully meaningless in aquifers where vertical heterogeneity is marked.

1.3.f Packers

Packers have been used for many years in testing and completing oil wells, but they have not been used extensively in hydrogeological studies for water supply. They are commonly used on engineering sites to assess grout take for ground treatment. Recent developments in design now make the use of inflatable straddle packers feasible for testing aquifers.

Both single and double-packer tests have been used by the Institute of Geological Sciences (Price et al 1982) for the study of the hydraulic conductivity of the Chalk in Hampshire.

One of the arguments frequently put forward against the use of packers is that they are complex to operate and relatively expensive. On the other hand although they could be ideal for isotropic formations when the case of fissured aquifers is considered such as the Chalk, the effect of fissure zones becomes very important. Barker (1981) has studied theoretically the problem of deriving the transmissivity of an infinite horizontal fissure in an injection zone and his method has recently been used by Price et al (1982) for the evaluation of the tests at Hampshire.

It is also quite usual for the packer not to achieve a successful seal because it is set against a fissure. Of course this problem can nearly be solved if the tests are supplemented by a television inspection of the walls of the well.

1.4 OUTLINE OF THE THESIS

The INTRODUCTION to this thesis has covered a preliminary discussion of the existing methods for the estimation of the hydraulic conductivity of fissured formations and an examination of the geophysical well logging methods currently in use by the water industry. The main body of the Thesis is divided into four PARTS.

PART I commences with Chapter II which deals with the fluid logging methods. Chapter III is devoted to a detailed theoretical and experimental study of the Heat-Pulse flowmeter. PART I concludes with Chapter IV which discusses the formation geophysical logs, how useful they

are in estimating the hydraulic properties of the fissured aquifers and how they are used today for the study of the Chalk aquifer.

The second PART of the Thesis starts with Chapter V where an attempt is made to study the hydraulic behaviour of fractured Chalk from the flow characteristics of a number of fissure elements. In the same Chapter the effect that fissure contact area and the local hydraulic gradient have upon the hydraulic conductivity of a fissure is being investigated. PART II continues with Chapter VI in which the Chalk is simulated by a numerical double porosity model and an attempt is made to correlate geophysical formation parameters measured by the logs with hydraulic conductivity. Special attention is given to the effect that fissures have on certain geoelectric parameters and a new formation parameter found to be very sensitive to fissure zones is introduced.

PART III commences with Chapter VII in which are described the construction details of microcomputer based hardware and software packages developed for the research. In Chapter VII, a method for modelling the response of a resistivity logging device is presented.

Finally, in PART IV, the methods introduced in PARTS I and III are applied to a number of wells and the results obtained are analysed in Chapter IX. The general conclusions of the research are presented in Chapter X where some recommendations for further studies are made.

The thesis contains a number of APPENDICES where technical aspects about the equipment and programs used are discussed and all relevant project information is presented.

PART I

This PART of the Thesis commences with Chapter II which studies to what extent the fluid geophysical logs can be used for estimating the hydraulic conductivity of the Chalk. Since flowmetering has proved to be very useful in understanding the hydraulic conditions in and around a borehole, special attention has been given to the heat pulse flowmeter whose limits of usefulness are defined by theoretical and experimental investigation: this is done in Chapter III. Finally in Chapter IV the formation geophysical logs are discussed.



Plate 1 Arrangement for geophysical well logging

C H A P T E R II

THE USE OF GEOPHYSICAL FLUID LOGS FOR EVALUATING THE HYDRAULIC PROPERTIES OF FISSURED AQUIFERS

2.1 INTRODUCTION

By means of a fluid log, the movement of the fluid filling the well under pumping conditions or at rest is determined together with some of its properties such as temperature and electric conductivity.

Fluid logs have been utilized for many years to gain information on fluid movement in and adjacent to wells. Much research, both field and laboratory, has been done in an attempt to apply mathematical standards to the information obtained. Detailed quantitative interpretation has been generally unsuccessful because of many factors such as borehole effects, unstable well conditions and equipment problems.

This Chapter discusses the results of an investigation of the fluid logs used by the water industry today, and examines the extent to which fluid logs can be used to estimate the hydraulic conductivity of the Chalk.

2.2 PROPERTIES OF THE FLUID COLUMN AS RELATED TO THE HYDRAULIC PROPERTIES OF THE AQUIFER

Three main properties of the fluid column measured by the fluid logging techniques used today are its velocity, its temperature and its electrical conductivity, which is linearly related to the total dissolved solids.

Often the total amount of information available to us at a given time or the properties of the fluids in the ground

exists in the form of fluid logs; therefore it is critical to be able to extract this data and, by determining what conditions affect it, to come to some conclusions about the hydraulic properties of the surrounding formation.

To do this, an understanding of the tools, their reactions and methods of reading, and the environmental reaction surrounding them is imperative.

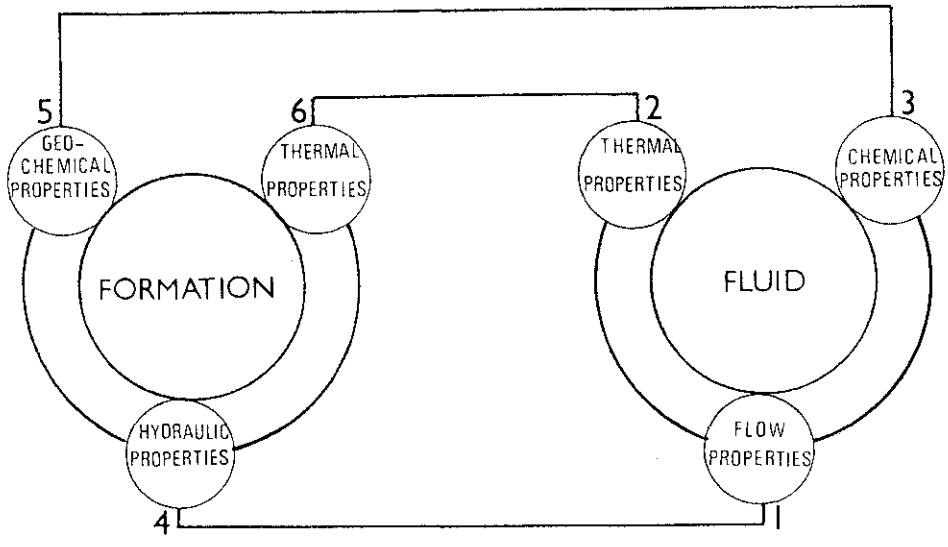


Fig. 2.1 The possible ways by which the three basic sets of properties of the formation and fluid affect each other

Fig. 2.1 represents in a diagrammatic form the various ways by which the three basic sets of properties of the formation and the fluid in the well can affect each other. In an idealized pumped borehole in a porous medium the fluid usually enters the borehole evenly at all points on the saturated face of the borehole, neglecting the capillary fringe. For most fissured aquifers such as the Chalk, the greater volume of water tends to enter the borehole at discrete levels, usually natural fissure zones.

The principle of operation of the flow log is that water from a particular fissure has some of its physical and physico-chemical properties slightly different from those in the fluid column. This is clearly shown in Fig. 2.1 by linking property 4 with properties 2 and 3 through 6 and 5 respectively.

It has become apparent in recent years that a knowledge of the distribution of these fissure zones is essential to the yield/drawdown studies and aquifer analysis associated with pumped wells.

Most fluid logs should permit the discrimination of the hydraulic properties (4 in Fig. 2.1) of the ground surrounding the well from the properties of the fluid in the well (1, 2 and 3 in Fig. 2.1).

Thermal and chemical properties (2 and 3 in Fig. 2.1), which are recorded in the form of temperature and conductivity logs respectively, give a qualitative estimate of the hydraulic properties (4 in Fig. 2.1) where flow property (1 in Fig. 2.1) which is recorded in the form of the fluid velocity log, can in some cases give a semiquantitative estimate of the hydraulic conductivity of the aquifer.

A considerable length of time, sometimes being of the order of several months is required for the water in most wells to reach thermal and chemical equilibrium, with the surrounding aquifer in the zones where there is no flow and every time a probe is moved through the well these conditions are disturbed.

Fig. 2.2 shows the arrangement usually used for flow logging and Fig. 2.3 shows some flow logging probes with their reference points.

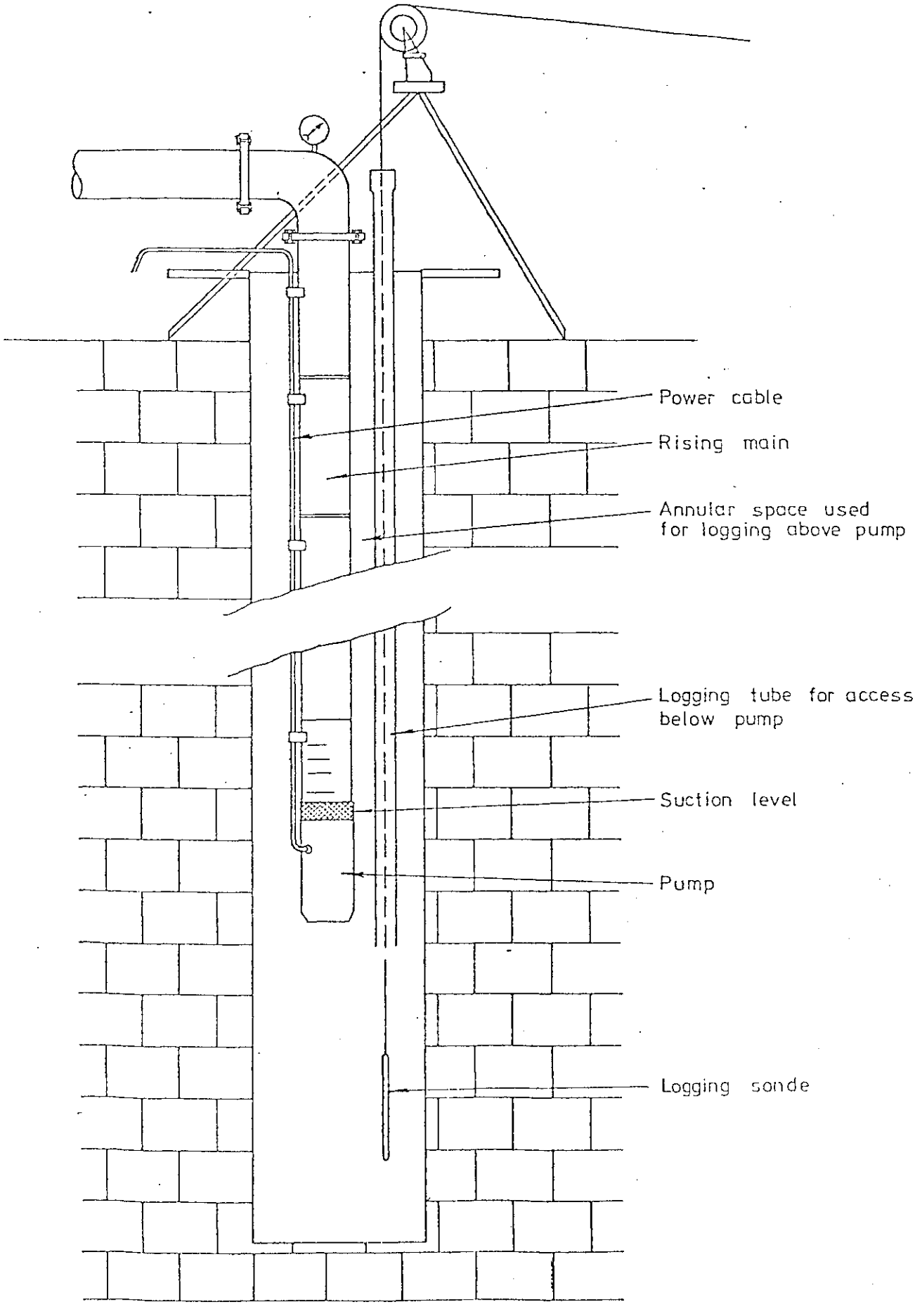
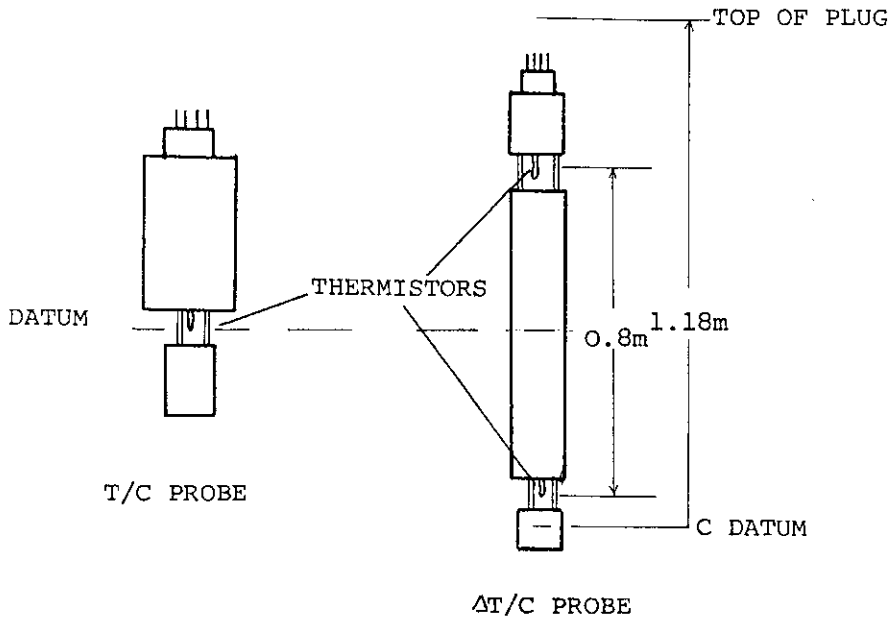


Fig. 2.2 Arrangement for a flow logging investigation



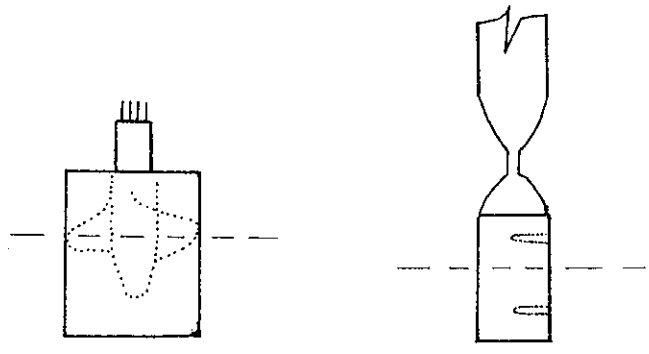


Fig. 2.3 Datum points for hydrologger probes. T/C: temperature-conductivity, ΔT/C: differential temperature-conductivity

2.3 THE USE OF FLOW VELOCITY MEASUREMENTS IN WELLS AND BOREHOLES

As the use of quantitative hydrologic methods has increased, the need for accurate methods of measuring flow within a well has also increased. Fluid velocity is a critical measurement and is very often sought in well logging programs (Tate et al 1970).

By means of a fluid velocity log, the vertical movement of the fluid filling the well under pumping conditions or at rest is determined.

The objectives may be:

- To detect flow from one fissure level to another when there is no pumping in the well;
- To determine, from existing wells, the optimum position and length of the screen for projected wells.
- To trace incrusted (screen) sections when a well has declined in production.
- To examine the outcome of well (re-)development, as might be accomplished by such development techniques as surging or jetting.
- And, mainly, to establish the inflow levels of a new well.

A fluid movement log run in a stagnant column of water would show a straight trace both in the up and down direction. Where vertical flow occurs, due to differences in the hydraulic gradient between the parts of the borehole, deflections in opposite directions are recorded on the up and down trip. With a moving flowmeter, rates of flow can be detected that are too small to affect the instrument when it is in a stationary position.

Many researches (Diment 1967; Gretener 1967) have shown that the thermal instability of the water column represent

water movements over a distance of no more than several times the diameter of the well. If the water column is viewed as a series of vertically juxtaposed convection cells or eddies, it can be said that the height of the cells would be no more than several times their width (Fig. 2.5).

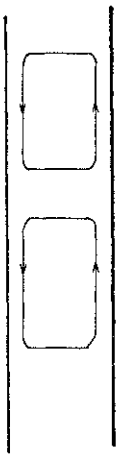


Fig. 2.5 Convection cells representing water movement due to thermal instability

Clearly, the actual motion is far more complex and probably involves the continual formation and breakdown of irregular eddies which move in response to the local density distribution within the water column.

2.4 THE FLOW REGIME INSIDE A WELL

It often happens that the water column inside a well becomes unstable because of the buoyancy forces resulting from a reduction in fluid density due to changes in temperature. Under such circumstances velocity measurements designed to record flows from non-thermal gradients encounter serious difficulties.

When a vertical tube filled with fluid is subjected to a thermal gradient, the fluid will become unstable and start

to convect as soon as the gradient exceeds a certain critical value.

Hales (1937) treated this problem from a theoretical point of view and derived the following formula for the critical gradient

$$G_c = \frac{g\beta T}{C_p} + \frac{C\nu\hat{k}}{g\beta D^4} \qquad (2.1)$$

where g = acceleration of gravity
T = absolute temperature
β = coefficient of thermal expansion
Cp = specific heat at constant pressure
ν = kinematic viscosity
$\hat{\kappa}$ = thermal diffusivity
D = radius of the borehole, and
C = a constant, which is 216 for a hole whose length is great compared to its diameter

The first term of the above formula gives the onset of convection in the absence of viscosity, whereas the second term ($C\nu\hat{k}/g\beta D^4$) takes into consideration the fluid viscosity. For a fluid such as water the first term is usually small, so small (0.2°C/Km) that any well be unstable under normal gradient conditions. It is, thus, the second term that is decisive.

By using the physical properties of water at 10°C given in Appendix I, the above formula can be simplified as follows:

$$G_c = \frac{216 \times 1.3 \times 10^{-6} \frac{m^2}{sec} \times 1.395 \times 10^{-7} \frac{m^2}{sec}}{9.81 \frac{m}{sec^2} \times 0.5 \times 10^{-4} \frac{1}{°F} \times D^4 m^4} \Longrightarrow$$

$$\boxed{G_c = \frac{0.4433 \times 10^{-7}}{D^4} \; °C/m}$$

An attempt is made below to calculate the critical gradient for wells of various diameters and these values are presented in the form of a graph in Fig. 2.4.

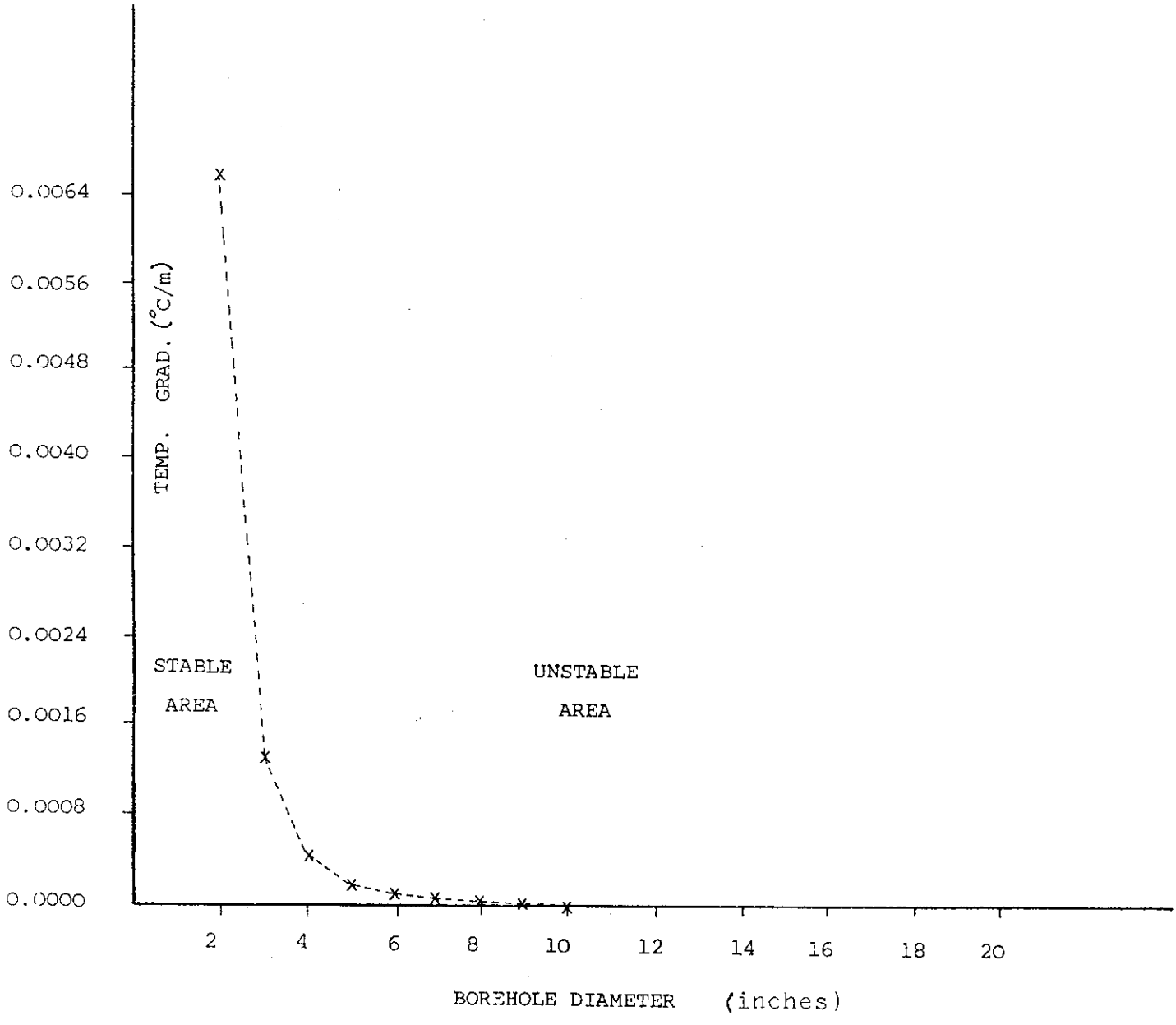


Fig. 2.4 Critical temperature gradient for different borehole diameters

Since in sedimentary areas the geothermal gradient is seldom less than 0.01, °C/m most wells in the Chalk (where much of the later fieldwork for this research was undertaken) must be thermally unstable.

In order to examine the flow regime inside a well at the level of a fissure zone, a perspex model was used (Plates 2 and 3). By injecting at the parallel plate inlet a blue dye and observing the subsequent dye front it was found that the flow at the output of the fissure was laminar (Figures 2.6 a,b,c), but as more dye continued to travel through the water column, turbulence started to develop above and below the fissure plane (Figures d and e).

Next an attempt was made to change the smooth output of the fissure plane to an irregular one. This was done by coating the fissure output by a mixture of sand and glue. The experiment was repeated and it was found that at certain points on fissure's output, turbulence started to develop from the point of entry to the well (Fig. 2.6f). This suggests that in actual situations one must bear in mind the irregularities of the fissure plane and it is more likely to expect the flow regime inside the well at the fissure level to be turbulent than laminar. This explains the phenomenon (Robertson, A., personal communication 1981) in which when an attempt is being made to operate a heat pulse flowmeter at a level where fissure flow exists, the obtained results are unusable.

2.5 METHODS OF FLOW MEASUREMENT

The several methods and devices of flow measurement in boreholes and wells which have been developed and are in use by the water industry today are briefly described below.

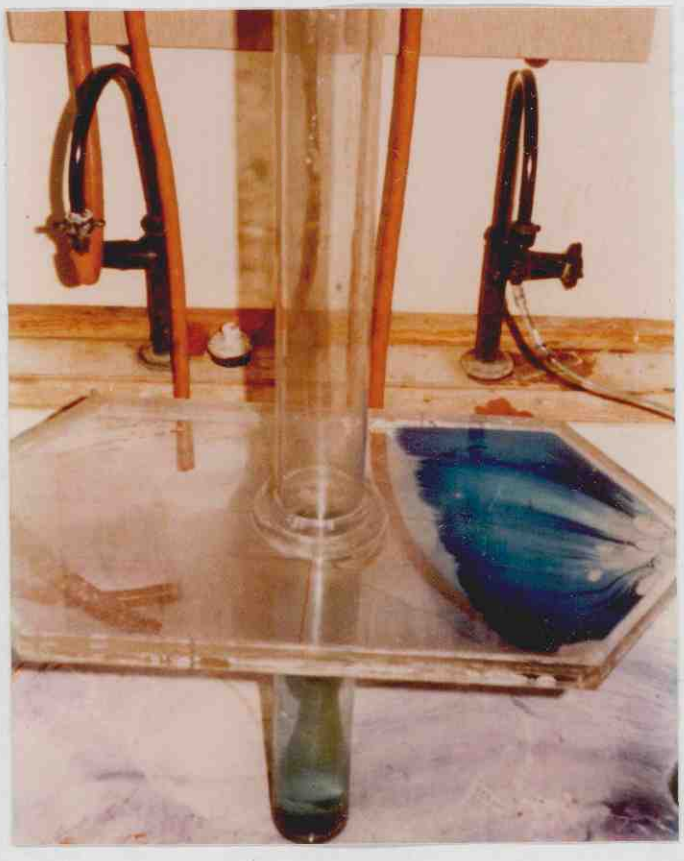


Plate 2 Perspex model used to simulate fissure flow

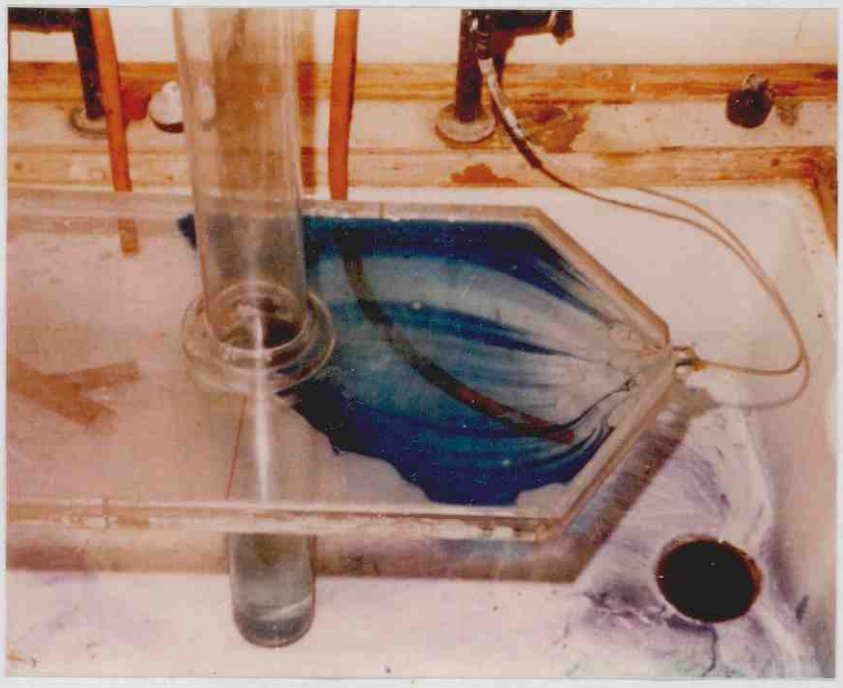


Plate 3 Fissure flow clearly illustrated by dye

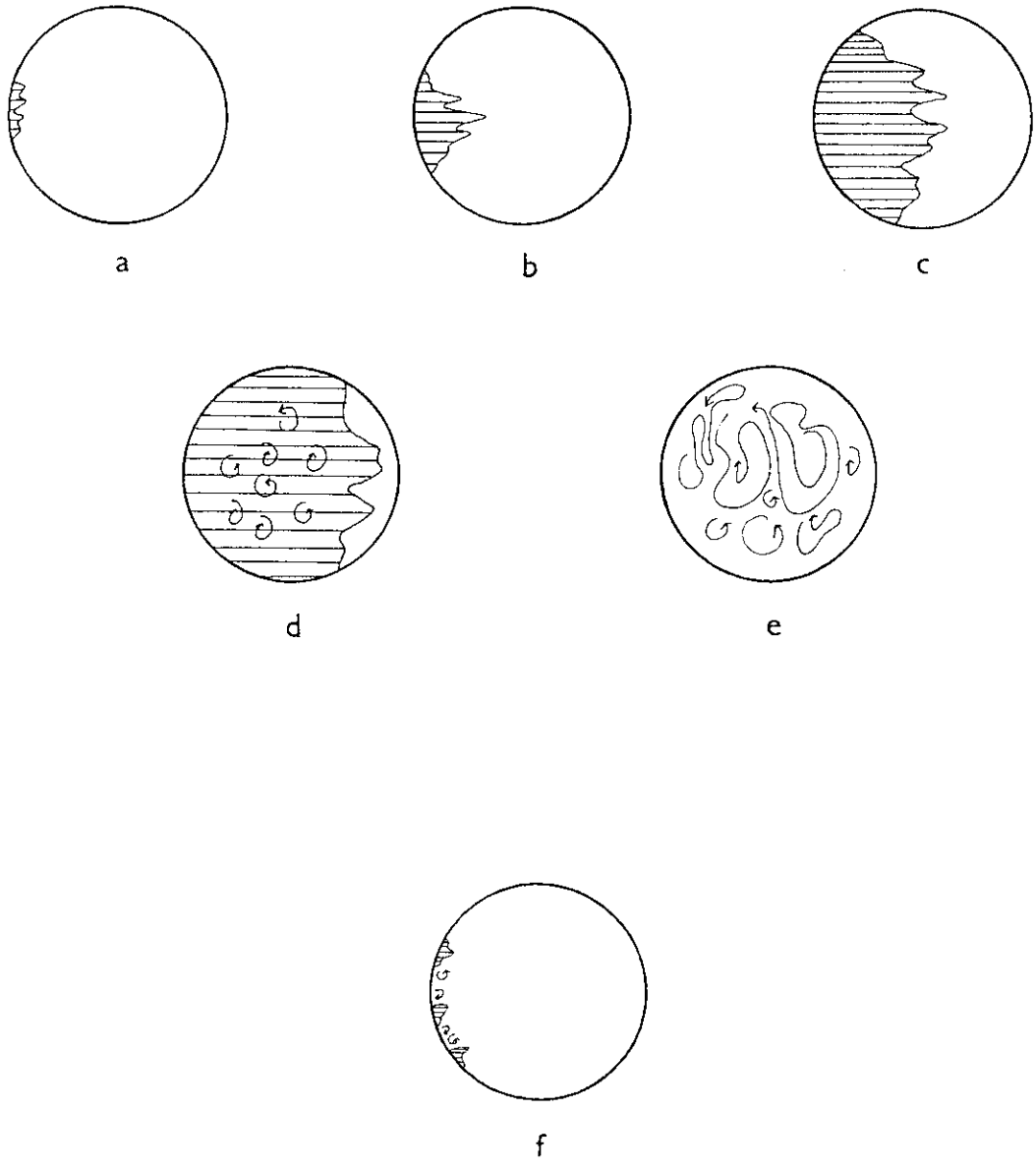


Fig. 2.6 Subsequent dye fronts inside the tube representing the well, at the level of the fissure

DIRECT METHODS

These methods depend on measuring either the velocity of the moving water or the velocity of a signal propagating with the moving water column. Such signals can be portions of dye introduced into the water, or locally produced changes of one of the physical parameters of the water, i.e. temperature, ion concentration, radioactivity. In all these cases the flow velocity is calculated from the time interval between the injection and the moment of tracing.

Impeller Flowmeter

Principle of operation: It converts flow rate to electric pulses by sensing the rotation of an impeller exposed to the water column.

Advantages: It is the more widely used flowmeter by the water industry today. It is simple in its operation, and continuous data can be obtained.

Limitations: Below velocities of the order 30 to 50 mm/s the effect of bearing friction has a serious reduction on the accuracy of the measurement.

Dye Propagation Method

Principle of operation: A portion of dye of similar density to water is introduced into the water and its travel time is measured.

Advantages: It can be used to study the horizontal flow opposite fissure zones.

Limitations: Very impractical method, requires a TV camera for observing the movement of the dye into the well or some appropriate timed sampling arrangement.

Ion Propagation Method

Principle of operation: A discrete slug of brine is injected in the water; its movement is then traced with a fluid-conductivity cell.

Advantages: The method is very simple; the equipment need no calibration, it utilizes a readily available tracer that does not require licensing.

Limitations: Continuous logging of the flow velocity versus depth is not possible; radial inflow of water in screened sections tends to disrupt the shape of the brine slug. There is an upper limit of velocities above which the measurements become inaccurate.

Radioactive Tracer Propagation Method

Principle of operation: The passage of radioactivity-tagged water past a pair of gamma-ray detectors is timed.

Advantages: It is more accurate than the above methods. It can be used to measure flow behind the casing.

Limitations: It uses radioactive elements which by many are considered as unacceptable for use in the water.

In the water industry today, various substances chosen to act as water tracers are selected depending on the strength of public opinion, (it took almost half a century for the use of radiotracers to be regarded as part of the normal range of techniques available to the hydrologist), the magnitude of the velocity range, the sensitivity of instrumentation available, the cost, the remoteness of the site and the accuracy required. When high accuracy is sought and the field conditions are such that the accuracy will be limited only by the tracer characteristics, there are very few tracers to choose from, the best being chloride, bromide (bromine-82), and tritium, as they have all proved to be reliable.

INDIRECT METHODS

These methods depend on measuring a physical process which is strongly dependent on velocity.

Dilution Methods

Principle of operation: A known quantity of salt solution of known concentration is introduced into the water. The rate of dilution is a function of the velocity of the water.

Advantages: It is very effective in measuring horizontal flow velocities opposite fissure zones.

Limitations: It is necessary to isolate each section of the well under study in order to define the dilution volume.

A variation in the above method is to measure the rate of dilution of a high gamma ray emitting tracer, by a gamma detector.

Hot Film Method

Principle of operation: The wire (film) is heated above the temperature of the surrounding water by passing an electric current through it. The rate of cooling is a function of the velocity of the water.

Advantages: The sensitivity of the method increases with decreasing velocity.

Limitations: The deposition of a layer of dirt on the wire, the formation of bubbles on the sensor and the variation of water-temperature result in the reduction of the accuracy of the measurement.

Thermal Flowmeter

Principle of operation: The water is heated continuously with an electric heater and the temperature difference between a point below and a point above the heater is measured. This difference is related to the water velocity.

Advantages: Since the temperature difference is measured, the ambient temperature variation does not affect the accuracy of the measurement.

Limitations: The continuous heating of the water generates thermal convection currents which can reduce the instrument's accuracy at the low velocity range.

Nuclear Magnetic Resonance Flowmeter

Principle of operation: A magnetic field is generated by means of a coil placed in the water column, inducing an electromotive force in the water which is directly proportional to the velocity of the water. This method is in the experimental stage.

The advantages and limitations of each method has been discussed and the choice of the appropriate method depends on a number of factors such as: site conditions, equipment, and resources available to the gauging authorities etc.

Resume

Table 2.1 summarizes all the above methods in a diagrammatic form with the optimum range of velocities within which they can operate with accepted accuracy.

Today the most common in use flowmeter device is the mechanic flowmeter (borehole spinner). It is the simplest and least expensive device but it is limited to higher velocities and must be carefully calibrated for quantitative use. Recently a new device under the name of heat pulse flowmeter has shown considerable promise in water velocity measurements as low as 1 mm/s and is examined in detail in the next Chapter.

2.6 THE RELATION OF FLOW VELOCITY MEASUREMENTS TO THE HYDRAULIC CONDUCTIVITY OF AN AQUIFER

It has already been shown in Fig. 2.1 that the flow regime,

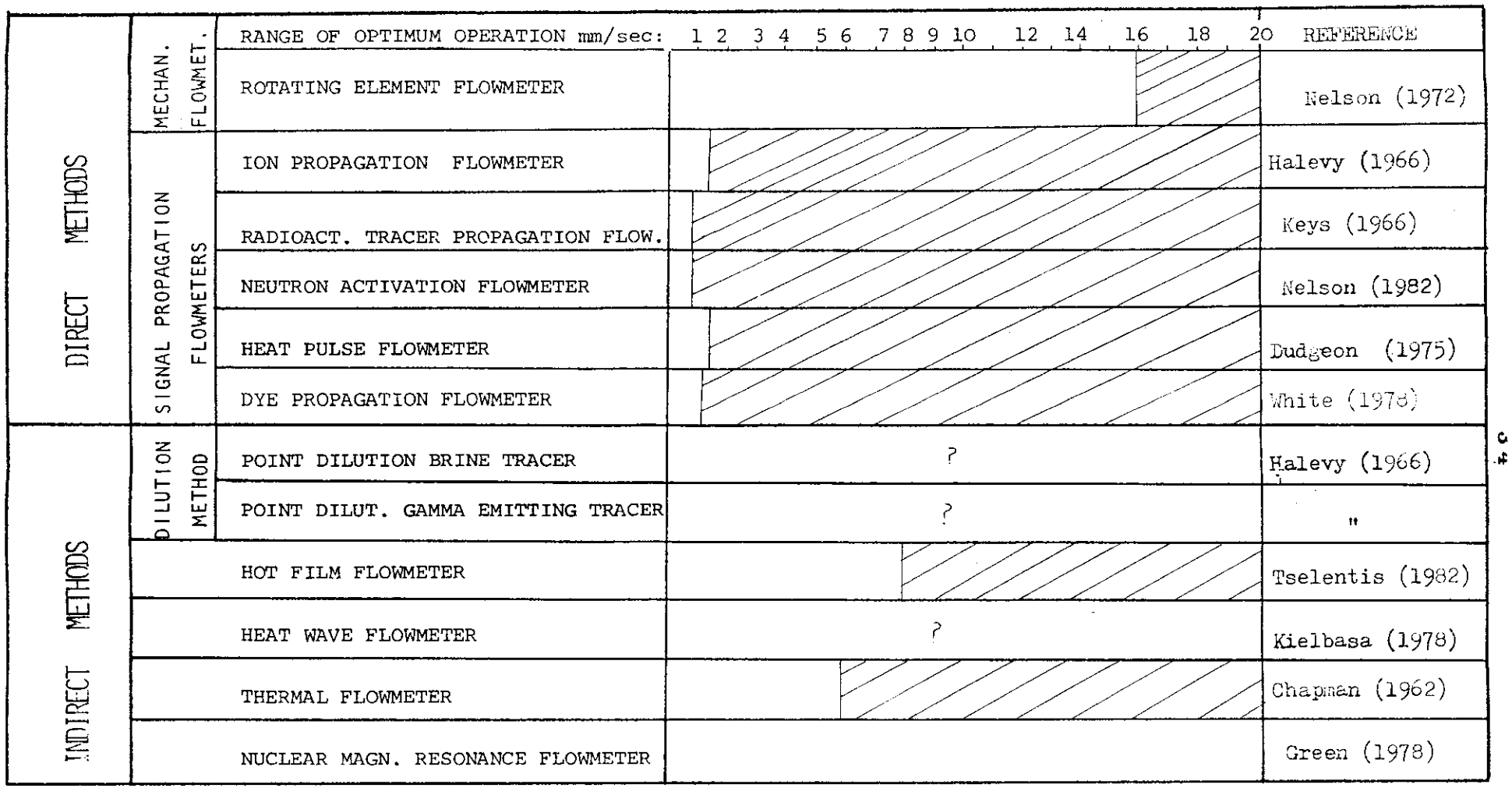


Table 2.1 Methods of flow velocity measurements and their optimum range of operation

under no pumping, inside a well is a function of the thermal properties of the water column and the hydraulic characteristics of the aquifer.

A very common question put often to the hydrogeologist or geophysicist is: "Given available measurements of velocity in a borehole, what is the transmissivity of the aquifer?". Unfortunately, even today, the answer to this sort of question continues to be an elusive goal, except for some special cases. Perhaps it is better to modify this question in the following form: "Given available measurements in a borehole, what can we deduce about the hydraulic characteristics of the surrounding material?". Here is where the flow velocity log can give, in most of the cases, a definite answer.

Measurements of the rates of vertical flow at different depths in a well can reveal the location, thickness and relative productivity of water bearing fissure zones. Imagine logging a well whose vertical hydraulic conductivity distribution is K(z) and let $V_{f,z}(z)$ be the measured velocity profile (Fig. 2.7). In general $V_{f,z}(z)$ can be related to K(z) for a constant pressure gradient as follows:

$$V_{f,z}(z) = F(K(z)) + C(z,D,T) \qquad (2.2)$$

where F is an unknown function and C depends on the diameter of the well (D) and the thermal gradient (T).

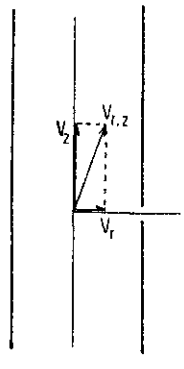


Fig 2.7 Velocity components at a point inside a borehole

Concentrating on the horizontal component of the velocity and neglecting the second term on the righthand side, the hydraulic conductivity function can be written as:

$$K(z) = G(V_r(z)) \qquad (2.3)$$

where G is an unknown function.

It is worth here to refer to an experimental attempt by the Bhabha Atomic Research Centre, Bombay (1978), in examining the relative permeability of bedrock foundation on a future dam. In this experiment radiotracer was injected all along the length of the borehole and the horizontal velocity profile across the axis of the borehole was studied by measuring the rate of disappearance of the tracer at different depths by repeated logging with a Geiger-Muller counter.

In general this approach of examining the hydraulic conductivity of the formation from measurements of the horizontal component of the velocity versus depth is feasible only when the rate of dilution at the suspected fissure zone (if we use one of the dilution methods to measure the velocity) is expected to far exceed the rate of vertical transport of the tracer by diffusion or vertical currents generated by thermal instability. Comparison of the profiles of the logs taken at different intervals will indicate whether this condition is satisfied because vertical currents would cause significant variations in the tracer concentration profile.

If we were to use the vertical component of the velocity, since this is what usually is measured by the commercial flowmeters, then the following relation should be used:

$$K(z) = G(V_z(z)) + C(z,D,T) \qquad (2.4)$$

where the second term is due to the thermal instability of the water column. Assuming that $\frac{\partial}{\partial z} C(z,D,T) = 0$, the following expression for K(z) can be obtained:

$$K(z) = \int F\left(\frac{\partial V_z(z)}{\partial z}\right) dz \qquad (2.5)$$

where G, C, and F are unknown functions.

All the above equation means is that in some cases it is better to look at changes of the vertical velocity profile than in absolute values themselves. Or in other words, that the vertical variation of the hydraulic conductivity can more easily be identified from the variations of the velocity profile.

2.7 THE USE OF FLOW TEMPERATURE LOG

Wells up to a certain diameter, left quiet for some time, enable the measurement of the temperature as a function of depth to be made. By comparing the measurement profiles with "normal" undisturbed temperature profiles, information may be gathered regarding the geohydrological conditions which have led to the thermal gradients measured.

This is based on the fact that the geothermal gradient is considerably modified by fluid movement in the borehole and adjacent rocks.

2.7.a The temperature regime inside a borehole

Let T be the observed temperature at depth z: it is well known (Beck et al 1969) that T can be written as:

$$T = T_o + g.z + V_s \qquad (2.6)$$

where T_o is the surface temperature before the onset of any climate change, g is the undisturbed temperature gradient in the area and V_s is the temperature disturbance at depth z due to a surface temperature variation of any form.

In order to make the above formula more complete, another term $V_d(z)$ is added, representing the temperature disturbance at depth z due to some change of the thermal properties of the formation at this depth.

The above formula shows that the temperature field inside a well is also a function of time, since V_s and $V_d(z)$ depend on time.

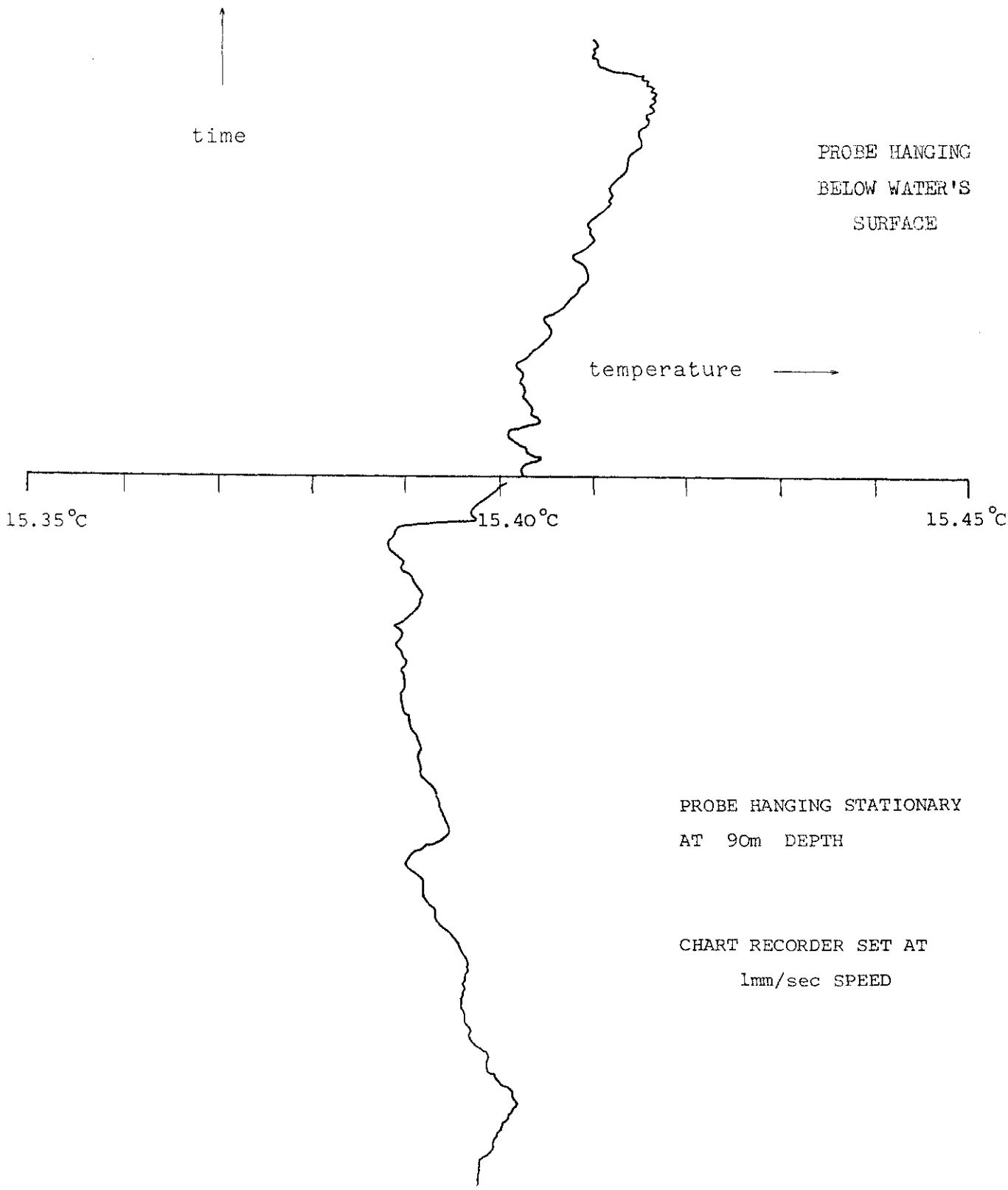
On the other hand, during the drilling of the borehole, the temperature profile at the drilling site is disturbed, and a period of rest of approximately half a year will normally be needed for the real temperature gradient to recover.

In addition to this, convection currents occurring in the fluid column can cause some errors, but it has been found (Samme 1968) that these are relatively small of the order of a few 1/100°C. In order to test this assumption, the following experiment was carried out: Before disturbing the fluid column in a borehole (No. 12) at Brighton, the temperature probe was placed in two positions inside the fluid column, and was left for some time. The variations in the temperature were recorded and the obtained results are shown in Fig. 2.8.

As it can be seen from the above graphs, there was not any serious disturbance of the temperature field since the maximum variations observed were of the order of 0.01°C.

Since the temperature observed at a specific point is the result of the total environment, a method of defining the variables and eliminating or computing their effect is necessary before valid quantitative work can be accomplished.

Fig. 2.8 Temperature variations inside the borehole



2.7.b Methods of temperature logging

Temperature logging tools used by the water industry today can be divided into two basic methods.

Absolute method: A single element tool calibrated and aligned to detect the existing temperature downhole and transmit this information to the surface, where it is recorded as actual temperature versus depth. By this method the temperature of the borehole water at a single point is measured and the measurement is subject to the sum of the vertical and lateral effects of temperature transition in the zone containing the point of measurement. Sharp definition of temperature interfaces is improbable unless the differential is extreme, and slight changes often go unnoticed unless recording sensitivity is high. Total transition from one temperature to another is usually averaged over a long vertical interval.

Differential methods: The differential method utilizes two elements physically separated by a given distance. Both elements detect the absolute temperature of the fluids at their respective depths. These temperatures are impressed upon a "comparison circuit" and the difference between them is transmitted to the surface and recorded.

The actual difference in temperature would be determined by the deflection of the curve. During most logging operations, the progress downhole is usually continuous; therefore, both the rate and the amount of temperature

change affect the readings, and the log is used as a relative temperature change indicator.

The actual temperature is recorded simultaneously on a separate circuit. The advantage in this usage is a more prominent indication of temperature change over a given interval.

Recently, a modification of the above method has been used. It makes use of a single element and an electronic "memory circuit". The single element detects the temperature of the well water and sends this information to a memory cell or delay circuit. The difference in temperature recorded at two time intervals is recorded as a differential.

2.7.c The Relation of temperature measurements to the hydraulic conductivity of the aquifer

Imagine measuring the temperature along the axis of a borehole in which there is no reason to suspect any significant influence from fissure flow.

Under these conditions what is represented by the temperature log is the normal geothermal gradient which is caused by the continuous flow of heat outward from the interior of the earth.

There should be no argument that a static column of fluid will present a different temperature profile from that in which the fluid is moving. Further, different rates of fluid flow will produce correspondingly different changes in the temperature profile.

The effect of water entering a well on the temperature

profile has been recognised and documented in the literature (Jones et al 1956; Tate et al 1970).

In the case that a fissure zone crosses the well at a certain level, a change in the thermal gradient at that level is expected because:

(a) The thermal gradient at the corresponding interval depends upon the thermal resistivity of the formation which is altered by the presence of the fissure.

(b) The entrance of fissure water (usually being of different temperature than that of the water column), causes the generation of convection currents disturbing the temperature field at the particular level in a very complicated way.

By looking at the temperature log for regions where changes in the temperature gradient occur, it is quite often possible to recognize zones of high hydraulic conductivity.

Similar results can be obtained by using the differential temperature log. Since the temperature and differential temperature logs are very sensitive to extraneous effects such as instrumental noise, changes in the speed of logging velocity, thermal instability of the water column etc., it is very common for these logs to show variations which could be misinterpreted as due to fissure effects.

A very effective method to recognize true fissure effects on the T and dT logs is, after running the log on the way down, to leave the logging probe for a while near the bottom of the hole for equilibrium to re-establish and then repeat the same process on the way upwards. By this method when we compare the two sets of logs, the true fissure effects should show as mirror images, whereas all the other effects should show in one of the two logs only and so can easily be removed.

Date	26-10-82	Plumbed depth	91.4 m	Casing	305 mm ϕ to 16 m depth
Time	1135 GMT	Depth datum	Recorder baseboard		
R.W.L.	30.8 m down	Datum m A.O.D.	39.64 m	Pumping	N/A
Depth		Logged From	32m To 90m.		

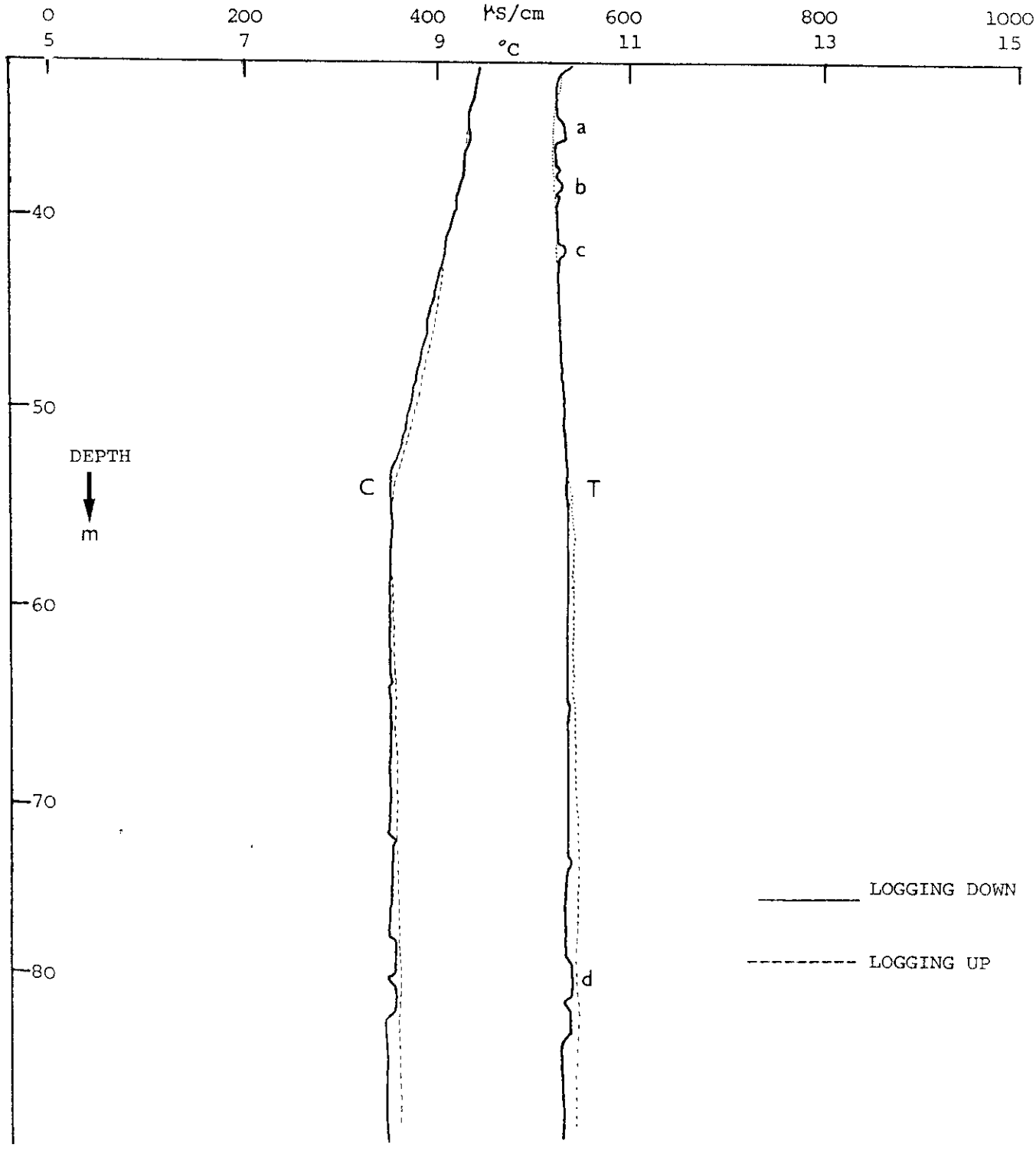


Fig. 2.9 Conductivity and temperature logs in both the ways up and down

The following Fig. 2.9 contains a copy of a conductivity and a Temperature while Fig. 2.10 contains a copy of a Differential temperature log carried out by the author in a borehole located in the Brighton Chalk.

A number of features a,b,c,d where recorded on the Temperature log on the way down but these features are missing from the same log when it was run on the way up. This suggests that these features have nothing to do with fissure flow effects and probably are due to external noise. These sort of variations on the Temperature log are very common in logging practice (Ellis, J. personal communication 1982) and cause a lot of problems during the interpretation stage.

By comparing the two traces on the Differential Temperature log, one can confirm that the feature existing at about 52 m is reproduced on the way up, thus it can be interpreted as the result of fissure activity at that specific level.

Fig. 2.11 shows a copy of a temperature and Differential Temperature log carried out by the WRC at borehole No. 2 in the Chalk of Brighton.

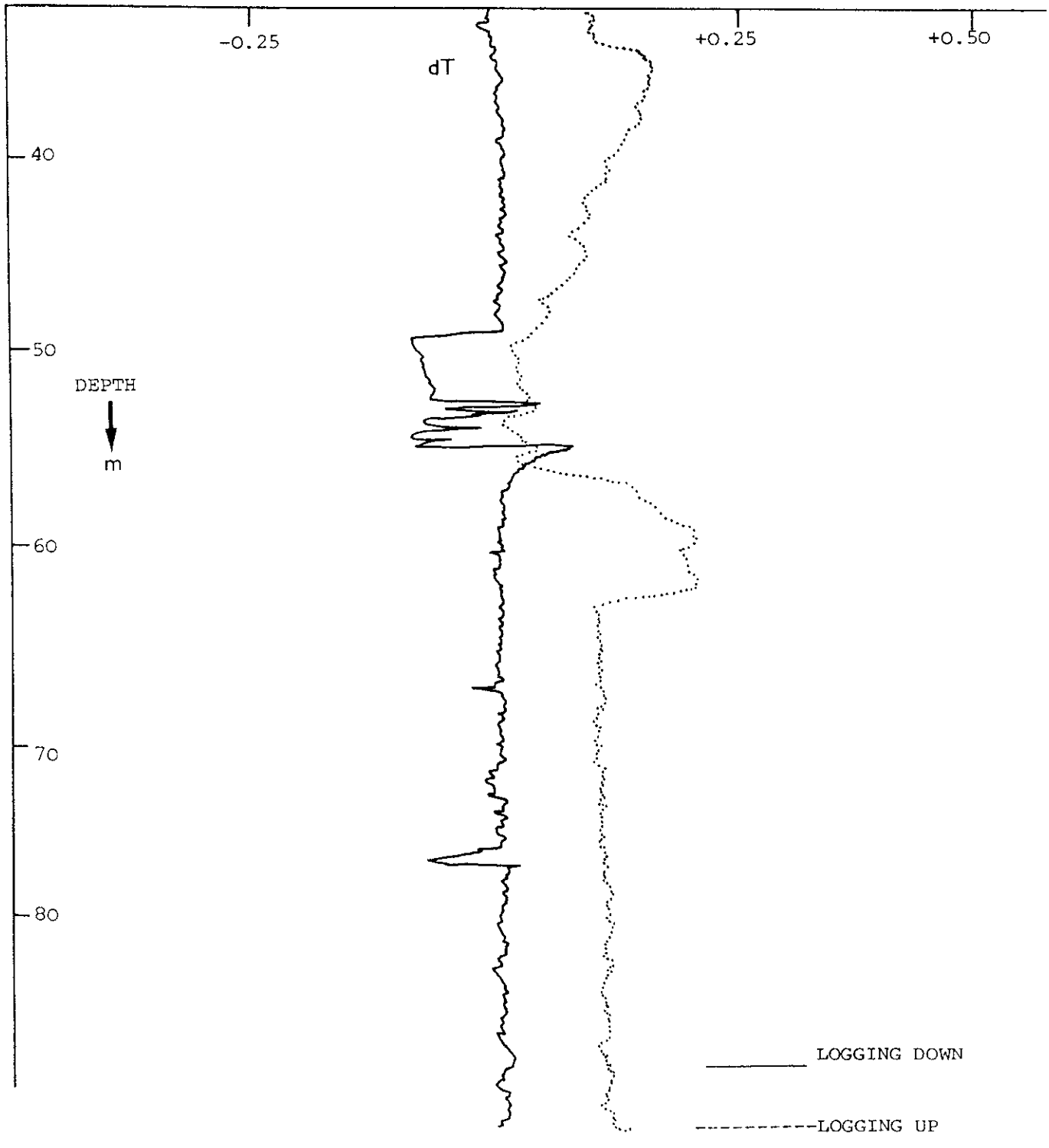
There are the following areas of interest in the log:

(a) Between 38 to 79m there is a slight temperature gradient of about 0.61°C/100m. In the same interval the differential temperature log shows little evidence of inflow or outflow points.

(b) Between 79 to 120m, there is a slight temperature gradient which now approximately becomes 1.95°C/100m with numerous peaks in the differential temperature log suggesting inflow/outflow levels.

(c) At the level of 120m there is a temperature jump of 0.6°C.

Fig. 2.10 Differential temperature log in both the ways up and down



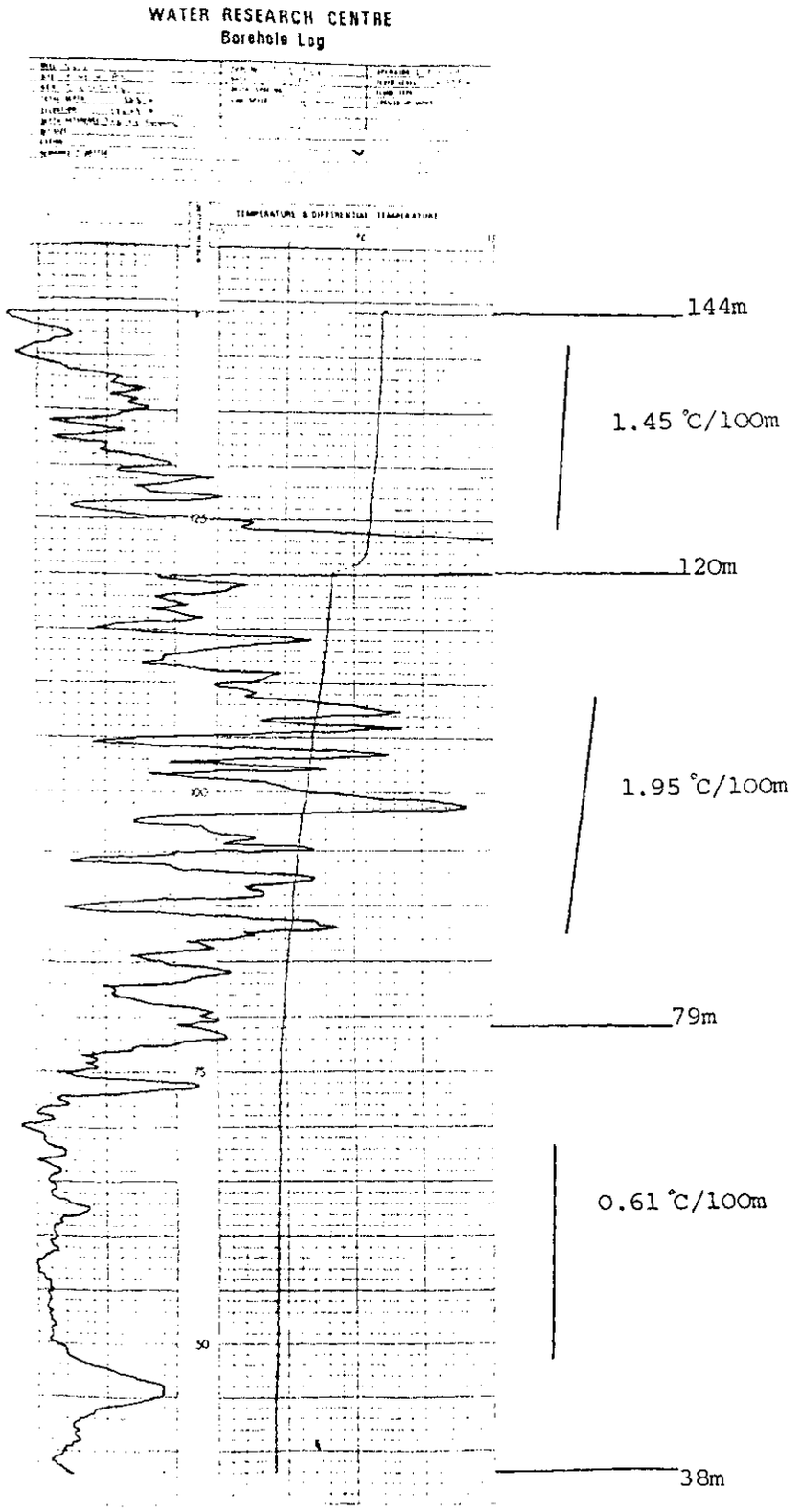


Fig. 2.11 Differential temperature and temperature logs

(d) Between 120 and the bottom of the well, a slighter gradient exists, together with differential temperature peaks.

Quite often distinct changes in borehole fluid temperature are generally observed at the depths where the resistivity lows occur.

Fig. 2.12 is an example of this showing the resistivity and temperature logs for a borehole in the Chalk at Brighton. The arrows show changes in the temperature gradient.

2.8 THE USE OF THE FLUID CONDUCTIVITY LOG

The fluid conductivity log provides information regarding the groundwater's electrical conductivity as a function of depth.

The principle of operation of the fluid conductivity log is that water from a particular fissure has an electrical conductivity which is slightly different from that in the fluid column.

2.8.a The fluid conductivity regime inside a borehole

The electrical conductivity of the water in a borehole at a given depth depends upon the concentrations, mobilities, and valences of the ions in the water at that depth. It is, therefore, controlled partly by the processes of ionic diffusion and dispersion and ion transport by moving fluids. Imagine measuring the fluid conductivity along the axis of a borehole in which there is no fissure flow. Under these conditions the conductivity profile may be representative of the porewater in the adjacent formation, nevertheless this is not necessarily so for the case of fissure flow.

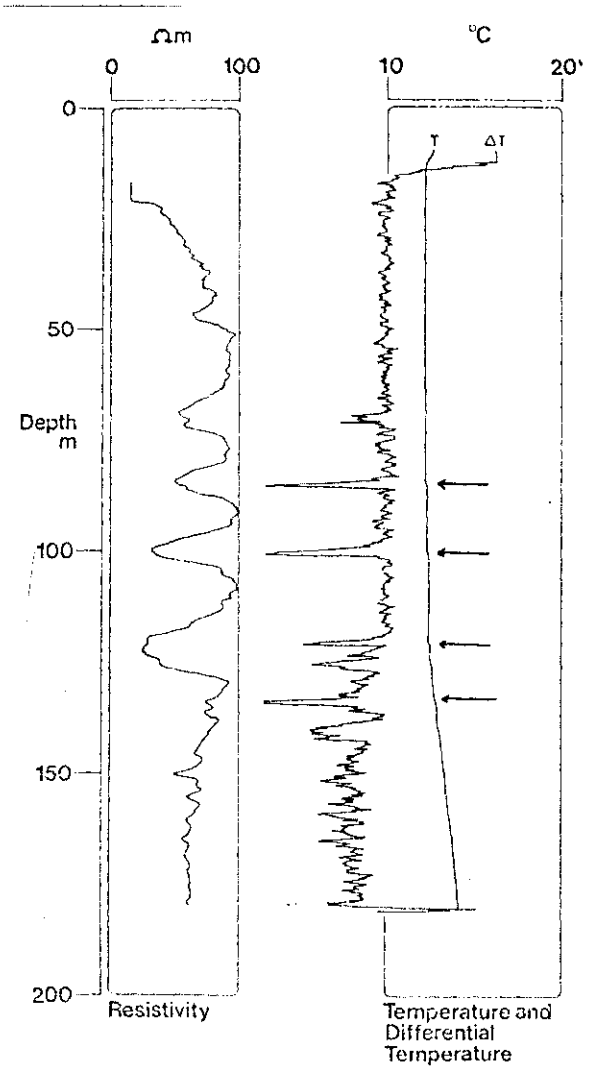


Fig. 2.12 Resistivity, temperature and differential temperature logs

Interstitial water extracted by centrifuge from core material from a borehole in the Chalk of Southern England (Edmunds et al 1973) was found to have a variable chemical composition and to be more mineralised, by as much as a factor of 10, compared with the fissure derived water found in the water columm.

Fig. 2.13 demonstrates compositional differences between interstitial water and water in the fissure zones for the above borehole.

Fig. 2.14 is an example of a borehole for which the Institute of Geological Sciences carried out detailed permeability inspection tests in conjunction with fluid geophysical logging and CCTV inspection (Price et al 1982). The conductivity log was made shortly after pumping from the nearby pumping station borehole had ceased. The flow velocity profile was made while the pumping station was abstracting 17 lt/sec. The solid circles represent horizontal intergranular permeability values while the vertical lines represent the measured permeability value for each injection-test interval. A major fissure at 29.3m was clearly indicated by the electrical conductivity log and is shown in Fig. 2.15. Another major fissure near the base of the borehole did not show on the electrical conductivity. The later fissure was indicated by heat pulse measurements and was also confirmed by CCTV inspection (Fig. 2.16).

Another important factor which could have a strong influence on the conductivity profile is the effect of saline intrusion in some coastal boreholes. Fig. 2.17 represents conductivity profiles for 10 boreholes (Table 2.2), in the Brighton's Chalk block coastal area, and was drawn from data kindly supplied by the Southern Water Authority. Continuous lines represent the maximum conductivity observed at the peak of the 1976 drought and broken lines represent the conductivity after three months of relatively heavy rainfall (December).

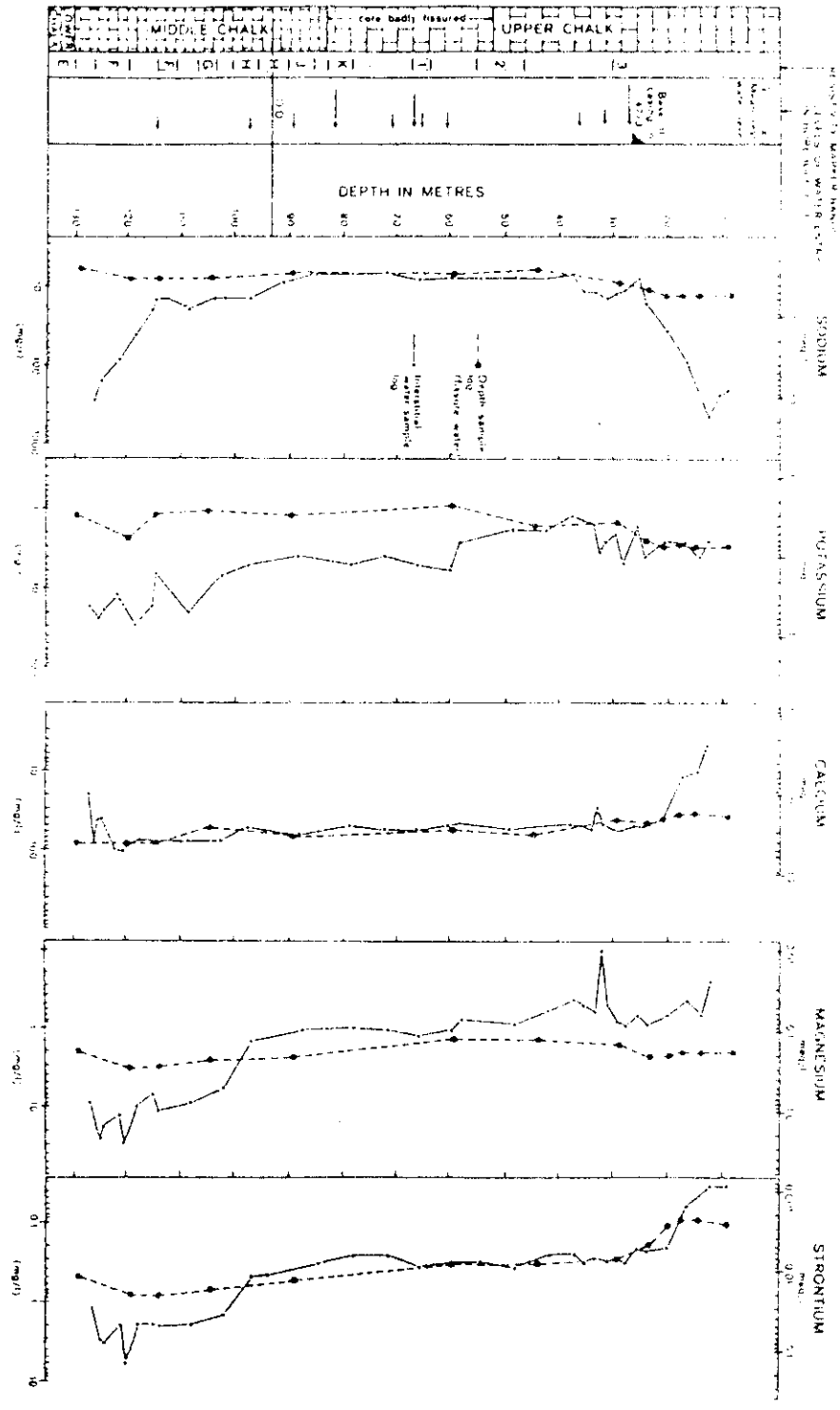


Fig. 2.13 Compositional differences between interstitial water in the fissure zones

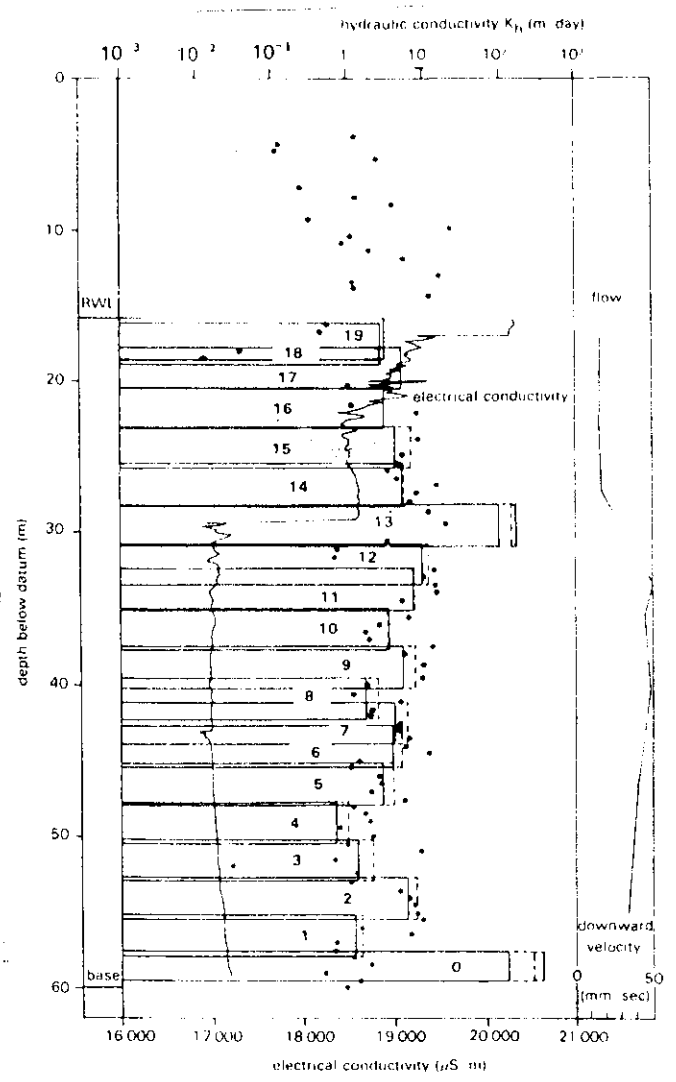


Fig. 2.14 Permeability values together with conductivity and flow logs (Price et al 1980)

A large variation in fluid conductivity values is evident between boreholes only short distances apart. As might be expected the boreholes near the coast show a greater variation in conductivity than those sited farther inland, since the effect of saline intrusion becomes more significant as the borehole is closer to the coast.

Another important factor which could influence the fluid conductivity of coastal boreholes is the effect of tide cycles. Southern Water Authority and the Water Research Centre have studied this phenomenon in a number of coastal boreholes (SWA 1979, Monkhouse and Fleet 1975). Fig. 2.18 shows the results of a tide cycle log carried out at



Fig. 2.15 Radial view of the fissure at 29.3m below datum



Fig. 2.16 Radial view of the fissure at 58.8m below datum

TABLE 2.2

Borehole No.	Name	O.S. Grid Reference	Datum M.O.D.	Depth (m)	Approximate depth W.L. (m)
1	Victoria Gardens N.	314044	11.26	250	4
2	St. Peter's Church	315049	13.56	250	5
3	Preston Park N.	303065	27.45	92	25
4	Roedean	348034	39.36	94	38
5	Ovingdean	359032	27.37	87	29
6	Daniels Barn	191053	2.12	63	10
7	Pembroke Gardens	282049	13.39	250	12
8	Goldstone	282066	53.03	210	52
9	New Salts Farm	203050	1.83	200	1
10	Soupting No. 3	167064	-	-	-

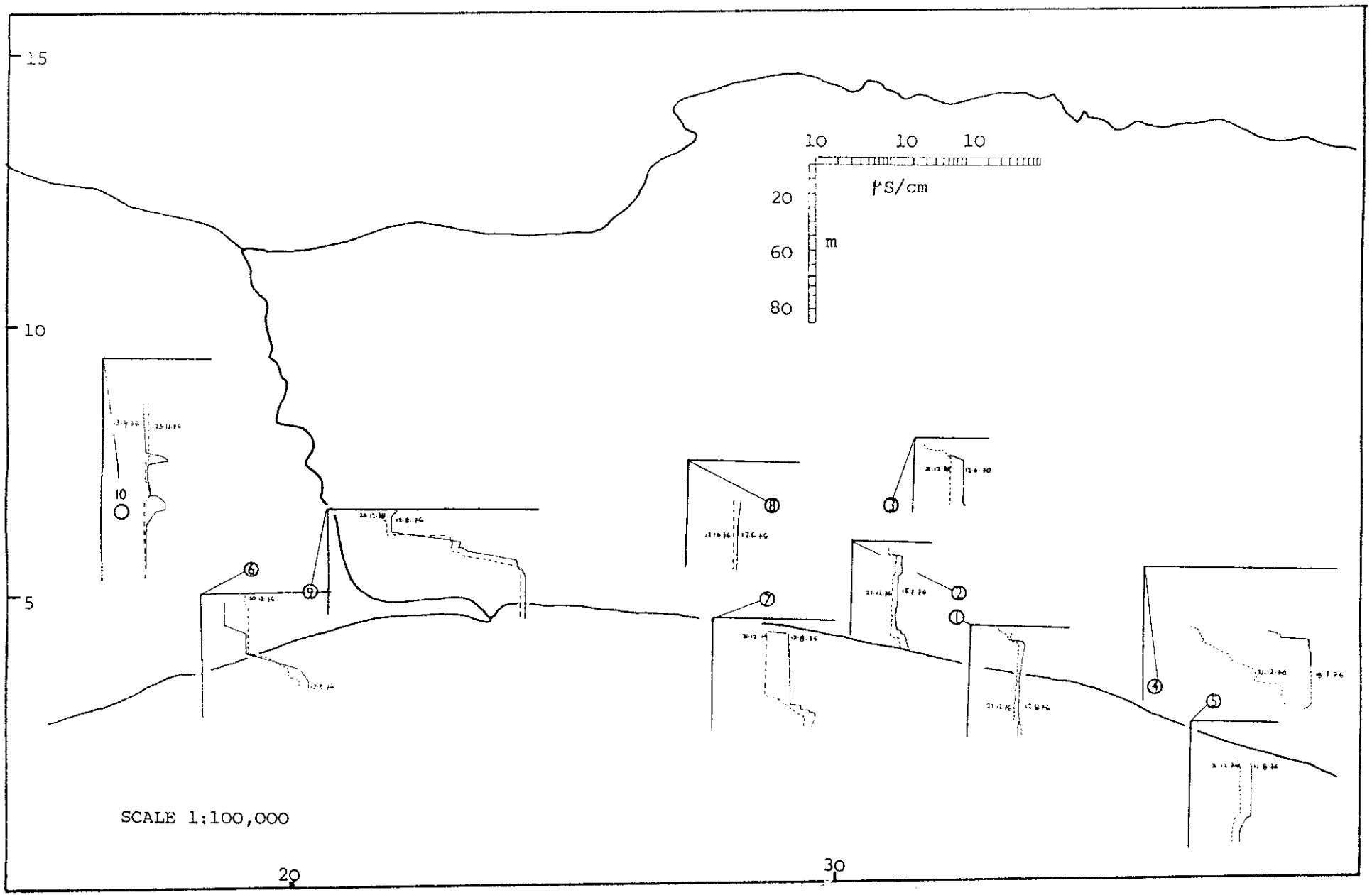


Fig. 2.17 Conductivity profiles for 10 boreholes in the Brighton Chalk

borehole No. 7 on 14th July 1977. Fig. 2.18.b shows the movement of the saline interface as observed from the log. One can see that it had been displaced over a range of 21m.

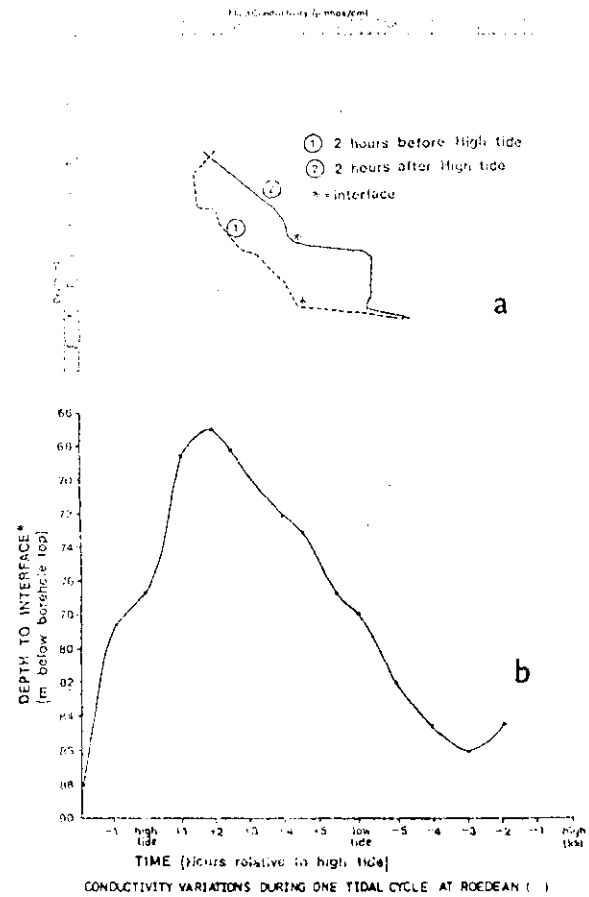


Fig. 2.18 Tide cycle log

2.9 GENERAL CONCLUSIONS

This Chapter has examined the role which the fluid logs play in the water industry today, and an attempt has been made to discuss how useful they are for estimating the hydraulic properties of the surrounding well formation. The general conclusions made can be summarized as follows:

(a) Fluid logs have been found to be very useful in helping to define the limits of fluid entry but at this time not in a quantitative sense.

(b) Calculations showed that a degree of movement must be expected in the water column of most of the wells due to thermal instability.

(c) A number of new techniques for measuring velocities as low as 1mm/sec look very promising.

(d) Experiments with a model showed that the velocity regime was laminar just in front of the simulated fissure with regular surfaces; and that turbulence was developed above and below the fissure zone, but by introducing irregularities on the output of the fissure plane, turbulence started to develop from the point of entry to the well.

(e) The Temperature and Differential Temperature logs are very sensitive to a number of effects and a method for recognizing the effects of fissure flow has been proposed.

Fluid geophysical logging can offer a great deal in the way of practical applications to hydrogeology, such as the detection of permeable zones, and the more complete the set of fluid logs that is available, the greater the benefits than can be expected from the logging.

C H A P T E R III

THEORETICAL AND EXPERIMENTAL INVESTIGATION OF THE HEAT-PULSE FLOWMETER

3.1 INTRODUCTION

The measurement of axial flow in a borehole is an established procedure. This information, in conjunction with other geophysical logs, aids the understanding of the behaviour of individual boreholes and of local and regional groundwater flow.

The main limitation of velocity measuring devices that have been available for use down boreholes is that they will not operate properly or at all below velocities of the order 30-50mm/sec. Recently, a new type of instrument for velocity measurements as low as 1 mm/sec has been used in the water industry with a lot of success (Dudgeon et al 1975). A substantial portion of the time spent on the present research was devoted to a detailed theoretical and experimental study of the principles of operation of this instrument in view of its promise for the water industry. The decision to do this research was taken because no analysis existed that examined the behaviour of the instrument from a theoretical point of view, even though the instrument is being used extensively by the water industry. Fluid velocity logs are essential for the study and analysis of in situ flow and hence for the assessment of in situ hydraulic conductivity. Obviously these logs rely on tools that must be capable of operating over a wide range of flows and the accurate measurement of low flows can be as valuable to analysis as that of high flows. The purpose of this Chapter is to define the limits of usefulness of the heat pulse flowmeter.

The basic idea of the heat pulse flowmeter is to use the thermal wake of a heated wire, submerged into the moving fluid, as a tracer.

The technique described here is not original. The first attempt to use such a method but for the case of air was the work of L. Kovasznay published in 1949 and some years later the work of R. Walker and A. Westenberg published in 1956.

All of these authors were interested in producing a periodical temperature field by applying a sinusoidal current in the probe, and trying to correlate the fluid velocity with phase measurements of the thermal wake.

The first who applied a single heat pulse into fluid (air) was A. Bauer, in work published in 1965. More recently, L. Bradbury and I. Castro (1971) in England and I. Tombach (1969) in the USA have been using modified versions of Bauer's original probe for use in highly turbulent flows.

The following table presents the velocities in which the above authors have been interested:

Table 3.1 Velocities studied by other authors

Author	Velocities
Kovasznay	500 cm/sec
Walker and Westenberg	50-300 cm/sec
Bauer	75 m/sec
Bradbury and Castro	200 cm/sec
Tombach	200 cm/sec

As it can be seen from Table 3.1, all these workers have used the instrument in a velocity range where the probe works essentially by convection with thermal diffusion having secondary influence.

The analysis presented here is opposite to the previous efforts in that with low flows, of the type that can be found in boreholes, there is essentially a thermal diffusion problem being influenced by convection. If the influence of diffusion, as in the case of Bradbury and Castro, and Bauer was secondary, the time of travel for the heated cloud of fluid would correspond to the time between the pulse and the initial response of the downstream sensor. The response would then rise with a linear slope determined by the thermal inertia of the sensor wire, and with the thermal-diffusion tending to eradicate this response.

Fig. 3.1 represents the response of the sensor with conditions of differing thermal diffusion and sensor wire inertia. The data from this diagram have been taken from the work of Bradbury and Castro (1971) and corresponds to Peclet numbers between 20 and 50. (See APPENDIX A.3.3 for definition of thermodynamic terms).

The analysis of the convection-diffusion problem was performed by both Bradbury and Castro, and Tombach in order to find when the effects of diffusion would pass the sensor. They could then extrapolate back to zero response and find the precise travel time. Tombach's approach was to digitize the signals and analyse them on a computer. Bradbury and Castro used a convenient voltage offset to indicate the travel time. Unfortunately in the present case, because of the large effect of diffusion the initial response of the sensor is going to be insensitive to convection at the low velocities that are of interest to borehole logging. This is the reason why it is preferred to use the location of the maximum signal for measuring travel time, since it is quite sensitive to the fluid

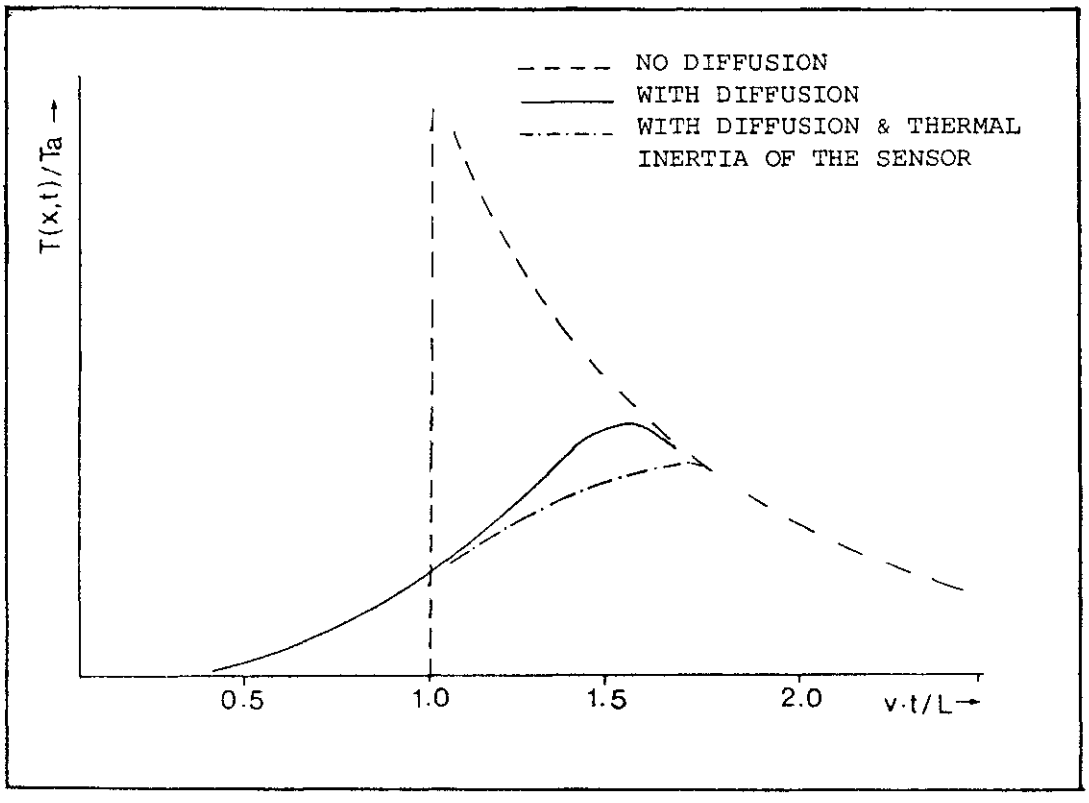


Fig. 3.1 Response of the sensor with conditions of different thermal diffusion and sensor wire inertia

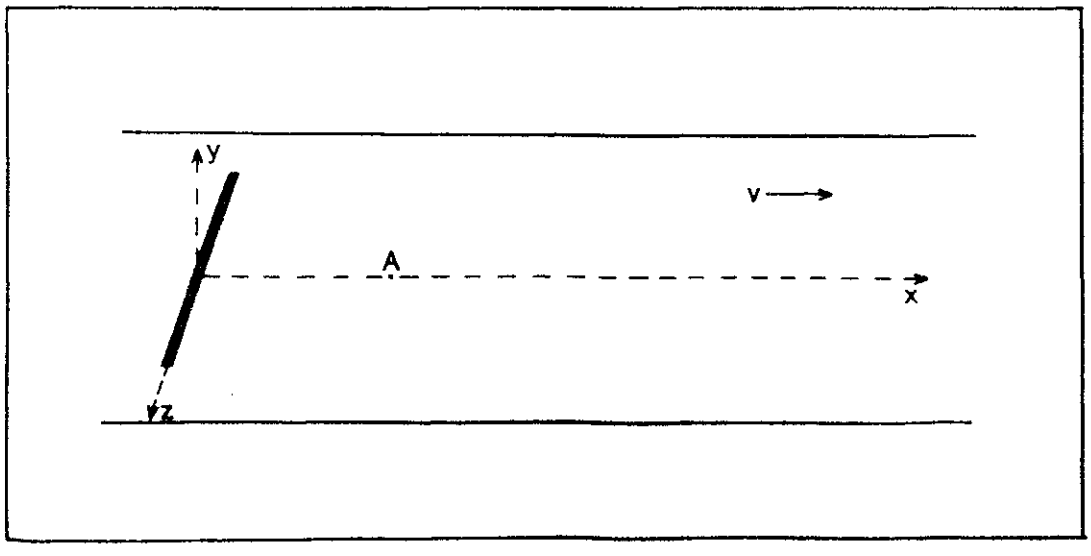


Fig. 3.2 The temperature field to be described, at Point A

velocity (Dudgeon et al 1975). It is obvious that in order to locate the maximum signal in the sensor the whole shape of the thermal cloud produced by the pulsed wire, the effect of diffusion on this cloud, the convection pattern of the viscous wake and of course the response of the sensor wire have to be predicted. This problem is extremely difficult to be analysed theoretically and in order to simplify it the thermal inertia of the sensor and the pulsed wire as well as the conduction of heat to the wire supports have been considered as unimportant. On the other hand the most important aspects of the problem are: determining the initial shape of the thermal cloud and assessing the convection diffusion interaction.

3.2 THEORETICAL CONSIDERATIONS

3.2.1 Formulation of the Problem

A tracer of heated water is introduced into the flow by pulsing a wire grid with a rectangular voltage pulse and the time taken for this tracer to reach the downstream sensor is measured.

In the following paragraphs, the physics of the phenomenon are going to be described in order to determine the characteristic parameters of the instrument.

Instead of starting the analysis with a wire grid, it is convenient to solve the problem for the case of a single wire, in other words the problem is resolved to the following:

Water in laminar flow with initial temperature T_a passes by a small wire of length l and diameter d. If the wire is heated by an electric pulse of known characteristics, what is the temperature field at a point A, which is at a distance x from the wire, downstream? (Fig. 3.2).

The differential equation of conduction of heat in an isotropic medium, whose conductivity is independent of the temperature, is given by equation(3.1)

$$\frac{\partial^2 T}{\partial x^2} + \frac{\partial^2 T}{\partial y^2} + \frac{\partial^2 T}{\partial z^2} - \frac{1}{\hat{k}} \frac{\partial T}{\partial t} = 0 \qquad (3.1)$$

On the other hand the total amount of heat released into the medium is given by Carslow and Jaeger (1959) as;

$$\int_{-\infty}^{\infty}\int_{-\infty}^{\infty}\int_{-\infty}^{\infty} \rho c T \, dx\,dy\,dz = \frac{Q\rho c}{(8\pi k t)^{3/2}} \int_{-\infty}^{\infty} e^{-\frac{(x-x')^2}{4\hat{k}t}} dx \int_{-\infty}^{\infty} e^{-\frac{(y-y')^2}{4\hat{k}t}} dy \int_{-\infty}^{\infty} e^{-\frac{(z-z')^2}{4\hat{k}t}} dz = Q\rho c \qquad (3.2)$$

From this it can be said that the solution of (3.1) may be interpreted as the temperature due to a quantity of heat Q.p.c. released instantaneously at t=0 at the point (x',y',z').

Transferring Eq. (3.1) to a coordinate system fixed with respect to the source it becomes:

$$\frac{\partial^2 T}{\partial x^2} + \frac{\partial^2 T}{\partial y^2} + \frac{\partial^2 T}{\partial z^2} - \frac{1}{\hat{k}} \left(\frac{\partial T}{\partial t} + U \frac{\partial T}{\partial x} \right) = 0 \qquad (3.3)$$

If the heat emitted at the origin by the point source is described by the function q(t), then the temperature at time t, at the point (x,y,z) due to the quantity of heat q(t').dt' released at time t' is

$$\frac{q(t')\,dt'}{8\rho c \left[\pi \hat{k}(t-t')\right]^{3/2}} \cdot \exp\left[- \frac{[x-U(t-t')]^2 + y^2 + z^2}{4\hat{k}(t-t')} \right] \qquad (3.4)$$

and the temperature at time t due to the heat emitted at the origin from time 0 to time t is:

$$T(x,y,z,t) = \frac{1}{8\rho c (\pi \hat{k})^{3/2}} \cdot \int_0^t \frac{q(t')}{(t-t')^{3/2}} \cdot \exp\left[- \frac{x-U(t-t')+y^2+z^2}{4\hat{k}(t-t')} \right] \qquad (3.5)$$

$$\frac{l}{d} => 1000.$$

For a large aspect ratio, $\frac{l}{d}$ the point source becomes an infinite line source, and Eq. (3.5) can be written

$$T(x,y,t) = \frac{1}{4\pi\hat{k}\rho c}\int_{o}^{t} q(t').e^{-r^2/(4\hat{k}(t-t'))}\frac{dt'}{(t-t')} \qquad (3.6)$$

where

$$r^2 = [x - U(t-t')]^2 + y^2 \qquad (3.7)$$

From Eq. (3.6) it becomes clear that in order to determine the temperature distribution downstream, we have to know the functional form of q(t), i.e. the physical law which describes the heat transfer from the pulsed wire. This can be easily calculated as long as the temperature history of the probe can be found. q(t) can be written as:

$$q(t) = \pi k Nu\,(T(t) - T_a).\,l \qquad (3.8)$$

Where Nu is the dimensionless Nusselt number. Recent measurements have shown that at low Reynolds numbers, the Nusselt number depends on the Reynolds number, the Prandl number and the angle of inclination of the fluid stream to the wire, neglecting the buoyance effect. The determination of the precise functional form of Nu(Re,Pr) is a classical problem in fluid mechanics, and although it is of great importance for the study of hot-wire anemometers, it is not so important in the present analysis, where the modified Kramers equation has been adopted for representing the heat convection process (Castaldin et al 1980).

$$Nu = 0.42\,Pr^{0.2} + 0.57\,Pr^{0.33}.\,Re^{0.36} \qquad (3.9)$$

From the principle of conservation of energy, the following equations can be written:

$$\left\{\begin{array}{l}\text{Electric Energy}\\ \text{entering the}\\ \text{pulsed wire}\end{array}\right\} = \left\{\begin{array}{l}\text{Heat stored}\\ \text{in the wire}\end{array}\right\} + \left\{\begin{array}{l}\text{Heat convected}\\ \text{by the water}\end{array}\right\}$$

$$\frac{V^2}{R} = \rho_w \cdot C_w \pi \frac{d^2 \cdot \ell}{4} \cdot \frac{dT}{dt} + \pi K \ell Nu (T - T_a) \qquad (3.10)$$

From which the time constant for appreciable convection becomes

$$T_p = \frac{\rho_w \cdot C_w \cdot d^2}{4 K Nu} \qquad (3.11)$$

and by keeping the duration of the electric pulse well below Tp the heat convection term in Eq. (3.10) can be ignored and it reduces to the following form:

$$\frac{V^2}{R} = \rho_w \cdot C_w \cdot \frac{\pi \cdot d^2 \cdot \ell}{4} \cdot \frac{dT}{dt} \qquad (3.12)$$

By solving this equation, the temperature history of the probe during the "pulsing time" can be found from:

$$\frac{a_0}{2} (T - T_a)^2 + (T - T_a) = \left(\frac{V}{\ell}\right)^2 \frac{1}{\rho C G_0} \cdot t \qquad (3.13)$$

After the almost impulsive rise of temperature the pulsed wire temperature decays exponentially due to heat convection, according to the equation

$$(T - T_a) = (T_1 - T_a) \cdot e^{-t/T_p} \qquad (3.14)$$

Where T_1 is the initial temperature of the probe at the end of the pulse. When the water velocity is low, then the time for the temperature decay in the pulsed wire will be much shorter than the time of diffusion between the pulsed wire and the sensor, a fact which permits the assumption to be made of an instantaneous source, at the velocity range of interest.

3.2.2 Analytical solution

Eq. (3.3) is expressed in terms of dimensionless variables, because with this procedure the mathematics becomes more concise:

(3.15)

where $\hat{T} = \frac{T-T_a}{T_a}$

$\xi = x/L$

$\eta = y/L$ (3.16)

$\tau = tU/L$

$p = UL/k$

Because

$$\frac{\partial^2 T}{\partial x^2} = \frac{1}{L^2}\frac{\partial^2 T}{\partial (x/L)^2} = \frac{1}{L^2}\frac{\partial^2 T}{\partial \xi^2}$$

$$\frac{\partial^2 T}{\partial y^2} = \frac{1}{L^2}\frac{\partial^2 T}{\partial (y/L)^2} = \frac{1}{L^2}\frac{\partial^2 T}{\partial \eta^2}$$

$$\frac{\partial T}{\partial t} = \frac{U}{L}\frac{\partial T}{\partial (tU/L)} = \frac{U}{L}\frac{\partial T}{\partial \tau}$$

The solution of Eq. (3.15) can be written as

$$T(\xi,\eta,\tau) = \frac{P}{4\pi\rho c}\int_0^{\tau} q(t').e^{-\frac{P}{4}[(\xi-\tau')^2+\eta^2]/\tau'}\, d\tau'/\tau' \qquad (3.17)$$

and since

$$q(t) = \pi K_f Nu \cdot \hat{T}_1 e^{-\tau/\tau_p} \quad , \quad \left(\tau_p = \frac{T_p U}{L}\right)$$

Eq. (3.17) can be written as

$$T(\xi,\eta,\tau) = \frac{\pi k_f Nu}{4\pi \hat{k} \rho c} \int_0^{\tau} \hat{T}_1 e^{-(\tau-\tau')/\tau_p} \cdot e^{-\frac{P}{4}[(\xi-\tau')^2+\eta^2]/\tau'}$$

and by substituting

$$\hat{k} = \frac{k_f}{\rho c}$$

$$T(\xi,\eta,\tau) = \frac{Nu \cdot T_1}{4} \int_0^{\tau} e^{-(\tau-\tau')/\tau_p} \cdot e^{-\frac{P}{4}[(\xi-\tau')^2+\eta^2]/\tau'} \qquad (3.18)$$

Considering the plane which passes through A and contains the wire, the dimensionless variable n takes the value 0 and to study the temperature field at the point A, ξ takes the value 1. For this case, Eq. (3.18) can be written as:

$$T(\tau) = \frac{Nu \cdot T_1}{4} \int_0^{\tau} e^{-(\tau-\tau')/\tau_p} \cdot e^{-P/4(1-\tau')^2/\tau'} d\tau'/\tau' \qquad (3.19)$$

Because the velocities being studied with the heat pulse flowmeter, when it is used for groundwater measurements, are very low, the dimensionless decay time of the pulsed wire is very small compared to the dimensionless travel time between the wire and the sensor, so the assumption of having an instantaneous pulse is made.

It is well known from the theory of the conduction of heat that the solution of Eq. (3.3) for the case of an instantaneous heat source has the form (Carslow and Jaeger 1959):

$$T(x,y,t) = \frac{Q}{4\pi \hat{k} t} \cdot e^{-r^2/4\hat{k}t} \qquad (3.20)$$

In dimensionless form Eq. (3.20) can be written as:

$$T(\xi,\tau) = \frac{Q\rho}{4\pi\tau} \cdot e^{-(\xi-\tau)^2 \cdot P/4\tau} \qquad (3.21)$$

and in order to find the time to the maximum signal the following Equation has to be solved:

$$\frac{\partial}{\partial\tau}\left(T(\xi,\tau)\right) = 0 \implies \qquad (3.22)$$

$$P\xi^2 - P\tau^2 = 4\tau \qquad \text{and by substituting } \xi = 1$$

$$\tau = \frac{-1 + \sqrt{1+(P/2)^2}}{P/2} \simeq P/4 \qquad (3.23)$$

because $\sqrt{1+\delta} \simeq 1+\delta/2$ for $\delta \ll 1$ (or for $U \to 0$)

It is convenient, therefore, to rescale the dimensionless time τ in Eq. (3.17) by putting $\tau = \delta\mu$ and $\tau' = \delta\lambda$ where $\delta = P/4$

$$T(\tau) = \frac{Nu \cdot T_i}{4} \int_0^{\mu} e^{-\frac{\delta}{\tau_p}(\mu-\lambda)} \cdot e^{-\frac{1}{\lambda}(1-\delta\lambda)^2} \frac{d\lambda}{\lambda} \qquad (3.24)$$

and because $\tau_p/\delta \ll 1$ the above integral is very small for all the values of λ except for $\lambda = \mu$ so by defining a new variable of intergration:

$$\lambda = \mu - \frac{\tau_p}{\delta} \cdot \lambda' \qquad (3.25)$$

---

* Because for $\lambda = \mu \Rightarrow \lambda' = 0$ and for $\lambda = 0 \Rightarrow \lambda' = \mu\delta/\tau_p$

the following intergral equation is obtained:

$$T(\tau)=\frac{Nu\cdot T_1}{4}\cdot\frac{\tau_p}{\delta}\int_0^{\frac{\mu\delta^*}{\tau_p}} e^{-\lambda'}\cdot e^{-\frac{(1-\delta\mu+\tau_p\lambda')}{(\mu-\tau_p\lambda'/\delta)}}\cdot\frac{d\lambda'}{\mu-\frac{\tau_p}{\delta}\cdot\lambda'} \qquad (3.26)$$

By expanding the factor $\frac{1}{\mu(1-\frac{\tau_p\lambda'}{\delta\mu})}$ in terms of $\frac{\tau_p\cdot\lambda'}{\delta\mu}$

$$T(\tau)=\frac{Nu\cdot T_1\cdot\tau_p}{4\delta}\int_0^{\frac{\mu\delta}{\tau_p}} e^{-\lambda'}\cdot\exp-\left\{\frac{1}{\mu}(1-\delta\mu+\tau_p\lambda')^2\cdot\left[1+\frac{\tau_p\lambda'}{\delta\mu}+\left(\frac{\tau_p\lambda'}{\delta\mu}\right)^2+\dots\right]\right\}\times$$

$$\times\left\{\frac{1}{\mu}\left[1+\frac{\tau_p\lambda'}{\delta\mu}+\left(\frac{\tau_p\lambda'}{\delta\mu}\right)^2+\dots\right]\right\} \qquad (3.26b)$$

Rearranging the exponential in orders of τ_p/δ

$$\exp\{\dots\}=\exp\left\{-\frac{1}{\mu}\left(\left[(1-\delta\mu)^2+\frac{\tau_p}{\delta}\left(2\delta(1-\delta\mu)+\frac{(1-\delta\mu)^2}{\mu}\right]\lambda'+\right.\right.$$

$$\left.\left.+\left(\frac{\tau_p}{\delta}\right)^2\cdot\left(\delta^2+\frac{2\delta}{\mu}(1-\delta\mu)+\frac{1}{\mu^2}(1-\delta\mu)^2\right)\lambda'^2+O\left[\left(\frac{\tau_p}{\delta}\right)^3\right]\right.\right.$$

$$=\exp\left\{-\frac{(1-\delta\mu)}{\mu}-\frac{\tau_p}{\delta}\cdot\frac{(1-\delta\mu)\cdot\lambda'}{\mu^2}-\left(\frac{\tau_p}{\delta}\right)^2\cdot\frac{\lambda'^2}{\mu^3}+O\left[\left(\frac{\tau_p}{\delta}\right)^3\right]\right.$$

Substituting the above result back to Eq. (3.26.b) and expanding in terms of exp. (τ_p/δ) and exp $(\tau_p/\delta)^2$ the following expression is taken

$$T(\tau)=\frac{Nu\cdot T_1}{4}\cdot\frac{\tau_p}{\delta}\int_0^{\frac{\mu\delta}{\tau_p}} e^{-\lambda'}\cdot\exp\left[-\frac{(1-\delta\mu)^2}{\mu}-\frac{\tau_p}{\delta}\frac{(1-\delta^2\mu^2)^2}{\mu^2}\cdot-\right.$$

$$\left.-\left(\frac{\tau_p}{\delta}\right)^2\cdot\frac{\lambda'^2}{\mu^3}+O\left[\left(\frac{\tau_p}{\delta}\right)^3\right]\right]\cdot\frac{1}{\mu}\left[1+\frac{\tau_p}{\delta}\cdot\frac{\lambda'}{\mu}+\left(\frac{\tau_p\cdot\lambda'}{\delta\mu}\right)^2+\dots\right]d\lambda' \qquad (3.27)$$

from which:

$$\hat{T}(\tau)=\frac{Nu\cdot\hat{T}_1\cdot\tau_p}{4\delta\mu}\cdot e^{-(1-\delta\mu)^2/\mu}\cdot\left[1+\frac{\tau_p}{\delta}\left(\frac{\delta^2\mu^2+\mu-1}{\mu^2}\right)+\left(\frac{\tau_p}{\delta}\right)^2\cdot\left[\left(\frac{\delta^2\mu^2+\mu-1}{\mu^2}\right)^2+\right.\right.$$

$$\left.\left.+1-\frac{2}{\mu}\right]+O\left[\left(\frac{\tau_p}{\delta}\right)^3\cdot e^{-\delta\mu/\tau_p}\right]\right] \qquad (3.28)$$

or by making the (inverse) transformation:

$$\hat{T}\longrightarrow\frac{T-T_a}{T_a}$$

$$\hat{T}_1\longrightarrow\frac{T_1-T_a}{T_a}$$

$$\tau\longrightarrow\frac{tU}{L}$$

$$\mu\longrightarrow\frac{\tau}{\delta}=tU/(L\delta)$$

$$\tau_p\longrightarrow\frac{T_pU}{L}$$

The following expression for the temperature field at point A is obtained:

$$(T-T_a) = \frac{(T_i-T_a)\cdot Nu\cdot T_p}{4t}\cdot \exp\left[-\frac{\delta(1-t\cdot U/L)^2}{t\cdot U/L}\right]\cdot\left[1+\frac{T_p}{t^2\cdot U/L}\cdot\left(t^2\cdot\delta\cdot(U/L)^2+t\cdot U/L-\delta\right)\right] \qquad (3.29)$$

3.2.3 Mathematical modelling of the temperature field produced by a grid

In the following, an assumption of using a square grid consisting of 10 wires each of length 1 cm and 1 mm apart, is made. Fig. 3.3 contains the construction details of the heating grid used in the experiment.

By taking L = 10 cm the dimensionless variable η takes the following (See Fig. 3.3.2) values:

$$\pm\frac{0.5}{10} = 0.05$$

$$\pm\frac{1.5}{10} = 0.15$$

$$\pm\frac{2.5}{10} = 0.25$$

$$\pm\frac{3.5}{10} = 0.35$$

$$\pm\frac{4.5}{10} = 0.45$$

from which n can be written as:

$$\eta = \frac{1}{L}(0.5+k) \qquad (3.30)$$

where k = 0, 1, 2, 3, 4, ..., n-1

Thus the temperature field at Point A downstream can be described by:

$$T(\eta,\tau) = \frac{Nu\cdot T_i}{2}\sum_{k=0}^{\eta-1}\int_0^{\tau} e^{-(\tau-\tau')/\tau_p}\cdot e^{-\frac{P}{4}\cdot\left[(1-\tau')^2+\left(\frac{0.5+k}{L}\right)^2\right]/\tau'}\frac{d\tau'}{\tau'} \qquad (3.31)$$

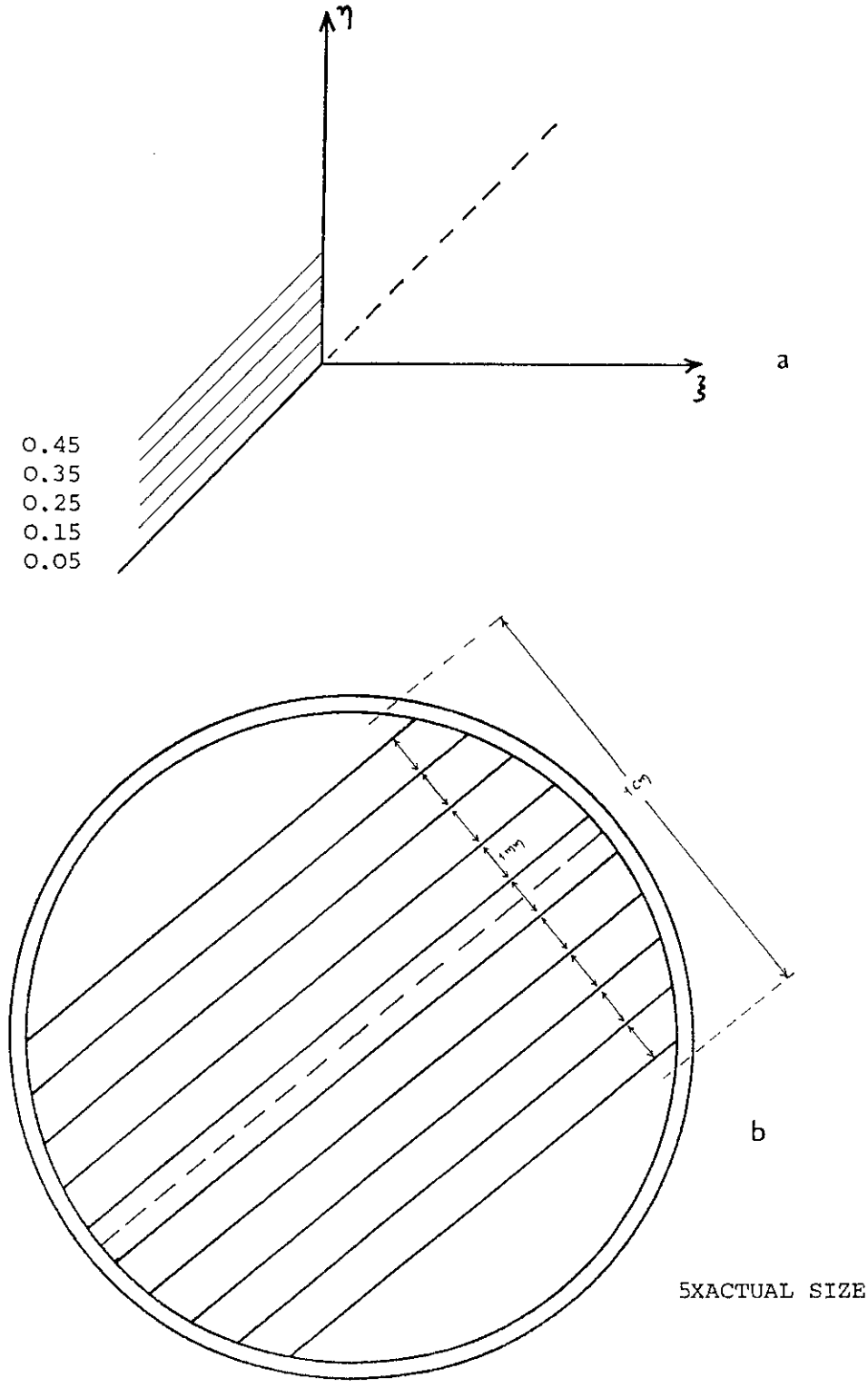


Fig. 3.3 Construction details of the heating grid used in the experiment

By using the same analytical methods as described in the previous paragraphs, Eq. (3.31) becomes, see APPENDIX (A.3.4).

$$T(\eta,\tau) = \frac{n \cdot Nu \cdot T_1 \cdot \tau_P}{4\delta\mu} \cdot e^{-(1-\delta\mu)^2/\mu} \cdot \left\{ 1 + \frac{\tau_P}{\delta}\left(\frac{1}{\mu} - \frac{1-\delta^2\mu^2}{\mu^2}\right) + 2\left(\frac{\tau_P}{\delta}\right)^2 \cdot \left[\frac{(1-\delta^2\mu^2)^2}{2\mu^4} - \frac{1}{\mu^3} - \frac{1}{\mu^2} - \frac{(1-\delta^2\mu^2)}{\mu^3}\right]\right\} + \frac{Nu \cdot T_1 \cdot \tau_P}{2\delta\mu} \cdot e^{\frac{-(1-\delta\mu)^2}{\mu}} \cdot \sum_{k=0}^{n-1} e^{-\eta(k)/\mu} \cdot \left\{ \eta(k) \cdot \left[2 \cdot \left(\frac{\tau_P}{\delta}\right)^2 \cdot \frac{(1-\delta^2\mu^2)}{\mu^4} - \frac{\tau_P}{\delta} \cdot \frac{1}{\mu^2}\right] + \left(\frac{\tau_P}{\delta}\right)^2 \cdot \frac{(\eta(k))^2}{\mu^4} \right. \tag{3.32}$$

By comparing Eq. (3.32) with Eq. (3.29), it becomes obvious that when using a grid of n-wires, the temperature field at point A is n times the temperature field caused by a single wire, plus a negative factor which is here named the "Grid Factor" or GF.

Calculations of GF for the case of a grid consisting of 10 wires gave very small values (10^{-6}) so the second term in Eq. (3.32) can be neglected without introducing any error in the calculation of the temperature field.

A computer program in FORTRAN IV was written in order to perform all the calculations and is presented in APPENDIX A.3.6.

Figures 3.4 and 3.5 are graphical representations of Eq. (3.32) for n = 10 and for a 0.25mm Pt-wire heated up to 75°C and where the sensor is 10mm and 15mm downstream respectively. In each case the ambient temperature is assumed to be 25°C.

These figures clearly illustrate the effect of the diffusion of the heat when the velocity of the water decreases.

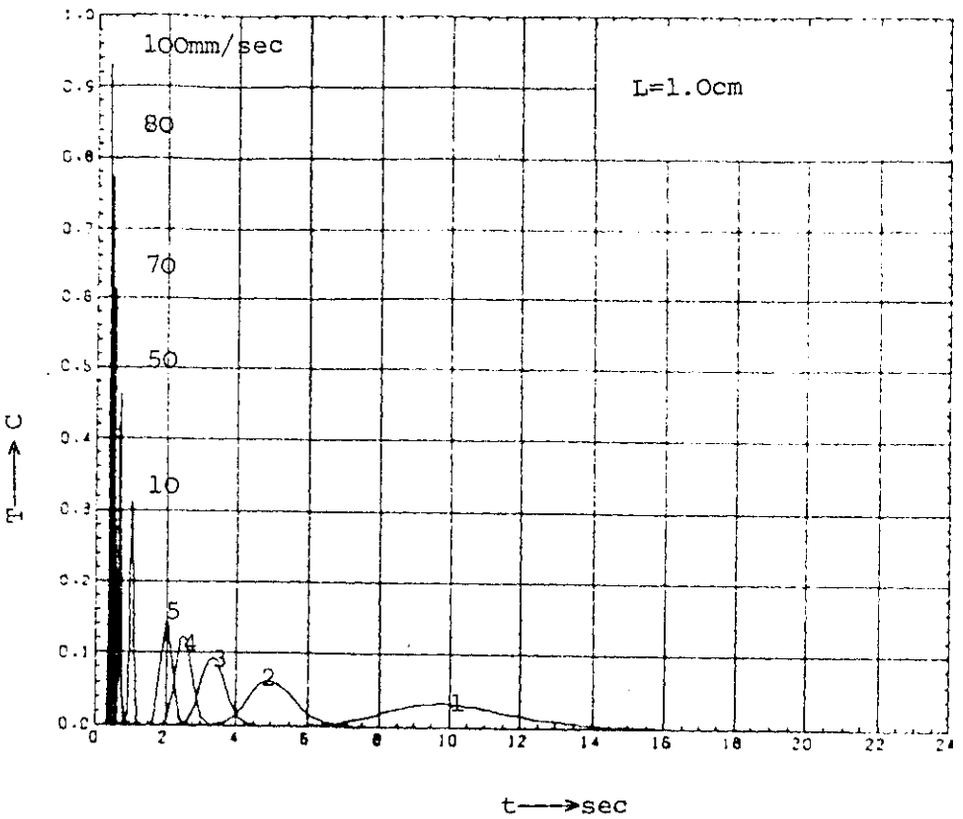


Fig. 3.4 Temperature field at a point 10mm downstream from a heating grid consisting of 10 wires of 0.25mm diameter and heated up to 75°C

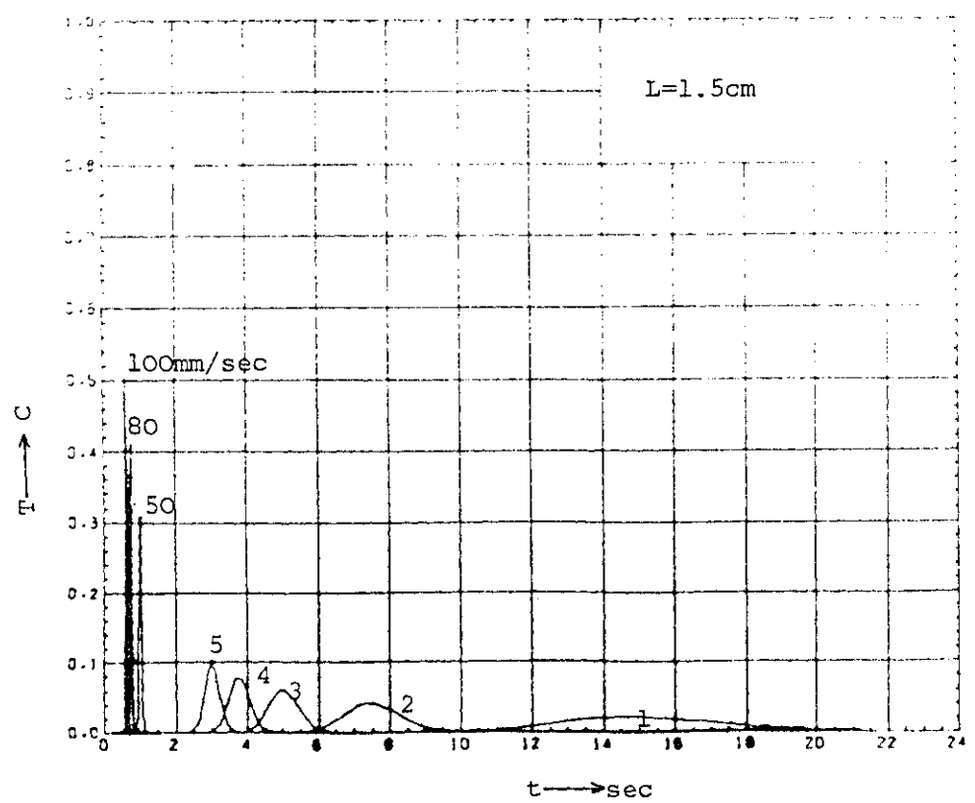


Fig. 3.5 Temperature field at a point 15mm downstream from a heating grid consisting of 10 wires of 0.25mm diameter and heated up to 75°C

3.3 EXPERIMENTAL CONSIDERATIONS

The design of a heat pulse flowmeter, and the way it operates depend not only on the dynamics of the convection and diffusion of the heat pulse but also on some of the practical electronic and mechanical constraints that arise.

These are problems of signal-to-noise ratio and the influence of electrical coupling between the pulsed wire and the sensor circuit.

3.3.1 Probe design

It is evident that the temperature decay of the pulsed wire is faster with a smaller wire. This produces a more sharply peaked thermal cloud moving between the pulsed grid and the sensor. Therefore, it is easier to determine the position of maximum signal in the sensor. Unfortunately, as there is an upper limit to the temperature which we can heat the pulsed wire, the dimension of the pulsed wire cannot be reduced a lot if enough energy is to be transferred into the water.

The most important parameter in the present experiment is the distance between the pulsed wire and the sensor, because both the convection time and the Peclet number depend on it.

Although from heat conservation arguments, it is expected that the amplitude of the thermistors signal is not strongly affected by the changing of spacing between the thermistor and the grid, in our case the effect of longitudinal diffusion is so strong that the peaked signal decays very rapidly with the spacing.

On the other hand, noise will be directly proportional to the total wire length of the grid; this includes both

electronic noise from the amplifier and also any response that the sensor has directly to the water stream flowing past it either to temperature fluctuations as a resistance thermometer or to velocity fluctuations as a hot wire anemometer. It would appear therefore that there is a strong motive to reduce the spacing between the wire and the thermistor as much as possible, keeping of course in mind the effect of the grid's viscous wake on the sensor.

In the present experiment a grid made from 0.025cm of Pt wire has been used. The design of the grid is shown in Fig.(3.3).

Another difficult task of the present design was to choose the appropriate sensor. The decision must be based on the following objectives:

(a) Provide as far as possible a direct means of the heat wave measurement without the need of complex corrections.
(b) Have a sufficiently good response characteristic.
(c) Provide a sensing element which is reliable in water environment, up to temperatures of about 100°C, without drift problems with time, and giving a long working life.

The ideal sensor would be a fine wire, but because of contamination due to dirt problems, the next choice is a thermistor, capable of measuring at least 0.01°C and having a response time not greater than 0.1 sec.

A number of sensors from those available in the market were tested during the first stages of the experiment in order to find the most appropriate.

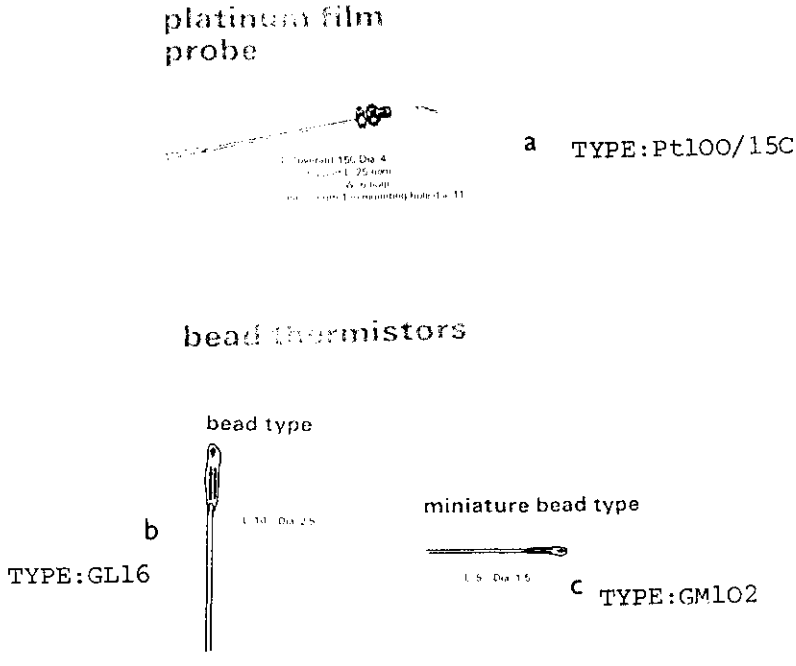


Fig. 3.6 Typical sensors tested in the research. All lengths are in mm

The first sensor that was tested was Pt 100/15C of the platinum film element type, supplied by Sensing Devices Ltd. (Fig. 3.6.a). Although its response time was claimed to be of the order of 0.05 sec. the results obtained were very poor, probably because of the effect of the stainless steel sheath which was used in order to keep the sensor waterproof. After this, it was decided to concentrate on the semiconductor type (thermostors) sensors and Fig. 3.6.b and c represents the two types supplied by Radio Spares Components Ltd., for which the best results were obtained. Type GM102 was selected for the rest of the experiment.

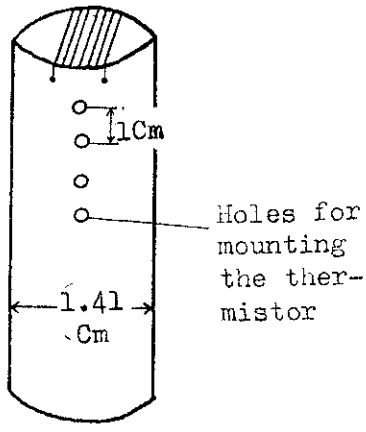


Fig. 3.7 Construction details of the probe containing the heating grid and the sensor

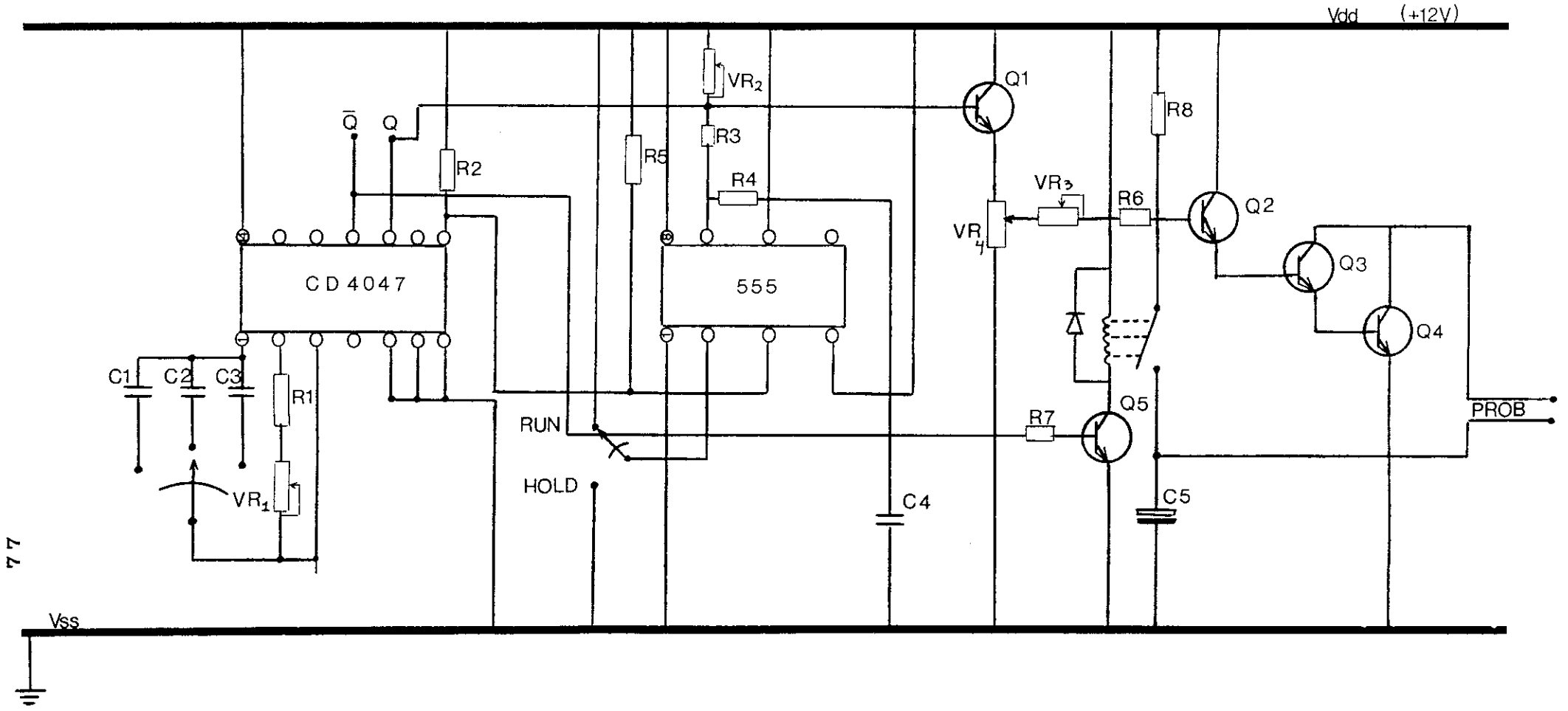
The sensor and the pulsed wire were built on a cylindrical plastic tube. The wire was kept in position by 20 slots cut on the top of the cylindrical tube and a number of holes were drilled on the face of the tube providing the facility of placing the thermistor at various distances from the grid (Fig. 3.7).

3.3.2 The Electronic Circuit

In this particular experiment, the duration of the pulses used to produce the tracer of heated water, ranges from a few microseconds up to about 100 m/sec with peak currents as high as 3 Amps.

There is nothing intrinsically difficult about making a circuit to produce such pulses, Fig. 3.8 shows the circuit designed and used in the present experiment.

Generally in the design of the electric circuit of a heat pulse flowmeter capacitor discharge must be employed for pulsing the heating element. This technique permits the



77

Fig. 3.8 Electronic circuit of the pulse generator

COMPONENTS

R1 = 10K	C1 = 0.022 F	Q1 = BC107
R2 = 22K	C2 = 0.22 F	Q2 = BC107
R3 = 1M	C3 = 2.2 F	Q3 = 2N3054
R4 = 100K	C4 = 2.2 F	Q4 = 2N3055
R5 = 10K	C5 = 2000 F	Q5 = BC107
R6 = 27K		
R7 = 100K		
R8 = 1K		

high power pulses required to be generated down the hole with minimal difficulty and results in a smooth and continuous supply of power flowing in the cable link.

This is a desirable feature since cross coupling, in a system where the input peak power is considerably greater than the signal power, invariably results in sacrificed sensitivity.

The circuit designed produces a series of pulses of the following form (Fig. 3.9):

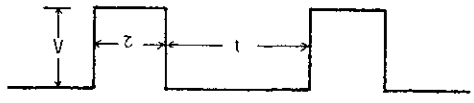


Fig. 3.9 Typical waveform produced by the pulse generator

where: time τ is controlled by Potentiometer VR_1
time t is controlled by Potentiometer VR_2
and the amplitude of the pulse can be controlled by potentiometers VR_3 and VR_4. A sample of pulses of different periods and duration are presented in Fig. 3.10.

A conservative estimate, including losses, for peak pulse power would be 5KW for the values quoted. The relation to the maximum available peak signal power (as produced by the laminar flow model) of approximately 0.5 nW gives an idea of the high degree of isolation required between the two circuits (pulsed wire and sensor) in the probe.

For the sensor a standard Wheatstone bridge consisting of 100ohm resistors was used. The recorded signal was fed from the bridge into a microamplifier and then it was recorded either on a oscilloscope or on a y-t plotter.

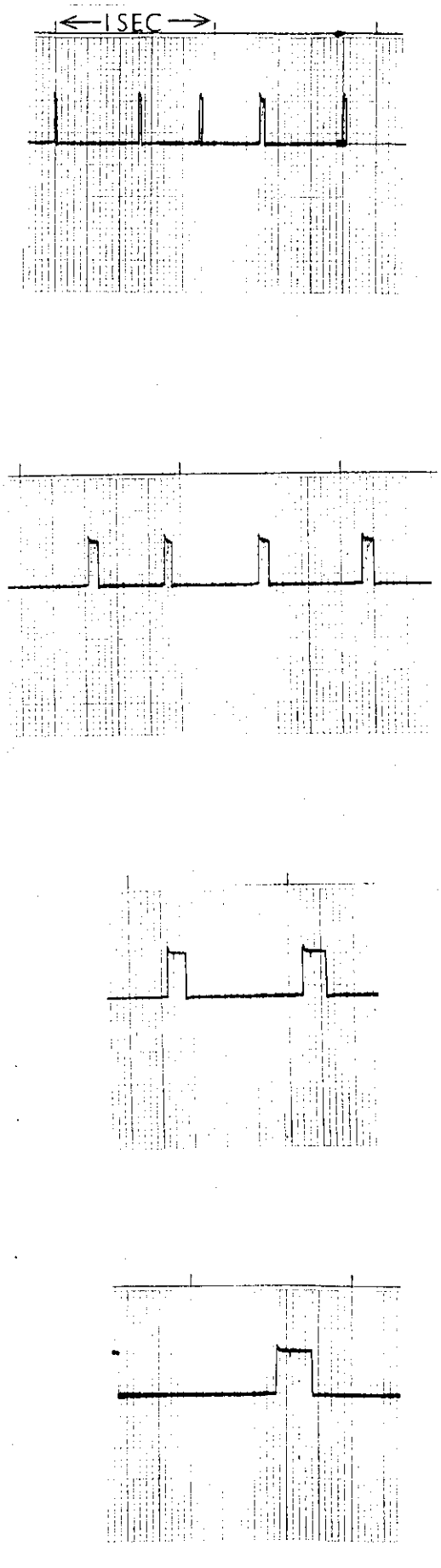


Fig. 3.10 Typical pulses of different periods and duration produced by pulse generator

3.3.3 The Calibration Device

The most common method used for the calibration of standard flowmeters is to place the probe in a flow and to measure the velocity by a second "standard" method, e.g. with a pilot static probe. Unfortunately these standard methods become inaccurate at very low velocities.

A second method consists of holding the fluid stationary and moving the probe through it (Newman 1967). The major shortcoming of this method is the resulting mechanical vibration of the probe.

A similar method is to hold the probe stationary and move the container with the fluid (Dring and Gebhart 1969). Various other arrangements have been used, such as towing, towed and rotating tanks etc.

In the present case because of the low velocities encountered in the flow, the buoyance effects must have the same direction to the flow. Keeping this in mind and trying to minimize the amount of equipment, money and trouble required, a constant-head device (Plate 4) has been used.

An adjustable reservoir tank supplies water through a flexible hose to the bottom of a vertical calibration tube of 7.5 cm diameter. The reservoir can be moved very accurately by a mechanism so that the difference in head can be easily changed, allowing of course for the water to overflow in both the reservoirs and the calibration tube in order to achieve constant head.

By having a wire screen (15-20 mesh/inch), below the probe (Plate 5) and leaving an opening of about 2mm between the rim of the screen and the tube wall (Plate 6), a more flattened velocity profile near the centre line (Callagher 1973) can be obtained. This makes exact probe placement less critical than in the case of unobstructed flow.

On the other hand, the velocity at the tube axis can be made very close to the cross-tube average by adjusting the gap between the screen and the tube wall. So the tube output can be related directly (by weighing or volumetric methods) to the measured mean-flow speed and eliminate computations involving the velocity profile (see APPENDIX A.3.5 for results of measurements).

The system itself is calibrated by adjusting the reservoir surface at various elevations and measuring the volume outflow or weight during some known time.

Of course the best method for the calibration of the heat pulse flowmeter in order to use it into boreholes, would be to use a calibration rig (Dudgeon et al 1975) having the same diameter as the borehole.

Plate 4 represents the general layout of the experiment where:

a. movable reservoir tank
b. pulse generator
c. power supply
d. electrolytic capacitor
e. microamplifier
f. bridge
g. timer
h. flow tube
k. y-t thermal plotter
m. oscilloscope

A sample of the recorded signal is shown in Fig. 3.11. The distance between the maxima of the signal to the right and the spike to the left represent units of travel time.

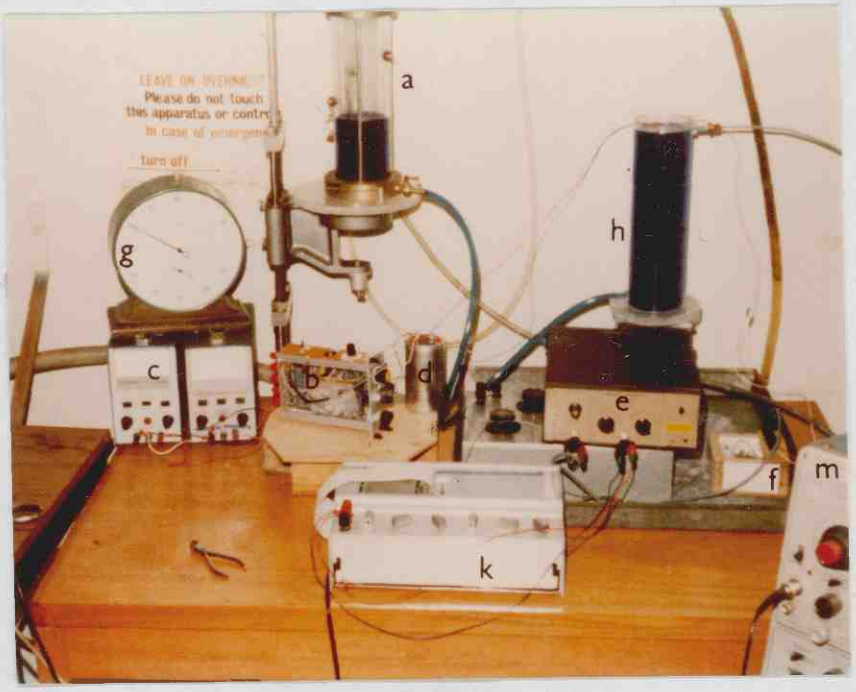


Plate 4 General layout of the experiment

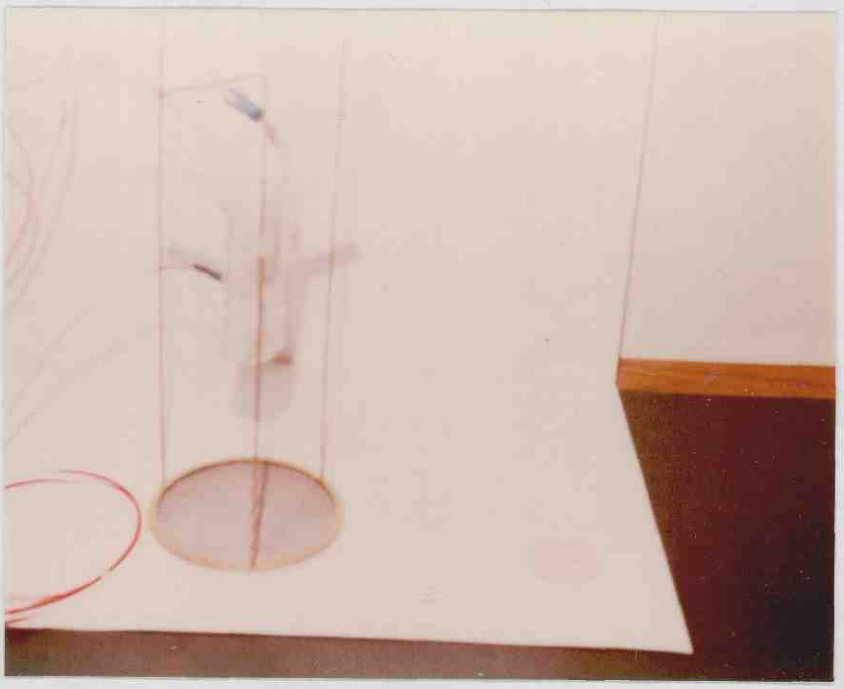


Plate 5 The probe mounted just above the grid



Plate 6 The effect of the grid on flow

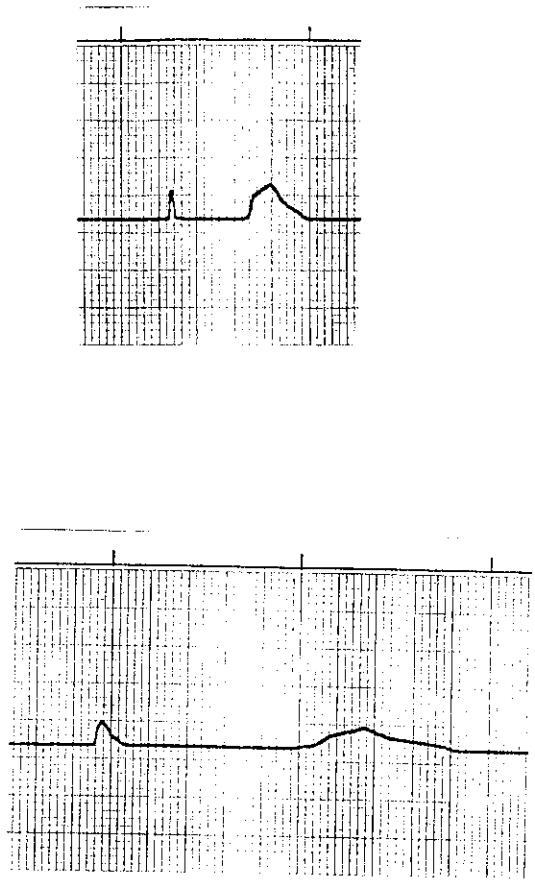
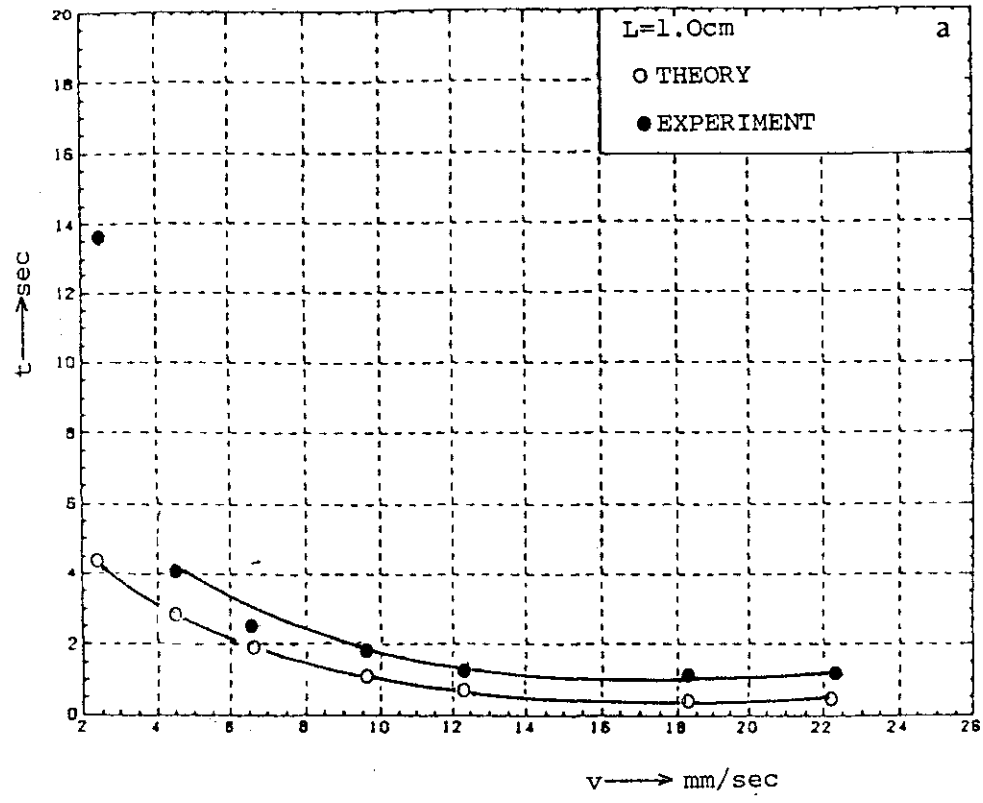


Fig. 3.11 Sample of a recorded signal

3.4 DISCUSSION OF THE RESULTS

Measurements of the travel time taken to the maximum amplitude of the thermistor's signal, have been obtained from chart recorder traces. These measurements can conveniently be used to give an indication of the agreement between the theoretical and experimental results and are presented in Fig. 3.12a and Fig. 3.12b for a 0.25 Pt-wire and for separations 10mm and 15mm respectively.

The agreement is quite satisfactory in showing the general trends although very precise agreement cannot perhaps be expected because of reasons that will be explained.



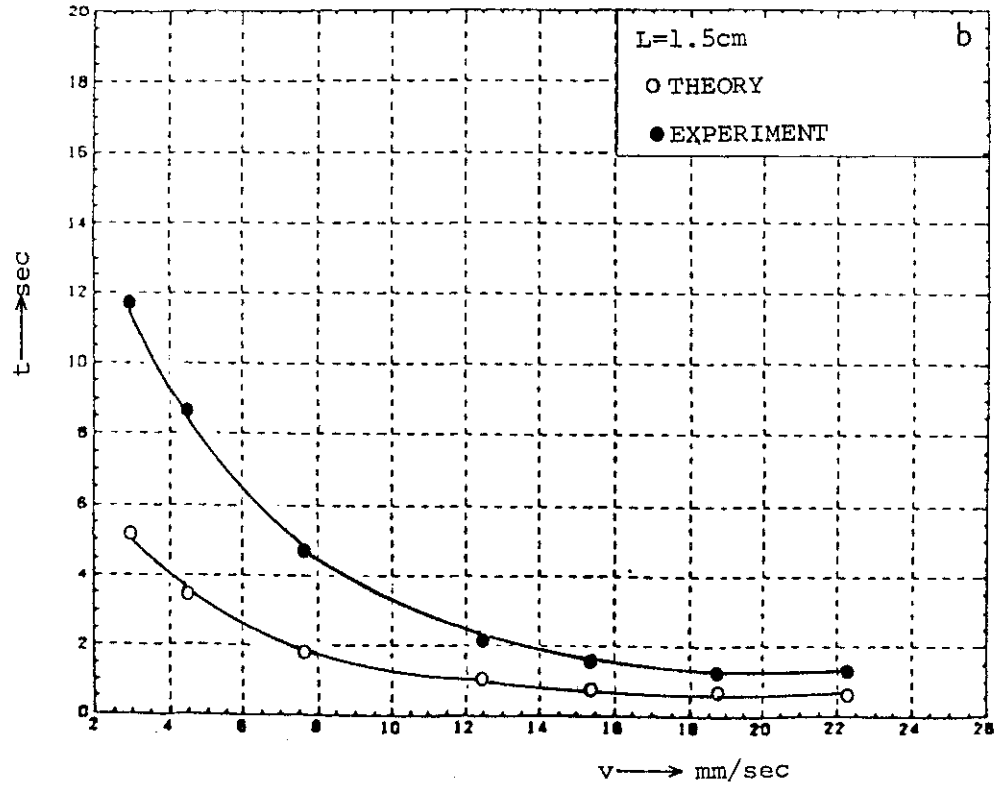


Fig. 3.12 Comparison between theoretical and experimental results for a 0.25mm Pt-wire and for separations 10mm (Fig. 3.12.a) and 15mm (Fig. 3.12.b).

One fundamental limitation of the theoretical analysis for low velocities is the assumption that the thermal diffusivity of water is constant, in order to solve equation (3.1). As it is known, the thermal diffusivity of water varies significantly with temperature, so that as the thermal pulse diffuses, it cools, decreasing the value of $\hat{k}$.

The comparison between experimental and theoretical results gives a significant increase in the difference between the two as the velocities decreases and this is shown more clearly in Fig. 3.13.

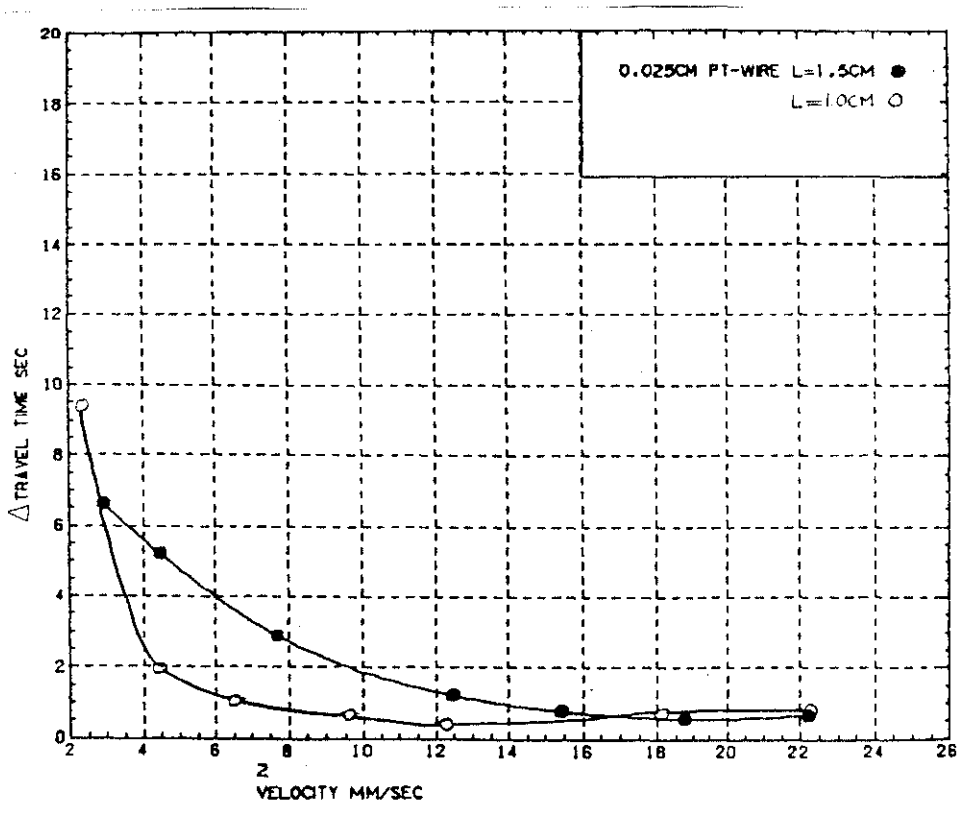


Fig. 3.13 Difference between theoretical and experimental results as a function of the fluid velocity

One obvious reason for this is because the time of travel is longer, thus giving the thermal pulse more time to diffuse and cool.

On the other hand, in the previous discussion of heat transfer from the grid to the water only considered the calculation of forced convection where water is forced through the heat transfer grid.

In the following case because of the very low velocities encountered, the forced flow velocity is coupled with the convective velocity which is generated by the buoyancy forces resulting from a reduction in fluid density near the grid.

As the water velocity increases, the forced convective velocity would be expected to overshadow most free-convection effects encountered in the system.

On the other hand flow situations of very low water velocities might be appreciably influenced by free convection currents.

An order of magnitude analysis of the free-convection boundary layer equation will indicate that the natural convection is significant when (Holman 1976)

$$Re < Gr^{1/3} \tag{3.33}$$

Where Gr is a dimensionless number representing the ratio of typical buoyancy force to a typical viscous force and is known as Grashof's number.

For a 0.025 cm wire Gr is calculated to be 2.55, for $T-T_a = 50°C$

If β is the volume coefficient of expansion of the water, then Gr can be calculated from Eq. (3.34)

$$Gr = \frac{g \cdot \beta \cdot d^3}{\nu^2} \cdot (T - T_a) \qquad (3.34)$$

For the system below, this means that Re numbers are less than 1.36, but if during the calculations the actual dimensions of the probe are considered, buoyancy effects for Re numbers at least up to 10 can be expected.

V	RE	NU	TP	PECLET NUMBER
.100000	2.636073	1.781446	.012585	64.338
.200000	5.272145	2.132216	.010514	128.677
.300000	7.908218	2.381843	.009412	193.015
.400000	10.544290	2.582403	.008681	257.354
.500000	13.180363	2.752922	.008144	321.692
1.000000	26.360726	3.379033	.006635	643.385
1.500000	39.541089	3.824608	.005862	965.077
2.000000	52.721451	4.182601	.005360	1286.770
2.500000	65.901814	4.486970	.004996	1608.462
3.000000	79.082177	4.754464	.004715	1930.155
3.500000	92.262540	4.994734	.004489	2251.847
4.000000	105.442903	5.213921	.004300	2573.540
4.500000	118.623266	5.416199	.004139	2895.232
5.000000	131.803629	5.604556	.004000	3216.925
5.500000	144.983991	5.781211	.003878	3538.617
6.000000	158.164354	5.947864	.003769	3860.310
6.500000	171.344717	6.105848	.003672	4182.002
7.000000	184.525080	6.256233	.003583	4503.695
7.500000	197.705443	6.399891	.003503	4825.387
8.000000	210.885806	6.537543	.003429	5147.080
8.500000	224.066169	6.669793	.003361	5468.772
9.000000	237.246531	6.797152	.003298	5790.465
10.000000	263.607257	7.038895	.003185	6433.850

Table 3.2 Thermodynamic parameters for different velocities

This means that for velocities less than 4mm/sec (see Table 3.2) a mixed convection situation is expected.

3.5 GENERAL CONCLUSIONS

In this Chapter has been described the results of both theoretical and experimental investigations into a

pulse-grid probe using a time of travel technique for water velocity measurements.

Important advantages of the heat pulse method are its stability and repeatability. Having no moving parts, the system operates over a wide dynamic range by a wide variety of conditions.

The analysis made in this Chapter has shown that below velocities of 4mm/sec, the influence of buoyancy effects becomes very important, thus introducing an error in the measurements. Probably the above effects could be reduced to a maximum by a more careful design of the probe, but even in the present case the technique seems to have considerable potential for exploring fissure flows into water wells (even under natural gradient conditions), which hitherto have not been amenable to proper experimental investigation.

However, although the present work represents a start on the theoretical and practical analysis of the method, it is clear that there are many aspects of the device behaviour that require further investigation. Such as:-

- The effect that the shape of the probe may have upon the accuracy of the measurements
- A detailed study of various sensors in order to find the most appropriate one
- Possible ways of reducing the effect of turbulence occurring at fissure levels which have an adverse effect upon the accuracy of the instrument.

Such development was considered to be beyond the scope of the present research.

C H A P T E R IV

GEOPHYSICAL FORMATION LOGS USED IN THE WATER INDUSTRY

4.1 INTRODUCTION

Formation logs permit a study to be made of the physicochemical properties of the formations surrounding the well.

The purpose of this Chapter is to review the necessary elements of the theory of formation logging, examine the role that they play in the water industry today and see to what extent they can be used for the evaluation of the Chalk aquifer.

A rather common combination of logging analyses used for hydrogeological purposes consists in the determination of formation resistivity, natural gamma radiation and spontaneous potential of the surrounding the borehole formation. The changes in the borehole diameter are also recorded since they are needed for the accurate interpretation of the above logs.

All variables are recorded continuously as a function of probe depth and logging speed which depending on the type of tool, varies between 3 and 15 m/min.

During the recent years some attention has been paid to a number of new logging methods such as the sonic log, nuclear logs and the guard log and these are going to be discussed as well.

The theoretical basis of quantitative formation log interpretation, required to investigate the relation between the recorded formation parameters and the hydraulic conductivity of the aquifer, is examined in detail in PART II.

4.1 RESISTIVITY LOGS

In 1927 the first resistivity log was run in a boring near Pechelbron, France, by Schlumberger brothers, and 1947 saw the first catalogue of resistivity departure curves published by Schlumberger Well Survey corporation.

The technology of resistivity logging comes largely from the oil industry and during the last twenty years the use of these devices was gradually increased in the field of Hydrogeology. Many of the principles, advantages, disadvantages and uses of resistivity logs that apply to the petroleum industry are also relevant to groundwater applications.

4.1.1 Instrumentation and Theory

The following discussion is confined to the single-point resistance, the 16-inch and 64-inch normal arrangement resistivity methods, since they remain the most popular methods of resistivity logging in hydrologic work.

A typical resistivity logging apparatus might be arranged according to the diagram represented in Fig. 4.1.

The measurements are commonly made using alternating current with frequency of a few tens of Hz; the short distance between the electrodes in the borehole precluding any harmful influences of the skin effect.

During the measurement the current intensity is kept constant between the electrodes by means of a stabilized circuit; in this condition the measured potential is directly proportional to the apparent resistivity. This apparent resistivity is recorded continuously while the measuring device is pulled up through the borehole at a constant speed. A recording galvanometer may be set to read the voltage between N and either A,M or M1. The

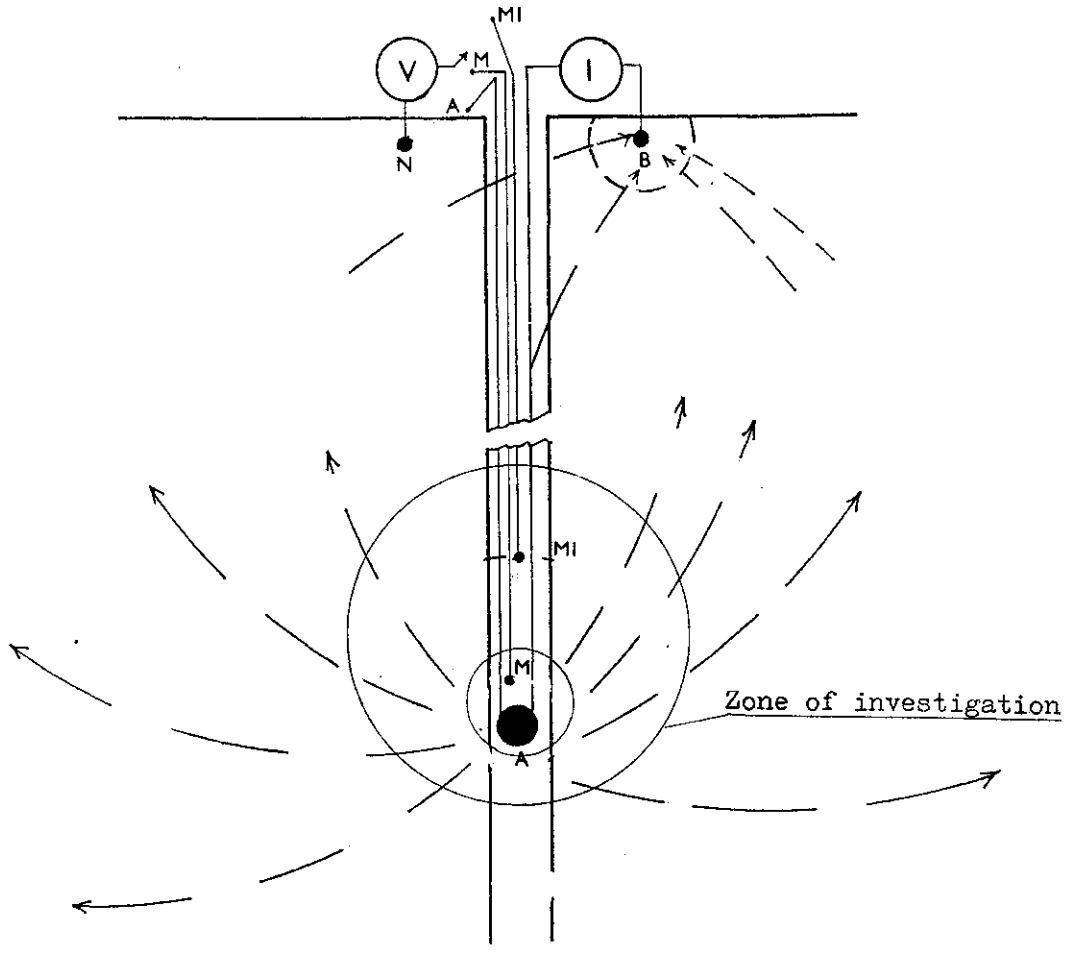


Fig. 4.1 Typical resistivity logging arrangement

distance AM is approximately 16 inches, and AM1 is approximately 64 inches. The distances AB and AN are large relative to AM and AM1.

If the galvanometer is set to read the potential difference between A and N, the apparatus is termed a single-point device; if it is set to read the potential between M and N, the apparatus is called a short normal device; and if it is set between N and M1 the apparatus is a long normal service.

To understand the relationship between the quantities measured and the parameters defining the resistivity stratification in the ground, and so to pave the way for a

quantitative interpretation of the measurements, it is necessary to find the relationship between the electric potential at the wall of the borehole and the strata.

The derivation of this relationship will be considerably simplified if the potential field set up by a single point source of current (monopole) is first considered, because in the above derivation the axial symmetry of the potential field can be used. The case for which the potential will be derived in this section is defined by the following specifications:

1. The formation consists of a finite number of layers separated from each other by horizontal boundary planes extending laterally to infinity.
2. Each of the layers is electrically isotropic.
3. The field is generated by a point source of current that is located at the wall of the borehole.

These specifications regarding the configuration of the subsurface are commonly used as the basis for the interpretation of resistivity sounding data. Nevertheless, it is generally recognized that these specifications are no more than a schematization of the real conditions in the subsurface which are considerably more complex.

On the assumption that all the beds are horizontal, the borehole is vertical and the current sources lie on the axis of the borehole, one may say that the potential surfaces and the lines of current flow possess a cylindrical symmetry.

In a cylindrical coordinate system (p,z,θ), Ohm's law may be generalized to state that the current density J is given in terms of the potential V by the equation:

$$-J = \frac{1}{R}\left(\frac{\partial V}{\partial p}p_1 + \frac{\partial V}{\partial z}z_1\right) \qquad (4.1)$$

where z_1 is a unit vector parallel to the axis of the borehole and p_1 a unit vector perpendicular to z_1 and directed away from the borehole axis.

The absence of current sources or sinks, everywhere except on the borehole axis, is expressed by assuming that the divergence of the current density vanishes for $p \neq 0$. This leads to the differential equation:

$$\nabla \cdot j = \frac{1}{\rho} \frac{\partial}{\partial \rho} \left(\frac{\rho}{R} \frac{\partial V}{\partial \rho} \right) + \frac{\partial}{\partial z} \left(\frac{1}{R} \frac{\partial V}{\partial z} \right) = 0 \qquad (4.2)$$

$$\nabla \cdot j = \frac{\partial^2 V}{\partial \rho^2} + \frac{1}{\rho} \frac{\partial V}{\partial \rho} + \frac{\partial^2 V}{\partial z^2} + \frac{1}{\rho^2} \frac{\partial^2 V}{\partial \theta^2} = 0 \qquad (4.3)$$

and by assuming cylindrical symmetry:

$$\frac{\partial^2 V}{\partial \theta^2} = 0 \qquad (4.4)$$

The solution of this equation must be found subject to the following boundary conditions:

1. The current source is an isotropic point source located at the axis of the borehole and near it the potential must approach infinity as:

$$V_n \longrightarrow \frac{I R_m}{4 \pi r} \quad , \; r \longrightarrow 0 \qquad (4.5)$$

2. At infinite distance from the axis of the borehole the potential must approximate zero:

$$V_n, V_f \longrightarrow 0, \; r \longrightarrow \infty \qquad (4.6)$$

3. At the wall of the borehole the vertical component of the current density must be continuous:

$$\frac{1}{R_m}\frac{\partial V_m}{\partial \rho} = \frac{1}{R_f}\frac{\partial V_f}{\partial \rho} \quad , \rho = a \tag{4.7}$$

4. At the wall of the borehole the electrical potential must be continuous:

$$V_m = V_f \quad , \rho = a \, , (r = \sqrt{\rho^2 + z^2}) \tag{4.8}$$

This is equivalent to the statement that there is no charge double layer on the surface.

A formal solution of this problem can be constructed in a fashion analogous to the treatment given in the Appendix of the Schlumberger Corporation's Interpretation Handbook (1950) for Resistivity Logs. The notation adopted is that in the previous section, but now the origin is at the current electrode, and thus z is the spacing of the normal device.

The potential in the borehole, expressed in terms of the modified Bessel functions K_0, K_1, I_0 and I_1, is found to be:

$$V_m(\rho, z) = \frac{I R_m}{4\pi}\left[\frac{1}{r} + \frac{2}{\pi}\int_0^\infty A(x)\cdot I_0(x\rho/a)\cos(xz/a)\cdot dx/a\right] \tag{4.9}$$

where

$$A(x) = \frac{K_0(x/2)\cdot K_1(x) - \frac{R_m}{2R}\cdot K_0(x)\cdot K_1(x/2)}{K_0(x/2)\cdot I_1(x) + \frac{R_m}{2R}\cdot I_0(x)\cdot K_1(x/2)} \tag{4.10}$$

and where the apparent resistivity for the normal device is given by the formula:

$$R_a = \frac{4\pi z}{I} V(0,z) \qquad (4.11)$$

As can be seen from the above equation, the essential step in the computation of the potential at the wall of the borehole due to a current source at its axis, is the evaluation of the following Fourier integral:

$$F(\lambda, R/R_m, z/a) = \frac{2}{\pi} \int_0^\infty A(x) \cos(xz/a)\, dx \qquad (4.12)$$

A technique for the numerical evaluation of such an integral for large values of z/a and slowly varying function A(x) has been described by Filon (1928) and used by Kunz and Moran (1958) in their study of anisotropic formations.

Recently in a paper by Gianzero and Ray (1977) the solution for the potential was recasted as a Fourier exponential transform by using Fast Fourier Transform techniques (Cooley et al 1969). The FFT is a clever computational device which drastically reduces the number of operations in the integration procedure.

The results of these computations have been published by many oil companies as a set of departure curves. Documents 3 and 7, published by Schlumberger Well Surveying Corporation, contain departure curves for a wide variety as shown in Fig. 4.2.

The axes are the ratio of the AM spacing to the hole diameter, and the ratio of the apparent resistivity to the resistivity of the mud.

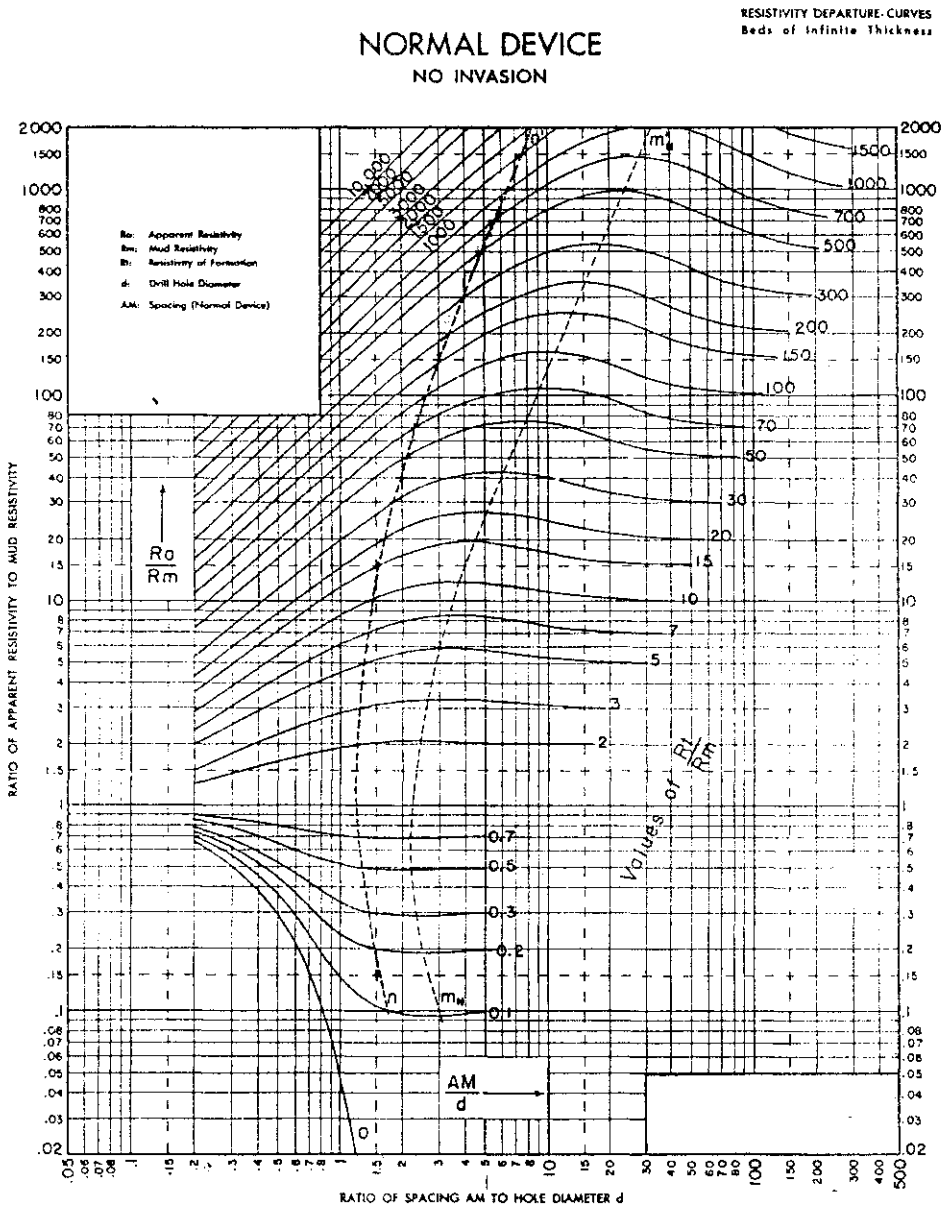


Fig. 4.2 Departure curves for normal device - infinitely thick bed, no invasion (courtesy Schlumberger Well Surveying Corp.)

It can be seen from these curves that the measured resistivity may be greater than, less than, or equal to the true resistivity of the bed, depending on the magnitude of the various factors listed above.

As the ratio of the spacing to the hole diameter becomes very small, all the curves approach a value of Ra/Rm of 1; or the measured resistivity approaches the resistivity of the mud.

As the AM/d ratio increases, the apparent resistivity approaches the true resistivity, then exceeds it for as while (or is less than the resistivity for low resistivity beds), and then for very large ratios approaches the true value assymptotically.

The curve n-n' represents the locus of points where the apparent and true resistivity are equal.

4.1.2 Volume of Ground Investigated by Normal Resistivity Logs

In order to visualize the zones of investigation of the resistivity devices, the introduction of the geometric factor is very useful, since it indicates the relative contribution of the various parts of the formation to the recorded signal. The intergrated geometric factor is defined as the sum of all the geometric factors starting from the current electrode.

Let g(r,z) be the geometric factor and let p(r,z) be the formation resistivity, then the apparent resistivity indicated by the logging sonde, as computed on the basis of the geometric factor alone, will be given by:

$$\rho_a = \int_{-\infty}^{\infty} dz \int_{0}^{\infty} g(r,z) \cdot \rho(r,z)\, dr \qquad (4.13)$$

Fig. 4.3 shows the intergrated geometric factors for the short and long normal devices as compared with the lateral device which is going to be described later in this Chapter. One can see that no signal of the 16-inch normal comes from the formation between the current electrode A and the M electrode (refer to Fig. 4.2); 50% of the signal is from that part of the formation between the M electrode and a point 32 inches from the current electrode; 90% of the signal is caused by that part of the formation within about 13 ft. of the current electrode, thus one can assume that for the short normal curve, the formation that is about 2 to 6 ft. from the current electrode will dominate the reading of the device.

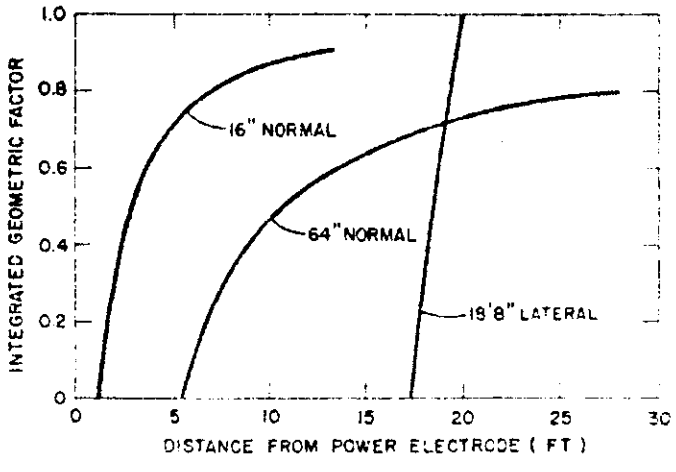


Fig. 4.3 Theoretical geometric factors for normal and lateral measuring systems in an infinite homogeneous medium (Lynch 1962)

Similar calculations show that for the long normal the formation from 6 to 16 ft. from the current electrode contributes more strongly to the signal as compared to the lateral curve from which one can see that the formation between 17 and 20 ft. contributes to the entire signal.

All the above conclusions were based upon the assumption

that there were no borehole effects. In the general case the volume of investigation of each device has gradational limits and depends partly on the resistivity of the fluid in the borehole and the adjacent formation. Therefore, the volume sampled constantly varies as the sonde travels the borehole.

4.1.3 Thin bed effects

Fig. 4.4 shows the response of a normal device as it passes opposite beds of various thicknesses. As the bed thickness decreases relative to spacing Fig. 4.4b, the resistivity peak at the centre of the bed gradually shrinks in size. When the bed thickness becomes equal to the spacing (Fig. 4.4.c), or less than the spacing (Fig. 4.4.d), the centre resistivity hump disappears altogether; the curve actually reverses and shows the resistivity bed as if it were even more conductive than the surrounding beds.

The reversal of the normal curve opposite a thin resistive bed is a serious limitation on the use of two electrode devices. Fig. 4.5 shows the fraction of the resistivity that is recorded by a normal device as a function of the bed thickness (Lynch 1962). It can be seen that when the bed thickness becomes less than three to four AM spacings, the needed correction to the recorded resistivity becomes very large but as the resistivity contrast with the adjacent beds becomes less, then slightly thinner beds may be logged successfully.

As far as bed thickness effects are concerned, it is desirable to use an electrode spacing that is small in comparison to the thickness of the average stratum. From the standpoint of determining true resistivity, however, it is desirable to use a long electrode spacing. These two requirements are opposed to each other and may be said to be the dilemma of normal electric logging systems. This condition of diametrically opposed requirements again demonstrates the desirability of recording more than one apparent resistivity curve.

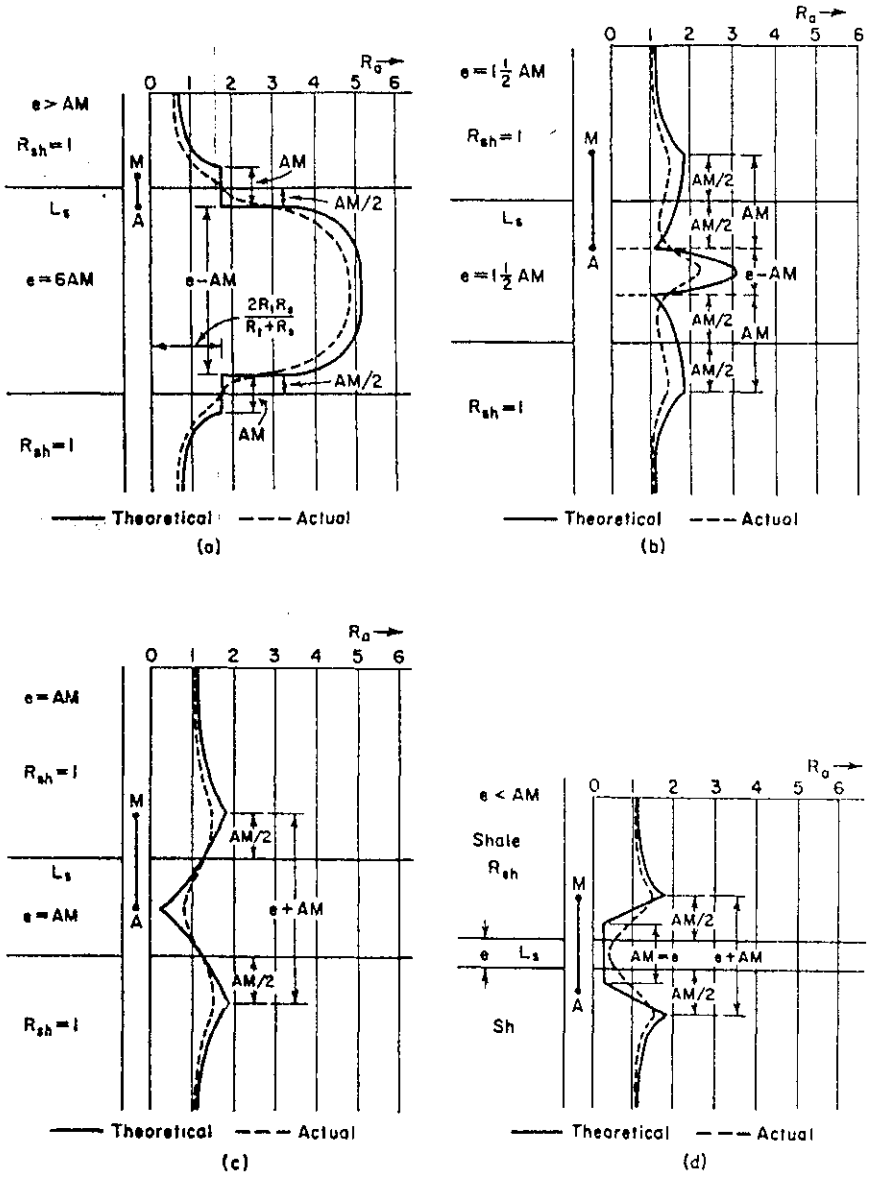


Fig. 4.4 Response of a normal device opposite beds of various thicknesses (courtesy of Schlumberger Well Surveying Cor.)

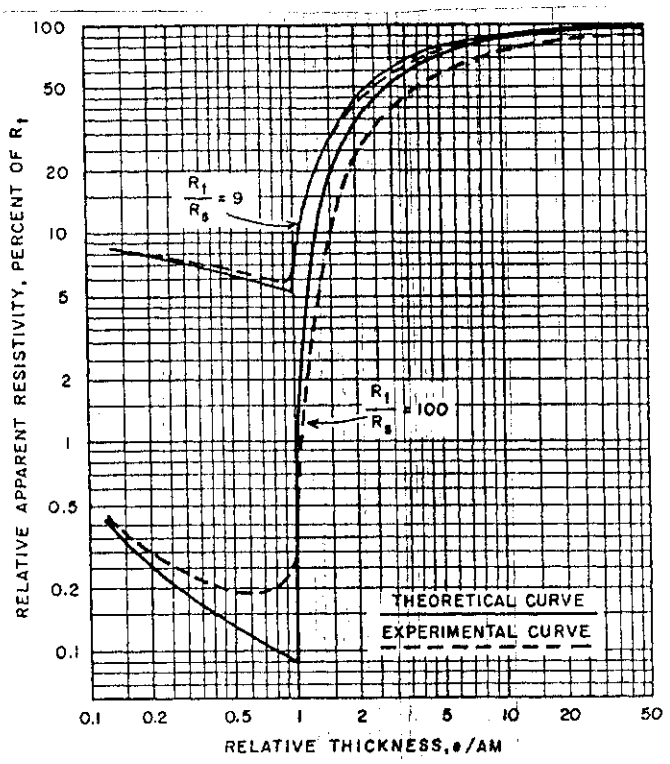


Fig. 4.5 Apparent resistivity indicated by a normal device for various bed thicknesses (Lynch 1962)

4.2 THE SPONTANEOUS POTENTIAL LOG

The spontaneous potential log is a measure of the natural potentials developed between the borehole fluid and the surrounding material.

The electrical spontaneous potential is considered to represent the algebraic sum of:

(a) the diffusion potential which is a result of the flow of drilling mud into the fresh water bearing formations surrounding the hole due to differences in concentration. The magnitude of this potential can reach the maximum value given by Eq. (4.14)

$$E_d \simeq \frac{v-u}{v+u} \cdot \frac{R \cdot T}{n \cdot F} \ln c_m / c_w = + k_d \log p_w / p_m \qquad (4.14)$$

where v = anion mobility
u = cation mobility
c_m, p_m = salinity, resistivity of the mud
c_w, p_w = formation water salinity, resistivity
R = universal gas constant (= 8,314 Joule/kg.mol.°K
T = absolute temperature in Kelvin degrees (°K)
F = Faraday constant (= $9,65.10^3$ Coulomb/kg.aeq.)
n = ion valence

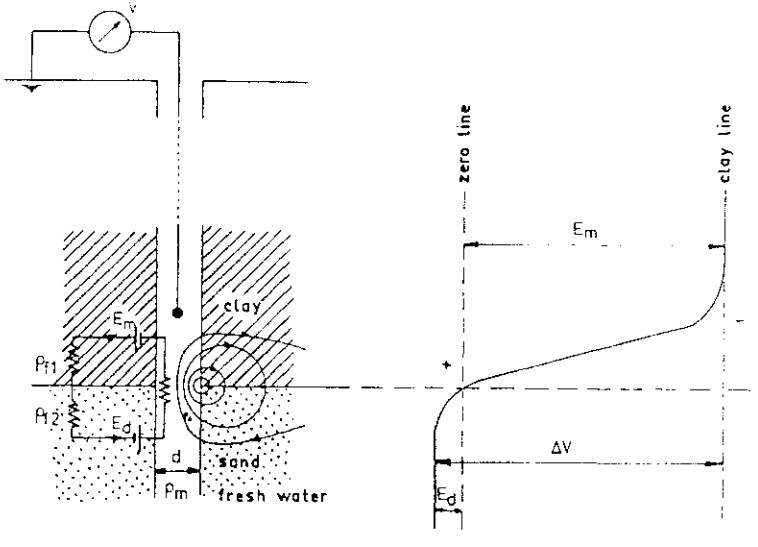


Fig. 4.6 Schematic representation of the spontaneous potential (S.P.)

(b) The membrane potential which occurs opposite a clay layer. As the clay particles bear negative electrical charges, they will jointly behave as a membrane that is more or less impervious to anions. The magnitude of this potential can be taken from Eq. (4.14) by taking v = 0:

$$E_m = -\frac{RT}{nF} \ln C_m/C_w \simeq -K_m \log \rho_w/\rho_m \qquad (4.15)$$

(c) The electrokinetic potential, which is a result of mud invasion due to over-pressure into the formation. At the relatively shallow depths reached in geohydrological investigations, this potential is negligible.

The main point is the combined effect of the diffusion and membrane potentials as described in Fig. 4.6. The maximum potential drop in the mud at the interface between a sandy layer and a clay bed that contains pore water with equal resistivity will hence amount to:

$$\Delta V = E_d - E_m \simeq (k_d + k_m) \log \rho_w/\rho_m = k \log \rho_w/\rho_m \qquad (4.16)$$

The spontaneous potential is measured by lowering a single electrode into the borehole. A second electrode is located at the surface. Measurements are obtained from a recording potentiometer in millivolts.

4.3 THE GAMMA RAY LOG

The gamma ray log is a measure of the amount of natural gamma radiation emitted by the rocks adjoining the borehole.

The gamma-ray emitting isotopes responsible for the radioactivity in most rocks are K and daughter products of the uranium and thorium decay series. Fig. 4.7 represents the range of radioactivity of some sedimentary rocks.

The gamma ray sonde contains a detector (usually a scintillation counter with pulse amplification and shaping

circuits), to measure the natural gamma radiation originating in the volume of the formation near the sonde.

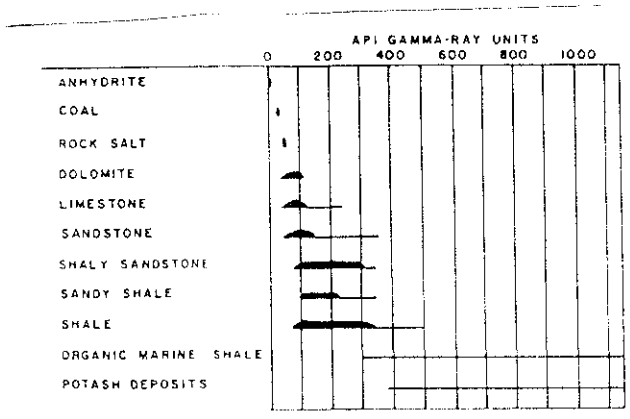


Fig 4.7 Range of radioactivity of some sedimentary rocks

The number of gamma rays reaching the counter fluctuates even when the sonde is stationary in the hole, the phenomenon being statistical in nature. A combination of factors cause a divergence of the recorded radioactivity with respect to the true radioactivity of a formation. An important factor of all radiation logging equipment is the time constant which is the time in seconds over which radiation pulses are averaged. Commonly the time constant can be chosen between 1 and 30 seconds. The true radiation intensity of a bed can be determined only if the logging speed is less than the bed thickness divided by the time constant. Fig. 4.8a shows the influence of these factors on the measuring results when the statistical variations have been omitted. One can see that with rising probe speed, the curve becomes more "rounded" and thin layers become more difficult to reproduce. Fig. 4.8b is a more realistic example since it contains statistical variations as well. If the time constant becomes small, the logging speed can be relatively high, the main disadvantage being the rather large statistical variation. If the statistical

variation is suppressed by a longer time constant, the logging speed must be slower. In practice, a proper choice of time constant and logging speed is determined by the accuracy wanted or needed. The recorded radiation level can be affected also by the eccentricity of the probe in the borehole and the borehole rugosity.

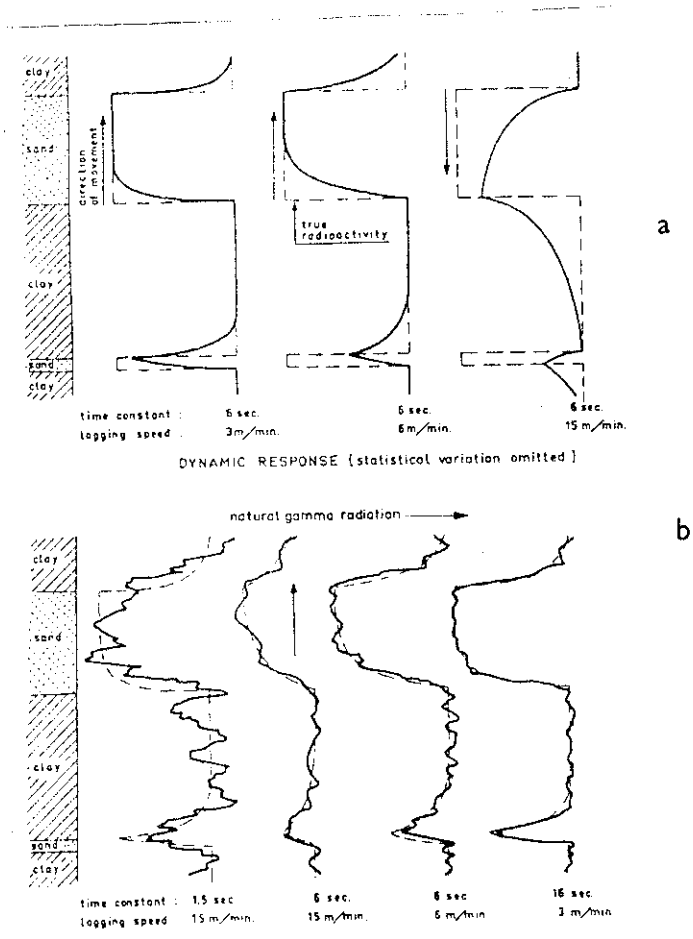


Fig. 4.8 Dynamic response of a natural gamma probe

4.4 THE CALIPER LOG

The caliper log represents the average diameter of the borehole at various depths. Its major use is to evaluate the environment in which other logs are made in order to correct them for hole diameter effects and to provide

lithographic information (some rocks are more liable to be washed out than others), stratigraphic correlation and to locate the fractures and other openings.

Caliper sondes consist of devices, such as arms (Plate 7) capable of sensing the wall of the hole. Averaging of the hole diameter is achieved by recording the diameter rather than the radius of the hole at a given depth.

4.5 INTERPRETATION PRACTICE OF FORMATION RESISTIVITY LOGS IN THE CHALK

It is well known that the methods of analysis of the resistivity logs which exist in the oil industry cannot be applied in groundwater rock.

Let us discuss the assumptions upon which these standard methods, for the analysis of oil reservoirs, have been developed and examine their limitations when they are applied to groundwater.

During the logging of an oil well, the borehole is usually filled with drilling mud, with resistivity of the order of 5 ohm.m. The formation may contain brine having a resistivity of 0.05 ohm.m. Considering a formation factor of 20 the true formation resistivity becomes 1 ohm.m which is roughly five times less than that of the borehole fluid.

If the drilling mud has invaded the formation to a certain radius, the borehole will be surrounded by a region of high resistivity, given by the product of the formation factor and the resistivity of the saturation fluid, thus being 100 ohm.m.

In such a case the following characteristic relationship between the apparent resistivity curves is to be expected:



Plate 7 Caliper probe with the arms open

obviously $P_{LN} < P_S < P_{SN}$

where P_{LN} is the resistivity measured by the long normal
P_S " " " obtained by the single point resistance
P_{SN} is the resistivity measured by the short normal

In the case where a formation is not invaded by drilling fluid, the difference between P_{LN} and P_{SN} is smaller and is due only to the greater effect of the borehole in the zone of investigation of the short normal. These are the conditions which have been used by the oil industry for the identification of permeable zones, on the assumption that only permeable zones will be invaded.

Thus, zones for which

$$P_{SN} >> P_{LN}$$

are considered to be permeable, and zones for which the apparent resistivities are closer together are considered to be impermeable. It is useful to examine to what extent the above assumptions are valid for groundwater aquifers (e.g. Chalk). As most of the boreholes are drilled with formation water, the value of the resistivity of the water in the borehole P_W is considered to be equal to the value of the resistivity of the water in the pore space of the formation. This assumption is valid if the logging process is to take place some weeks after drilling, in order for the fluid column to settle down to something like the average resistivity at each level, and if the water in the borehole at the specific level can be considered as chemically identical to the water in the formation.

Under these circumstances, there will be no invaded zone and the effect of the borehole will be to lower the apparent resistivity, according to the relative influence of the open borehole in the zone of investigation of the device (Fig. 4.1).

In this case we would expect the relation:

$$P_{LN} > P_{SN} > P_S$$

Formation resistivity measurements made in boreholes driven in Chalk containing fresh water depend strongly upon the porosity of the formation. A very common result of this effect is the higher values which are obtained for the resistivities of the Chalk rock and the Melbourn Rock (Fig. 4.10).

In the special case where the phenomenon of saline intrusion into the borehole occurs, the interpretation of the formation resistivity logs becomes complicated, since in this case the apparent formation resistivity which is measured by the logs is a function of salinity.

Monkhouse and Fleet (1975) have investigated the phenomenon of saline water intrusion in the Chalk of the South coast of England and have concluded that when the borehole and aquifer contain highly saline fluid, the apparent formation resistivity will be low. Conversely, when the fluid is fresh, the apparent formation resistivity will be high. Intermediate values will occur when the borehole fluid is saline and the aquifer fluid is fresh or vice versa.

From the extensive recent literature (Reeves 1979), about the general hydraulic behaviour of the English Chalk, it seems that the average horizontal hydraulic conductivity of the extruded rock appears to be greater than the vertical one. Therefore, there is a possibility of having two or more fissure horizons containing water of different qualities (i.e. electrical conductivities). this phenomenon is more likely to happen when dealing with coastal boreholes because of the effect of saline intrusion. The following Fig. 4.9 represents some of the possible combinations between fluid and formation, which could exist in a borehole with saline water intrusion.

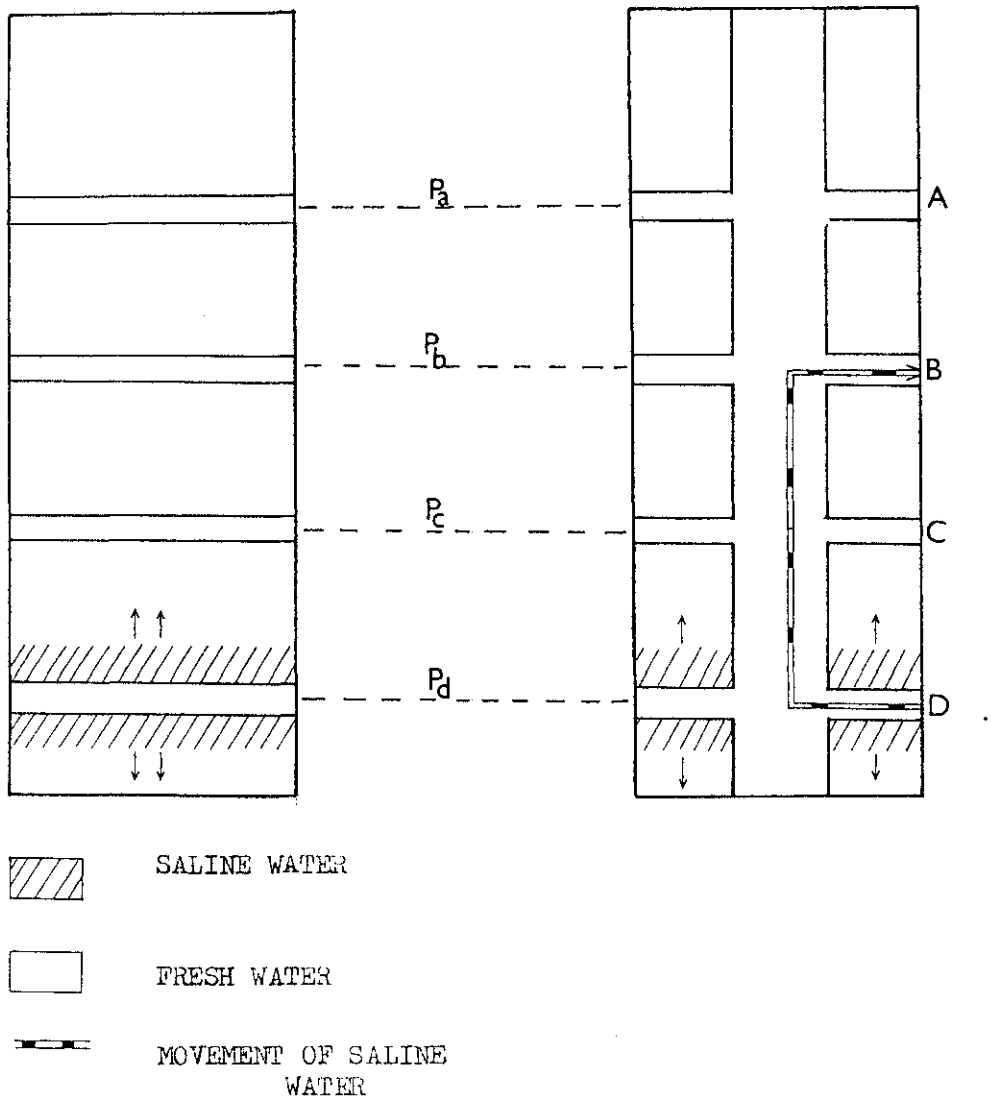


Fig. 4.9 Possible combinations between fluid and formation in a borehole with saline intrusion

Considering first the horizon which contains saline water (D in Fig. 4.9), it can be assumed that the pore water content of the surrounding formation is of similar composition, although things are complicated from the fact that the salinity of the groundwater in these levels responds to both tidal and long-term seabed effects (see Fig. 2.18).

By drilling a borehole through the formation, there is a possibility of vertical groundwater movement into the borehole due to differences in the piezometric heads between the different fissure zones. Thus, it is quite common for saline water in the borehole to be present at a level where the pores and fissures or only the pores

contain fresh water. (Zones C and B in Fig. 4.9 respectively). Eventually the water in fissure zone B becomes saline because of long term flushing of D type water. Real situations are more complicated, but from the above discussion one can consider that the following four basic extremes of groundwater conditions (shown in Table 4.1) exist:

Table 4.1 Typical groundwater conditions in a borehole with saline intrusion

Zone	Borehole water	Pore water	Fissure water	Apparent Formation resistivity
D	Saline	Saline	Saline	Low
B	Saline	Fresh*	Saline	Medium
C	Saline	Fresh	Fresh	Medium
A	Fresh	Fresh	Fresh	High

From all the above discussion, one can conclude that the interpretation practice of formation resistivity logs is more complicated than that used in the oil industry, and it must be carried out, always bearing in mind the local hydrogeological conditions.

4.6 THE RELATION OF FORMATION LOGGING MEASUREMENTS TO THE HYDRAULIC CONDUCTIVITY OF AN AQUIFER

Extensive borehole geophysical logging has been carried out in the Chalk aquifer of England. The purpose of this paragraph is to discuss to what extent the formation logs described previously have been used for the assessment of the hydraulic conductivity of fissured aquifers such as Chalk.

---

* eventually becomes saline

4.6.1 Resistivity Logs

Electrical resistivity logs have been classified in terms of resistivity marker bands (Gray 1958, 1965; Tate 1971), and have long been used for stratigraphic correlation. These marker bands have enabled stratigraphic correlation of Chalk horizons from Surrey, in the south, through the London Basin to East Anglia.

This is of particular importance because the drilling methods employed during the construction of the boreholes frequently provided very poor drilling samples making the Chalk subdivisions difficult to identify. Fig. 4.10 shows an idealized resistivity log for the full Chalk to Gault succession showing the electrical marker bands and some other features.

Apart from the use of the normal resistivity logs for stratigraphic correlation, very little use has been made of them in order to evaluate the hydraulic properties of the adjacent well formations, thus the question naturally arises as to why such a little information has been gained.

This is mainly due to the fact that the fissure zones which are the main water bearing zones and are characterized by a relatively low electrical resistivity, fail to show clearly at all on the resistivity curves.

This failure is either due to the poor resistivity contrast between the fissure zone and the formations adjacent to the well or to some other factors. For example it is well known that in some horizons in the Chalk, one can find flint bands which are more resistive than the formation of the Chalk. These flint bands can generate some irregularities on the logs which could either be misinterpreted as fissure effects or make the interpretation very difficult. Fig. 4.11 is an example of

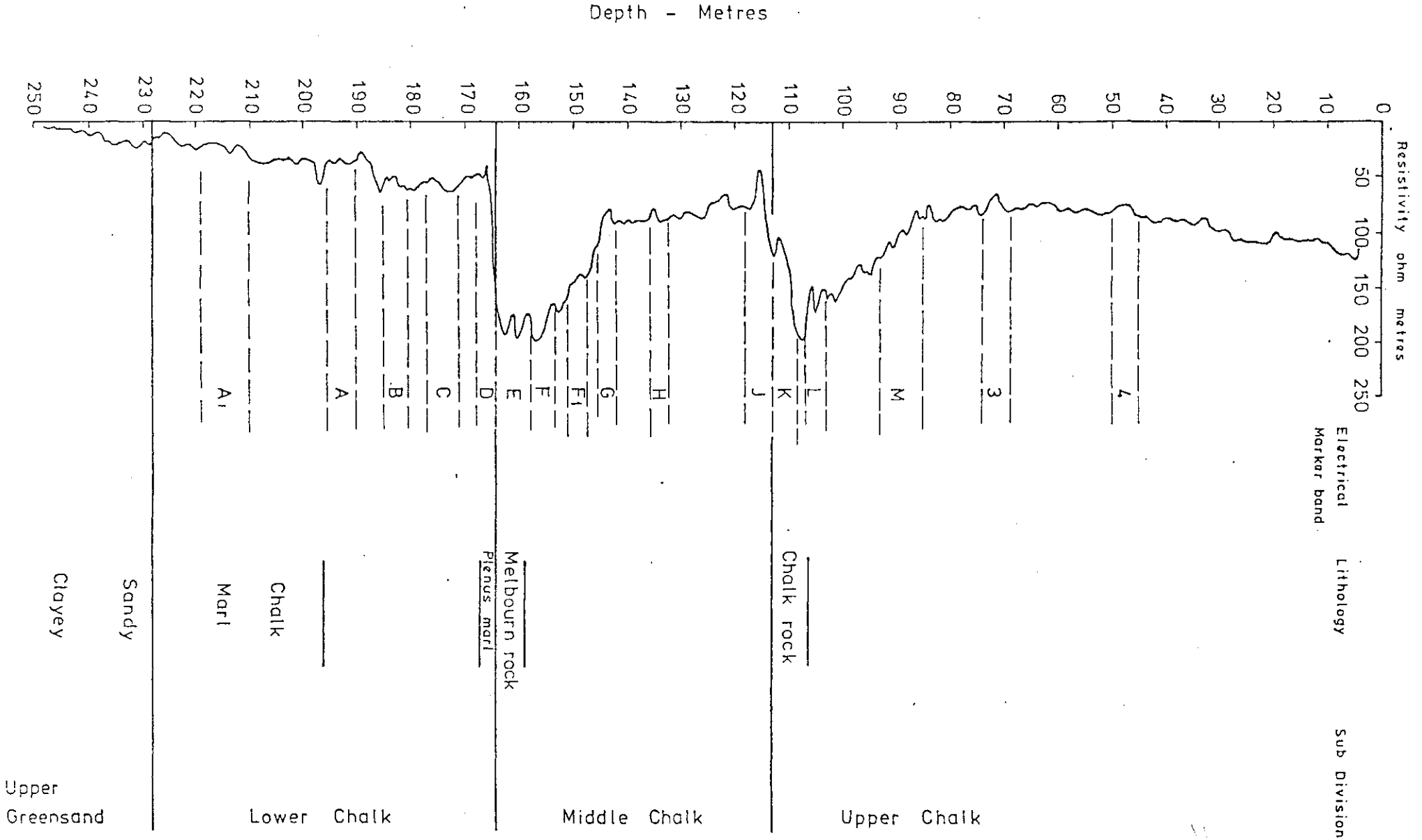


Fig. 4.10 Idealised 16-inch normal resistivity log for the Chalk

a normal resistivity log carried out in borehole No. 5 in the Brighton Chalk. By observing only the long normal curve, one could misinterpret the recorded minimals A,B,C,D as the effect of fissuring of the formation, but by referring to the short normals it becomes apparent that the inversion of the long normal curve at these points is due to some thin resistive beds, probably flint bands.

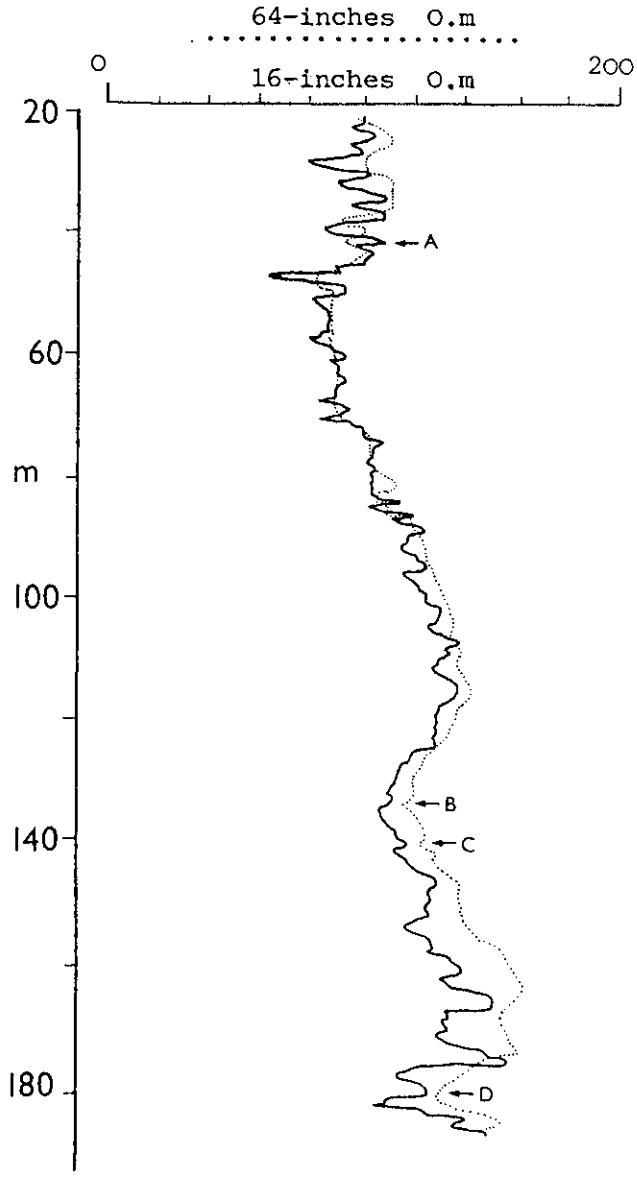


Fig. 4.11 Normal resistivity logs showing thin bed reversal effects

Fig. 4.12 represents a 16-inch normal resistivity log carried out in a borehole in Hampshire by the IGS (Price et al 1977) together with the results of packer tests. During the packer tests, three main fissure zones were detected and were confirmed by flow logging methods. The resistivity log shows little or no evidence at all of these fissure levels. Attempts to extract fissure information from the normal resistivity logs may be successful in some cases, especially when dealing with large fissure zones in a non-flinty Chalk formation (or generally in a homogeneous fissured formation), but it is doubtful whether this approach will result in a successful method that will be generally applicable. Thus one can conclude that the quantitative evaluation of the characteristics of individual fissure zones, and hence their hydraulic properties, from normal resistivity devices by applying standard interpretation procedures, is almost impossible.

4.6.2 Gamma ray logs

Interpretive procedures for utilizing gamma ray logs have, for the most part, been restricted to qualitative identification of lithology and formation contacts. By observing laboratory and x-ray logs of the Chalk, Ponsford (1955) came to the conclusion that Chalk is one of the least radioactive of the British sediments. This was confirmed by the work of Smart et al (1964) and Taylor (in Gray 1965).

The Upper and Middle Chalk produce a rather featureless gamma ray log but in the Lower Chalk detailed logs are obtained which can be used for correlation, since marly bands in the Chalk have a substantially higher level of radioactivity than normal Chalk. Fig. 4.13 contains a part of a natural gamma log carried out in borehole No. 1 in Brighton.

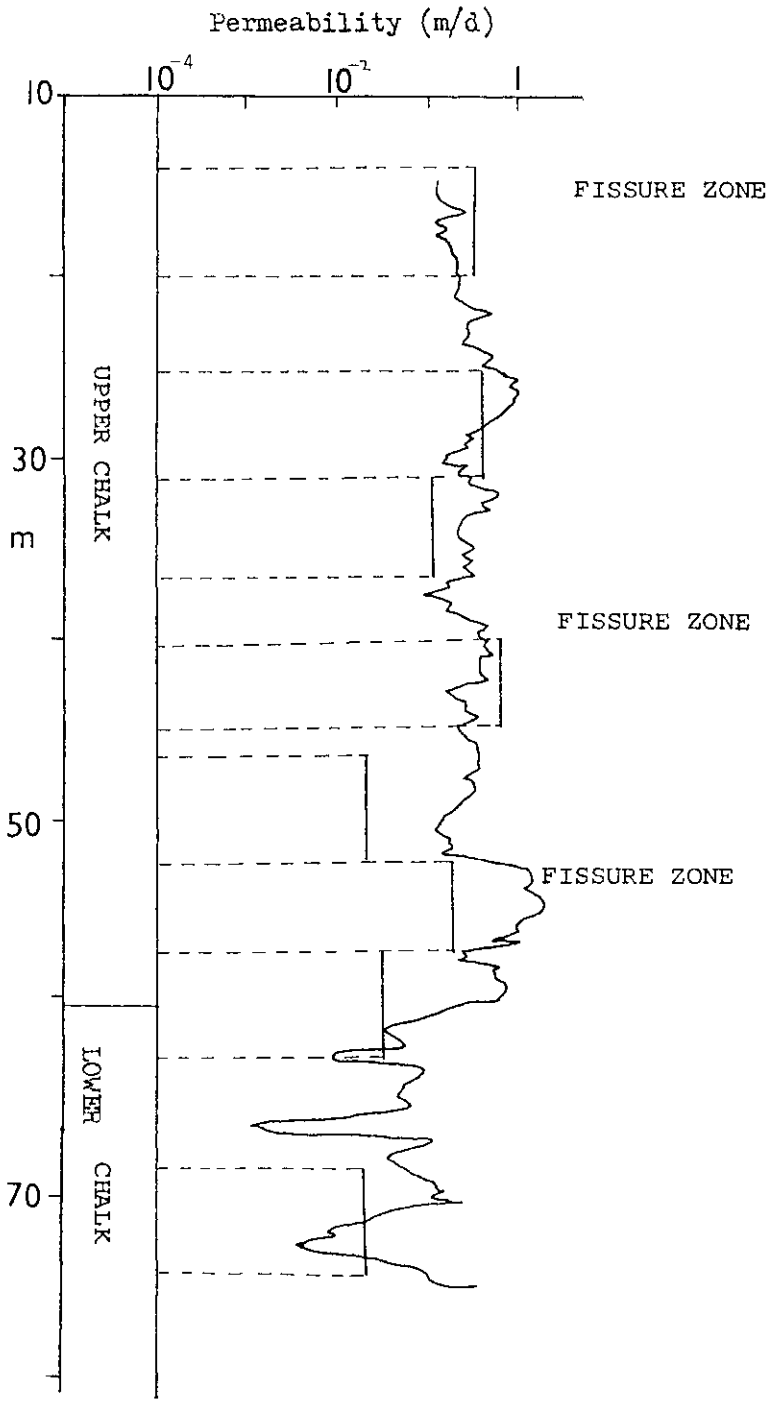


Fig. 4.12 Comparison of 16-inches resistivity log with results from packer tests

One can easily identify the effect of Plenus Marl horizon on the log at the depth of 190 metres. The distinctly higher gamma count of the lower Chalk is also obvious. Apart from its use for the location of marl horizons, it seems that there will be no use of the natural gamma log for the location of permeable zones.

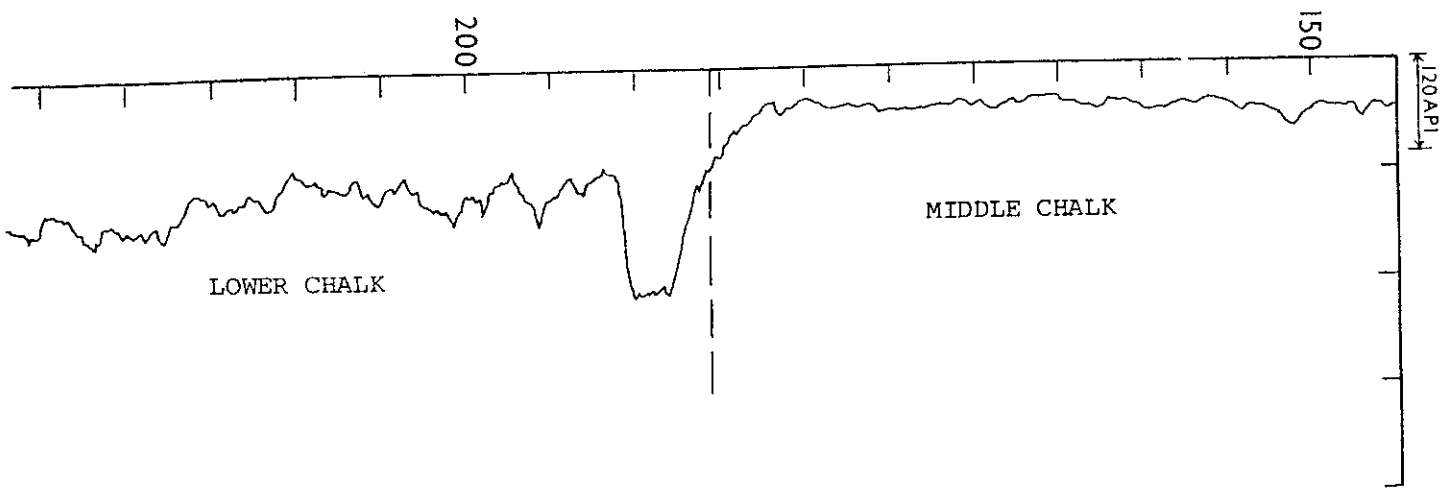


Fig. 4.13 Part of the natural gamma log in a Chalk borehole

4.6.3 Spontaneous potential log

The assumptions involved in the quantitative interpretation of the spontaneous potential log are seldom satisfied in groundwater work. In most of the cases of SP logging, a flat and featureless spontaneous potential is obtained indicating that the ion content between the water in the formation penetrated by the borehole and the borehole fluid opposite the formation is only slightly different. Thus the use of this method as a quantitative tool is therefore likely to produce erroneous results.

SP logs are usually run together with electric resistance or electric resistivity logs and are recorded on the left column of the Chart. In some cases reading of the log consists in identifying positive or negative deflections from a recognizable, arbitrary baseline, which represents a permeable or impermeable formation.

Fig. 4.14 contains a part of a spontaneous potential log of borehole No. 1 in the Brighton Chalk. Several permeable zones can be shown in the log. The SP deflection is produced by the difference in composition of the borehole and aquifer fluids. The "shale line" appears to be to the right and therefore, deflections to the left are caused by borehole fluid entering permeable Chalk horizons.

4.2 OTHER DEVICES FOR FORMATION LOGGING

Apart from the systems already described, which are the most common logging methods for the water industry, there are some others which are less common: they also originate from the oil industry. Some of them can be of particular help for the solution of hydrogeological problems.

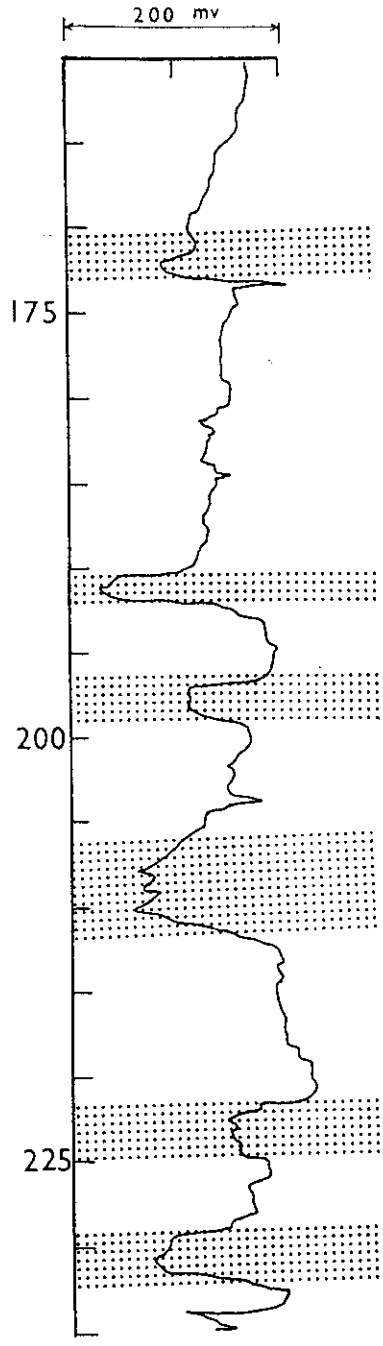


Fig. 4.14 Part of the S.P. log indicating permeable zones

4.7.1 Lateral Device

The lateral is a "deep-looking" device and gives best results in beds whose thickness exceeds twice the electrode spacing.

Three effective electrodes are present in the borehole (Fig. 4.15). The potential electrodes M and N are positioned below the current electrode A. The reference point is the mid-point O between electrodes M and N. In most of the devices the distance AO (spacing), has been standardized at 18 ft. 8 in.

The advantages of the lateral device, compared to the normal ones, is that it provides greater penetration of the formations, and always shows a positive deflection when passing through a resistive bed, regardless of the bed thickness.

Its limitation is that it does not record abrupt deflections at the top and bottom of the beds because of the wide spacing of the electrodes, therefore it is of limited value for stratigraphic correlations. In addition to this, the lack of symmetry of the obtained logs about a given bed is another major disadvantage of the method.

In the water industry the lateral device is of limited use since the shadow peaks and dead zones (Fig. 4.16) obtained on the logging curve make the delineation of fissure zones very difficult.

4.7.2 The Gamma-gamma Log

Gamma-gamma logs are records of the intensity of gamma radiation originating from an artificial source (usually ^{60}Co or ^{137}Cs) located in the probe, after the radiation has been backscattered and attenuated in the borehole and the surrounding rocks. The gamma radiation absorbed is

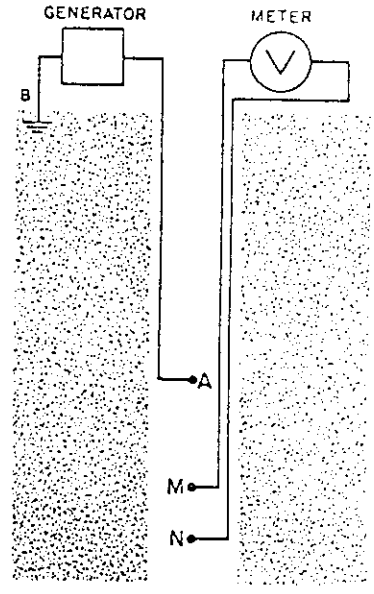


Fig. 4-5 Theoretical arrangement for the lateral logging system

proportional to the electron density of most materials penetrated by logging. Electron density in turn, is approximately proportional to the bulk density of the materials. For this reason, the gamma-gamma log is also called the density log, and Eq. 4.17 is applied:

$$\text{Porosity} = (\text{grain density} - \text{bulk density}) / (\text{grain density} - \text{fluid density}) \qquad (4.17)$$

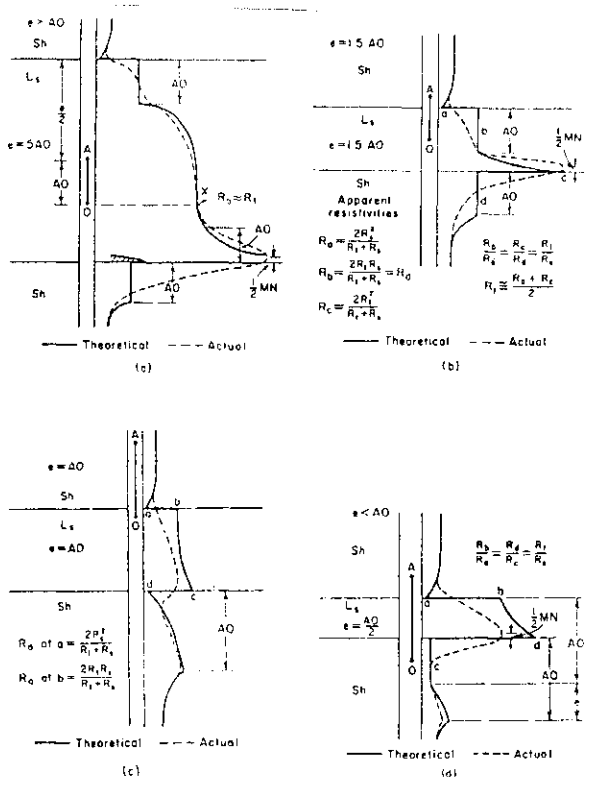


Fig. 4.16 Response of a lateral device opposite beds of various thickness. (Courtesy of Schlumberger Well Surveying Corp.)

Fig. 4.17 represents the physical principles of the gamma-gamma log. If the same lithology unit is present above and below the water table (or if gamma-gamma measurements can be made before and after drawdown), the specific yield of aquifers can be assessed by the gamma-gamma log, as the difference between the bulk density of the saturated and drained sediments.

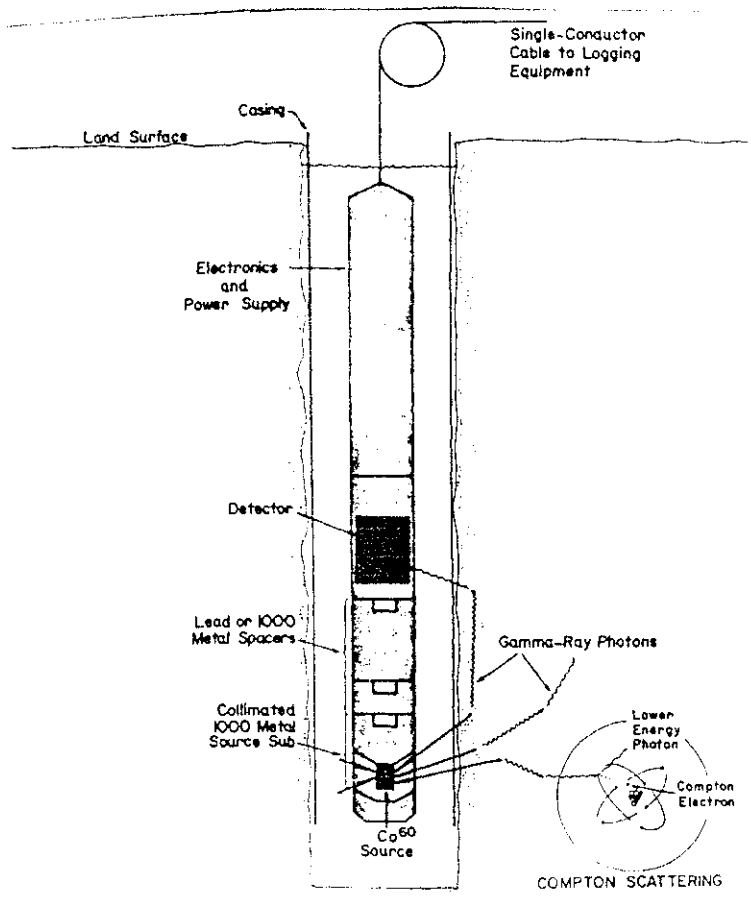


Fig. 4.17 The equipment, principles and interpretation of gamma-gamma logs (Keys et al 1971)

4.7.3. Neutron Log

Neutron logs are records of the intensity of gamma rays emitted from a formation under the influence of neutron bombardment.

The neutrons are captured by the atomic nuclei of certain elements resulting in gamma ray emission which are recorded by the probe. Fig. 4.18 shows the physical principles of the method. Since neutrons have no electric charge the only way of losing energy when passing through matter is by elastic collision. This process is called moderation, and the slowed-down neutrons are described as thermalized.

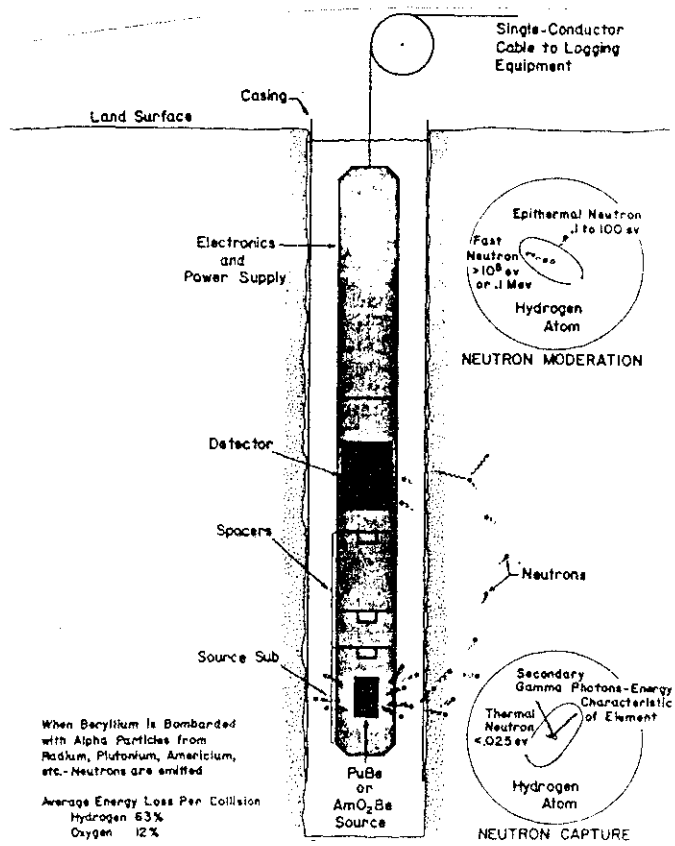


Fig. 4.18 The equipment, principles, and interpretation of neutron logs (Keys et al 1971)

The most effective element in moderating neutrons is hydrogen. Because of the great number of hydrogen atoms in the fluid contained in the pore space of the rock, the induced gamma radiation provides an indication of the amount of fluid in a rock, hence of the porosity (in the saturation zone).

Neutron logs are used mainly for the measurement of moisture content above the water table.

Recently a number of new logging techniques based on the physical processes of moderation and absorption of neutrons when passing through matter, have been applied in the oil industry and are represented in a diagrammatic form in Fig. 4.19.

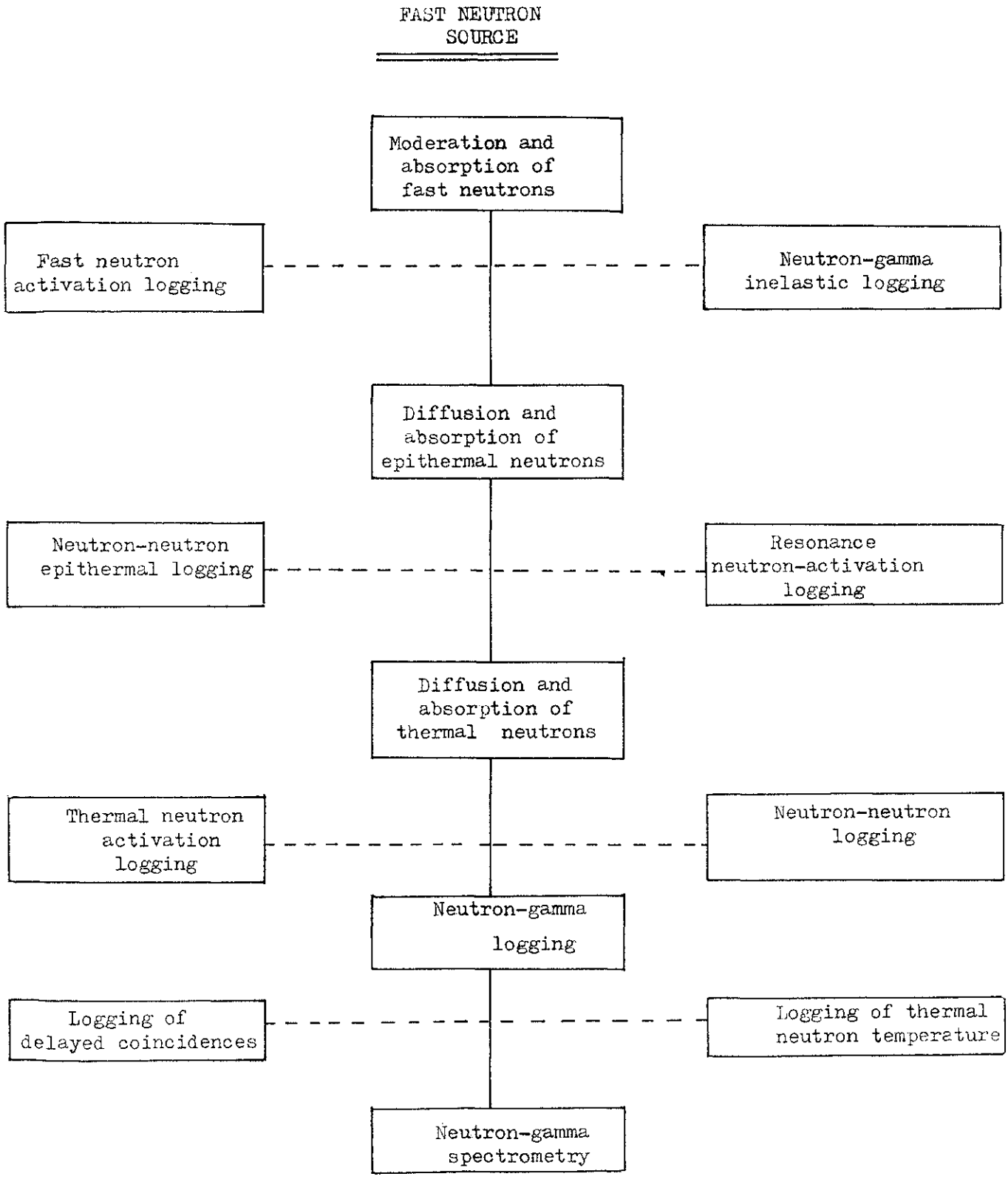

FAST NEUTRON SOURCE
Moderation and absorption of fast neutrons
Fast neutron activation logging
Neutron-gamma inelastic logging
Diffusion and absorption of epithermal neutrons
Neutron-neutron epithermal logging
Resonance neutron-activation logging
Diffusion and absorption of thermal neutrons
Thermal neutron activation logging
Neutron-neutron logging
Neutron-gamma logging
Logging of delayed coincidences
Logging of thermal neutron temperature
Neutron-gamma spectrometry

Fig 4.19

The present application of the gamma-gamma or neutron logging methods in the geophysical logging of Chalk boreholes is very limited and all the existing tools are used in a qualitative way.

The basic reason for this is that all the information which can be obtained by using the above methods about fissure zones can also be obtained by conventional logging methods (i.e. caliper, single point resistance) and the high porosity of the Chalk results in restraining the depth of investigation of the nuclear logging tools.

In addition to this, all the logging techniques utilizing an active radiation source require precautionary measures to protect personnel as well as the environment from radiation damage.

4.7.4 The Sonic Log

The sonic log was originally developed as an aid in the interpretation of seismic data, but it has been proved so effective in the determination of porosity that it has already become the standard wireline method of porosity estimation in the oil industry.

The sonic device measures the time of transit of a sonic impulse through a given length of rock, usually either 1 ft. or 3 ft. The rate of propagation of the compression wave through the rock depends on the elastic properties of the rock matrix and its contained fluids. Fig. 4.20 shows a sonic logging probe which is compensated for borehole-diameter changes, where Fig. 4.21 shows an illustrative received waveform.

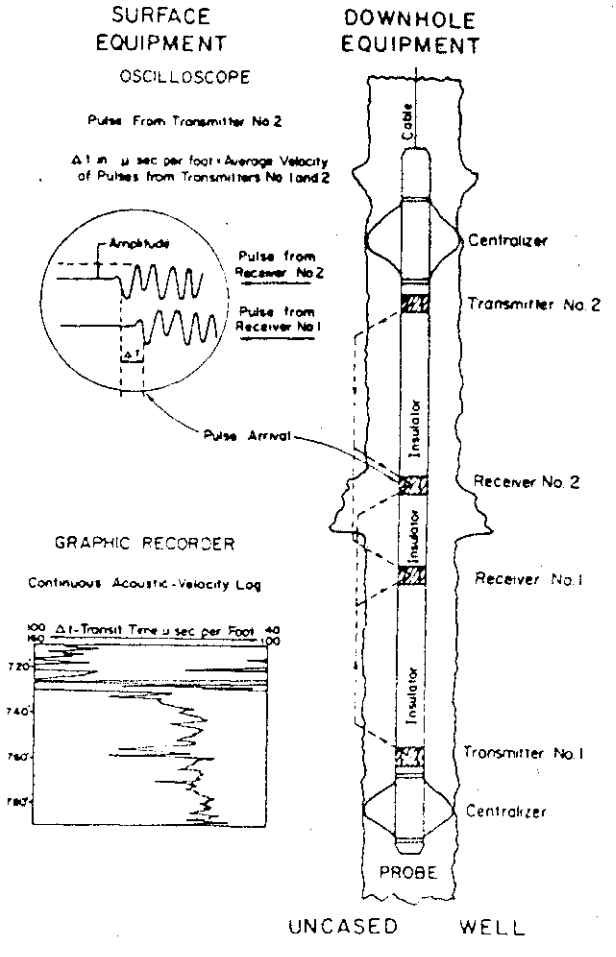


Fig. 4.20 Principles and equipment for making borehole adjusted acoustic velocity logs

By a sonic device the following acoustic-wave parameters and the ratios between them can be measured: P and S wave velocity; P and S wave amplitude, or attenuation; and frequency.

Many empirical relations have been established in the oil industry between the various acoustic parameters and permeability of porous formations.

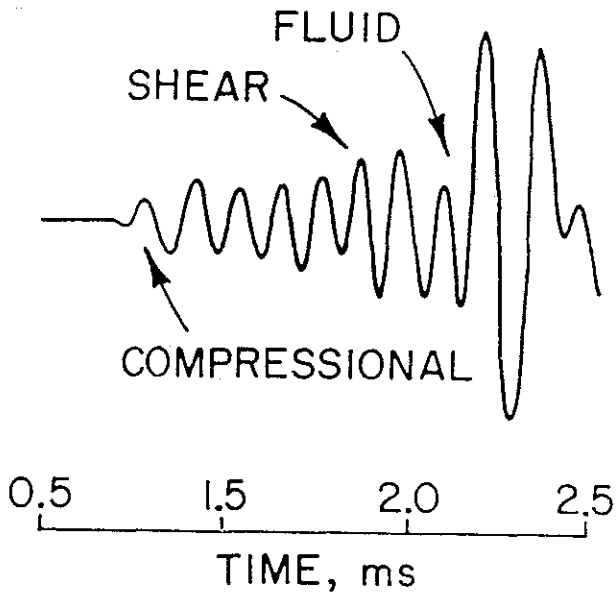


Fig. 4.21 Illustrative waveform of received signal showing compressional, shear, and fluid arrivals

There is also much literature concerning the effect of fractures on acoustic wave propagation. Unfortunately, it is all theoretical and not always supported by field examples; often it is contradictory (Suau et al 1980). Nevertheless, the sonic log may well prove to be the best fracture finder, considering the new wave-train recording capabilities obtainable with acoustic imaging methods (Nelson 1982). Fig. 4.22 is an example of a VDL* (Variable Density Log) opposite a fracture zone.

The main advantages of the sonic log are that it is basically a mechanical properties tool, not too sensitive to borehole effect and free of statistical variations. On the other hand, the sonic log may respond to formation features other than fractures. In theory, the compressional wave travel time is little affected by fractures so long as there is a free matrix path between transmitter and receivers (as would be expected for vertical fractures), but shear wave energy should be strongly affected and so should its amplitude.

* Note of Shlumberger Corp.

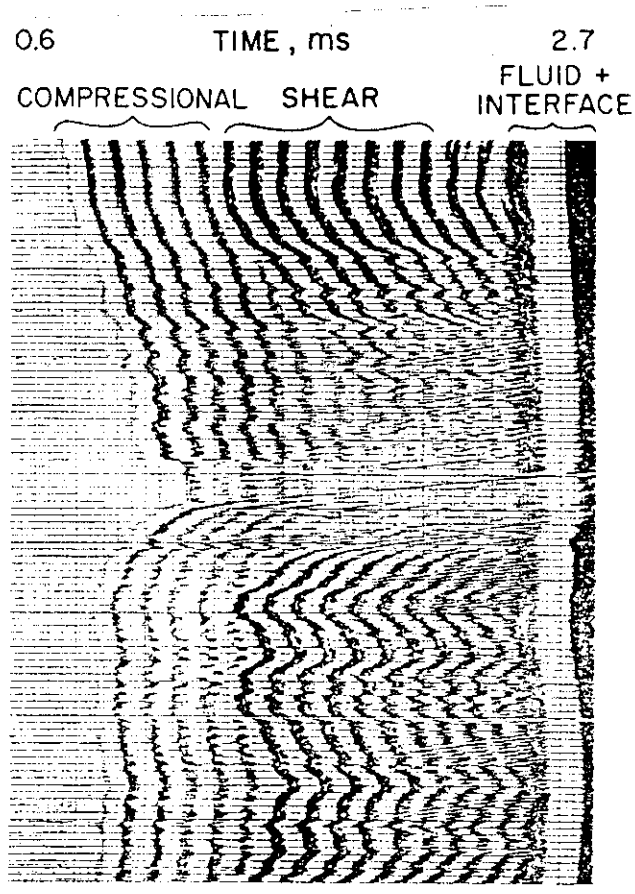


Fig. 4.22 Use of variable density log for identification of arrivals

Morris et al (1964) based on the selective effect of fracture orientation on P and S wave arrival and amplitude were able to locate fracture zones and interpret their primary orientations although they were not able to determine fracture intensity. Although no similar work for the location of fissures in the Chalk has been carried out, the technique looks very promising.

4.7.5 The Focused Devices

Measurement of the resistivity of a homogeneous and isotropic material can be made, simply, when (a) the body of the material is infinite in all dimensions and (b) the measuring electrodes can be placed within the body. In such a case, the current leaving an electrode follows a

spherical distribution and the mathematical expression for the potential level at any distance from that electrode can readily be derived.

If it is considered that the active electrodes are within a borehole filled with fluid of a resistivity different from that of the formation, the current does not flow in a spherical pattern near the current source or sink (Fig. 4.24) and the calculations of potential levels become more difficult. Should the vertical dimensions of the formations be considered as finite, such as the case of fissured formations, the problem becomes so complex as to preclude reasonable solution.

In efforts to eliminate the above problem, combinations of two, three, and four electrode logging configurations of the conventional types have been used. In the guard logging method, the current is forced to flow in a thin disk normal to the axis of the logging tool.

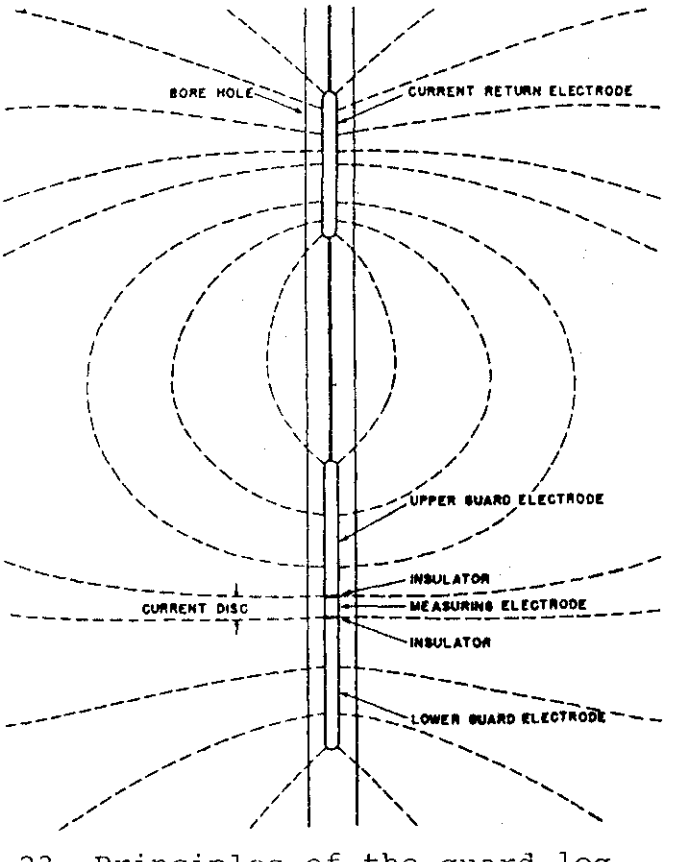


Fig. 4.23 Principles of the guard log

The principles of the guard logging device are illustrated in Fig. 4.23. The guard electrode assembly is made up of an upper guard electrode, a measuring electrode, and a lower guard electrode. The thickness of the current beam is approximately the length of measuring electrode M and, in commercial logging systems, ranges from 3 to 12 inches. Variations in each resistivity within this disk-shaped current beam control the amount of current flowing from the measuring electrode.

Another focusing system is the laterolog method where the solid conductors of the guard method are replaced by a series of conventional electrodes A_1A_2, $M_1'M_2'$ and M_1M_2 to focus the current (Fig. 4.24). The advantage of the laterolog compared with the guard log is that SP can be measured at the potential electrode almost to the bottom of the borehole because the metallic guards are eliminated.

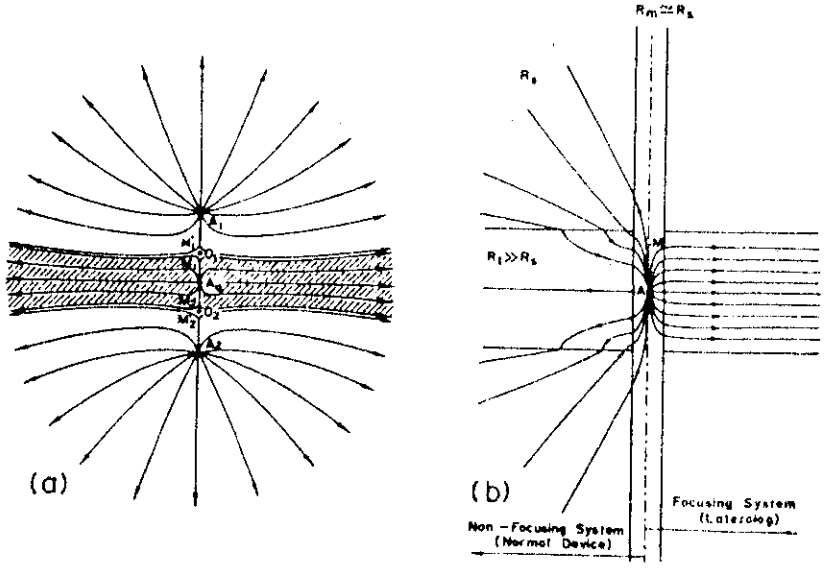


Fig. 4.24 Principles of the laterolog and schematic comparison of current patterns from laterolog and normal device

The instrumentation employed to furnish the necessary current to the electrode system at the focused device and to measure the voltage and exploring current values and

transmit them to the surface is rather complicated and until now the advantages of groundwater exploratory have been considered to be rather small.

The author believes that the focused devices could play an important role in the evaluation of the hydraulic characteristics of the Chalk, when it is to be used together with other conventional resistivity methods.

Recently, a similar device has been built and tested in a borehole in S.E. England (Bear, T., personal communication 1982) and the results were very promising.

4.8 GENERAL CONCLUSIONS

For many years there has been a notable lack of equipment specifically designed for logging in water boreholes in contradiction to the oil industry which developed many sophisticated logging techniques for use in mud-filled boreholes. Recently a number of companies are attempting to provide a fairly good selection of devices which are purpose designed equipment of minimal diameter for use in either new or existing production boreholes in which the presence of a pump and ancillary equipment poses access problems.

Although the water industry has been slow to adopt logging techniques, the use of logging devices and interpretation methods in groundwater work for the exploration, evaluation and the measurement of geophysical parameters of aquifers is increasing. There are about half a dozen borehole measurements which are in common use by the water industry compared to the several dozen currently available for the oil industry. One can say that the stage of groundwater borehole geophysics today is that of the oil borehole geophysics 10 to 20 years ago. Nevertheless, potential application of the existing techniques have important

ramifications towards making useful conclusions about the aquifer properties.

A review of the necessary elements of the theory of the logging techniques most common to the water industry has been done, and a discussion of the limitations of these methods when they are applied for obtaining information about the hydraulic properties of the Chalk has been made.

- The apparent formation resistivity measured by the logs depends upon the porosity of the formation.
- For boreholes which are affected by saline water intrusion the apparent formation resistivity depends on the electric conductivities of the borehole and formation fluids and the local pressure heads of the fissure zones. Four basic extreme cases have been described.
- Attempts to extract fissure information from the electric resistivity logs are complicated by the presence of flint and marl bands but may be successful when dealing with large fissure zones in a pure Chalky formation.
- Apart from its use for stratigraphic correlation, the natural gamma log has no application for the location of fissure zones.
- Most of the SP logs in the Chalk are flat and featureless indicating that the ion content between the borehole and formation fluid is only slightly different.
- SP logs can be useful in locating permeable zones in coastal boreholes where the phenomenon of saline intrusion occurs.
- From the rest of the formation logging methods the guard log and the sonic log look very promising for the study of fissure zones.

A detailed study of the relation between the geophysical properties of the formation, measured by the logs, and its hydraulic conductivity is needed and is the subject of PART II of this Thesis.

PART II

Having studied in PART I the principles of operation of the different logging methods and the extent to which they have been used for the evaluation of the hydraulic properties of Chalk, the next step in the research is to examine the possible ways of learning more about the hydraulic conductivity from parameters measured by the geophysical logs. Such a study constitutes PART II of this thesis.

Before being able to correlate the measured geophysical parameters with the hydraulic conductivity of the formation, a clear understanding of its hydraulic structure must be established since this would permit us to simulate the Chalk by realistic models, necessary for the accurate evaluation of the possible relations that exist between geophysical and hydraulic parameters.

This PART contains two Chapters: Chapter 5 deals with the hydraulic structure of Chalk and Chapter 6 introduces the theoretical basis for the relationship between geophysical and hydraulic parameters.

C H A P T E R V

HYDRAULIC PROPERTIES OF THE CHALK

5.1 INTRODUCTION

In this Chapter the hydraulic characteristics of Chalk are examined by adopting a discrete model approach. This is achieved by applying a conduit geometry embedded in the matrix of the Chalk in order to represent the fissures. Conduits are assumed to have smooth parallel plane walls of finite extent, with variable orientations, openings and spacings.

Before proceeding to the task of finding the combined influence of these idealized properties the hydraulic conductivity of a single parallel plane is evaluated, then the equivalent conductivities of parallel sets of openings are derived.

Next to be considered is the replacement of the matrix, which up to now was assumed to be impervious, by a semipervious media and to examine the overall effect of this change.

An understanding of the Chalk's hydraulic structure is necessary before trying to correlate the geophysical parameters measured from the logs with the hydraulic properties of the rock and the Chapter opens with a consideration of primary and secondary porosity.

5.2 PRIMARY POROSITY AND HYDRAULIC CONDUCTIVITY

Electron microscopy has shown that the matrix of the Chalk consists of calcium carbonate which usually takes the form

of calcite particles about one micron or less in size and being almost entirely or organic derivation (Coccoliths etc.). Generally the Chalk can be divided into coarse and fine fractions. The coarse fraction, which may constitute 20-30% of the Chalk, falls within the 10-100μ range. This contains material derived from the mechanical breakdown of large shelled organisms and, to a lesser extent, Foraminifera. The fine fraction is almost entirely composed of coccoliths and may form up to, and sometimes over, 80% of certain horizons.

In some Chalks many of the coccoliths are preserved (Fig. 5.1) whilst in others most of the coccoliths have broken into their component laths.



Fig. 5.1 Electron microscope photograph of a sample of Upper Chalk (Price et al 1976)

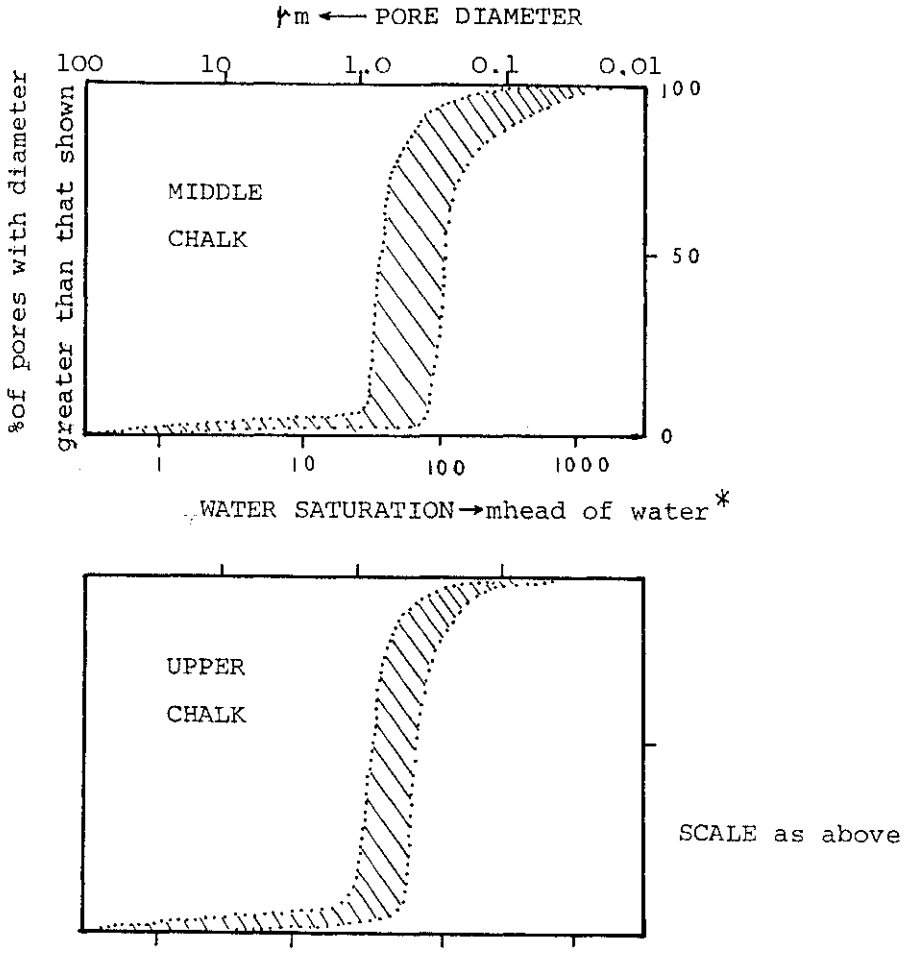


Fig. 5.2 Envelopes of available pore-size distribution curves for the Upper and Middle Chalk (Price et al 1976)

---

* The pressure required to force a liquid into a spherical cavity of diameter d is:

$$p = \frac{-4\sigma\cos\theta}{d}$$

writing $p = pgh$ we obtain

$$h = \frac{-4\sigma\cos}{dgp}$$

For water at 10°C, $\sigma = 0.074$ N/m and θ for most materials is effectively zero thus

$$h_w = \frac{-3.0 \times 10^{-5}}{d} \text{ m head of water}$$

(The negative sign implies that water is drawn into the cavity and that a suction or tension is needed to remove it).

The most impressive feature of the texture of Chalk is how little of the rock is actually occupied by the calcite. Pore-size distributions of the Chalk measured using the mercury injection method, have been made by Price et al (1976) and some of their results for the Middle and Upper Chalk of S.E. England are shown in Fig. 5.2 from which one can see the degree of uniformity of Chalk pore size. Laboratory experiments (Price et al 1976) have shown an approximate correlation between intrinsic permeability and porosity (Fig. 5.3). The poor correlation obtained in Fig. 5.3 might be due to the influence of occasional larger pores.

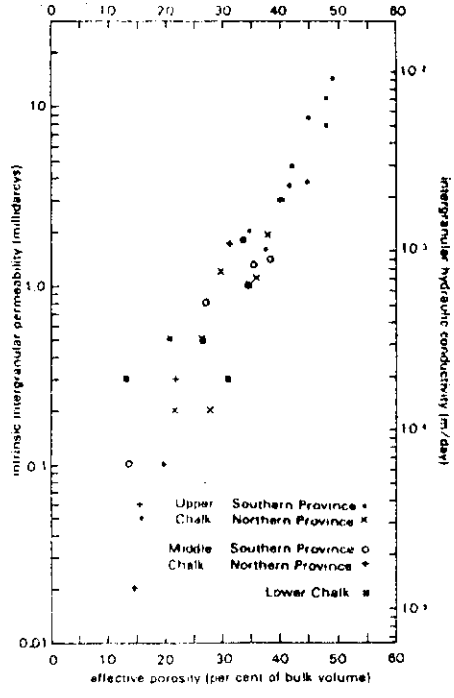


Fig. 5.3 Intergranular permeability against effective porosity for 36 Chalk samples (Price et al 1976)

A number of characteristic values for the porosity and intrinsic permeability of the Chalk have been collected from the existing literature and are presented in Table 5.1.

TABLE 5.1

Author	Porosity %	Permeability md
Scholle 1974	40-46	6-12
Carter and Mallard 1974	35-47	
Ineson 1962		0.001-0.25
Edmunds et al 1973	35-45	0.87-1.91
Bell 1977	28-45	0.14-2.85

From Table 5.1, one can see that Chalk has exceptionally low intrinsic permeability for a rock with such high porosity. Because of its high interstitial porosity the Chalk contains large volumes of water. Each km of saturated Upper Chalk contains on average some 300,000 to 400,000 Ml of interstitial water. On the other hand, because of the small dimensions of the pores, nearly all the water which they contain is held by capillary and molecular forces, and very little can drain or move under gravity. Of course in the unsaturated zone both evaporation and transpiration can be expected to be the only processes which can substantially deplete the water content (Foster 1975).

The extent to which pore drainage occurs under field conditions will depend on the relationship between the larger and smaller pores and between the large pores and

the fissures, but it is worth noting that interstitial specific yield is more likely to be evenly distributed throughout the aquifer and therefore available at all groundwater stages (Foster 1975).

5.3 SECONDARY POROSITY AND HYDRAULIC CONDUCTIVITY

Despite the very small value of the intrinsic permeability of the Chalky matrix, it is not uncommon for a great number of wells sunk into the Chalk to have yields up to 250 m^3/h for a depression of water level of only up to 3m. Since the Chalk is essentially a soft limestone with very low primary conductivity, the source for the above high yields is an extensive anastomizing system of fissures with a high proportion of the groundwater discharging into the well flowing through them.

The conductivity of the Chalk is determined essentially, therefore, by the effective conductivity of the fissures as conduits.

The analysis of the pumping tests is one of the most useful means of determining the hydrogeological characteristics of an aquifer but for the case of some Chalk, great hydraulic anisotropy would not be likely to lead to an accurate determination of transmissivity: rather it provides evidence of the overall hydraulic response of the aquifer and its boundary parameters.

Whilst it is not the primary purpose of this thesis to discuss in detail the hydrogeology of Chalk, certain aspects of it are of fundamental importance to the better understanding of the hydrodynamics of fissure flow.

(a) Time-drawdown response

Time-drawdown analysis of a number of pumping tests of various duration in the Chalk has revealed the following (Fig. 5.4) typical time-drawdown response in most of the pumped wells (Connoston and Reed 1978).

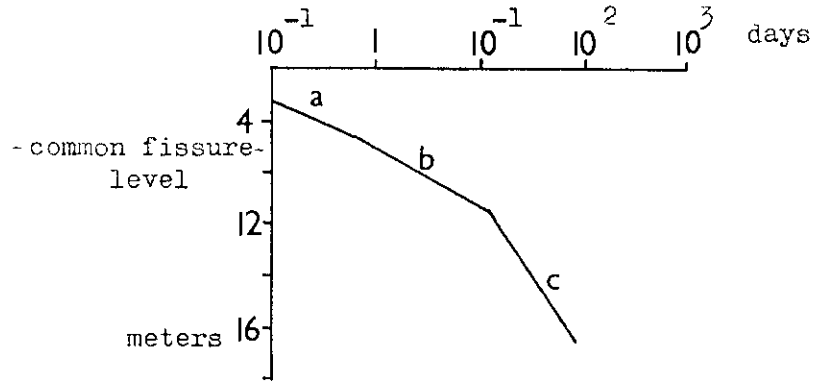


Fig. 5.4 Typical time-drawdown response in a Chalk well.

The early time data appear to show the characteristic relationship between instantaneous release from pressure storage and delayed yield by gravity drainage (Boulot 1963; Streltsova 1972; Neuman 1975). This is followed by a straight line portion (portion b) which is a typical example of a homogeneous, isotropic and infinite in areal extend aquifer (Freeze and Cherry 1980).

The "straight line" response is followed by an abrupt breakway departure (portion c) with the precise timing of the departure depending upon the hydrogeological regime of the borehole (and its cone of depression) under consideration.

If the decrease in aquifer parameters associated with variations of topography is neglected, the main factor which determines the shape of the response curves is the dewatering of major yielding fissures in the immediate vicinity of the pumped well.

(b) Fissure Distribution

Geological and geophysical logs of Chalk boreholes often indicate that saturated flow is largely dependent on a limited number of contributing flow horizons. The accumulation of recent work on the Chalk supports the above indication. Foster (1977) observed from geophysical logs that in East Anglia Chalk, discrete high permeability horizons are concentrated above -20m OD. Price et al (1977) have demonstrated by using water injection tests in cored boreholes in Hampshire, that except from a discrete number of flow horizons, the in situ conductivity of the Chalk is very low. Headworth (1978) from the analysis of geophysical logs for a confined aquifer in the same area, showed that a number of distinct flow levels could be identified. Connorton and Reed (1978) presented convincing evidence for this in the chalk aquifer of Berkshire.

It is now believed that most of the Chalk's discrete high-permeability horizons can be related to recent and historic zones of water table fluctuation (Foster et al 1974). Fig. 5.5 shows a histogram of the occurrence of major yielding fissures, with depth, constructed from the results of geophysical logging investigations (Robinson, V. personal communication 1982).

The overall picture obtained shows that fissures appear to be grouped in the upper part of each borehole from test water level down to a certain depth generally regardless of stratigraphic subdivision but with certain exceptions.

(c) Vertical variation of hydrogeologic parameters

The non-linear decline of the number of fissures per depth can be directly connected with the decline of hydrogeological parameters of some boreholes at increasingly lower rest water levels. Fig. 5.6 represents the variation of storativity and transmissivity with defining rest water level for an observation borehole in the Lambourn Wellfield (Connorton and Reed 1978). Similar results have been obtained by Foster and Milton (1974).

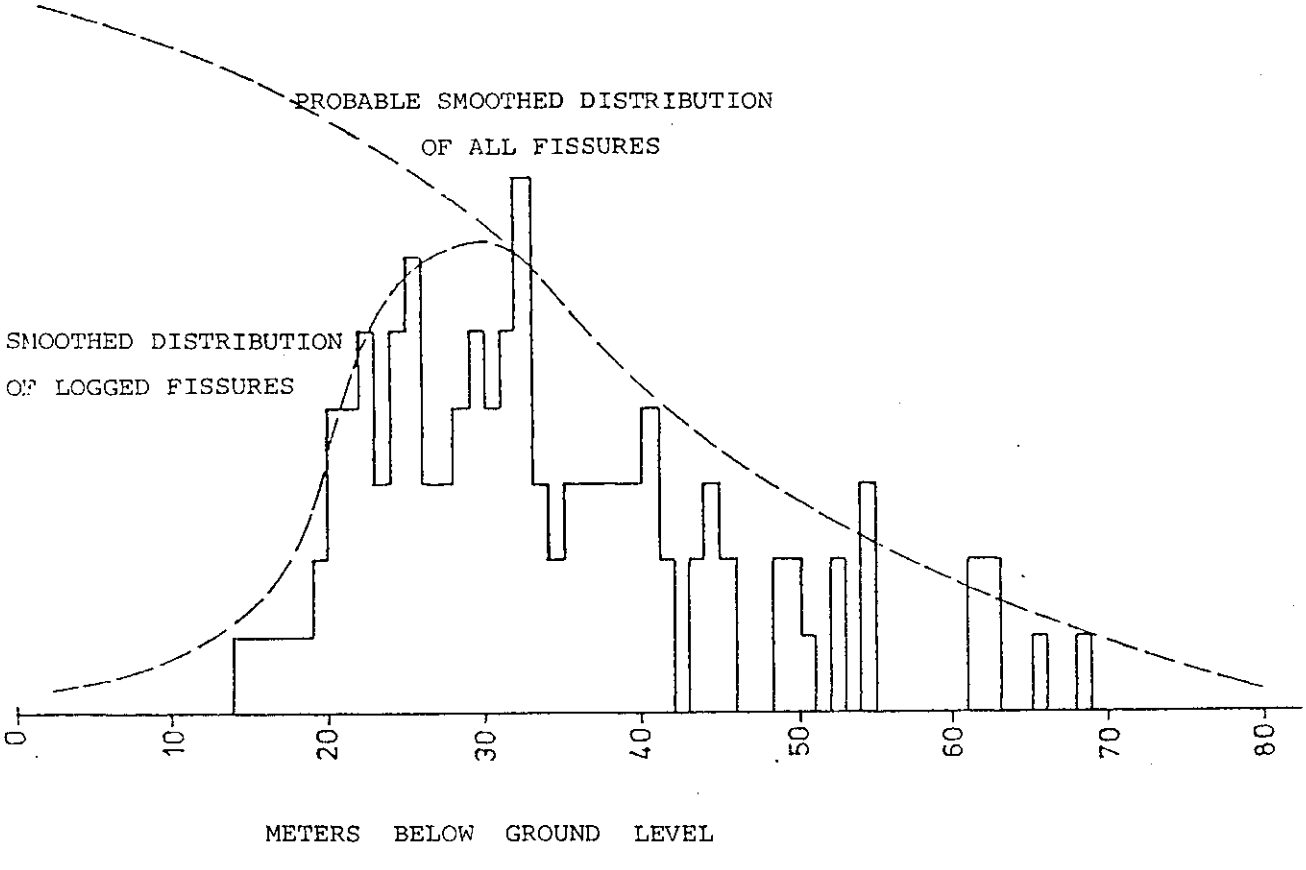


Fig. 5.5 Histogram of the occurrence of major yielding fissures constructed from the results of geophysical logging. The presence of the casing prevented results to be obtained from all the boreholes for depths less than 30m and this is shown by the two smoothed distribution curves

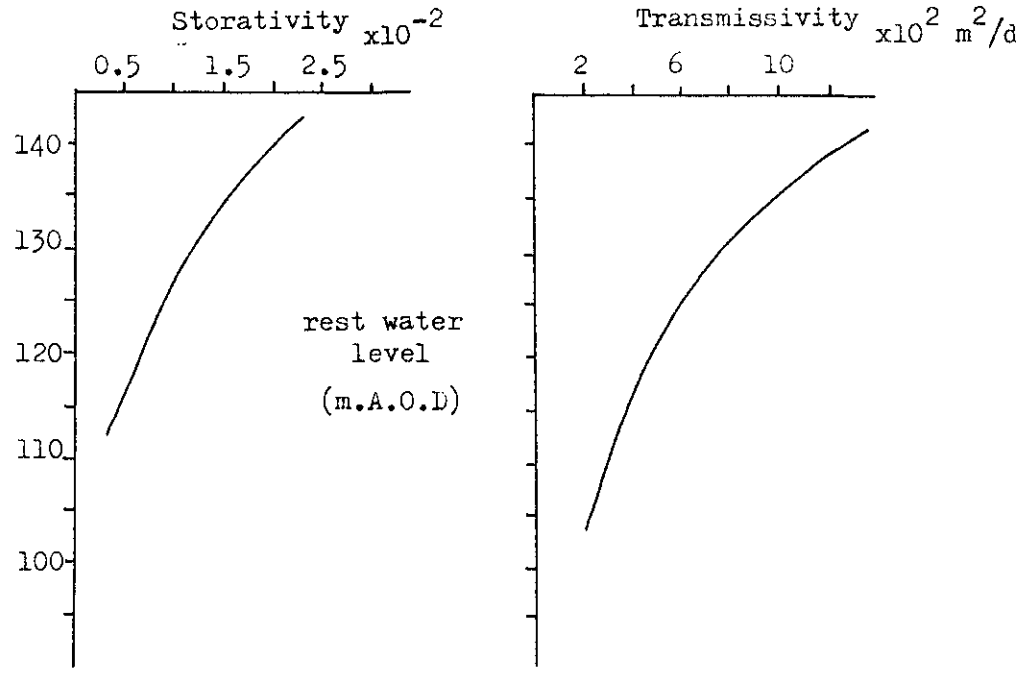


Fig. 5.6 Storativity and transmissivity against rest water level

From the above one can deduce that in fissure flow aquifers, it is not sufficient to know the overall transmissivity T; the three dimensional distribution of permeability which it represents, is also required.

The level and thickness of main permeability development is more important than the overall saturated thickness, since it directly relates to the heads that can be utilized in groundwater abstraction and therefore the behaviour of individual boreholes (Foster and Milton 1974).

This relationship between aquifer transmissivity, radial position and water table level can be summarized by Equation (5.1) (Rushton and Chann 1977):

$$T = m.K(r,m) \qquad (5.1)$$

where T Transmissivity
r radial distance from the well
m saturated aquifer thickness
K hydraulic conductivity

The above equation shows that transmissivity is a nonlinear function of (decreasing) hydraulic conductivity and a linear function of (decreasing) saturated aquifer thickness.

Thus, the understanding of the fissure patterns in the area of a well is of great importance because the saturated permeability will be a function of the configuration of the physical discontinuities of the Chalk mass with respect to the external or applied head.

5.4 FLOW MECHANISM THROUGH THE CHALK

Detailed analysis of data suggests that the Chalk aquifer possesses two major and distinct physical components each with highly contrasting permeability and porosity; one of these components, the integranular pore space, is almost fully saturated with static water unless in the zone where evapotranspiration is active. The other one, the fissure space, is of varying levels of saturation and is responsible for water transmission and free draining storage.

For the case of infiltration it is now believed that this mechanism involves piston displacement of water through the fissure network via a discontinuous air phase. In addition a slow seepage from the mass of the Chalk into the fissures is operative, occurring where a pressure differential is created between ground water in the fissure channel and in the surrounding Chalk.

Brooks and Corey (1966) have made a detailed experimental study of the flow characteristics of both consolidated and unconsolidated porous media. Applying their results for the case of the Chalk, the following infiltration mechanism is suggested (Reeves 1979).

First of all there is a making up of any pore water deficit induced by evapotranspiration, followed by making up of any microfissure flow threshold deficit induced either by evapotranspiration or gravity drainage. Only when these two stages are completed does the saturation of increasingly large fissures start until the vertical unsaturated hydraulic conductivity is sufficient to match the rate of inflow.

Detailed study of the movement of pollutants in the ground and especially of the thermonuclear tritium (Barker and Foster 1981), suggests that over most of the Chalk 80-90% of the infiltration rates do not exceed 1mm/d although for some cases the flow rates through macrofissures can be of the order of 1m/d (Smith et al 1970). In the saturated zone, the movement of the groundwater is mainly controlled by the intercommunicating fissure system and joints, the later being most commonly associated with bedding.

Fig. 5.7 describes the processes which operate to produce the variability of the Chalk aquifer (Robinson V., personal communication 1982). The two main parameters controlling the development of the hydraulic conductivity of the Chalk are: (a) the solution potential of the meteoric water when it reaches the water table, (b) the flux of groundwater which passes through any particular unit area. According to this model, an assumption is made that meteoric water on reaching the water table moves in a laminar fashion down gradient with increasing velocity towards the perennial streams, where there is a large flux of water with a high solution potential passing through al relatively narrow zone which is not deeply buried.

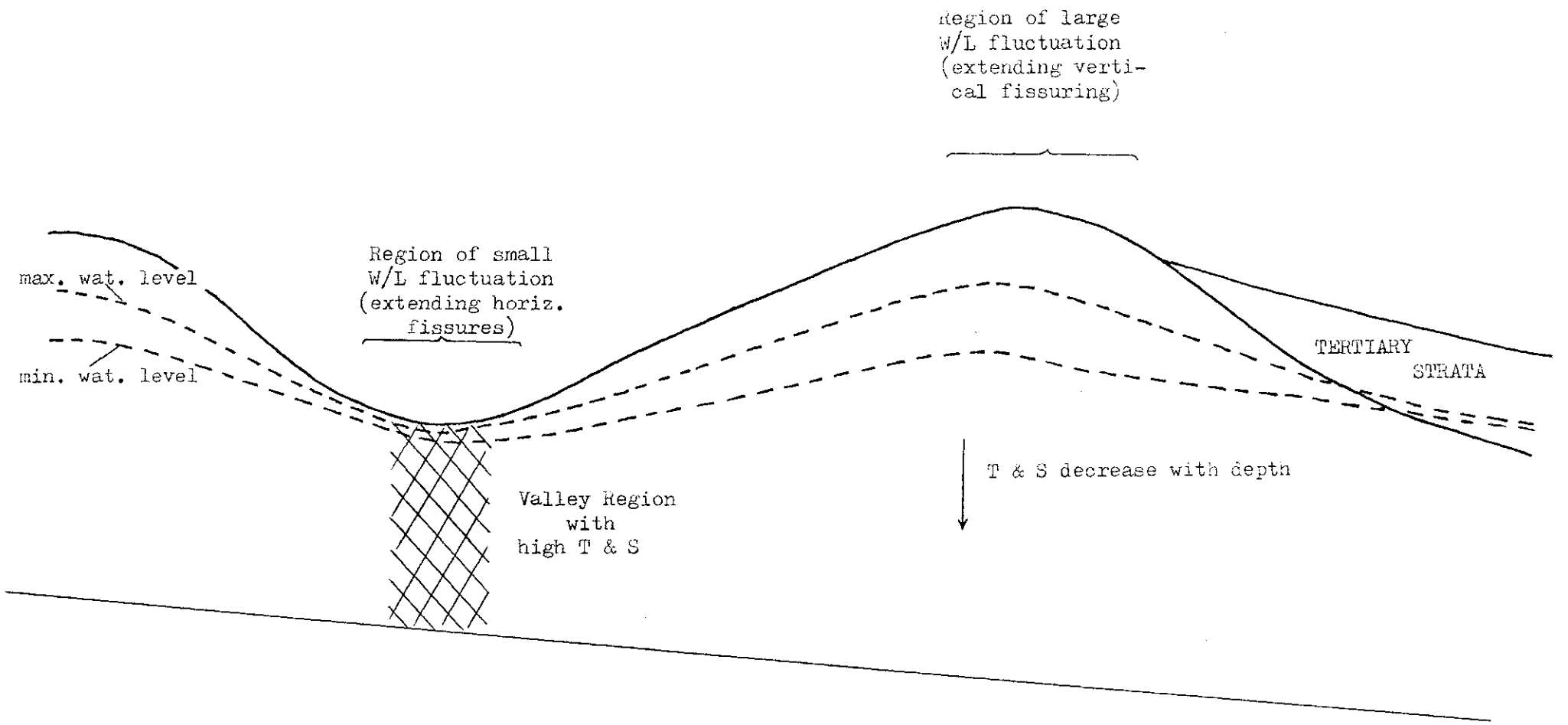


Fig. 5.7 Diagram of aquifer model



Plate 8 Well bedded Upper Chalk with vertical and horizontal fissures in a fresh face of Caistor St. Edmund Quarry, Norwich

From the extensive recent literature a picture of the fissure geometry of the Chalk can be constructed, and is shown in Fig. 5.8.

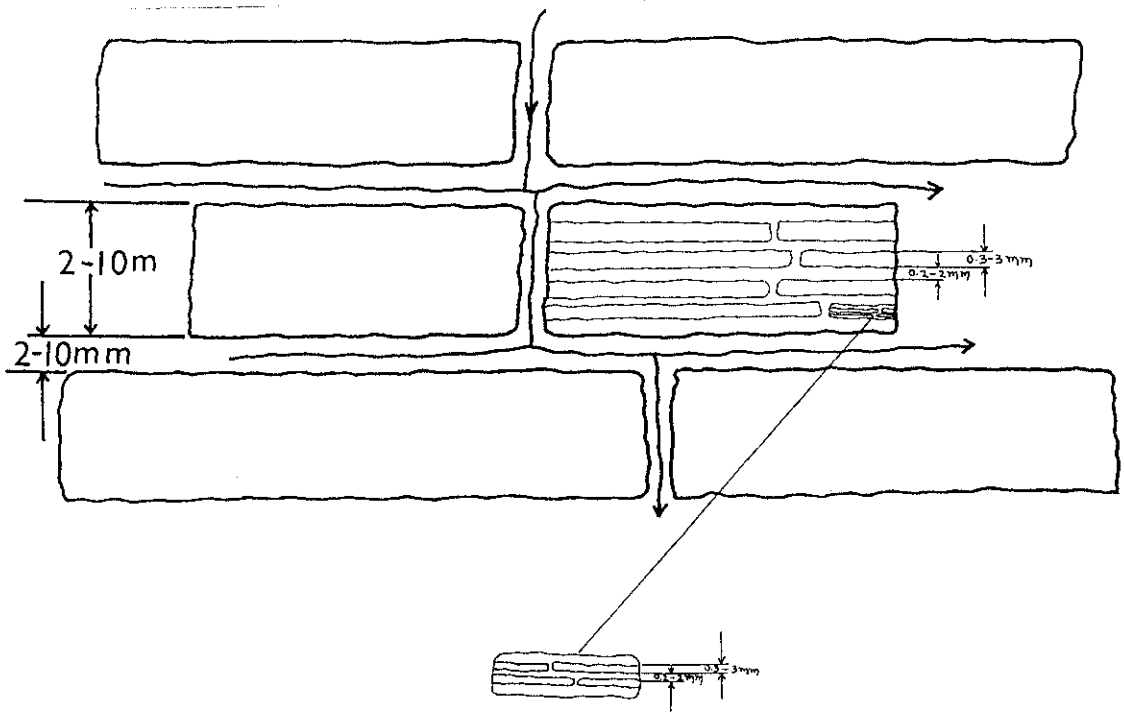


Fig. 5.8 Fissure geometry of the Chalk

In the saturated zone, where flow is essentially horizontal certain lateral fissures tend to become enlarged. On the other hand in the unsaturated zone enlargement of vertical fissures occurs.

As it has already been stated above, in the zone of water table fluctuation both horizontal and vertical enlarged fissures are present providing a zone of advanced permeability.

From the above model of the Chalk aquifer, it is evident that at every point in the aquifer there is one direction in which the permeability is greater than in any other. In other words the Chalk aquifer is characterized by a high degree of anisotropy.

Verslugs (1915) was the first to explain anisotropic permeability by modelling conductors as arbitrarily oriented bundles of tubes. Many authors (Ferrandon 1948; Sheidegger 1954; Childs 1957; Snow 1965) have derived the tensor form of Darcy's law and proved that the coefficient of permeability is a second rank tensor. As a result of this, the velocity is parallel to the gradient only along the eigenvectors (principal axes) of the tensor.

In the hydrodynamic research of the Chalk aquifer, it should be useful to study two different fissure networks, resulting in two types of aquifers with nearly different regimes. In the first type, there is a regular and homogeneous fissuration consisting of independent fissures and joints, with no hydraulic connection between them, so that we would expect a different piezometric level at a certain level between two aquiferous fissures.

In the second type, there is an irregular and heterogeneous fissuration with very many orientations so that there is a possibility of hydraulic continuity and hence of a proper aquifer.

Somewhere between these two principal cases, we could locate the Chalk aquifer. Even if it were possible to overcome the enormous mathematical difficulties involved in solving the fluid mechanics equations for a fissured system, there has first of all to be determined the configuration of this system: this is not possible.

It would be easier to follow the trend which is characteristic of the mechanics of continuous media generally, namely, the introduction of mean characteristics of the media and flow (porosity, permeability, pressure, velocity etc.). From this, the basic concepts of homogeneity and isotropy appear strictly related to the choice of an appropriate volume and a corresponding scale of representation. The larger the scale at which the phenomena are examined, the more the detailed peculiarities

disappear and the more the configuration becomes homogeneous and isotropic. Such a criterion leads to the adoption of the so called scale of homogeneity which has been fruitfully applied in several practical situations (Louis 1968). In the present thesis, the hydraulic properties of the Chalk are going to be examined by using the discrete model approach.

5.5 THE FUNDAMENTAL EQUATIONS FOR FISSURE FLOW

The importance of the investigation of flow phenomena in fissures is great since these are the phenomena which determine the groundwater movement through the Chalk aquifer. In the following, the physics of flow through fissures are going to be described, starting from the well known Navier Stokes equations.

The motion of a fluid is geometrically described if the position of every material point of the fluid is known at every instant. Three conditions determine such motion: continuity, the rheological equation of state, and the third Newton's law of motion.

These physical conditions are expressed mathematically as a system of differential equations together with an additional set of initial or boundary conditions. The best known of these equations is that of Navier and Stokes which are applicable to incompressible viscous fluids (Lamb 1932, p.577; Muskat 1937, p.126). The Navier and Stokes equation for the case of laminar stationary flow in arbitrarily inclined fissure has the form:

$$g.\mathrm{grad}(z + p/\gamma) = \nu \nabla^2 \vec{u} \qquad (5.2)$$

where:

- p static pressure
- z vertical coordinate
- γ specific weight of water
- $\vec{u}$ velocity
- ν kinematic viscosity

By substituting $\phi = z + p/\gamma$ for the hydraulic potential, the above equation reduces to the following three equations, written in matrix form:

$$\rho \cdot \begin{vmatrix} \frac{\partial \phi}{\partial x_1} \\ \frac{\partial \phi}{\partial x_2} \\ \frac{\partial \phi}{\partial x_3} \end{vmatrix} = \nu \cdot \begin{vmatrix} \frac{\partial u_1}{\partial x_1^2} & \frac{\partial u_1}{\partial x_2^2} & \frac{\partial u_1}{\partial x_3^2} \\ \frac{\partial u_2}{\partial x_1^2} & \frac{\partial u_2}{\partial x_2^2} & \frac{\partial u_2}{\partial x_3^2} \\ \frac{\partial u_3}{\partial x_1^2} & \frac{\partial u_3}{\partial x_2^2} & \frac{\partial u_3}{\partial x_3^2} \end{vmatrix} \qquad (5.3)$$

According to the boundary conditions of Fig. 5.9 u_3, the component of the velocities in the direction of the axis (x_3) perpendicular to the fissure plane must be zero:

$$u_3 = 0 \qquad (5.4)$$

On the other hand x_1, x_2 is the plane of symmetry of the fissure, across which there can be no shear:

$$\frac{\partial u_2}{\partial x_1} = 0 \quad ; \quad \frac{\partial u_1}{\partial x_2} = 0 \qquad (5.5)$$

and because of incompressile continuity

$$\frac{\partial u_2}{\partial x_2} = 0 \quad ; \quad \frac{\partial u_1}{\partial x_1} = 0 \qquad (5.6)$$

Thus the above matrix equation reduces to:

$$\rho \cdot \begin{vmatrix} \frac{\partial \phi}{\partial x_1} \\ \frac{\partial \phi}{\partial x_2} \\ \frac{\partial \phi}{\partial x_3} \end{vmatrix} = \nu \cdot \begin{vmatrix} 0 & 0 & \frac{\partial^2 u_1}{\partial x_3^2} \\ 0 & 0 & \frac{\partial^2 u_2}{\partial x_3^2} \\ 0 & 0 & 0 \end{vmatrix} \qquad (5.7)$$

Hydraulic potential is seen to be constant along lines normal to the flow, while the gradient in the flow direction is proportional to the rate of change of shear, or the velocity gradient, as one moves normal to the boundary.

$$g \cdot \frac{\partial \phi}{\partial x_1} = \nu \cdot \frac{\partial^2 u_1}{\partial x_3^2} \quad ; \quad g \cdot \frac{\partial \phi}{\partial x_2} = \nu \cdot \frac{\partial^2 u_2}{\partial x_3^2} \tag{5.8}$$

Since ϕ is independent of x_3:

$$\frac{\partial \phi}{\partial x_1} = -\jmath_1 \quad ; \quad \frac{\partial \phi}{\partial x_2} = -\jmath_2 \tag{5.9}$$

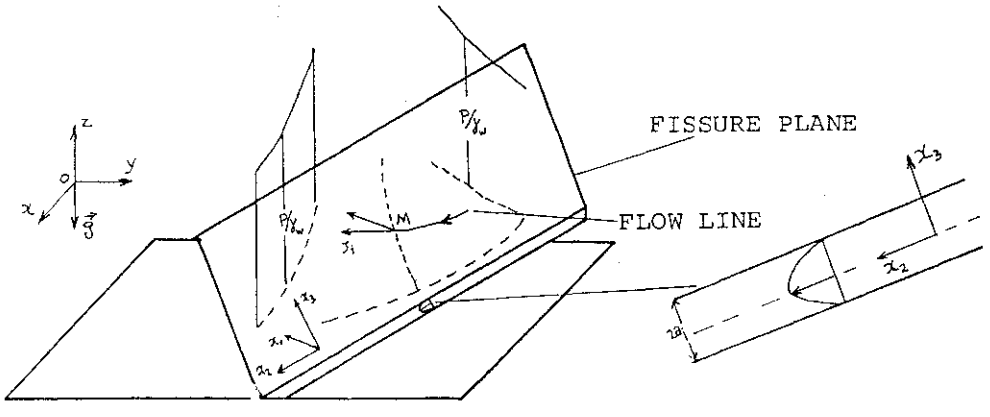


Fig. 5.9 General flow in a fissure plane

Two successive integrations of the above equations, bearing in mind the boundary conditions

$$\frac{\partial u_1}{\partial x_3} = \frac{\partial u_2}{\partial x_3} = 0 \quad \text{for } x_3 = 0 \; ; \quad u_1 = u_2 = 0 \quad \text{for } x_3 = \pm a_i$$

give

$$u_1 = \frac{g \jmath_1}{2\nu}(a_i^2 - x_3^2) \quad ; \quad u_2 = \frac{g \jmath_2}{2\nu}(a_i^2 - x_3^2) \tag{5.10}$$

so the mean velocities are

$$\bar{u}_1 = \frac{g \jmath_1 (2a_i)^2}{12\nu} \qquad \bar{u}_2 = \frac{g \jmath_2 (2a_i)^2}{12\nu}$$

and by substituting the potential gradients

$$\bar{u}_1 = \frac{-g(2a_i)^2}{12\nu} \cdot \frac{\partial \phi}{\partial x_1} \quad ; \quad \bar{u}_2 = \frac{-g(2a_i)^2}{12\nu} \cdot \frac{\partial \phi}{\partial x_2} \tag{5.11}$$

These classic equations for parallel plate flow are given in various forms in many texts (Lamb 1932, p.583; Long 1961, pp.135-137; Borg 1963, p.246; Louis 1969, pp.21-22; Snow 1965, pp.89-92).

Comparison of Eq. (5.11) with the original Darcy's equation shows that for this case the hydraulic conductivity of the opening is given by:

$$\boxed{k = \frac{g(2a_i)^2}{12\nu}} \tag{5.12}$$

5.6 REVIEW OF SOME EXPERIMENTAL RESULTS

The flow laws through joints were experimentally tested by numerous scientists and some important empirical laws for flow in joints have been proposed (Lomize 1951; Louis 1969; Rissler 1977; Sharp and Maini 1972).

Flow in a fissure may be well ordered and smooth (laminar), or it may assume a chaotic fluctuating motion (turbulent) superimposed on the mean flow.

The character of the flow is determined by wall roughness and Reynolds number. It is found that the pressure losses occurring in the flow are given by the following functional relationship:

$$\Delta P = f(4a_i^*, \bar{v}, L, \mu, \rho, k) \tag{5.13}$$

---

* $4a_i$ is the "hydraulic diameter" = $2x(2a_i)$

where:

$2a_i$	opening of the fissure
V	mean velocity
L	travelling distance
p	fluid density
k	wall roughness
μ	dynamic viscosity of the fluid

From dimensional analysis (Lamb 1932) the above equation can be written in terms of four dimensional parameters:

$$\frac{\Delta P}{\rho \bar{V}^2} = f\left(\frac{\rho V 4a_i}{\mu}, \frac{k}{4a_i}, \frac{L}{4a_i}\right) \qquad (5.14)$$

and experiments (Louis 1969) have shown that the parameters may be combined to give

$$\frac{\Delta P}{\frac{1}{2}\rho \bar{V}^2} \cdot \left(\frac{4a_i}{L}\right) = \lambda\left(\frac{\rho V (4a_i)}{\mu}, \frac{k}{4a_i}\right) \qquad (5.15)$$

where λ is the so called dimensionless resistance coefficient. For the case of zero wall roughness this equation can be written:

$$J_i = \lambda \cdot \frac{1}{4a_i} \cdot \frac{V^2}{2g} \qquad (5.16)$$

According to the different functional relations that occur between λ, k/D and Re the laminar-turbulent flow can be divided in three flow domains (Schlichting 1965):

1. hydraulic smooth where $\lambda = f(Re)$
2. transition zone where $\lambda = f(Re, k/D)$
3. completely rough where $\lambda = f(k/D)$

The functions f are called the laws of resistance, for parallel flow.

In nature, often fissures occur which have irregular shaped walls and which are uneven. Unfortunately the general flow laws, which presume parallel flow, cannot be considered for those cases which are beyond a relative roughness limit.

It has been found (Petzny 1964) that for the case of a non-parallel fissure, this can be considered as equivalent to a plane fissure if the resistance coefficient λ is replaced (Fig. 5.10) by the following:

$$\lambda' = \frac{\lambda}{\cos\theta_i} + \sin 2\theta_i \cdot \frac{4a_i}{l_i} \qquad (5.17)$$

Fig. 5.11 (Louis 1969) represents the different laws of resistance which exist for flow in a joint.

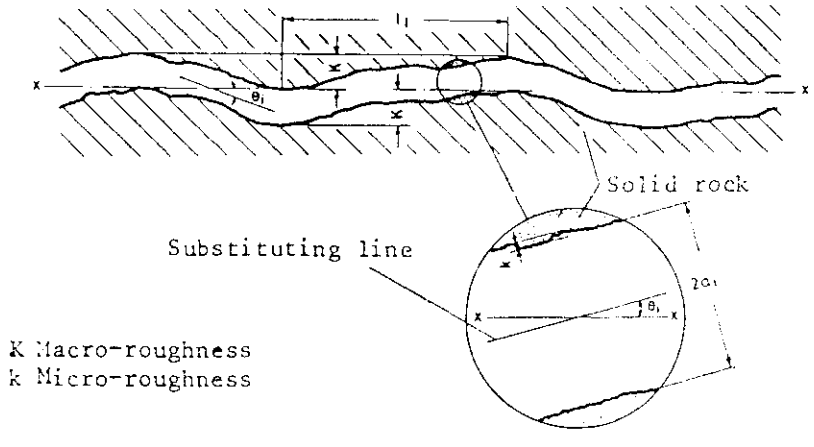


Fig. 5.10 Illustration of a fissure surface

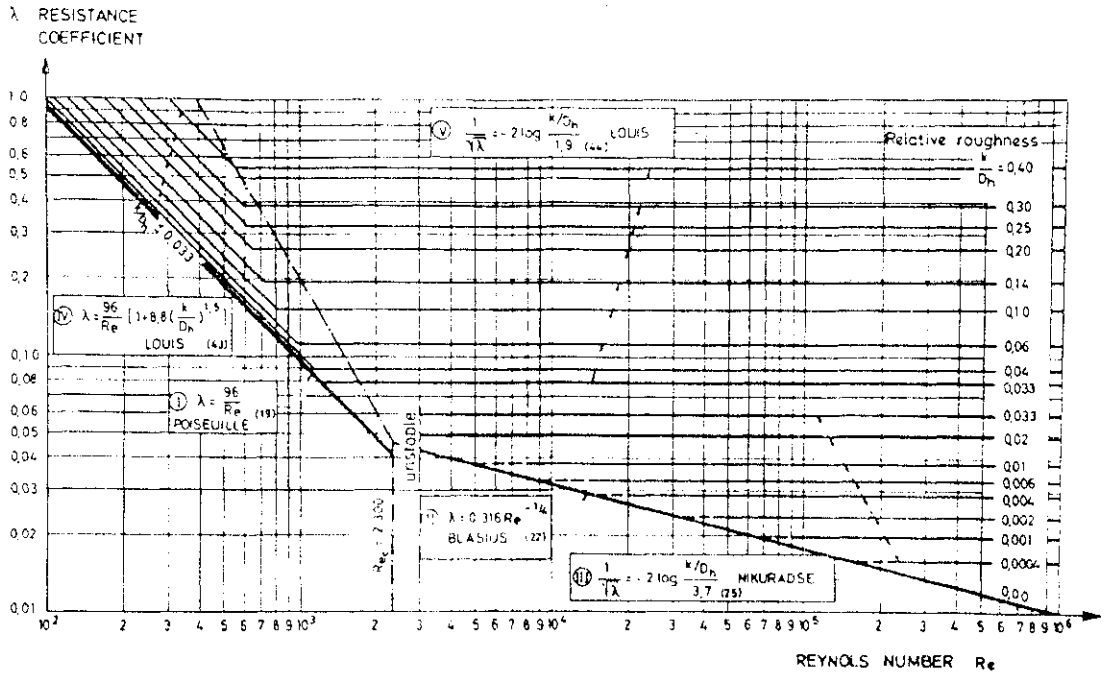


Fig. 5.11 Laws of resistance for flow in a joint (Louis 1969)

5.7 EQUIVALENT HYDRAULIC CONDUCTIVITY OF A SET OF PARALLEL (HORIZONTAL) FISSURES

In order to describe the total hydraulic behaviour of a Chalk mass which is rendered discontinuous by several sets of parallel fissures, it is possible to separate the individual joint systems and to study each system in detail.

The fundamental hydraulic parameters which are required are the hydraulic conductivity of each fissure system, which depends upon the elemental fissure conductivity and the joint spacing.

After describing the hydraulic parameter of each individual fissure system, it is necessary to relate the systems one with another. This relation depends on the position and orientation of each system in space.

Assuming that the hydraulic characteristics of each single fissure are isotropic all over its plane, then the discharge for a single fissure (Fig. 5.12) is given by Eq. (5.18):

$$Q = \frac{2\pi \cdot (2a_i) \cdot k_i}{\log(r_o/r_i)} \cdot (J_1 - J_o) \qquad (5.18)$$

Similarly, from the principle of superposition, for the case where the number of fissures is m one can write for the total discharge:

$$Q = \frac{2\pi \cdot (2a_i) \cdot m \cdot k_i}{\log(r_o/r_i)} \cdot (J_1 - J_o) \qquad (5.19)$$

where the hydraulic gradient $J_1 - J_0$ is assumed to be the same, which is not always true.

Let K_e be the equivalent hydraulic conductivity of the system, then

$$Q = \frac{2\pi \cdot b \cdot k_e}{\log(r_o/r_i)} \cdot (J_1 - J_o) \qquad (5.20)$$

so from Eq. (5.19) and (5.20) K_e can be written as follows:

$$k_e = m \cdot \frac{(2a_i)}{b} \cdot k_i \qquad (5.21)$$

Consider that the Chalk is built up of n blocks each one containing the same number of fissures m (Fig. 5.13).

One can write for the equivalent hydraulic conductivity, K_T , of the system:

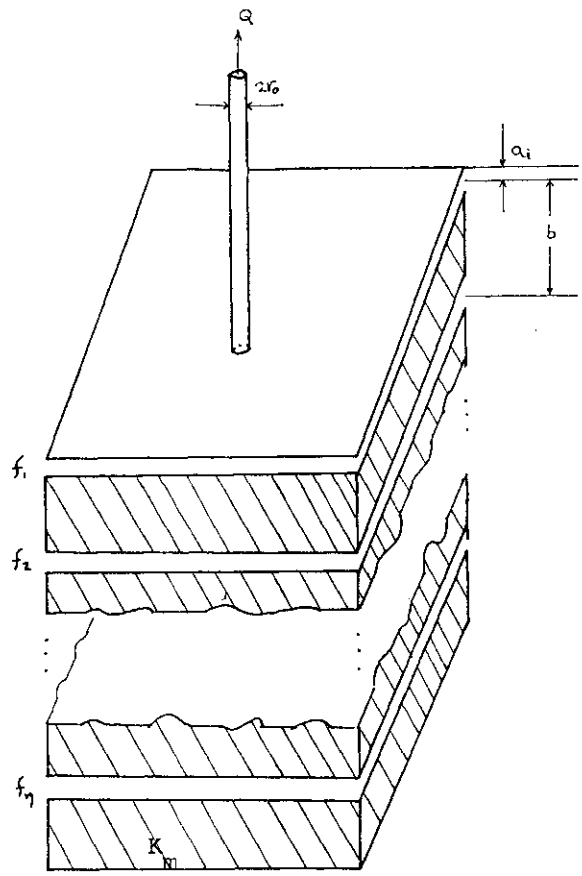


Fig. 5.12 Set of equispaced fissures of the same opening

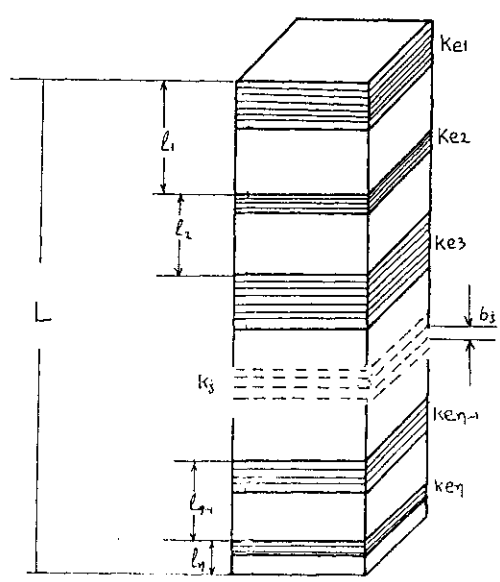


Fig. 5.13 Set of non-equispaced fissures of different openings

$$K_T = \frac{\sum_{j=1}^{n} K_{ej} \cdot \ell_j}{L} \qquad (5.22)$$

where K_{ej} is the equivalent hydraulic conductivity of the Jth block.

By replacing K_{ej} from Eq. (5.21), Eq. (5.22) becomes:

$$K_T = \frac{1}{L} \sum_{j=1}^{n} m \frac{2a_j}{b_j} \cdot K_j \cdot \ell_j \qquad (5.23)$$

and because $K_j = g \cdot (2a_j)^2 / 12\nu$ Eq. (5.23) takes the following form:

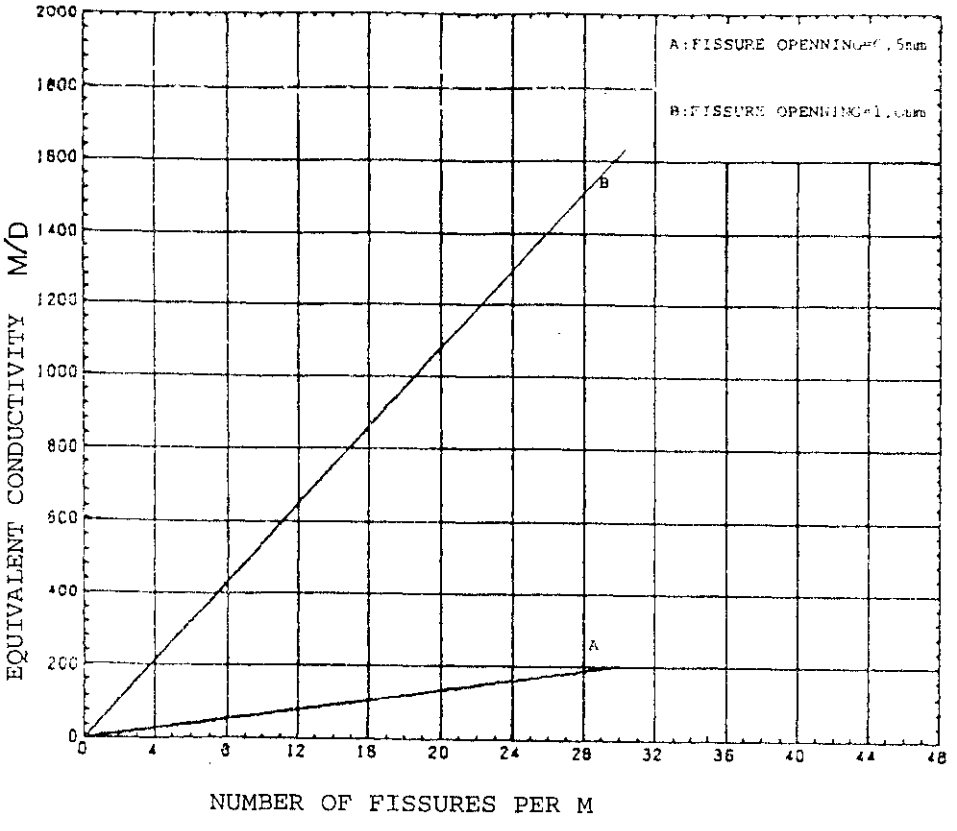
$$\boxed{K_T = \frac{g}{12L\nu} \sum_{j=1}^{n} m \cdot \frac{(2a_j)^3}{b_j} \cdot \ell_j} \qquad (5.24)$$

The above equation can be used to study the hydraulic conductivity of a Chalk aquifer containing specific conduit patterns. For example, if a well is crossing a single block of joints of the same hydraulic characteristics, by substituting in Eq. m = 1 and $b_j = 1_j$, it reduces to the following Equation (L = 1).

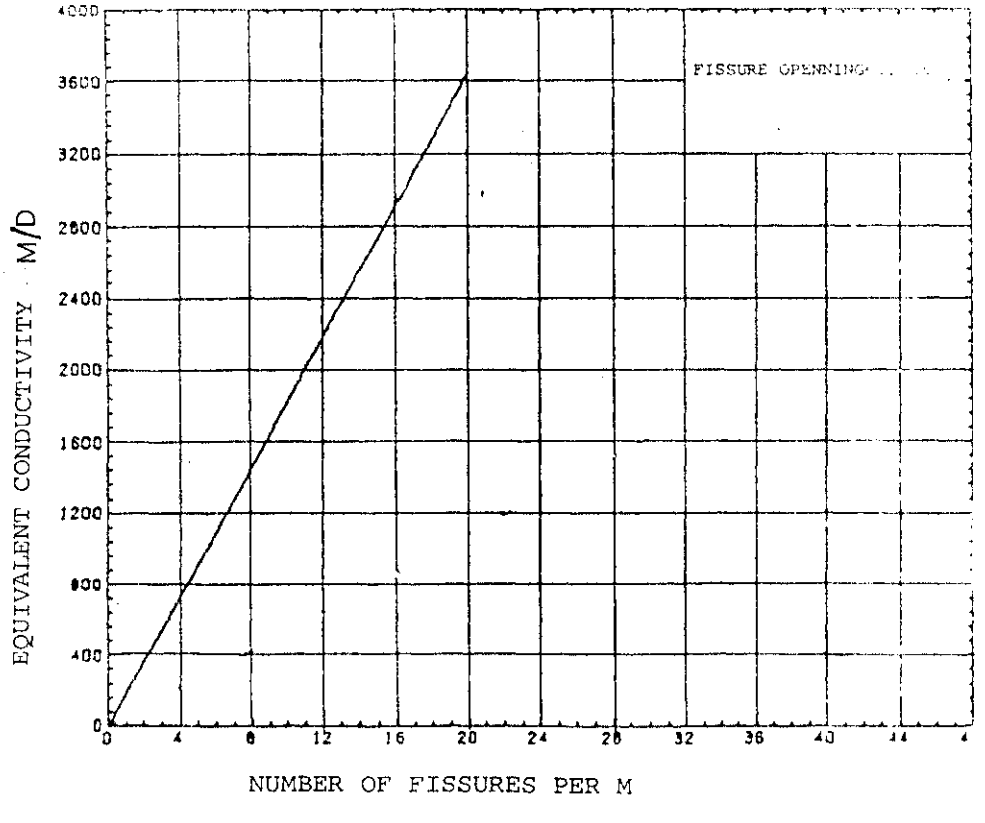
$$K_T = \frac{(2a_i)^3 \cdot \eta \cdot g}{12\nu} \qquad (5.25)$$

which is the one used by Foster and Milton (1974) to study the hydrogeological properties of some Chalk aquifers.

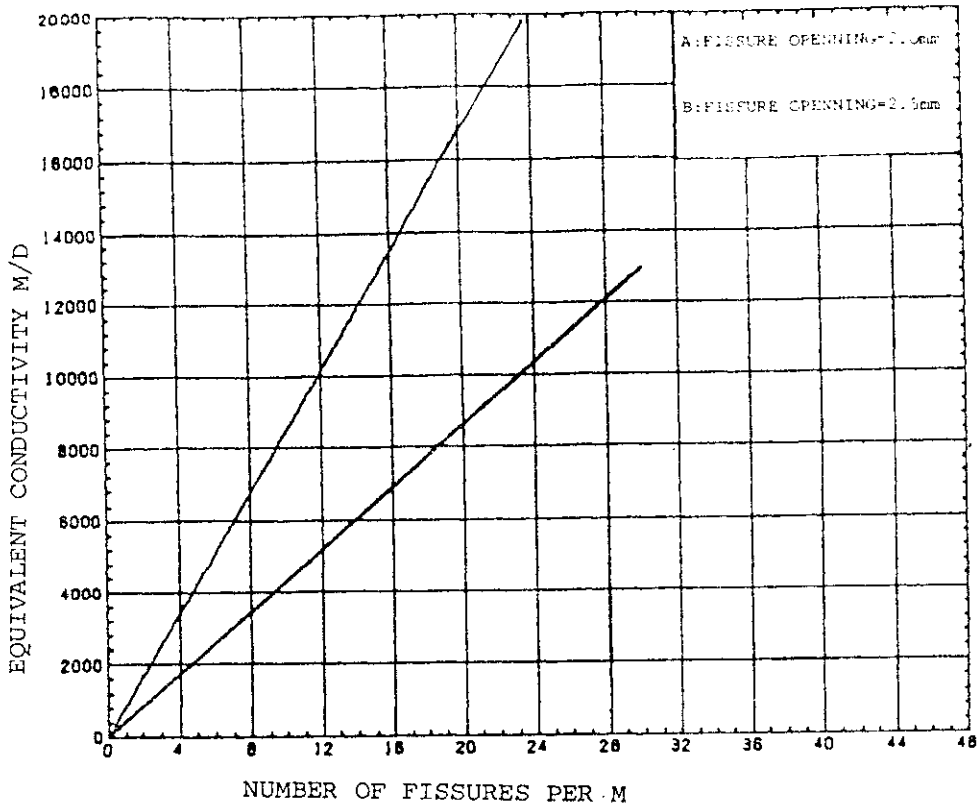
A family of diagrams has been constructed for this specific case, relating the fissure opening and the fissure frequency to the equivalent conductivity.


EQUIVALENT CONDUCTIVITY M/D
NUMBER OF FISSURES PER M
A:FISSURE OPENNING
B:FISSURE OPENNING
A
B

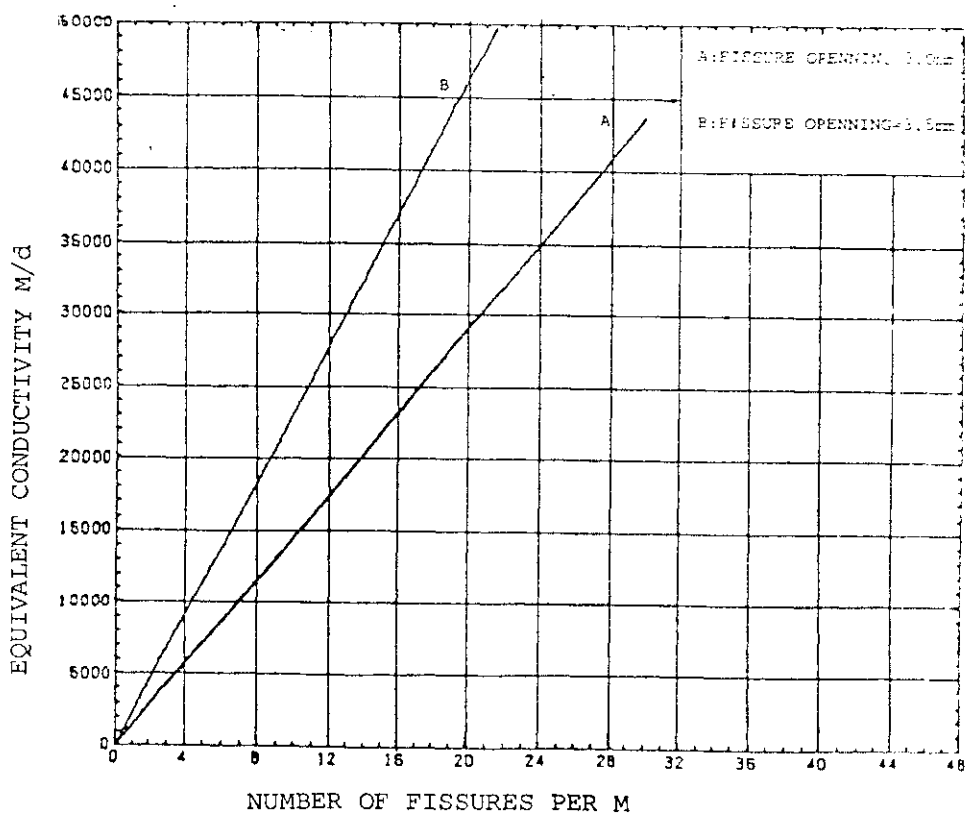
a


EQUIVALENT CONDUCTIVITY M/D
NUMBER OF FISSURES PER M
FISSURE OPENNING

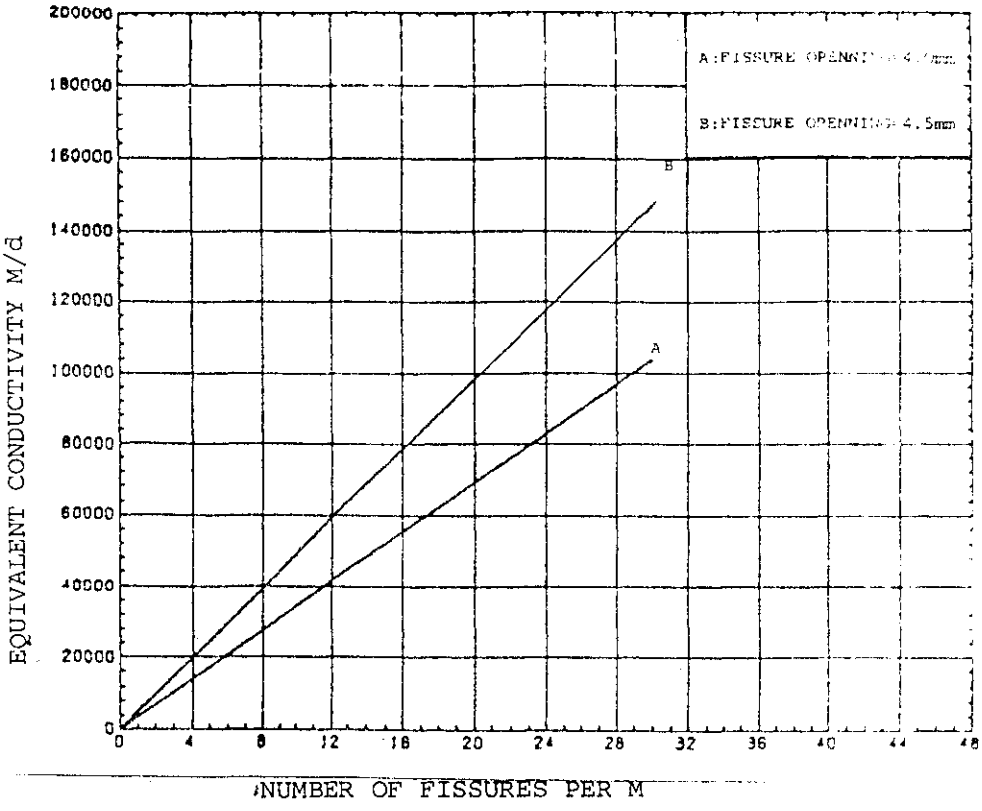
b


EQUIVALENT CONDUCTIVITY M/D
NUMBER OF FISSURES PER M
A:FISSURE OPENNING=
B:FISSURE OPENNING=2.5mm
20000
16000
16000
14000
12000
10000
8000
6000
4000
2000
0
0
4
8
12
16
20
24
28
32
36
40
44
48

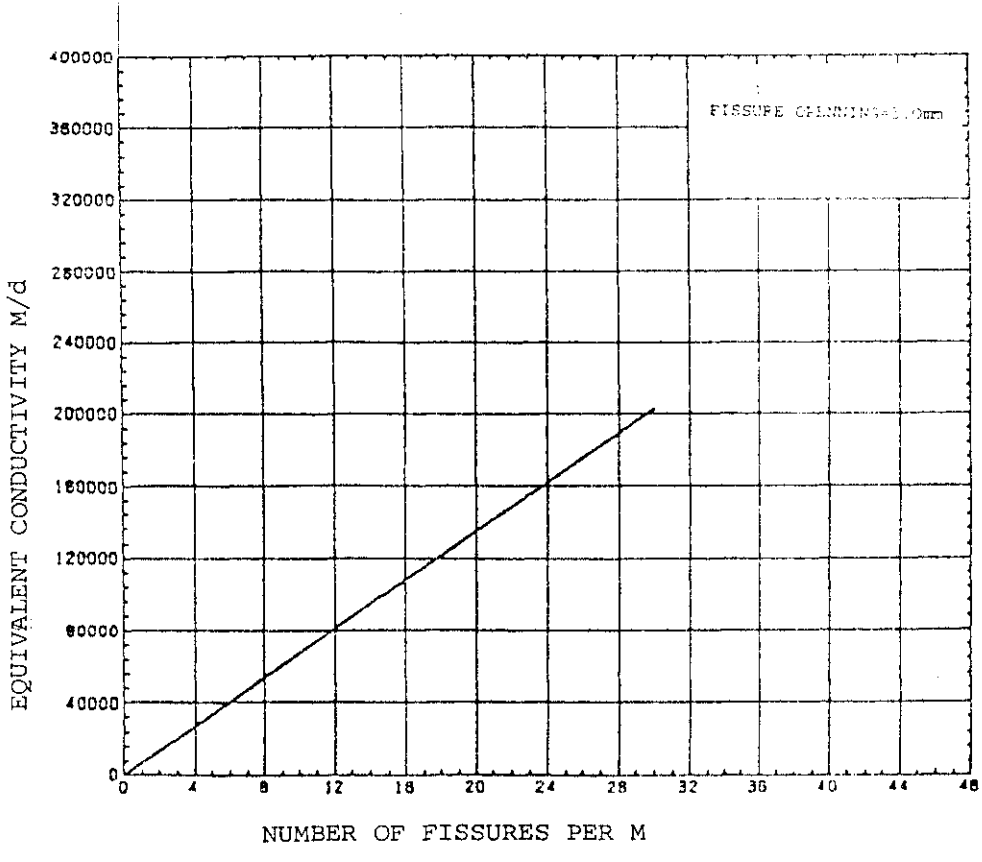
c


EQUIVALENT CONDUCTIVITY M/d
NUMBER OF FISSURES PER M
A:FISSURE OPENNING=
B:FISSURE OPENNING=3.5mm
B
A
45000
40000
35000
30000
25000
20000
15000
10000
5000
0
0
4
8
12
16
20
24
28
32
36
40
44
48

d


EQUIVALENT CONDUCTIVITY M/d
200000
180000
160000
140000
120000
100000
80000
60000
40000
20000
0
0
4
8
12
16
20
24
28
32
36
40
44
48
A:FISSURE OPENNI
B:FISSURE OPENNING=4.5mm
B
A
NUMBER OF FISSURES PER M

e


EQUIVALENT CONDUCTIVITY M/d
400000
360000
320000
280000
240000
200000
160000
120000
80000
40000
0
0
4
8
12
16
20
24
28
32
36
40
44
48
FISSURE OPENNING=
NUMBER OF FISSURES PER M

f

5.8 INCLINED FISSURES

Considering a Chalk block containing three mutually inclined sets of fissure planes, the equivalent hydraulic conductivity of the medium takes the form of a symmetrical second rank tensor with three mutually orthogonal principal directions and three invariants, which depend only on the geometry of the fissure. Only when the fissure sets are mutually orthogonal and of the same geometry may K_T be replaced by the scalar coefficient of permeability, as Darcy found empirically in 1856.

Thus for a general case the hydraulic conductivity tensor is given by Eq. (5.26):

$$K_T = \begin{vmatrix} K_{xx} & K_{xy} & K_{xz} \\ K_{yx} & K_{yy} & K_{yz} \\ K_{zx} & K_{zy} & K_{zz} \end{vmatrix} \tag{5.26}$$

Snow (1965) has found that for an inclined fissure (Fig. 5.15) the above tensor takes the following form:

$$k_e = \frac{2a_i}{b} k_i \begin{vmatrix} 1-n_x n_x & -n_x n_y & -n_x n_z \\ -n_y n_x & 1-n_y n_y & -n_y n_z \\ -n_z n_x & -n_z n_y & 1-n_z n_z \end{vmatrix} \tag{5.27}$$

where $\vec{n} = \{n_x, n_y, n_z\}$ the normalized vector, perpendicular to the fissure plane. For the special case of a horizontal plane $n_x = n_y = 0$ and the above equation takes the form

$$k_e = \frac{2a_i}{b} k_i \begin{vmatrix} 1 & 0 & 0 \\ 0 & 1 & 0 \\ 0 & 0 & 0 \end{vmatrix} \tag{5.28}$$

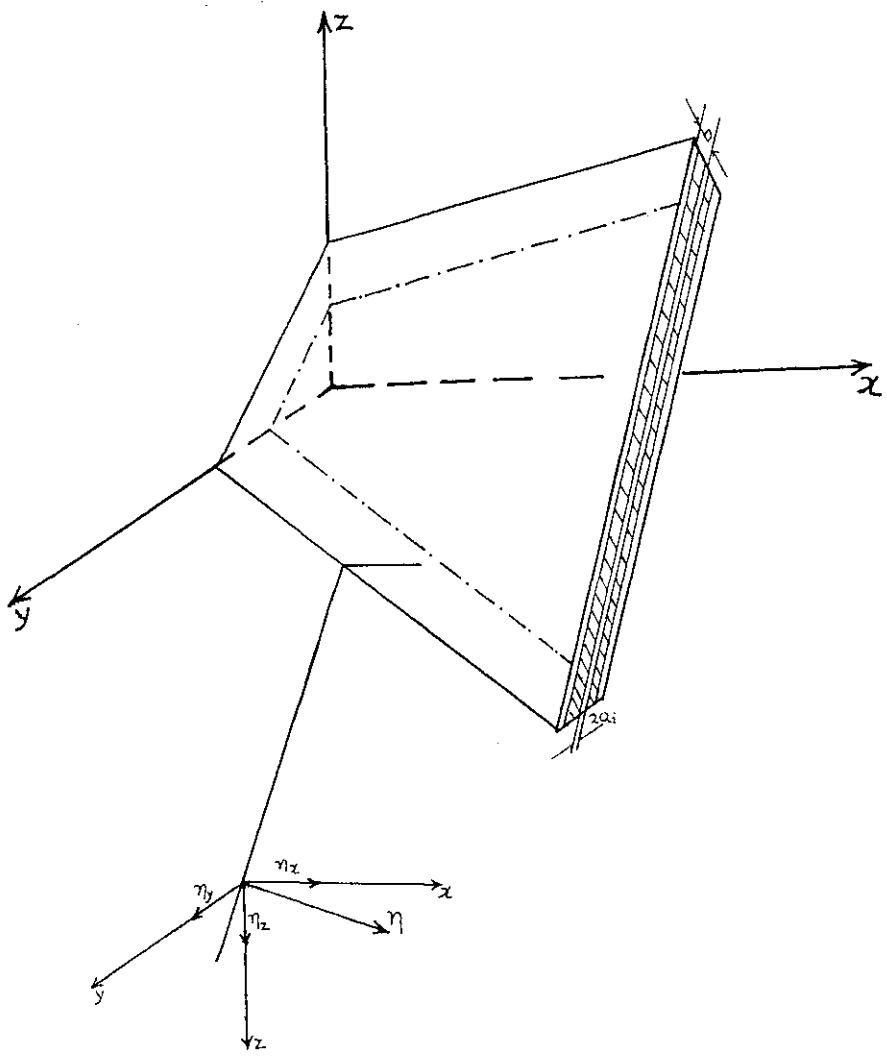


Fig. 5.15 Coordinate reference for a set of inclined fissures

It is known, in general, that the permeability forms a second rank tensor, so Darcy's law can be written as follows:

$$\vec{V} = -(\hat{k}_{ij} \cdot \rho g/\mu) \cdot \vec{J} \qquad (5.29)$$

where the matrix of k_{ij} is assumed to be Hermitian (Szabo 1968; Whitaker 1969; Guin et al 1971; Chas and Cochran 1972).

During the usual laboratory measurements, the so called "dimensional" permeability rather than the components $\hat{k}_{ij}$ of the permeability tensor are measured.

Scheidegger (1954) investigated the problem of relating the directional permeabilities measured by many workers (Johnson et al 1948; Johnson et al 1951) to the components $\hat{k}_{ij}$ of the permeability tensor. He distinguished two mathematically equal possible cases:

(A) The fluid velocity is measured directly and the component of the pressure gradient in the direction of the velocity must be used in Darcy's law.

(B) The component of the fluid velocity taken in the direction of the pressure gradient is measured directly and used in Darcy's law.

In the following, the second case is adopted. Let $\hat{k}_f$ be the directional permeability in the direction of the hydraulic gradient given by the unit vector $\vec{f}$, and let $_f$ be the measure of the velocity component, of the flow, in the direction of $\vec{f}$. One can write (The reader is reminded that the symbol $\hat{k}$ is used to denote permeability).

$$v_f = -\frac{\hat{k}_f \cdot \rho \cdot g}{\mu} \cdot |\vec{J}| \tag{5.30}$$

But

$$v_f = \vec{f} \cdot \vec{v} = -\frac{\rho g}{\mu} \cdot \vec{f} \cdot \hat{k}_{ij} \cdot |\vec{J}| \cdot \vec{f} \tag{5.31}$$

comparing Eqs. (5.30) and (5.31), the following result is obtained:

$$\hat{k}_f = \vec{f} \cdot \hat{k}_{ij} \cdot \vec{f} \tag{5.32}$$

Since $\hat{k}_{ij}$ is Hermitian it can be diagonalized; using the new principal axes, $\hat{k}_f$ can be written:

$$\hat{k}_f = (f_1, f_2, f_3) \cdot \begin{vmatrix} \hat{k}_1 & 0 & 0 \\ 0 & \hat{k}_2 & 0 \\ 0 & 0 & \hat{k}_3 \end{vmatrix} \cdot \begin{vmatrix} f_1 \\ f_2 \\ f_3 \end{vmatrix} \tag{5.33}$$

where f_1, f_2, f_3 are the components of $\vec{f}$ along the principal axes and $\hat{k}_1$, $\hat{k}_2$, $\hat{k}_3$ are the principal permeabilities.

If now α, β, γ are the angles enclosed by $\vec{f}$ and the principal axes the above Equation (5.33) becomes

$$\hat{k}_f = \hat{k}_1 \cos^2\alpha + \hat{k}_2 \cos^2\beta + \hat{k}_3 \cos^2\gamma \tag{5.34}$$

which of course gives our familiar elipsoid if $1/\sqrt{k_f}$ is plotted for various vectors $\vec{f}$. Before proceeding with the evaluation of the equivalent directional hydraulic conductivity for the general case represented in Fig. 5.16, it is worth discussing the problem of superposition of flows.

It has been proved (Snow 1965; Louis 1969) that there can be no mutual interference of flows at the intersection of two or more planar conduits, provided that they are not dislocated, interrupted or otherwise changed at the intersection. It is also known that the driving force acting on the fluid in joints of various orientation may be represented by a gradient field vector not necessarily lying within the conduits but generally crossing the solid, whether or not there be continuous pore-fluid connection within the solid.

In order to determine the equivalent conductivity, (K_{fT}) in the direction of the vector $\vec{f}$, which is assumed to be the direction of the regional gradient (Fig. 5.16).

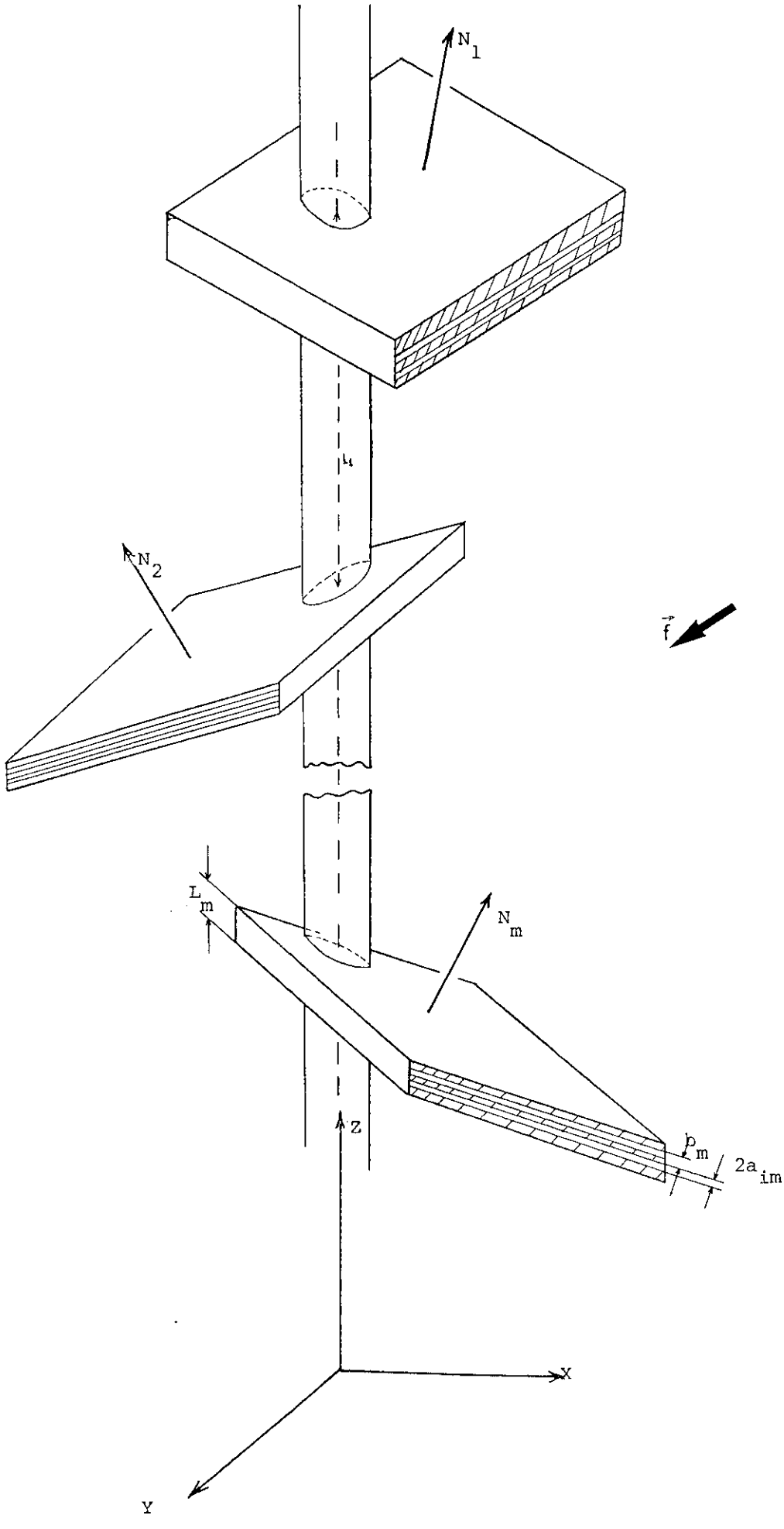


Fig. 5.16 General case of a borehole intersecting sets of inclined fissures of different orientations

Equation (5.34) together with Equations (5.21) and (5.24) have to be applied for each one fissure system. Thus K_{fT} is found to be:

$$K_{fT} = \sum_{\eta=1}^{m} \frac{1}{L_\eta} \cdot \frac{g}{\nu} \cdot \frac{(2a_{i\eta})}{b_\eta} \cdot \left(\hat{k}_{1\eta} \cdot \cos^2 a_\eta + \hat{k}_{2\eta} \cos^2 \beta_\eta + \hat{k}_{3\eta} \cos^2 \gamma_\eta \right) \cdot l_\eta \qquad (5.35)$$

where

$\hat{k}_{1\eta}, \hat{k}_{2n}, \hat{k}_{3n}$ are the principal permeabilities of the n^{th} fissure system.

$a_\eta, \beta_\eta, \gamma_\eta$ are the corresponding angles between $\vec{f}$ and the principal permeability axes.

5.9 AN ALGORITHM FOR THE FAST CALCULATION OF THE EQUIVALENT DIRECTIONAL HYDRAULIC CONDUCTIVITY OF AN INCLINED FISSURE ZONE

The method developed in this paragraph concerns the direct calculation of the equivalent directional hydraulic conductivity of an inclined set of parallel fissures from a knowledge of the orientation of the fissure plane, the direction of the local hydraulic gradient and the number and the geometric characteristics of the fissures.

The purpose of the development of such a method was to provide a fast and efficient computer algorithm which could be used with a portable microcomputer system and given to the hydrogeologist an opportunity to estimate the hydraulic conductivity of certain fissure patterns indicated by geophysical logging methods.

The general structure of the algorithm is shown in Fig. 5.17. In step 1 the operator inputs the fissure opening and the number of fissures per meter. In step 2 the hydraulic conductivity of a single fissure is calculated

using Eq. 5.12. In step 3 the operator inputs the X and Y direction cosines of the normal to the fissure plane where in step 4 the third direction cosine is calculated and the orientation matrix is constructed as in Eq. 5.27.

In order to save computer time and memory instead of using standard "off the shelf" algorithms for the direct calculation of the eigenvalues and eigenvectors of the orientation matrix, it was decided to proceed as follows:

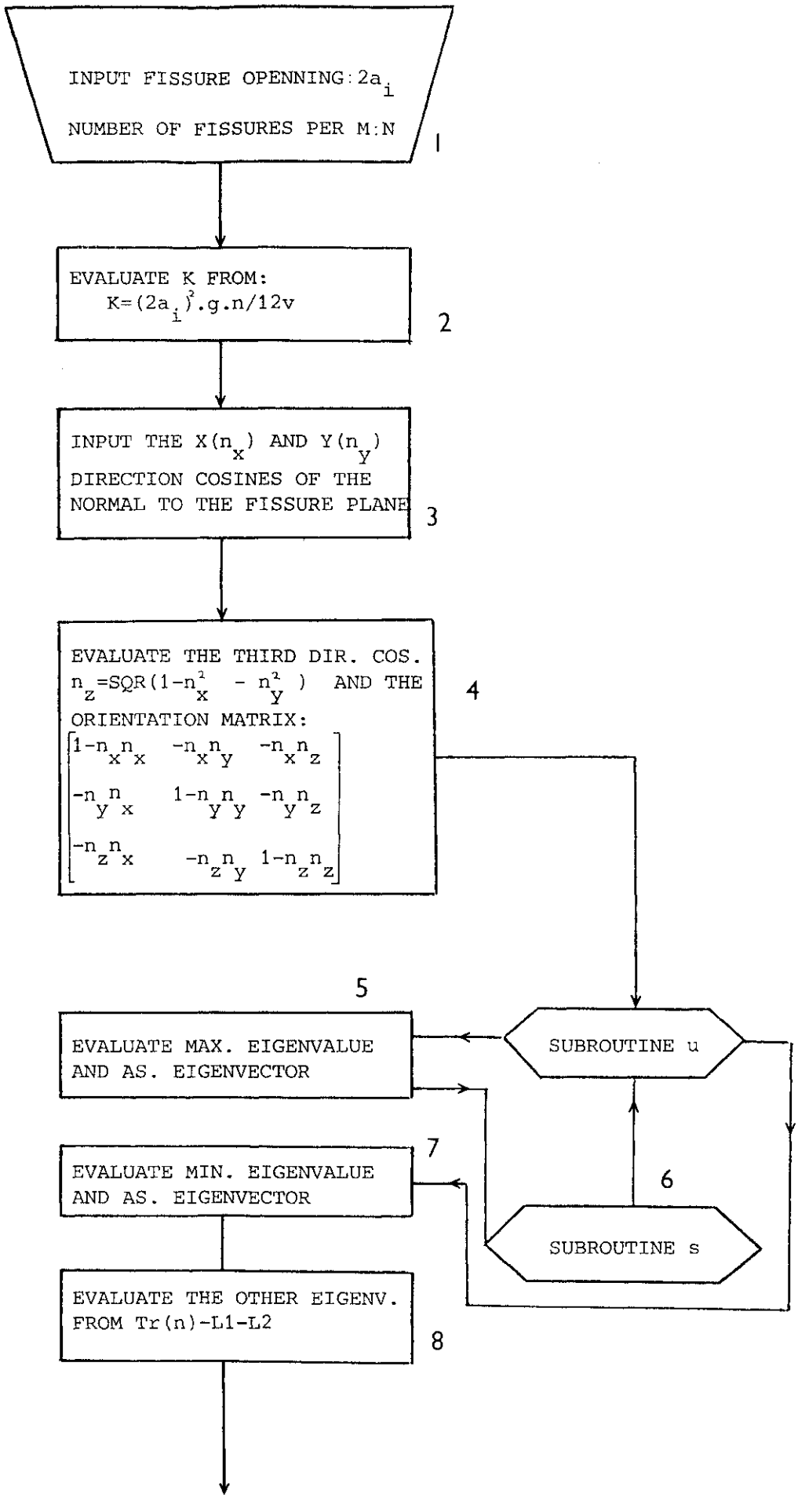
(a) Use the Ruckdeschel (1981) power method for the calculation of the maximum eigenvalue of a matrix.

(b) Use the following two theorems for the theory of linear algebra:

Theorem 1. The maximum eigenvalue of a matrix becomes the minimum eigenvalue of the inverse matrix.

Theorem 2. The sum of the diagonal elements of a matrix (trace) is equal to the sum of its eigenvalues.

In step 4 the subroutine (u) calculates the maximum eigenvalue of the orientation matrix by means of the power method. In step 6 subroutine(s) is used to invert the orientation matrix and control is passed back to subroutine (u) which calculates the minimum eigenvalue. Then control is passed to step 8 where theorem 2 is used for the evaluation of the third eigenvalue. In step 9 the components of the third eigenvector are evaluated by using the orthogonality and normalisation conditions. In step 10 the principal hydraulic conductivities are evaluated and in step 11 the operator inputs the two components of the hydraulic gradient: the third is calculated. In step 12 the components of the hydraulic gradient across the principal directions are calculated and finally in step 13 Eq. 5.32 is used for the calculation of the equivalent directional hydraulic conductivity.


INPUT FISSURE OPENNING: $2a_i$
NUMBER OF FISSURES PER M:N
1
EVALUATE K FROM:
$K=(2a_i)^2.g.n/12v$
2
INPUT THE $X(n_x)$ AND $Y(n_y)$ DIRECTION COSINES OF THE NORMAL TO THE FISSURE PLANE
3
EVALUATE THE THIRD DIR. COS. $n_z=SQR(1-n_x^2-n_y^2)$ AND THE ORIENTATION MATRIX:
$\begin{bmatrix} 1-n_x n_x & -n_x n_y & -n_x n_z \\ -n_y n_x & 1-n_y n_y & -n_y n_z \\ -n_z n_x & -n_z n_y & 1-n_z n_z \end{bmatrix}$
4
5
EVALUATE MAX. EIGENVALUE AND AS. EIGENVECTOR
SUBROUTINE u
7
EVALUATE MIN. EIGENVALUE AND AS. EIGENVECTOR
6
SUBROUTINE s
EVALUATE THE OTHER EIGENV. FROM Tr(n)-L1-L2
8

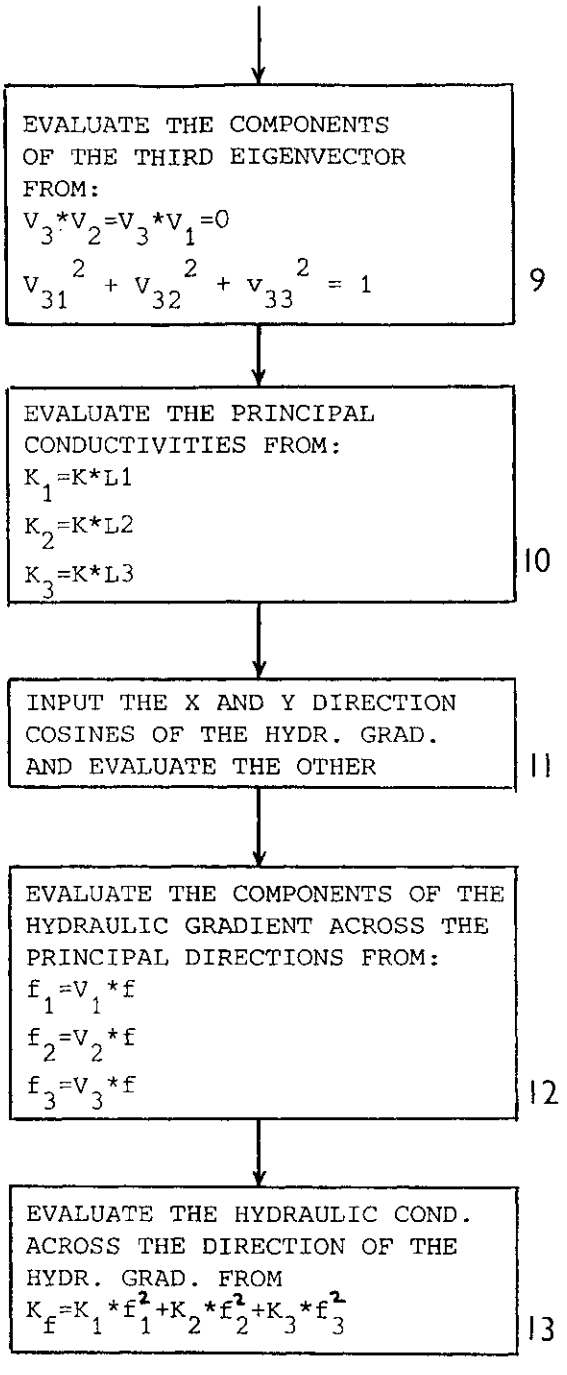


Fig. 5.17 Logic diagram of the algorithm for the calculation of the equivalent hydraulic conductivity of an arbitrary fissure set

A computer program in a basic dialect incorporating the above algorithm has been written and is presented in Appendix A.5.1

5.10 THE DEPENDENCE OF THE HYDRAULIC CONDUCTIVITY OF A FISSURE ZONE UPON THE PRESSURE HEAD DISTRIBUTION NEAR THE WELL

So far, a great deal of emphasis has been placed on the particular case of flow from a set of parallel horizontal or inclined fissures into a well which intersects them.

The purpose of this section is to examine the effect of the pressure drop which occurs within the vicinity of a well on the directional hydraulic conductivity of a fissure zone.

Pressure drop occurs as fluid flows towards the well. In the case of fissure flow the drop is a very much more severe one, probably this behaviour is due to the limited area available for flow of a fluid in a fissure and the acceleration of the fluid as it approaches the cavity.

It is worth considering a hypothetical numerical model to illustrate this point because of its great importance. From the theory of well hydraulics it is known that the discharge of a confined aquifer can be expressed as:

$$Q = \frac{2\pi b k_j}{\ln(r_1/r_0)} \cdot (P_1 - P_0) \qquad (5.36)$$

A similar relation of course holds for a single fissure discharging aquifer. For example, assuming the following conditions (Fig. 5.18):

$b = 2.a_i = 0.1\text{mm}$
$k_j = (2a_i)^2.g/12$
$Q = 1$ lt/min
$P_o = 800$ cm
$r_o = 3$ cm
$r_1 = 6$ cm

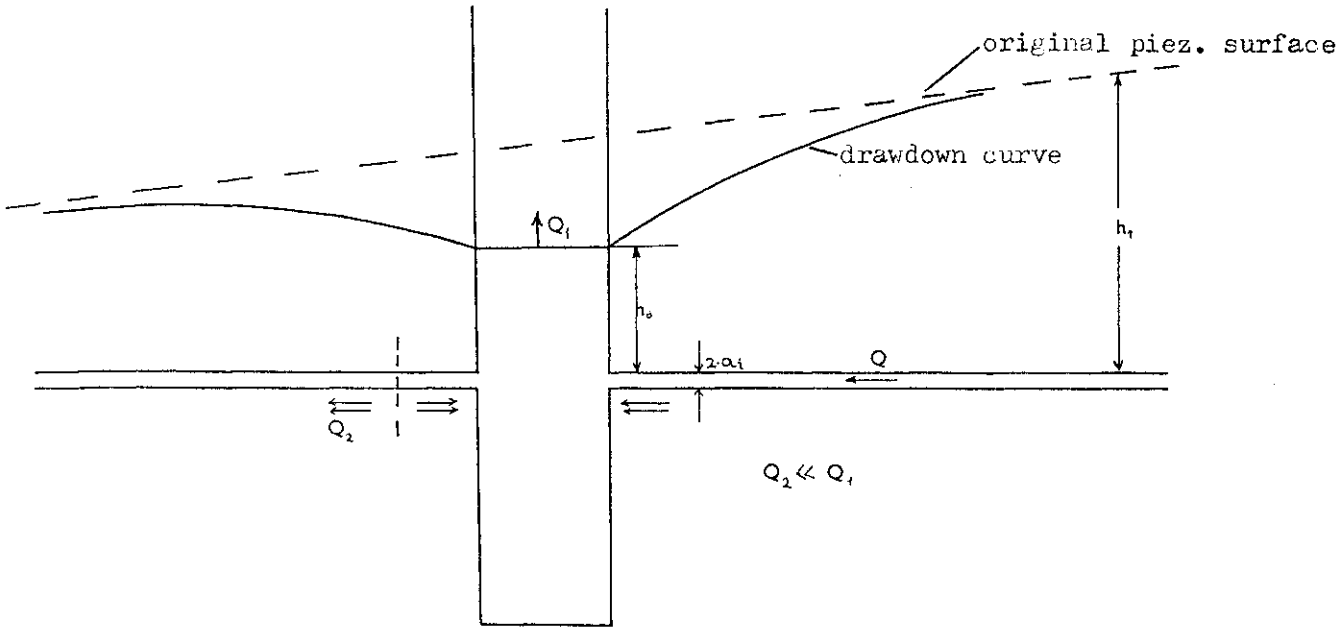


Fig. 5.18 Pumping well intersecting a single fissure

Then by substituting these values in the above expression one can see that for a distance r_1 = 6 cm from the well the pressure P_1 becomes 467 cm; in other words there is a pressure drop of 58.5% in a distance twice the radius from the well.

It is known from the literature that the potential lines in the vicinity of the well are described by Eq. (5.37):

$$\phi = \frac{Q/2a_i}{2\pi k_j} \log \sqrt{x^2+y^2} + J_o x \qquad (5.37)$$

where

Q is the pumping rate

k_j is the permeability of the fissure

J_o is the natural gradient

A computer program was written making use of standard graphic packages already existing in ICCC (Imperial College Computer Centre) and of Eq. (5.37) in order to plot the pressure distribution in three dimensions. Fig. 5.19 shows the drastic drop in pressure occurring in the vicinity of a pumped well.

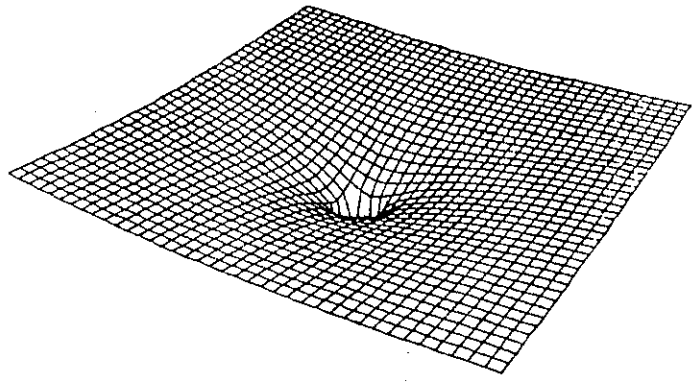


Fig. 5.19 Pressure distribution in the vicinity of a pumped well

In order to study the dependence of the directional equivalent hydraulic conductivity of a fissure zone upon the changes of the direction of the local hydraulic gradient occurring during pumping, the following diagram (Fig. 5.20) was constructed.

The orientation of the fissure zone is described by the directional cosines of its normal vector with reference to the coordinate axes XYZ. In this particular example a fissure zone inclined at 45° to the horizontal is shown.

The algorithm described in the previous section is used to calculate the directional hydraulic conductivity of the fissure zone as the hydraulic gradient changes during pumping. The results obtained (units of hydraulic conductivity) are plotted against the angle between the hydraulic gradient $\vec{f}$ and the normal to the fissure plane N.

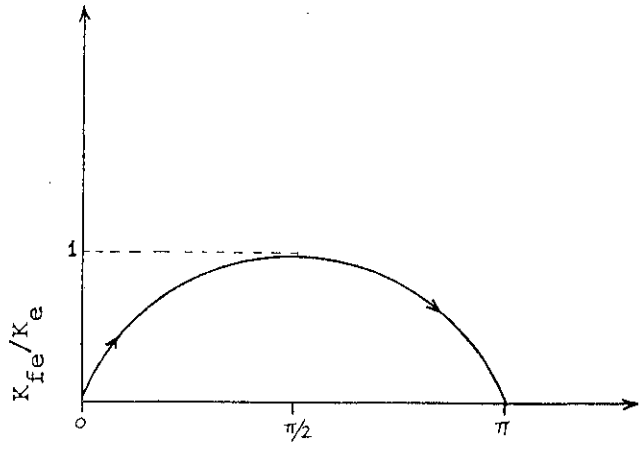


Fig. 5.20 Usual variation of the direction of the local hydraulic gradient during pumping

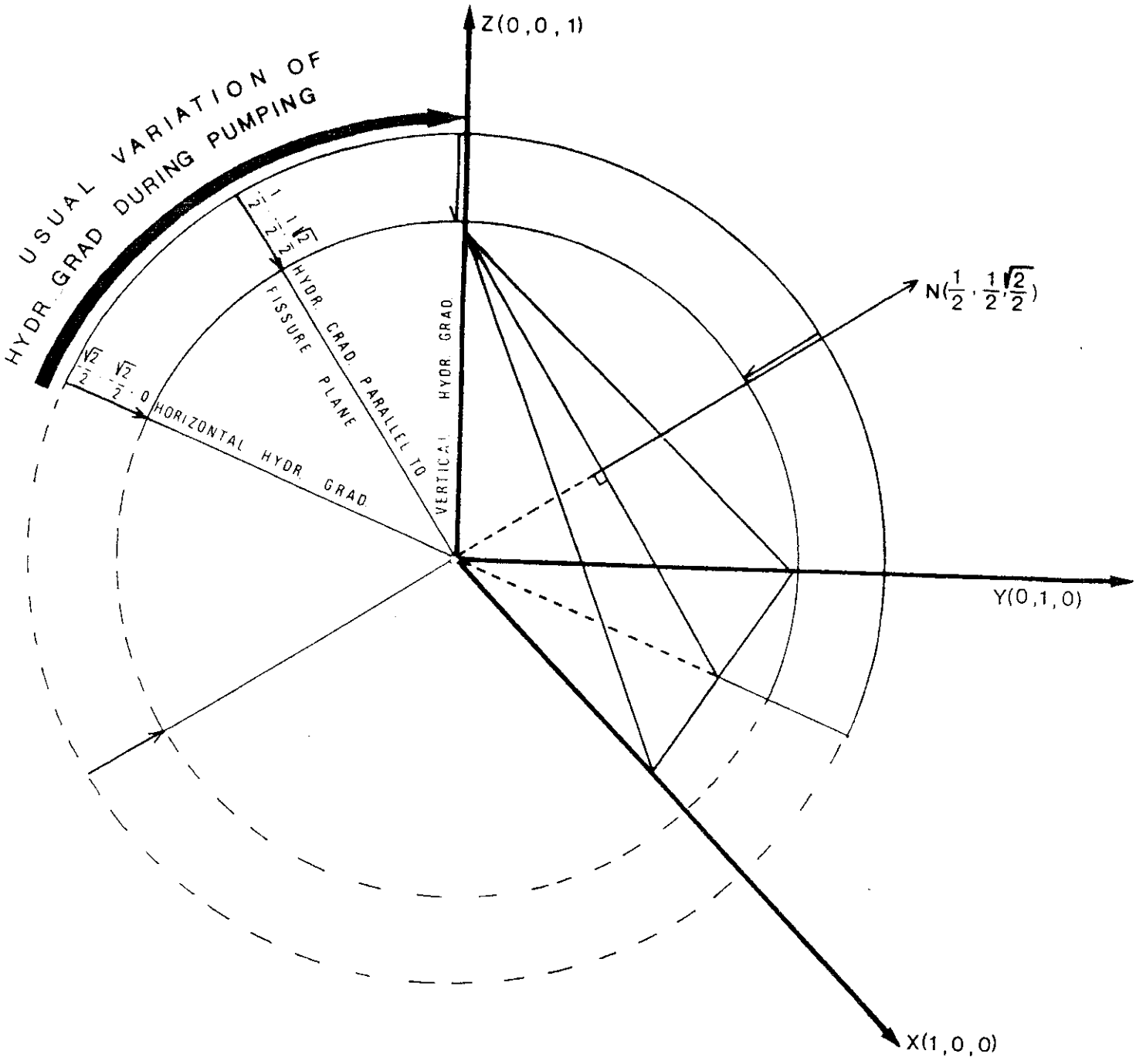


Fig. 5.20 Direction equivalent hydraulic conductivity of a fissure zone K_{fe}, during pumping

From these results (Fig.5.21), one can see that when the angle between $\vec{f}$ and N is zero (the hydraulic gradient is normal to the fissure plane), the directional equivalent hydraulic conductivity, K_{fe}, becomes negligible: by increasing the angle between $\vec{f}$ and N there is an increase in the hydraulic conductivity which takes its maximum value, Ke, when the hydraulic gradient becomes parallel to the fissure plane (where Ke is given by Eq. 5.24). This example shows that the performance of any set of fissure zones is consequently governed largely by what happens to the pressure head near the well.

5.11 THE DEPENDENCE OF THE HYDRAULIC CONDUCTIVITY OF A FISSURE UPON ITS CONTACT AREA

Since the hydraulic characteristics of fissures are mainly governed by aperture size, it is expected that the hydraulic conductivity of a fissure zone will also depend upon the elastic properties of the formation, which describe the deformability of the Chalk with the changes of the stress field occurring during pumping in the vicinity of the well.

Gangi (1975) has derived an analytical expression for the variation of fracture hydraulic conductivity with confining pressure and similar works are presented by Katsuhiko (1975).

The purpose of this section is to investigate the relation between the hydraulic conductivity of a fissure and its contact area, which is expected to increase during pumping. This is because the Chalk is a non-elastic particularly deformable rock as its low modulus of deformation (Table 5.20) shows.

The method that was adopted was to use an electric analogue approach. A 30cm diameter circle of electrical conductive

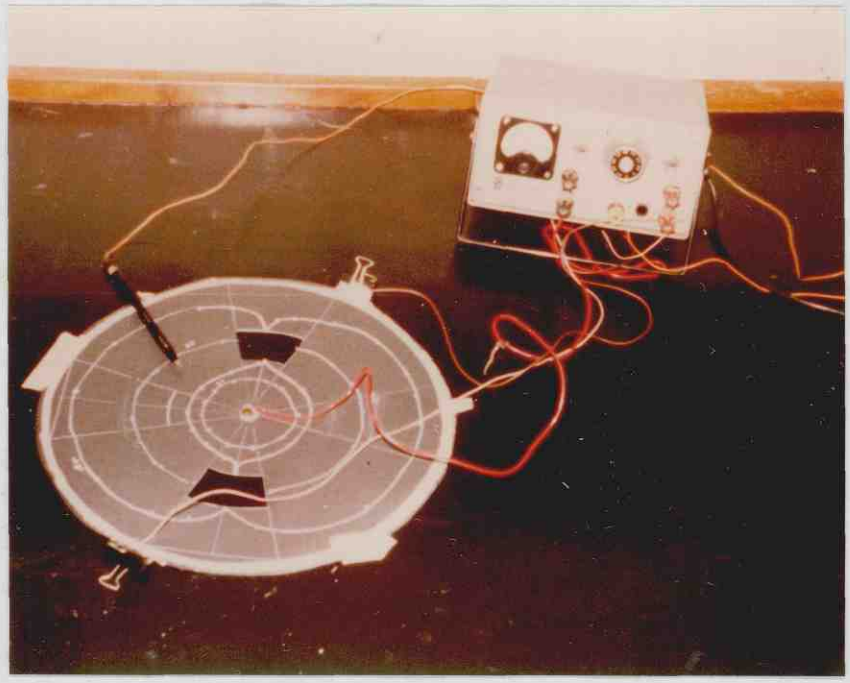


Plate 9 Electric analogue arrangement used to study the effect that the contact area of fissure has upon its discharge

paper was used to represent the fissure. The pumping process was modelled by driving a current from the perimeter of the circle towards its centre which represented the well as shown in Plate 1. The contact area was simulated by cutting circle sectors of increasing area laterally and radially. Next, the potential lines were drawn using a standard Wheatstones bridge and the discharge was calculated as usual. The diagrams obtained, together with the calculated results, are included in Appendix A.5.2.

Strength of the Chalk

	Lower Chalk (Yorkshire)	Middle Chalk (Norfolk)	Upper Chalk (Kent)
Unconfined compressive strength (MN/m^2)*			
maximum	38.2	36.3	6.2
minimum	20.1	22.1	4.8
mean	28.4	27.2	5.5
Saturated unconfined compressive strength (MN/m^2)			
maximum	15.2	17.5	2.2
minimum	9.6	8.9	1.4
mean	13.7	12.3	1.7
Brazilian tensile strength (MN/m^2)			
maximum	3.4	2.8	0.6
minimum	1.0	0.9	0.4
mean	2.6	2.1	0.5
Point load test (MN/m^2)			
maximum	0.9	0.7	—
minimum	0.4	0.2	—
mean	0.7	0.4	—

*Unconfined compressive strength: < 1.25, very weak; 1.25—5, weak; 5—12.5, moderately weak; 12.5—50, moderately strong; 50—100, strong; 100—200, very strong; > 200, extremely strong (in MN/m^2).

Table 5.2 Elastic properties of Chalk

Fig. 5.22 is a graphic representation of the results obtained. From this, one can see that the flow carried by a fissure decreases with increasing contact area but that the decrease is a function of the areal distribution of the contact area; in other words, it depends on the path of fluid flow.

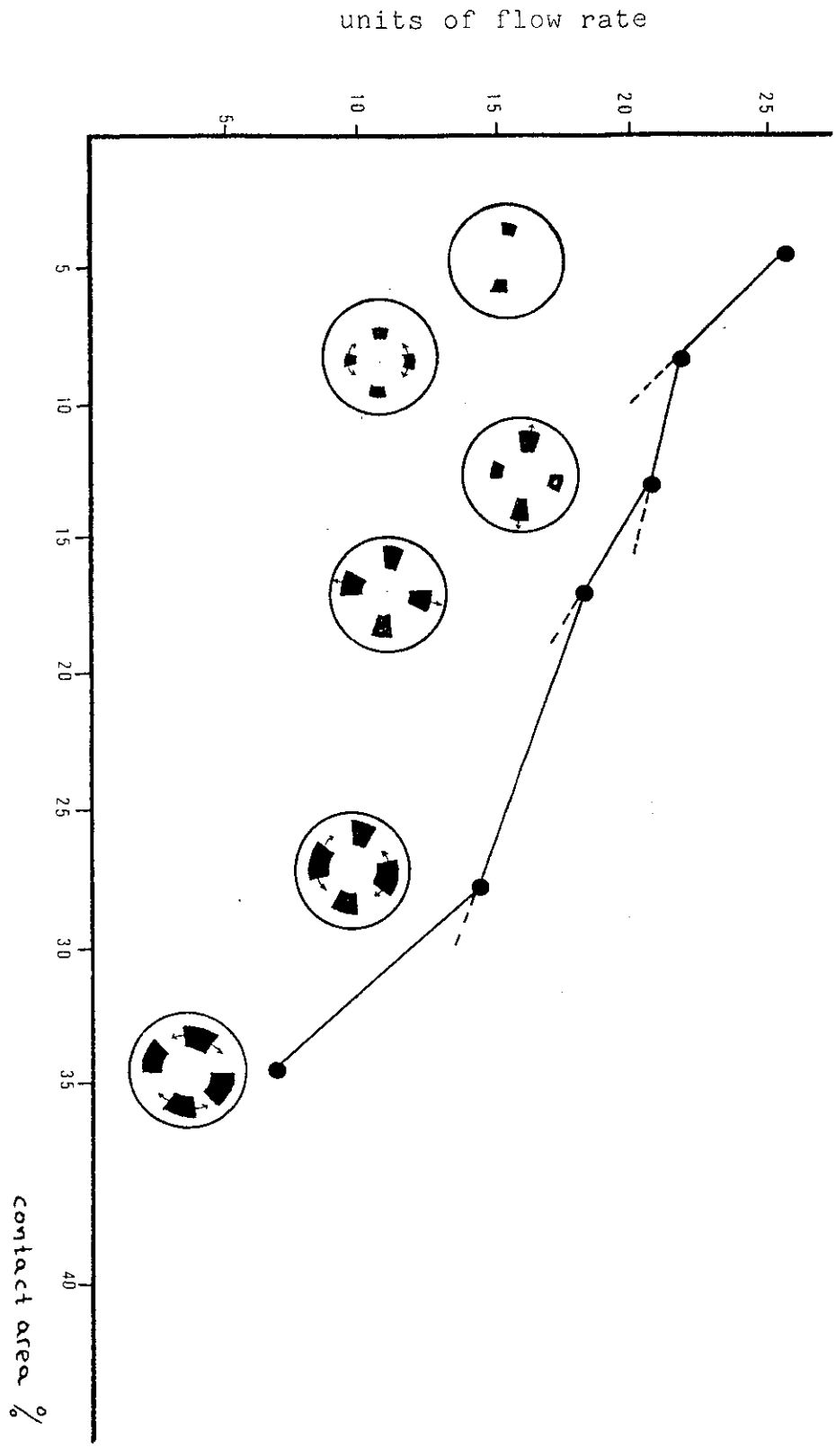


Fig. 5.22 Flow rate as a function of contact area

5.12 FLOW THROUGH A CONDUIT BISECTING A SEMIPERMEABLE MATRIX

Although it has already been mentioned that the groundwater flow through the Chalk cannot be treated in the same manner as that through porous media, because of the irregular occurrence of fissures in the former, which play a large part in the flow characteristics, it nevertheless appears to be reasonable to apply such treatment in the limiting case in which the Chalk as a whole is largely free of fissures, except for a limited number of extended length.

In this case the flow system may be considered as a composite synthesis of a uniform medium representing the Chalk matrix bisected by others of different permeability corresponding to the fissures.

While these fissures are, in principle, flow channels free of any porous medium they may be given conductivities to correspond to their carrying capacity, as has already been determined by classical hydrodynamics.

As these conductivities will be very much higher than that of the Chalk matrix itself, which has a $\hat{k}$ of the order of 1md the flow will be essentially one in which the Chalk's matrix feeds its water into the highly permeable fissures and these bring the fluid directly or by complex interconnection through the joints of the outlet wells.

(a) Mathematical formulation of the problem

The diagrammatic representation of the problem is given in Fig. 5.23.

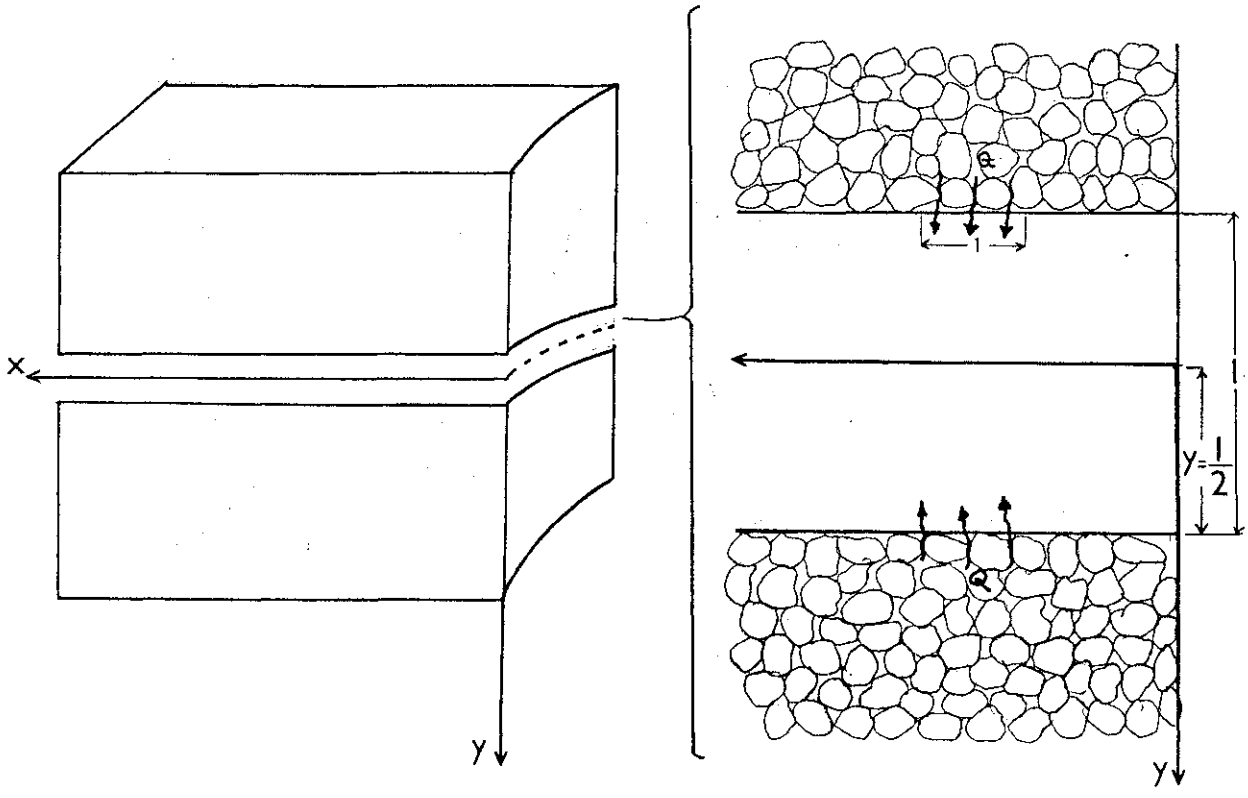


Fig. 5.23 Fissure bisecting a semipermeable matrix

An assumption is made that there is only one fissure in the system, which bisects the otherwise extended and uniform Chalk proper. Because of the very low conductivity of the Chalk's matrix as compared to that of the conduit, the flow into the well directly from the Chalk's matrix may be neglected.

It will be convenient to take the fissure's width as the unit length and both the media representing the fissure and the Chalk to be of infinite extent, the latter also to be of infinite thickness. Because of the obvious symmetry of the system, only one single quadrant of the (x,y) plane needs to be considered.

The analytical formulation of the problem follows from the application of the equation of continuity to Darcy's law, which in the presence of the fissure for the case of steady flow gives:

$$\operatorname{div}(\rho V_1) - Q = 0 \qquad \therefore \qquad \frac{\rho \hat{K}_1 g}{\nu} \Delta P_1 + Q = 0$$

$$V_1 = -\frac{\hat{K}_1 g}{\nu} \operatorname{grad} P_1 \tag{5.38}$$

similarly, in the presence of the pores one can write

$$\frac{\rho \hat{K}_2 g}{\nu} \Delta P_2 + Q = 0 \tag{5.39}$$

so the problem can be described:
locating pressure distributions P_1 and P_2 such that:

$$\frac{\rho \hat{K}_1 g}{\nu} \left(\frac{\partial^2 P_1}{\partial x^2} + \frac{\partial^2 P_1}{\partial y^2} \right) + Q = 0$$

$$\frac{\rho \hat{K}_2 g}{\nu} \left(\frac{\partial^2 P_2}{\partial x^2} + \frac{\partial^2 P_2}{\partial y^2} \right) - Q = 0 \tag{5.40}$$

gives, with the boundary conditions stated:

$$y \leq 1/2 \begin{cases} x = 0 \;, \; \dfrac{\partial P_1}{\partial x} = 1 & ; \text{ assuming unit flux} \\ y = 0 \;, \; \dfrac{\partial P_1}{\partial y} = 0 & \\ y = \dfrac{1}{2} \;, \; \dfrac{\partial P_1}{\partial y} \cdot x = \hat{K}_2 \dfrac{\partial P_2}{\partial y} \cdot x = Q & ; \text{ for unit width} \end{cases} \tag{5.41}$$

$$y > 1/2 \begin{cases} x = 0, \; \dfrac{\partial P_2}{\partial x} = 0 \end{cases} \tag{5.42}$$

(b) Solution of the differential equations

It is well known that the general problem of the steady state flow of fluids through porous media (Sheidegger 1960), may be reduced to the solution of Laplace's equation

with the appropriate boundary conditions. Since this equation is so well known in other branches of physics, the general method of solution and in some cases even the explicit solutions themselves for a number of flow problems of practical interest, may be taken over from those that have already been derived for other purposes in other branches of physics (Carslow and Jaeger 1980), by simply translating them into their proper hydrodynamic equivalent.

In our case reference is made to a similar homogeneous set of equations describing an analogous electrical problem, published by Muskat (1935). In order to use Muskat's analytical results the system of equations (5.41) and (5.42) has to be reduced to an homogeneous one, modifying of course the boundary conditions.

In order to simplify the calculations:

$$\frac{Q \cdot \nu}{\rho \hat{K}_1 g} = Q_1$$
$$\frac{Q \cdot \nu}{\rho \hat{K}_2 g} = Q_2 \qquad (5.43)$$

then obviously system (5.40) is equivalent to the following homogeneous one:

$$\frac{\partial^2 \Phi_1}{\partial x^2} + \frac{\partial^2 \Phi_1}{\partial y^2} = 0$$
$$\frac{\partial^2 \Phi_2}{\partial x^2} + \frac{\partial^2 \Phi_2}{\partial y^2} = 0 \qquad (5.44)$$

where $$\Phi_1 = P_1 + Q_1 x^2$$
$$\Phi_2 = P_2 - Q_2 x^2 \qquad (5.45)$$

with the boundary conditions

$$y \leq 1/2 \begin{cases} x=0, \ \frac{\partial \Phi_1}{\partial x} = 1 \\ y=0, \ \frac{\partial \Phi_1}{\partial y} = 0 \\ y=1/2, \ \frac{\partial \Phi_1}{\partial y} \cdot x = \hat{k}_2 \frac{\partial \Phi_2}{\partial y} \cdot x = Q \end{cases} \qquad (5.46)$$

$$y > 1/2 \begin{cases} x=0, \ \frac{\partial \Phi_2}{\partial x} = 0 \end{cases} \qquad (5.47)$$

the solution of the later homogeneous system is already known from Muskat's electric analogue problem (Muskat 1935)

$$P_1(x,y) = \left(\tfrac{1}{2}-y\right)\cdot \log\left\{x^2+(1/2-y)^2\right\} + y\log(x^2+y^2) - 1 + 2x\tan^{-1}\frac{x}{2x^2+2y^2-y} +$$

$$+2\int_0^\infty \frac{da}{a}\left[\left(\frac{1}{\delta}-\frac{1}{2}\right)e^{-a} + \frac{2\cos xa}{a\Delta}\cdot\left\{e^{-ya}(\delta\cosh a/2+\sinh a/2-\delta)+\right.\right. \quad (5.48)$$

$$\left.\left. + (1-\delta)e^{-a/2+ya}\cdot\sinh a/2\right\}\right] - Q_1x^2$$

$$P_2(x,y) = 2\int_0^\infty \frac{da}{a}\left[\operatorname{cth} y e^{-a} - 2e^{-(y-\frac{1}{2})a}\cdot\frac{\cosh\gamma\cdot\sinh a/2\cdot\cos xa}{a\cdot\sinh(a/2+\gamma)}\right] + Q_2x^2 \quad (5.49)$$

where

$$\delta = k_2/k_1 = \tanh\gamma, \text{ assuming that } \delta < 1$$
$$\Delta = -2(\delta\cosh a/2 + \sinh a/2) \quad (5.50)$$

for computation purposes the integretation constants are removed by subtracting the value of p at x = 0. Thus by looking across the line y = ½ one takes:

$$P_1(x,1/2) - P_1(0,1/2) = \frac{1}{2}\log(1+4x^2) + 2x\tan^{-1}(1/2x) +$$

$$+4\int_0^\infty \frac{\sin^2 xa/2\,da}{a^2\sinh(a/2+\gamma)}\cdot\left\{e^{-a/2}\cdot\sinh(a/2+\gamma)+\sinh(a/2-\gamma)\right\} - Q_1x^2$$

$$\pi x + 2\int_0^\infty \frac{\sin^2 xa\cdot\sinh(a-\gamma)}{a^2\sinh(a+\gamma)}\,da - Q_1x^2 \quad (5.51)$$

for large values of x the above result can be written

$$P = \frac{2\cosh\gamma}{\gamma}\cdot\left[1.2704+\log\gamma x\right] - Q_1x^2 \quad (5.52)$$

from which

$$\frac{\partial P}{\partial x} = \frac{2\cosh\gamma}{\gamma x} - 2Q_1x - x^2\frac{\partial Q_1}{\partial x} \quad (5.53)$$

multiplying both sides with $\hat{k}_1 . p . g/v$

$$\frac{\hat{K}_1 \rho g}{\nu} \cdot \frac{\partial P}{\partial x} = \frac{\hat{k}_1 \rho g}{\nu} \cdot \left(\frac{2\cosh\gamma}{\gamma x} - 2Q_1 x - x^2 \frac{\partial Q_1}{\partial x} \right) \qquad (5.54)$$

and because of Equations (5.43)

$$x^2 \frac{\partial Q}{\partial x} + 2Qx = \frac{\hat{k}_1 \rho g}{\nu} \cdot \frac{2\cosh\gamma}{\gamma x} - \frac{\hat{k}_1 \rho g}{\nu} \cdot \frac{\partial P}{\partial x} \qquad (5.55)$$

which can be written as follows

$$\frac{\partial Q}{\partial x} + \frac{2}{x} \cdot Q = \frac{A}{x^3} + \frac{C}{x^2} \qquad (5.56)$$

where

$$A = \frac{\hat{K}_1 \rho g}{\nu} \cdot \frac{2\cosh\gamma}{\gamma}$$

$$C = -\frac{\hat{K}_1 \rho g}{\nu} \cdot \frac{\partial P}{\partial x} = 1 \qquad \text{for unit conduit discharge}$$

The solution of this equation is

$$Q(x) = \frac{\ln x}{x^2} \cdot A + \frac{1}{x} + \frac{C}{x^2} \qquad (5.57)$$

This relation is very useful for studying the dependence of Q on the permeability ratio $\hat{k}_2/\hat{k}_1$.

EXAMPLE By considering a distance of 10^4 units, $\hat{k}_1 = 8.3 \times 10^{-4}$ cm², p = 1gr/cm³, g = 10^3gr.cm/sec², v = 1.3×10^{-2} cm²/sec. The above relation can be written

$$Q = 11.7 \times 10^{-6} \frac{\cosh\gamma}{\gamma} + C'$$

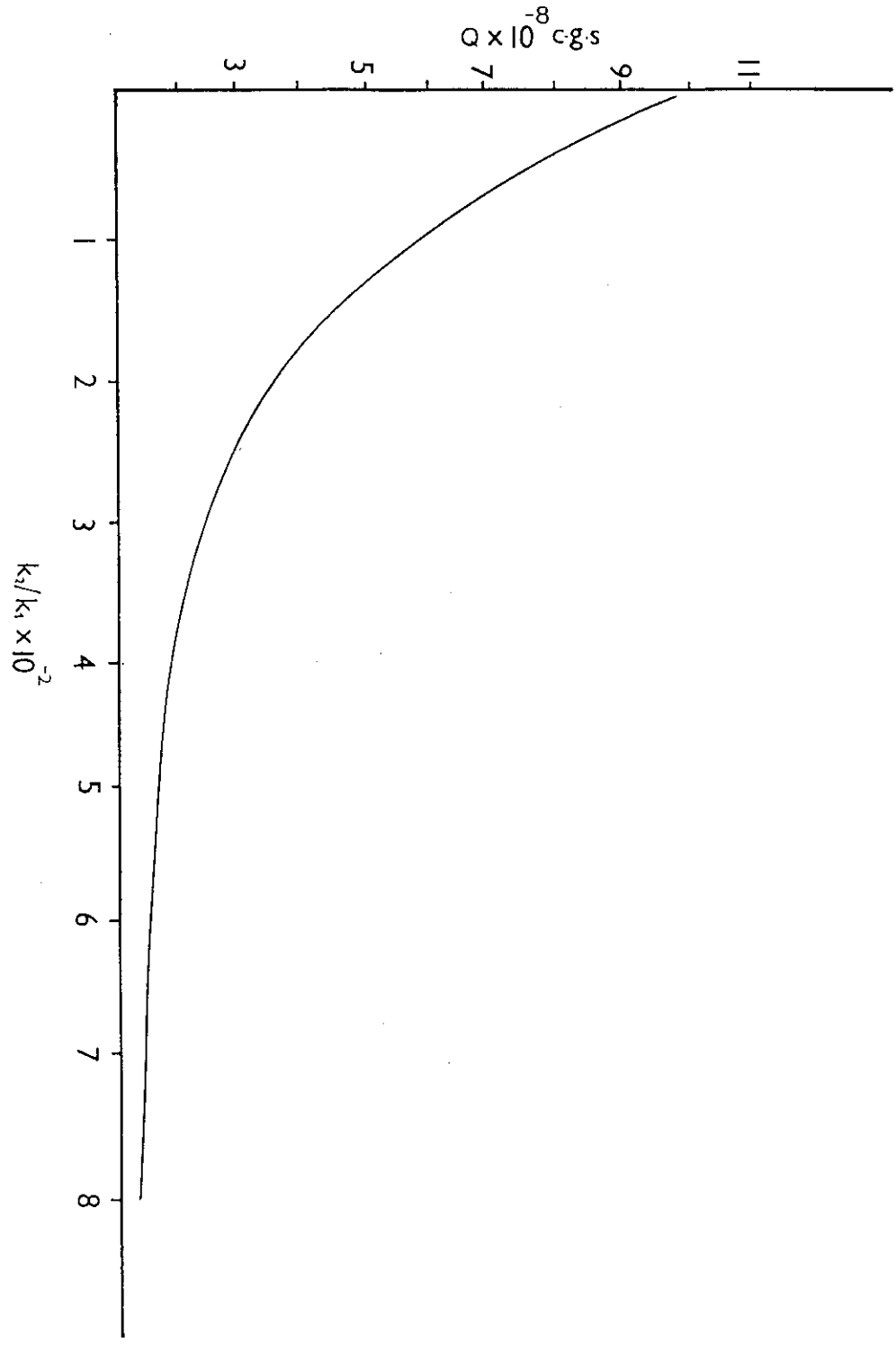


Fig. 5.24 Fissure discharge as a function of the permeability ratio between matrix and formation

and by taking in mind that

$$\text{Cosh}\,\gamma = \frac{1}{\sqrt{1-(\tanh\gamma)^2}}$$

and $$\gamma = \tanh^{-1}(\hat{K}_2/\hat{K}_1) = 1/2\,\ln\left(\frac{1+\hat{K}_2/\hat{K}_1}{1-\hat{K}_2/\hat{K}_1}\right)$$

we take the following expression

$$Q\left(K_2/K_1\right) = 11.7\times10^{6}\cdot\frac{2}{\sqrt{1-(\hat{K}_2/\hat{K}_1)^2}\cdot\ln\left(\frac{1+\hat{K}_2/\hat{K}_1}{1-\hat{K}_2/\hat{K}_1}\right)} \qquad (5.58)$$

This result is represented graphically in Fig. 5.24. From this one can see that for a constant fissure hydraulic conductivity $\hat{k}_1$, fissure discharge decreases with increasing matrix hydraulic conductivity $\hat{k}_2$. In other words less fluid is carried by the fissure as the matrix becomes more permeable.

5.13 GENERAL CONCLUSIONS

The primary porosity and hydraulic conductivity of the Chalk have been discussed, showing that the Chalk has exceptionally low intrinsic permeability as compared with its high porosity. An extensive anastomizing system of fissures is responsible for the yield of wells driven in the Chalk with a high proportion of the groundwater discharging into the wells flowing through them. The fissure space is of varying levels of saturation.

Geological and geophysical logs of Chalk boreholes have

indicated that saturated flow is largely dependent on a limited number of contributing flow horizons. Thus, the understanding of the fissure patterns in the area of a well is of extremely great importance since the saturated permeability will be a function of the configuration of the physical discontinuities of the Chalk mass with respect to the external applied head.

After discussing the flow mechanism through the Chalk, the conclusion that the Chalk aquifer is characterized by a high degree of anisotropy has been reached. The fundamental equations of fissure flow have been discussed and the hydraulic conductivity of a single parallel plane has been derived. Some experimental results of flow lows through joints have been described. From this the equivalent hydraulic conductivity of a set of parallel fissures grouped in blocks, has been calculated and a number of diagrams relating fissure opening and fissure frequency with the equivalent hydraulic conductivity have been constructed.

The tensor form of the permeability of an inclined fissure has been discussed and an analytical formula for the calculation of the equivalent hydraulic conductivity of an arbitrary set of inclined fissure zones in the direction of the pressure gradient has been derived. A new computer algorithm has been constructed for the assessment of the equivalent hydraulic conductivity of certain fissure patterns.

The pressure head distribution near a pumped well has been studied and the previously constructed computer algorithm has been used to study the dependence of the directional hydraulic conductivity upon the changes of the direction of the local hydraulic gradient which occur during pumping. The results indicated that during pumping the directional hydraulic conductivity of a fissure zone is not constant and that it is largely governed by what happens to the pressure head near the well.

A new technique using an analogue electric model for studying the relation between contact area and flow rate through a fissure has been introduced. The measurements showed that the flow rate through a fissure decreases with increasing contact area and that depends on the path of fluid flow.

Eventually an analytical formulation of the problem of flow through a fissure bisecting a semipermeable matrix has been given and a formula correlating the discharge through the conduit as a function of the permeability ratio (between matrix and conduit), has been derived.

After studying the hydraulic structure of Chalk and the main factors which are responsible for its hydraulic properties, the next step is to try to derive any possible relations between geophysical parameters measured from the logs and the hydraulic conductivity of the Chalk.

CHAPTER VI

SIMULATION OF CHALK CONDUCTIVITY BY A DOUBLE POROSITY MODEL AND EVALUATION OF IN SITU HYDRAULIC CONDUCTIVITY FROM GEOPHYSICAL FORMATION LOGS

6.1 INTRODUCTION

The purpose of this Chapter is to examine the extent to which the hydraulic conductivity of a fissured Chalk aquifer can be assessed from parameters measured by the geophysical formation logs. This can be achieved by simulating the Chalk aquifer with a simplified double porosity model consisting of a set of parallel conduits embedded in the matrix of the Chalk and by the use of the existing empirical relations for porous media (eg. Archie's law).

Before proceeding to the task of investigating the physical aspects of the relationship which is presumed to exist between geophysical and hydraulic parameters, the formation factor - porosity relation is investigated and is applied to a simplified double porosity model.

The possibility is examined of being able to obtain from geophysical logs alone enough data to permit a quantitative evaluation of the hydraulic conductivity to be made. Consideration is also given to the problem of formulating, for use in the field, simple semiempirical relationships between structural features such as number and opening of fractures, and the hydraulic characters of the ground.

Finally the effect of fissures on some geophysical parameters determined by the formation resistivity logs is being discussed and the principles of operation of a new logging technique are introduced.

6.2 FORMATION FACTOR-POROSITY RELATION

An important, clearly defined, and easily measurable property of porous media is the so called formation factor F which is defined as the ratio of the resistivity of a porous sample that is 100% saturated with an ionic solution to the bulk resistivity of the same ionic solution:

$$F = R_o/R_w \tag{6.1}$$

where R_o is the resistivity of the 100% saturated sample and R_w the resistivity of the electrolyte solution.

The formation factor measures the influence of pore structure upon the resistance of the sample.

Obviously according to the above definition F is a dimensionless quantity whose value is always greater than one, and it is defined only for porous matrices of negligible electrical conductivity.

The influence of pore structure on the electrical conductivity may be attributed to:

(1) the reduction of the cross-section which is available for conduction.
(2) the orientation and topography of the conducting pores.

It is evident that for isotropic disordered media, the ratio of the cross section available for conduction to the bulk cross section is equal to the bulk porosity $\emptyset$, so an inverse relation between F and $\emptyset$ is expected. In fact it has been found empirically that F varies more than just in inverse proportion.

Maxwell (1881) first derived a relation between porosity and formation factor for uniform nonconducting spheres embedded in a fluid continuum:

$$F = (3 - \phi)/(2\phi) \qquad (6.2)$$

Empirical relations between porosity and formation factor have been used extensively in the oil industry, and have also been applied frequently to hydrological problems. Archie (1942) first recognized a relation between porosity and formation factor, as a result of experiments on various sands from the Gulf Coast region. Archie restricted the validity of his equation to sandstones ranging from 10 to 40% porosity, and saturated with brine containing from 20,000 to 100,000 ppm of sodium chloride.

Archie's relation had the form

$$F = \emptyset^{-m} \qquad (6.3)$$

where m is the "cementation exponent" and was supposed to have values between 1.3 and 2.5 for various types of rock.

A great deal of further experimentation followed Archie's work. De La Rue and Tobias (1959) studied random suspensions of spheres, cylinders, and sand in an aqueous solution of zinc bromide of approximately the same density as the particles and they found the above equation to hold with m = 1.5 with a high degree of precision over a range of $\emptyset$ extending from about 0.25 to 0.55.

Researchers following Archie proposed covering the same sandstone spectrum as studied by Archie, a light modified relationship (Winsauer et al 1952) of the type:

$$F = C.\emptyset^{-m} \qquad (6.4)$$

where C and m are constants.

The most famous examples of such constant m and C relations are the Humble formulae in which C = 0.52 and m = 2.15 and the Wyllie formula in which C = 0.75 and m = 2.0.

In Fig. 6.1, typical examples of the above relations are shown.

It is seen that Archie's lines for m = 1.8 to m = 2.0 and the Humble line essentially yield the same Ø range for a given F value or conversely the same F range for a given Ø value for a fairly wide band of porosities.

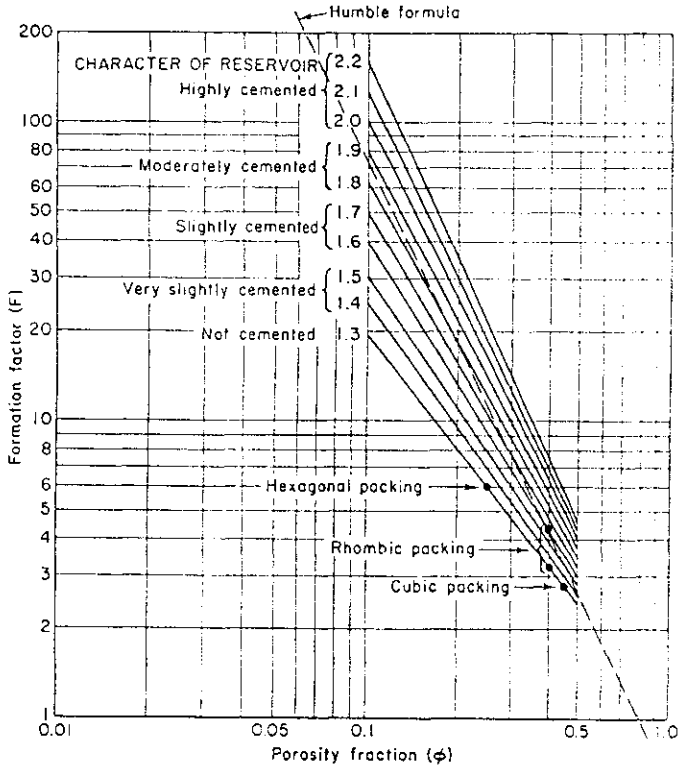


Fig. 6.1 Formation factor vs. formation porosity for the Archie equation

A great many determinations of m have been made over the years on cores from various carbonate reservoirs throughout the world. From the available data it appears certain that the exponent m does vary in carbonate rocks (Chokbart 1960) within a range which is a good deal wider than, and different from, that found in sandstones.

In a paper, important to formation evaluation, Carothers (1968) measured a large sample (981 samples) of formation factor data. This wealth of data suggested that the formation factor-porosity relation for sandstones was:

$$F = 1.45/\phi^{1.45} \quad \text{rather than } F = 0.62/\phi^{2.15}$$

which was the relation suggested by Humble and for carbonates was:

$$F = \phi.85/\phi^{2.14} \text{ rather than } F = 1/\phi^{2}$$

Carothers et al in further work (1970) used log measurements to determine the formation factor-porosity relation in the Pliocene in South California as

$$F = 2.45/\phi^{1.8} \text{ and } F = 1.97/\phi^{1.29}$$

as the relation for the Miocene in the Texas-Louisiana Gulf Coast. These relations differ from Carothers' initial relation and the Humble relation.

Recent work by other workers (Lang 1972) indicated that different average relations may be more applicable than those commonly used. The Archie, Humble and Willie equations have been around a long time and unfortunately are the keystone of analysis techniques, as witnessed by all of the service companies' interpretation manuals.

Keller and Frischknecht (1966) having summarized the findings of a number of workers concluded that the value for the parameter 'C' in Eq. (6.4) varies from slightly less than 1 for rocks with intergranular porosity to slightly more than 1 for rocks with joint porosity, while the exponent m is somewhat larger than 2 for cemented and well-sorted granular rocks and somewhat less than 2 for poorly sorted and poorly cemented granular rocks.

It appears, however, that no "worldwide" average relation accurately fits a specific reservoir rock. Thus no one of the above equations should be applied to a formation until experimental control has established:

(a) the validity of the equation in the formation
(b) the value of the constants C and m for the formation

Sen et al (1981) have investigated a theoretical model of clay free sedimentary rocks and have shown that it yields Archie's law. For spherical grains these authors found that the constant C in Archie's law has the value of 1, and the constant m has the value of 1.5. The value of m fails in the observed range and in fact is close to the minimum observed value.

Measurements by Jackson et al (1978) on marine sands indicated that the value of m depends upon grain shape, the lowest values associated with spherical grains and larger values arising from oblate grains.

Veinberg (1966) investigated a theoretical model consisting of grains which were approximated by ellipsoids of revolution at random orientations. A more generalized approach to the later model has been published recently by Mendelson and Cohen (1982). The later authors found that the presence of aspherical grains leads to an increase of m above its minimum value of 1.5. The presence of oblate spheroids is more significant, prolate spheroids having little effect on m.

This observation becomes reasonable since disk-shaped grains will have a greater effect that needle shaped ones, in blocking current paths and so increasing the resistivity, i.e. increase m. They found also, that even the presence of spheroids with quite large eccentricities will not raise m above the maximum observed value of 4.

It has long been recognized that the value of m in some way reflects the texture of the rock. However, it has been supposed that it also reflects the degree of consolidation of the rock.

From the analysis of Mendelson and Cohen (1982) it also appears that grain anisotropy has an important affect on m, and that for unconsolidated sediments is the main factor governing m.

Under the conditions prevailing in the oil industry Eq. (6.3) can be a very useful relation. From a small amount of core analysis in an oil field, it is frequently easy to establish the correct porosity-formation factor relations for the various strata and porosity determinations in the remainder of the wells can be made on the basis of electric logging data alone. Because most of the oil fields are of limited extent, it is seldom necessary to apply the relations at any great distance from the region represented in the laboratory control. In addition to this, the reservoir rocks are at a depth where the stresses are such that most of the fissures are closed and pores are the main voids. These conditions, however, are rarely duplicated in hydrological work, where aquifers are normally of much greater size than oil fields, in their areal extent, and are normally near the surface, and thus at low stress, and have open fissures. In addition to this, the opportunities to obtain core data are far fewer in a hydrologic study than in any oil reservoir investigation.

Because of the difficulty in obtaining adequate control, there has been a tendency among hydrogeophysicists to make use of Eq. (6.4) without such control, using arbitrarily chosen values for C and m. Used without control, therefore, the equation is at best a method of rough approximation.

6.3 THEORETICAL INVESTIGATION OF THE FORMATION FACTOR-POROSITY RELATION

Although the porosity-formation factor relation is an empirical one, its basic form can also be derived from theoretical considerations. Consider a porous block with a non-conducting matrix and introduce into the left face of the block an electric current which flows out of its right face as shown in Fig. 6.2.

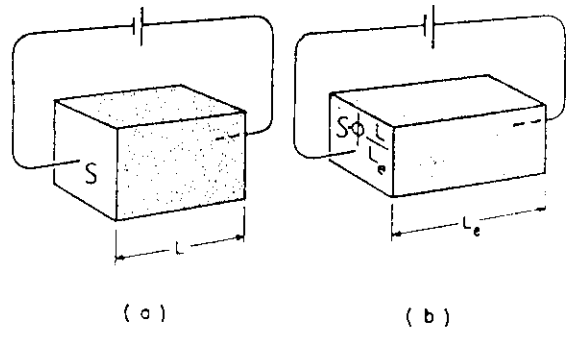


Fig. 6.2 Models illustrating the resistivity and equivalent resistivity of a porous block

Let R_o be the resistivity of the block under 100% saturation

R_w be the resistivity of the water in the pores

ϕ be the porosity of the block

L be its length

S be its cross sectional area

Since the only conducting medium in this block is water, it is possible to draw an equivalent block of water which has the same resistance as the pore block. The current flown through the porous block takes a tortuous path so that the length Le of the equivalent block is greater than the actual length L.

Since the total amount of water must be the same, the cross sectional area of the equivalent block is

$$Se = \phi \cdot S \cdot L / Le \qquad (6.5)$$

On the other hand, the resistances of the porous block and the equivalent block respectively are:

$$r_o = R_o \cdot L/S \quad ; \quad r_w = R_w \cdot \frac{Le^2}{L} \cdot \frac{1}{\phi \cdot S} \tag{6.6}$$

since $r_o = r_w$ one takes the equation:

$$R_o = \left(\frac{Le}{L}\right)^2 \cdot \frac{1}{\phi} \cdot R_w \tag{6.7}$$

which indicates that the resistivity of a porous block filled with water should be directly proportional to the resistivity of the water contained within the block.

The constant of proportionality depends only on the "electric tortuosity" $(Le/L)^2$ and the porosity ϕ of the rocks, and is independent of the water in the pore space.

By introducing the formation factor

$$F = R_o/R_w \tag{6.8}$$

Eq. (6.7) reduces to:

$$F = \left(\frac{Le}{L}\right)^2 \cdot \frac{1}{\phi} \tag{6.9}$$

which is in the form of Archie's law.

By comparing Eq. (6.9) with Archie's relation (Eq. 6.3) the following relation between cementation factor m, electric tortuosity T and porosity ϕ can be obtained:

$$m = \ln\left(\phi/T^{1/2}\right)/\ln\phi \tag{6.10}$$

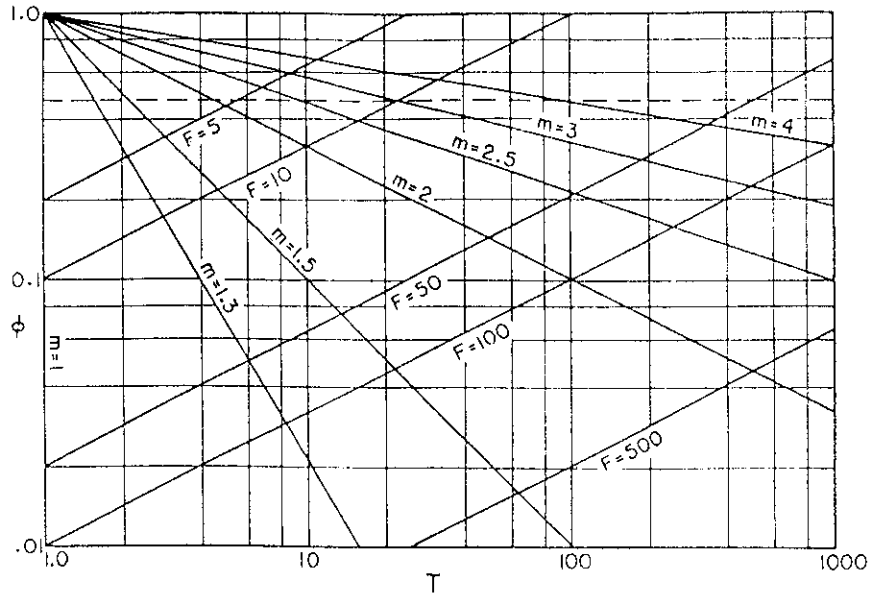


Fig. 6.3 Porosity as a function of tortuosity for constant values of formation factor and cementation factor (Willie et al 1950)

Fig. 6.3 is a plot of the porosity as a function of tortuosity for constant values of formation factor and cementation factor. The dashed horizontal line relates to the porosity of the cubic packing of spheres, which is the maximum theoretical regular packing porosity that can be obtained.

6.4 TYPICAL FORMS OF ARCHIE'S LAW FOR CHALK

Chombart (1960) writing on well logs in carbonate reservoirs, stated that for pure Chalky type-II carbonates (these possess a very fine structure with a high porosity associated with extremely low permeability), the cementation factor in Archie's original equation varies between 1.7 and 1.9.

Smart et al (1964) and Gray (1965) used these values in the evaluation of the borehole geophysical logs in the chalk. Schlumberger (1972a) recommended the use of the relation $F = \phi^{-2}$ for Chalky rocks.

Philips petroleum (written communication 1982) have established a relatively narrow range for m between 1.92-2.00 for the North Sea Chalk reservoirs.

Oteri (1982) studying the formation factor porosity relation of the Upper Chalk in the Tiltmastone area of SE England, suggested the relation $F = 1.22\emptyset^{-1.55}$; this falls in the range given by Chombart indicating that the results obtained are correct.

The following Fig. 6.4 shows, in a log-log plot, typical examples of the formation factor-porosity relation for Chalk which have been collected from the literature.

6.5 SIMULATION OF THE CHALK AQUIFER BY A DOUBLE POROSITY MODEL

The following approach uses the empirical relations that have been derived for porous media in the hope that it will be useful in the study of fissured formations.

Fissures have always been attractive to the hydrogeologists because they frequently provide the key to the producibility of water wells.

The hydraulic conductivity of a Chalk aquifer, as has already been shown (Chapter 5), is a function of the configuration of its physical discontinuities, with respect to the external head.

By assuming the permeability of the intact matrix to be negligible, the yield of a well could be directly related to the number of fissures intersected by the well. Of course, detection of even a large system of fissures will never guarantee production. It will only raise the possibility of production.

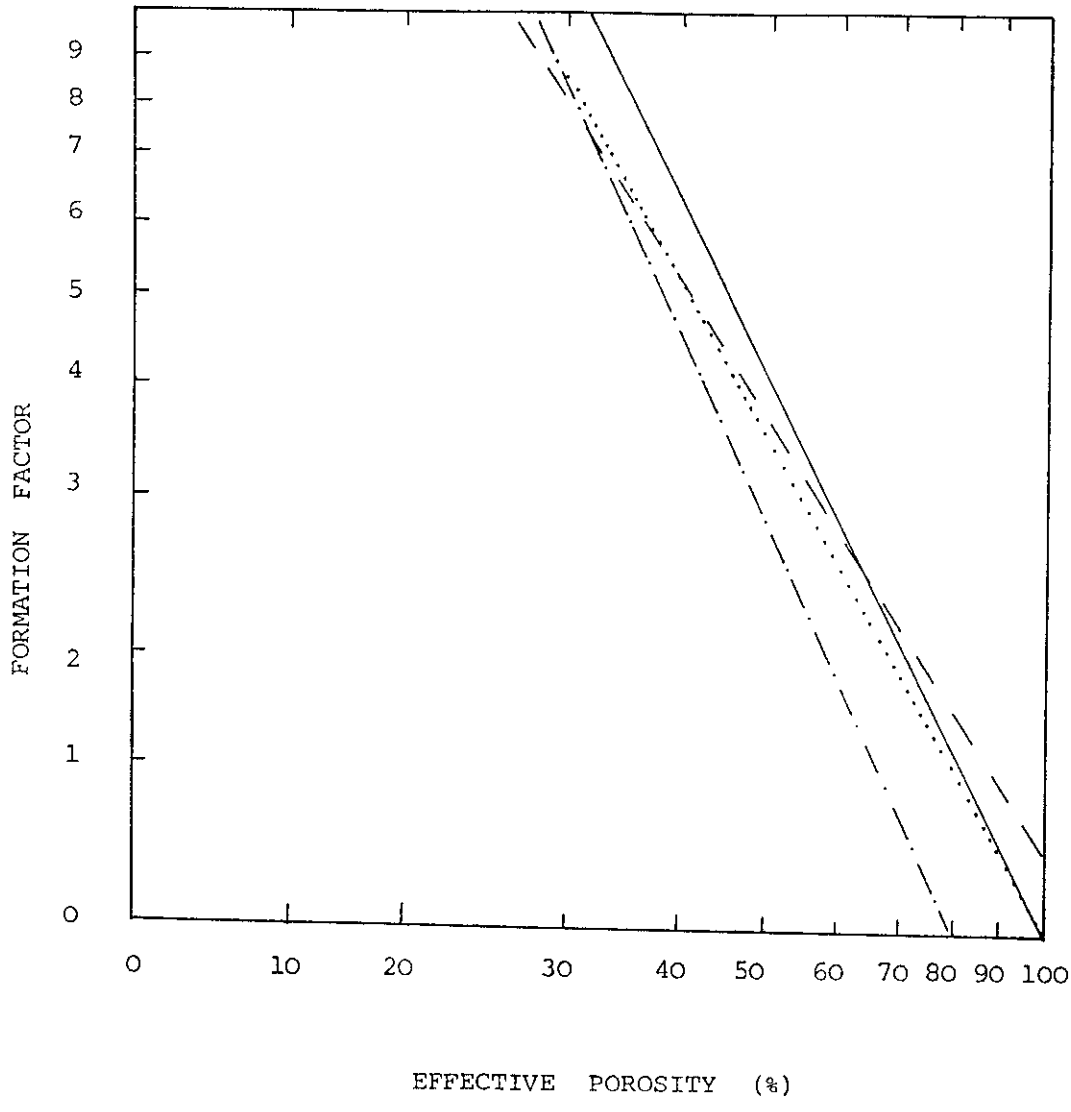


Fig. 6.4 Typical forms of Archie's law for Chalk

Adequate hydraulic conductivity of each fissure system is necessary for a reasonable production of water but this is not easy to evaluate from the formation logs. Expressed simply; what is in the Chalk, and what will come out of it are often two different matters. The formation logs pertain chiefly to the former.

Numerical investigations have been made concerning the relationship between formation factor and permeability of porous media. Many of these have been experimental (Tixier 1958; Schlumberger 1958; Komarov and Keivszar 1962; Barker and Worthington 1973; Griffiths 1976) while others have been theoretical (Schopper 1966; Dullien 1979).

For example, Fig. 6.5 shows the relations obtained by Archie (1950) between the permeability and the formation factor for a number of consolidated sandstone cores of the Gulf Coast oil reservoir. From this figure one can see that the permeability decreases with increasing formation factor.

Fig. 6.6 shows a similar relation obtained by Jones and Budford (1951) for a sandstone aquifer. In this case, the permeability increases with increasing formation factor. This relation was used by Croft (1971) to estimate transmissivity from electric log measurements. Clearly, formation factor alone is insufficient for the needs of the hydrogeologist.

6.5.a Pore system description and analysis

Although an important characteristic of Chalk is that the total amount of its fissure (secondary) porosity, when compared to its matrix porosity, is very small, when the logging probe is opposite a fissure zone, then the effect of fissure porosity becomes very important to the response of the logging tool.

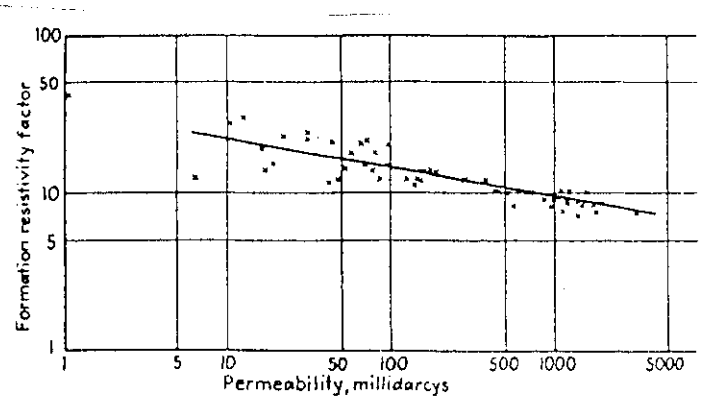


Fig. 6.5 Relation of permeability to formation resistivity factor for consolidated sandstone cores of the Gulf Coast (Archie 1952)

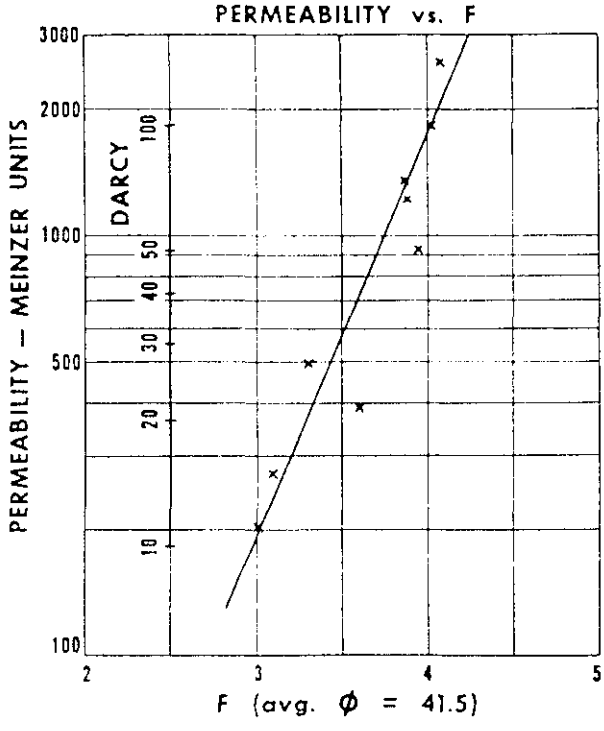


Fig. 6.6 Permeability vs. formation factor (Jones et al 1951)

In the following analysis the Chalk is being treated as a double porosity system. The idealized model considered in this analysis is presented in Fig. 6.7.

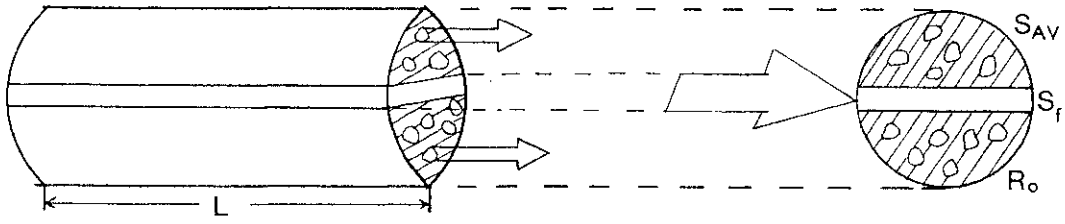


Fig. 6.7 Double porosity system for the Chalk

Let S_{AV} be the average cross section
S_f be the fissure cross section
S_o be the voids cross section
R_o be the matrix resistivity at 100% saturation
R_w be the water resistivity
R_{eq} be the equivalent resistivity
$\emptyset$ be the total porosity
$\emptyset_f$ be the fissure porosity
$\emptyset_o$ be the matrix porosity

In the above definitions, all the porosities are considered as areal porosities (Freeze and Cherry 1979). Because the matrix of the Chalk can be considered as non-conductive (Oteri 1980), the electric current on its way through the Chalk can be considered to follow two paths, one of which is throughout the fissures and the other throughout the saturated pore space of the Chalk's matrix. In other words, it is like having two different porosity systems connected in parallel.

By considering Fig. 6.2, the following relations can be written:

$$\sqrt{o} = \frac{R_o \cdot \ell}{S_{AV} - S_f}$$

$$\sqrt{w} = \frac{R_w \cdot \ell}{S_f} \quad , \quad \frac{1}{\sqrt{eq}} = \frac{1}{\sqrt{o}} + \frac{1}{\sqrt{w}} \tag{6.11}$$

$$\sqrt{eq} = \frac{R_{eq} \cdot \ell}{S_{AV}}$$

from which

$$\frac{S_{AV}}{R_{eq}} = \frac{S_f}{R_w} + \frac{S_{AV} - S_f}{R_o}$$

$$\frac{1}{R_{eq}} = \frac{S_f}{S_{AV}} \cdot \frac{1}{R_w} + \left(1 - \frac{S_f}{S_{AV}}\right) \cdot \frac{1}{R_o} \tag{6.12}$$

Because an important parameter in this analysis is the apportioning of total porosity between matrix porosity and fissure porosity, the term "Chalk Fissure Index" (f) is introduced as the fraction of total pore volume contained in the fissures:

$$f = \frac{\Phi_f}{\Phi} \tag{6.13}$$

obviously for the total porosity one can write:

$$\Phi = \left[(S_{AV} - S_f) \cdot \Phi_o + S_f \right] / S_{AV} \tag{6.14}$$

on the other hand

$$\Phi_f = S_f / S_{AV} \tag{6.15}$$

so the above relation becomes

$$\Phi \cdot S_{AV} = S_{AV} \cdot \Phi_o - S_f \cdot \Phi_o + S_f \rightarrow S_f / S_{AV} \cdot (1 - \Phi_o) = \Phi - \Phi_o \tag{6.16}$$

and because of Eq. (6.13)

$$f = \frac{\phi - \phi_o}{\phi(1-\phi_o)} \tag{6.17}$$

and

$$\phi_f = \frac{\phi - \phi_o}{1-\phi_o} \tag{6.18}$$

Returning to Eq. (6.12) one can write:

$$\boxed{\frac{1}{Req} = \frac{f\phi}{R_w} + \left(1 - f\phi\right)\frac{1}{R_o}} \tag{6.19}$$

This is a very important equation because it is the link between the two pore systems.

Similar equations have been met in the literature of fractured oil reservoirs (Pirson 1963; Pirson 1967; Aguilera 1974; Aguilera 1977), but these appear to contain errors as outlined below:-

Pirson (1967) , on his analysis of the multiple porosity systems gives the equation:

$$\frac{1}{Req} = \frac{f\phi}{R_w} + (1-f)\cdot\frac{\phi}{R_o} \tag{6.20}$$

The difference between the above equation and Eq. (6.21) occurred because Pirson during his evaluation of the resistance of the matrix, used the formula

$$r_o = R_o \cdot \ell / (\phi_o \cdot S_{AV})$$

Of course, using S_{AV} instead of $S_{AV}-S_f$ has little effect but using the term $\phi_o.S_{AV}$ means that the term R_o describes the pore's water resistivity and not the 100% saturated matrix resistivity as Pirson intended.

Aguilera (1977), in his very interesting paper about the analysis of fractured reservoirs, states that he is using Pirson's formula, but quotes it as:

$$\frac{1}{R_{eq}} = \frac{f\phi}{R_w} + \frac{1-f}{R_o} \tag{6.21}$$

in which it is clear that he omitted the factor Ø in the second term of the right hand side factor. If this was intentional, it introduces a significant error in his later analysis. It is therefore concluded that Eq. (6.19) is similar in form to the relationships derived by others, but differs in detail and is considered to be the more correct relationship between resistivity and porosity than those presently in print.

Rearranging Eq. (6.19) results in:

$$R_{eq} = \frac{R_w \cdot R_o}{f\phi R_o + R_w(1-f\phi)} \tag{6.22}$$

and by introducing the system formation factor

$$F = R_{eq}/R_w$$

one can write

$$F = \frac{R_o}{f\phi R_o + R_w(1-f\phi)} \tag{6.23}$$

It is worth examining the behaviour of Eq. (6.24) in the following limited cases:

(a) fissure porosity is zero.

In this case the chalk fissure index becomes zero and Eq. (6.23) turns out to be the defining relation for the formation factor of the porous medium

$$F = R_o/R_w \tag{6.24}$$

(b) matrix porosity is zero.

In this case the Chalk fissure index becomes one and since there is no matrix porosity and the assumption has to be made that the matrix of the Chalk is non conductive R_o must be infinite so Eq.(6.23) can be written as:

$$F = 1/\phi \quad \left(= \lim_{R_o \to \infty} \frac{1}{\phi + \frac{R_w}{R_o}(1-\phi)}\right) \tag{6.25}$$

indicating that for a pure fissured system the cementation exponent should be close to one.

Introducing into Eq. (6.23) the matrix formation factor F_o, yields

$$F = \frac{1}{f\phi + \frac{R_w}{R_o}(1-f\phi)} = \frac{1}{f\phi + (1-f\phi)/F_o} \tag{6.26}$$

and by using Archie's expression, the following interesting formula is obtained:

$$\boxed{\phi^{-m} = \frac{1}{f\phi + \phi_o^{m_o}(1-f\phi)}} \tag{6.27}$$

This, together with Eq. (6.17), is going to be used in order to study some possible combinations of the porous system needed to describe fissured Chalk aquifers.

The reader is remined that in the above formula (6.27), m_o represents the initial cementation factor of the porous formation, where m is the total cementation factor for porous and fissured formation.

6.5.b Discussion of the results

Starting from the two important equations (6.17) and (6.27), computer runs were made (the computer program is given in Appendix A.6.1), in order to study all possible combinations of a two porosity system representing a Chalk aquifer.

The analysis has considered the following ranges:

range of m_o: 1.5 - 2.00
range of $\emptyset$: 0.2 - 0.45
range of f: 0.02 - 0.22

The complete results are given in a form of a table in APPENDIX A.6.1.

Figures 6.8a to 6.8f represent in graphic form the results for the cases: m_o = 1.60, 1.64, 1.66, 1.70, 1.74, 1.80. From these charts, one can see the following:

(a) For a constant Chalk fissure index "f", the total cementation factor increases with increasing matrix porosity. An obvious explanation of this result is that when the channels of current flow are changing from straight and are relatively constant area to tortuous, the cementation factor increases. It has already been mentioned that for a single porosity model consisting of straight hydraulic channels, the cementation factor tends to be 1. Obviously by introducing in a single (fissure) porosity system some more channels (pores), more current is going to travel through the pore system with an obvious increase in tortuosity. The effect of the "fissure porosity" $\emptyset_f$ on the total cementation factor is shown in Fig. 6.9.

It is very clear that with increasing $\emptyset_f$, m decreases; also that the slope of the curves $m = g(\emptyset_f)$ becomes less as

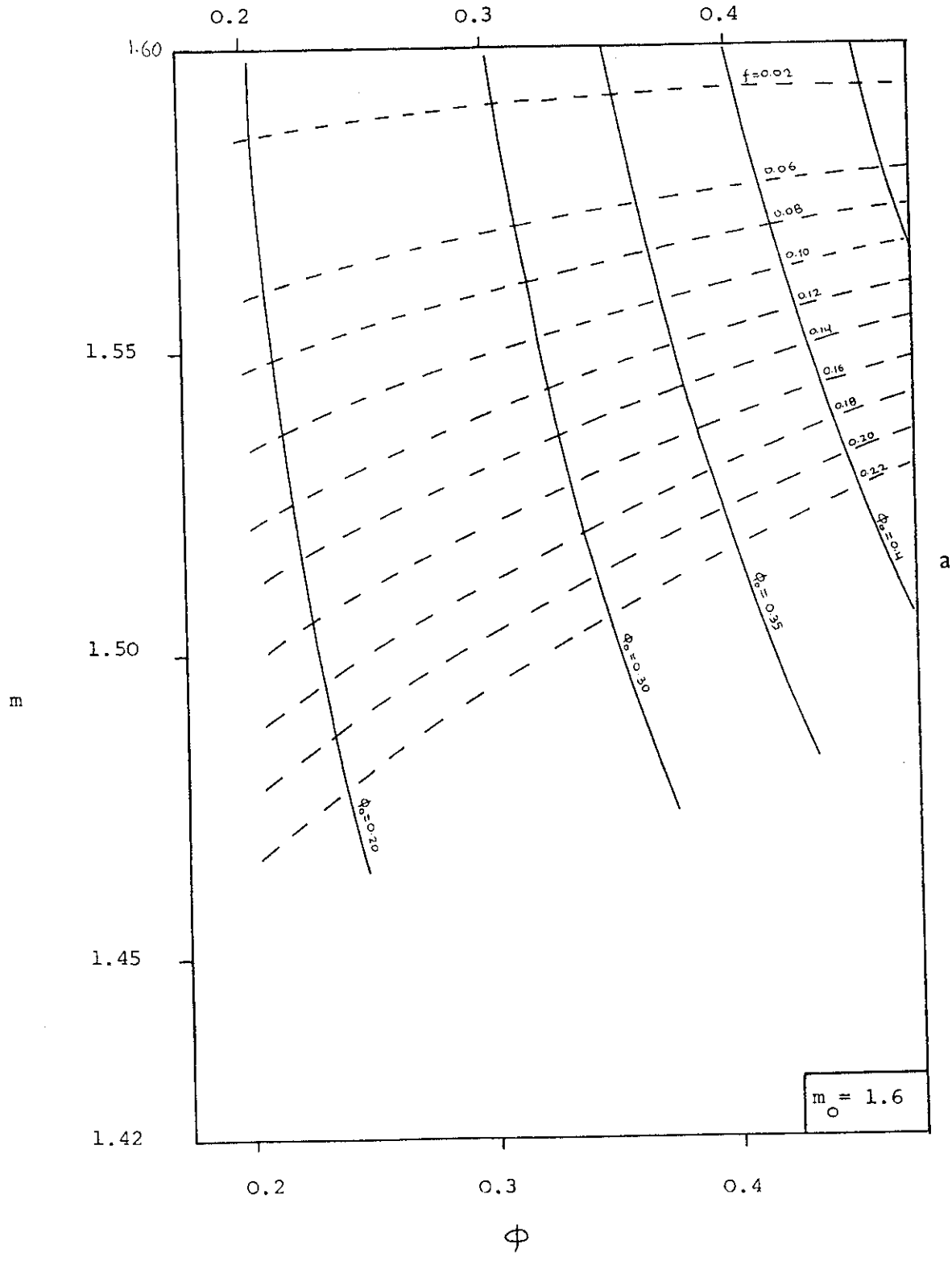
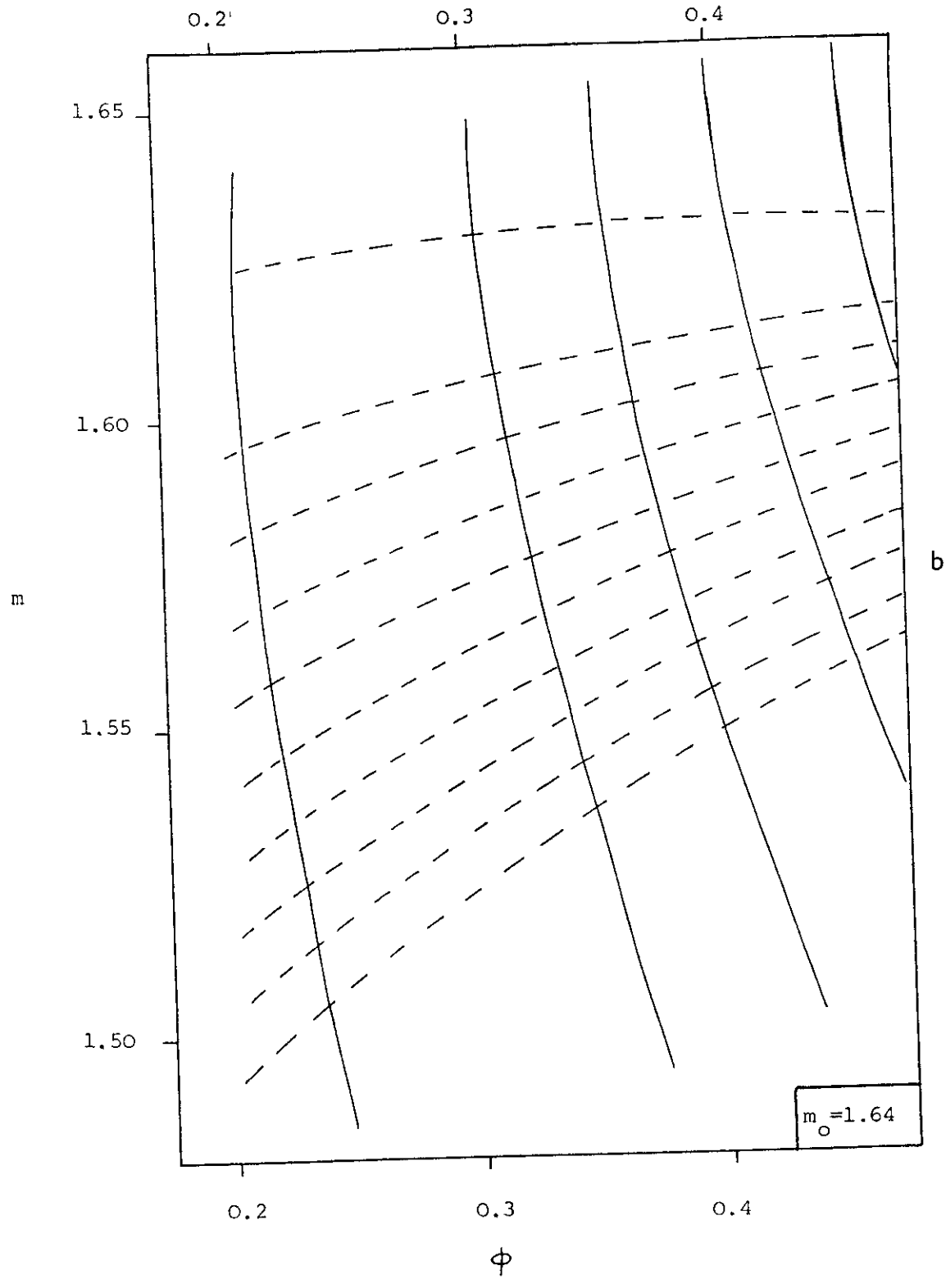
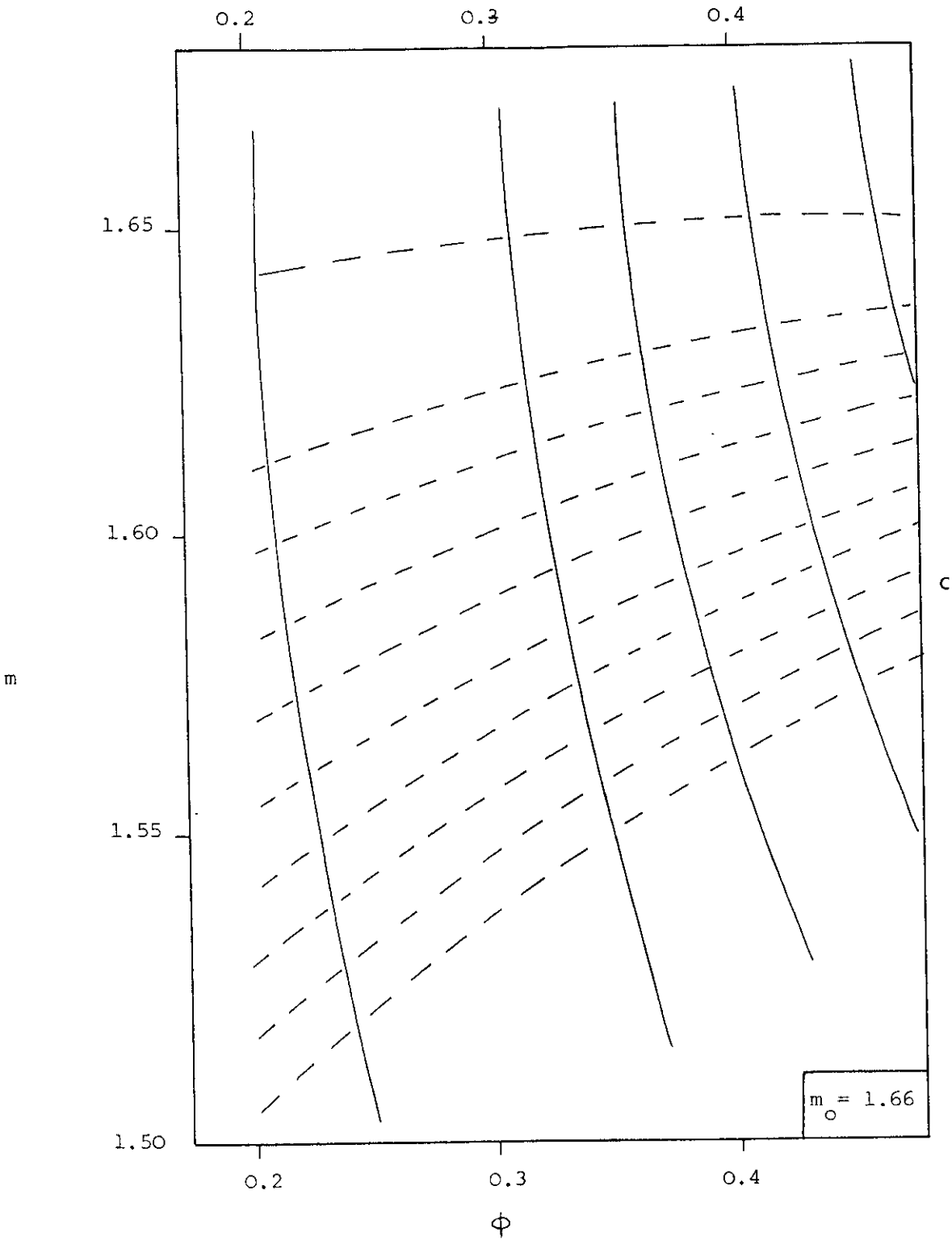
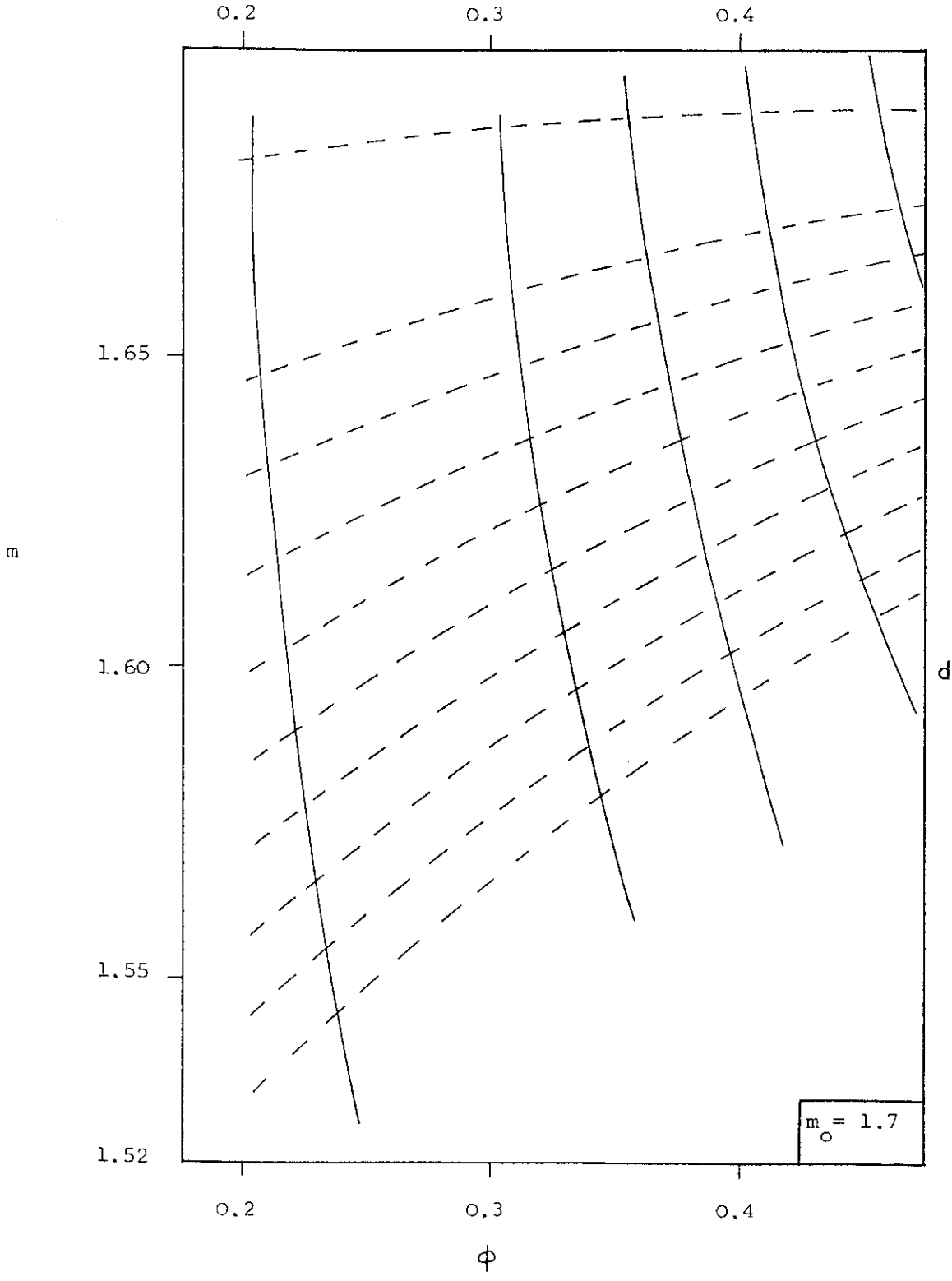
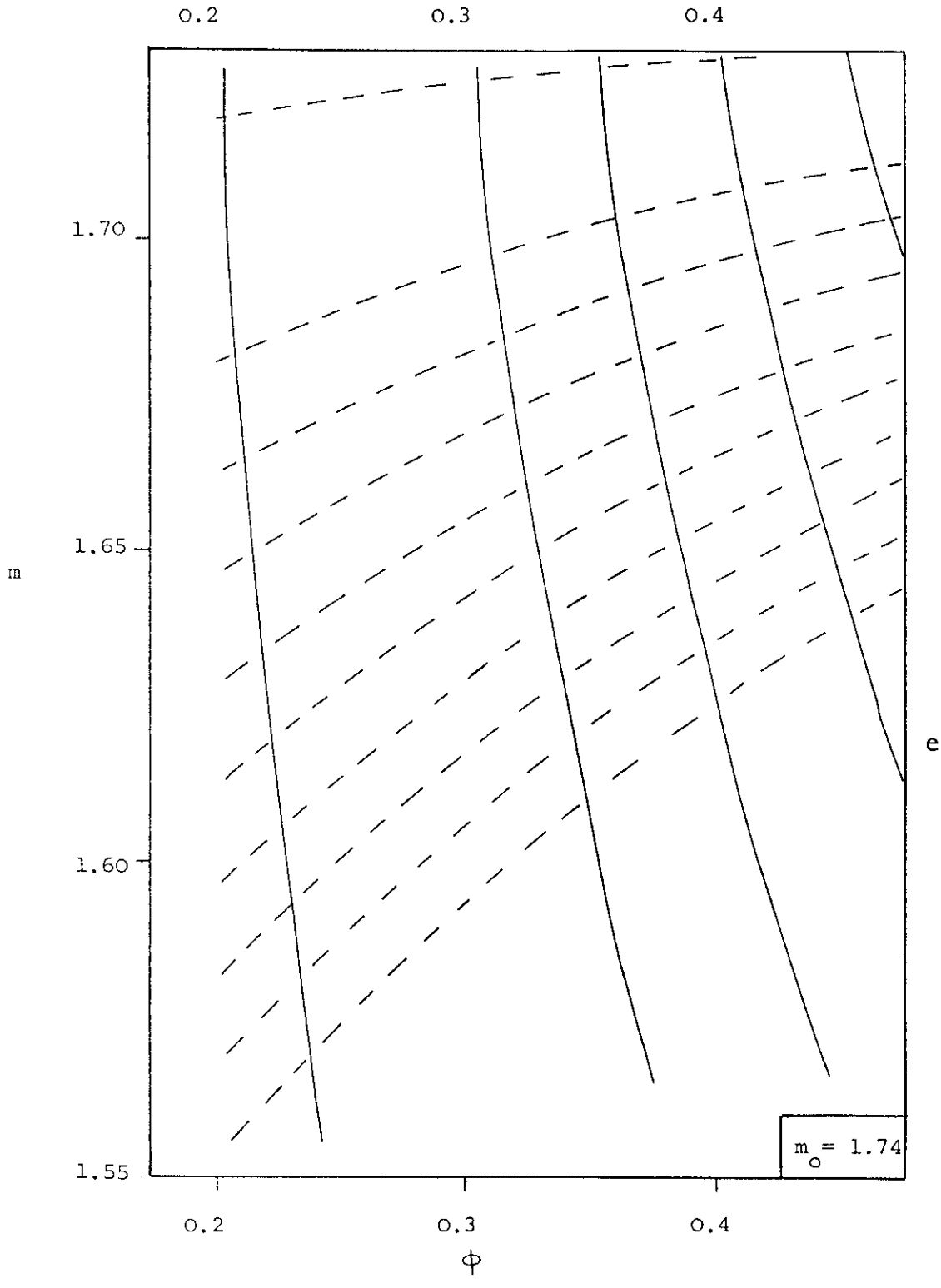


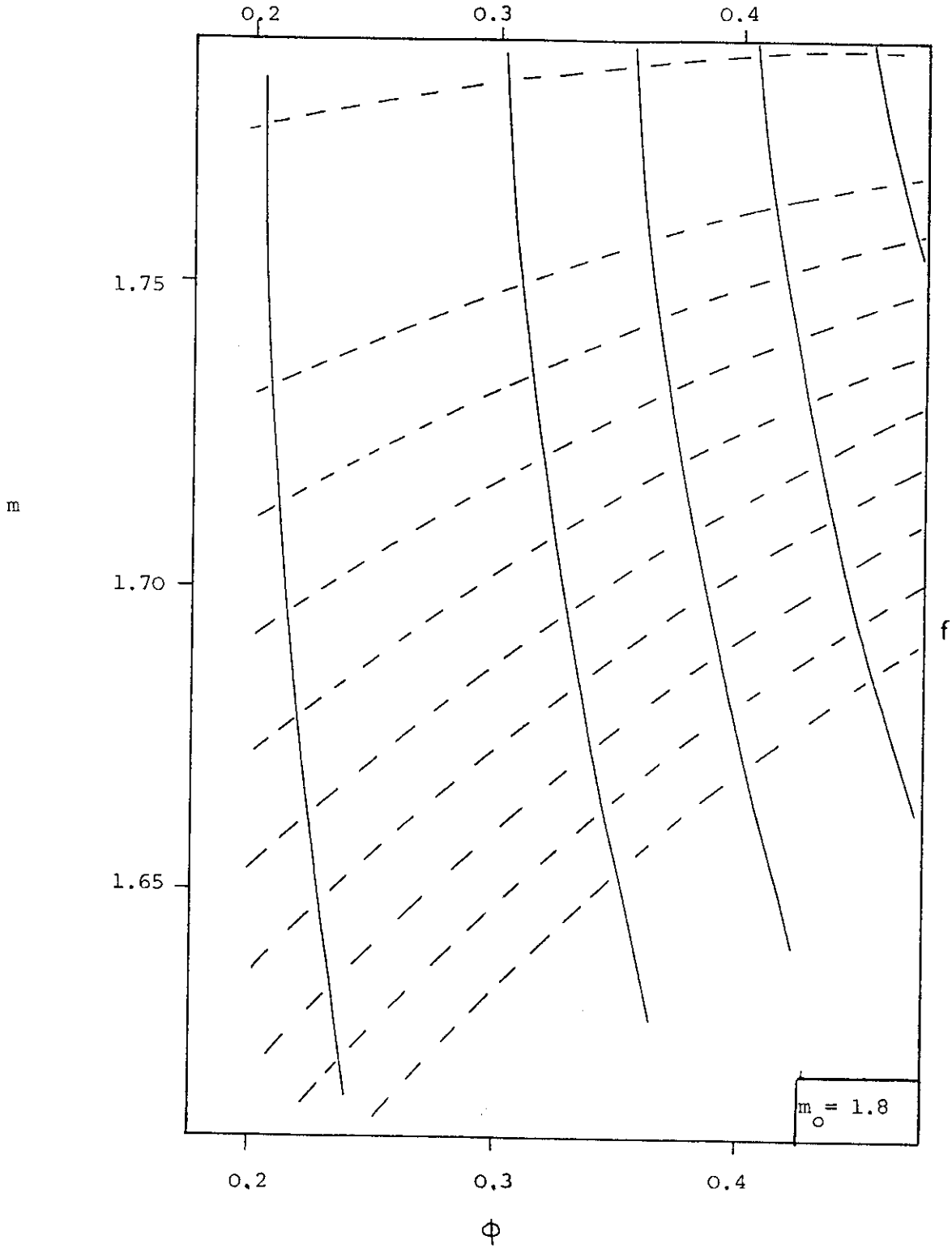
Fig. 6.8 Relation between the formation parameters of the double porosity model


0.2
0.3
0.4
1.65
1.60
1.55
1.50
m
b
m_o=1.64
0.2
0.3
0.4
φ


0.2
0.3
0.4
1.65
1.60
1.55
1.50
m
c
m_o = 1.66
0.2
0.3
0.4
Φ


0.2
0.3
0.4
1.65
1.60
1.55
1.52
m
d
m_o = 1.7
0.2
0.3
0.4
φ


0.2
0.3
0.4
1.70
1.65
1.60
1.55
m
e
m_o = 1.74
0.2
0.3
0.4
Φ


0.2
0.3
0.4
1.75
1.70
1.65
m
f
m_o = 1.8
0.2
0.3
0.4
Φ

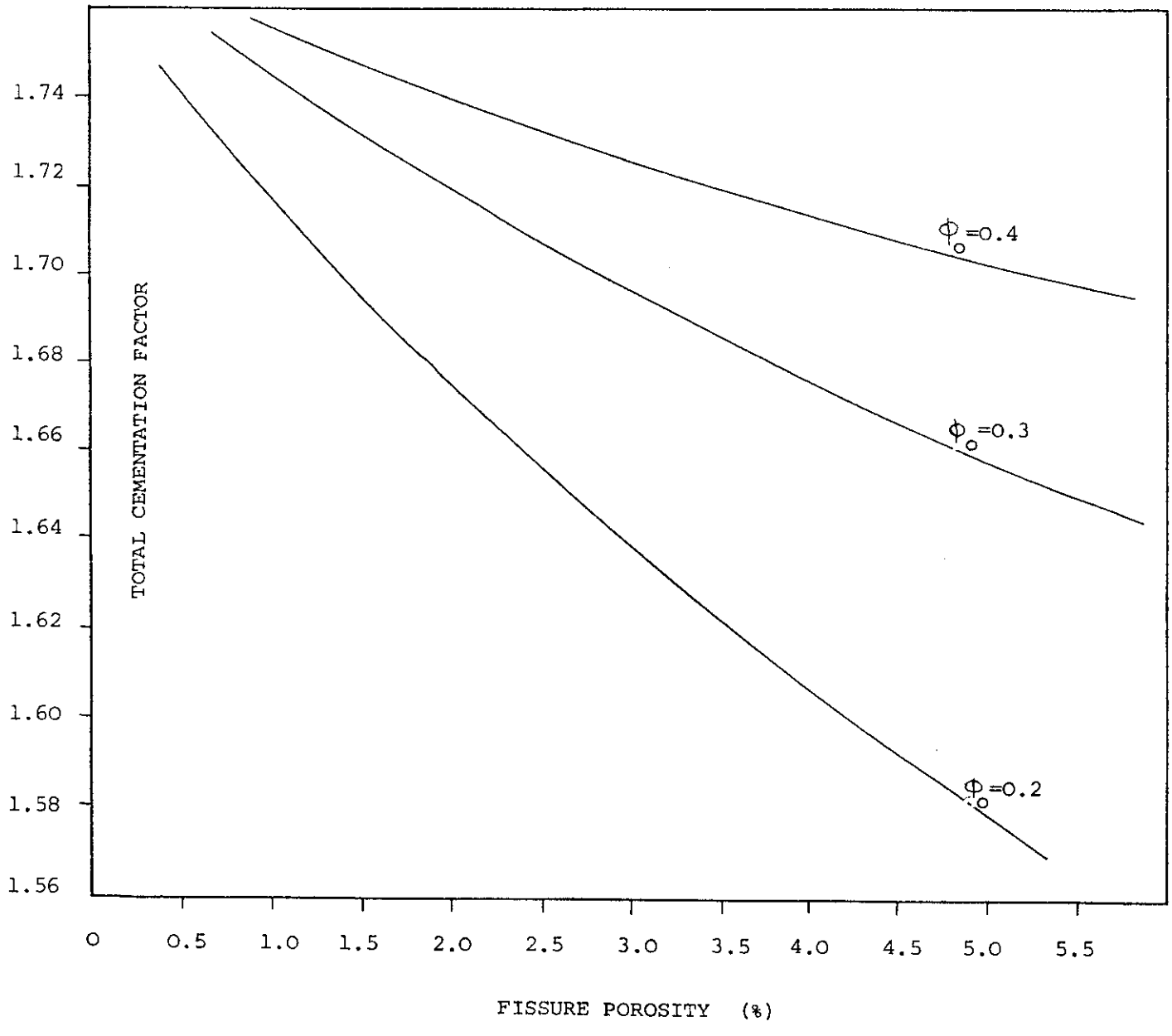


Fig. 6.9 Total cementation factor vs. fissure porosity

the matrix initial, porosity increases. In other words, the effect of ϕ_f on m becomes less important with increasing ϕ_o.

From the above argument, one can say that for a double porosity system m is mainly controlled by the degree of change of the initial porosity.

(b) For constant ϕ_o, m increases with decreasing f. This is due to the fact that the more compact the "rock" becomes, the bigger becomes the cementation factor

(c) Another important result which is shown on the interpretation charts, and which verifies the correctness of the model, is that when f tends to zero, the total porosity tends to the initial porosity; the same also happens when the total cementation factor m becomes equal to the initial cementation factor m_o.

From all the above, one can conclude that a characteristic property of the total cementation factor m of a double porosity system, is that it decreases appreciably with increasing f. Since f is a quantitative measure of the degree of fissuring of the Chalk, if m could be measured (methods of measuring m from resistivity and porosity logs are an established procedure in the logging industry), then for a given primary porosity ϕ_o and for a given matrix cementation factor m_o one could, by using the interpretation charts, estimate f and from this the total fissure porosity ϕ_f.

In the following paragraphs, the possible ways of correlating f with the hydraulic conductivity of the Chalk are going to be examined.

6.6 RELATION BETWEEN THE FISSURE INDEX OF CHALK AND ITS HYDRAULIC CONDUCTIVITY

The dramatic effect of fissures on the hydraulic conductivity of the Chalk has already been stressed. In the previous section, a method for measuring the degree of fissuring of the Chalk has been introduced by using for its quantitative measurement, the fissure index of the Chalk (f). Thus it would be logical to investigate the existing relation between f and the hydraulic conductivity.

The following analysis starts from the fact that f represents the fraction of the total porosity through which a path of least resistance to fluid flow exists.

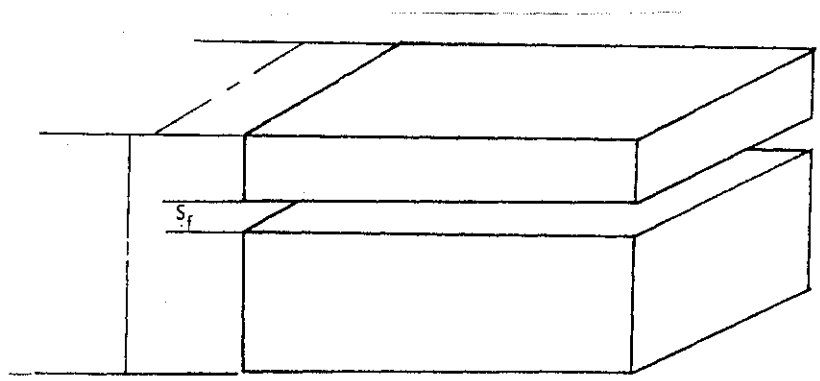


Fig. 6.10 Chalk block with one fissure per unit length

By considering a unit block of Chalk cointaining a single fissure of width s, (Fig. 6.10) and assuming the hydraulic conductivity of the matrix of the Chalk to be negligible, one can write for the equivalent hydraulic conductivity:

$$k = \frac{g}{12\nu} \cdot (s_f)^2 \qquad (6.28)$$

By referring to the following relations:

$$f = \Phi_f/\phi \;,\; \phi_f = S_f/1 \;,\; \phi_f = \frac{\phi - \phi_o}{1-\phi_o} \tag{6.29}$$

The equivalent hydraulic conductivity of the block can be easily expressed as a function of the Chalk's fissure index f or as a function of the total porosity Ø:

$$k = \frac{g}{12\nu} \cdot \left(\frac{\phi-\phi_o}{1-\phi_o}\right)^2 \tag{6.30}$$

$$k = \frac{g\,\phi^2}{12\nu} \cdot f^2 \tag{6.31}$$

which, by expressing Ø in terms of ϕ_o and f, becomes:

$$k = \frac{g\,\phi_o^2}{12\nu} \left[\frac{f}{1-f(1-\phi_o)}\right]^2 \tag{6.32}$$

By writing k as $\hat{k}.g/\nu$ where $\hat{k}$ is the permeability, the above formulae can be written as follows:

$$\hat{k} = \frac{1}{12} \left(\frac{\phi-\phi_o}{1-\phi_o}\right)^2 \tag{6.33}$$

and

$$\hat{k} = \frac{1}{12} \cdot \phi_o^2 \left[\frac{f}{1-f(1-\phi_o)}\right]^2 \tag{6.34}$$

A graphic representation of these results is shown in Figures 6.11 and 6.12.

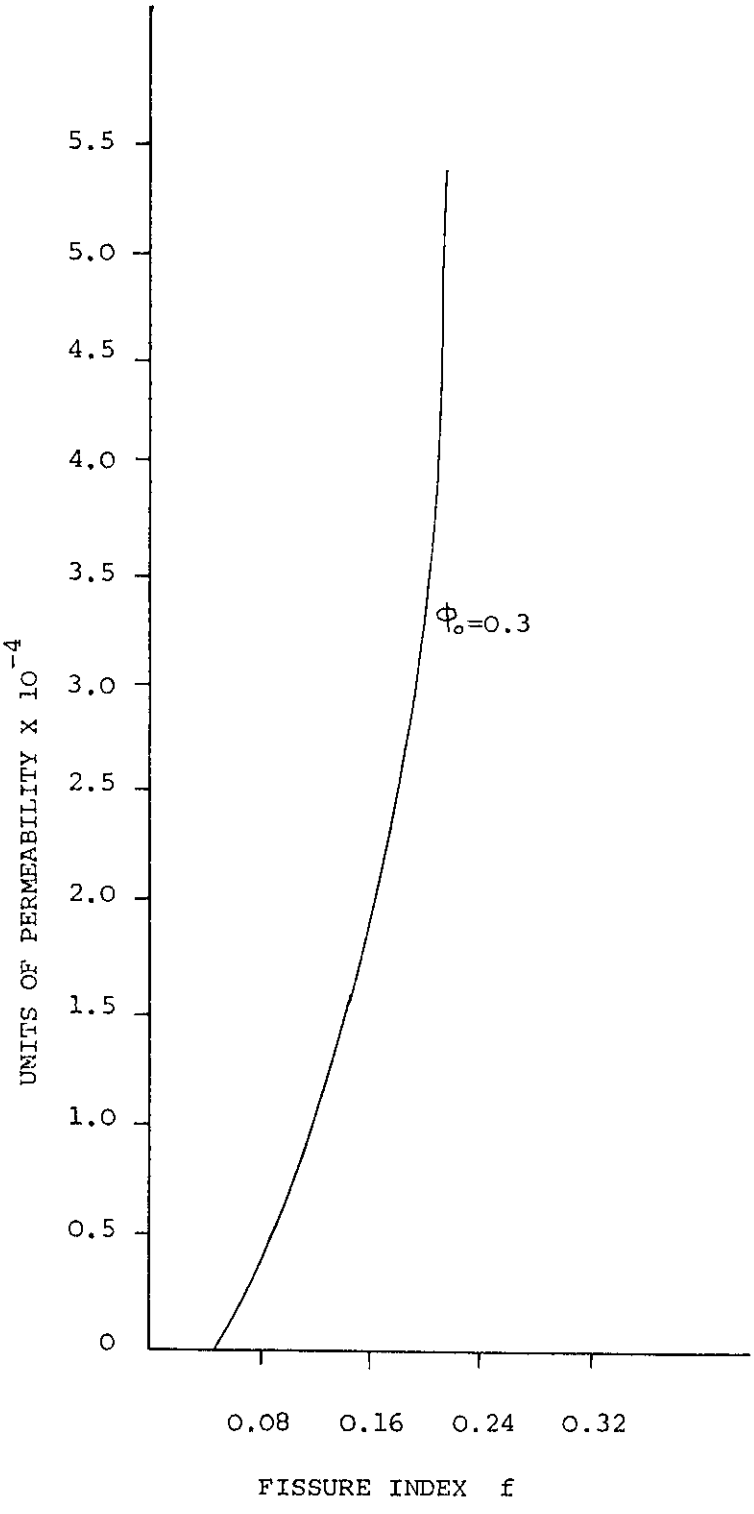


Fig. 6.11 Permeability vs. fissure index

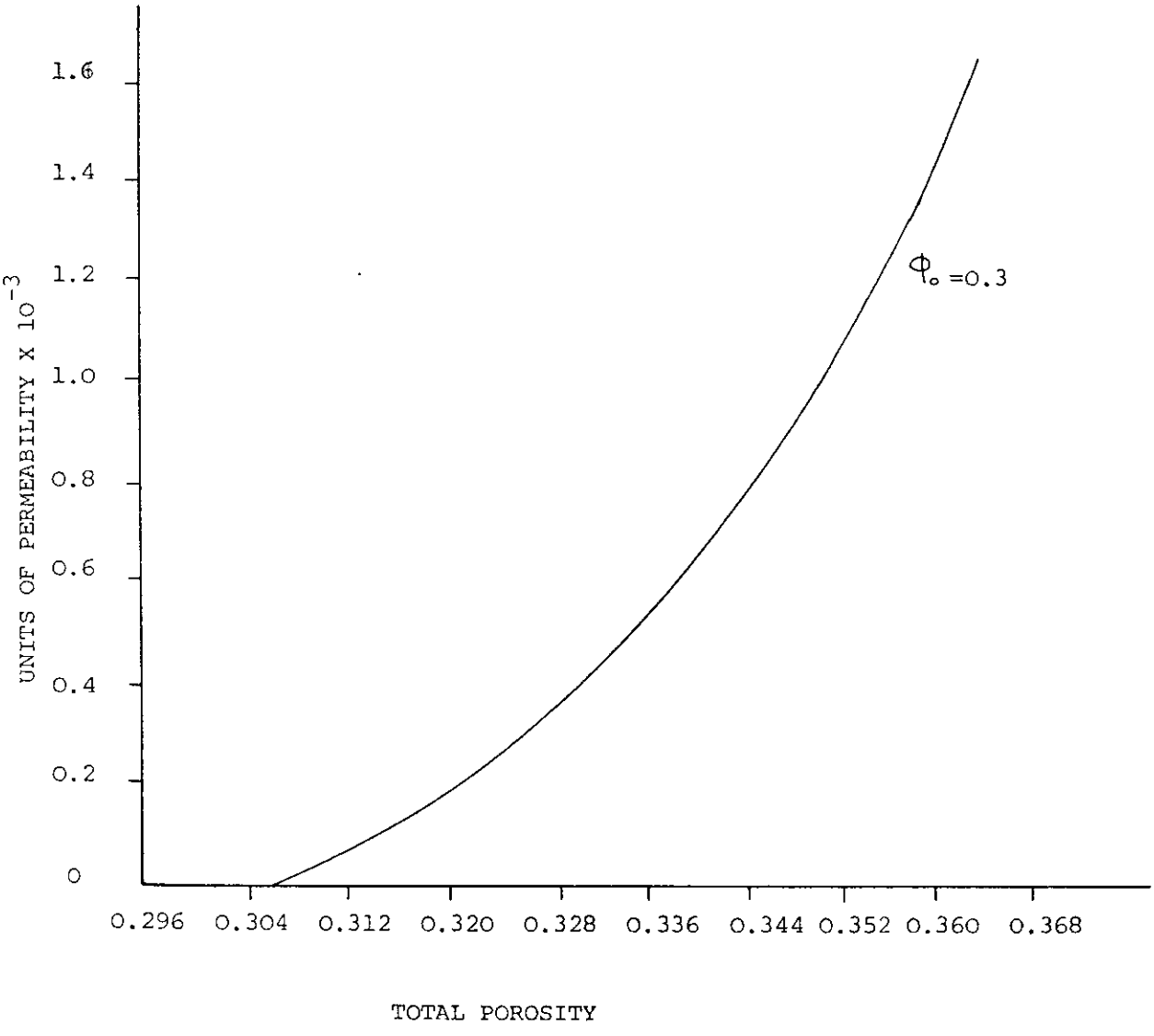


Fig. 6.12 Permeability vs. total porosity

By observing Fig. 6.11 which is the graphical representation of the relation between the permeability and the degree of fissuring of the formation, one can deduce that even a small error in the calculation of the fissure index introduces a large error in the calculation of the permeability.

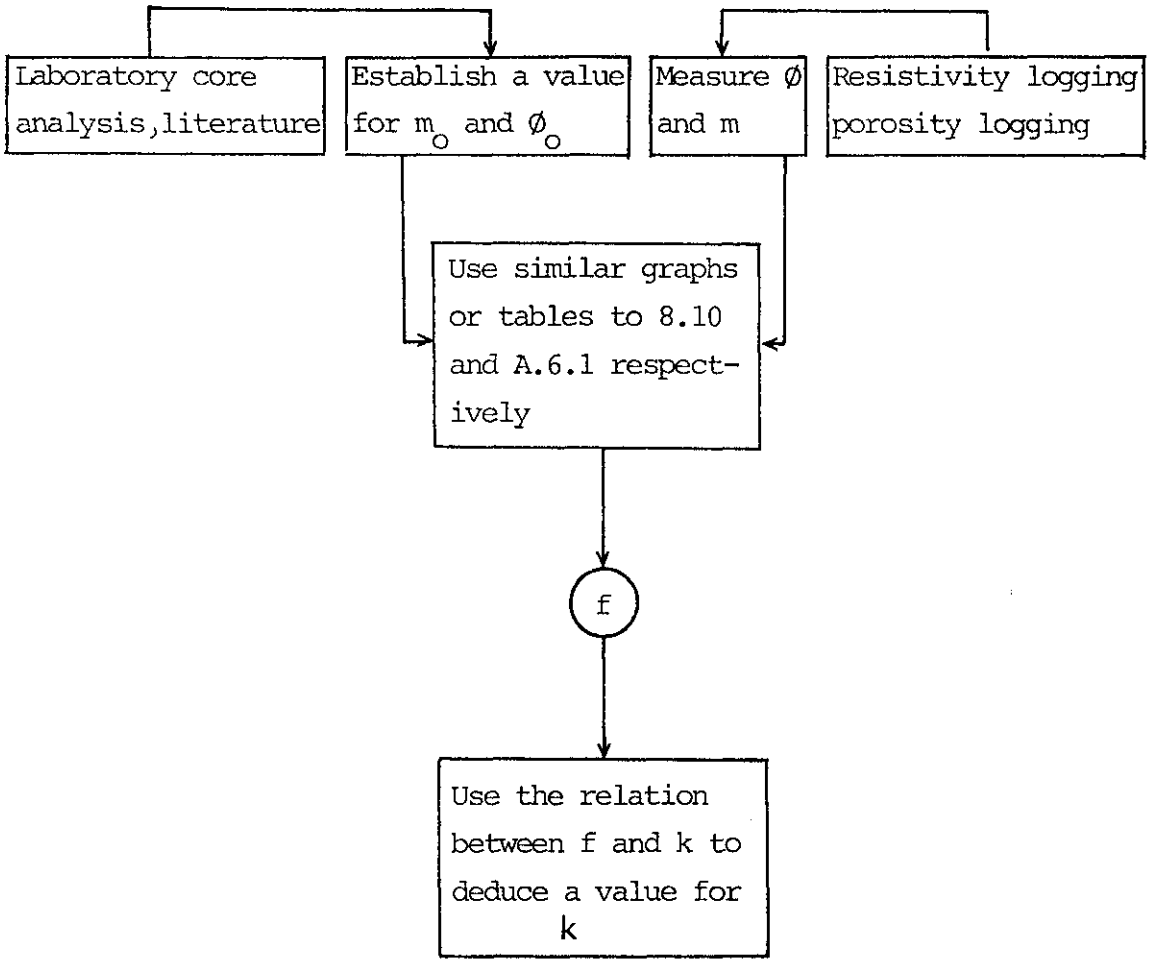
This result explains the great difficulty encountered in any attempt to measure the hydraulic conductivity of a fissured formation from standard formation logging techniques. Fig. 6.12 represents the relation between permeability and the total porosity of the formation, considering a constant matrix porosity $\emptyset_o$. One can again see that a small increase in the total porosity (due to fissuring) produces a larger increase in the permeability.

Since the most important factor in deducing a quantitative estimate of the hydraulic conductivity of fissured formations from geophysical formation logs is the degree of accuracy with which this secondary porosity can be measured, it is evident that the higher the initial porosity becomes, the less accurate the evaluation of the hydraulic conductivity. For formations with high initial porosities such as the Chalk, it is doubtful whether it is possible to obtain accurate measurements for the hydraulic conductivity from geophysical measurements alone.

For the case of fissured formations with low initial porosity, such as highly cemented limestones, igneous or metamorphic rocks, one should be more optimistic about the existing possibilities of deducing a quantitative measure of the lamation's hydraulic conductivity from geophysical formation logs alone.

In the above analysis, a single fissure per unit length of formation was considered but similar relations can be derived for the most general case of having fissures of different orientations and conductivities and by using the formulae for the equivalent hydraulic conductivity developed in Chapter V.

The following diagram represents the basic principles of the method proposed in this Chapter for the evaluation of the hydraulic conductivity of fissured formations from geophysical formation logs.



6.7 HYDRAULIC CONDUCTIVITY-VS.-ELECTRIC CONDUCTIVITY

It would be very useful if the mutual relation between hydraulic and electric conductivities could be emphasized, as it has already been shown that both of them depend on the degree of fissuring of the Chalk, or in other words, its fissure index.

The main difference between the two conductivities arises from the fact that they originate from two different

physical laws: the Hagen-Poissuele and Ohm's law. Because of this, the electric conductivity varies in proportion with the area S of the conductor whereas the hydraulic conductivity in laminar flow varies with S^2.

It is instructive to consider a hypothetical sample consisting of n identical parallel capillaries with a total constant cross-sectional area equal to S. Obviously the cross-sectional area of each capillary is $S_i = S/n$. Imagine that n is increased beyond any limit, while S is kept constant, thus leaving the electric conductivity of the system unchanged. The hydraulic conductivity, however, is proportional to $n.S_i^2 = n.(S/n)^2 = S^2/n$; which becomes vanishingly small with increasing n.

From the above simple example, one can see that the determination of the electric conductivity or equivalently, the formation factor, are not enough to determine the hydraulic conductivity, since the first two are sensitive to a different aspect of pore structure whose contribution to the permeability is only negligible. This relation between the two conductivities becomes even purer when we consider the typical Chalk aquifers in which the fissure porosity becomes a minor part of total porosity.

6.8 AN INVESTIGATION OF THE EFFECT THAT FISSURES HAVE UPON SOME PARAMETERS MEASURED FROM THE FORMATION RESISTIVITY LOGS

In surface-based resistivity soundings, the measured resistivities are controlled by the average response of the earth over very large volumes, volumes with dimension comparable to the depth to which measurements are being made. On the other hand, resistivity measurements made in well logging are highly detailed over distances of a few cm to a few metres vertically through a well. One must

therefore ask the question: how sensitive are these resistivity measurements for defining fissure zones and what is the best way of treating the data?
Consider a hypothetical section in the Chalk consisting of layers with two resistivities, p_1 for the fissures and p_2 for the formation, Fig. 6.13.

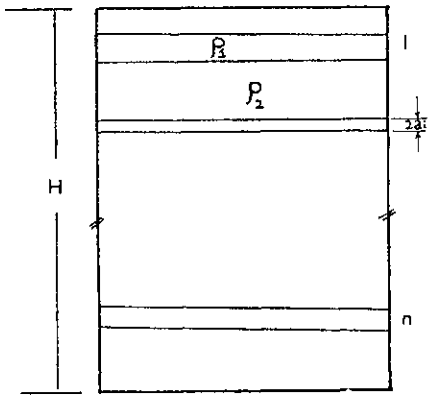


Fig. 6.13 Geoelectric model of fissured formation

By definition the transverse resistivity p_{tr} is given by:

$$\rho_{tr} = \frac{\sum_1^n h_i \rho_i}{H} = \left[\sum_1^n \frac{2a_i}{\rho_1} + \left(H - (2a_i)\cdot\eta\right)/\rho_2 \right] \cdot \frac{1}{H} \qquad (6.35)$$

from which:

$$\rho_{tr} = \frac{2a_i}{H}\cdot\eta\cdot(\rho_1 - \rho_2) + \rho_2 \qquad (6.36)$$

Similarly the longitudinal conductivity is given by:

$$\sigma_\ell = \frac{\sum_1^n (h_i/\rho_i)}{H} = \left[\sum_1^n \frac{2a_i}{\rho_1} + \left(H-(2a_i)\cdot\eta\right)/\rho_2\right]\cdot\frac{1}{H} \qquad (6.37)$$

from which

$$\sigma_\ell = \frac{2a_i}{H}\cdot\eta\cdot\left[\frac{1}{\rho_1} - \frac{1}{\rho_2}\right] + \frac{1}{\rho_2} \qquad (6.38)$$

The coefficient of anisotropy is given by:

$$\lambda = \left(\rho_{tr}\cdot\sigma_\ell\right)^{1/2} \qquad (6.39)$$

which by using the above relations becomes:

$$\lambda = \left[\frac{(\rho_1-\rho_2)^2}{\rho_1\cdot\rho_2}\cdot\left(\frac{2a_i\cdot\eta}{H}\right)\cdot\left(1-\frac{2a_i\cdot\eta}{H}\right)+1\right]^{1/2} \qquad (6.40)$$

From this later equation, one can see that for the case where there are no fissures in the formation ($\rho_1=\rho_2$) the coefficient of anisotropy becomes equal to unity.

Figures (6.14) and (6.15) represent the dependence of the above geoelectric parameters upon the percentage of fissures per unit cross section ($\frac{2a_i\cdot\eta}{H}$ x 100%), for a hypothetical section with ρ_1 = 25 and ρ_2 = 150 ohm.m.

The fraction of low resistivity beds in the section was varied by increasing the number of fissures.

The values of longitudinal and transverse resistivity vary from 25 ohm.m for the case in which the entire section is composed from water to 150 ohm.m in the case that there are no fissures at all (Fig. 6.15). In the case of the longitudinal resistivity, the value remains close to 25 ohm.m until the fraction of fissures becomes less than 80%.

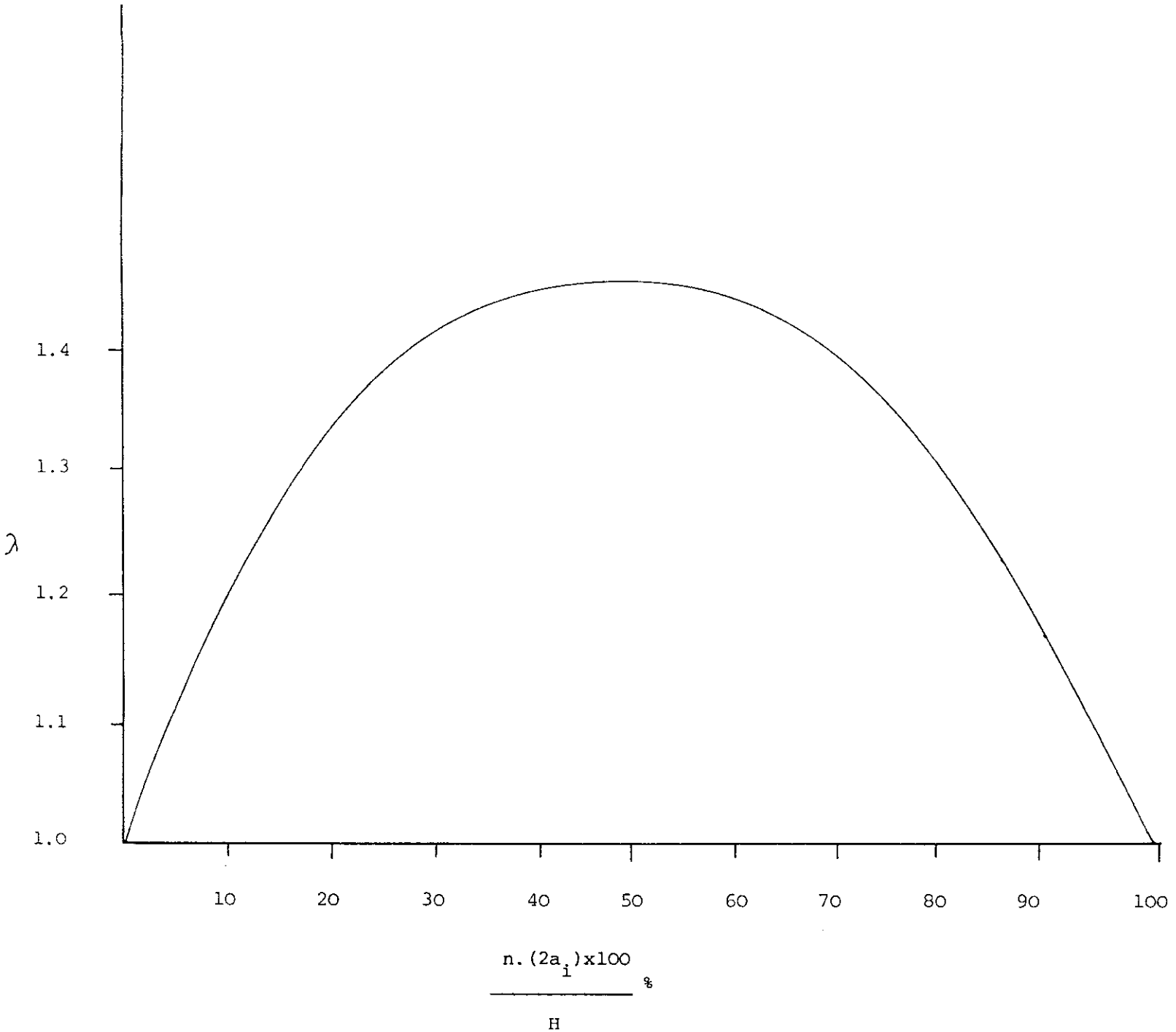


Fig. 6.14 Anisotropy index vs. fissure porosity

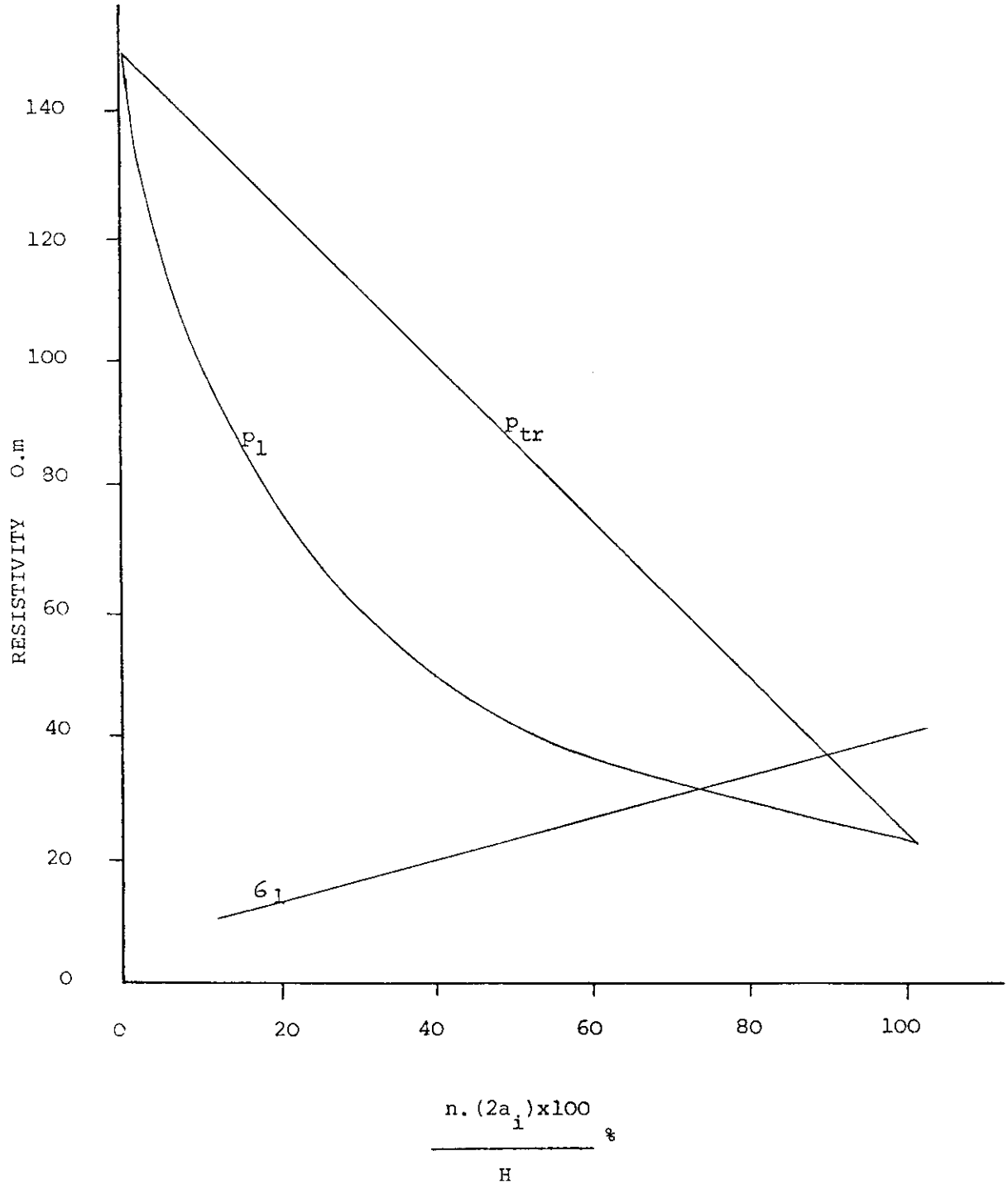


Fig. 6.15 Transverse resistivity P_{tr}, longitudinal resistivity P_l and longitudinal conductivity σ_l vs. fissure porosity

On the other hand, the transverse resistivity decreases rapidly over 150 ohm.m even for a small fraction of low resistance beds in the section.

From the above observation one can say that:

(1) the longitudinal resistivity is dominated by the fissures in the section.
(2) the transverse resistivity is less sensitive to the fissures in the section and depends more on the high resistive beds.

From the above analysis, it is evident that, even if it was possible to correct for the effect of limited bed thickness upon the measured apparent resistivity, it would not be possible to determine the geometric characteristics of the individual fissures (i.e. $2a_i$) from the values of p_{tr} or p_R, since both p_{tr} and p_R depend on the product n x $(2a_i)$, and different combinations of n and $(2a_i)$ can produce the same value for the product n x $(2a_i)$.

Although it has been shown that the values of the longitudinal and transverse resistivities are not adequate for getting a quantitative estimate of the opening of the individual fissures, hence their hydraulic properties, an accurate knowledge of the values of p_{tr} and p_l versus depth could be very useful in defining fissure zones.

By looking in the diagram of Fig. 6.15, one can see that fissures have a different effect upon the values of the longitudinal and transverse resistivities. From this result, it is logical to think that calculating the difference $p_{tr}-p_l$ and plotting this difference with depth would be very indicative of the degree of fissuring of the formation. It is worth noting here an important result which brought to light by Maillet and Doll (1932). These authors found that the resistivity measured with a system of electrodes aligned perpendicular to the bedding planes

is not affected by the effect of microanisotropy (produced by the microscopic structure of sediments), and that the values obtained are close to the values of longitudinal resistivity (Paradox of anisotropy). In the analysis presented in the present section, the strata were considered to consist of a series of isotropic beds whose resistivity were determined from the resistivity logs.

A theoretical proof of the fact that the difference $p_{tr}-p_l$ is more sensitive to the percentage of fissure volume per unit cross section is given below, for the simple case of Fig. 6.13.

From equations 6.35 and 6.38 one can write:

$$\rho_{tr}-\rho_l = h\cdot(\rho_1-\rho_2)+\rho_2-\frac{\rho_1\cdot\rho_2}{h\cdot(\rho_2-\rho_1)+\rho_1} \quad , h=(2a_i)\cdot n/H \longrightarrow$$

$$\rho_{tr}-\rho_l = -h^2(\rho_1-\rho_2)^2+h(\rho_1-\rho_2)^2 \qquad (6.41)$$

The latter shows that the difference between transverse and longitudinal resistivities depends on the second power of the percentage of fissure volume.

6.8.a Example of Borehole No. 5

Here the variation of the difference between p_{tr} and p_l versus depth is going to be examined for a real case. No reference is made here on how the data are treated, since this is described in detail in PART III of the thesis. The general approach followed is to divide the normal resistivity logs into a number of different zones and then to calculate for each zone an average value for p_{tr}, p_l and $p_{tr}-p_l$ which are considered representative for the specific interval.

Fig. 6.16 represents the variation of the difference $p_{tr}-p_l$

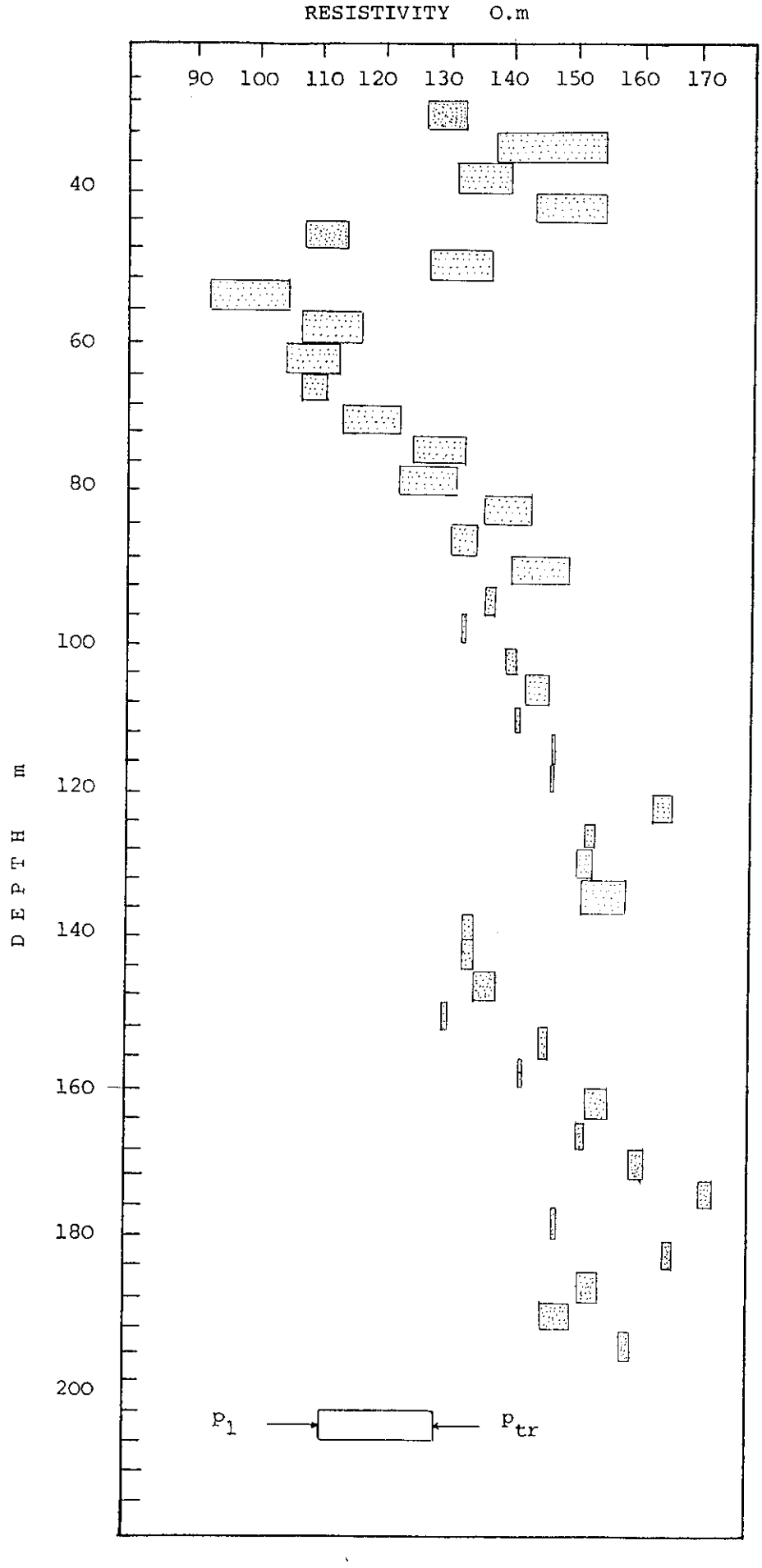


Fig. 6.16 Difference between transverse and longitudinal resistivities vs. depth

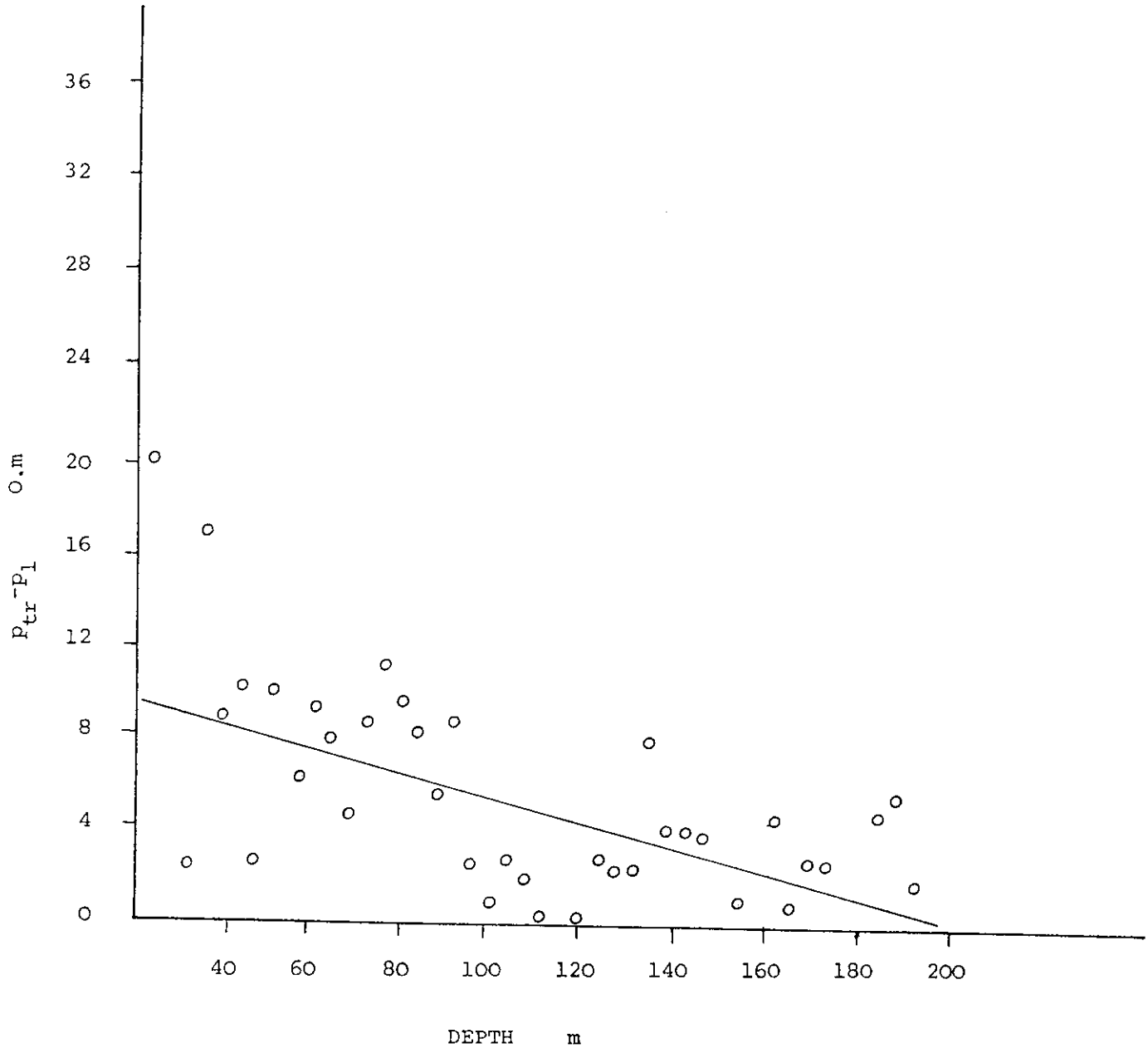


Fig. 6.17 Difference between transverse and longitudinal resistivities vs. depth with regression line fitted through the data.

as a function of depth for borehole No. 5 in Brighton, and shows that this difference tends to decrease with depth. This is shown more clearly in Fig. 6.17 where a regression line has been fitted through the data. This observation is in agreement with the well known fact that the degree of fissuring of the Chalk decreases with depth.

The difference between the p_{tr} and p_l values plotted as a function of depth is referred to as T-L log (Transverse-Longitudinal) and will be examined in detail in PARTS III and IV of this thesis. It is sufficient to note here that this T-L log holds considerable potential for the geophysical assessment of in situ hydraulic characters of fractured aquifers.

6.9 GENERAL CONCLUSIONS

In this Chapter the existing possibilities of measuring the hydraulic conductivity of a fissured formation from geophysical formation logs alone have been examined. After studying the formation factor-porosity relation (Archie's law) and its most common forms for the case of Chalk, a simplified double porosity model has been introduced in order to study the possible relations between geophysical formation parameters measured from the logs and hydraulic conductivity in detail.

The general conclusions reached can be summarised as follows:

(a) A quantitative measure of the degree of fissuring of the formation has been introduced by the "fissure index".

(b) A generalized form for the formation factor corresponding to a fissured formation has been evaluated and has been shown to be in agreement with existing results for the limited cases of pure porous and pure fissured formations.

(c) The way that the different formation parameters introduced by the model, correlate with each other has been given in a form of graphs or tables which show that they describe correctly the limiting cases.

(d) A theoretical relationship between the formation's fissure index and its hydraulic conductivity has been established and has explained the great difficulties encountered in the problem of deducing a quantitative value for the hydraulic conductivity from geophysical formation measurements alone.

(e) A general procedure for measuring the equivalent hydraulic conductivity of a fissured section from geophysical formation logs has been proposed although its application is limited by the present low level of accuracy in porosity measurements when carried out in high porosity formations such as the Chalk.

(f) A detailed investigation of the effect that fissures have upon some geoelectric parameters measured from the resistivity logs has been made and a new parameter, very sensitive to the degree of fissuring, has been introduced.

Since the analysis carried out in this Chapter has shown the advantages of knowing the values of some new parameters developed from standard geophysical logs, the next step in the present thesis will be to develop some fast and accurate methods for obtaining the above parameters. Obviously the only way to achieve this is by employing a microcomputer system, and this will be discussed in PART III.

PART III

The purpose of this Part is to describe the development of a microcomputer based software and hardware package for the automatic evaluation of the geophysical well logs.

Having already shown in Chapter VI how the different geophysical parameters measured by the logs could be linked together in order to provide, in certain cases, useful information about the hydraulic characteristics of the formation, the necessity of the existence of a method to process the data in a fast and accurate way becomes obvious. The amount of calculation involved in analysing a log is enormous and if one was to use standard hand calculating methods, the number of cases that could be studied would be very limited. In addition the difficulties of using the methods revealed by this research would prevent its application in practice.

The Part contains two Chapters: Chapter VII describes the hardware and software of the designed system and Chapter VIII describes the procedure for modelling the response from a geophysical normal resistivity tool; a procedure which could be very useful to the hydrogeologist and geophysicist when using normal resistivity logs to study fissure zones.

C H A P T E R VII

DESIGN OF A MICROCOMPUTER SYSTEM FOR THE AUTOMATIC EVALUATION OF THE LOGS

7.1 INTRODUCTION

In the previous Chapter, the importance of being able to process the information which is contained in the geophysical well logs was emphasized. It was also shown that certain parameters, such as the difference between transverse and longitudinal resistivities, could be very indicative in certain cases of the hydraulic characteristics of the formations logged. It is thus desirable to apply the proposed techniques to a number of real cases.

The geophysical log, by being a continuous signal representing the measure of some geophysical parameter, contains a large amount of information. One can thus see that any attempt to perform by hand all the necessary operations for the evaluation of the previously described parameters, would be a very tedious and time consuming process, thus only a few cases could have been examined. This is why it was decided, before proceeding in the discussion of some actual cases, to look for a fast and accurate method which could be used to perform all the necessary calculations. It was decided to use a microcomputer. The objective of the present Chapter is to describe the design of a cheap but effective portable microcomputer system, and its necessary software, that is able to evaluate geophysical well logs in a fast and accurate way. A number of useful computer algorithms have been designed and the problem of how to combine them in order to obtain a useful package for hydrogeologists and geophysicists is discussed.

7.2 CURRENT STATUS OF THE USE OF MICROCOMPUTERS IN HYDROGEOPHYSICAL LOGGING

Digital computing methods have proved to be very useful for the analysis of well log data and for the development of new techniques of data processing, and their use has resulted in a more accurate knowledge of the properties of the formations encountered. This is achieved by applying standard signal theory techniques to extract and enhance all the information which is included in the signal rather than treating the signal solely as a measuring device.

In the oil industry today, the advent of digital and logging equipment and associated interpretive software allows sophisticated handling of sonde calibrations, trouble-free logging operations, and accurate wellsite log interpretation analysis.

Logging engineers and geophysicists in the oil industry have been quick to adapt most of the log interpretation procedures to portable microcomputers and in doing so, they have eliminated much of the tedium of calculating by hand calculators, nomograms and charts. In the water industry, the digital processing of geophysical logs has just begun to be developed. This is probably due to the fact that it has taken a lot of time for the hydrogeologists to realize how useful the geophysical well logging methods can be for the solution of many hydrogeological problems. Most of the logs are interpreted from a qualitative point of view, which obviously does not require computer processing methods, apart from some applications in lithostratigraphic correlations. The main reason for this may be the fact that most of the instruments used in the water industry for geophysical well logging were designed with the qualitative use of the obtained geophysical logs in mind. Therefore, the obtained measurements were not suitable for quantitative work.

Furthermore, the full advantage of the geophyusical logs come when quantitatively interpreted on site; for example, they give an idea of the distribution of permeable beds permitting the correct placing of well screens etc. Obviously it is not possible for the small water contractor to carry with him a digital computer costing thousands of pounds, being very complicated in its operation and very sensitive to tough field conditions, and this may also have been a strong disincentive for the provision of logs and logging systems suitable for quantitative analysis. These probably are the main reasons which constrained the use of digital computers for the evaluation of geophysical logs in the water industry.

Recently, mainly due to an ever increasing use of geophysical well logging methods by the water industry, the growth rate of geophysically derived data has been increasing. In addition to this, the microelectronic revolution, which started a few years ago, has now come to a point where it can change the position of the computer in hydrogeophysical well logging. The new logging instruments, incorporating the microelectronic technology, have been very effective in the accurate measurement of the different physical parameters of the formations crossed by the well. In addition to this, the introduction of portable microcomputers in every-day life, costing less than £1,000, can be extremely useful to the water contractor. For these reasons, there is now new interest by hydrogeologists and geophysicists in the processing capabilities offered by the microcomputer.

7.3 DESIGN OF A MICROCOMPUTER SYSTEM - GENERAL REQUIREMENTS

This Section outlines the guiding philosophy behind the design of the microcomputer system and the development of its software. The system is designed to eliminate tedious,

time consuming and error-prone wellsite hand calculations and to permit new interpretation procedures by offering several unique advancements for fast, reliable, computerized interactive formation evaluation at the wellsite.

7.3.1 The Hardware

The development of the hardware of the system has been based on the following requirements:

- to provide a method to digitize the logs
- to provide a microprocessor to process the data
- to provide a system of data storage and retrieval
- to provide an interactive graphic system to display and update the information
- to be cost effective, simple, portable, fast and accurate

To fulfil the above requirements, a 6502 8-bit microprocessor based microcomputer was used and Table 7.1 shows the type and price of the instrument and auxillary equipment purchased.

TABLE 7.1

INSTRUMENT	MANUFACTURER-TYPE	1982 PRICE (£)
Digitizer	Lynton Computer System	1,400
Microcomputer	Acorn Atom	250
Printer	Microline 80	340
XY Plotter	Phillips	500
Recorder	Panasonic	45
TV Monitor	Boots Audio	70
D/A/D	Constructed (Acorn Type	100

7.3.2 The Software

Before proceeding in the description of the software package, it is essential to emphasize some basic principles.

Computer programs are available to perform operations on various classes of geological data, such data usually are used for statistical analysis, but other uses include mapping, reduction of geophysical measurements, modelling of geophysical parameters etc., such programmes are usually parts of large data-handling systems.

In the present case, what is needed is a set of programs to (i) replace the work of a human well log analyst and probably (ii) to derive some new methods of analysis which could be used on site to provide some useful information about the hydraulic characteristics of the different formations crossed by the well.

Since the software are mainly going to be used for on-site investigation, they have to run on a limited memory machine, they must be as simple as possible and also be economic in computing time.

As a part of the digital processing of the geophysical logs, it is generally required that the output from one program be used as an input to another program. Thus a computerized quantitative study of a series of logs might result in the steps shown in Fig. 7.1 below.

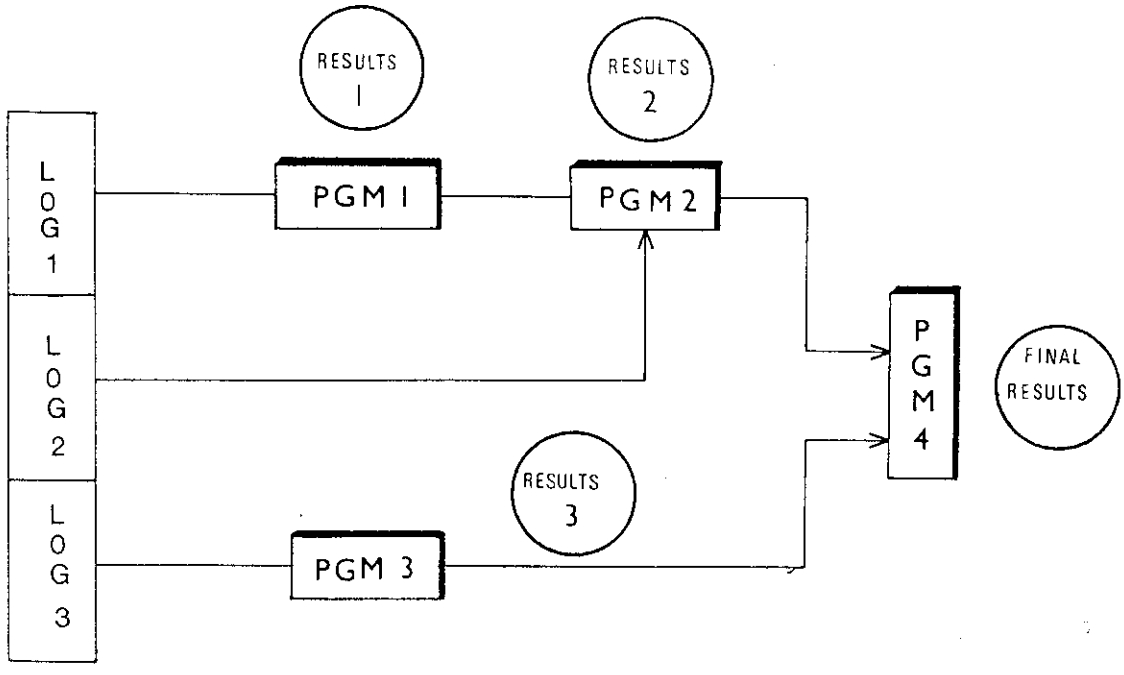


Fig. 7.1 Typical procedure for the automatic processing of geophysical logs

From the above, it is evident that several computer runs incorporating different programs would be required to do the various computations needed for the quantitative evaluation of the geophysical logs. In the following, the main requirements of the software package developed in this work are listed:

(1) simplicity of operation

(2) economy in program memory

(3) accuracy

(4) ability to apply various corrections on the log data

(5) ability to calculate various petrophysical parameters for a specific section of the well, defined by the operator

(6) ability to correlate between different logs

7.4 THE STRUCTURE OF A MICROCOMPUTER

Before proceeding with the details of how the data representing a geophysical log can be stored and processed by a microcomputer, it is essential to describe the general architecture of the computer.

The three main units of a computer are:

1. The central processor - the 'brain' of the computer - which, under the instructions of the computer program, co-ordinates and controls the activities of the other units, and performs all the arithmetic and logic processes applied to the raw data stored in the memory.

2. A storage - or memory - device which holds the instructions forming the computer program, and stores the raw information, ready for retrieval for processing. The computer's memory can be likened to a large number of locations or addresses each one containing a single number between zero and 255 (00000000 to 11111111 in binary). Computers use binary code to store information, so the largest number that can be held in an address in binary is 11111111, which is eight bits (Binary Digits) long. This unit of eight bits is often called a byte. A computer with one byte (1K) of memory has 1024 bytes. In cases where numbers greater than 255 have to be stored by the computer, it is possible (by a dimension statement) to set aside four bytes for each number so that values approximately between minus 2000 million and 2000 million can be stored.

3. Input and output devices - the peripherals - through which data are fed into and read out of the computer.

7.5 ORGANIZATION OF THE INFORMATION CONTAINED IN THE LOGS

In order to be able to process with a digital computer the analog information represented by the logs, a sampling technique of digitization must be used for converting all the analog signals into digital form. In doing so, one can incorporate an analog to digital converter in the output of the logging instrument, in order to record the analog signal directly in a digital form or, in the case where the information already exists in the form of logs, to use a digitizer.

The digitization of geophysical logs must take into account a number of important considerations. These involve the precision with which the log should be sampled and how often the samples should be taken.

A basic sampling theorem states that in order to reconstruct any given signal from discrete samples, the

sampling frequency must be at least twice that of the highest frequency which is desired to be maintained in the sampled digitized signal. This is known as the Nyquist theorem, and the limit of the frequency which can be reconstructed from a given sampling rate is often termed as Nyquist frequency.

Another very important section of the Nyquist theorem states that not only will frequencies higher than the limit imposed by the sampling rate be lost, but they will also produce a false signal which will appear as a much lower frequency. This process is defined as aliasing.

Fig. 7.2 illustrates an example of a 64-inches resistivity log carried out at borehole No. 1 in Brighton. If the log were to be reconstructed from a number of sample points picked up through a digitization process from the original analog signal, the accuracy of the resulting log would depend on the digitization interval. As this figure shows, most of the essential details of the original log are present in the two-meters sampling process although some thin streaks have been lost. If the log had been sampled every four or eight meters, then the reconstructed log would have lost considerable detail, as it is shown in the figure. In the present work, the digitization interval taken was 0.2m, and was considered to be more than adequate to prevent any aliasing effects. The usual depth scale of the logs is 2m/cm, and thus a digitizing interval of 0.2m means that a sample is taken every one millimeter of actual log record and that for 200m of logged formation, one takes 1000 numbers. If these numbers are scaled to be between 0 and 255 in value (see Section 7.4), then it is possible to allocate only a single byte of computer memory per number, instead of four. (A set of numbers stored in this way is called a byte vector). This is especially useful when memory is restricted.

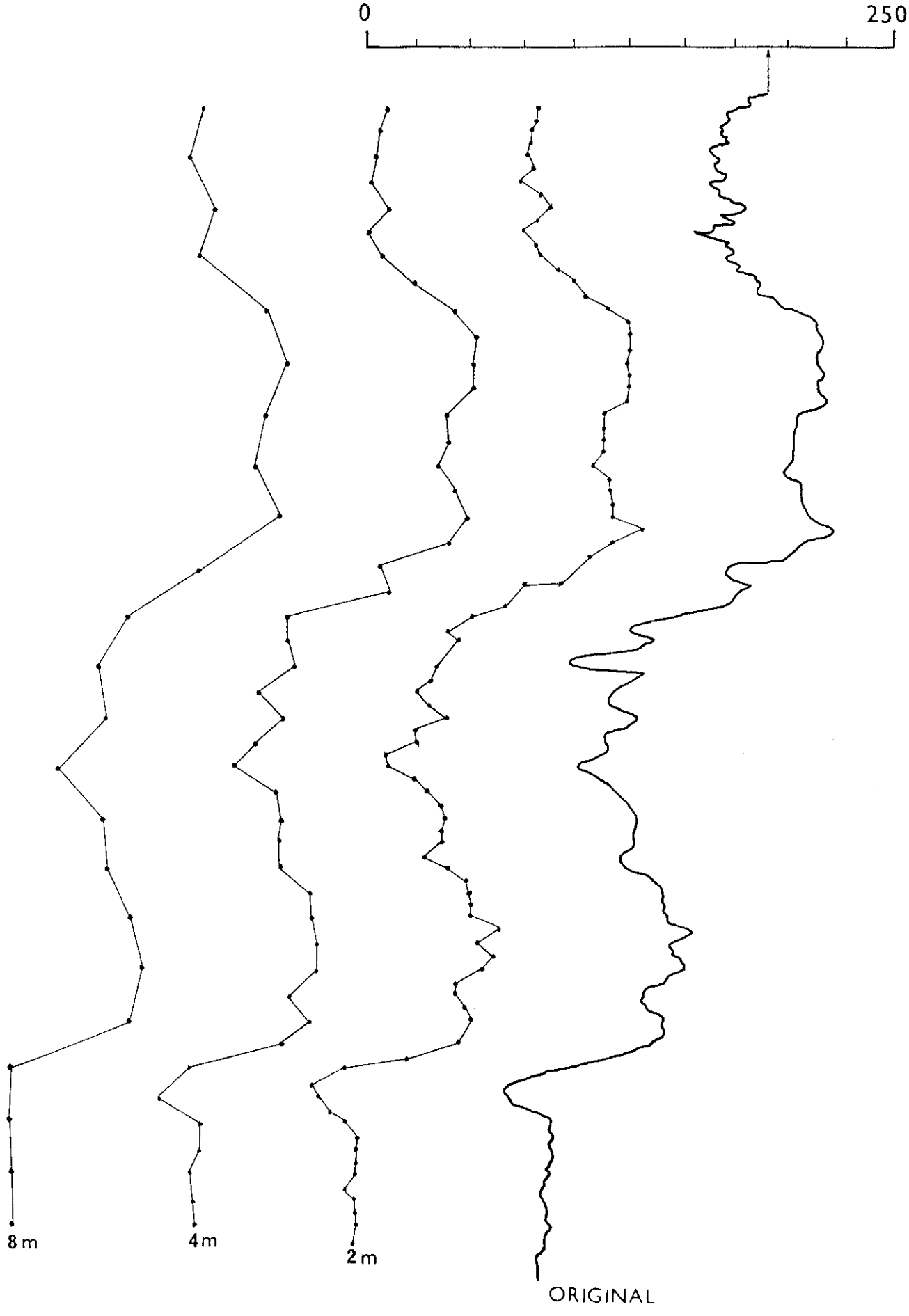


Fig. 7.2 Example of log digitization with different sampling intervals

From the above one can see that the memory requirements for storing a geophysical log representing 200m of logged strata are 200m x (1/0.2m) = 1000 bytes = 1K byte

Together with the sample data, one must provide information about the kind of the log being digitized, the construction characteristics of the well, its location etc. in order to create an efficient data bank that is easy for later use. A special program was written to ask the operator during the digitization process about the above information which is automatically stored in the first 100 bytes of the byte vector representing the sampled data themselves. A printout of this information is listed below.

```
--------------------

WELL No: 7
TYPE OF LOG: 16N
TOTAL DEPTH: 200m
BIT SIZE: 200mm
CASING: 20.5m
DATE: 16-6-76

--------------------
```

7.6 CORRECTIONS

Theory and experience demonstrate that geophysical logs yield "apparent", rather than "true" values of the petrophysical properties which they reflect. Whether or not the apparent values read off the logs can be corrected back to the true values depends upon the facts of each individual situation. The gap between apparent and true values in a given formation depends upon the following elements:-

1. the nature of the property being measured

2. the property contrast with the adjacent formation

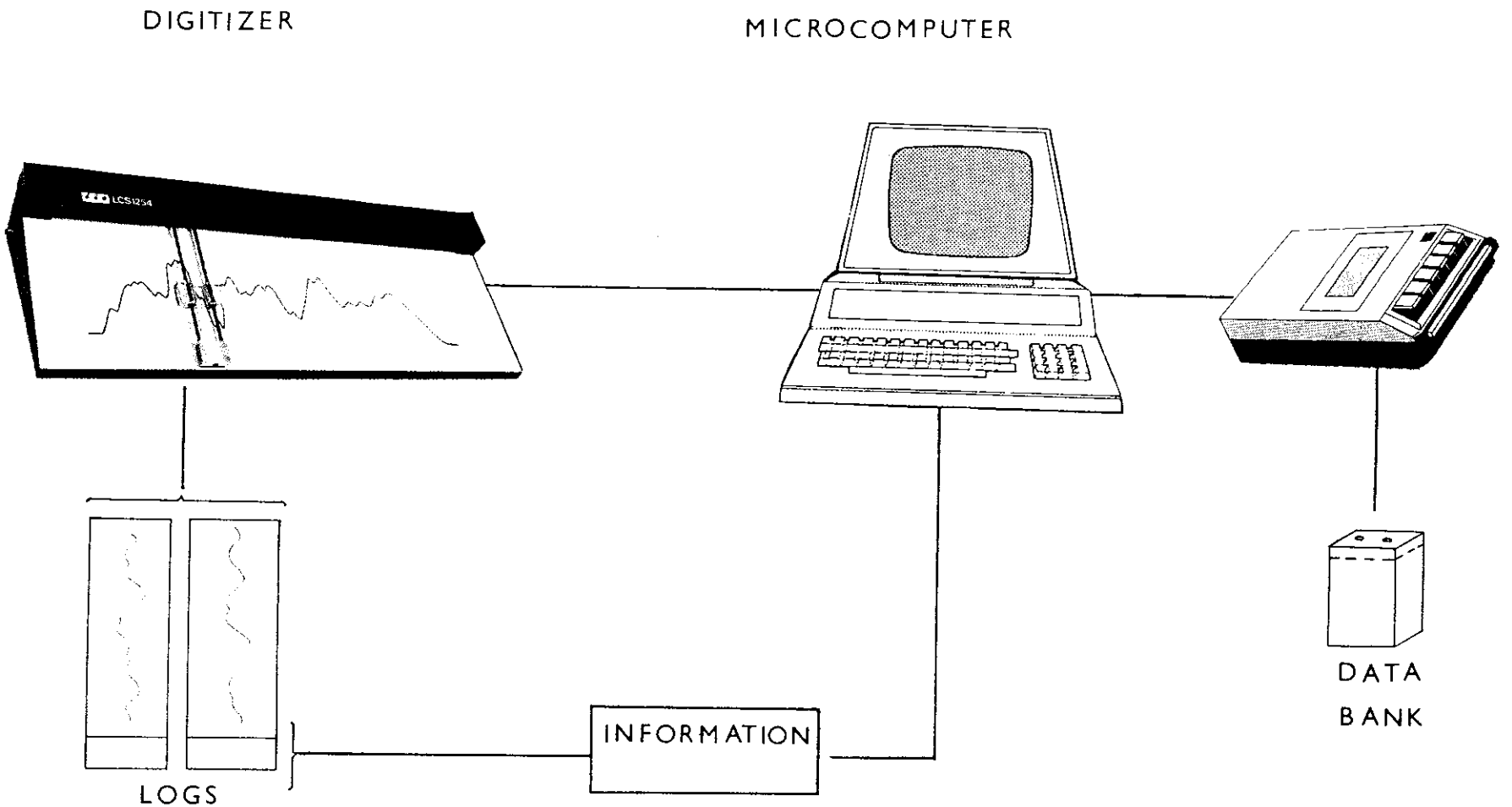


Fig. 7.3 Arrangement used for the automatic processing of the logs

3. the spacing of the device

4. the thickness of the given volume possessing the true property value considered

5. the diameter size of the hole

6. the properties of the water (fluid) filling the hole

7. the position or "eccentricity" of the device with relation to the walls of the hole

8. the effect of noise on the measurements

Since the spacing of the logging devices have non-negligible dimensions, all logs mark the boundary from one true level of properties to another true level by "transition patterns" straddling the boundary, rather than by sharp, instant level change at the boundary. Again the shapes of transition patterns and the thickness over which they extend depend upon all the elements listed above.

Generally speaking, the following facts should be remembered when selecting values from logs:

(a) Apparent property values shown by transition patterns are most generally beyond correction. The one use of such patterns is to indicate that changes in property level occur.

(b) For a device of given spacing, the property logged must maintain the same level over a minimum thickness before this level can make its existence known on the log.

(c) Because of geometrical effects, apparent values suitable for possible corrections and use in quantitative analysis appear in the form of peaks or plateaus towards the high property levels and depressions or valleys towards the low property levels.

(d) Again, for a device of a given spacing the property logged must maintain the same level over a certain thickness if the log is to yield a "representative point" or preferably a "representative segment" for that level, whose apparent value can be adequately corrected for thickness and fluid effects, thus resulting in a value that is sufficiently good to be entered into the relationships for later quantitative analysis. This thickness again is a complex function of the factors a,b,c previously stated.

In the following the problem of obtaining true resistivities from the apparent resistivities shown in the normal resistivity logs is going to be examined.

7.6.a Corrections for changes in the conductivity of the fluid column

It has already been stated in CHAPTER IV of this thesis that the formation resistivity when measured with a normal resistivity device depends upon the conductivity of the fluid column and the diameter of the well. The functional relation between the apparent resistivity shown by the logs, the true formation resistivity, the conductivity of the fluid column and the diameter of the well is calculated from Eq. 4.9.

A common method which is used in the water industry today for the determination of true resistivity values from the apparent resistivities measured by the normal resistivity logs, is to use a graphical representation of Eq. 4.9 sometimes known as departure curves. Obviously in the present case where the microcomputer has to perform all the necessary corrections, these departure curves are of little use. On the other hand, any attempt to program the microcomputer to perform the mathematical operations described by equation 4.9 would result in a substantial loss of memory and computing time.

The method adopted in the following discussion was to represent each one of the departure curves corresponding to different well diameters, by a third degree polynomial through a least squares process.

The departure curves used were taken from the manual "LOG INTERPRETATION CHARTS", page 46, published by Schlumberger Inc. 1969. An adequate number of evenly distributed points was picked from the curves. These points were fitted by a cubic polynomial using the subroutine E202 of the CERN Library.

According to the above the true resistivity can be written:

$$\rho_{tr} = \rho_f \cdot \left[A \cdot \left(\frac{\rho_a}{\rho_f} \right)^3 + B \cdot \left(\frac{\rho_a}{\rho_f} \right)^2 + C \left(\frac{\rho_a}{\rho_f} \right) + D \right] \qquad (7.1)$$

where the values for the constants A, B, C and D are given in Appendix A.7.3. Because of the great importance of the subject of curve fitting, a special APPENDIX has been included in the present Thesis. In it the necessary elements of the theory are presented together with a computer program for curve fitting written in Standard Basic. Programming a microcomputer to perform the above correction is an easy process. One has to start from the memory map of the particular microcomputer used (see APPENDIX A.7.1) and define three spaces. One for the program which has to carry out the calculations, one for the apparent resistivity values contained in the log and one for the fluid conductivity values. The results of the calculation (true resistivity values) can be sent directly to an output device (printer, cassette, disc), written over the apparent resistivity values, or stored in a 4th place in the computer's memory for use in a latter stage.

7.7 ZONATION OF THE LOGS

A common technique used during the interpretation of geophysical logs is to employ a zonation process. By this method, a number of boundaries that divide the log into intervals are selected such that the measurement being considered is relatively constant compared to the change in the measurement from that interval to the depth adjacent intervals. For example, the following Fig. 7.4 is a schematic representation of a part of the 16N resistivity log of Borehole No. 5.

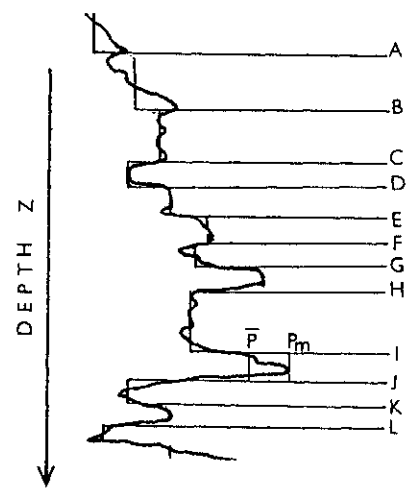


Fig. 7.4 Typical zonation of a log

The log consists of measurements of some value P (resistivity in this case) displaced as a continuous function of depth z. A log interpreter might, by visual inspection, select a number of zone boundaries as shown in Fig. 7.4. In addition to the zonation, the interpreter has to select a representative value of P in order to represent any interval, say I-J. The average value of P within the interval is often used.

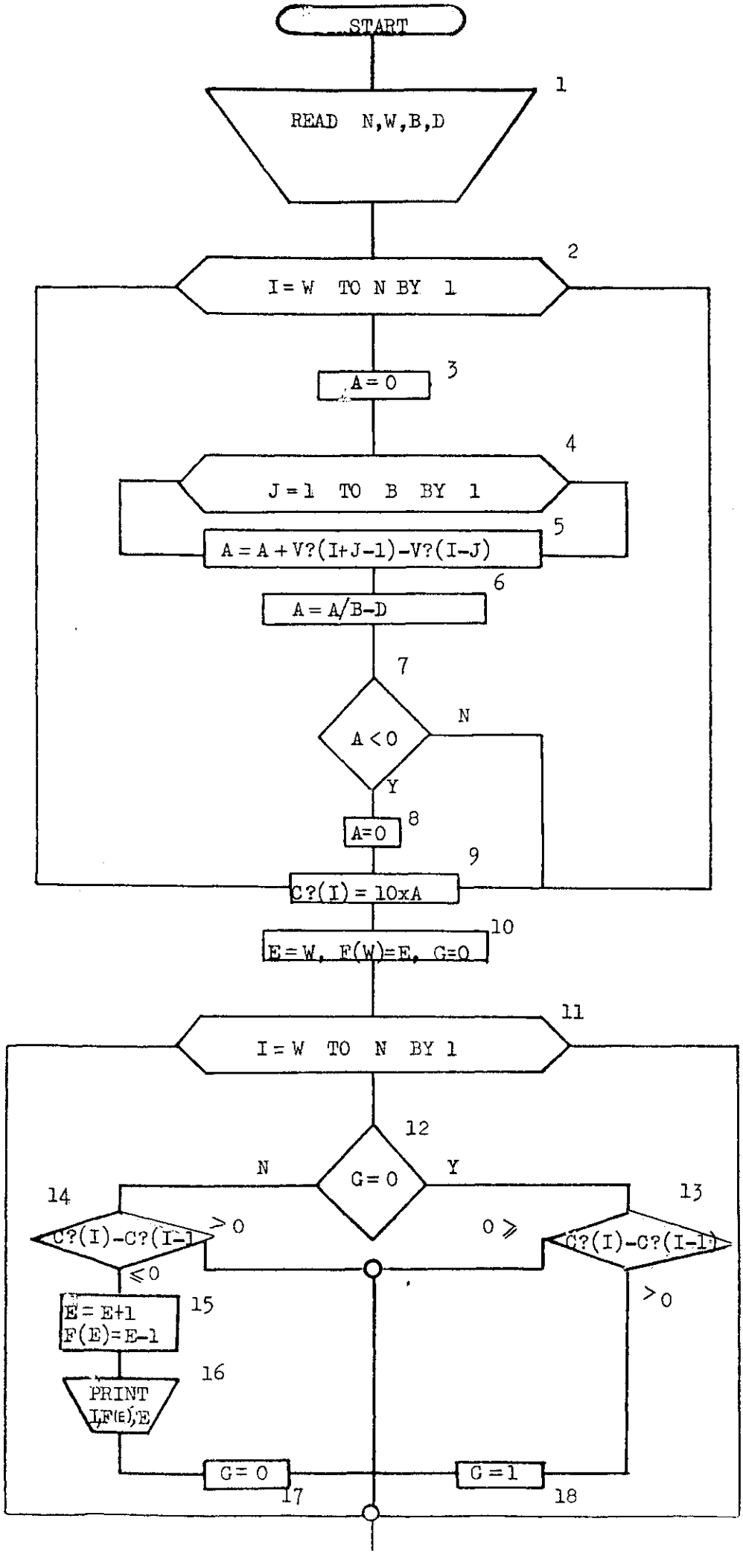
In order to design the algorithm for the automatic zonation of the logs, one can either use the variation of the data with depth, by locating the different boundaries at points where the data exceed a pre-defined threshold value, or use some functional relation of the data. Such a function could be, for example, the standard deviation of a number of data or their average value. In the literature, there are quite a few such algorithms for the zonation of sequences of data. (Testerman 1962; Gill 1970; Hawkins et al 1978; Webster 1978). Since these algorithms were mainly designed for use with large computers and in the present case the software have to be compatible with the restrictions imposed by microcomputers an N point moving average of the data was used. A similar technique was used by Sounder et al 1973.

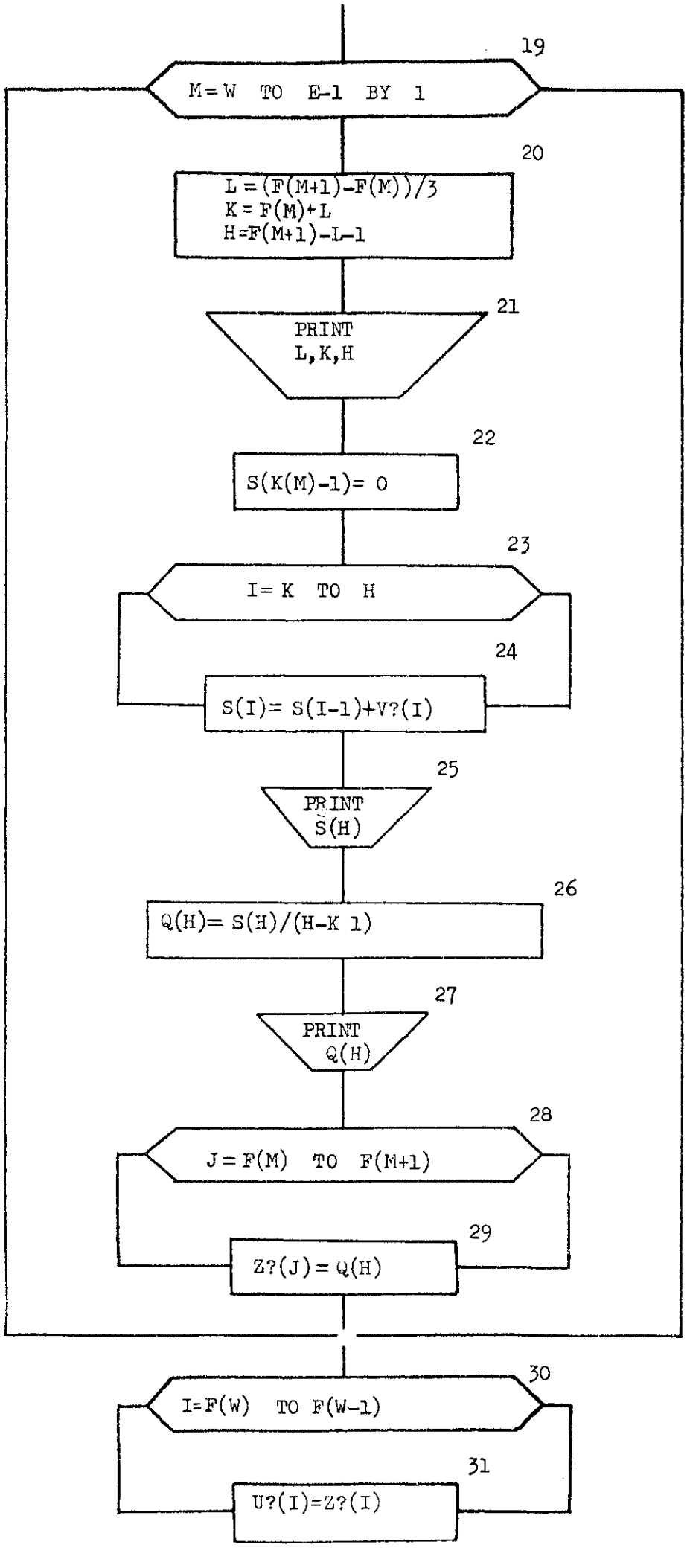
7.7.1 The Program "WINDOW"

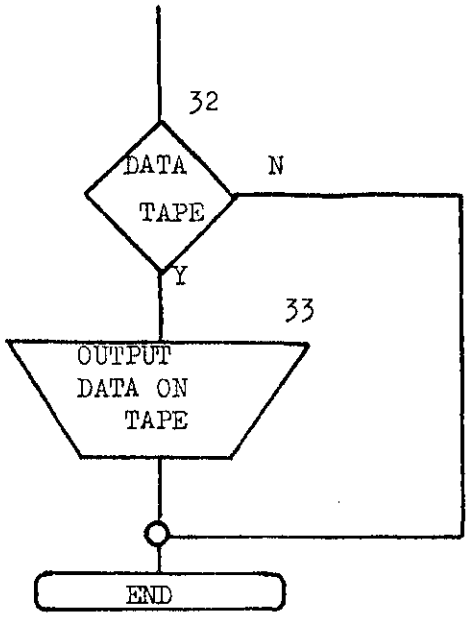
A computer algorithm was designed by applying the N point moving average technique of Sounder et al (1973). The way in which the algorithm operates is as follows. An average amplitude of a segment consisting of N data is compared to the average amplitude of the adjacent segment. If the difference between the two averages are greater than a predefined threshold value D, the program assigns a zone boundary at the corresponding point.

After the zone boundaries have been chosen, the program divides each zone by 3, and then computes the mean value of the central portion, assigning the later to the total zone interval. It is also possible, by a small modification of the software, to use a picked value for each zone instead of a mean value.

Fig. 7.5 shows the detail structure of the algorithm designed for this.


START
1
READ N,W,B,D
2
I = W TO N BY 1
3
A = 0
4
J = 1 TO B BY 1
5
A = A + V?(I+J-1) - V?(I-J)
6
A = A/B-D
7
A < 0
N
Y
8
A=0
9
C?(I) = 10xA
10
E = W, F(W)=E, G=0
11
I = W TO N BY 1
12
G = 0
N
Y
13
C?(I)-C?(I-1)
> 0
0 ⩾
14
C?(I)-C?(I-1)
> 0
⩽ 0
15
E = E+1
F(E)=E-1
16
PRINT
I,F(E),E
G = 0
17
G = 1
18


19
M=W TO E-1 BY 1
20
L=(F(M+1)-F(M))/3
K=F(M)+L
H=F(M+1)-L-1
21
PRINT
L,K,H
22
S(K(M)-1)= 0
23
I= K TO H
24
S(I)= S(I-1)+V?(I)
25
PRINT
S(H)
26
Q(H)= S(H)/(H-K 1)
27
PRINT
Q(H)
28
J=F(M) TO F(M+1)
29
Z?(J)=Q(H)
30
I=F(W) TO F(W-1)
31
U?(I)=Z?(I)


32
DATA
TAPE
N
Y
33
OUTPUT
DATA ON
TAPE
END

At step 1, the operator enters the number of data, N, which have to be processed, the starting point W, the width of the smoothing interval B and the threshold value D. A loop is initiated at Step 2, and Step 3 sets the dummy parameters, A, to null each time loop 2 is executed. Loop H is initiated each time loop 2 is executed and the computation of function

$$\frac{1}{B}\left|\sum_{j=1}^{i+N-1} V_j - \sum_{j=i-N}^{i-1}\right| - D \qquad (7.2)$$

is made and assigned to A, where V_j is the array containing the data from the digitized log. Steps 7 and 8 force A to be positive or zero and in Step 9 the value of A for each I from 1 to N is stored in the array C(I). Step 10 assigns initial values to the dummy variables E, F(W), G and indicates the location of the first zone boundary as the starting point on the log N. The parameter G is a device by which the computer will compare two successive points in the data array C(I) to determine if one of such points is a maximum in that local region of the array. E is a counter that will be increased by unity each time a maximum is found so that at the completion of loop 11 the value of E will be the total number of zone boundaries. At step 12, G is tested to be "true" (moved towards a maximum from I-2 to I-1) or "False" (moved away from a maximum). If "false", C(I) is tested against C(I-1) in step 13 to determine whether C(I) is increasing or decreasing in magnitude. If it is not increasing, control is simply passed to the end of the loop and loop 11 continues. If C(I) is increasing, G is changed to "true" in Step 18 and control passes to the end of the loop. If G is "true" in test 12, C(I) is compared to C(I-1) in Step 14. If C(I) >C(I), (the magnitude continued to increase), control is passed to the end of the loop. Note that C(I) <C(I-1), means the array has passed the maximum which was at I-1. Therefore E is updated and the array F(E), which contains the zone boundaries, is set to E-1. Next G is set to "false" and

control passes to the end of the loop. In 19, a loop is initiated which will step the value of M through all the zones. Step 20 calculates the length of the subzones lying adjacent to the zone boundaries and the middle subzone. K is the location of the upper boundary of the middle subzone and H is the other boundary. At Step 22, the variable S is set to zero. Step 23 initiates a loop which will cycle the dummy index I from the first point K of the middle subzone to the last point H of the middle subzone. At the end of the loop in Step 24, the accumulating variable S will be the sum of all the data V(I) lying on the middle subzone. The value of S is divided by the length of the middle subzone to obtain the average value of the amplitudes lying on the middle subzone in Step 26. This average value is given a subscripted variable Q(H), and is assigned to the corresponding zone in Steps 29 to 31.

A program "WINDOW" was written in a Basic dialect (ATOM'S BASIC) from the above algorithm and is presented in APPENDIX A.7.4.

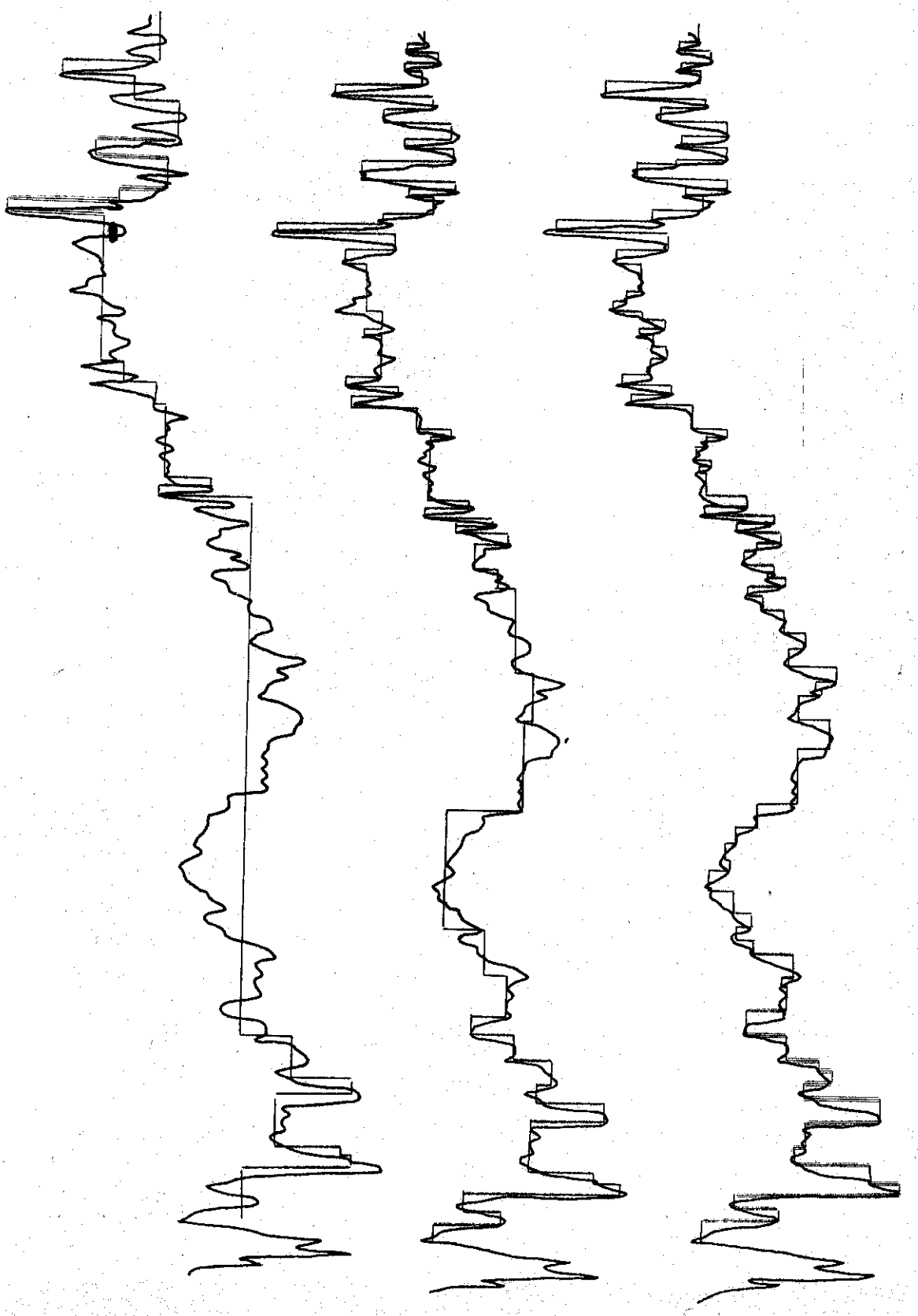
The following Figure 7.6 contains one example of the automatic zonation which was carried out by the above program for the 16-inches resistivity log of Borehole No. 5 in Brighton. Three different values for the parameters B and D were used and resulted, as one can see from the figure, in a change in the accuracy of the zonation process. Table 7.4 contains some values of the parameters used by the program in part of the above log.

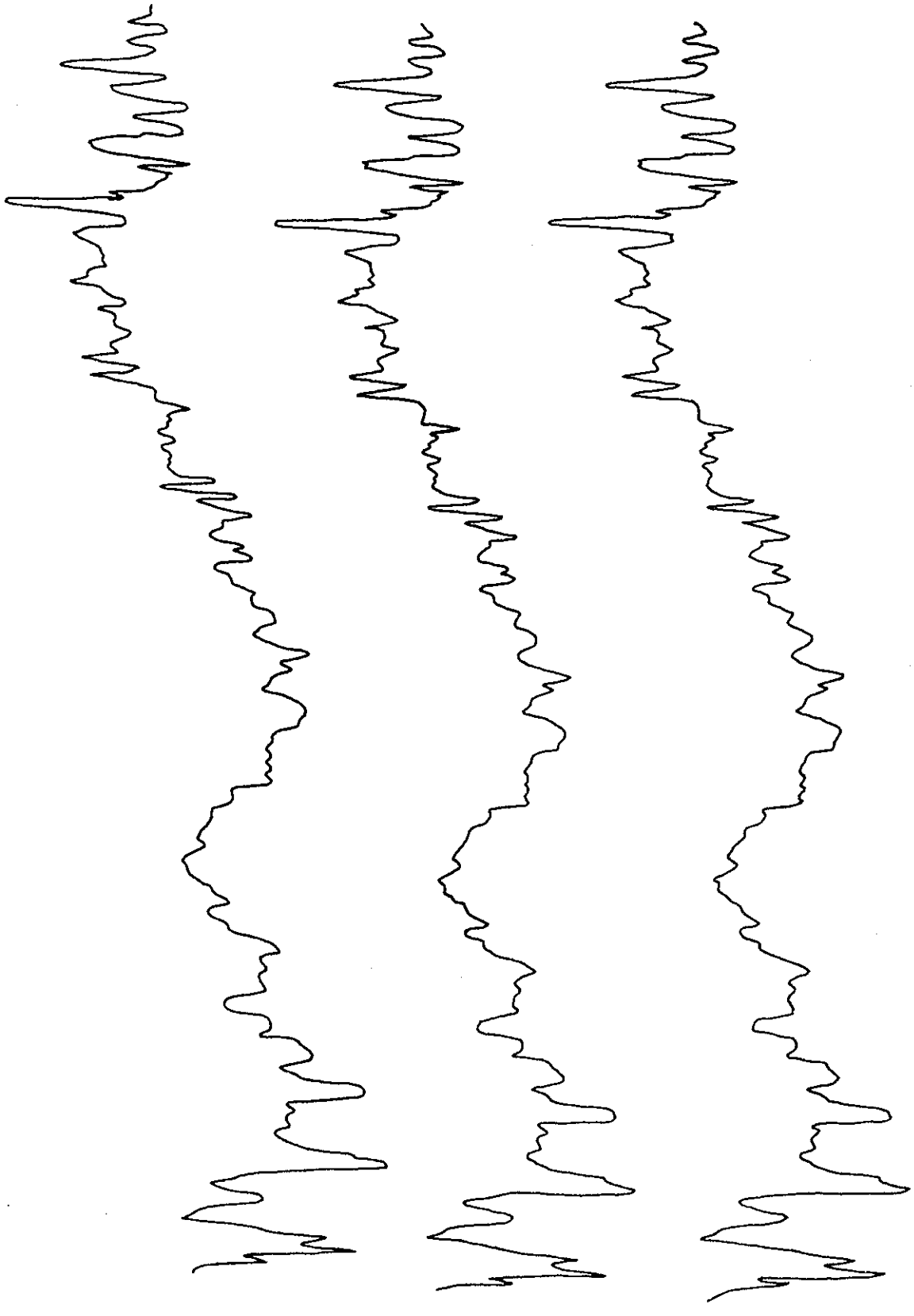
7.8 EVALUATION OF THE FORMATION PARAMETERS

The use of electrical resistivity well logs for the direct evaluation of the formation geoelectric parameters, and from them the T-L logs, is very important since in certain cases it can provide an indication of the formation's hydraulic properties, as has been shown in Chapter VI.

Fig. 7.6 Examples of the zonation of a geophysical log by using program "WINDOW"

D=8 , B=2 D=4 , B=2 D=2 , B=2





The purpose of this paragraph is to set the theoretical basis of a procedure which could be used with a microcomputer for the fast and accurate evaluation of the formations geoelectric parameters, and the T-L log from normal resistivity logs.

It is reasonable that equations 6.35 and 6.37 of Chapter VI might be used directly in compiling average transverse and longitudinal resistivities from electric logs. A log would be interpreted in terms of a series of beds, each having a specific thickness and resistivity. However, it is felt that this procedure would be too tedious for a microcomputer. The procedure used in the following analysis is based on the fact that the sums involved in equations 6.35 and 6.37, which give the transverse and longitudinal resistivities, were not ordered. Thus if there are several beds with the same resistivity, they could be replaced by a single bed having the same resistivity, and thickness equal to the sum of the thicknesses of the single bed.

By sampling a specific section H, of the log, randomly, one could estimate the equivalent portion of the section having any particularly resistivity, and from this construct the resistivity frequency distribution, with a density function $N(\rho)$. The transverse and longitudinal resistivities may now be directly computed as follows:

$$\rho_{tr} = \frac{\int_0^\infty \rho \cdot (\rho) \cdot d\rho}{H} \tag{7.3}$$

$$\rho_{l} = \frac{H}{\int_0^\infty \frac{N(\rho)}{\rho} d\rho} \tag{7.4}$$

The determination of a resistivity frequency distribution has been the approach used in the following. A computer algorithm was designed to perform all the necessary calculations and Fig. 7.7 shows the way in which this algorithm treats the data.

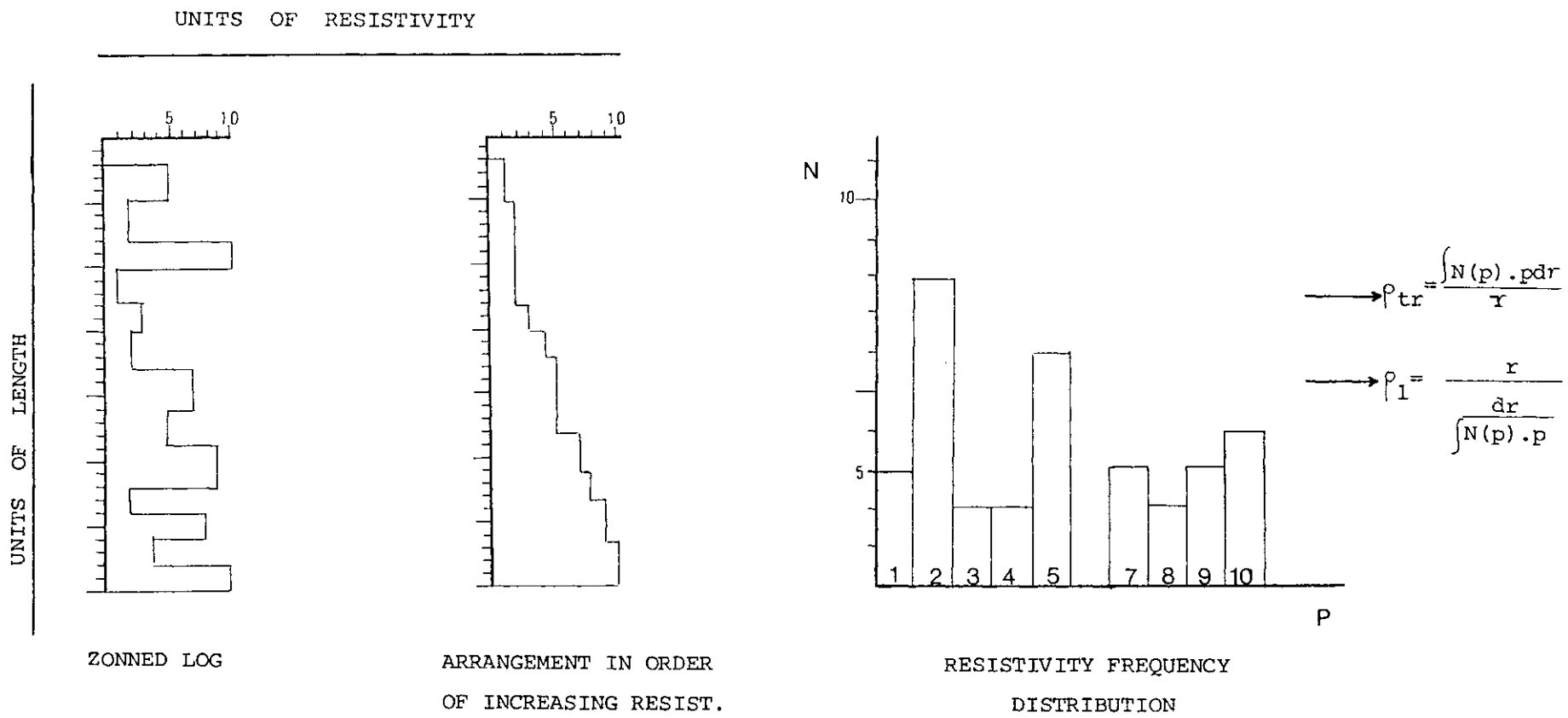


Fig. 7.7 Diagram showing the manipulation of the data

Fig. 7.8 contains the detailed structure of the above algorithm. A computer program was written to perform the above operations and is presented in APPENDIX A.7.7. Table 7.2 contains a sample output of this program.

```
***INTERVAL BETWEEN68.0000000METERS AND72.0000000METERS***
TRANSVERSE RESISTIVITY IS150.6000000.m
LONGITUDINAL RESISTIV.  IS141.8469280.m
Rtr-Rl IS:8.753072200.m
ANISOTROPY INDEX IS1.03039210

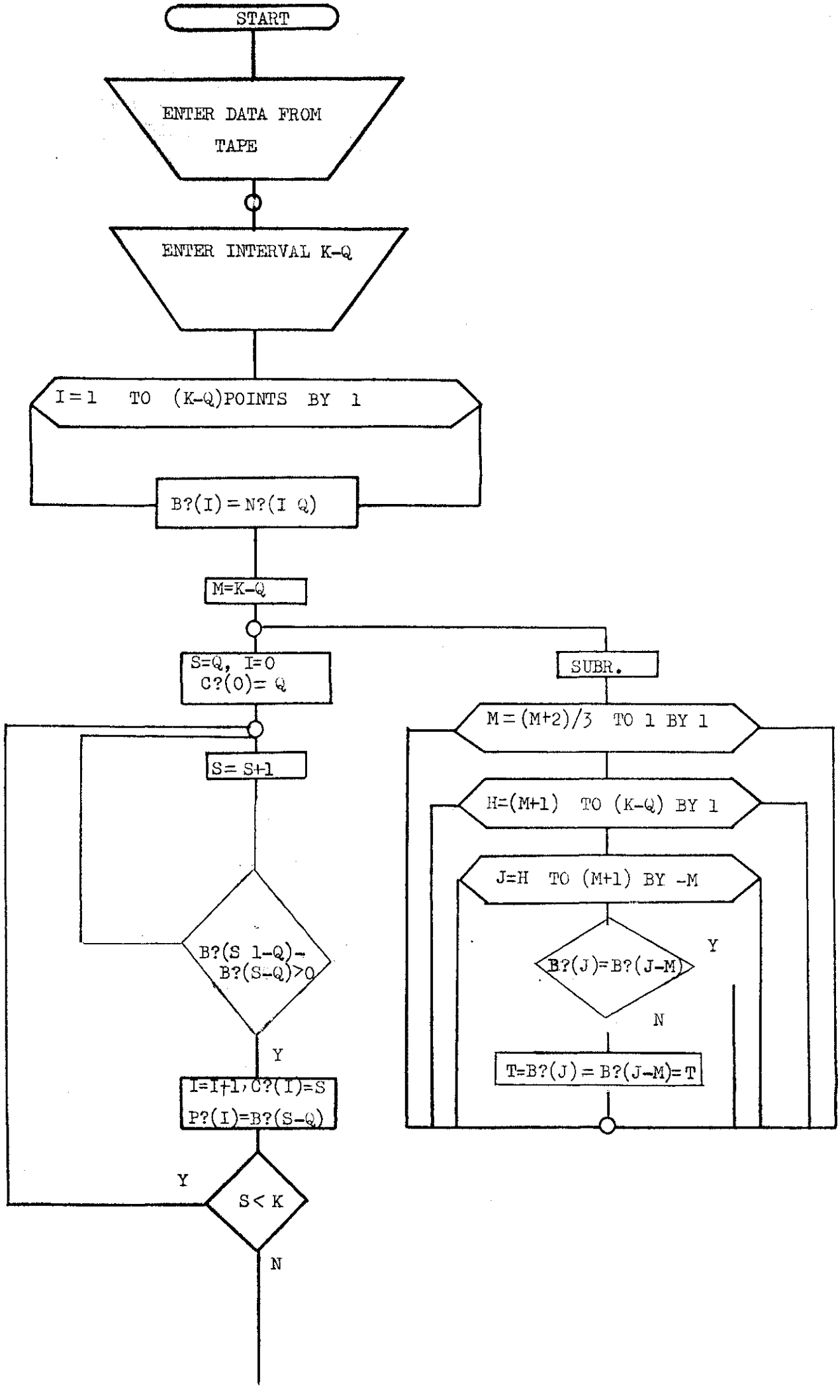
INTERVAL'S DATA ARE
     137     137     125     125     125     125     131     131     131     131
     205     205     140     140     140     131     131     131     131     131
SORTED DATA ARE:
     125     125     125     131     131     131     131     131     131     131
     131     131     131     137     137     140     140     140     205     205
     364     125
     373     131
     375     137
     378     140
     380     205
RES. DISTRIB. FROM72.0000000TO76.0000000METERS
-------------------------------------------------
       4     125
       9     131
       2     137
       3     140
       2     205
***INTERVAL BETWEEN72.0000000METERS AND76.0000000METERS***
TRANSVERSE RESISTIVITY IS179.1500000.m
LONGITUDINAL RESISTIV.  IS136.5322850.m
Rtr-Rl IS:2.617714460.m
ANISOTROPY INDEX IS1.00954091

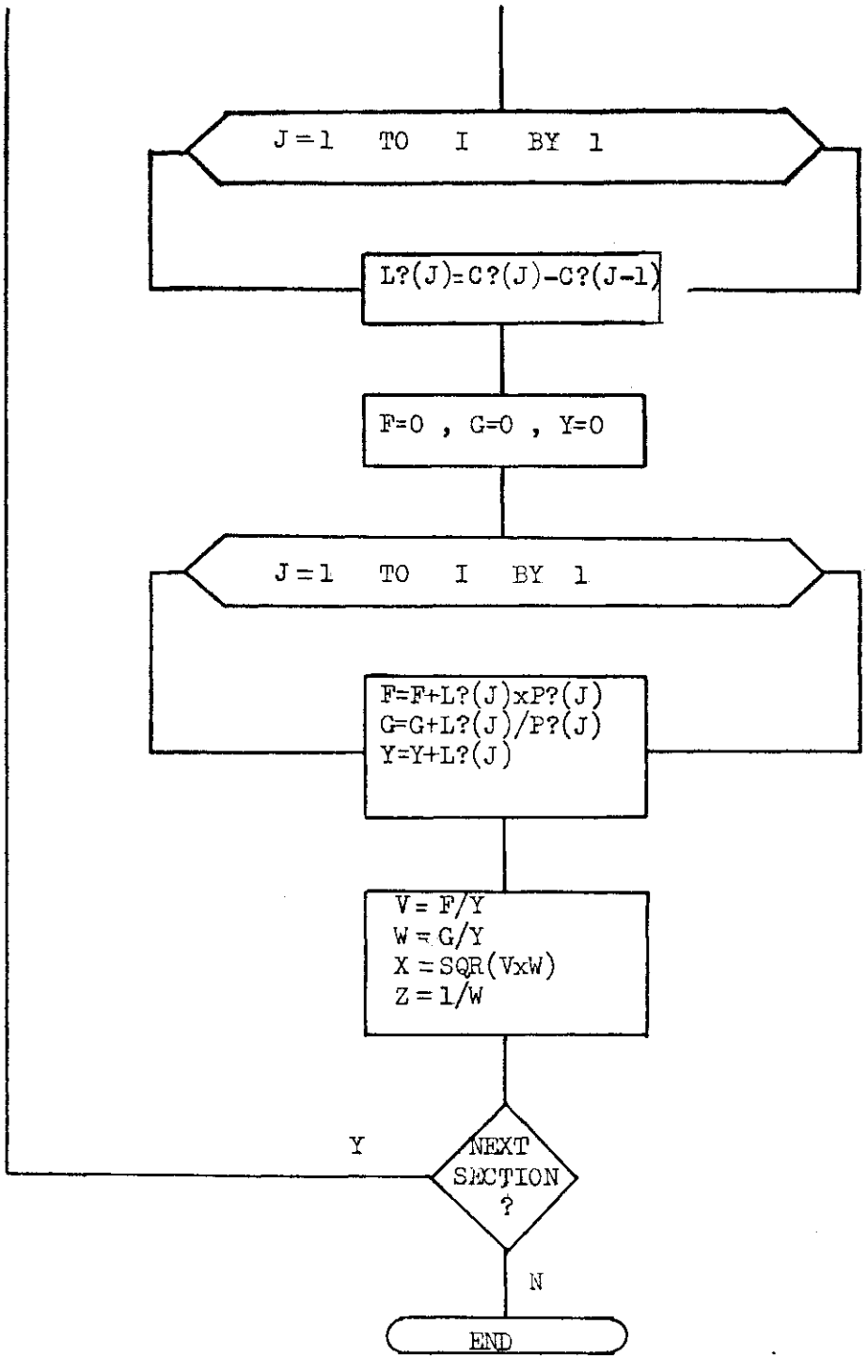
INTERVAL'S DATA ARE
     131     131     131     131     131     131     131     131     131     131
     131     138     138     138     138     138     138     138     138     141
SORTED DATA ARE:
     131     131     131     131     131     131     131     131     131     131
     131     138     138     138     138     138     138     138     138     141
     391     131
     399     138
     400     141
RES. DISTRIB. FROM76.0000000TO80.0000000METERS
-------------------------------------------------
      11     131
       8     138
       1     141
```

Table 7.2 Sample output from program "WINDOW"

7.9 DIGITAL FILTERING OF LOGS

The processes of smoothing, differentiating, integrating and removing noise from measurements are very common options. Often such processes are linear transformations on the data and here is where the great importance of digital filters comes, since a digital filter is a linear


START
ENTER DATA FROM TAPE
ENTER INTERVAL K-Q
I=1 TO (K-Q)POINTS BY 1
B?(I)=N?(I Q)
M=K-Q
S=Q, I=0
C?(0)=Q
S=S+1
B?(S 1-Q)-B?(S-Q)>0
Y
I=I+1, C?(I)=S
P?(I)=B?(S-Q)
Y
S<K
N
SUBR.
M=(M+2)/3 TO 1 BY 1
H=(M+1) TO (K-Q) BY 1
J=H TO (M+1) BY -M
B?(J)=B?(J-M)
Y
N
T=B?(J)=B?(J-M)=T


J = 1 TO I BY 1
L?(J)=C?(J)-C?(J-1)
F=0 , G=0 , Y=0
J = 1 TO I BY 1
F=F+L?(J)xP?(J)
G=G+L?(J)/P?(J)
Y=Y+L?(J)
V = F/Y
W = G/Y
X = SQR(VxW)
Z = 1/W
NEXT SECTION ?
Y
N
END

compilation of the input data and possibly the output data, and includes many of the operations that are performed when processing a signal.

In the following paragraphs, various types of digital filters are introduced and their application to the evaluation of geophysical logs used by the water industry will be discussed. One of the most obvious types of data filtering is the smoothing by a simple moving average. The smoothed value P is calculated as

$$\bar{P} = \frac{\sum_{i-k}^{i+k} P_j}{m} \qquad (7.5)$$

where:

k = (m-1)/2
m is the length of the smoothing interval.

One of the most serious consequences of this type of filtering is the shift of peaks and troughs in the smoothed curve. Fig. 7.9 represents a digitized 16N log of Borehole No. 5, and the log smoothed by 5-, 10-, 15-, and 20-term moving average filtering. Note how the long term features of the record are emphasized at the expense of shorter variations.

In Fig. 7.10, the 64N log of the same borehole is included and is compared with the 20-term average version of the 16N. Note the similar appearance of the 20-term filtering of the 16N and 64N logs.

Fig. 7.11 contains the caliper log of the same borehole together with its versions filtered by 5-, 10- and 15- term moving average filters. From this example, one can see that th high frequency content of the log is reduced drastically when the moving average filter used is more than 5 terms long. Obviously when filtering very high

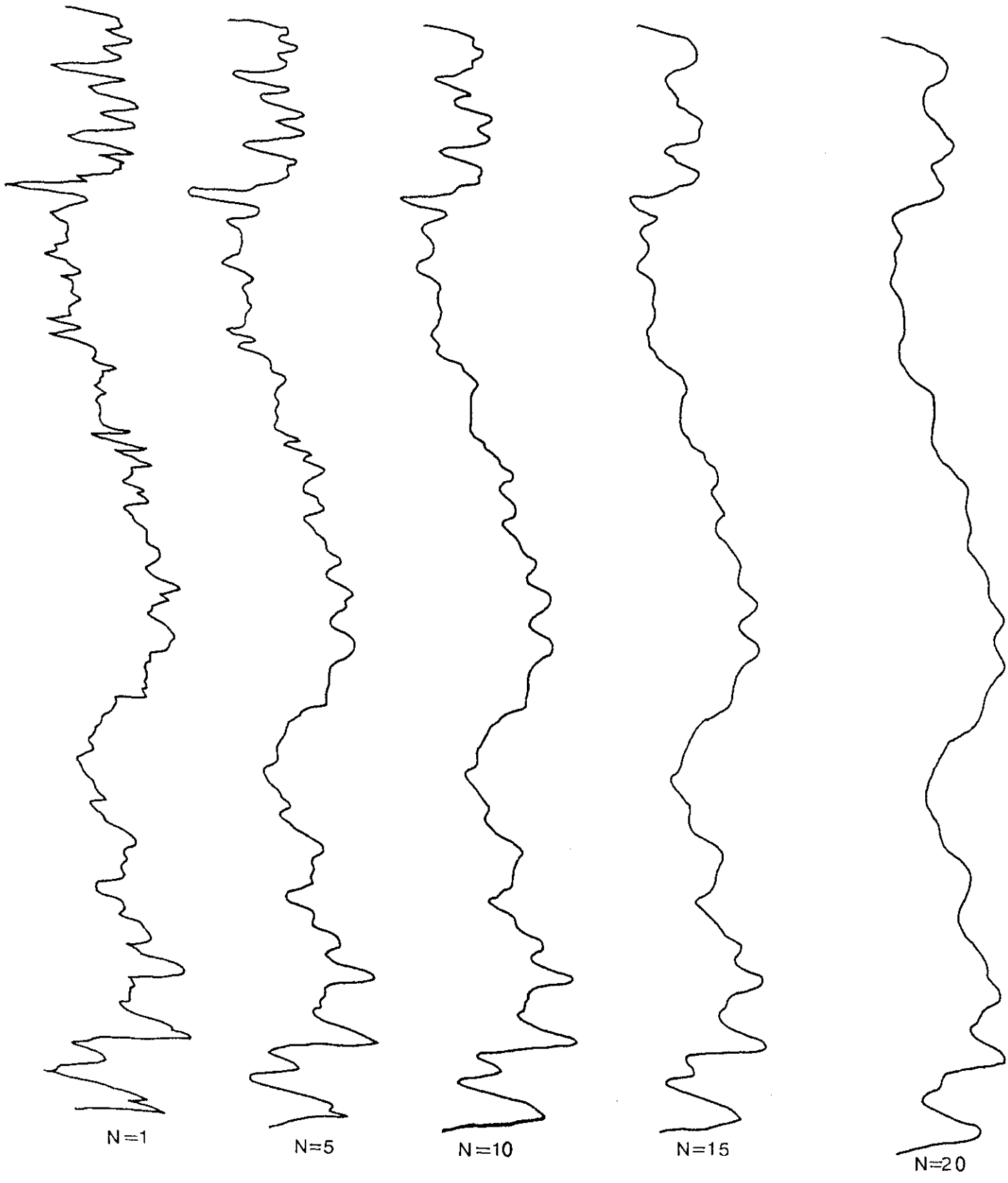


Fig. 7.9 Example of a 16-inches resistivity log filtered by 5-, 10-, 15-, and 20-term moving average filtering

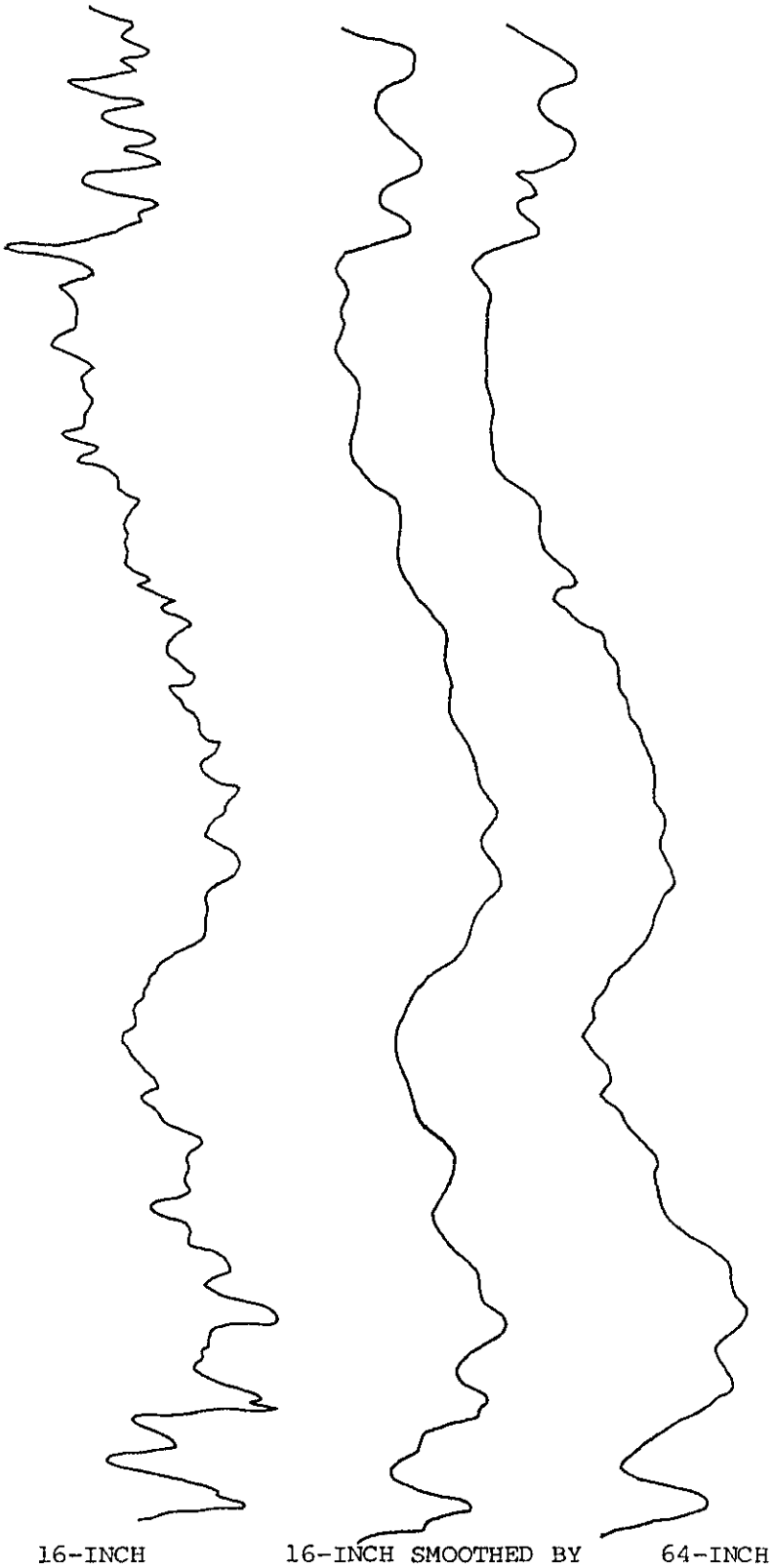


Fig. 7.10 Comparison between 20-term moving average filtered version of 16-inches resistivity log with the 64-inches resistivity log

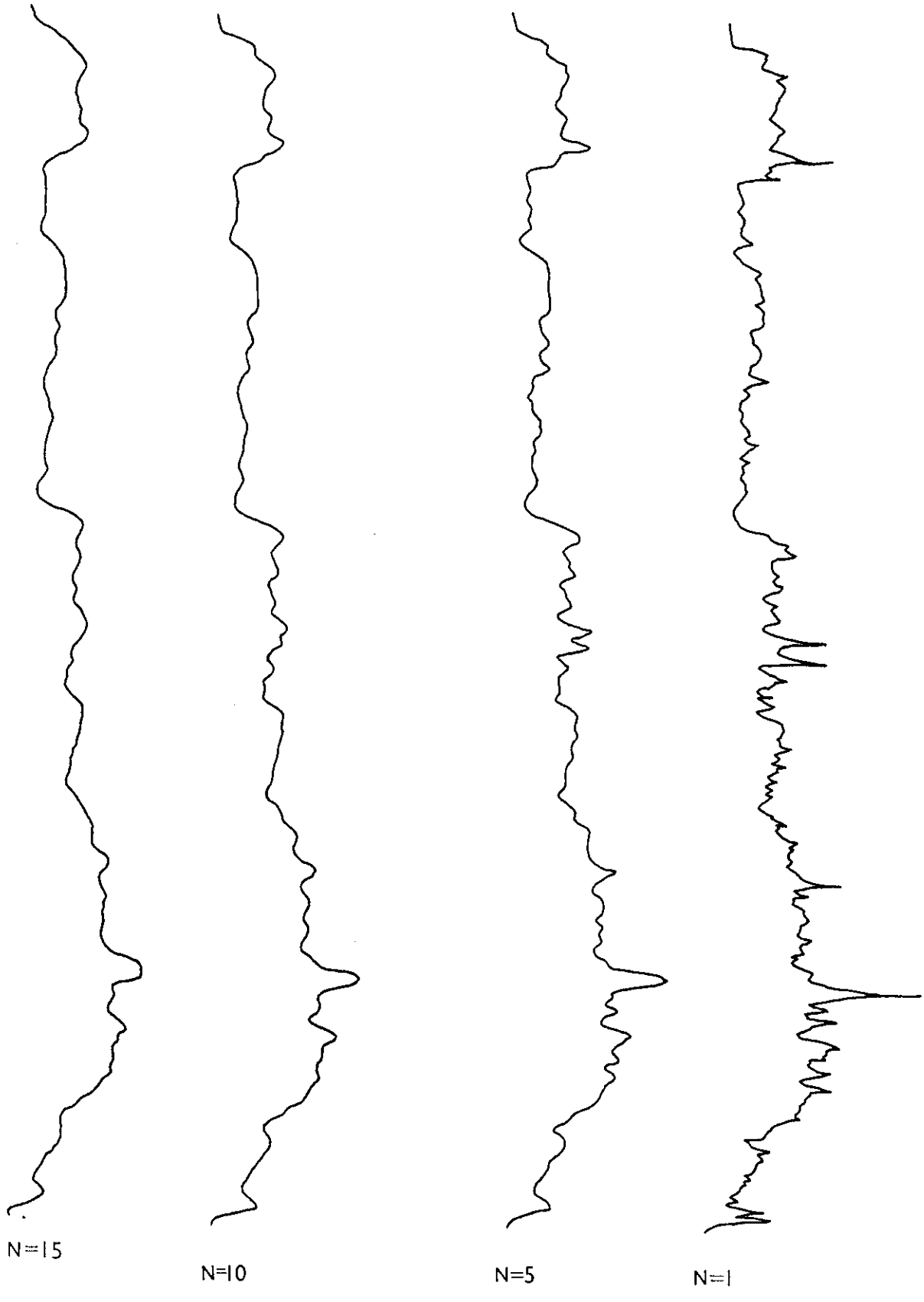


Fig. 7.11 Example of 5-, 10-, and 15-term moving average filtering of a caliper log

frequency logs such as the caliper, the moving average technique is not the ideal one. Some other simple smoothing filters have been collected from the literature and are discussed below.

(a) Sheppard's 5-term equation

$$\bar{P}_i = \frac{1}{35}\left[17P_i + 12(P_{i+1}+P_{i-1}) - 3(P_{i+2}+P_{i-2})\right] \tag{7.6}$$

(b) Spencer's 21-term equation

$$\bar{P}_i = \frac{1}{350}\left[60P_i + 57(P_{i+1}+P_{i-1}) + 47(P_{i+2}+P_{i-2}) + 33(P_{i+3}+P_{i-3}) + \right.$$
$$+ 18(P_{i+4}+P_{i-4}) + 6(P_{i+5}+P_{i-5}) - 2(P_{i+6}+P_{i-6}) - 5(P_{i+7}+P_{i-7}) -$$
$$\left. - 5(P_{i+8}+P_{i-8}) - 3(P_{i+9}+P_{i-9}) - (P_{i+10}+P_{i-10})\right] \tag{7.7}$$

(c) A 7-term equation having properties intermediate between Spencer's and Sheppard's equations

$$\bar{P}_i = \frac{1}{21}\left[7P_i + 6(P_{i+1}+P_{i-1}) + 3(P_{i+2}+P_{i-2}) - 2(P_{i+3}+P_{i-3})\right] \tag{7.8}$$

Fig. 7.12 shows the filter response of the above equation.

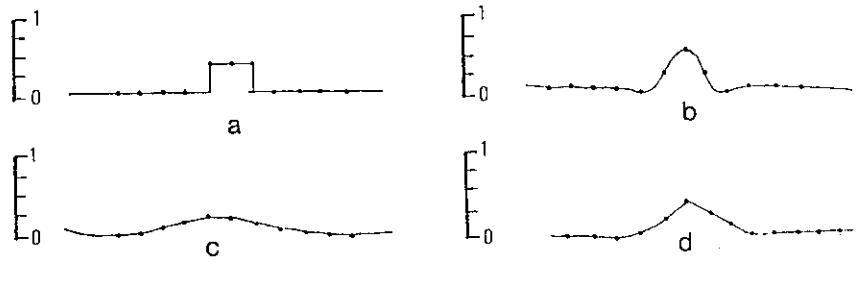


Fig. 7.12 (a) Three-term moving average, (b) Sheppard's five-term equation, (c) Spencer's twenty-one-term equation, (d) Spencer's and Sheppard's seven term equation.

Fig. 7.13 is an example of the caliper log of Borehole No. 5 and the result obtained when it was filtered by 7-term Spencer's-Sheppard's and a 21-term Spencer's filters. One can see that although the high frequency has been removed, the individual "microfissures" show quite clearly in the filtered versions.

A computer program able to carry out an L points moving average (L defined by the operator), Sheppard's and Spencer's filtering has been written (in ATOM'S BASIC) and is presented in APPENDIX A.7.5.

7.10 OPTIMUM OPERATION OF THE SOFTWARE PACKAGE

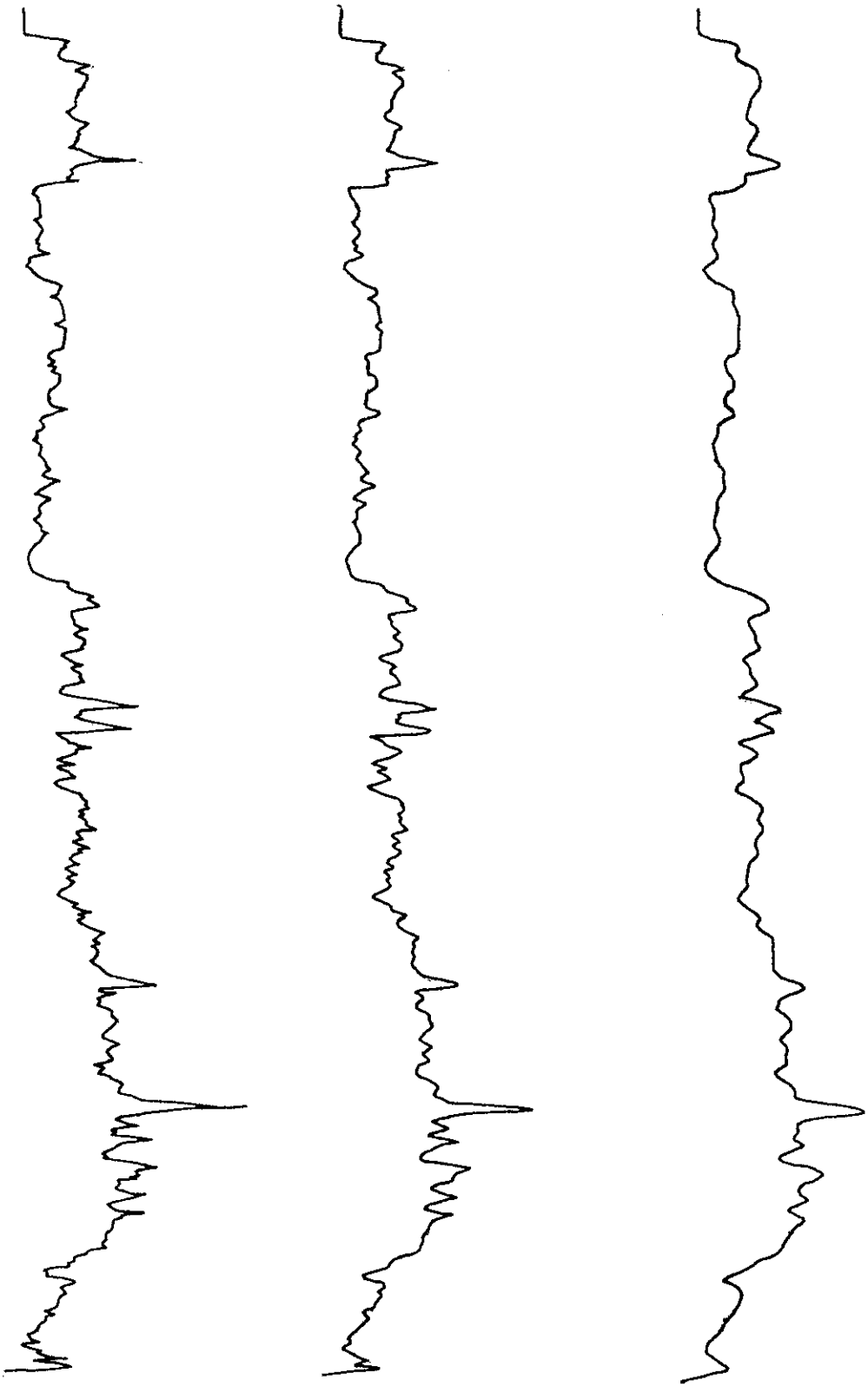
After having designed the individual algorithms and presented the corresponding microcomputer programs, it is necessary to describe the way in which these programs can be combined for a fast and an effective evaluation of the geophysical well logs.

Fig. 7.14 illustrates how the software package was used, for the evaluation of a number of normal resistivity logs which are going to be discussed in the next Chapter.

An important fact in this process is the general structure of the memory of the microcomputer which is used, since the operator has to define the parts of the memory which will contain the data, the programs and the results.

By referring to Fig. 7.14, one can see that the data from the digitized log can either be fed directly to a memory location or, in the case where filtering is necessary, to pass them through a filtering process, with the help of program "FILTER".

Next program "WINDOW" is called to perform the zonation of the log and after this the zoned data are corrected for



CALIPER

CALIPER SMOOTHED BY Sh-Sp FILTER

CALIPER SMOOTHED BY SPENCERS FILTER

Fig. 7.13 Example of a caliper log filtered by 21-term Spencer's filter and 7-term Spencer's and Sheppard's filter

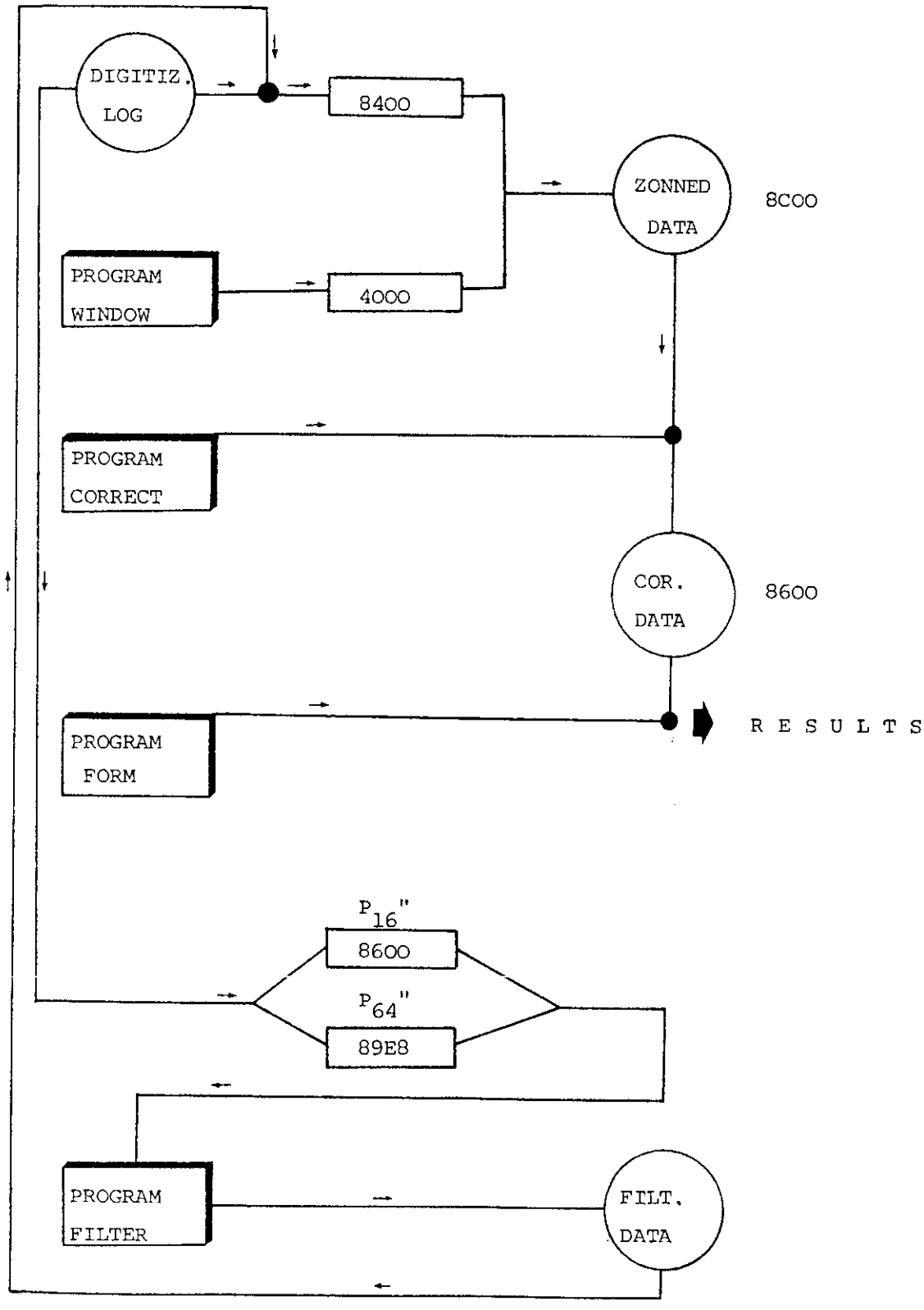


Fig. 7.14 Operation of the software package

fluid conductivity effects with program "CORRECT". If the changes in the fluid conductivity are small, instead of using the fluid conductivity (or resistivity) log a representative mean value for the fluid resistivity could be used. Program "CORRECT" provides such a facility.

After having obtained the true resistivity values from the apparent resistivity values program "FORM" is called to evaluate the geoelectric parameters as specified by the operator over a section of the well. "FORM" will perform all the necessary calculations for the construction of the T-L log, which can be presented in a graphic form on an X-Y plotter by passing the data through a Digital to Analogue 12-bit convertor especially constructed for this process (APPENDIX A.9.3).

It is very useful to have in the computer's memory, the data representing the 16-inches and 64-inches normal resistivity logs because a number of other parameters can now be possibly found. For example, by using the true resistivity values and a defined form of Archie's law, one can directly construct a porosity log. Fig. 7.15 contains an example of a caliper log of Borehole No. 1 and compares it with a porosity log derived by the above process from a 16-inches resistivity log assuming an Archie's formula of the form $F = \phi^{-1.77}$. The good degree of correlation between the two logs is obvious. Having the 16-inches and 64-inches resistivity logs in two different parts of the memory, further allows one to evaluate the difference between them and to plot this difference in the form of a new log. It was found that the later can be very useful in defining the boundaries between Upper-Middle and Lower Chalk.

Fig. 7.16 combines a $P_{16"}-P_{64"}$ log together with its filtered version, using a Spencer's filter. It is obvious that the boundaries between the different sections of the Chalk can be defined very easily.

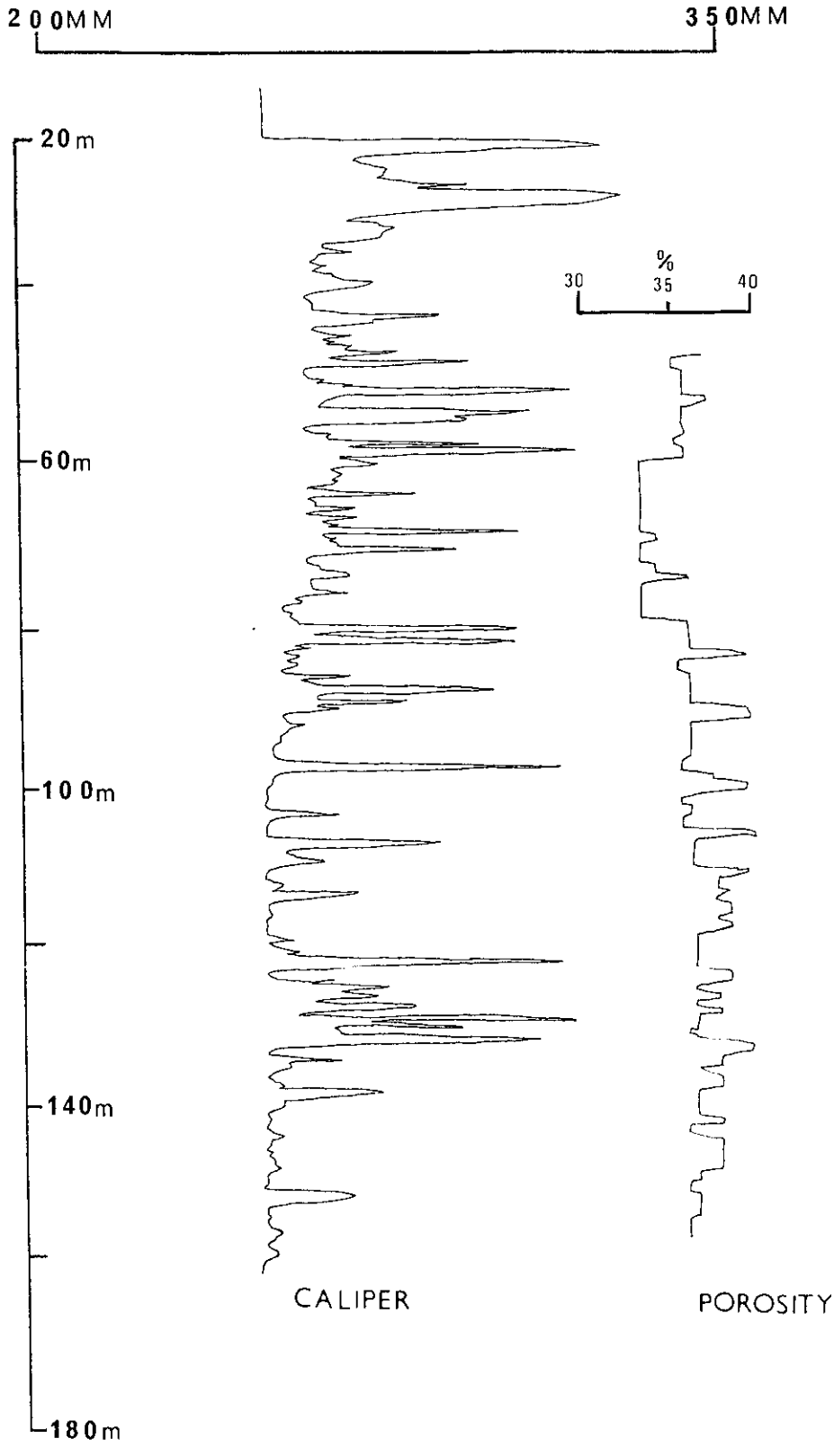


Fig. 7.15 Comparison between caliper and porosity logs

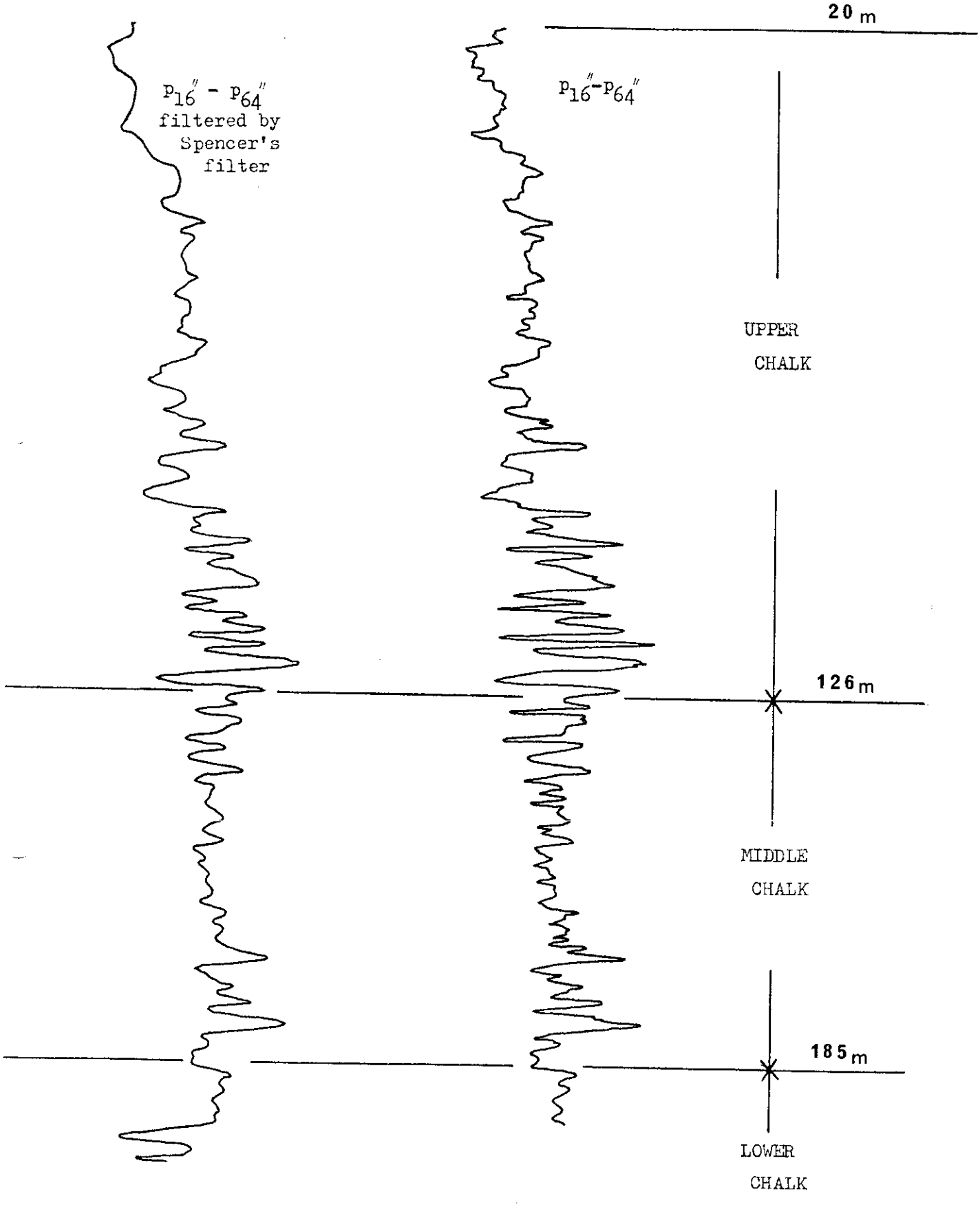


Fig. 7.16 Difference between 16N and 64N vs. depth

7.11 GENERAL CONCLUSIONS

In this Chapter, the construction details of a portable microcomputer software and hardware package have been described. After discussing the optimum way of transferring the analog signal, representing the geophysical well log, into a digital form so that it may be processed by a microcomputer, a number of very powerful computer algorithms are presented, as follows:-

(a) A method for the automatic correction of the normal resistivity logs from the effect of fluid conductivity has been proposed. This was achieved by fitting the existing "departure" curves through a least squares process with a third degree polynomial and by keeping its coefficients in the memory of the microcomputer.

(b) An algorithm for the automatic zonation of various geophysical logs to varying degrees of sensitivity, as specified by the operator, has been designed and demonstrated to be very effective.

(c) A new method for the automatic evaluation of the geoelectric parameters, from a section of the formation has been proposed.

(d) The effect of different digital filters on the geophysical logs has been discussed and a general purpose filtering program has been proposed.

From all the above, it has been shown that it is possible to build and put into operation in a limited period of time a very powerful, cheap and useful system for the hydrogeologists and geophysicists.

CHAPTER VIII

MATHEMATICAL-MODEL SIMULATION, USING A MICROCOMPUTER, OF THE RESPONSE OF AN ELECTRIC LOGGING TOOL

8.1 INTRODUCTION

From the early days of the application of the resistivity logging method, an important tool in the interpretation of the data has been the comparison of the apparent resistivity curves derived from field observations with apparent resistivity model curves for assumed models of the subsurface stratification.

Such models, for a limited number of cases, can be found in the logging manuals of the major logging companies (Schlumberger, 1949, 1950, 1969; Dresser Atlas 1975) and in many other publications (Lynch 1962; Pirson 1963).

Although the expected response of the electric resistivity tool for some characteristic subsurface stratifications (thick or thin, resistive or conductive beds) is well documented in the above publications, it would be very useful if it were possible to determine the expected response of the resistivity logging tool to a bed that has arbitrary geoelectrical/geometrical characteristics.

The electric potential distribution about a point source in the vicinity of one or more parallel plane interfaces separating two or more homogeneous isotropic materials has been solved previously by many researchers (Guyod 1944; Jakosky 1950; Smythe 1950; Keller et al 1977; Koefoed 1979) and has been successfully used for the evaluation of surface resistivity surveys. Subsurface electrical measurements about a thin bed with material of equal resistivity above and below and with all electrodes in a line normal to the interfaces is another practical case of the problem.

Usually the mathematical model computations for the potential distribution are too laborious and costly (see Eq. 4.9), to be used directly in the field. In the following paragraphs, a method for the rapid calculation of the response of the electric resistivity logging tool as it passes through a horizontal bed with arbitrary geoelectric and geometric characteristics is described. This method can be inexpensively handled by means of a microcomputer in the field, using the approach developed during this research and reported in this Chapter.

8.2 GENERAL PROBLEM

Consider a material of resistivity p_1, a plane interface at $z = B > 0$ with material p_2 above and a second plane interface at $z = B+D$ with material p_2 below and $p_3 = p_1$ above (Fig. 8.1).

If a point current source is placed at the origin of a cylindrical coordinate system $(z,r,\emptyset)$ then the potential distribution is described by the Laplace equation:

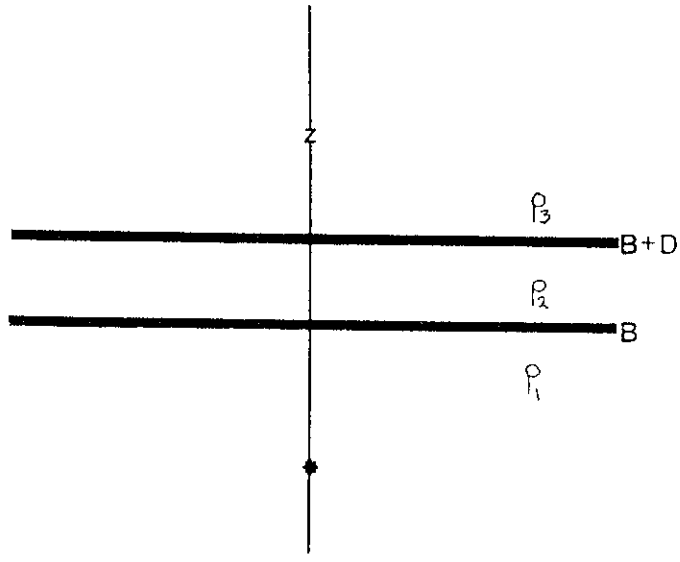
$$\frac{\partial^2 V}{\partial r^2} + \frac{1}{r}\cdot\frac{\partial V}{\partial r} + \frac{1}{r^2}\frac{\partial^2 V}{\partial \phi^2} + \frac{\partial^2 V}{\partial z^2} \qquad (8.1)$$

with the following boundary conditions:

$$z = B \;,\; V_1 = V_2 \;,\; \rho_2 \frac{\partial V_1}{\partial z} = \rho_1 \frac{\partial V_2}{\partial z}$$

$$z = B+D \;,\; V_2 = V_3 \;,\; \rho_3 \frac{\partial V_2}{\partial z} = \rho_2 \frac{\partial V_3}{\partial z}$$

$$V \to 0 \;,\; r^2+z^2 \to \infty \qquad (8.2)$$

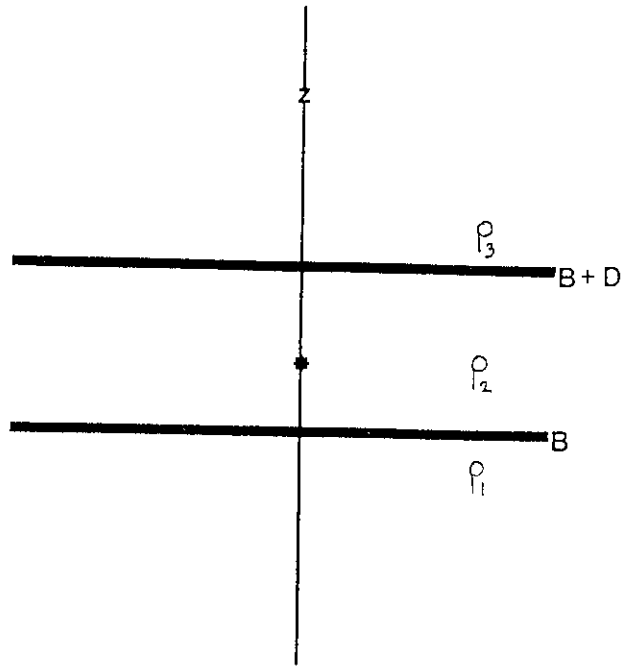


$$V_1 = \frac{\rho_1 \cdot I}{4\pi} \cdot \left\{ \frac{1}{(r^2 + z^2)^{1/2}} + \frac{A}{(r^2 + (2B-z)^2)^{1/2}} - (1-A^2) \cdot \sum_{n=0}^{\infty} \frac{A^{2n+1}}{(r^2 + (2nD\ 2\cdot(B+D)-z)^2)^{1/2}} \right\}$$

$$V_2 = \frac{\rho_1 \cdot I}{4\pi} \cdot (1+A) \cdot \left\{ \sum_{n=0}^{\infty} \frac{A^{2n}}{(r^2 + (2nD+z)^2)^{1/2}} - \sum_{n=0}^{\infty} \frac{A^{2n+1}}{(r^2 + (2nD + 2\cdot(B+D)-z)^2)^{1/2}} \right\}$$

$$V_3 = \frac{\rho_1 \cdot I}{4\pi} \cdot (1-A^2) \sum_{n=0}^{\infty} \frac{A^{2n}}{(r^2 + (2nD + z)^2)^{1/2}}$$

Fig. 8.1 Current source outside the thin bed



$$V_1 = \frac{\rho_2 \cdot I}{4\pi} \cdot (1-A) \left\{ \sum \frac{A^{2n}}{(r^2+(2nD-z)^2)^{1/2}} - \sum \frac{A^{2n+1}}{(r^2+(2nD+2\cdot(B+D)-z)^2)^{1/2}} \right\}$$

$$V_2 = \frac{\rho_2 \cdot I}{4\pi} \cdot \left\{ \frac{1}{(r^2+z^2)^{1/2}} - \sum \frac{A^{2n+1}}{(r^2+(2nD-2B+z)^2)^{1/2}} + \sum \frac{A^{2n}}{(r^2+(2nD+z)^2)^{1/2}} - \sum \frac{A^{2n+1}}{(r^2+(2nD+2\cdot(B+D)-z)^2)^{1/2}} + \sum \frac{A^{2n}}{(r^2+(2nD-z)^2)^{1/2}} \right\}$$

$$V_3 = \frac{\rho_2 \cdot I}{4\pi} \cdot (1-A) \cdot \left\{ \sum \frac{A^{2n}}{(r^2+(2nD+z^2)^{1/2}} - \sum \frac{A^{2n\ 1}}{(r^2+(2nD-2B+z)^2)^{1/2}} \right\}$$

Fig. 8.2 Current source inside the thin bed

If $J_0(r)$ is a Bessel function of zero order and $\Theta(\lambda)$ and $X(\lambda)$ are arbitrary functions chosen to satisfy the above boundary conditions, then the 3 solutions of equation (8.1) can be written as follows (Koefoed 1979):

$$
\begin{aligned}
V_1 &= \frac{\rho_1 I}{4\pi} \int_0^\infty \left\{ e^{-\lambda z} + \Theta_1(\lambda) e^{-\lambda z} + X_1(\lambda) e^{+\lambda z} \right\} \cdot J_0(\lambda r)\, d\lambda \\
V_2 &= \frac{\rho_1 I}{4\pi} \int_0^\infty \left\{ e^{-\lambda z} + \Theta_2(\lambda) e^{-\lambda z} + X_2(\lambda) e^{+\lambda z} \right\} \cdot J_0(\lambda r)\, d\lambda \\
V_3 &= \frac{\rho_1 I}{4\pi} \int_0^\infty \left\{ e^{-\lambda z} + \Theta_3(\lambda) e^{-\lambda z} + X_3(\lambda) e^{+\lambda z} \right\} \cdot J_0(\lambda r)\, d\lambda
\end{aligned}
\qquad (8.3)
$$

The solution of the system of equations (8.3) with boundary conditions described above is one of the classical problems in the theory of partial differential equations and is well documented in the literature (Smythe 1950). Figures 8.1 and 8.2 contain the solution of the problem for the case where the current source is outside and inside the thin bed respectively.

8.3 EVALUATION OF THE POTENTIAL

The use of the above expressions for evaluating the potential distribution is too laborious and costly to be practical, because of the infinite series involved.

In the following, these expressions are simplified in order to reduce them to a more useful form. All the calculations have been calibrated to a base unit of one by introducing all the physical parameters in terms of bed thickness. In this way, it can be assumed that the unit impulse response of the logging tool that is to be simulated is known. Since the points along the Z-axes are of interest, r = 0 can be replaced, and from the expressions it can be seen that all the infinite series reduce to the same form, if the thickness of the bed is replaced by 1.

$$
\sum_{n=0}^{\infty} \frac{A^{2n}}{2n+t} \qquad (8.4)
$$

where t is a variable term.

F(t) is defined as $$F(t) = \sum_{n=1}^{\infty} \frac{A^{2n}}{2n+t} \qquad (8.5)$$

since the zero term does not appear in all the series. Another important fact is that the value of F does not depend on the sign of A. In other words, it has the same value if the resistivities of the bed and the surrounding medium are interchanged.

With this notation, the solutions can be rewritten as a function of F(t) and since the apparent resistivity given from a two-electrode device is

$$\rho_a = \frac{4\pi s}{I} V \qquad (8.6)$$

Thus its calculation is straightforward. Expressions for the apparent resistivity in units of ohm.bed thickness are shown below.

Table 8.1 contains the calculated values of the functional F for t between -1 and 10 and for ρ_2/ρ_1 = 2 or 0.5. By following the above approach, it is easy to construct similar tables for different resistivity values.

The method adopted here for the rapid calculation of the theoretical response of the logging tool was to approximate the functionals F(t) by third degree polynomials of t. The program contained in APPENDIX A.7.3 has been used and the following polynomial form F(t) was found:

$$F(t) = -0.000254t^3 + 0.0039683t^2 - 0.02094t + 0.060855 \quad (8.3)$$

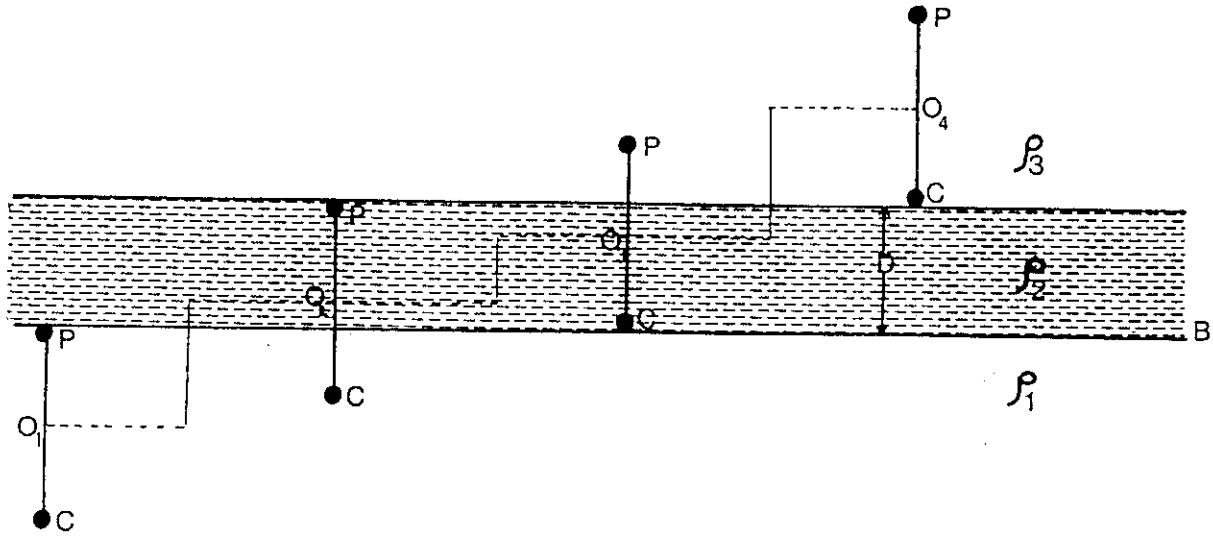
corresponding to a resistivity ratio of 2 or 0.5.

t	F
-1	0.086017
0	0.060855
1	0.043629
2	0.032816
3	0.026892
4	0.024332
5	0.023612
6	0.023209
7	0.021599
8	0.017258
9	0.008661
10	-0.005715

Table 8.1 Values of functional F for different values of t and for resistivity ratio 2 or 0.5

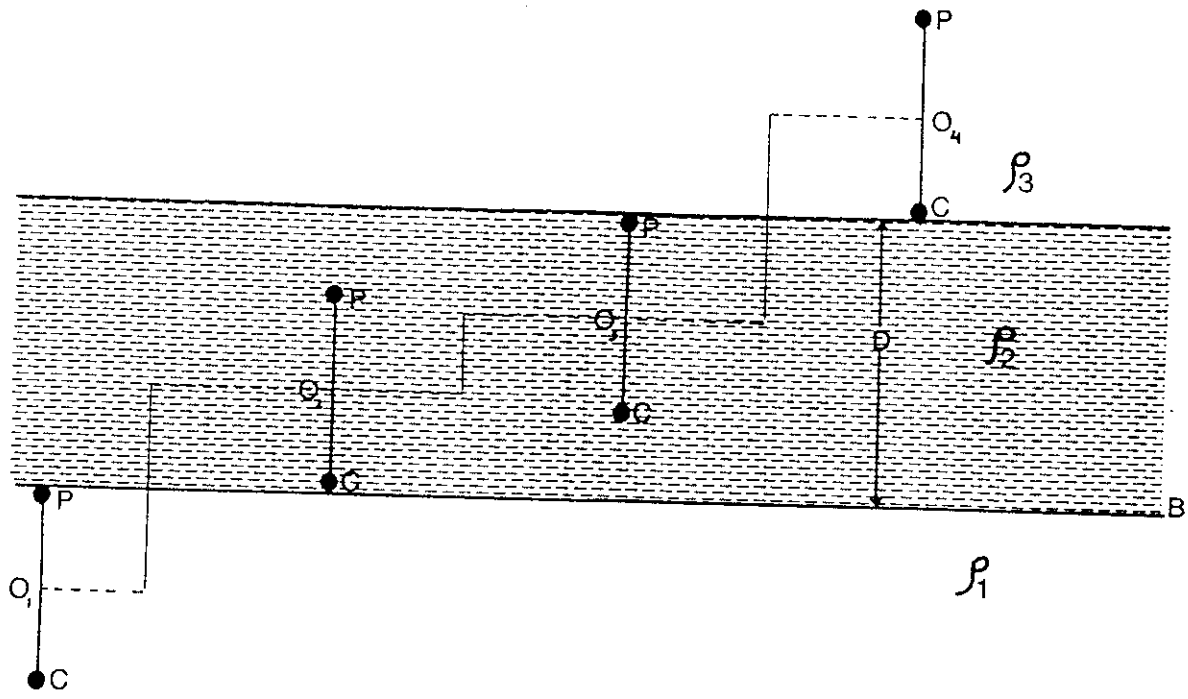
8.4 RESISTIVITY LOG SIMULATION

Imagine logging a zone of thickness D with a hypothetical normal resistivity tool. The values of the apparent resistivity that are expected for the different locations of the current electrode are already known. For the case where the spacing of the tool is larger than the thickness of the bed, the values of the apparent resistivity as the tool passes through the intervals $-oo0_1 0_2 0_3 0_4 +oo$ are given in Fig. 8.3 and for the case where the bed thickness is larger than the spacing, in Fig. 8.4.



LOGGING INTERVAL	R_a GIVEN BY FORMULA
$-\infty \quad O_1$	A
$O_1 O_2$	B
$O_2 O_3$	C
$O_3 O_4$	F
$O_4 \quad \infty$	A

Fig. 8.3 Example of log simulation for the case that the tool spacing is larger than the bed's thickness



LOGGING INTERVAL	R_a
$-\infty$ O_1	A
O_1O_2	B
O_2O_3	E
O_3O_4	F
O_4 ∞	A

Fig. 8.4 Example of log simulation for the case that the tool spacing is shorter than the bed's thickness

CURRENT ELECTRODE OUTSIDE

$$\rho_{1}a = \rho_{1} \cdot s \cdot \left(\frac{1}{|z|} + \frac{A}{2B-z} - \frac{(1-A^2).A}{2(B+1)-z} - (1-A^2).A.F(2(B+1)-z)\right) \quad A$$

$$\rho_{2}a = \rho_{1} \cdot s \cdot (1+A) \cdot \left(\frac{1}{z} + F(z) - \frac{A}{2(B+1)-z} - A.F(2(B+1)-z)\right) \quad B$$

$$\rho_{3}a = \rho_{1} \cdot s \cdot (1-A^2) \cdot \left(\frac{1}{z} + F(z)\right) \quad C$$

CURRENT ELECTRODE INSIDE

$$\rho_{1}a = \rho_{2} \cdot s \cdot (1-A) \cdot \left(-\frac{1}{z} + F(-z) - \frac{A}{2(B+1)-z} - A.F(2(B+1)-z)\right) \quad D$$

$$\rho_{2}a = \rho_{2} \cdot s \cdot \left(\frac{1}{z} - \frac{A}{z-2B} - A.F(z-2B) + F(z) - \frac{A}{2(B+1)-z} - A.F(2(B+1)-z) + F(-z)\right) \quad E$$

$$\rho_{3}a = \rho_{2} \cdot s \cdot (1-A) \cdot \left(\frac{1}{z} + F(z) - \frac{A}{z-2B} - A.F(z-2B)\right) \quad F$$

A computer program was written to simulate the above process, a flowchart of which is presented and explained in Section 8.5.

The program permits the following factors to be varied:

(a) The thickness of the bed D.
(b) The electrode separation S.
(c) The logging interval.

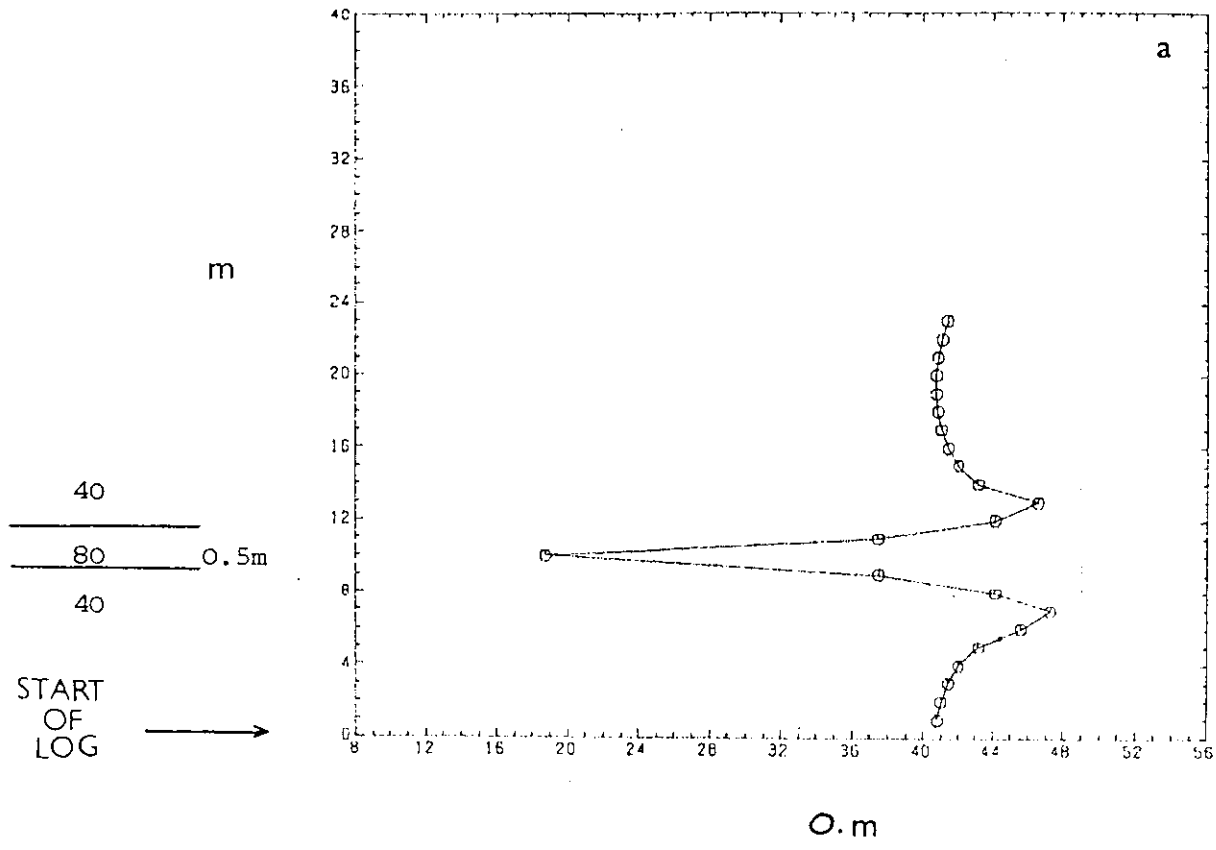
A number of subroutines can be added at the end, giving the functional term of the factor F(t) for the specific resistivity ratios. In the present program, there is only one subroutine corresponding to the resistivity ratio of 2 or 0.5.

A plotting routine can be added at the end of the program in order to plot directly the values of the apparent resistivity.

Figures 8.5.a to 8.5.f show the theoretical response of a normal resistivity logging device of spacing CP 0.7m, as it was calculated from the algorithm, when passing through some beds of different resistivity thicknesses. Note the characteristic reversal of the normal curve opposite thin resistive beds (Fig. 8.5.a and 8.5.b). Also, the thickness for "non-thin" beds appears on the resistivity curve to be one electrode spacing CP more than it actually is, the main resistivity hump being one half an electrode spacing CP above the bottom boundary and one half an CP spacing below the top (Fig. 8.5.d,e,f).

8.5 FLOW DIAGRAM OF COMPUTER PROGRAM

In step 1 (Fig. 8.6), the operator has to give the computer the geometric and geoelectric characteristics of the bed, the resistivity of the surrounding formation, the starting



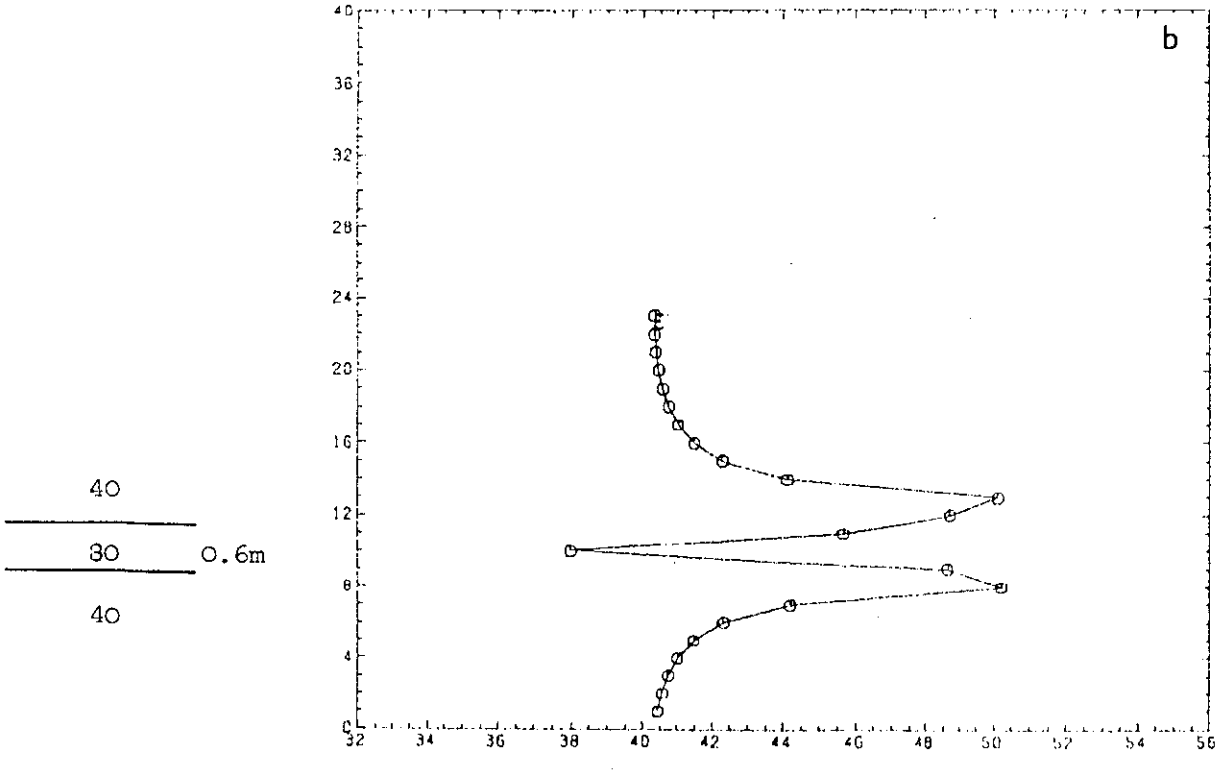
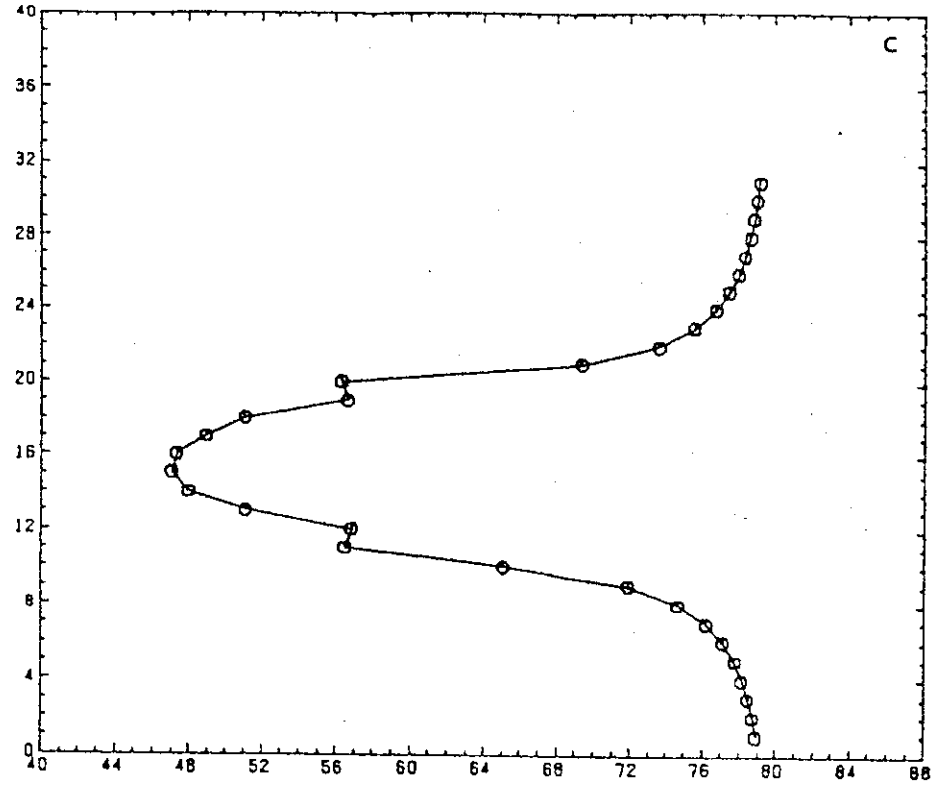


Fig. 8.5 Examples of theoretcial simulation of the normal resistivity logging process

80

40 1.5m

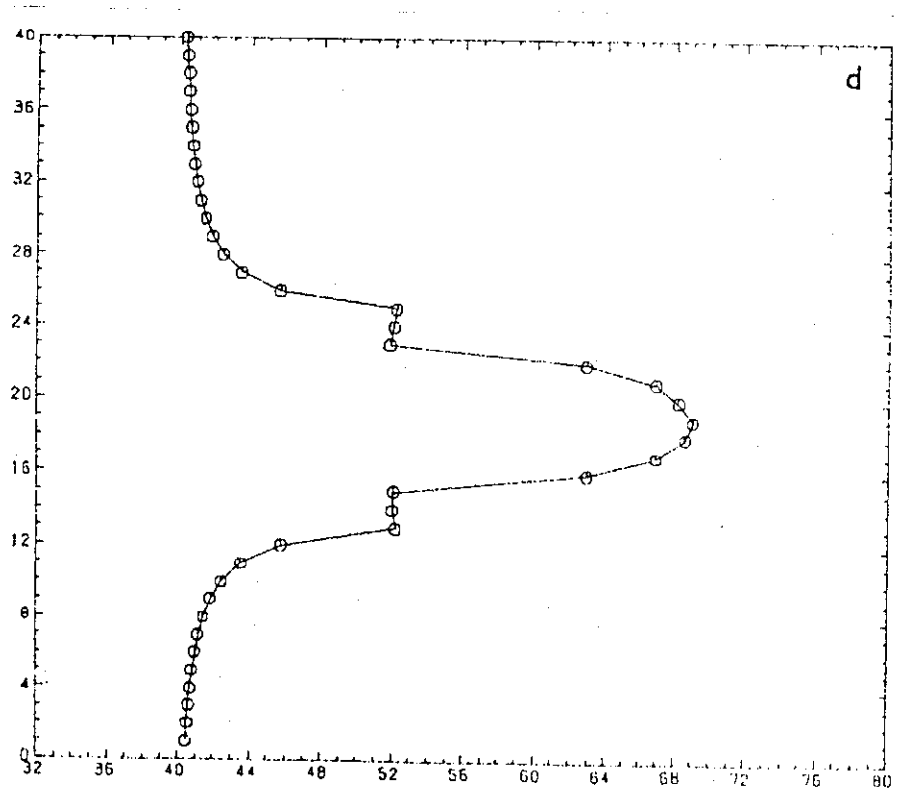
80



40

60 2.0m

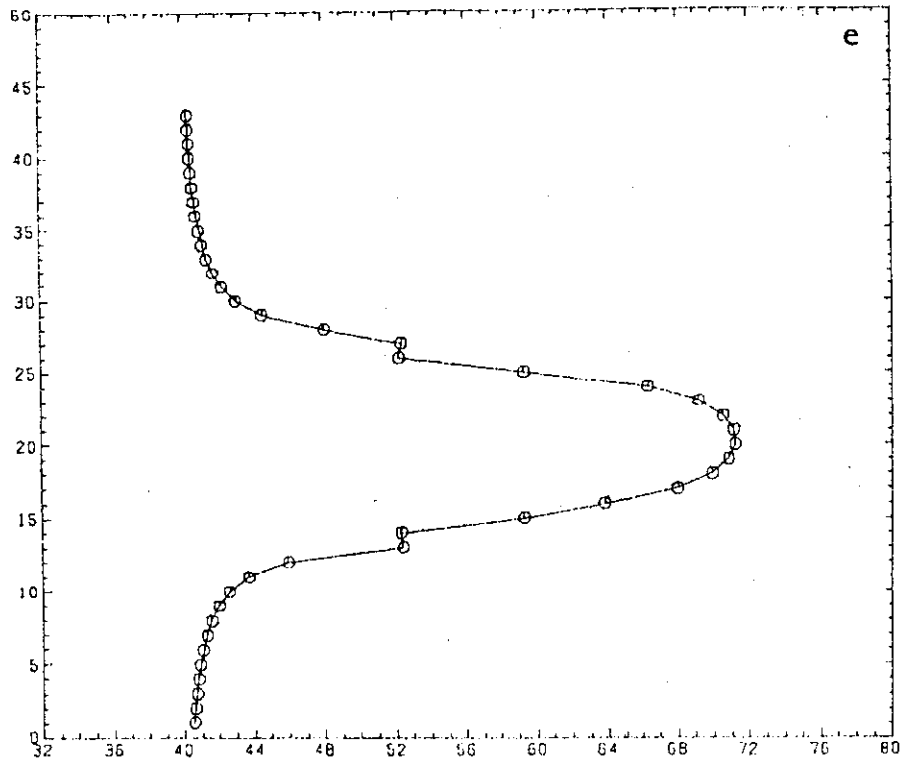
40



40

80 2.5m

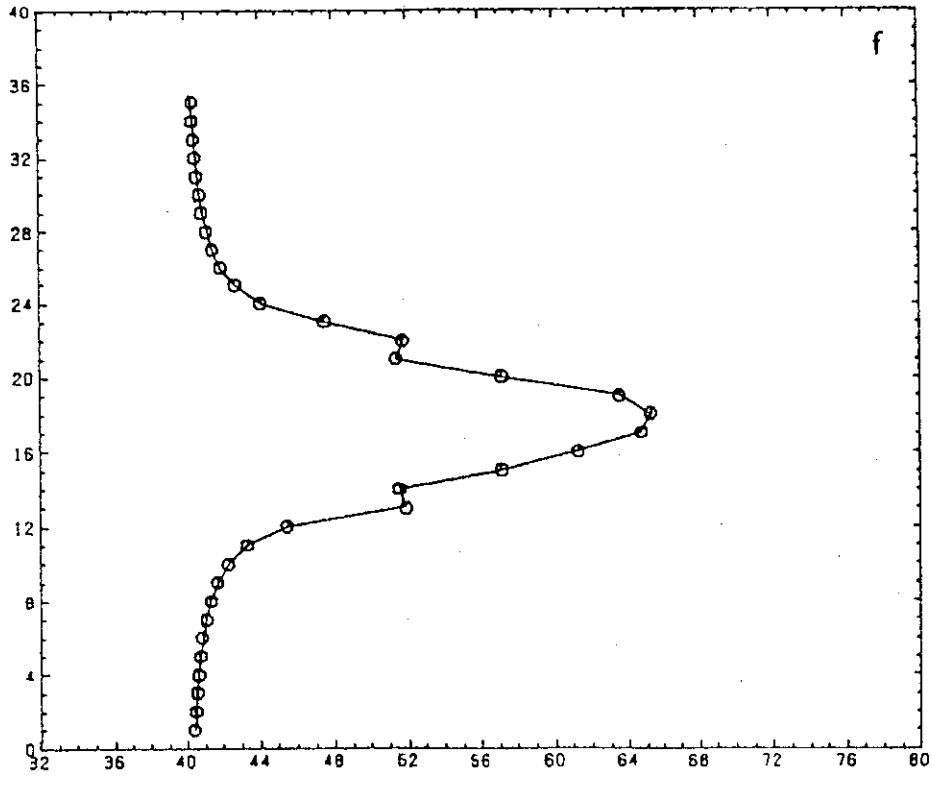
40



40

80 1.5m

40



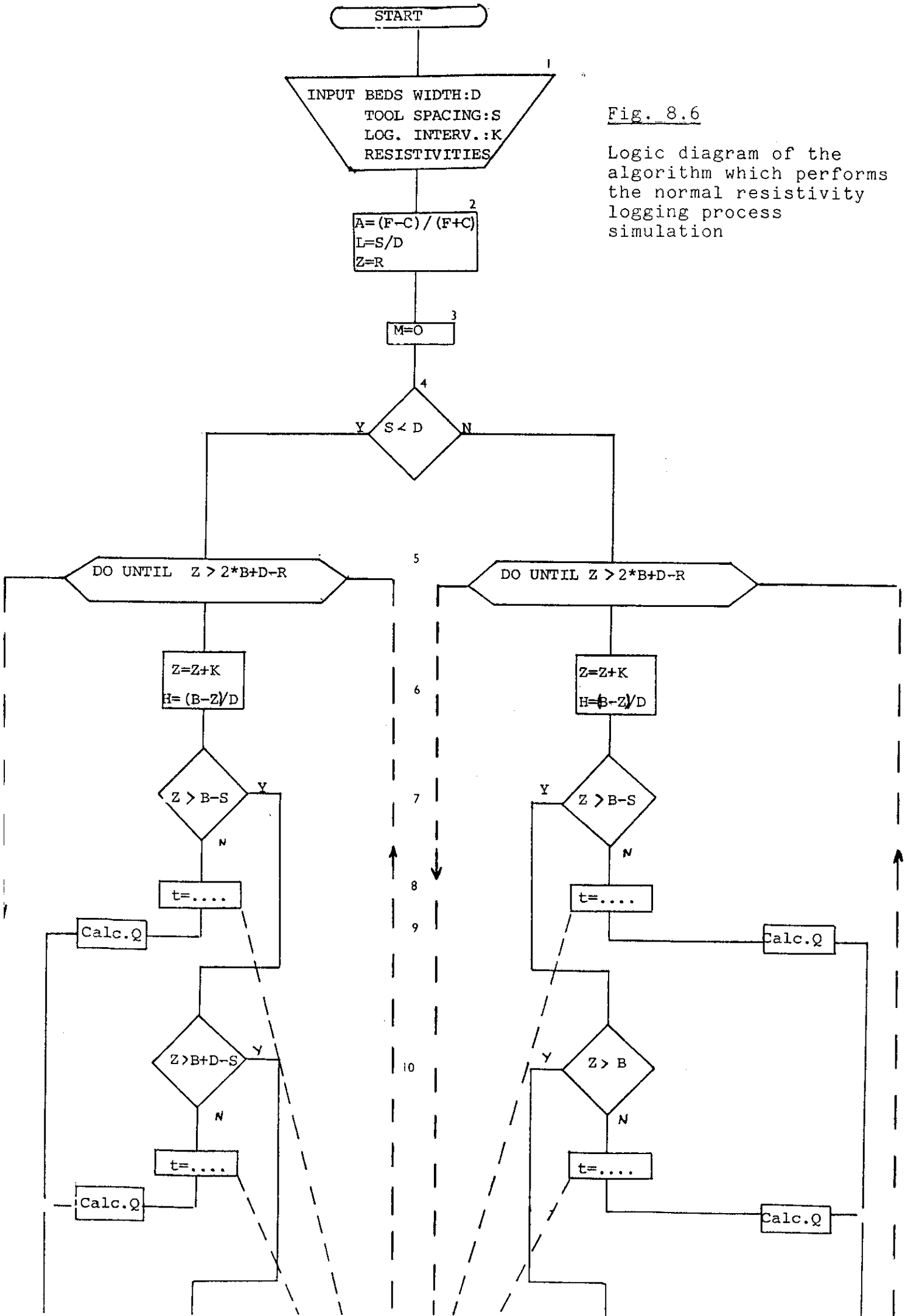
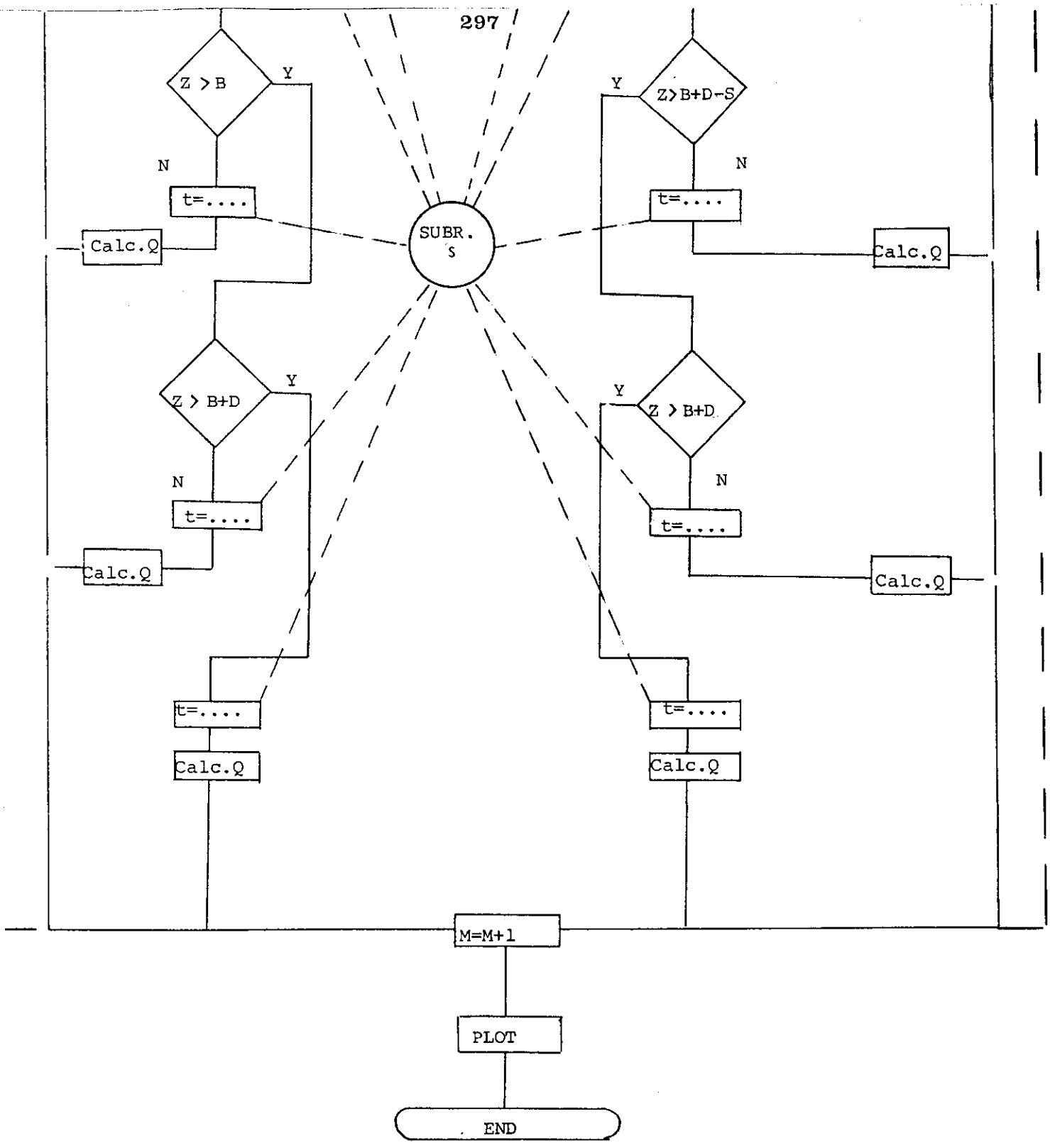


Fig. 8.6

Logic diagram of the algorithm which performs the normal resistivity logging process simulation


Z > B
Y
N
t=....
Calc.Q
SUBR.
S
Y
Z>B+D-S
N
t=....
Calc.Q
Z > B+D
Y
N
t=....
Calc.Q
Z > B+D
Y
N
t=....
Calc.Q
t=....
Calc.Q
t=....
Calc.Q
M=M+1
PLOT
END

point of the log (with reference to any point on the axis of the borehole), and the spacing of the logging tool.

In step 2 the parameter A (reflection coefficient) is evaluated, and the spacing of the tool is reduced in units of bed thickness. In the same step the parameter z is initiated to the starting point of the log.

Step 3 assigns an initial value of zero to the dummy variable M which increases by one each time the logging tool is displaced by the appropriate logging interval.

In step 4 a decision is made on whether the spacing of the tool is bigger or smaller than the width of the bed and the control is passed in one of the two branches of the program.

A loop is initiated at 5 and is executed until the parameter z exceeds the value 2B+D-R (see Fig. 8.7). Each time the loop is executed, parameter z is increased by the logging interval K (step 6). In the same step also the distance between the current electrode and the lower boundary of the bed is reduced to units of ohm.bed thickness.

In step 7 a decision is made as to whether the potential electrode has entered the bed.

If it has the control is passed to the next decision, step 10.

In step 8 the appropriate value of the parameter t is assigned and control passes to subroutine s for the evaluation of F(t).

The next step calculates the value of the apparent resistivity for the specific interval and control passes to the end of the loop where the dummy variable M is increased by 1.

Inside the loop there are four decision steps where the appropriate equations (see Figures 8.3 and 8.4) are used accordingly for the evaluation of the apparent resistivities. The present algorithm is designed for only one resistivity ratio but an unlimited number of them can be included in the program simply by inserting a "switch" just after step 1 according to which the control passes to the appropriate subroutine for the evaluation of F(t).

At the end of the program a plotting subroutine can be added to provide a direct plot of the results.

8.6 RANGE OF VALIDITY OF THE ALGORITHM

Since the functionals F(t) were calculated for a specific range of the parameter t (between -1 and 35 except for the resistivity ratio of 2 for which they were calculated for the range between -1 and 10), it is necessary to investigate the range above and below the bed in which the above algorithm, which calculates the values of the apparent resistivity, is valid (Fig. 8.7).

The following variables have been used during the various stages of the calculation:

$$t = 2(H + 1) - L, \quad \text{(Eq. A, B, E)}$$
$$t = L - 2H, \quad \text{(Eq. E and F)}$$

where L has a negative sign for Z > B+D.

In each case, t must satisfy the condition

$$-1 < t < 35$$

Substituting t = L-2H gives

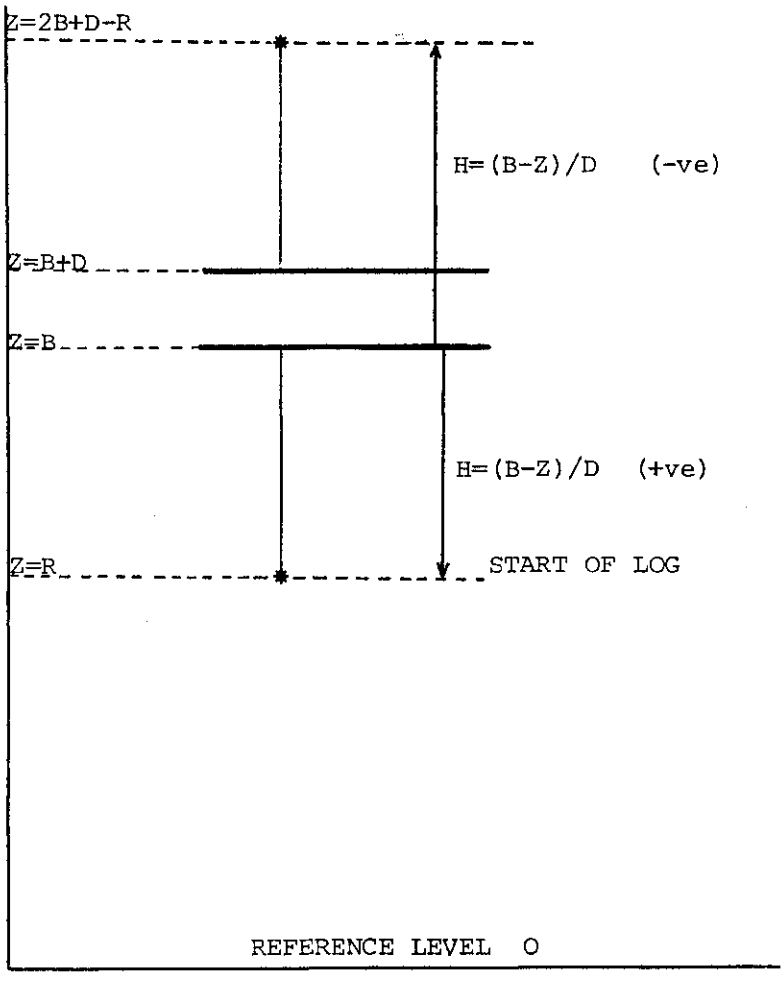


Fig. 8.7 Range of validity

$$
\begin{aligned}
&-1<L-2H<35\\
&-(L+1)/2<-H<(35-L)/2\\
&-(L+1)/2<(Z-B)/D<(35-L)/2\\
&B-(L+1)D/2<Z<B+(35-L)D/2
\end{aligned}
\qquad (8.8)
$$

The latter condition is always true since Eq. E and F correspond to the case where the current electrode is inside the bed.

Substituting t = 2(H+1)-L gives

$$
\begin{aligned}
&-1<2H+2-L<35\\
&(L-3)/2<H<(33+L)/2\\
&(L-3)/2<(B-Z)/D<(33+L)/2
\end{aligned}
\qquad (8.9)
$$

For example, let D = 0.5m, S = 0.7m and B = 30m.

Then L = S/D = 1.4 and the above condition gives

$$21.4<Z<30.4 \qquad (8.10)$$

which is the condition satisfying the limits of validity of Equations A,B,E. When the current electrode passes the upper boundary of the bed, the parameter L takes a negative value and the upper limit is extended to 31.4m (by replacing L with 1 in the right hand side of the above equation).

Concluding, in the specific example, the above algorithm can be used safely for the simulation of a logging process for the interval between 21.4m and 31.4m.

8.7 CONCLUSION

An attempt has been made to demonstrate that it is possible for a microcomputer to handle, by relatively simple operations, complex analytical processes which may be used to advantage by the log analyst to simulate directly in the field the response of a logging tool.

Imagine, for example, a typical Chalk section made up of a series of fissures of varying openings. Each individual fissure will have some effect on the response of the logging system. A continuous log would record a curve which would show the response of the system to each successive fissure, and usually the recorded curve will appear quite different from the individual components which make it up, but it will nevertheless truly represent the sum of all the effects of the formation's properties on the logging system. By applying the approach developed in this Chapter, the hydrogeologist could simulate the combined effect of all the individual fissures zones by replacing them with a low resistivity layer, for which he will vary its length until the obtained curve from the model matches the field curve. Obviously in this case the thickness of the "model layer" is directly related to the degree of fissuring of the formation and hence its hydraulic conductivity.

Finally the above method can be easily adapted to simulate a three electrode resistivity tool (lateral log). Flexibility and the speed of execution should make this method of analysis a valuable tool for its direct application on site.

PART IV

This PART contains two Chapters: Chapter IX detailing the case histories of logging in various boreholes, and Chapter X, which is devoted to a statement of the general conclusions of the research.

CHAPTER IX

9.1 INTRODUCTION

The purpose of this Chapter is to apply the methods introduced in PARTS II and III to a number of boreholes and discuss the results obtained.

The author has taken part in the geophysical logging of a number of boreholes during the summer of 1980 with the geophysical logging section of the Anglian Water Authority at Cambridge and at certain intervals between September 1980 and October 1982 with the geophysical logging section of the Southern Water Authority at Brighton.

The geophysical logs were digitized and then processed by the software package introduced in Chapter VII following the procedure shown in Fig. 7.13. All the relevant details for the studied boreholes are contained in APPENDIX A.9.1.

9.2 BOREHOLE NO. 1: VICTORIA GARDENS NORTH (BRIGHTON CHALK BLOCK)

Introduction

The 16 and 64-inches normal resistivity logs together with the caliper log were digitized and scaled to 0.08 cm/m in order to fit an A4 size page. Fig. 9.1 contains these logs together with a lithologic information log obtained from the driller's log. The procedure shown in Fig. 7.14 of Chapter 7 was followed. First of all, the resistivity logs were zoned by using program "WINDOW" and the obtained zones were superimposed on top of the logs. After the data have been corrected for fluid conductivity effects, program "FORM" was used in order to evaluate the geoelectric parameters of the formations crossed by the borehole. This evaluation was carried out at 4 meter intervals (every 20 samples) and a detailed output of the program for the 64-inches log is contained in APPENDIX A.9.1. A copy of the differential temperature and spontaneous potential logs (reduced by 8) is presented in Fig. 9.2.

Discussion of the results

By looking at the resistivity logs and the driller's logs, the base of the Middle Chalk is expected to be around 185m and the base of the Upper Chalk is expected to be around 126m.

Since the values of the formation's geoelectric parameters are already known and are contained in the output of program "WINDOW", it was decided to check if these parameters could be indicative of the boundaries between Upper, Middle and Lower Chalk. The values obtained for the longitudinal resistivity were plot versus depth and are presented in Fig. 9.3. The data points have been joined together by a cubic curve and a regression line of order 9 has been fitted throughout them as well. It is evident

that the boundaries between Upper, Middle and Lower Chalk are shown very clearly in this graph.

The caliper log shows that below the lining which extends to 18m, down to about 50m there are many diameter enlargements to more than 400mm. Some distinct diameter enlargements occur at depths of 103, 106, 120, 188 meters, where at 203 and 205 meters there are two unusually large enlargements.

The fluid temperature increases from 10.7°C at the top of the borehole to 11.5°C at 123m. This increase is in the form of continuous steps of the depths 42, 44, 54.5, 59.5, 66, 72.5, 90 and 123m and are not shown very clearly in Fig. 9.2 due to the large reduction. It is obvious to suspect that there might be some fluid entry points at the above depths.

From 123m to the bottom of the borehole, the temperature increases continuously to 13.5°C. In this latter interval the differential temperature log suggests that minor water movement might occur at the depths 138, 171, 204m.

The spontaneous potential log on the other hand, indicates several permeable zones in the bottom half of the borehole at the following depths:

FROM	TO
171.5	173
190.5	192
197	199
205.5	212
223	225
229.5	232

The differences between Transverse and Longitudinal resistivities were computed for the complete length of the borehole and plotted versus depth in a form of a new log (T-L log). This was done for both the 16-inches and 64-inches normal resistivity curves, and the obtained results are shown in Fig. 9.1.

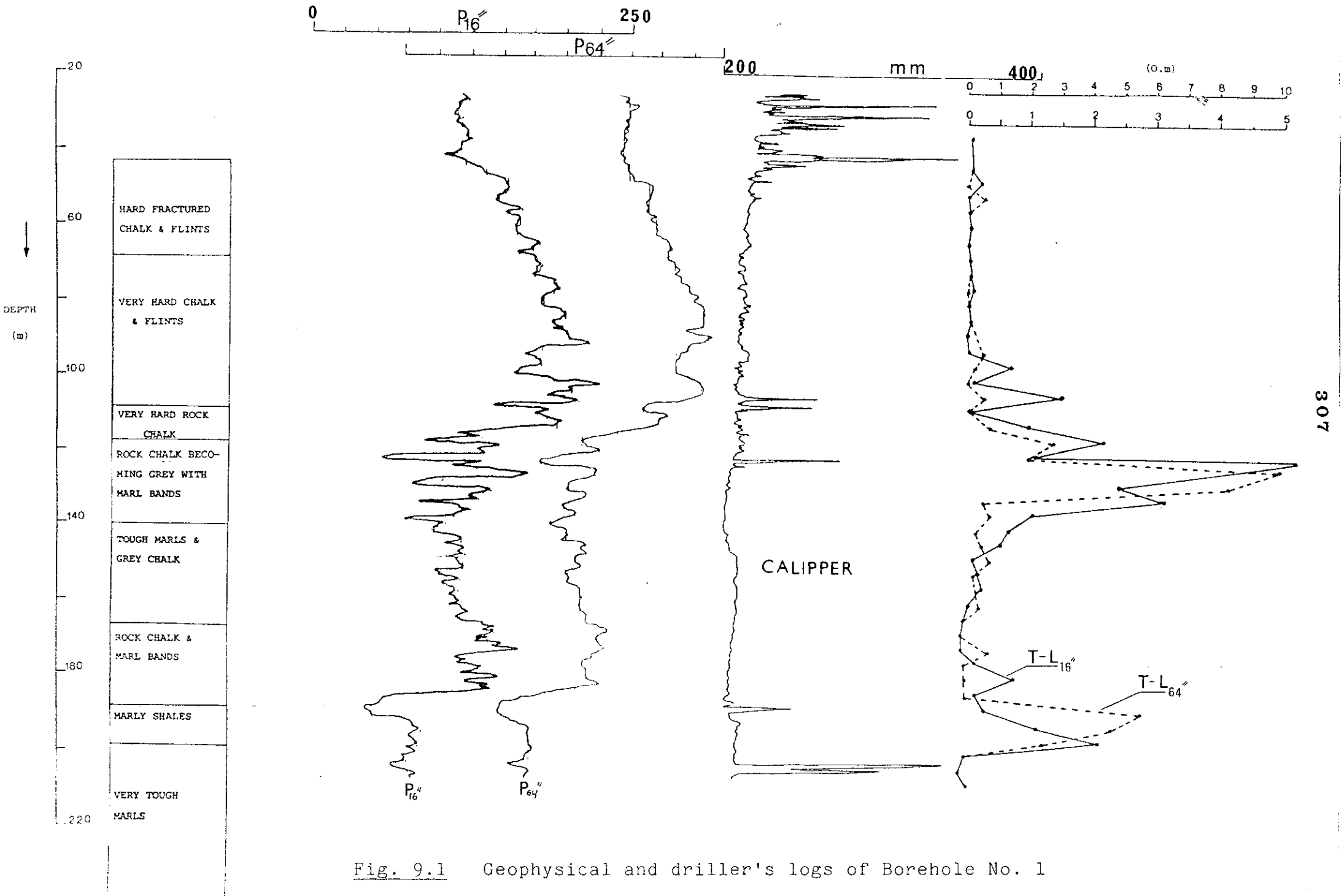


Fig. 9.1 Geophysical and driller's logs of Borehole No. 1

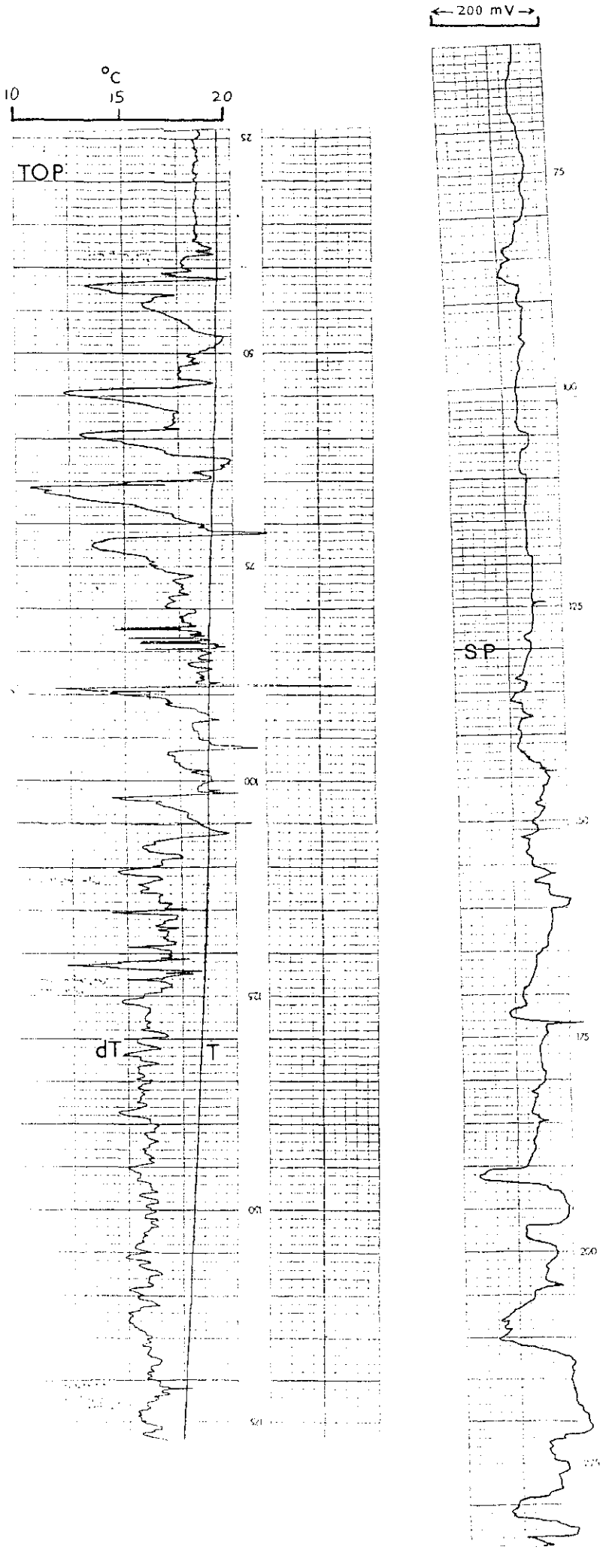


Fig. 9.2 Temperature, differential temperature and S.P. logs of Borehole No. 1

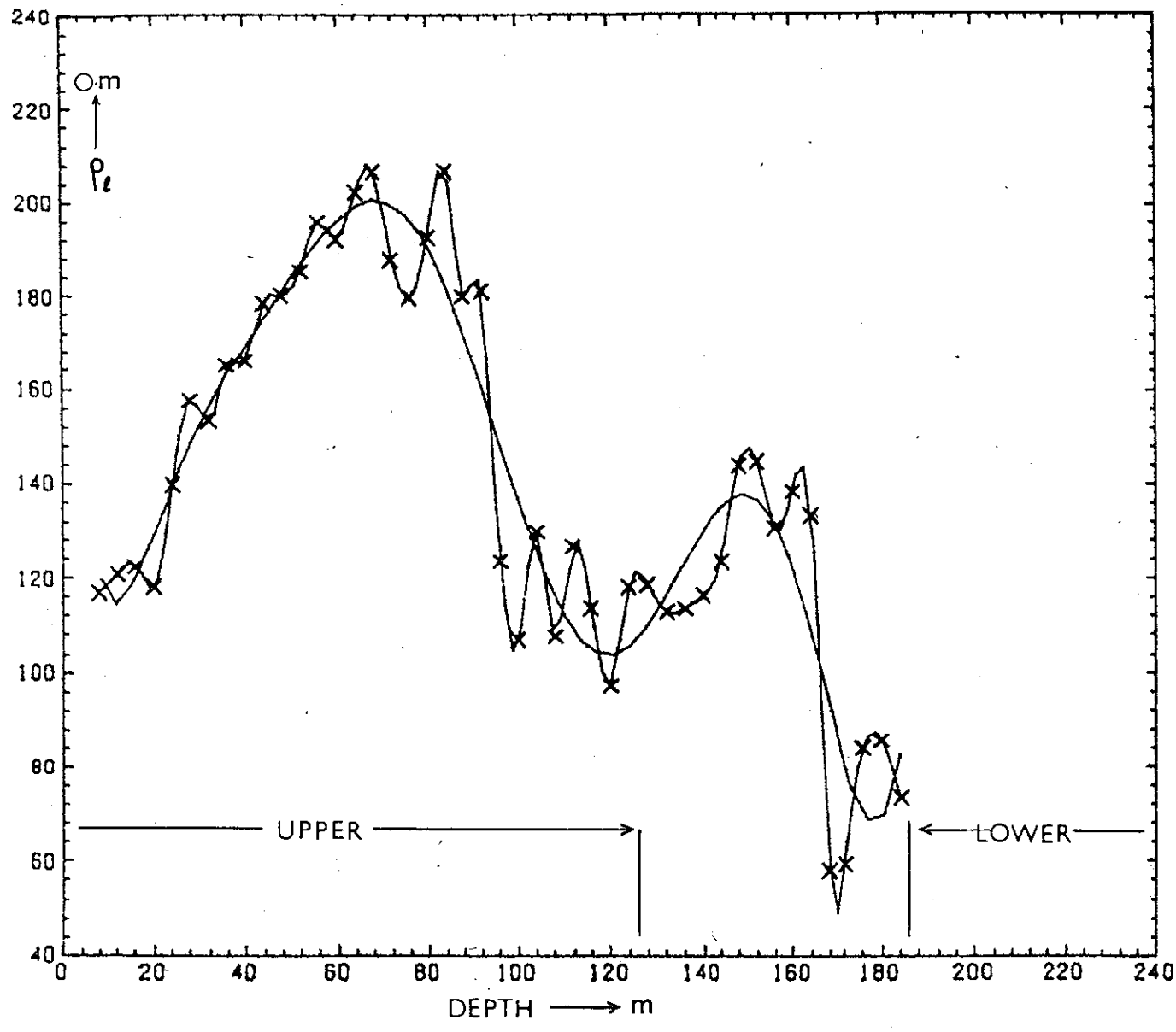


Fig. 9.3 Values of longitudinal resistivity vs. depth for Borehole No. 1

9.3 BOREHOLE NO. 2: FINDON (BRIGHTON CHALK BLOCK)

The 16-inches, 64-inches, caliper and differential temperature logs were digitized and scaled to 0.08cm/m. These logs together with a driller's log are represented in Fig. 9.4.

As the resistivity logs show the borehole is constructed in the Upper and Middle Chalk, the base of the Upper Chalk being at approximately 105m. The borehole was acidized and this is revealed by the rough, caliper log. The level of acid injection was probably around 90m as one can deduce from the greatest hole enlargement which has taken place at this depth. The effects of the acid appear to extend from approximately 100m to the base of the casing.

The digitized data representing the 64-inches log were processed and the corresponding T-L log was plotted, as is shown in Fig. 9.4. Until the depth of 105m the T-L log showed no variations, indicating the uniformity of the formation. Two maxima occur at the depths of 112 and 121m indicating an abrupt change in the geoelectric properties of the formation at the specific levels and probably the presence of fissure zones. This is confirmed by looking at the differential temperature peak occurring at 119 meters.

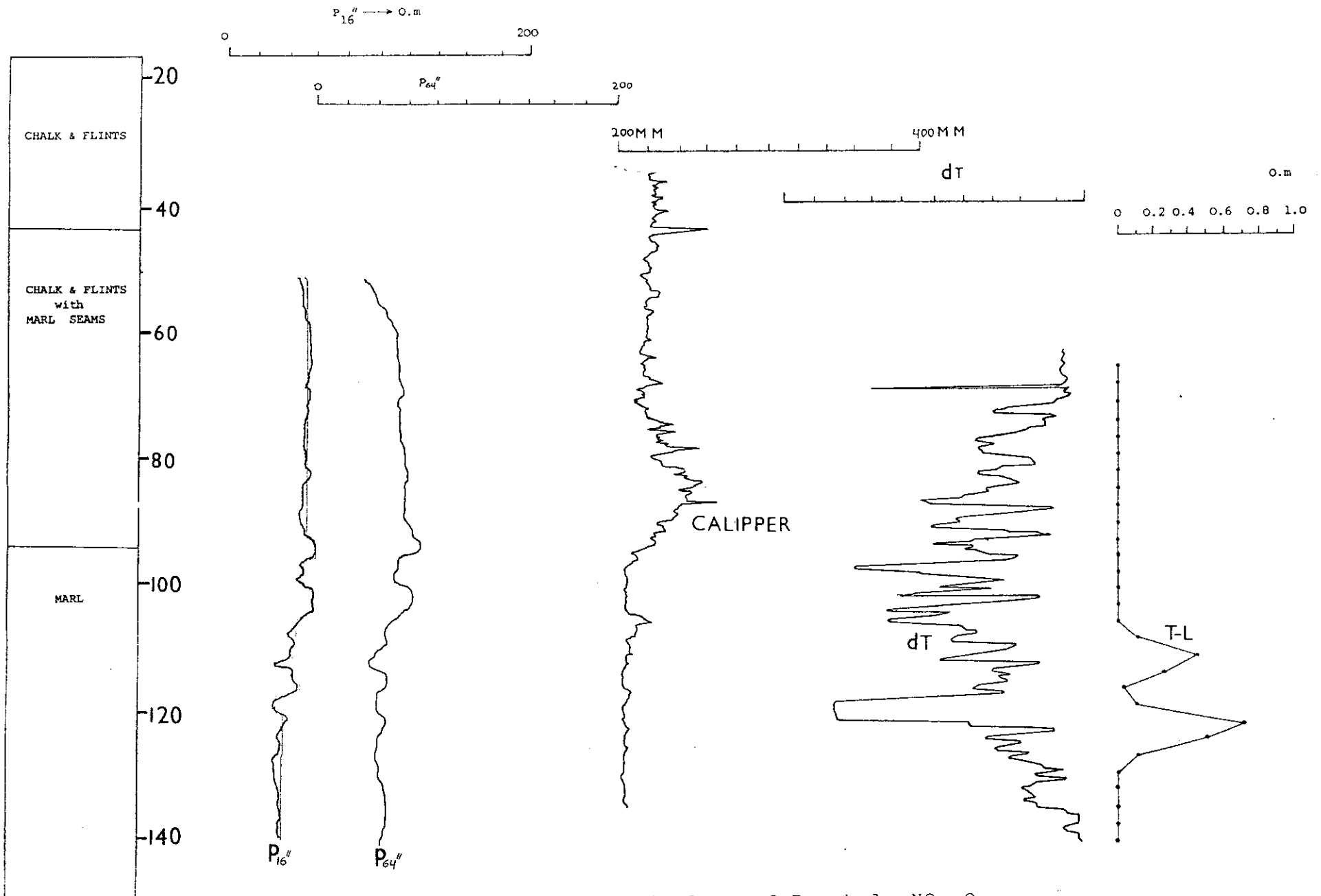


Fig. 9.4 Geophysical and driller's logs of Borehole NO. 2

9.4 BOREHOLE NO. 3: BRICK KILN FARM (CHICHESTER CHALK BLOCK)

This is an example of a borehole in highly fissured Chalk. The 16-inches, 64-inches, caliper and differential temperature logs were digitized and these logs are shown in Fig. 9.4.

The fissured nature of the formation is indicated by the caliper log. The calculated T-L log for the 16-inches is characterized by a great variation being in agreement with the caliper but, the same curve obtained for the 64-inches tool is much smoother indicating that most of the fissures indicated by the caliper are concentrated near the face of the borehole and do not continue deep into the formation. Intervals most likely to contain productive fissure, might be expected at 38, 45, 52, 61 and 75m. There is also a characteristic variation on the differential temperature log occurring as a depth of about 45m.

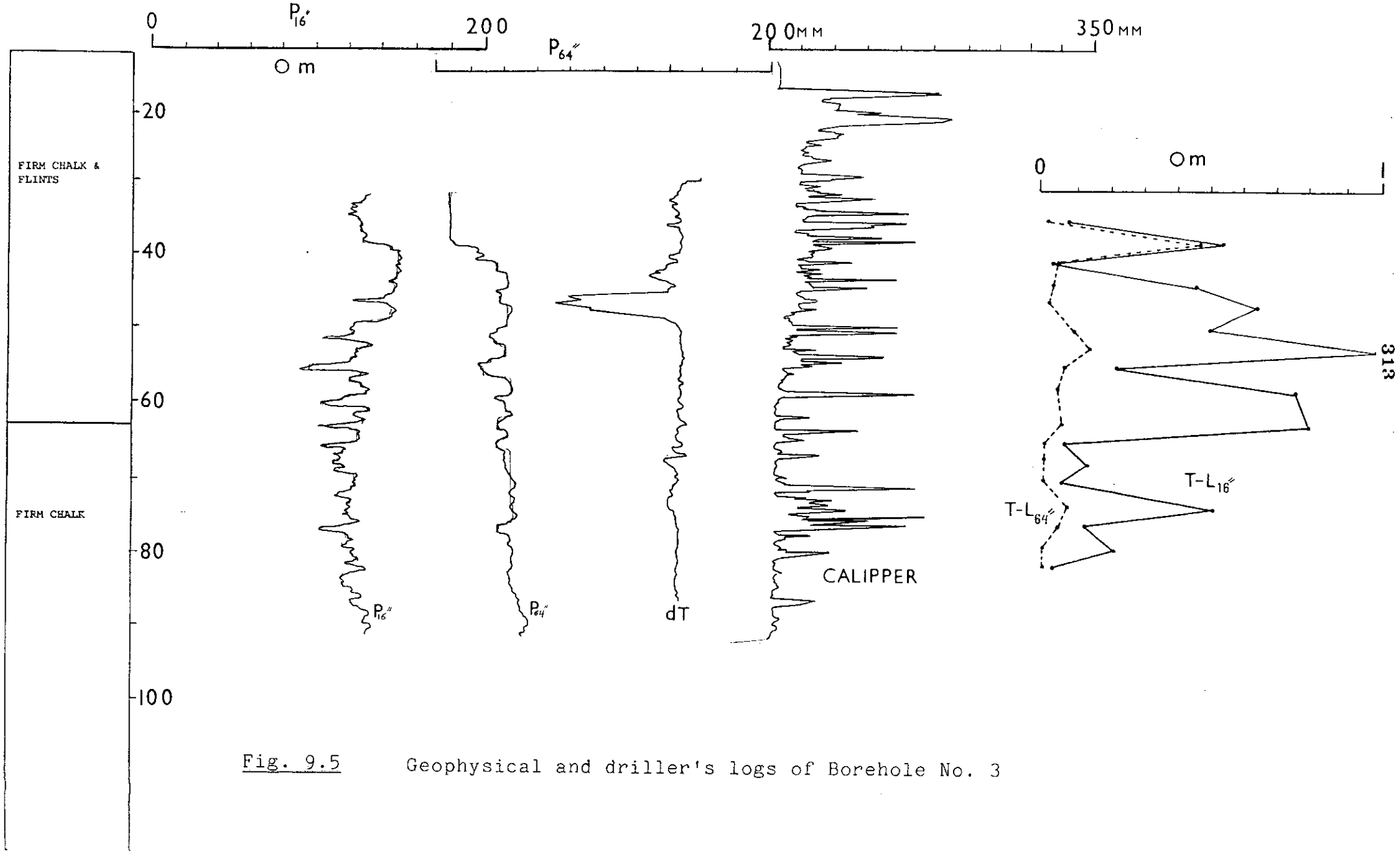


Fig. 9.5 Geophysical and driller's logs of Borehole No. 3

9.5 BOREHOLE NO. 4: PARK BOTTOM BARN ARUNDEL (CHICHESTER CHALK BLOCK)

The 16-inches, 64-inches and caliper logs were digitized and are shown in Fig. 9.6.

The caliper log suggests possible fissure zones between 49 and 57m. This is confirmed by the shape of the T-L log for both the 16 and 64 inches tools. The T-L log shows another two maxima at about 81 and 101m which probably are indicative of fissure zones at these levels.

The fluid conductivity and temperature logs (kept by the Southern Water Authority) have confirmed the existence of a fissure zone at the depth around 81m.

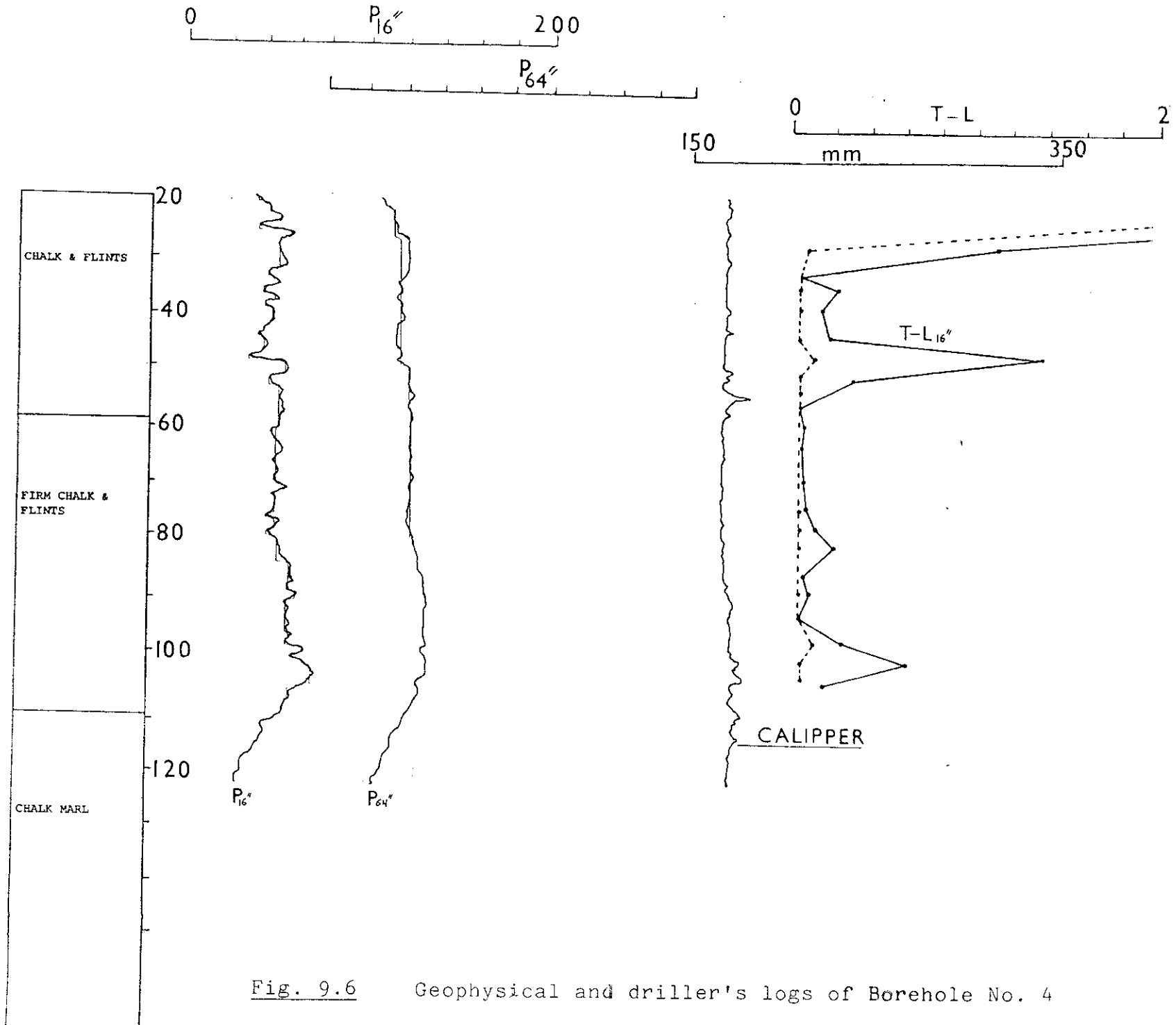


Fig. 9.6 Geophysical and driller's logs of Borehole No. 4

9.6 BOREHOLE NO. 5: KINGSTONE MIDDLE RD. (BRIGHTON CHALK BLOCK)

The 16-inches, 64-inches and caliper logs of this borehole after have been digitized and rescaled, are presented in Fig. 9.7 together with the driller's log. As one can see from the driller's log, this is an example of a borehole driven in a very anisotropic Chalk formation. The same result is obtained from the T-L logs whose oscillating nature reveals the variation of the formation's geoelectric properties.

In this case, the T-L log is of little use in indicating fissure zones since it is not possible to distinguish from the T-L log alone which variations of the formation's geoelectric properties depend upon fissure activity and which depend upon other factors such as the effect of flints etc.

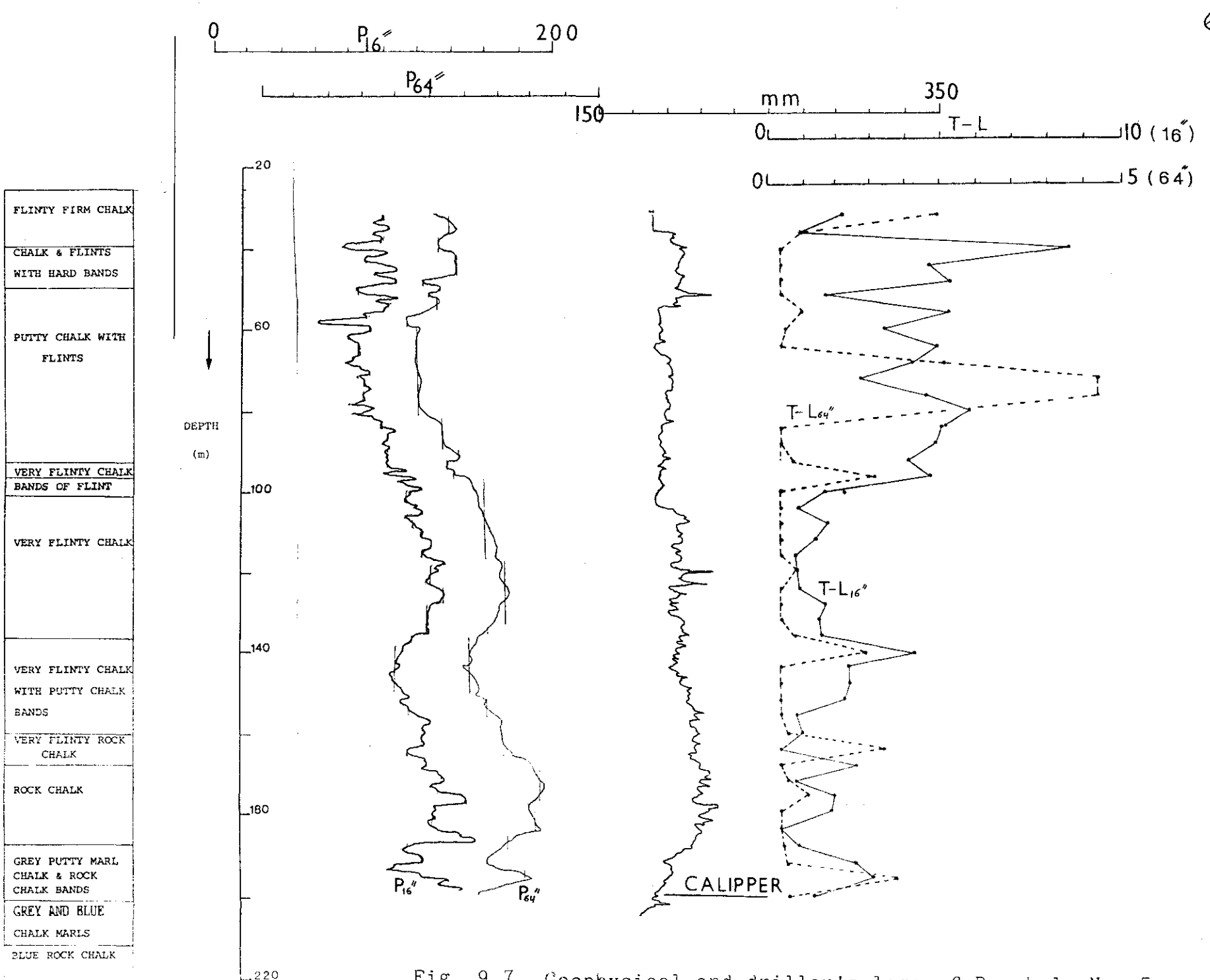


Fig. 9.7 Geophysical and driller's logs of Borehole No. 5

9.7 BOREHOLE NO. 6: ST. PETER'S CHURCH (BRIGHTON CHALK BLOCK)

The 16-inches, 64-inches and caliper logs were digitized, scaled and are represented in Fig. 9.8 together with the driller's log. As one can see, this borehole passes through the Upper, Middle and Lower CHalk. The base of the Middle Chalk occurs at 178m where the base of the Upper Chalk occurs around 115m.

Although the caliper log indicates that the Chalk is heavily fissured between the base of the casing and a depth of about 40m, it is more likely these diameter variations are the result of placing the casing or dislodging isolated blocks from the well wall, rather than of true fissures. This can be confirmed by looking at the T-L logs.

The highly anisotropic nature of the formation makes the T-L log difficult to separate the effect of fissure zones from the effect of variations in the lithology itself. The high oscillating nature of the T-L log occurring around 115m is indicative of the transition between Upper and Middle Chalk: and the same happens at 178m where the transition between Middle and Lower Chalk occurs. Any fissure activity existing in these zones is very difficult to recognize from the T-L log alone, and the use of fluid logs is necessary. By looking at the temperature and differential temperature logs (Fig. 9.9), one can see a change in the gradient at 120m and there is a similar variation on the differential temperature log at this level. Similar features occurring on the conductivity log (not included in the present thesis but are kept in the Southern Water Authority) suggest the presence of inflow levels at around 118m. The SP log indicates that there is a well developed self potential below the depth of 150m indicating the presence of fissures at this interval. This is in agreement with the variations indicated by the T-L log.

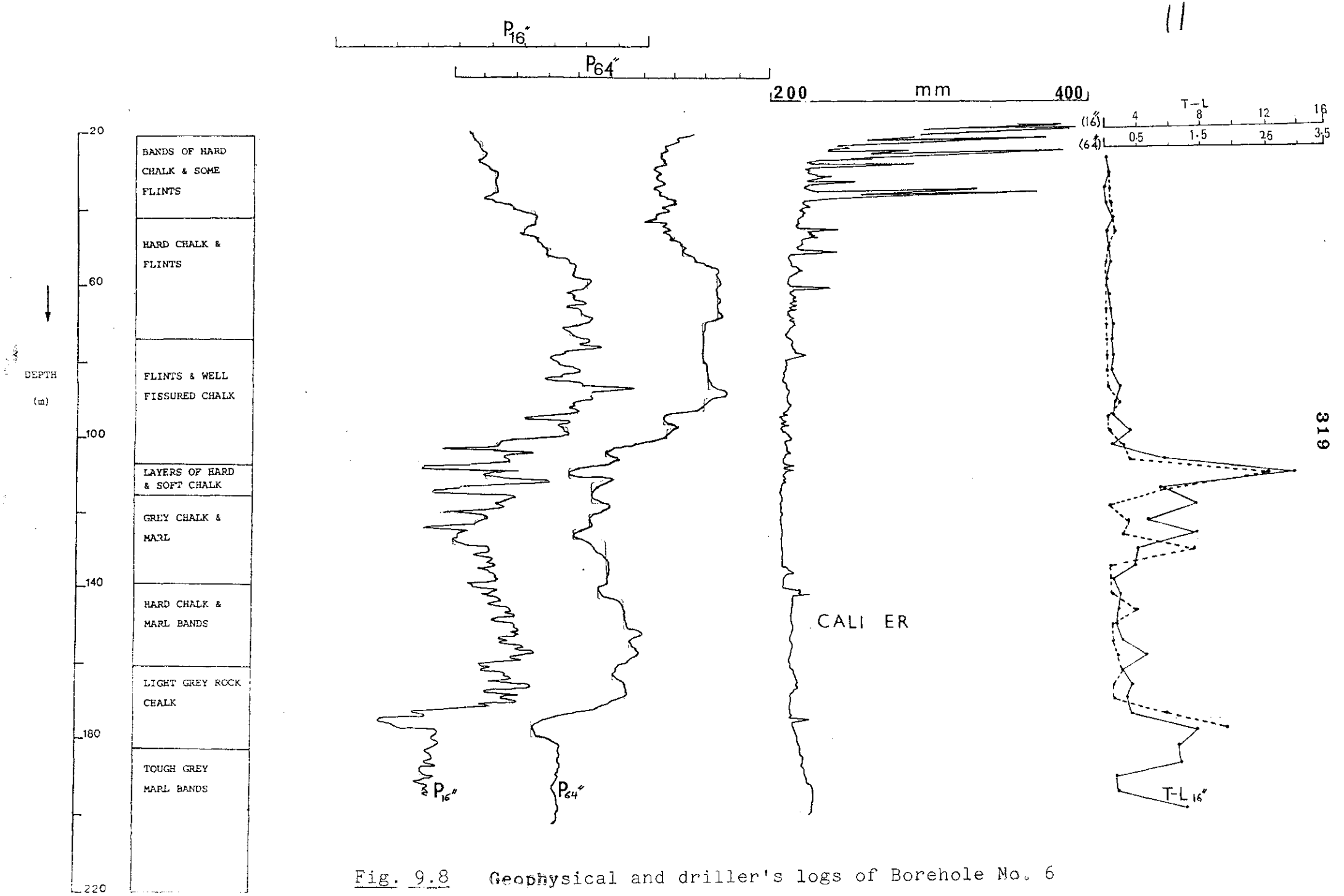


Fig. 9.8 Geophysical and driller's logs of Borehole No. 6

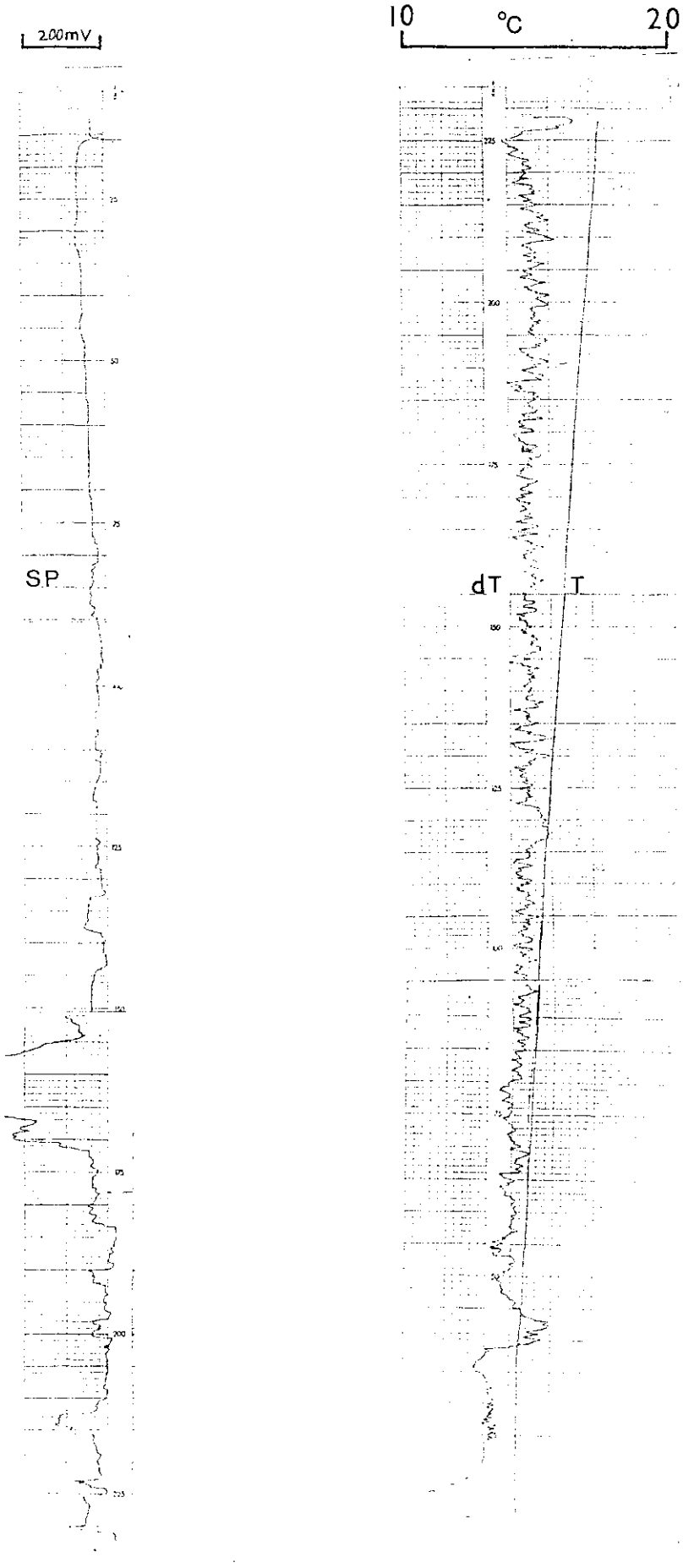


Fig. 9.9 Temperature, differential temperature and S.P. logs of Borehole No. 6

9.8 BOREHOLE NO. 7: ST. CATHERINES HILL, WINCHESTER (THAMES CHALK)

Fig. 9.10 represents the 16-inches, 64-inches and caliper logs together with the driller's log where Fig. 9.11 contains the temperature and differential temperature logs. In the same figure, a flow velocity log obtained by the heat pulse flowmeter is shown. The T-L log suggests two fissure zones at about 45m and 80m. Both of these fissure zones are confirmed by the features occurring on the differential temperature log at the corresponding levels. Note the change in the temperature gradient at 80m and the measured increase in the fluid velocity above the above levels.

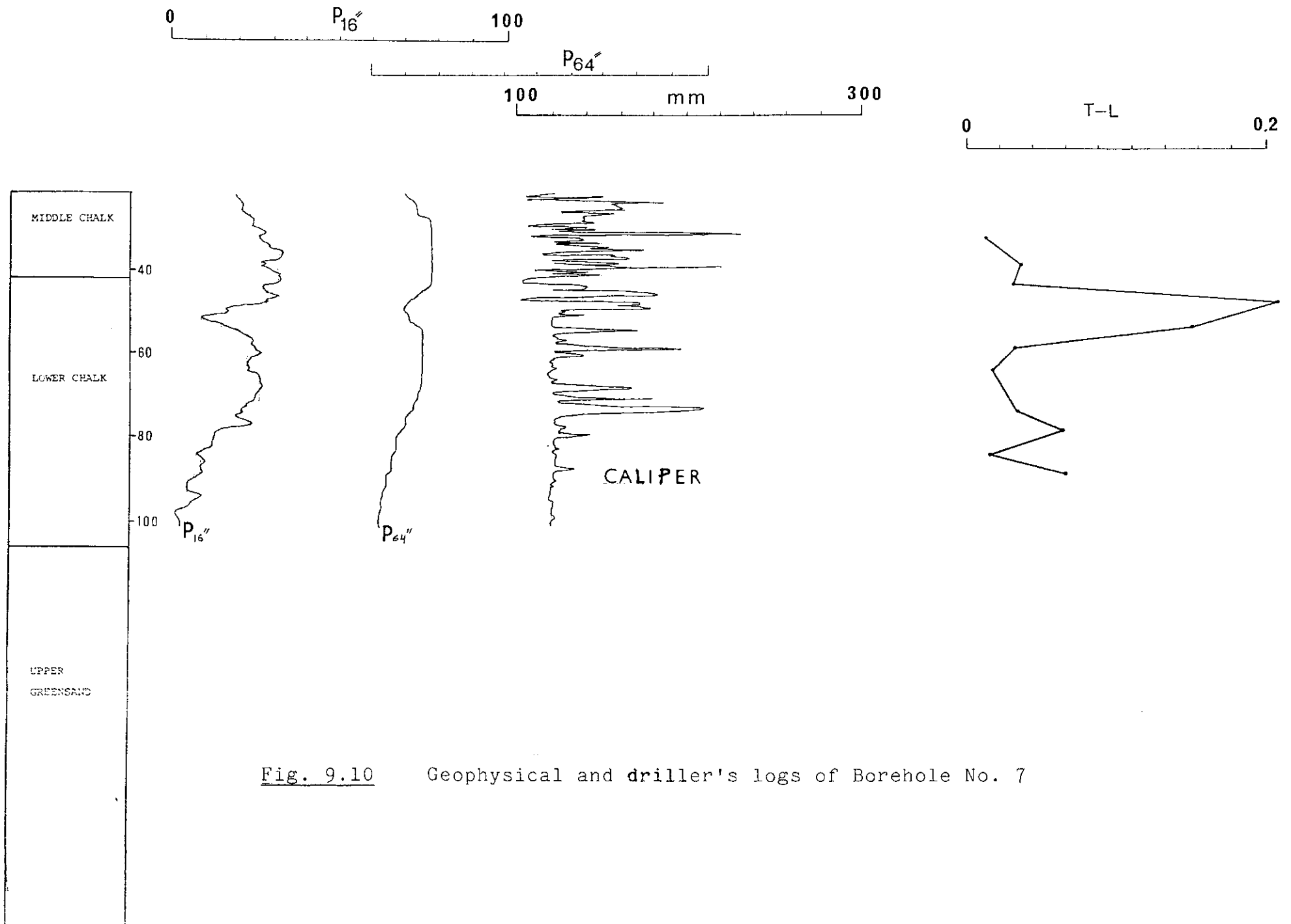


Fig. 9.10 Geophysical and driller's logs of Borehole No. 7

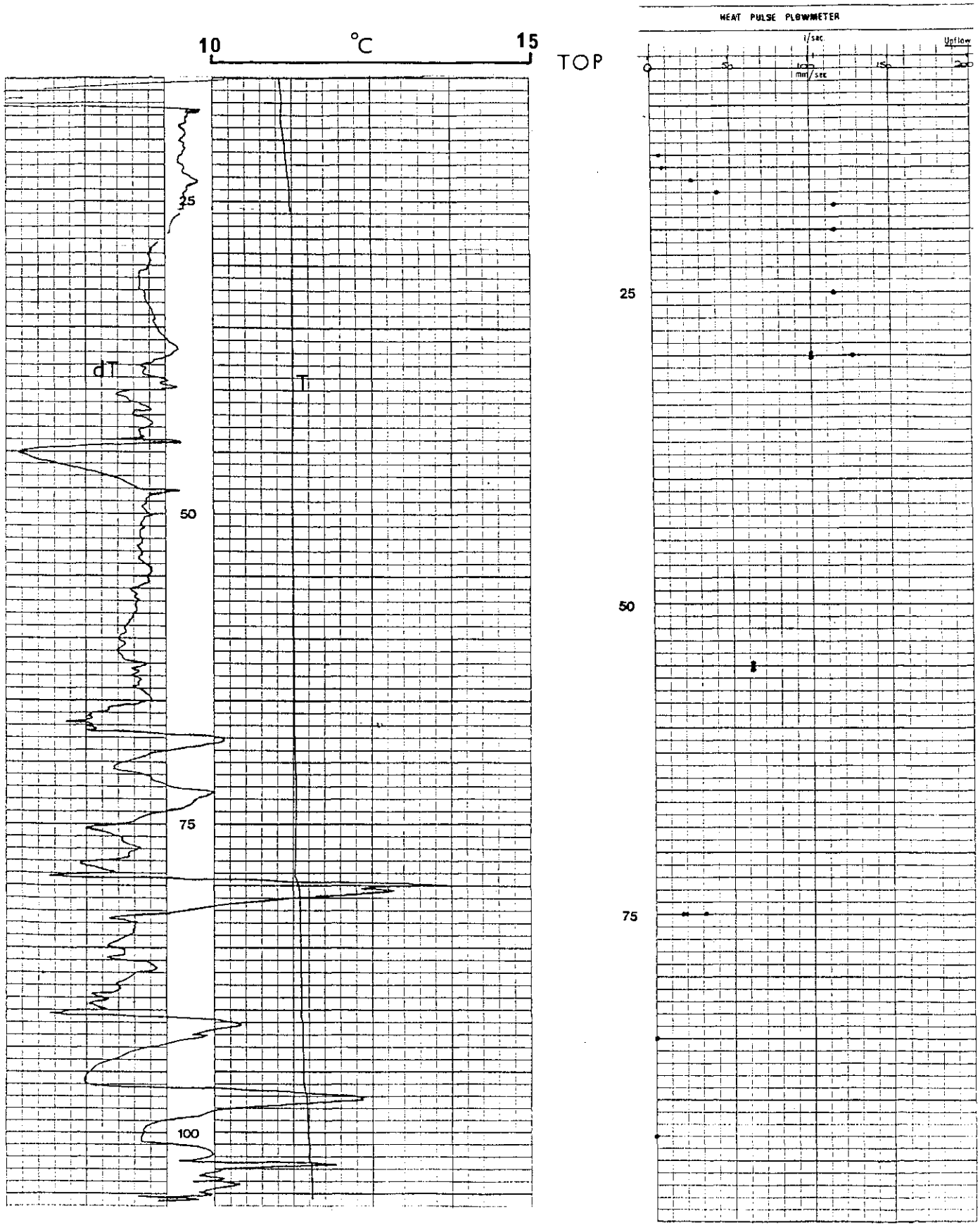


Fig. 9.11 Temperature, differential temperature and flow velocity logs for Borehole No. 7

9.9 BOREHOLE NO. 8: MADEHURST (THAMES CHALK)

This is an example of a relatively large diameter borehole (550mm), and the effect of the high diameter seems to occur in both the 16-inches and 64-inches resistivity logs (Fig. 9.12). The caliper log is not indicative of any fissure zones but the shape of the T-L and the fluid logs suggest the permeable nature of the formation. For example, the recorded high on the T-L log curve at around 108m corresponds very well with both the change in the temperature gradient and the feature on the differential temperature log occurring at this level (Fig. 9.13).

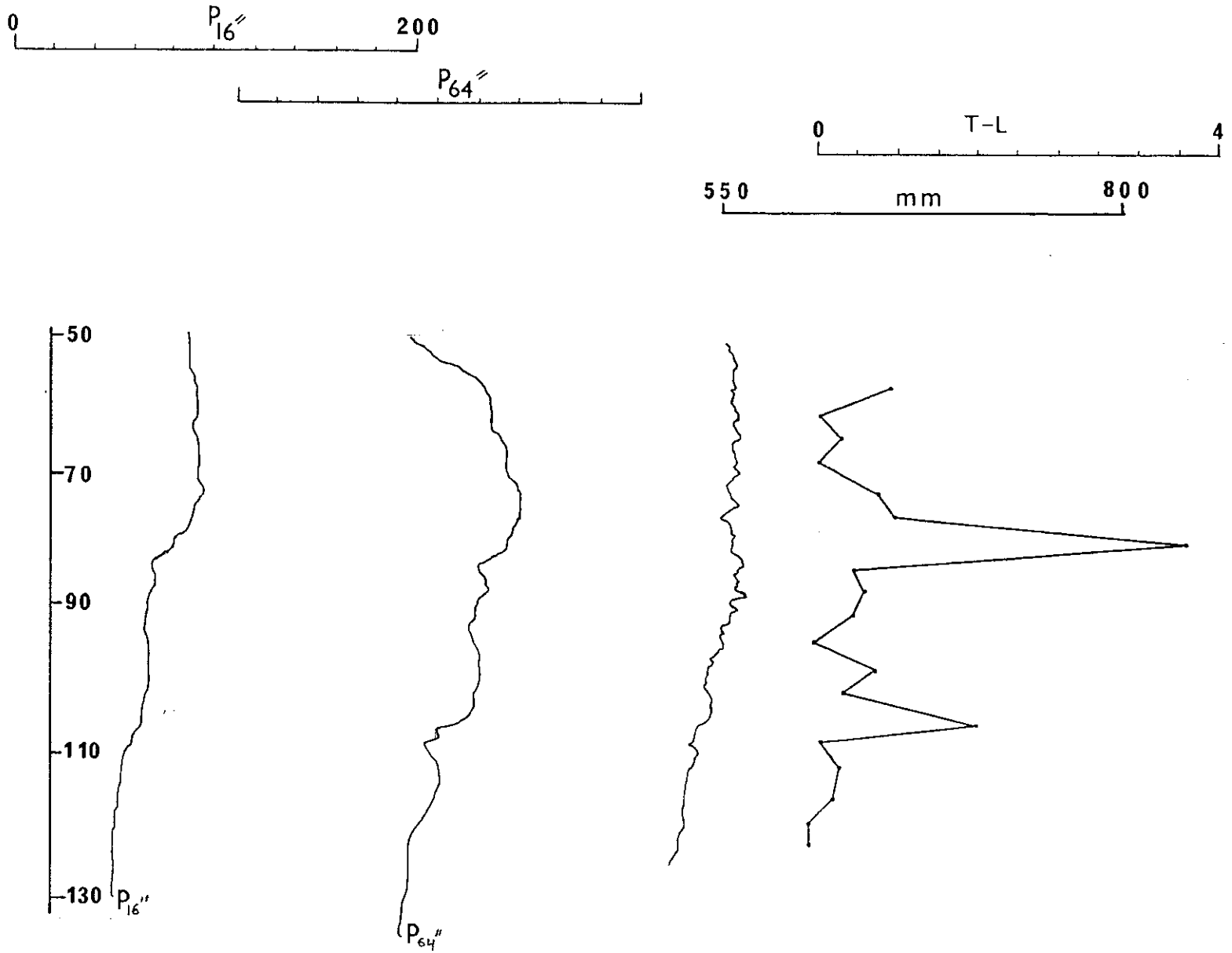


Fig. 9.12 Geophysical logs of Borehole No. 8

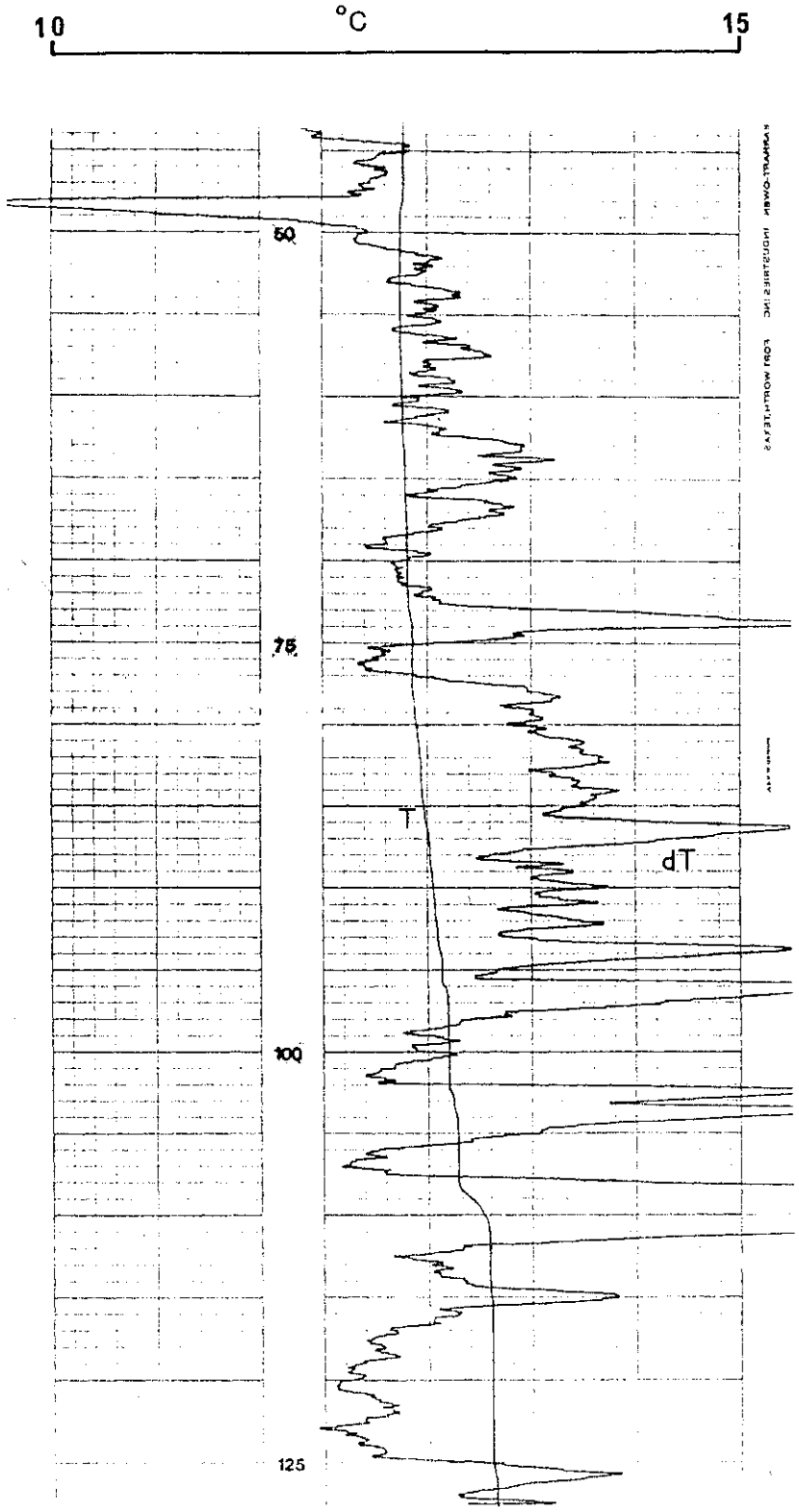


Fig. 9.13 Temperature and differential temperature logs of Borehole No. 8

9.10 BOREHOLES NO. 9 AND 10: LUDGERSHALL (THAMES CHALK)

The 16-inches, 64-inches and caliper logs of these boreholes were digitized and are shown in Fig. 9.14. The nature of the T-L log of borehole No. 9 suggests the existence of an anomaly in the geoelectric properties of the formation at around 40m. This corresponds with the feature recorded on the differential temperature log and with the change in the temperature gradient occurring at the same level (Fig. 9.15). The T-L log of borehole No. 10 suggests the occurrence of similar variations in the formation's geoelectric properties at the same level although this cannot be confirmed by the fluid logs (Fig. 9.16).

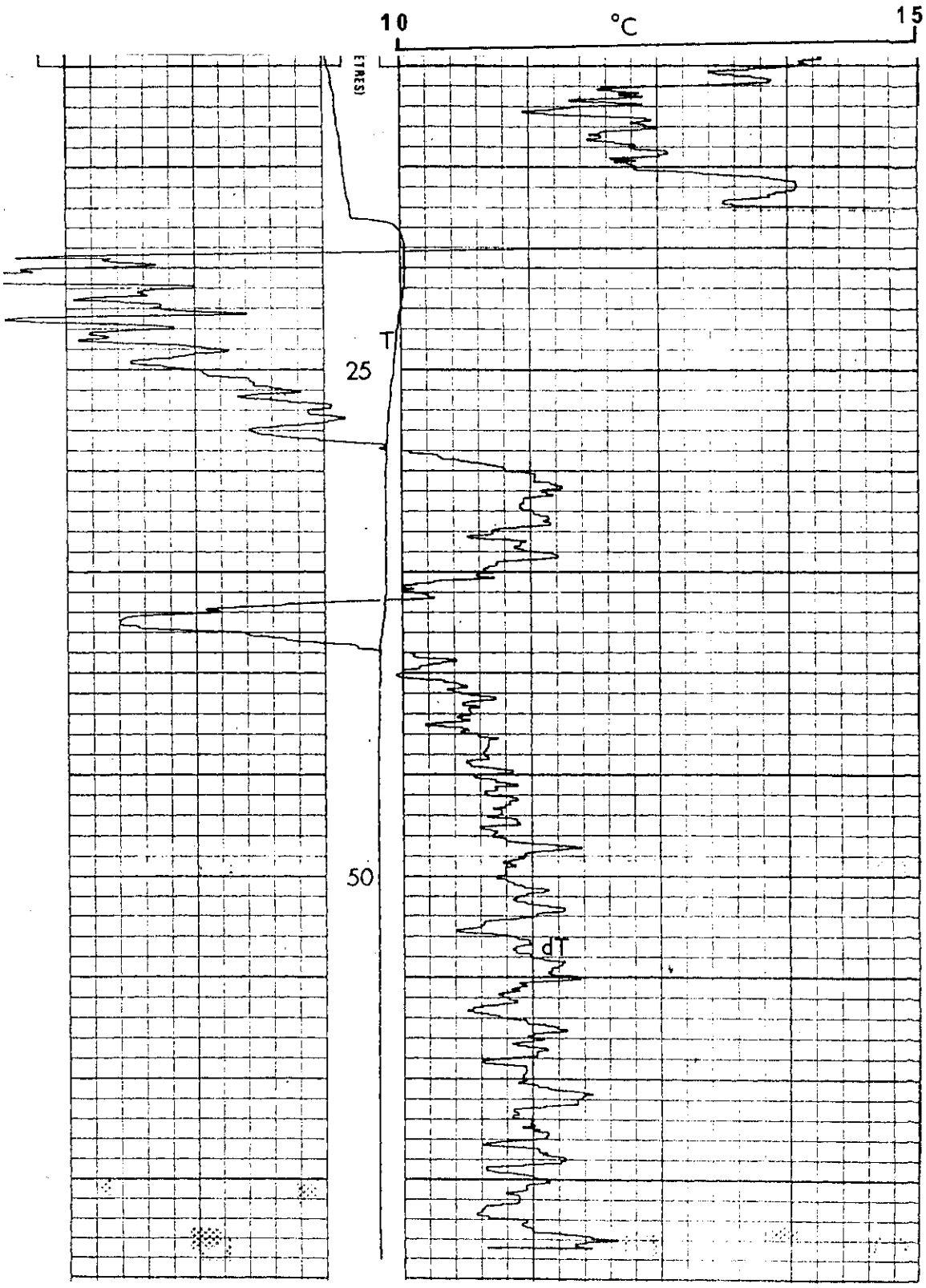


Fig. 9.15 Temperature and differential temperature logs of Borehole No. 9

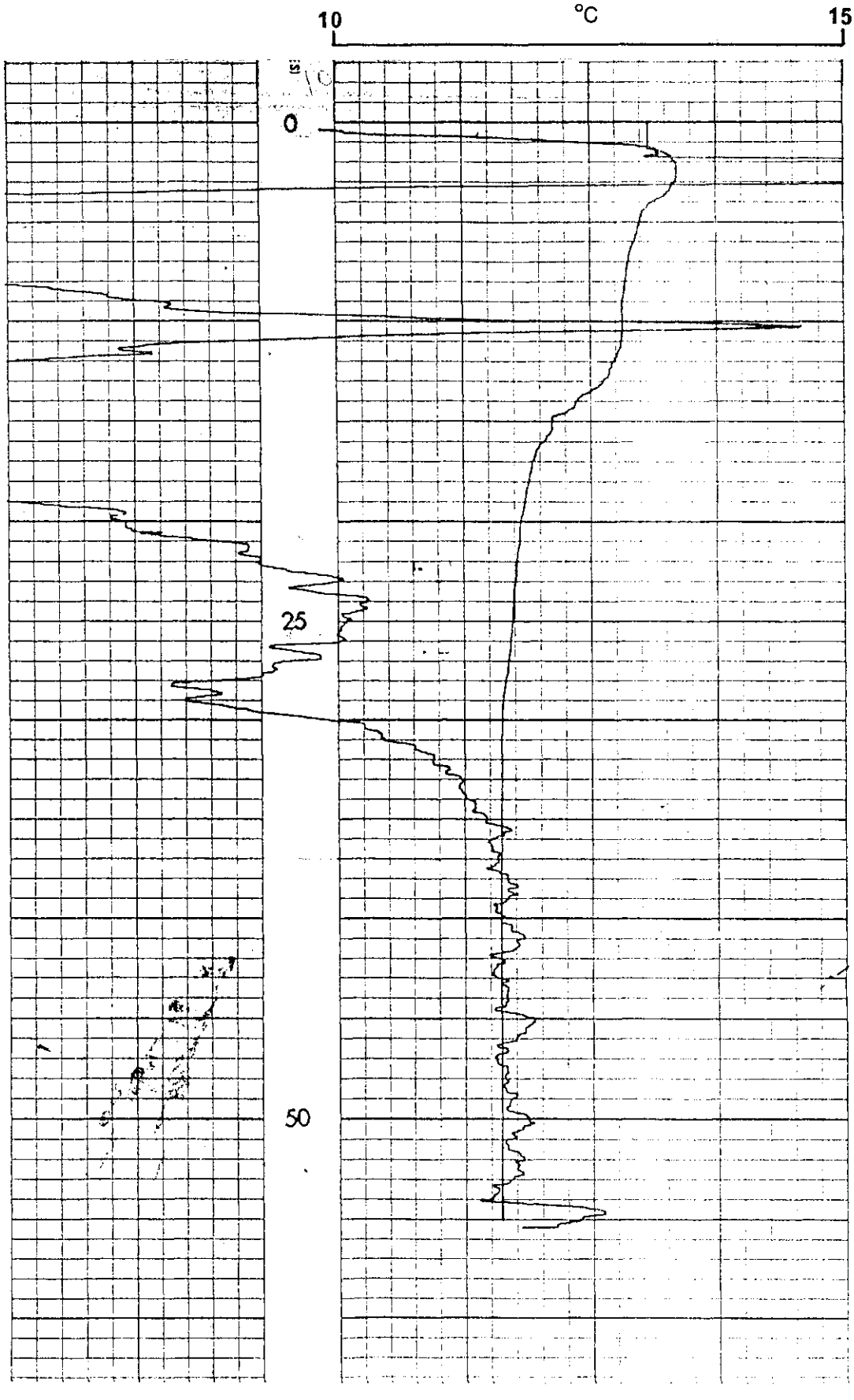


Fig. 9.16 Temperature and differential temperature logs of Borehole No. 10

9.12 BOREHOLE NO. 11: ADCOTE (THAMES CHALK)

The 16-inches and 64-inches resistivity logs were digitized and are presented in Fig. 9.17. A copy of the caliper log together with a fluid velocity log obtained by the heat pulse flowmeter is shown in Fig. 9.18.

From the features indicated by the T-L log, the one occurring at about 75m corresponds very well with the fissure zone indicated by the caliper and the measured increase in fluid velocity recorded at the same level.

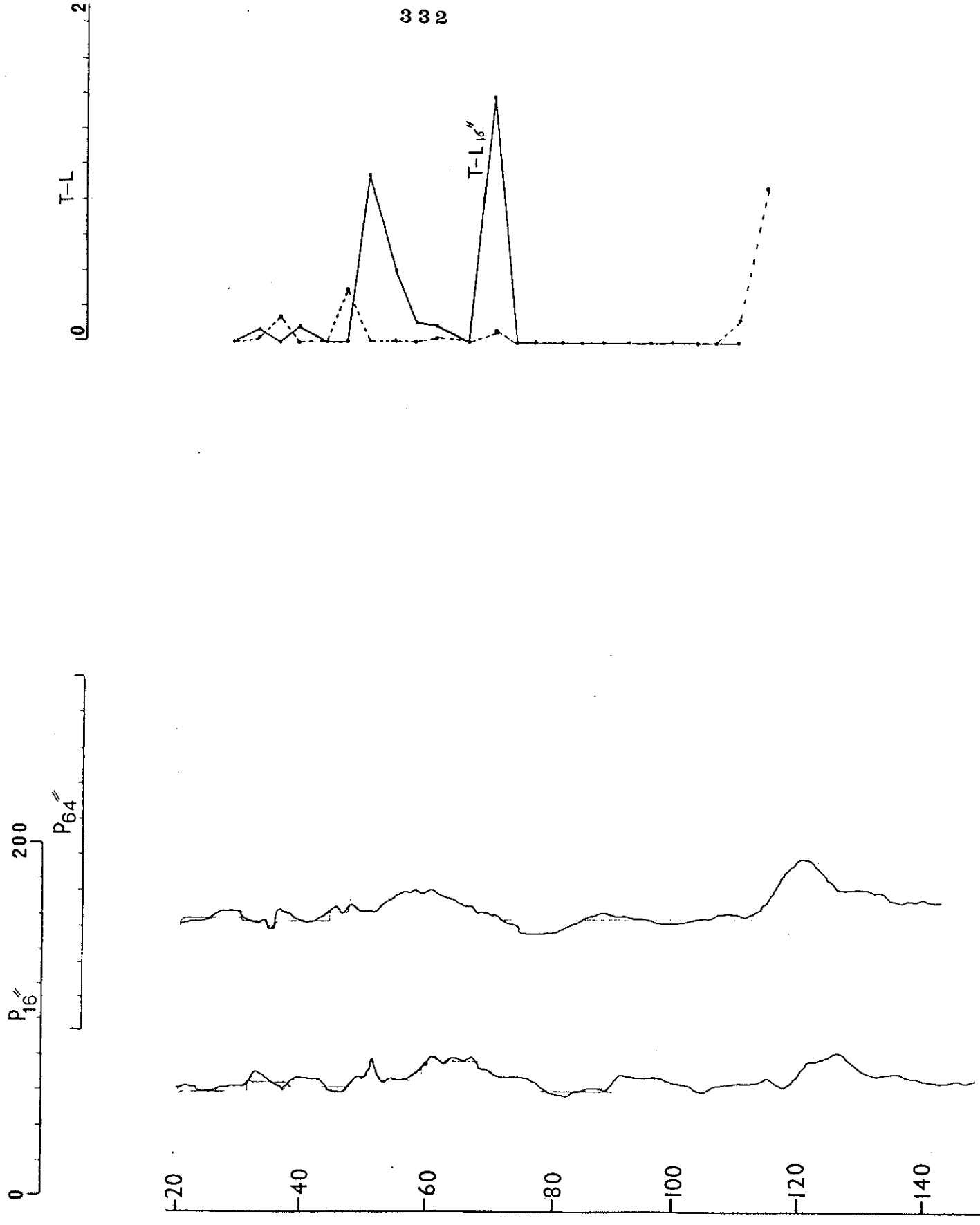


Fig. 9.17 Geophysical logs of Borehole No. 11

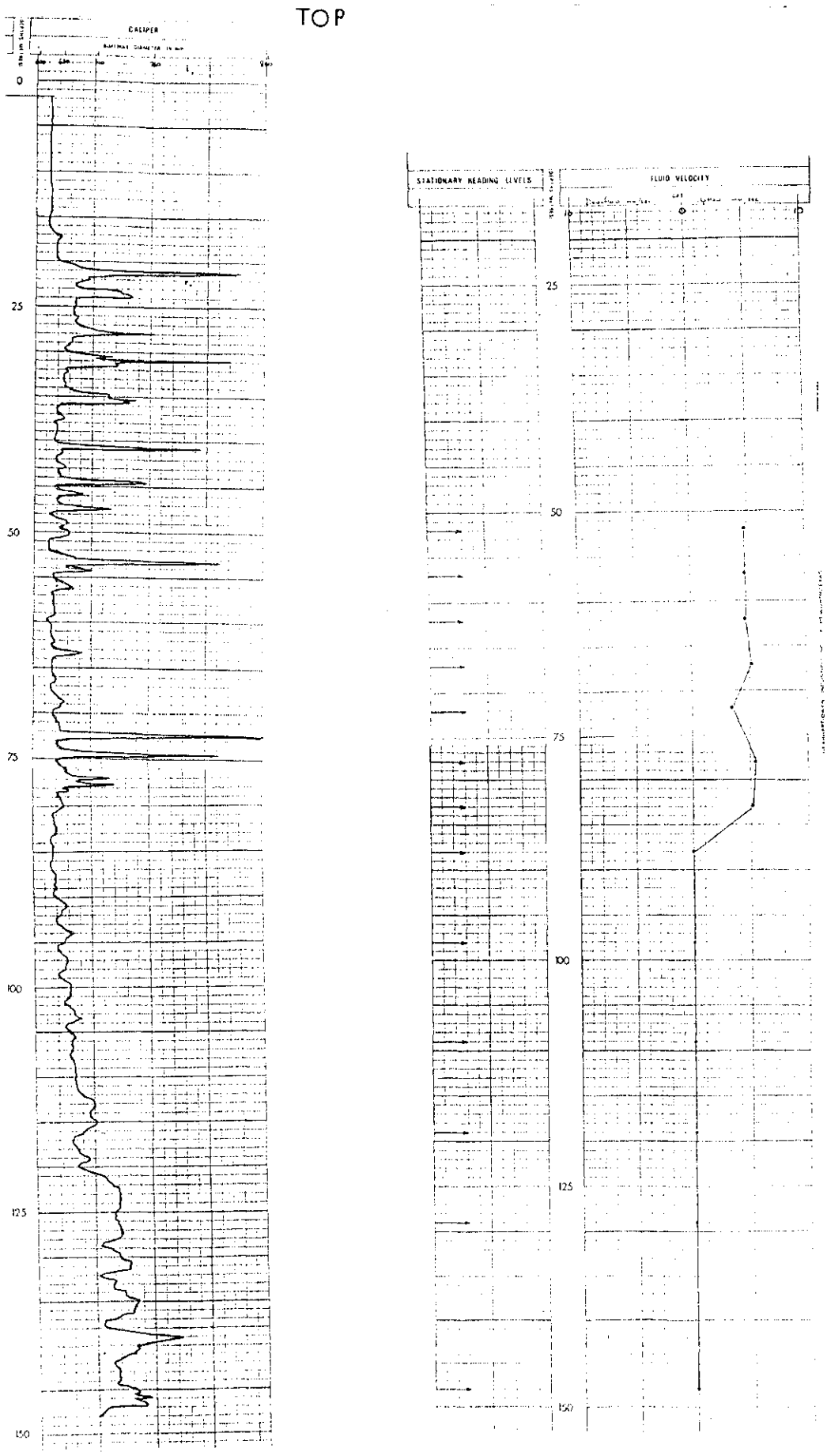


Fig. 9.18 Caliper and flow logs of Borehole No. 11

9.13 BOREHOLE NO. 12: HOUNDEAN BOTTOM (BRIGHTON CHALK BLOCK

An example of an in-situ application of the above methods.

After the analysis of a number of geophysical logs and the discussion of the obtained results, it was decided to try to apply the same methods of analysis directly in the field. For this reason a 12 bit Analog to Digital converter manufactured by ACORN COMPUTERS was modified in order to link the microcomputer with the logging unit (APPENDIX A.9.3). The idea was to feed directly the analog signals obtained by the logging unit through the AD converter into the microcomputer's memory in a digital form. In order to keep the number of accessories needed to a minimum (TV monitor, tape recorder, cassettes etc.), all the necessary software were stored in the computer's memory in the form of EPROM (Eraseable Programmable Read Only Memory). For this reason, an EPROM Programmer was constructed and all the technical details are given in APPENDIX A.9.4. A small portable printer was linked to the computer so that the calculated values of the T-L log could be printed directly as a function of depth. The hardware were tested successfully in the laboratory after simulating the output of the logging unit by a variable voltage obtained from a potentiometer.

On the 26th October 1982, the Areal Resource Planning Office of the Southern Water Authority permitted the author to make use of its geophysical logging unit for the logging of a well for which fissure flow was suspected. Unfortunately because of reasons outside control, the idea of linking directly the microcomputer with the logging unit was abandoned and the author decided to develop a method to derive a simplified form of a T-L log directly in the field.

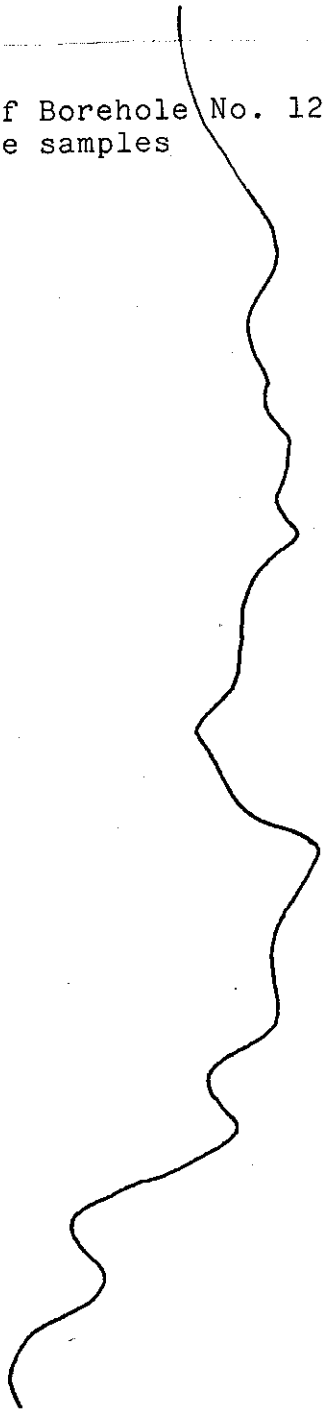
Since the geophysical logs are usually plotted on charts which are divided in one meter intervals, it is relatively



Plate 10 Adjusting the geophysical logging probe inside Borehole No.12

Fig. 9.20

64N resistivity log of Borehole No. 12 reconstructed from the samples



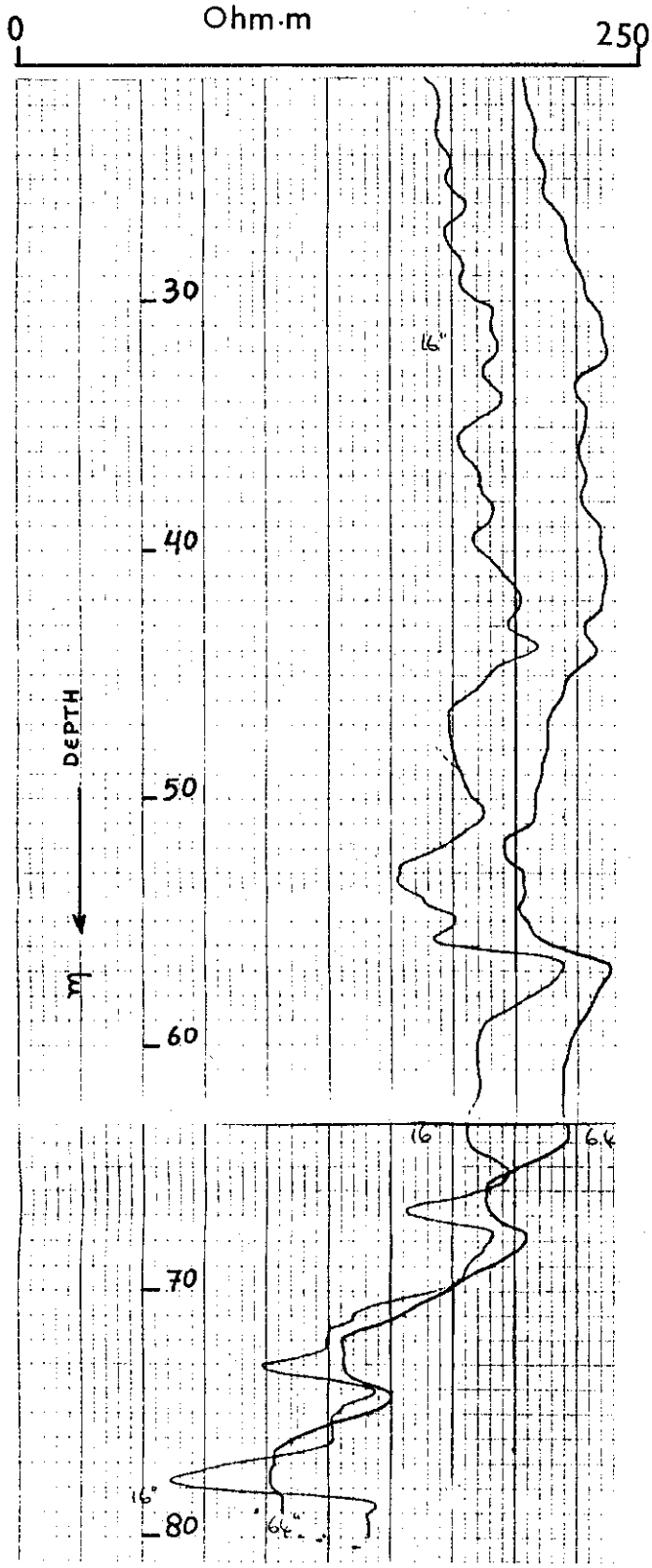


Fig 9·19

TABLE 9.1 Hand calculation of the T-L log

DEPTH (m)	ρ_a (O.m)	$\rho_{a,zon.}$ (O.m)	DEPTH INT. (m)	h_i (m)	ρ_i (O.m)	$\sum h_i \cdot \rho_i$ (O.m.m)	$\sum h_i/\rho_i \times 10^{-3}$ (Ω^{-1})	$\rho_{tr} = (h_i \cdot \rho_i)/4m$ (O.m)	$\rho_1 = 4/\sum h_i/\rho_i$ (O.m)	T-L (O.m)
30	210									
31	205									
32	205	208	30-34	4	208	832	0.019	208	208	0
33	208									
34	210									
35	213			1	208					
36	215			3		865	0.018	216.25	216.22	0.03
37	220	219	34-38							
38	223				219					
39	227									
40	230			4						
41	235	232	38-42		232	928	0.017	232	232	0
42	237									
43	225									
44	227									
45	228	227	42-46	4	227	908	0.017	227	227	0
46	225									
47	230			2						
48	227				227					
49	235			2		924	0.017	231	229.88	1.12
50	235	235	46-50		235					
51	236			2						
52	235				235					
53	228	228	50-54	1	228	936	0.017	234	233.91	0.09
54	238	238		1	238					
55	223									
56	219	221	54-58	2	221					
57	214					862	0.018	215.5	215.47	0.03
58	212			2	210					
59	210	210		3						
60	207		58-62		210					
61	206					825	0.0194	206.25	206.04	0.207
62	195	195		1	195					
63	202									
64	203	203	62-66	3	203					
65	205					824	0.019	206	205.87	0.13
66	215	215		1	215					

DEPTH (m)	ρ_a (O.m)	$\rho_{a,zon.}$ (O.m)	DEPTH INT. (m)	h_i (m)	ρ_i (O.m)	$\sum h_i \cdot \rho_i$ (O.m.m)	$\sum h_i/\rho_i \times 10^{-3}$ (σ^{-1})	$\rho_{tr} = (h_i \cdot \rho_i)/4m$ (O.m)	$\rho_1 = 4/\sum h_i/\rho_i$ (O.m)	T-L (O.m)
67	238	235	66-70	2	235	912	0.0176	228	227.79	0.21
68	232									
69	225			2	221					
70	221									
71	220	221	70-74	4	221	884	0.0181	221	221	0
72	220									
73	221									
74	220									
75	200	200	74-78	1	200	785	0.0204	196.25	196.04	0.21
76	190	190		2	190					
77	190									
78	205	205		1	205					
79	190	190	78-82	1	190	645	0.0253	161.25	158.17	3.08
80	170	170		1	170					
81	155	155		1	155					
82	130	130		1	130					
83	130	145	82-86	1	130	526	0.031	131.5	129.37	2.13
84	150			2	145					
85	140			1	106					
86	110									
87	103	106	86-90	4	106	424	0.0377	106	106	0
88	103									
89	106									
90	106									

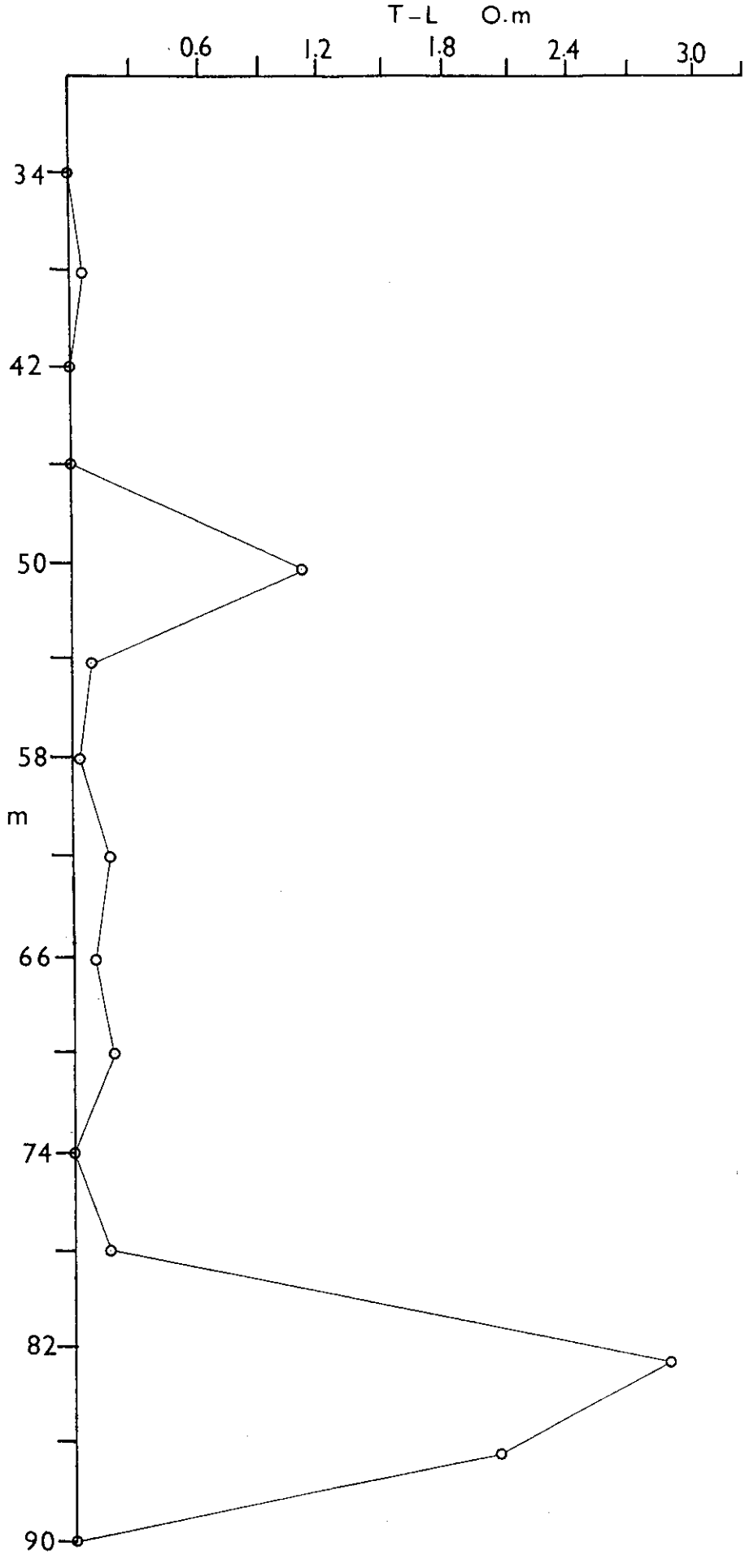


Fig. 9.21 T-L log of Borehole No. 12

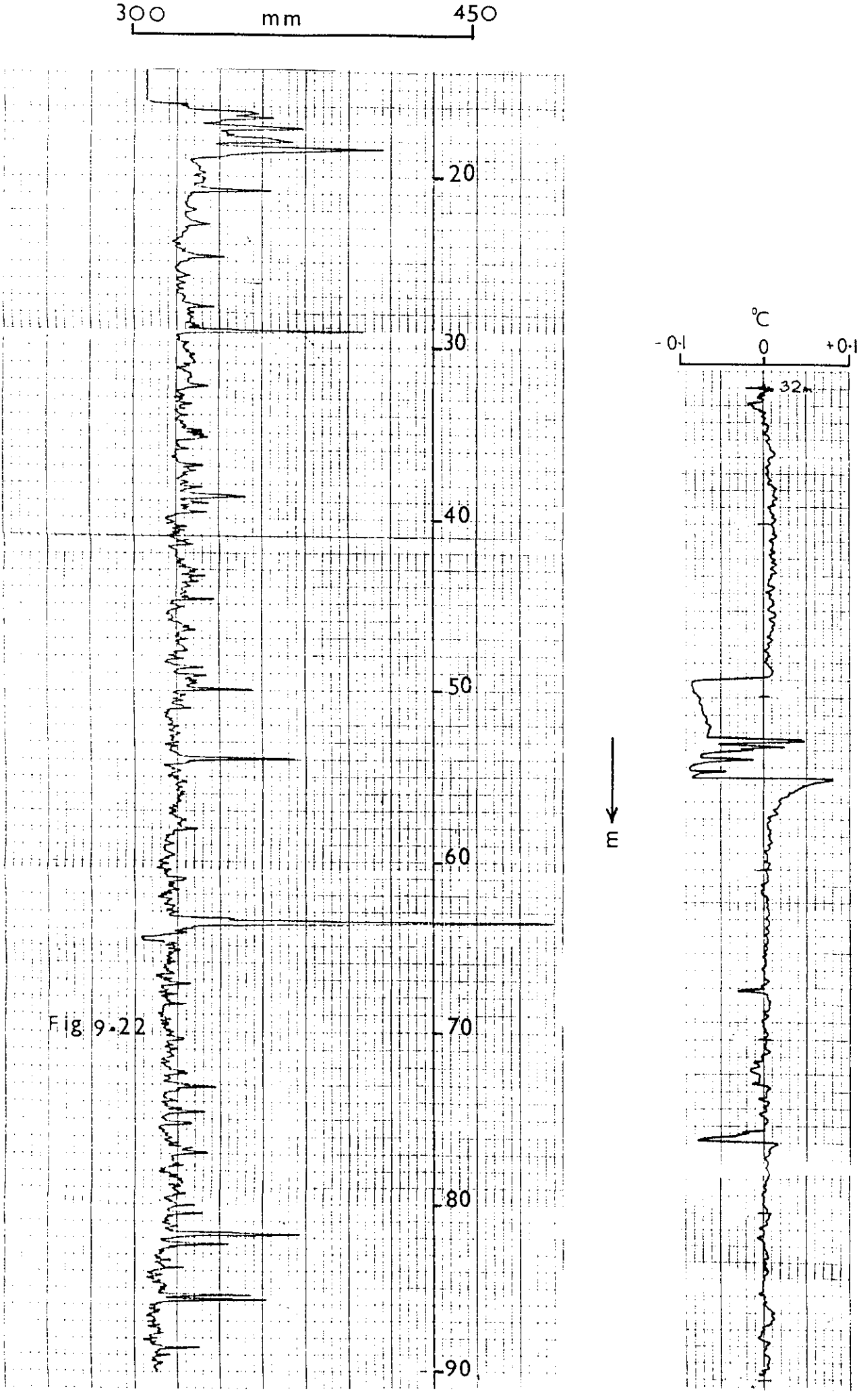


Fig 9.22

easy to digitize the log by hand every one meter. After having the log in a form of a column of numbers, it can be divided into a number of individual zones. Within each zone the variation of the resistivity is less than a predefined limit (for example 10 ohm.m). The next thing to be done is to calculate the Transverse and Longitudinal resistivities over a predefined depth interval (for example 4m) from the thicknesses and resistivities of the individual zones contained in this depth interval, and then plot the difference T-L as a function of depth. This method was applied to the 64-inches normal resistivity log of the borehole examined after the log was taken from the logging unit. Fig. 9.19 contains the 16-inches and 64-inches resistivity logs and Table 9.1 describes all the above procedures. Fig. 9.20 represents the 64-inches resistivity log replotted from the digitized samples. By comparing Fig. 9.19 with Fig. 9.20, one can notice that almost all the information contained in the original log is also contained in its version reconstructed from the hand digitization process.

The obtained T-L log is shown in Fig. 9.21 and suggests that there is a change in the geoelectric properties of the formation at around fifty and eighty meters. The differential temperature log confirmed the existence of a fissure level at about fifty meters and a similar feature was recorded at the depth of 76m. This log is shown in Fig. 9.22 together with the caliper log which confirmed the existence of the fissure levels suggested by the T-L log as well.

9.14 GENERAL CONCLUSIONS

This Chapter has recorded the practical application of the analytical methods introduced in Chapters VI and VII to a number of Chalk boreholes and the Transverse-Longitudinal (T-L) logs. The general conclusions from this part of the research can be summarised as follows:

- The software and hardware package proved to be very efficient for the processing of the geophysical logs of the examined boreholes.

- In almost all the cases, there was a satisfactory correlation between the T-L log and the other conventional fissure sensitive logs such as the caliper and the fluid logs.

- For a uniform formation, it is possible from the T-L log alone to identify existing fissure zones.

- Since the T-L log depends only upon the geoelectric properties of the formation, it is difficult to distinguish between anomalies caused by changes in the formation's lithology, such as boundaries between Upper, Middle and Lower Chalk, flints, etc. and anomalies caused by the presence of fissure zones. In this case the caliper and fluid logs must be used as well.

- By comparing the caliper and T-L logs, it is possible to distinguish between real fissures and borehole enlargements. For example, it was found that very few of the fissure-like responses recorded by the caliper for most of the boreholes just below the casing represented real fissures.

- A simplified method for the manual construction of the T-L log proved to be very efficient when applied in the field.

CHAPTER X

GENERAL CONCLUSIONS OF RESEARCH AND RECOMMENDATIONS

The purpose of this research was to examine the use of borehole geophysical measurements for assessing the in situ hydraulic character of fractured aquifers and in particular the Chalk.

In doing this, it became necessary that the subject of the research be broadened somewhat towards the following directions:-

A detailed study of the philosophy and techniques of borehole geophysics used by the water industry today in examining the hydraulic character of fractured aquifers was made. This pointed out that there has not been any serious attempt to correlate the geophysical and hydraulic parameters of the surrounding well formation.

An attempt was made to link the geophysical parameters measured from the normal resistivity logs with the hydraulic conductivity of the formation. In doing this, the aquifer was simulated by a double porosity model and from the laws of fluid mechanics an analytical evaluation of the hydraulic conductivity of the model was done. This was followed by correlating the geoelectric parameters of the model with some very close related to its hydraulic conductivity properties such as total and fissure porosity.

A procedure for the automatic evaluation of the geophysical logs was introduced. This was consisted of a microcomputer based software package which when applied to a number of actual situation, proved to be very efficient.

The fundamental conclusions obtained during the research are summarized below:-

1. Fluid geophysical logs play a very important role in the water industry since they can be useful in defining the limits of fluid entry, but they cannot provide any quantitative measure of hydraulic conductivity of the formation surrounding the well. The accuracy of these logs can be affected by many factors such as the thermal instability of the fluid column and special care is needed during their interpretation.

2. Detailed theoretical and experimental work was carried out in order to define the limits of usefulness of the heat pulse flowmeter. The analysis has shown that below velocities of 4mm/sec the influence of buoyancy effects becomes very important. Even so, with the present design, the device can be very useful for exploring fissure flows into water wells, even under nature gradient conditions, which hitherto have not been amenable to proper experimental investigation.

3. A review of the most common geophysical techniques to the water industry has pointed out that for many years there has been a notable lack of equipment specifically designed for logging in water boreholes, in contradiction to the oil industry where many sophisticated logging techniques have been developed. Nevertheless, potential applications of the existing techniques have important ramifications for making useful conclusions about aquifer properties. There has not been any attempt to correlate geophysical parameters measured from the geophysical logs with the hydraulic conductivity of fissured formations. Attempts to correlate normal resistivity measurements with fissure zones may be complicated by the presence of flint and marl bands and the effect of saline intrusion. In the later case, four basic extremes have been discussed. The spontaneous potential log was found to be useful in locating permeable zones in coastal boreholes.

4. The hydraulic characteristics of Chalk have been examined by adopting a distinct model approach consisting of a conduit geometry embedded in the matrix of the Chalk in order to represent fissures. From the fundamental equations of fissure flow, formulae for the equivalent hydraulic conductivity of sets of parallel fissures have been derived and a new computer algorithm for the on site assessment of the equivalent hydraulic conductivity of certain fissure patterns has been introduced. The dependence of the directional hydraulic conductivity upon the change of the direction of the local hydraulic gradient which occur during pumping was investigated and the results indicated that during pumping the directional hydraulic conductivity of a fissure zone is largely governed by the pressure head near the well. A new technique incorporating the use of an analogue electrical model for the study of the relation between fissure contact area and its hydraulic conductivity has been introduced and the results showed that flow rate through a fissure decreases with increasing contact area and that it also depends upon the path of fluid flow. The problem of flow through a fissure bisecting a semi-permeable matrix was examined and a formula giving the fissure's discharge as a function of the permeability ratio between fissure and matrix was derived.

5. The existing possibilities of expressing the hydraulic conductivity of a fissured formation from geophysical parameters measured from the logs were examined with the help of a double porosity model, and a quantitative measure of the degree of fissuring of the formation was made by the introduction of the Chalk's fissure index. The way in which the different formation parameters introduced by the model correlate with each other was described in terms of a generalised equation which proved to be in agreement with existing results for the limited cases of pure porous and pure fissured formations. It was also possible to express the hydraulic conductivity of the formation in terms of the formation's fissure index and a general procedure for measuring the equivalent hydraulic

conductivity of a fissured section from geophysical formation logs alone, has been proposed. After a detailed study of the relation between geoelectric and hydraulic properties of a fissured formation, a new formation parameter very sensitive to fissures was found and a new formation geophysical log capable of indicating permeable zones was introduced.

6. A microcomputer based on software and hardware package was designed in order to process the geophysical data in a fast and accurate way. In doing so a method for the automatic correction of the normal resistivity logs from the effect of changes in the hydraulic conductivity of the fluid column was proposed. In addition to this, an algorithm for the automatic zonation of the logs and a new method for the automatic evaluation of the geoelectric parameters of the surrounding well formation were introduced. An attempt was also made to simulate the response of a normal resistivity logging tool with the help of a microcomputer and the proposed method proved to be very efficient.

7. After applying the above methods of analysis to a number of Chalk boreholes and constructing the Transverse-Longitudinal (T-L) log, it was observed that almost in all cases the correlation between the T-L log and the other conventional fissure sensitive logs was satisfactory. It was also found that in many cases it was possible to distinguish between true fissure zones and borehole enlargements by comparing the caliper and the T-L logs, and this was verified by the fluid logs. The results also suggested that very few of the fissures recorded by the caliper just below the casing represented real fissures and they were probably borehole enlargements produced during drilling or the placement of the casing. The T-L log proved to be a very effective method of indicating fissure zones but one must be careful in its interpretation when the stratigraphy is complex, since any changes in the

geoelectric properties of the formation could produce the same effects as that derived from the fissure zones. In this case the T-L log should be examined in conjunction with the caliper and fluid logs.

Geophysical well logging can offer a great deal in the way of practical applications to hydrogeology but unfortunately the use of geophysical logging is generally restricted to either research projects or to a small number of municipal wells.

A very common argument used to support this approach is that the cost of well logging is not justified by the marginal benefits gained on small-yield domestic wells (Fetter 1980). This is not quite true and if one compares the drilling costs with that of geophysical logging, he will realize that drilling is the most expensive item on the budget of a groundwater investigation, and that in most of the cases the cost of geophysical logging turns out to be less than 2 per cent of the drilling costs per meter of borehole. Bearing in mind that correctly interpreted geophysical logs can be used to reduce future drilling costs by guiding the location, proper drilling and construction of wells, one will realize that the above argument is not valid.

If one comes now to the case of the Chalk aquifer, it will be seen that in most of the cases the geophysical logs are used in a qualitative way, mainly for stratigraphic correlation purposes and for defining the inflow levels and the extent of saline intrusion in boreholes. This qualitative approach to the problem of geophysical logging probably is based on a number of factors such as the fact that groundwater geophysical logging is an outgrowth of the oil industry and its application in groundwater investigations is still restricted and has not yet attained the scope it merits. The fact that in the case of fractured oil reservoirs any reliable definition of permeability from geophysical logs continues to be an

elusive goal does not mean that the water industry should not start to look at the problem of defining the permeability of fissured aquifers from geophysical logs. The author believes that it is a wrong attitude to expect all the progress in equipment and interpretation techniques to come directly from the oil industry; it is time for the groundwater geophysical logging to carry its own way.

As it was demonstrated by both experimental and analytical work, it became possible by taking advantage of the special geoelectric characteristics possessed by the fissures, to suggest a general methodology of location of fissure zones. This was achieved by using normal resistivity data alone, and introducing a new logging technique, the T-L log which proved to be a very useful tool during groundwater investigations but its use in the oil industry could prove rather limited because of the fact that there is a great difference between the geoelectric properties of water and oil.

This shows that there are research topics where the interests of the water and oil industries do not seem to converge, thus research results which could be of great importance when dealing with aquifers might be disregarded as useless when referred to oil reservoirs.

During the recent years, a dazzling variety of physical measurement techniques has been adapted to the oil well environment, while new applications are continuously making their debut. Many of these techniques are concerned with the task of calculating the permeability of fractured reservoirs from combination of new and existing logs and by using empirical techniques. This approach might be successful in specific areas or rock types, but it is doubtful that this will result in a generally applicable method for the water industry. The task of determining the hydraulic conductivity of fissured aquifers from geophysical methods alone is a very difficult one and more

research, both theoretical and experimental needs to be done. It seems that it is better at the present stage to work on methods that will not attempt to measure directly permeability but give an accurate quantitative measure of the factors upon which permeability depends. Such factors are the fissures, and their detection has been discussed extensively in the present thesis. The T-L log can prove to be a breakthrough in the accurate location of permeable zones in the Chalk if further research is carried out. Most of the present work was carried out by using a small do-it-yourself microcomputer, in a limited amount of time and with even a more limited amount of available money. There are many improvements which can be made to the method, and two of them are presented below:-

(a) Instead of calculating both the T and L resistivity values from the same normal resistivity device, it might be better to use the 64-inches normal for the calculation of the Transverse resistivity and the guard log for the longitudinal. Both these measurements could be taken simultaneously by using an appropriate electrode arrangement which should be linked to a microcomputer based device to provide directly the values of the T-L log.

b) Investigate the existing relations between T-L logs calculated from different electrode geometries (for example different electrode separations which would have as a result different depths of investigation) and fissure characteristics. Recent experiments carried out by the author and not included in the present thesis proved to be very promising.

Finally, as a general rule, the more complete the set of geophysical logs that is available for a single well and the more wells that are logged within a given geohydrologic environment, the greater the benefits than can be expected from the logging. Keys and MacCary (1971, p.15) state it more clearly:

> "The synergistic character of logs is due to the fact that each type of log actually measures a different parameter, and when several are analyzed together, each will tend to support or contradict conclusions drawn from others".

At the beginning of this thesis, it was stated that the main object of the research was to examine the use of geophysical well logs for assessing the in situ hydraulic character of fractured Chalk aquifers. This has now been done and it is clear that in geophysics linked to the data handling facilities of microcomputers, the water industry has a powerful and underdeveloped logging technology that is ripe for development as a low-cost quantitative investigation technique.

REFERENCES

AGUILERA, R. (1974): Analysis of naturally fractured reservoirs from sonic and resistivity logs. J. Pet. Tech. 1283-1238.

AGUILERA, R. (1976): Analysis of naturally fractured reservoirs from conventional well logs. J. Pet. Tech. 764-772.

ALGER, R.P. (1966): Interpretation of electrical logs in fresh water wells in unconsolidated formations. Soc. Prof. Well Log Analysts, 7th Ann. Logging Symposium, Tulsa Okla. CC1-CC25.

ARCHIE, G.E. (1942): The electrical resistivity log as an aid in determining some reservoir characteristics. Trans. AIME, 146, 54.

ARCHIE, G.E. (1952): Reservoir rocks and petrophysical considerations. Am. Assoc. Petr. Geologists Bull., 36, 2, 278.

ARNOLD, D.M. and PAAP, H.J. (1979): Quantitative monitoring of water flow behind and in wellbore casing. Journ. of Petr. Technology, 31, 2.

ATKINS, F.R. and SMITH, G.H. (1961): The significance of particle shape in formation factor-porosity relationships. J. Petr. Tech. 13, 285-291.

BAKER, W.J. (1955): Flow in fissured formations. Proc. 4, World Petroleum Congr., Section II/E, Paper 7, S.379-393.

BARENBLATT, G.I., ZHELTOV, I.P. and KOCHINA, J.N. (1960): Basic concepts in the theory of seepage of homogeneous liquids in fissured rock strata. Journ. Appl. Math. and Mech., 24, 5.

BARKER, J.A. (1981): A formula for estimating fissure transmissivities from steady-state-injection-test data. J. Hydrol., 52, 337-346.

BARKER, J.A. and FOSTER, S.S.D. (1981): A diffusion exchange model for solute movement in fissured porous rock. Q.J. Eng. Geol., 14, 17-24.

BARKER, R.D. and WORTHINGTON, P.F. (1973): Some hydrogeophysical properties of the BUNTER sandstone of N.W. England. Geoexploration 11, 151-170.

BAUER, A.B. (1965): Direct measurement of velocity by hot-wire anemometers. AIAA Journal, 3, 1189-1191.

BEAR, J. (1972): Dynamics of fluids in porous media. Elsevier, N.Y., p.764.

BECK, A.E. (1969): Techniques of measuring heat flow on land. Terrestial heat flow. Amer. Geophys. Union, Monograph 8, 24-51.

BECK, A.E. (1976): The use of thermal resistivity logs in stratigraphic correlation. Geophysics, 41, 2, 300-309.

BELL, F.G. (1977): A note on the physical properties of the Chalk. Eng. Geol., 11, 217-225.

BENEDINI, M. (1976): The Aquifers and their hydraulic characteristics. Geoexploration, 14, 157-178.

BHATTACHARYA, P.K. and PATRA, H.P. (1968): Direct current sounding principles and interpretation. Publ. Elsevier, N.Y., 135.

BLACKWELL, J.H. (1954): A transient flow method of determination of thermal constants of insulating materials in bulk. J. of Applied Physics, 25, 137-144.

BORG, S.F. (1963): Matrix-Tensor methods in continuum mechanics. D. Van Nostrand Co., N.Y., 313.

BOULTON, N.S. (1963): Analysis of data from non-equilibrium pumping tests allowing for delayed yield from storage. Proc. Instn. Civ. Engrs. 26, 469-482.

BRADSHAW, P. (1970): An introduction to turbulence and its measurement. Pergamon, London, 218.

BROOKS, R.H. and COREY, A.T. (1966): Properties of porous media affecting fluid flow. Proc. ASCE, J. Irrig. Drain. Div., 92, 61-88.

BROWN, B.L. (1971): Techniques for quality of water interpretation from calibrated geophysical logs. Atlantic coastal area. Ground water 9, 4, 25-38.

CALLAGHER, B. (1973): Calibration of probes in water at velocities under one meter per second. DISA information report No. 14.

CAROTHERS, J.E. (1968): A statistical study of the formation factor relation to porosity. The Log Analyst. IX, 5.

CAROTHERS, J.E. and PORTER, C.R. (1970): Formation factor-porosity relation derived from well log data. SPWLA Trans.

CARSLOW, H.S. and JAEGER, J.C. (1959): Conduction of heat in solids. Oxford Publ., 510.

CARTER, P.G. and MALLARD, D.J. (1974): A study of the strength, compressibility, and density trends within the Chalk of S.E. England. Q.Jl. Eng. Geol., 7, 43-55.

CASTALDINI, M., HELLAND, K.N. and MALVESTUTO, V. (1980): Hot film anemometry in aqueous NaCl solutions. Int. J. Heat Mass Transfer, 24.

CHAPMAN, H.T. and ROBINSON, A.E. (1962): A thermal flowmeter for measuring velocity flow in a well. USGS water-supply paper 1544-E.

CHILDS, E.C. (1957): The physics of land drainage. In drainage of agricultural lands (J. Luthin, editor). Amer. soc. Agric. Madison, Wisconsin 1-76.

CHOMBART, L.G. (1960): Well log interpretation in carbonate reservoirs. Geophysics, 25, 779.

COLEBROOK, C.F. (1939): Turbulent flow in pipes with particular reference to the transition region between the smooth and rough pipe laws. Journ. Instn. Civ. Engrs., London, Fe., 133.

COLLIS, D.C. and WILLIAMS, N.J. (1959): Two dimensional convection from heated wires at low Reynolds numbers. J. of Fluid Mechanics, 6, 357-384.

CONNORTON, B.J. and REED, R.N. (1978): A numerical model for the prediction of long term well yield in an unconfined Chalk aquifer. Q. Jl. Eng. Geol., 11, 127-138.

CROFT, M.G. (1971): A method of calculating permeability from electric logs. U.S.G.S. prof. paper 750-B, B265-B269.

DAVIS, S.N. and De WIEST, R.J.M. (1967): Hydrogeology. Publ. Wiley & Sons, N.Y., 462.

DAVIS, J.C. (1973): Statistics and data analysis in geology. J. Wiley Pub., 550.

De La RUE, R.E. and TOBIAS, C.W. (1959): J. Electrochemical Society, 106, 827.

DIMENT, W. (1967): Thermal regime of a large diameter borehole, instability of the water column and comparison of air and water filled conditions. Geophysics, 32, 4, 728.

DOLL, H.G. (1971): The spontaneous potential log. Theoretical analysis and principles of interpretation. SPE, Reprints Series No. 1, Well Logging 45-64.

DOWNING, R.A., SMITH, D.B. and WARREN, S.C. (1978): Seasonal variations of tritium and other constituents in groundwater in the Chalk near Brighton, England. J. Inst. Water Eng. Sci., 32, 123-136.

DRING, R.P. and GERHART, B. (1968): Hot wire anemometer calibration for measurements at very low velocity. Paper No. 69-HT-A.

DUDGEON, C.R., GREEN, M.J. and SMEDMOR, W.J. (1975): Heat pulse flowmeter for boreholes. WRC (U.K.), Technical Paper TR4.

DULLIEN, F.A.L. (1979): Porous media. Fluid transport and pore structure. Academic Press, 396.

DYCKE, J.H., KEYS, W.S. and MENELEY, W.A. (1972): Application of geophysical logging to groundwater studies in southern Saskatchewan. Canadian Journal of Earth Sciences, 9,1.

EDMUNDS, W.M., LOVELOCK, P.E.R. and GRAY, D.A. (1973): Interstitial water chemistry and aquifer properties in the Upper and Middle Chalk of Berkshire, England. J. Hydrol. 19, 159-165.

EMERSON, D.W. (1969): Laboratory electrical resistivity measurements of rocks. Proc. Austr. Inst. Mining Met. No. 230, 51-62.

FERRANDON, J. (1948): Less lois de l'ecoulement de filtration, Ge'nie Civie. An.68, 125, 24-28.

FILON, L.N.G. (1928): On a quadrature formula for trigonometric integrals. Proc. of the Royal Society of Edinburgh, 49, 38.

FLATHE, H. (1976): The role of a Geologic concept in geophysical research work for solving hydrogeological problems. Geoexploration, 14, 195-206.

FLATHE, H. (1955): Possibilities and limitations in applying geoelectrical methods to hydrogeological problems in coastal areas of northwest Germany. Geophysical Prospecting 3, 95-110.

FLATHE, H. (1967): Interpretation of geoelectrical resistivity measurements for solving hydrogeological problems. Mineral Groundwater Geophysics, Ottawa, Econ. Geol. Rep. 26, 560-597.

FLOWER, J. (1982): Atom EPROM Programmer, Practical Computing June,

FONS, L.C. (1958): Downhole camera helps solve production problems. World Oil, 151, 5, 150-152.

FORSYTHE, G.E. (1957): Orthogonal polynomials. J. of the Society for Industrial and Applied Mathematics, 5, 74.

FOSTER, S.S.D. and MILTON, V.A. (1974): The permeability and storage of an unconfined Chalk aquifer. Hyrol. Sci. Bull. 19, 485-500.

FOSTER, S.S.D. (1975): The Chalk groundwater tritium anomaly - a possibly explanation. J. Hydrol., 25, 159-165.

FOSTER, S.S.D. and CREASE, R.I. (1975): Hydraulic behaviour of the Chalk aquifer in the Yorkshire Wolds. Proc. Instn. Civ. Engrs., Dart 2, 59, 181-188.

FREEZE, A.R. and CHERRY, J.A. (1979): Groundwater, Publ. Prentice-Hall, 604.

GANGI, A.F. (1975): Variation of whole and fractured porous rock permeability with confining pressure. First Internat. Symp. on Induced seismicity. Banff, Alberta, Canada.

GIANZERO, S. and RAU, R. (1977): The effect of sonde position in the hole on responses of resistivity logging tools. Geophysics, 24, 642-654.

GILL, D. (1970): Application of a statistical zonation method to reservoir evaluation and digitized-log analysis. Bull., AAPG, 54, 5, 719-729.

GRAY, D.A. (1958): Electrical resistivity marker bands in the Lower and Middle Chalk of London basin. Bull. Geol. Surv. Gt. Britain 15, 85-95.

GRAY, D.A. (1965): The stratigraphical significance of electrical resistivity marker bands in the Cretaceous strata of the Leatherhead borehole. Bull. Geol. Surv. G.B., 23, 65-115.

GRETENER, P. (1967): On the thermal stability of large diameter wells - an observational report. Geophysics, 32, 4, 727-738.

GRIFFITHS, D.H. (1976): Application of electrical resistivity measurements for the determination of porosity and permeability in sandstones. Geoexplotation, 14, 207-213.

GUYOD, H. (1944): Electrical well logging: Series of articles in Oil Weekly, August 7 to December 4.

GUYOD, H. (1952): Electrical well logging fundamentals. Houston, Tex., Well Instrument Developing Co., 164.

GUYOD, H. (1966): Interpretation of electric and gamma ray logs in water wells. Log Analyst 6, 5, 29-44.

HALES, A.L. (1937): Convection currents in geysers. Monthly Notices Royal Astrom. Soc., Geophys. Supp., 4, 1, 122-132.

HALEVY, E., MOSER, H., ZELLHOFER, O., ZUBER, A. (1966): Borehole dilution techniques: a critical review. Isotopes in Hysdrology. Proc. Symp. Vienna. IAEA, 531.

HAMMING, R.W. (1977): Digital Filters. Prentice Hall Publ. N.Y., 226.

HANCOCK, J.M. (1975): The petrology of the Chalk. Geologists' Assoc. Proc. 86, 83-118.

HARDCASTLE, B.J. (1978): From concept to commissioning. Proc. Conf. Thames Groundwater Scheme Instn. Civ. Engrs., London, 1, 5-31.

HAWKINS, D.M. and KROODEN, J.A.T. (1979): Zonation of sequences of heteroscedastic multivariate data. Computers and Geosciences, 5, 189-194.

HEADWORTH, H.G. (1978): Hydrogeological characteristics of artesian boreholes in the Chalk of Hampshire. Q. Jl. Eng. Geol., 11, 139-144.

HEIGOLD, P.C., GILKESON, R.H., CARTWRIGHT, K. and REED, P.C. (1979): Aquifer transmissity from surficial electrical methods. Groundwater 17, 4, 338-345.

HOLMAN, J.P. (1976): Heat transfer, McGraw Hill publ. 530.

INESON, J. (1959a): Yield-depression curves of discharging wells, with particular reference to Chalk wells, and their relationship to variations in transmissivity. J. Instn. Wat. Engrs., 13, 119-162.

INESON, J. (1959b): The relation between the yield of a discharging well and its diameter with particular reference to a Chalk well. J. Instn. Wat. Engrs., 13, 299-316.

INESON, J. (1962): A hydrogeological study of the permeability of the Chalk. J. Instn. Wat. Engrs., 16, 449-463.

INESON, J. and GRAY, D.A. (1963): Electrical investigations of borehole fluids. Journ. of Hydrol. 1, 204-218.

INESON, J. and DOWNING, R.A. (1965): Some hydrogeological factors in permeable catchment studies. J. Inst. Wat. Engrs., 19, 59-80.

IRMAY, S. (1955): Flow of liquid through cracked media. Bull. Res. Conc. Israel, 5, L.

JACKSON, P.D., TAYLOR, S.D. and STANDORD, P.N. (1978): Resistivity-porosity-particle shape relationships for marine sands. Geophysics, 43, 6, 1250-1268.

JAKOSKY, J.I. (1950): Exploration geophysics, 2nd ed., Los Angeles, Trija publ. company.

JOHNSON, E.W. and HUGHES, R.V. (1948): Directional permeability measurements and their significance. Producer's monthly, 13, 17-25.

JOHNSON, W.E. and BRESTON, J.N. (1951): Directional permeability measurements on oil sandstones from various states. Producer's monthly, 14, 10-19.

JONES, P.H. and BUFORD, T.B. (1951): Electrical logging applied to groundwater exploration. Geophysics, 16, 1, 115-139.

JONES, P.H. and SKIBITZKE, H.E. (1956): Subsurface geophysical methods in groundwater hydrology. Advances in Geophysics, 3, 241-300.

KATSUHIKO, I. (1975): Fundamental studies of fluid flow through a single fracture. Ph.D. Thesis, Berkeley Univ.

KELLER, G.V. and FRISHCKNECHT, F.L. (1966): Electrical methods in geophysical prospecting. Pergamon Press, N.Y., 517.

KELLY, W.E. (1978): Geoelectric sounding for estimating aquifer hydraulic conductivity. Ground water, 15, 6, 420-425.

KEYS, W.S. (1967): The application of radiation logs to groundwater hydrology. Isotopes in Hydrology. Proc. Symp. Vienna. IAEA, 477.

KLINKENBERG, L.J. (1941): The permeability of porous media to liquids and gases. Drill and Prod. Prac. API, 200.

KOEFOED, O. (1968): The application of kernel function in interpreting geoelectrical measurements. Geoexploration Monographs Series I, No. 2, Gebruder Sorntraeger, Berlin-Stuggart.

KOEFOED, O. (1979): Resistivity sounding measurements. Elsevier, 276.

KOMAROV, S.G. and KEIVSAR, Z.I. (1962): Determining the permeability of oil-bearing strata from the specific resistance. In "Applied Geophysics USSR", edited by Rast, N., Publ. Pergamon Press, 328-349.

KOSINSKI, W.K. and KELLY, W.E. (1981): Geoelectric soundings for predicting aquifer properties. Ground water, 19, 2, 163-171.

KOWASZNAY, X.X. (1949): Thermal flowmeters. Proc. Royal Soc. of London, A-198, 174-190.

KRUSEMAN, G.P., DE RIDDER, N.A. (1979): Analysis and evaluation of pumping test data. Bull. 11, Inst. for Land Reclamations and Improvements, Netherlands.

KUNETZ G. (1966): Principles of direct current resistivity prospecting. Berling-Gebruder Borntraegger, 103.

KUNZ, K.S. and MORAN, J.H. (1958): Some effects of formation anisotropy on resistivity measurements in boreholes. Geophysics, XXIII, 4, 770-794.

LAMB, H. (1932): Hydrodynamics. Cambridge Univ. Press, 738.

LANG, W.H. Jr. (1972): Porosity-resistivity cross-plotting. SPWLA, 13.

LEE, J.D. and LEE, T.D. (1982): Statistics and computing methods in BASIC. Publ. Van Nostrand Reinhold Company, 198.

LE TIRANT, P. and BARON, G. (1972): Ecoulement dans les Roches fissurees et contraintes effectives: Application a le fracturation hydraulique des reservoirs. Proc. Symp. on percolation through fissured rock. T2-K, Stuttgart.

LLOYD, J.W. (1981): Case studies in Groundwater evaluation. Publ. Oxford Univ. Press.

LLOYD, J.W., HARKER, D. and BAXENDALE, R.A. (1981): Recharge mechanisms and groundwater flow in the Chalk and drift deposits of southern East Anglia. Q.J. Eng. Geol. 14, 87-96.

LOMIZE, G.M. (1951): Water flow in jointed rocks. Go senergoizdat (Russian).

LONG, R.R. (1961): Mechanics of solids and fluids. Prentiss-Hall, Englewood Cliffs, N.J., 156.

LOUIS, C. (1969): A study of groundwater flow in jointed rock and in influence on the stability of rock masses. Imperial College, Rock Mechanics, Research Report No. 10.

LYNCH, E.J. (1962): Formation evaluation, Publ. Harper Row, 422.

MAILLET, R. and DOLL, H.G. (1932): Sur an theoreme relatif aux milieux electriquement anisotropes et ser applications a la prospection electrique en courant continu Erganzungshefte fur angewandte Geophysik, 3, 109.

MANDEL, S. and SHIFTAN, Z.L. (1981): Groundwater resources - investigation and development. Publ. Academic Press, 269.

MAXWELL, J.C. (1881): A treatise on Electricity and Magnetism. 2nd ed. Oxford Univ. Press.

McCARY, L.M. (1978): Interpretation of well logs in a carbonate aquifer. U.S.G.S. Water Resources Investigations, paper 78-88.

MENDELSON, K.S. and COHEN, M.H. (1982): The effect of grain anisotropy on the electrical properties of sedimentary rocks. Geophysics, 47, 2, 257-263.

MONKHOUSE, R.A. and FLEET, M. (1975): A geophysical investigation of saline water in the Chalk of the South Coast of England. Q.J. Eng. Geol., B, 291-302.

MORRIS, R.L., GRINE, D.R. and ARKFELD, T.E. (1964): The use of compressional and shear acoustic amplitudes for the location of fractures. J. of Pet. Tech. June issue.

MUSKAT, M. (1935): Analog electric problem. Physics, 6, 14.

MUSKAT, M. (1937): The flow of homogeneous fluids through porous media. McGraw Hill, N.Y.. Reprinted 1948, J.W. Edwards Co., Ann. Arbor. Mich.

NELSON, P.H. (1982): Advances in borehole geophysics for hydrology. U.S.G.S. special paper 189, 207-219.

NEWMAN, L. (1966): A survey of the literature on transition from laminar to turbulent flow in natural convection and forced flow. M.Sc. thesis, Cornell Univeristy.

NEUMAN, S.P. (1975): Analysis of pumping test data from anisotropic unconfined aquifers considering delayed gravity response. Wat. Resour. Res. 11, 2.

OTERI, A.U.J. (1980): Geophysical and hydrogeological investigations of contaminated aquifers in Southern England. Thesis, Univ. of London, 424, (unpublished).

OTERI, A.U. (1982): Geoelectric investigation of saline contamination of a Chalk aquifer by mine drainage water at Tilmanstone, England. Geoexploration 19, 179-192.

OWEN, M. and ROBINSON, V.K. (1978): Characteristics and yield in fissured Chalk. Instn. Civ. Engrs. Symposium on Thames Groundwater Scheme, 2, 33-49.

PARSONS, R.W. (1966): Permeability of idealized fractured rock. Soc. Pet. Eng. J., 126-136.

PARSON, J.R. and MULLIGAN, J.C. (1978): Measurement of the properties of liquids and gasses using a transient hot-wire technique. Rev. Sci. Instruments, 49, 1460-1463.

PATTEN, E.P. and BENNETT, G.D. (1962): Methods of flow measurement in well bores, U.S.G.S. Water Supply paper 1544-C.

PATTEN, E.P. Hr. and BENNET, E.D. (1963): Application of electrical and radioactive well logging to ground water hydrology. U.S. Geol. Survey Water Supply Paper 15440.

PETZNY, H. (1964): On the practice of foundation rock investigation in Austria. Hydrostatic effects in jointed rock. Part C. 8th Congrs des Grands Barrages 1, 28, Edinburgh.

PIRSON, S.J. (1963): Comprehensive quantitative well log interpretation in multiple-porosity type reservoir rocks. In Handbook of well log analysis, Prentice-Hall Inc. 303-314.

PIRSON, S.J. (1967): How to map fracture development from well logs. World Oil, 106-198.

PODOLSKY, B. (1951): A problem in heat conduction. J. of Appl. Physics, 22, 581-585.

PONSFORD, D.R.A. (1955): Radioactivity studies of some British sedimentary rocks. Bull. Geol. Surv. Gt. Britain 10, 24-44.

PRICE, M., BIRD, M.J. and FOSTER, S.S.D. (1976): Chalk pore-size measurements and their significance. Water serv., 80, 968, 596-600.

PRICE, M., ROBERTSON, A.S. and FOSTER, S.S.D. (1977): Chalk permeability - a study of vertical variation using water injection tests and borehole logging. Water Serv., 81, 980, 603-610.

PRICE, M., MORRIS, B. and ROBERTSON, A. (1982): A study of intergranular and fissure permeability in Chalk and Permian aquifers, using double-packer injection testing. J. Hydrol., 54, 401-423.

RAST, N. (1962): Applied Geophysics U.S.S.R. Pergamon Press, 429.

REEVES, M.I. (1979): Recharge and pollution of the English Chalk. Some possible mechanisms. Eng. Geol., 14, 231-240.

ROBINS, N.S. and LLOYD, J.W. (1975): A surface resistivity investigation over an area of the English Chalk aquifer. J. Hydrol., 27, 285-295.

ROBINSON, V.K. (1974): Low cost geophysical well logs for hydrogeological investigations. Eng. Geol. Quart. Journ. 7, 207-215.

RUCKDESCHEL, F.R. (1981): Basic Scientific Subroutines. McGraw-Hill Publ., II, 790.

RUSHTON, K.R. and CHAN, Y.K. (1976): Pumping test analysis when parameters vary with depth. Ground water, 14, 2, 82-87.

RUST, C.F. (1952): Electrical rersistivity measurements on reservoir rock samples by the two electrode and four-electrode methods. Am. Inst. Met. Engrs. Trans., 195, 217-227.

SAMMEL, E.A. (1968): Convective flow and its effect on temperature logging in small diameter wells. Geophysics, 33, 6, 1004-1012.

SCHEIDEGGER, E.E. (1954): Directional permeability of porous media to homogeneous fluids. Geofisica Pura E Applicata, Milan, 30, 17-26.

SCHEIDEGGER, A.E. (1960): The physics of flow through porous media. Publ. McMillan Co., NY, 313.

SCHLIGHTING, H. (1965): Grenzschichtheorie, Verlag G. Braun, Karlsruhe, 5.

SCHLICHTING, H. (1968): Boundary layer theory. Publ. McGraw Hill, N.Y.

SCHLUMBERGER, C. (1920): Etude sur la prospection electrique du sous-sol Gotuthier-Villars, Paris.

SCHLUMBERGER WELL SURVEYING CORP (1950): Interpretation hand-book for resistivity logs.

SCHOLLE, P.A. (1974): Diagenesis of Upper Cretaceous Chalks from England, Northern Ireland and the North Sea. In K.J. Hsu and H.C. Jenkyns (edits.), Pelagic Sediments on land and under the sea. Spec. Publ. Int. Ass. Sediment 1, 177-210.

SCHOPPER, J.R. (1966): A theoretical investigation on the formation factor/permeability/porosity relationship using a network model. Geophysical prospecting, XIX, 301-341.

SEN, P.N. (1981): Relation of certain geometrical features to the dielectric anomaly of rocks. Geophysics, 46, 1714-1720.

SEN, P.N., SCALA, C. and COHEN, M.H. (1981): A self-similar model for sedimentary rocks with application to the dielectric constant of fused glass beads. Geophysics, 46, 781-795.

SHARP, J.C. (1970): Fluid flow through fissured media. Ph.D. thesis, Imperial College, Univ. of London.

SHARP, J.C. and MAINI, Y.N. (1972): Fundamental considerations on the hydraulic characteristics of joints in rocks. Proc. Int. Symp. Int. Soc. Rock Mech. "Percolation through fissured rock". Stuttgart, T1-F.

SHCHERBAKOVA, T.V. (1962): Optical methods of borehole investigation. In "Applied Geophysiks, U.S.S.R.". Edited by Rast, N., publ. Pergamon Press, 328-349.

SLATER, R.J. (1966): Notes on the use of closed circuit television for inspection of wells and boreholes. J.I.W.E., 404-406.

SMART, J.G., SABINE, P.A. and BULLERWELL, W. (1964): The geological survey exploration borehole at Canvey Island, Essex. Bull. Geol. Survey, Gt. Britain, 21, 1-36.

SMYTHE, W.R. (1950): Static and dynamic electricity. Publ. McGraw-Hill, New York.

SNOW, D.T. (1965): A parallel plate model of fractured permeability matrix. Ph.D. Thesis, University of California, Berkeley, 330.

SOUDER, W.W. and PICKETT, G.R. (1974): A computerized method for the zonation of digitized well logs. The Log Analyst. May-June issue, 3-8.

STEWART, C.R., CRAIG, F.F. and MORSE, R.A. (1953): Determination of limestone performance characteristics by model flow tests. Trans. AIME 198, 93.

STEWART, C.R. and OWENS, W.W. (1958): A laboratory study of laminar and turbulent flow in heterogeneous porosity limestones. Trans. AIME 213, 121-126.

STRELTSOVA, T.D. (1972): Unsteady radial flow in unconfined aquifer. Wat. Resourc. Res. 8, 1059-1066.

SUAV, J. and GARTNER, J. (1980): Fracture detection from well logs. The Log Analyst, March-April issue, 3-13.

TATE, T.K., ROBERTSON, A.S. and GRAY, D.A. (1970): The hydrogeological investigation of fissure flow by borehole logging techniques. Q.J. Eng. Geol., 2, 196-215.

TATE, T.K. (1971): Borehole logging investigations in the Chalk of the Lambourn and Winterbourn Valleys of Berkshire. Wat. Sup. Pap. I.G.S. Res. Rep. No. 5.

TATE, T.K. and ROBERTSON, A.S. (1975): Logging equipment for water boreholes. Wat. Serr. 79, 368-369.

TERZAGHI, K. and PECK, R. (1961): Soil mechanics and Engineering Practice. Publ. John Wiley & Sons. N.Y., 566.

TESTERMAN, J.D. (1962): A statistical reservoir-zonation technique. J. Pet. Tech. 889-893.

THE ART OF ANCIENT LOG ANALYSTS (1979): Published by the Society of Professional well log analysts.

TIXIER, M.P. (1958): Porosity balance verifies water saturation determined from logs. Trans. AIME, 213, 161.

TNO -GROUND-WATER SURVEY (1976): Geophysical well logging for Geohydrological purposes in unconsolidated formations. Published by the Netherlands Organization for Applied Scientific Research, 67.

TODD, D.K. (1959): Ground Water Hydrology, Publ. John Wiley and Sons, NY, 336.

TOLMAN, C.F. (1937): Ground Water. Publ. McGraw Hill, N.Y., 593.

TOMBACH, I.H. (1969): Velocity measurements with a new probe in inhomogeneous turbulent sets. Ph.D. thesis, California Institute of Technology.

TSELENTIS, A. (1977): Methods of mathematical analysis. Publ. Kronos, 177 (in Greek).

TSELENTIS, A. and STAURAKAKIS, G. (1978): Lessons of Linear Algebra. Publ. Kronos, 340, (in Greek).

TSELENTIS, A. (1982): On the use of hot wire (film) flowmeters for water velocity measurements into wells. J. of Hydrol. 58, 375-381.

VAN DAM, J.C. (1976): Possibilities and limitations of the resistivity method of geoelectrical prospecting in the solution of geohydrological problems. Geoexploration 14, 179-193.

VANDENBERG, A. (1977): Pump testing in heterogeneous aquifers. J. Hydrol., 34, 45-62.

WALKER, R.E. and WESTENBERG, A.A. (1956): Absolute low speed anemometer. Rev. Sci. Instruments, 27, 844-848.

WALTON, W.C. (1970): Ground water resource evaluation. Publ. McGraw-Hill, 664.

WEBSTER, R. (1978): Optimally partitioning soil transects. J. Soil Sci., 29.

WENNER, F. (1916): A method of measuring earth-resistivity. Bull. U.S. Bureau Stand., 12, 469-478.

WHITE, K.E. (1978): Dilution methods. In Hydrometry, edited by A. Herschy, publ. by J. Wiley & Sons, 111-148.

WYLLIE, M.R.J. (1949): A quantitative analysis of the electro-chemical component of the SP curve. Journ. Petr. Techn. 1, 17.

WYLLIE, M.R.J. (1951): An investigation of the electrokinetic component of the SP curve. Trans. AIME, 192, 1.

WYLLIE, M.R.J. and ROSE, W.D. (19590): Some theoretical considerations related to the quantitative evaluation of the physical characteristics of reservoir rock from electrical log data. Trans. AIME, 189, 105.

WINKLER, K. and NUR, A. (1978): Pore fluids and seismic attenuation in rocks. Proceedings, 48th annual meeting of Society of Exploration Geophysicists, San Francisco.

WINSAUER, W.O., SHEARIN, H.M., Jr., MASSON, P.H. and WILLIAMS, M. (1952): Resistivity of brine saturated sands in relation to pore geometry. Bull. AAPG, 36, 253.

WORTHINGTON, P.F. and BARKER, R.D. (1972): Methods for the calculation of true formation factors in the Bunter Sandstone of north west England. Eng. Geol., 6, 213-228.

WORTHINGTON, A.E. (1975): Errors in the laboratory measurement of formation factor. Soc. Prof. Well Log Analysts, Trans, Paper D, 17.

WORTHINGTON, P.F. and GRIFFITHS, D.H. (1975): The application of geophysical methods in the exploration and development of sandstone aquifers. Eng. Geol. Quart. Journ. 8, 73-102.

WORTHINGTON, P.F. (1976): Hydrogeological equivalence of water salinity, porosity and matrix conduction in arenaceous aquifers. Ground Water, 14, 224-232.

ZOHDY, A.A.R., EATON, G.P. and MABEY, D.R. (1974): Application of surface geophysics to ground water investigations. U.S. Geol. Survey Techniques, Water Resources Investigations Book 2, Chapter D1, 116.

APPENDIX A.1

A.1 CONVERSION FACTORS

Standard International (SI) units were used as units of measurement in this thesis. Conversion to the conventional F.P.S. system can be made by using the following table.

QUANTITY	EQUIVALENTS
Length	1 ft = 12 in. = 30.48 cm = 0.3048 m
	1 cm = 0.3937 in. = 0.03280 ft
	1 micron = 10^{-6} m
	1 mile (U.S. statute) = 5280 ft = 1609.3 m
	1 nautical mile (U.S.) = 6074.6 ft = 1852 m
Mass	1 lb_m = 453.59 gm = 0.45359 kg = 0.03108 slug
	1 kg = 2.2046 lb_m = 6.8521 × 10^{-2} slug
	1 slug = 32.174 lb_m
	1 lb_m-mole = 453.59 gm-moles
Force	1 lb_f = 4.448 × 10^5 dyne = 4.448 newtons
	1 newton = 0.2249 lb_f = 10^5 dynes
	1 kilogram force = 9.807 newtons
	1 poundal = 0.1383 newton
Time	1 hr = 60 min = 3600 sec
	1 day (mean solar) = 8.64 × 10^4 sec (mean solar)
	1 yr (calendar) = 3.1536 × 10^7 sec (mean solar)
Temperature	1°F = 1°R = $\frac{5}{9}$°C = $\frac{5}{9}$°K
	1°C = 1°K = 1.8°F = 1.8°R
	Absolute zero—0°R, 0°K, −459.67°F, −273.16°C
Energy	1 Btu (thermochemical) = 1054.35 joule = 251.99 cal
	= 1.054 × 10^{10} erg = 777.66 ft-lb_f
	1 cal = 3.97 × 10^{-3} Btu = 4.184 joules
	1 joule = 9.48 × 10^{-4} Btu
	1 Btu (Intern. Steam Table) = 1.0007 Btu (thermochemical)
Power	1 Btu/sec = 1054.35 watts
	1 hp = 550 ft-lb_f/sec = 2546.1 Btu/hr = 745.7 watts
	1 kw = 3414 Btu/hr
	1 cal/sec = 4.184 watts = 3.97 × 10^{-3} Btu/sec
Pressure	1 $lb_f/in.^2$ = 6894.8 newtons/m^2 = 68,948 dynes/cm^2
	= 27.69 in. H_2O = 2.036 in. Hg
	1 atm = 14.696 $lb_f/in.^2$ = 2116.2 lb_f/ft^2 = 29.92 in. Hg
	= 760 mm Hg = 101,325 newtons/m^2
	1 dyne/cm^2 = 145.04 × 10^{-7} $lb_f/in.^2$ = 0.1 newton/m^2
	1 kilogram force/m^2 = 9.807 newtons/m^2
	= 1.422 × 10^{-3} $lb_f/in.^2$
Volume	1 gal (U.S. liquid) = 0.13368 ft^3 = 3.785 liters
	= 0.003785 m^3
	1 liter = 1000 cm^3 = 0.001 m^3 = 0.2454 gal
	1 ft^3 = 0.028317 m^3 = 7.480 gal
Density	1 lb_m/ft^3 = 16.018 kg/m^3 = 1.6018 × 10^{-2} gm/cm^3
	= 0.03108 slug/ft^3
	1 slug/ft^3 = 515.4 kg/m^3
	1 kg/m^3 = 0.06242 lb_m/ft^3
Viscosity	1 lb_m/(hr ft) = 8.634 × 10^{-4} lb_f-sec/ft^2 = 8.634 × 10^{-4} slugs/(sec ft) = 0.03108 slug/(hr ft)
	= 4.133 × 10^{-4} newton-sec/m^2 = 0.4133 centipoise
	1 centipoise = 10^{-2} poise = 10^{-3} newton-sec/m^2 = 10^{-2} dyne-sec/cm^2 = 10^{-2} gm/(cm sec)
	= 2.419 lb_m/(hr ft) = 2.088 × 10^{-5} slug/(sec ft)
	1 slug/(sec ft) = 47.88 newton-sec/m^2 = 4.788 × 10^4 centipoise = 1.158 × 10^{-2} lb_m/(hr ft)
Kinematic viscosity, diffusivity	1 ft^2/hr = 0.2582 cm^2/sec = 2.582 × 10^{-5} m^2/sec
Energy flux	1 Btu/(hr ft^2) = 3.152 watts/m^2 = 3.152 × 10^{-4} watts/cm^2 = 7.529 × 10^{-5} cal/(sec cm^2)
	1 watt/cm^2 = 3172 Btu/(hr ft^2)
	1 cal/(sec cm^2) = 13,280 Btu/(hr ft^2)
Mass flux	1 lb_m/(hr ft^2) = 1.355 × 10^{-4} gm/(sec cm^2)
	= 1.355 × 10^{-3} kg/(sec m^2)
	1 gm/(sec cm^2) = 7380 lb_m/(hr ft^2)
Thermal conductivity	1 Btu/(hr ft^2 °F/ft) = 1.7293 watts/(m^2 °K/m)
	= 0.01729 watt/(cm^2 °K/cm)
	= 4.131 × 10^{-3} cal/(sec cm^2 °C/cm)
	1 watt/(cm^2 °K/cm) = 57.84 Btu/(hr ft^2 °F/ft)
Heat transfer conductance	1 Btu/(hr ft^2 °F) = 5.674 watts/(m^2 °K)
	= 5.674 × 10^{-4} watt/(cm^2 °K)
	= 1.355 × 10^{-4} cal/(sec cm^2 °C)
	1 watt/(cm^2 °K) = 1762 Btu/(hr ft^2 °F)
Specific heat	1 Btu/lb_m °F = 1 cal/gm °C = 4184 Joules/kg °K

APPENDIX A.3

A.3.1 PHYSICAL PROPERTIES OF THE WATER AT 10°C

Kinematic viscosity v (m^2/s)	Thermal conductivity $\hat{k}$ (W/m.°C)	Specific heat c (Kj/Kg.°C)	Thermal diffusivity k (m^2/s)	Density p (Kg/m^3)	Vol. coef. of expansion a (1/°C)
1.3×10^{-6}	0.585	4.195	1.39×10^{-7}	999.2	0.28×10^{-4}

A.3.2 PHYSICAL PROPERTIES OF Pt

Thermal conductivity : 41 Btu/hr.ft.F

Density : 1339 lb/ft^3

Specific heat : 0.031 Btu/lb.F

A.3.3 THERMODYNAMIC DEFINITIONS

Grashof number (Gr): This can be considered as a dimensionless group representing the ratio of buoyancy forces to viscous forces in a free-convection flow system.

Prandtl number (Pr): This can be considered as a dimensionless group representing the ratio of viscous effects to thermal effects.

Peclet number (Pe): This can be considered as a dimensionless group representing the ratio of buoyancy effects to thermal effects.

A.3.4 PROOF OF EQUATION 3.32

By substituting $A(k) = ((0.5+k)/L)^2$ in eq.3.31, one takes

$$T(\eta,\tau) = \frac{Nu \cdot T_1 \cdot \tau_p}{2\delta} \sum_{k=0}^{\eta-1} \int_0^{\mu\delta/\tau_p} e^{-\lambda'} \cdot \exp\left\{ -1/\mu \left[(1-\delta\cdot\mu+\tau_p\cdot\lambda')^2 + A(k) \right] \cdot \left[1 + \frac{\tau_p\cdot\lambda'}{\delta\mu} + \right.\right.$$

$$\left.\left. + \left(\frac{\tau_p\cdot\lambda'}{\delta\mu} \right)^2 + \cdots \right] \right\} \cdot \frac{1}{\mu} \cdot \left[1 + \frac{\tau_p\cdot\lambda'}{\delta\mu} + \left(\frac{\tau_p\cdot\lambda'}{\delta\mu} \right)^2 + \cdots \right] \qquad \text{A.3.1}$$

The exponent in the above equation can be written as

$$-\frac{(1-\delta\mu)^2}{\mu} - \frac{\tau_p}{\delta}\frac{(1-\delta^2\mu^2)}{\mu^2}\cdot\lambda' - \left(\frac{\tau_p}{\delta}\right)^2 \frac{\lambda'^2}{\mu^3} + \cdots - \frac{1}{\mu}\cdot A(k) - A(k)\frac{\tau_p\cdot\lambda'}{\delta\mu^2} -$$

$$- \frac{A(k)}{\mu} \cdot \left(\frac{\tau_p\cdot\lambda'}{\delta\mu} \right)^2 + \cdots \qquad \text{A.3.2}$$

So equation A.3.1 takes the following form

$$T(\eta,\tau) = \frac{Nu\cdot T_1\cdot\tau_p}{2\delta} \sum_{k=0}^{\eta-1} \int_0^{\mu\delta/\tau_p} e^{-\lambda'} \cdot e^{-\frac{(1-\delta\mu)^2+A(k)}{\mu}} \cdot e^{-\overbrace{\frac{[1-\delta^2\mu^2+A(k)]\cdot\lambda'}{\mu^2}}^{a\cdot\lambda'}\cdot\frac{\tau_p}{\delta}} \cdot e^{-\overbrace{[1-A(k)]\cdot\lambda'^2}^{\beta\cdot\lambda'^2}\cdot\left(\frac{\tau_p}{\delta}\right)^2} \cdot$$

$$\cdot \overbrace{\frac{1}{\mu}\cdot\left[1 + \frac{\tau_p\cdot\lambda'}{\delta\mu} + \left(\frac{\tau_p\cdot\lambda'}{\delta\mu}\right)^2 + \cdots\right]}^{c} \qquad \text{A.3.3}$$

and by expanding the terms involving $\frac{\tau_p}{\delta}$ and $\left(\frac{\tau_p}{\delta}\right)^2$ in terms of $\frac{\tau_p}{\delta}$ and $\left(\frac{\tau_p}{\delta}\right)^2$ respectively, one takes

$$e^{-a\cdot\lambda'\cdot\tau_p/\delta} = 1 - a\lambda'\cdot\frac{\tau_p}{\delta} + 1/2\cdot a^2\cdot\lambda'^2\cdot(\tau_p/\delta)^2$$

$$e^{-\beta(\tau_p/\delta)^2} = 1 - \beta\left(\frac{\tau_p}{\delta}\right)^2\cdot\lambda'^2 + \frac{1}{2}\beta^2\left(\frac{\tau_p}{\delta}\right)^4\cdot\lambda'^4$$

$\therefore$

$$T(\eta,\tau) = \frac{Nu\cdot T_1\cdot\tau_p}{2\cdot\delta} \sum_{k=0}^{\eta-1} \int_0^{\mu\delta/\tau_p} e^{-\lambda'} \cdot e^{-\frac{(1-\delta\mu)^2+A(k)}{\mu}} \cdot \overbrace{\left[1 - a\lambda'\cdot\frac{\tau_p}{\delta} + \frac{1}{2}\cdot a^2\cdot\lambda'^2\left(\frac{\tau_p}{\delta}\right)^2\right]}^{A} \cdot \overbrace{\left[1 - \beta\lambda'^2\left(\frac{\tau_p}{\delta}\right)^2 + \frac{1}{2}\beta^2\left(\frac{\tau_p}{\delta}\right)^4\lambda'^4\right]}^{B}$$

$$\cdot c\, d\lambda' \qquad \text{A.3.4}$$

$$A\cdot B = 1-\beta\cdot\left(\frac{\tau_p}{\delta}\right)^2\cdot\lambda'^2+\frac{1}{2}\cdot\beta^2\left(\frac{\tau_p}{\delta}\right)^4\cdot\lambda'^4-a\cdot\left(\frac{\tau_p}{\delta}\right)\cdot\lambda'+a\cdot\beta\cdot\left(\frac{\tau_p}{\delta}\right)^3\lambda'^3-$$

$$-a\cdot\frac{1}{2}\cdot\beta^2\cdot\left(\tau_p/\delta\right)^5\cdot\lambda'^5+\frac{1}{2}a^2\left(\tau_p/\delta\right)^2\lambda'^2-\frac{1}{2}a^2\cdot\beta\cdot\left(\frac{\tau_p}{\delta}\right)^4\cdot\lambda'^4+$$

$$+\frac{1}{4}\cdot a^2\cdot\beta^2\cdot\left(\frac{\tau_p}{\delta}\right)^6\cdot\lambda'^6$$

and ignoring the terms involving $(x_p/\delta)^n, n\geq 3$ Eq.A.3.4 becomes

$$T(\eta,\tau)=\frac{Nu\cdot T_1\cdot\tau_p}{2\delta\mu}\sum_{k=0}^{\eta-1}e^{-\frac{(1-\delta\mu)^2+A(k)}{\mu}}\int_0^{\mu\delta/\tau_p}\left\{e^{-\lambda'}-e^{-\lambda'}\cdot\lambda'\cdot a\cdot\frac{\tau_p}{\delta}+e^{-\lambda'}\cdot\lambda'^2\left(\frac{a^2}{2}\cdot\right.\right.$$

$$\left.\left.\left(\frac{\tau_p}{\delta}\right)^2-\beta\cdot\left(\frac{\tau_p}{\delta}\right)^2\right)+e^{-\lambda'}\cdot\lambda'\cdot\frac{\tau_p}{\delta\mu}-e^{-\lambda'}\cdot\lambda'^2\cdot\frac{a}{\mu}\cdot\left(\frac{\tau_p}{\delta}\right)^2+e^{-\lambda'}\cdot\lambda'^2\left(\frac{\tau_p}{\delta\mu}\right)^2\right\}d\lambda'$$

$$=\frac{Nu\cdot T_1\cdot\tau_p}{2\delta\mu}\sum_{k=0}^{\eta-1}e^{-\frac{(1-\delta\mu)^2+A(k)}{\mu}}\int_0^{\mu\delta/\tau_p}\left\{e^{-\lambda'}+e^{-\lambda'}\cdot\lambda'\cdot\left(\frac{\tau_p}{\delta\mu}-\frac{a\tau_p}{\delta}\right)+\right.$$

$$\left.+e^{-\lambda'}\cdot\lambda'^2\left[\frac{a^2}{2}\left(\frac{\tau_p}{\delta}\right)^2-\beta\left(\frac{\tau_p}{\delta}\right)^2-\frac{a}{\mu}\left(\frac{\tau_p}{\delta}\right)^2+\left(\frac{\tau_p}{\delta\mu}\right)^2\right]\right\}d\lambda' =$$

$$=\frac{Nu\cdot T_1\cdot\tau_p}{2\delta\mu}\sum_{k=0}^{\eta-1}e^{-\frac{(1-\delta\mu)^2+A(k)}{\mu}}\left\{\int_0^{\mu\delta/\tau_p}e^{-\lambda'}d\lambda'+\left(\frac{\tau_p}{\delta\mu}-\frac{a\cdot\tau_p}{\delta}\right)\int_0^{\mu\delta/\tau_p}e^{-\lambda'}\cdot\lambda'\,d\lambda'+\right.$$

$$\left.+\left[\frac{a^2}{2}\left(\frac{\tau_p}{\delta}\right)^2-\beta\left(\frac{\tau_p}{\delta}\right)^2-\frac{a}{\mu}\left(\frac{\tau_p}{\delta}\right)^2+\left(\frac{\tau_p}{\delta\mu}\right)^2\right]\int_0^{\mu\delta/\tau_p}e^{-\lambda'}\cdot\lambda'^2\,d\lambda'\right\} \qquad \text{A.3.5}$$

The above equation can be written

$$T(\eta,\tau) = \frac{Nu\cdot T_1\cdot \tau_P}{2\delta}\sum_{k=0}^{\eta-1}\int_0^{\mu\delta/\tau_P} e^{-\lambda'}\cdot e^{-\frac{(1-\delta\mu)^2+A(k)}{\mu}}\cdot\left[1-a\cdot\frac{\tau_P}{\delta}\cdot\lambda'+\left(\frac{a^2}{2}\left(\frac{\tau_P}{\delta}\right)^2-\right.\right.$$

$$\left.\left.-\beta\cdot\left(\frac{\tau_P}{\delta}\right)^2\right)\cdot\lambda'^2\right]\cdot\frac{1}{\mu}\cdot\left[1+\frac{\tau_P}{\delta\mu}\cdot\lambda'+\left(\frac{\tau_P}{\delta\mu}\right)^2\lambda'^2+\dots\right]d\lambda'$$

$$= \frac{Nu\cdot T_1\cdot\tau_P}{2\delta\mu}\sum_{k=0}^{\eta-1} e^{-\frac{(1-\delta\mu)^2+A(k)}{\mu}}\int_0^{\mu\delta/\tau_P}\left\{e^{-\lambda'}-e^{-\lambda'}\cdot\lambda'\cdot a\cdot\frac{\tau_P}{\delta}+e^{-\lambda'}\cdot\lambda'^2\left(\frac{a^2}{2}\cdot\left(\frac{\tau_P}{\delta}\right)^2-\right.\right.$$

$$\left.\left.-\beta\left(\frac{\tau_P}{\delta}\right)^2\right)\cdot\left[1+\frac{\tau_P}{\delta\mu}\cdot\lambda'+\left(\frac{\tau_P}{\delta\mu}\right)^2\right]\right\}d\lambda'$$

$$= \frac{Nu\cdot T_1\cdot\tau_P}{2\delta\mu}\sum_{k=0}^{\eta-1} e^{-\frac{(1-\delta\mu)^2+A(k)}{\mu}}\cdot\int_0^{\mu\delta/\tau_P}\left\{e^{-\lambda'}-e^{-\lambda'}\cdot\lambda'\cdot a\cdot\frac{\tau_P}{\delta}+e^{-\lambda'}\cdot\lambda'^2\left(\frac{a^2}{2}\cdot\left(\frac{\tau_P}{\delta}\right)^2-\right.\right.$$

$$\left.-\beta\left(\frac{\tau_P}{\delta}\right)^2\right)+e^{-\lambda'}\cdot\lambda'\cdot\frac{\tau_P}{\delta\mu}-e^{-\lambda'}\cdot\lambda'^2\cdot\frac{a}{\mu}\cdot\left(\frac{\tau_P}{\delta}\right)^2+e^{-\lambda'}\cdot\lambda'^3\cdot\frac{\tau_P}{\delta\mu}\left(\frac{a^2}{2}\left(\frac{\tau_P}{\delta}\right)^2-\right.$$

$$\left.-\beta\left(\frac{\tau_P}{\delta}\right)^2\right)+e^{-\lambda'}\cdot\lambda'^2\left(\frac{\tau_P}{\delta\mu}\right)^2-e^{-\lambda'}\cdot\lambda'^3\cdot\frac{a}{\mu^2}\cdot\left(\frac{\tau_P}{\delta}\right)^3+e^{-\lambda'}\cdot\lambda'^4\cdot\left(\frac{\tau_P}{\delta\mu}\right)^2\cdot$$

$$\left.\cdot\frac{a^2}{2}\left(\frac{\tau_P}{\delta}\right)^2-\beta\left(\frac{\tau_P}{\delta}\right)^2\right)\Big\}d\lambda'$$

$$T(\eta,\tau)=\frac{Nu\cdot T_1\cdot\tau_p}{2\delta\mu}\sum_{k=0}^{\eta-1}e^{-\frac{(1-\delta\mu)^2+A(k)}{\mu}}\left\{1-e^{-\mu\delta/\tau_p}+\left(\frac{\tau_p}{\delta\mu}-\frac{a\tau_p}{\delta}\right)\cdot\right.$$

$$\cdot\left[1-e^{-\mu\delta/\tau_p}\left(1+\frac{\mu\delta}{\tau_p}\right)\right]+\left[\frac{a^2}{2}\left(\frac{\tau_p}{\delta}\right)^2-\beta\left(\frac{\tau_p}{\delta}\right)^2-\frac{a}{\mu}\left(\frac{\tau_p}{\delta}\right)^2+\left(\frac{\tau_p}{\delta\mu}\right)^2\right]\cdot$$

$$\left.\cdot\left[2-e^{-\mu\delta/\tau_p}\left[\left(\frac{\mu\delta}{\tau_p}\right)^2+2\left(\frac{\mu\delta}{\tau_p}+1\right)\right]\right]\right\} \qquad \text{A.3.6}$$

and ignoring the terms which involve $e^{-\mu\delta/\tau_p}$ we take

$$T(\eta,\tau)=\frac{Nu\cdot T_1\cdot\tau_p}{2\delta\mu}\sum e^{-\frac{(1-\delta\mu)^2+A(k)}{\mu}}\left\{1+\frac{\tau_p}{\delta\mu}-\frac{a\tau_p}{\delta}+a^2\left(\frac{\tau_p}{\delta}\right)^2-\right.$$

$$\left.-2\beta\left(\frac{\tau_p}{\delta}\right)^2-\frac{2a}{\mu}\left(\frac{\tau_p}{\delta}\right)^2+2\left(\frac{\tau_p}{\delta\mu}\right)^2\right\}$$

$$T(\eta,\tau)=\frac{Nu\cdot T_1\cdot\tau_p}{2\delta\mu}\sum_{k=0}^{\eta-1}e^{-\frac{(1-\delta\mu)^2+A(k)}{\mu}}\left\{1+\frac{\tau_p}{\delta}\left(\frac{1}{\mu}-\frac{1-\delta^2\mu^2+A(k)}{\mu^2}\right)+\right.$$

$$\left.+\left(\frac{\tau_p}{\delta}\right)^2\left[\frac{(1-\delta^2\mu^2+A(k))^2}{\mu^4}-2\frac{1-A(k)}{\mu^3}-2\frac{1-\delta^2\mu^2+A(k)}{\mu^3}+\frac{2}{\mu^2}\right]\right\}$$

A.3.7

$$T(\eta,\tau) = \frac{Nu\cdot T_1\cdot \tau_p}{2\delta\mu} \sum_{k=0}^{\eta-1} e^{-\frac{(1-\delta\mu)^2}{\mu}} \cdot e^{-A(k)/\mu} \left\{ 1 + \frac{\tau_p}{\delta}\left(\frac{1}{\mu} - \frac{1-\delta^2\mu^2}{\mu^2}\right) + \right.$$

$$+2\left(\frac{\tau_p}{\delta}\right)^2 \left[\frac{(1-\delta^2\mu^2)^2}{2\mu^4} - \frac{1}{\mu^3} + \frac{1}{\mu^2} - \frac{(1-\delta^2\mu^2)}{\mu^3}\right] - \frac{\tau_p}{\delta}\cdot\frac{A(k)}{\mu^2} +$$

$$\left.\left(\frac{\tau_p}{\delta}\right)^2\cdot\frac{A^2(k)}{\mu^4} + 2\left(\frac{\tau_p}{\delta}\right)^2\cdot\frac{(1-\delta^2\mu^2)\cdot A(k)}{\mu^4}\right\} \qquad \text{A.3.8}$$

by separating the terms which do not involve k out of the series we finally take

$$T(\eta,\tau) = \eta/2\cdot\frac{Nu\cdot T_1\cdot\tau_p}{2\delta\mu}\cdot e^{-(1-\delta\mu)^2/\mu}\cdot\left\{1+\frac{\tau_p}{\delta}\left(\frac{1}{\mu}-\frac{1-\delta^2\mu^2}{\mu^2}\right)+\right.$$

$$\left.+2\left(\frac{\tau_p}{\delta}\right)^2\left[\frac{(1-\delta^2\mu^2)^2}{2\mu^4}-\frac{1}{\mu^3}+\frac{1}{\mu^2}-\frac{(1-\delta^2\mu^2)}{\mu^3}\right]\right\} + \frac{Nu\cdot T_1\cdot\tau_p}{2\delta\mu}\cdot$$

$$\cdot e^{-(1-\delta\mu)^2/\mu}\sum_{k=0}^{\eta-1} e^{-A(k)/\mu}\left\{A(k)\left[2\cdot\left(\frac{\tau_p}{\delta}\right)^2\cdot\frac{(1-\delta^2\mu^2)}{\mu^4}-\frac{\tau_p}{\delta}\cdot\frac{1}{\mu^2}\right]+\right.$$

$$\left.+\left(\frac{\tau_p}{\delta}\right)^2\frac{A^2(k)}{\mu^4}\right\} \qquad \text{A.3.9}$$

A.3.6 COMPUTER PROGRAM "THERM"

```
      PROGRAM THERM(VEL,OUTPUT,TAPE5=VEL,TAPE6=OUTPUT,TAPE7,
     +TAPE8,TAPE9)
      DATA DIAP,DH2O,TKH2O,VISC,PR,CPH2O,DPT,AOPT,RESPT,CPT,
     +TKPT,AL,THETAA,N,M/0.015,0.988,64200.0,0.005622,5.54,4.1807E7,21.37,
     +0.0038,8.58E-6,1.3233E6,7.111E6,1.0,25.0,23,1/
       DIMENSION MSG(4),MSG2(4),MSG3(4)
      DIMENSION U(50),RE(50),ANU(50),TP(50),X(180),TEMX(150),P(50),C(50),
     +THETA(50),A1(160),A2(160),T(50),VLOL(50),TEMAX(50),C2(50),C3(50),F1(180),
     +F2(180),F3(160),DSF(180),C1(50),A10(180),A20(180),S(10),SA1(10),SA2(10)
     +,ATE(50)
      READ(5,40) (U(I),I=1,N)
      BS=DIAP*DIAP*CPT*DPT/(4*TKPT)
      TDH2O=TKH2O/(DH2O*CPH2O)
      WRITE(6,45)
      REWIND 7
      DO 15 J=1,N
      RE(J)=DH2O*U(J)*DIAP/VISC
      ANU(J)=0.42*(PR**0.2)+0.57*(PR**0.33)*(RE(J)**0.33)
      TP(J)=BS/ANU(J)
      P(J)=U(J)*AL/TDH2O
      TEMAX(J)=(1.0+SQRT(1.0+P(J)*P(J)/4))/(P(J)/2.0)
      WRITE(6,50) U(J),RE(J),ANU(J),TP(J),P(J),TEMAX(J)
      WRITE(7,50) U(J),RE(J),ANU(J),TP(J),P(J),TEMAX(J)
   15 CONTINUE
      REWIND 7
      CALL PFREQ("REPLACE,TAPE7=RESULTS.",MSG,ICODE)
      IF(ICODE.NE.0)CALL REMARK(MSG)
   40 FORMAT (F5.2)
   50 FORMAT (4(2X,F10.3),2X,F10.2,2X F10.3)
   45 FORMAT (9X'V',9X'RE',10X'NU',10X'TP',5X'PECLET NUMBER',5X'TEMAX')
      WRITE(6,55),DIAP,DPT,TKPT,DH2O,VISC,PR,CPT,AL
   55 FORMAT(///'WIRE DIAMETER' F10.5'CM'///'WIRE DENSITY'
     +F10.2'GR/CM3'///'WIRE THERMAL CONDUCTIVITY ' F10.2
     +'ERG/CM.SEC'///'WATER DENSITY' F10.5 'GR/CM3'//
     +'WATER KINEMATIK VISCOSITY' F10.8'GR/CM.SEC'//
     +'PRANDL NUMBER'F10.2 ,3X'WIRE SPECIFIC HEAT ' F10.2
     +'ERG/GR.GRAD'///'DISTANCE BETWEEN WIRE AND SENSOR'F5.2'CM'////)
   70 FORMAT (///'WATER VELOCITY'F10.8'CM/SEC'////)
      REWIND 8
      REWIND  8
      DO 85 J=1,23
      C(J)=U(J)/AL
      C2(J)=TP(J)*P(J)/4
      C3(J)=C(J)*4/P(J)
      B0=(0.05/(10.0*M))*(0.05/(10.0*M))
      DL=P(J)/4
      WRITE(6,70),U(J)
      DO 85 I=1,100
      IF(J.LT.6) X(I)=1+0.202*I
      IF (J.GT.5.AND.J.LT.10) X(I)=0.337+0.00523*I
      IF(J.GT.8.AND.J.LT.14) X(I)=0.18+0.002*I
```

```
      IF(J.GT.13.AND.J.LT.18) X(I)=0.14+0.001*I
      IF(J.GT.17) X(I)=0.107+0.00051*I
      C1(J)=X(I)*C(J)
      TEMX(I)=50.0*(ANU(J)*TP(J))/(X(I))*EXP(-DL*
     +(1-X(I)*C(J))*(1-X(I)*C(J))/(X(I)*C(J)))*(1+(X(I)*X(I)*DL*
     +C(J)*C(J)+X(I)*C(J)-DL)*TP(J)/(X(I)*X(I)*C(J)))
      F1(I)=ANU(J)*TP(J)/(4.0*X(I))*EXP((-P(J)/4.0*(1.0-C1(J))
     +*(1.0-C1(J)))/C1(J))
      F2(I)=2.0*C2(J)*C2(J)*(1.0-C1(J))*(1.0-C1(J))/
     +(C1(J)*X(I)*X(I)*X(I))-C2(J)/(C1(J)*X(I))
      F3(I)=C2(J)*C2(J)*AL/(X(I)*X(I)*X(I)*X(I))
      A10(I)=EXP(-X(I)*C3(J)*B0)*B0
      A20(I)=EXP(-X(I)*C3(J)*B0)*B0
      DO 11 K=1,4
      B(K)=(0.05+K*0.1)*(0.05+K*0.1)/(10.0*M)
      A1(K)=EXP(-X(I)*C3(J)*B(K))*B(K)
      SA1(K)=A10(I)+A1(K)
      A10(I)=SA1(K)
      A2(K)=EXP(-X(I)*C3(J)*B(K))*B(K)*B(K)
      SA2(K)=A20(I)+A2(K)
      A20(I)=SA2(K)
   11 CONTINUE
      GSF(I)=F1(I)*(F2(I)*SA1(4)+F3(I)*SA2(4))
      WRITE(6,75)X(I),TEMX(I),GSF(I)
      WRITE(9,75)X(I),TEMX(I),GSF(I)
   85 CONTINUE
   75 FORMAT (F15.10,F10.5,F15.10)
      DO 80 I=80,85,5
      THETA(I)=I
      WRITE(6,85),THETA(I)
      ATE(I)=(THETA(I)-THETAA)*(THETA(I)-THETAA)*ADPT/2-
     +(THETA(I)-THETAA)
      A2S=DPT*CPT*RESPT/10
      WRITE(6,95)
      DO 80 K=5,50,5
      T(K)=K
      VLOL(K)=SQRT(ATE(I)*A2S/T(K))
          WRITE(6,90),T(K),VLOL(K)
      WRITE(9,90),T(K),VLOL(K)
   80 CONTINUE
      REWIND8
      REWIND 9
      CALL PFREQ("REPLACE,TAPE8=XVTEM.",MSG2,ICODE2)
      IF(ICODE2.NE.0)CALL REMARK(MSG2)
      CALL PFREQ("REPLACE,TAPE9=TVVLOL.",MSG3,ICODE3)
      IF(ICODE3.NE.0)CALL REMARK(MSG3)
   85 FORMAT(//'MAXIMUM WIRE TEMPERATURE'F5.1'GRADS CELCIUS'/)
   90 FORMAT(3X F10.2,10X F10.4)
   95 FORMAT(1X'PULSE DURATION',5X 'VOLTAGE PER UNIT LENGTH'
     +/3X'MICROSECS',12X'VOLTS/CM'//)
      STOP
      END
```

A.3.5 EXPERIMENTAL RESULTS OF HEAT PULSE PROPAGATION INVESTIGATION

FLOWRATE gr/sec	MEAN VELOCITY mm/sec	TRAVEL TIME sec	
49.2	2.8	11.7	L :1 cm
77.3	4.4	8.7	
135.4	7.7	4.9	
221.5	12.6	2.3	
	15.4	1.7	
330.5	18.8	1.1	
392	22.3	1.3	
45.7	2.6	13.7	L :1.5 cm
80.9	4.6	4.0	
117.8	6.7	2.7	
168.8	9.6	1.8	
216.2	12.3	1.6	
319.9	18.2	1.1	
393.8	22.4	1.2	

APPENDIX A.4

A.4.1 THE HYDROLOGGER

The geophysical logging unit used in the present research, was that manufactured by Guidard Ltd. and owned by the Southern Water Authority. It is shown in PLATE 11.

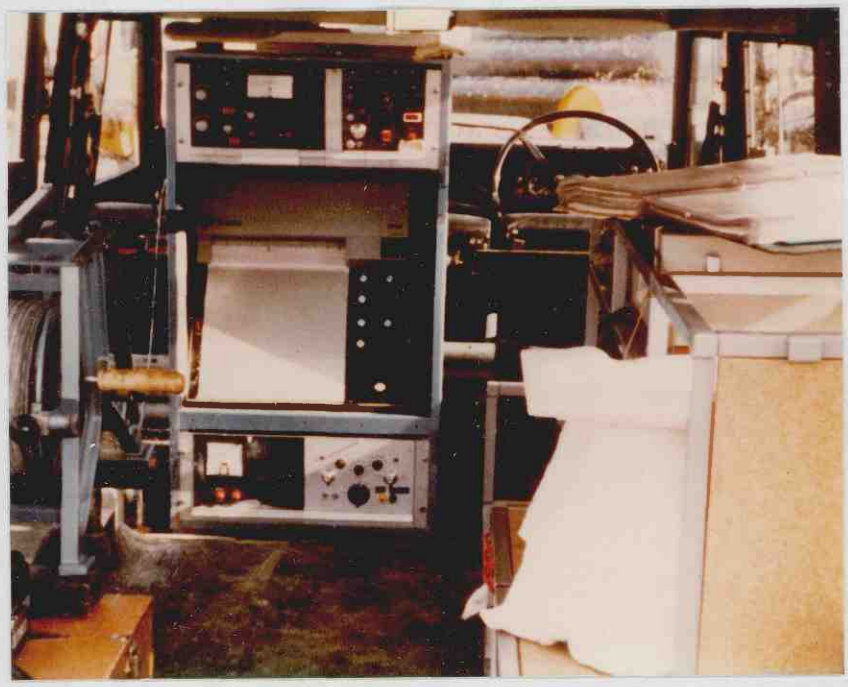


PLATE 11: A view of the hydrologer, mounted at the back of a LAND ROVER

The unit has the following specification:-

Measuring depth : 300m

Probes available:

FLUID LOGS - Temperature/Conductivity
Differential Temperature/Conductivity
Heat Pulse flowmeter
Impeller (Braystoke) flowmeter
Sampler

FORMATION LOGS - Natural Gamma
16/64" Normal Resistivity
4'8" Lateral Resistivity
Caliper
Spontaneous Potential
Point Resistance

The general layout of all the units and controls for the Hydrologger is shown in Fig. A.1 and the logging select module switch positions are as follows:-

LOG REQUIRED	SWITCH POSITION	
	TOP	BOTTOM
Temperature/Conductivity (T/C) Differential Temperature/Conductivity (ΔT/C) Point Resistance (PR)/Spontaneous Potential (SP) Normal 16"/64" Resistivities Lateral 4'8" Resistivity	5	A
Impeller Flowmeter	6	A
Heat Pulse Flowmeter	7	A
Sampler	8	A
Natural Gamma	X	F
Caliper	9	A

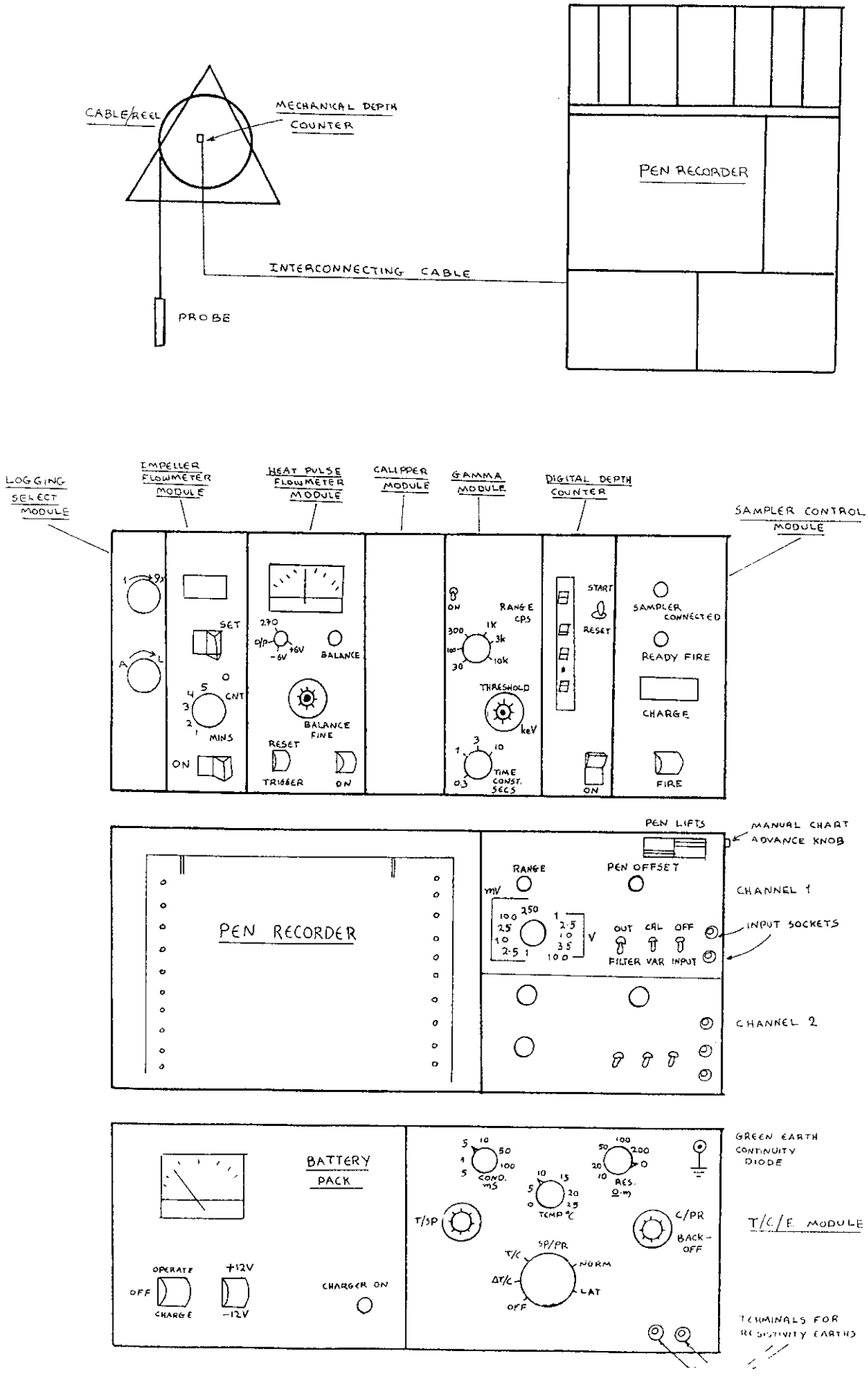
The pens are zeroed so that, as far as possible, all the logs have zero output on the left-hand side when the log is orientated with greatest depth at the bottom of the sheet.

The channels used on the pen recorder for each set of logs, together with the pen zero position and logging direction, are shown in the table below:-

LOG	CHART RECORDER CHANNEL 1	CHART RECORDER CHANNEL 2	PEN ZERO POSITION CHANNEL 1	PEN ZERO POSITION CHANNEL 2	LOGGING DIRECTION
T/C	T	C	RH	RH	UP/DOWN*
ΔT/C	ΔT	C	CENTRE	RH	DOWN
PR/SP	PR	SP	CENTRE	CENTRE	
Normal 16"/64" Resistivities	64"	16"	LH	LH	UP
Lateral Resistivity	Not	LAT	Not	LH	UP
Heat Pulse Flowmeter	Used	HPF	Used	CENTRE	-
Natural Gamma	↓	γ	↓	LH	UP
Caliper		CAL		LH	UP

NOTE:- * T/C is usually run down the hole, but if ΔT/C is required, this should be run first to reduce disturbance for ΔT as much as possible. In that case, T/C may be run up if required.

Fig. A.1: Hydrologer equipment layout



A.4.2 DETAILS OF HYDROLOGER FACILITIES

Specification and Ranges

The module has the following capabilities:-

(a) Temperature/Fluid Conductivity
(b) Differential Temperature/Fluid Conductivity
(c) Spontaneous Potential/Point Resistance
(d) 16"/64" Normal resistivities
(e) 4'8" Lateral resistivity

In the case of (a) to (d) inclusive, both parameters are recorded simultaneously on a dual pen chart recorder.

(i) Temperature

Uses Chart Recorder Channel 1 (top channel).
Measures temperatures between 0°C and 30°C (output = 100 mV/°C)
Five switchable scales, with ranges set by chart recorder sensitivity control (see section B.5.1.1.).
End points of chosen scales can be offset (reduced by up to 10°C using a 10-turn back-off potentiometer (1°C = 1 turn).
Absolute accuracy 1°C, calibration by external variable resistors adjustable from the front panel.

(ii) Fluid Conductivity

Uses Chart Recorder Channel 2 (bottom channel).
Measures conductivities up to 100 mS/cm (100,000 µS/cm).
Six switchable scales with ranges set by chart recorder sensitivity control (see section B.5.1.1.).
End points of chosen range can be offset by up to 100% of chosen scale using a 10-turn back-off potentiometer (10% = 1 turn).
Accuracy <5%, calibration by external resistor.

(iii) Differential Temperature

Uses Chart Recorder Channel 1 (top channel).
Measures difference in temperature recorded by two thermistors, within the range 0° and 30°C.
Scale ranges set by chart recorder sensitivity control.

(iv) Point Resistance

Uses Chart Recorder Channel 1 (top channel).
Measures PR up to 200Ω using five switchable ranges as follows:-

0 - 10Ω)
0 - 20Ω)
0 - 50Ω) top ends of ranges represent 100 mV output.
0 - 100Ω)
0 - 200Ω)

Calibration by external resistors.
End points of chosen range can be offset by up to 1 volt using a 10-turn back-off potentiometer.

(v) Spontaneous Potential

Uses Chart Recorder Channel 2 (bottom channel).
Output = I x Input.
Back-off approximately ±80 mV available using a 10-turn back-off potentiometer.

(vi) 64"/16" Normal Resistivities

Uses Chart Recorder Channels 1 and 2 respectively.
Measures resistivities up to 200Ωm, using five switchable ranges as follows:-

0 - 10Ωm)
0 - 20Ωm)
0 - 50Ωm) top ends of ranges represent 100 mV output.
0 - 100Ωm)
0 - 200Ωm)

Calibration by external resistors.

(vii) 4'8" Lateral Resistivity

Uses Chart Recorder Channel 2 (bottom channel).
Ranges and calibration as for 16"/64" Normal.

Power Supply

Operates off two lines:- + 12v @ 80 mA.
- 12v @ 80 mA.

APPENDIX A.5

A.5.1 COMPUTER PROGRAM FOR THE EVALUATION OF THE DIRECTIONAL HYDRAULIC CONDUCTIVITY OF AN INCLINED FISSURE ZONE (see Chapter V)

```
10REM THIS PROGRAM CALCULATES THE DIRECTIONAL HYDRAUL.CONDUCT.
20REM AS A FUNCTION OF THE ORIENTATION OF THE FISSURE PLANE
30REM THE DIRECTION OF THE HYDR.GRADIENT THE OPENNING OF THE
35REM FISSURES AND THE
40REM NUMBER OF FISSURES PER M CORRESPONDING TO THE FIS.ZONE
50REM IT USES THE POWER METHOD TO CALCULATE THE MAX EIGENVALU
60REM OF A MATRIX
70REM THE VISCOSITY OF THE GROUNDWATER IS CONSIDERED TO BE
80REM1.30MM.MM/SEC FOR10DEGREES CELCIUS
90FDIM%XX(8),%AA(8),%BB(8),%CC(8),%FF(50),%LL(50),%EE(9)
100FDIM%QQ(9),%ZZ(9),%SS(9),%AK(9),%WW(9),%JJ(9)
110P.$12
120REMCHARACTERISTICS OF FIS.ZONE
130P.$2
140P."ENTER FIS. OPENING IN MM"
150FINPUT%E
160P."ENTER NUMBER OF FIS. PER METER FOR THE SPECIFIC ZONE"
170INPUTN
180P."K IS";FPRINT%K;P."M/D"
190REMORIENTATION OF FIS.PLANE AND CALCULATION OF DIR.MATRIX
200F.I=1TO50:%LL(I)=2:%FF(I)=0:N.I
210P."ENTER THE X-DIR. COS. OF THE NORM. TO THE FIS. PLANE"
220FINPUT%X
230P."THE SAME FOR THE Y-DIR."
240FINPUT%Y
250P.$3
260%Z=SQR(1-%X*%X-%Y*%Y)
270%ZZ(4)=1-%X*%X
280%ZZ(5)=-%X*%Y
290%ZZ(6)=-%X*%Z
300%ZZ(7)=-%Y*%Z
310%ZZ(8)=1-%Y*%Y
320%ZZ(9)=-%Y*%Z
330%ZZ(10)=-%Z*%X
340%ZZ(11)=-%Z*%Y
350%ZZ(12)=1-%Z*%Z
360F.R=1TO3
370F.C=1TO3
380%XX(R*3+C)=%ZZ(R*3+C)
390N.C
400N.R
410P."THE MATRIX IS"
420P.
430F.R=1TO3
440F.C=1TO3
450FPRINT%XX(R*3+C);P.","
460N.C
470P.'
480N.R
490REM CALCULATION OF THE INVERSE MATRIX
500F.R=1TO3
510F.C=1TO3
520%FF(R*3+C)=%XX(R*3-C)
530N.C
540N.R
550GOSUBs
```

```
560%E=0.110:W=10
570GOSUBu
580P."max eigenvalue is"'
590P."--------------------"'
600%T=%A
610PRINT%T
620P.'
630P."EIGENVECTOR'S COMP. ARE"'
640F.I=1TO3
650%EE(I*3+1)=%BB(I*3+1)
660PRINT%EE(I*3+1)'
670N.I
680REMCALCULATION OFMIN EIGENVALUE AND AS.EIGENVECTOR
690F.R=1TO3
700F.C=1TO3
710%XX(R*3+C)=%LL(R*3+C)
720N.C
730N.R
7400GOSUBu
750P.'
760P."min eigenvalue is"'
770P."--------------------"'
780%V=1/%9
790PRINT%V
800P.'
810P."EIGENVECTOR'S COMP. ARE"'
820F.I=1TO3
830%QQ(I*3+1)=%BB(I*3+1)
840PRINT%QQ(I*3+1)'
850N.I
860REM CALCULATION OF THE THIRD EIGENVALUE
870%O=%ZZ(4)+%ZZ(8)+%ZZ(12)-%T-%V
880P.'
890P."medium eigenvalue is"'
900P."--------------------"'
910PRINT%O'
920REM CALCULATION OF THIRD'S EIGENVECTORS COMPONENTS
930%O=%EE(4)*%QQ(7)-%QQ(4)*%EE(7)
940%G=%QQ(10)*%EE(7)-%EE(10)*%QQ(7)
950%H=%EE(10)*%QQ(4)-%QQ(10)*%EE(4)
960%U=SQR(1/(%G*%G+%H*%H+1))
970%P=%H*%U
980%G=%G*%U
990%SS(4)=%G:%SS(7)=%P:%SS(10)=%U
1000P."EIGENVECTOR'S COMP. ARE"'
1010F.I=1TO3
1020PRINT%SS(I*3+1)'
1030N.I
1040%KK(4)=%K*%T:%KK(7)=%K*%O:%KK(10)=%K*%V
1050REM CALCULATION OF THE PRINCIPAL CONDUCTIVITIES
1060P."THE principal COND. ARE"'
1070P."k11=";FPRINT%KK(4)'
1080P."k22=";FPRINT%KK(7)'
1090P."k33=";FPRINT%KK(10)'
1100P.$2
1110P."ENTER THE X-DIR COS FOR THE HYDR. GRAD."'
```

```
1130FINPUT%F
1132P,"THE SAME FOR THE Y-DIR"
1140FINPUT%H
1150%Y=SQR(1-%F*%F-%H*%H)
1160%WW(4)=%F
1170%WW(7)=%H
1180%WW(10)=%Y
1190REM CALCULATION OF THE COMP. OF THE HYDR.GRAD.ACROSS THE
1200REM PRINCIPAL DIRECTIONS
1210%JJ(4)=%WW(4)*%EE(4)+%WW(7)*%EE(7)+%WW(10)*%EE(10)
1220%JJ(5)=%WW(4)*%SS(4)+%WW(7)*%SS(7)+%WW(10)*%SS(10)
1230%JJ(6)=%WW(4)*%QQ(4)+%WW(7)*%QQ(7)+%WW(10)*%QQ(10)
1240P,"COMP. OF HYDR. GRD IN THE PRINCIPAL DIRECTIONS"
1250P,"// TO X(1):";PRINT%JJ(4)'
1260P,"// TO X22:";PRINT%JJ(7)'
1270P,"// TO X33:";PRINT%JJ(10)'
1280REM CALCUL.OF THE HYDR.COND. IN THE DIR.OF THE HYDR.GRD
1290%D=%JJ(4)*%JJ(4)*%KK(4)+%JJ(7)*%JJ(7)*%KK(7)
1300%D=%D+%JJ(10)*%JJ(10)*%KK(10)
1310P,"hydr. cond. in the dir  of the hydr gradient"
1320P,"-------------------------------------"
1330FPRINT%D;P,"M/D"
1340END
1350REM SUBROUTIN TO FIND THE MAX EIGENVALUES&S.EIGENVECTOR
1360%B=0
1370H=3
1380P=1
1390F.I=1TO3
1400%BB(I*3+1)=1/SQR(3)
1410N.I
1420%B=1
1430D=0
1440%A=2
1450GOSUB*
1460F.I=1TO3
1470%BB(I*3+1)=%CC(I*3+1)
1480%A=%A+%BB(I*3+1)*%BB(I*3+1)
1490N.I
1500D=D+1
1510%A=SQR(%A)
1520F.I=1TO3
1530%BB(I*3+1)=%BB(I*3+1)/%A
1540N.I
1550FIFABS((%A-%B)/%A)(%E THEN GOTO1590
1560%B=%A
1570IFD)%N THEN GOTO1590
1580GOTO1440
1590RETURN
1600REM SUBROUTINE TO MULTIPLY TWO MATIXES
1610*F.I=1TOG
1620F.J=1TOP
1630%CC(I*3+J)=0
1640F.K=1TOH
1650%CC(I*3+J)=%CC(I*3+J)+%XX(I*3+K)*%BB(K*3+J)
1660N.K
1670N.J
```

```
1580%I
1590RETURN
1700REM SUBROUTINE TO INVERT A MATRIX
1710FI=1TO3
1720FJ=1TO3
1730%LL(I*3+J)=1-ABS(SGN(I-J))
1740%J
1750%I
1760FI=1TO2
1770IF ABS(%FF(I*3+I))0.110THEN GOTO1790
1780P"CAN'T COPE WITH MATRIX"
1790FJ=I+1TO3
1800%Y=%FF(J*3+I)/%FF(I*3+I)
1810FK=1TO3
1820%FF(J*3+K)=%FF(J*3+K)-%Y*%FF(I*3+K)
1830%LL(J*3+K)=%LL(J*3+K)-%Y*%LL(I*3+K)
1840%K
1850%I
```

A.5.2 DRAWINGS SHOWING FLOW PATTERNS OBTAINED FROM AN ELECTRICAL ANALOGUE USING TELEDELTOS PAPER

The following drawings (1-6), represent 1/2 the actual size of the patterns used for the calculation of current flow. The results obtained are shown in the following Table.

TABLE A.5.2

No	1	2	3	4	5	6
S	13.6	3.84	4.12	5.46	2.83	1.15
L	1.20	0.70	0.80	1.20	0.80	0.70
S/L	11.33	5.48	5.15	4.55	3.54	1.60
S_t/L	25.67	21.93	20.63	18.20	14.15	6.60
E	7.42	14.84	22.75	30.66	48.83	61.54
%E	4.20	8.40	12.88	17.36	27.64	34.84

S: length of a section of a potential line

L: distance between two potential lines

S_t/L: sum of the ratios S/L for all the sections

E: fissure contact area

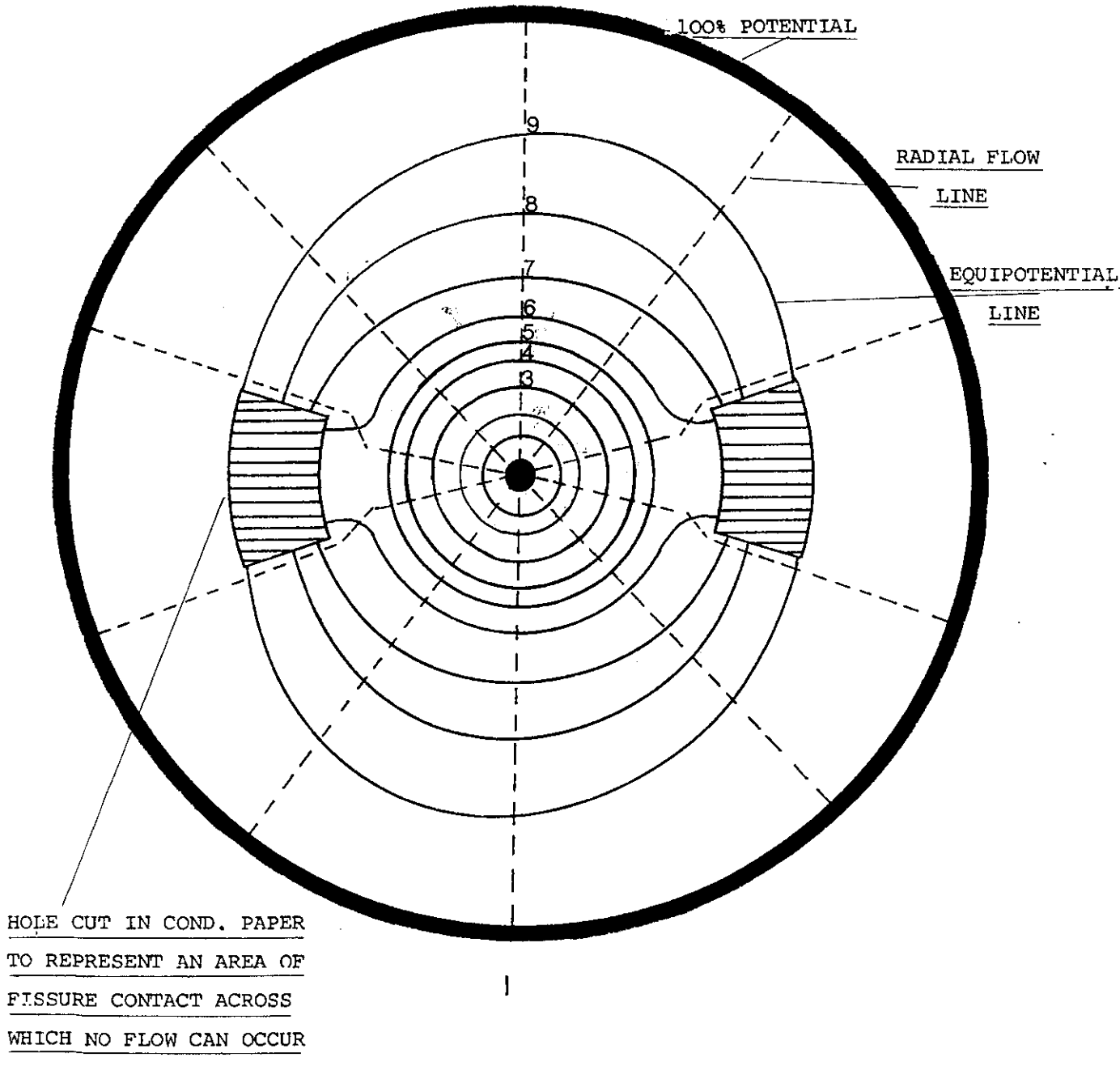
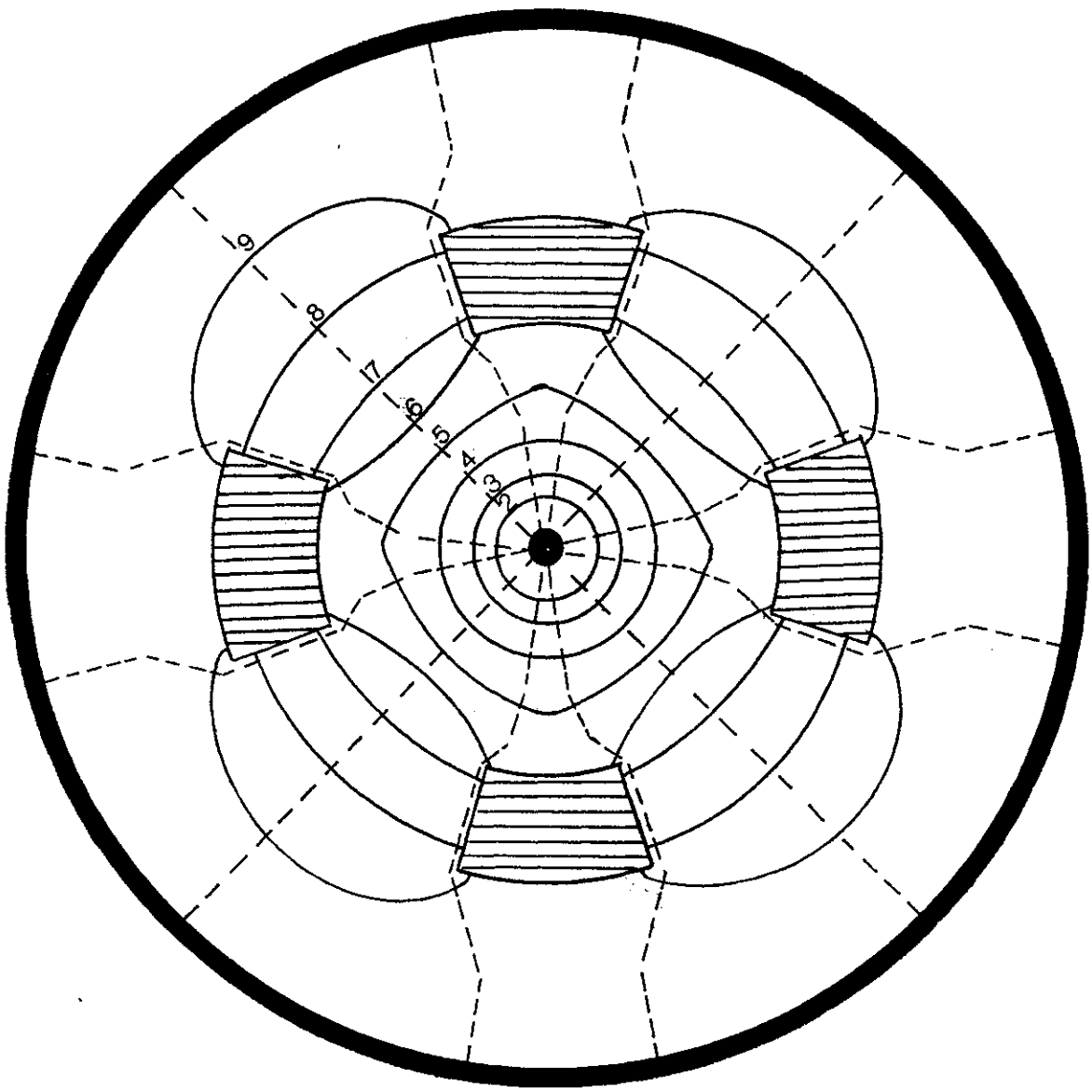
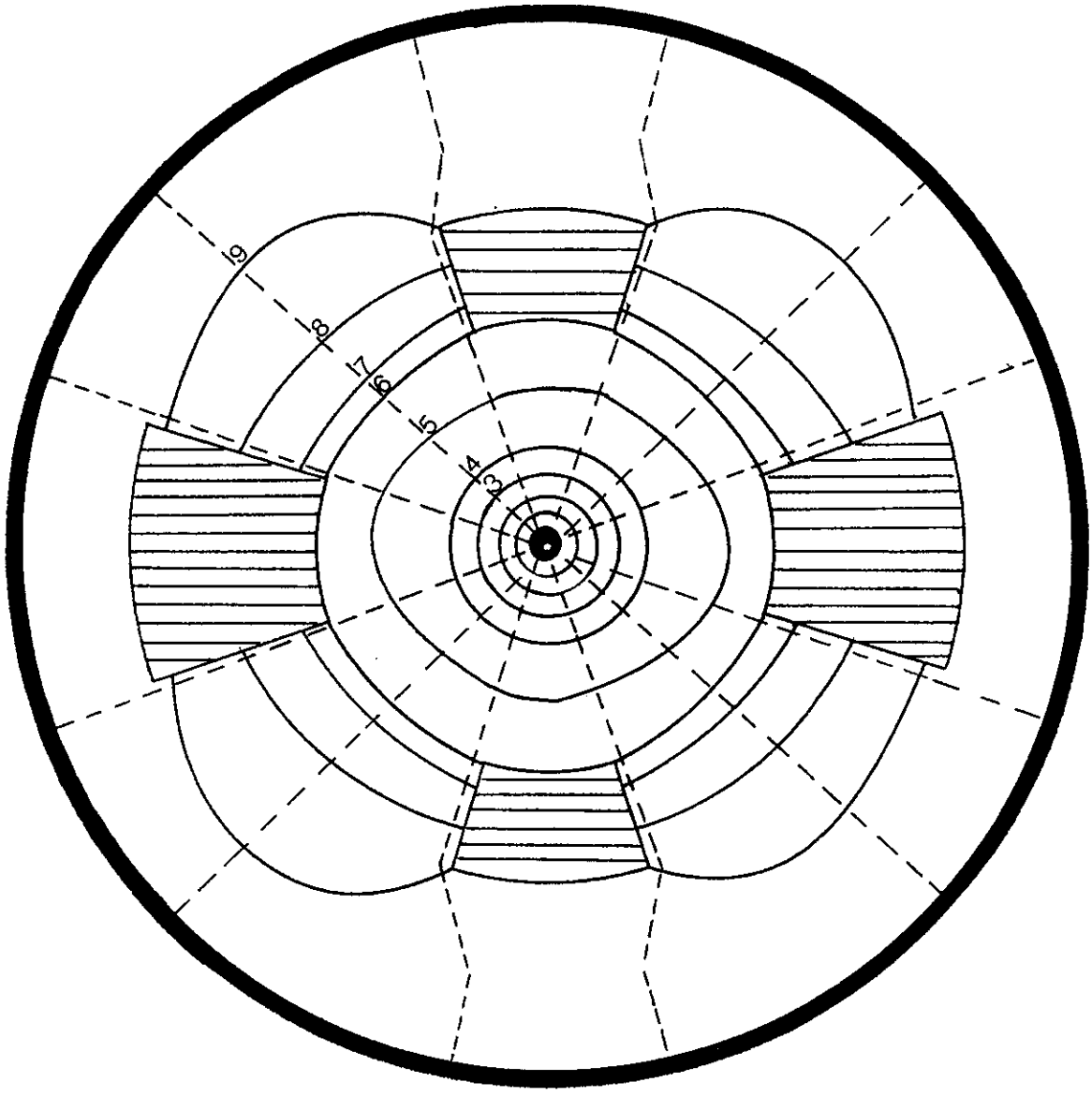


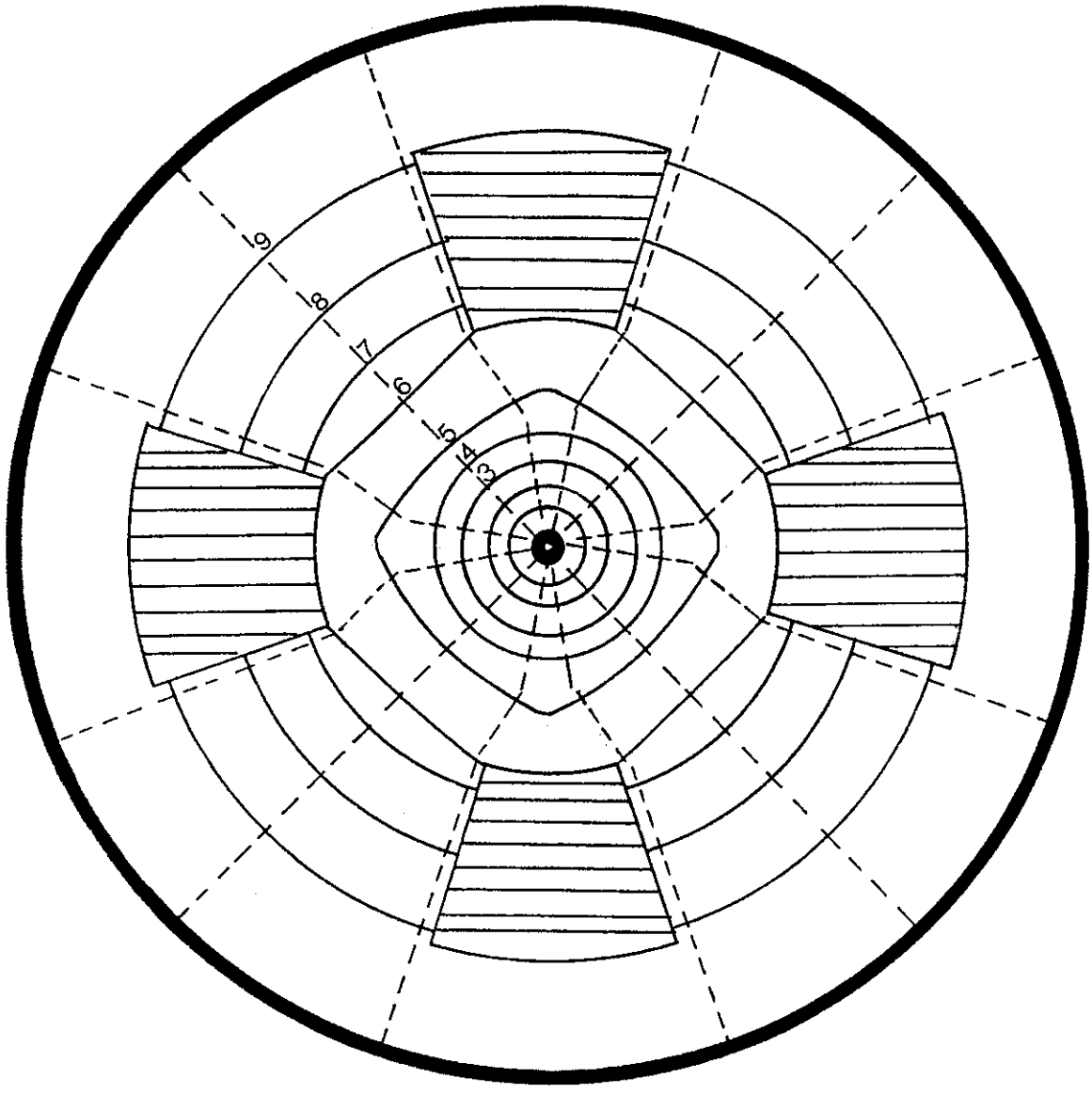
FIG. A.2. Equipotential and flow lines



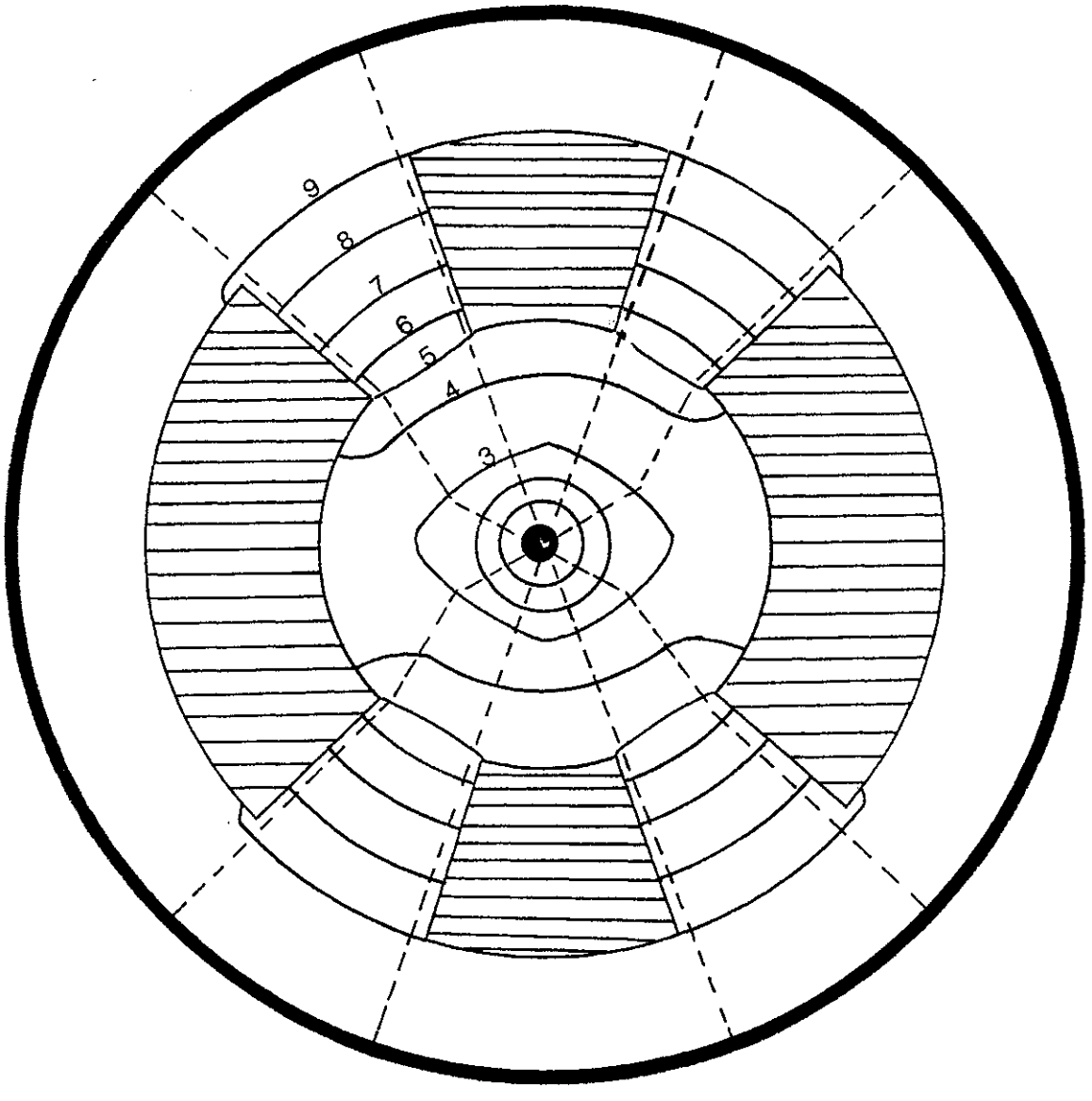
2



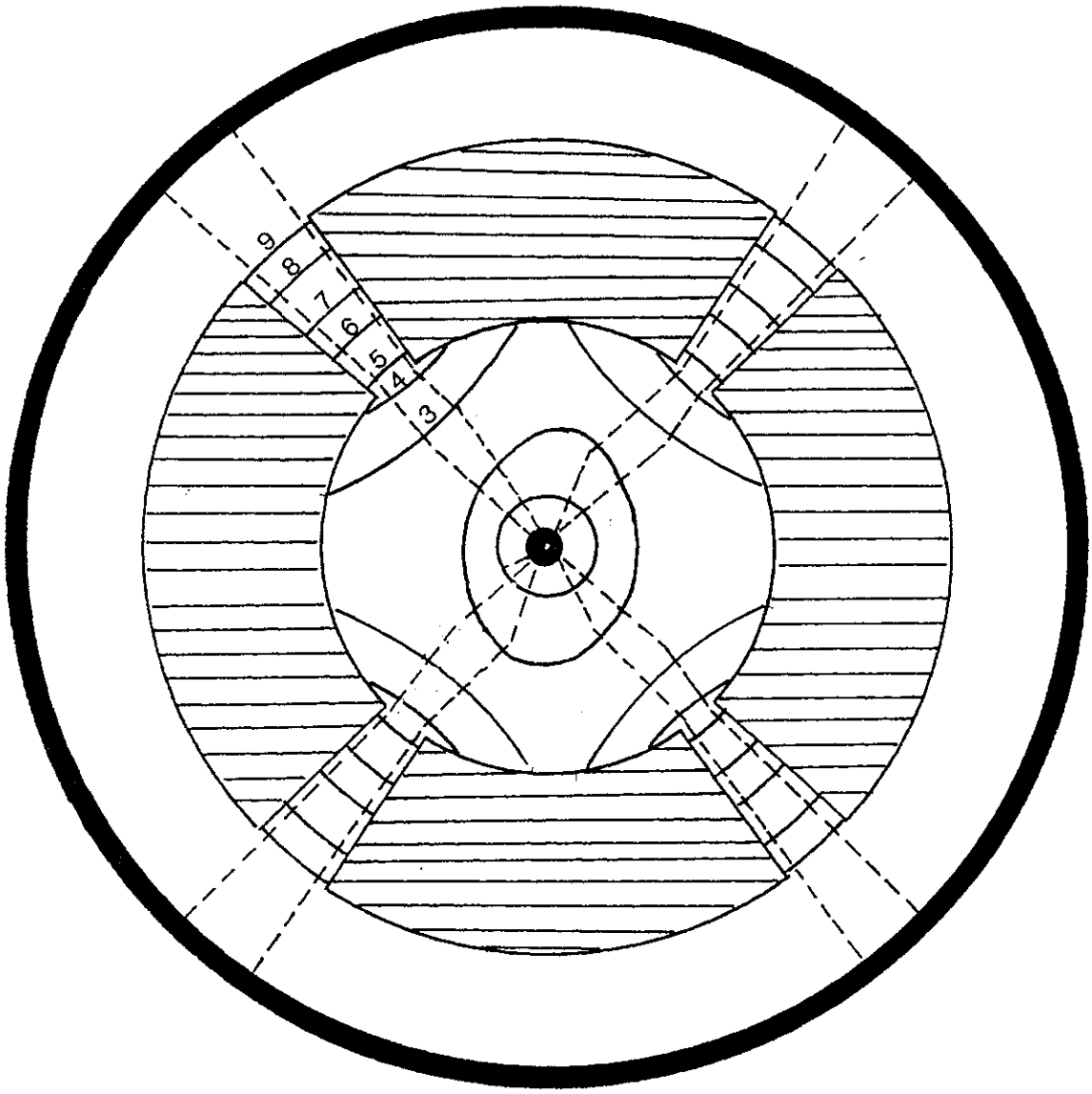
3



4



5



6

APPENDIX A.6

A.6.1 PROGRAM FOR GENERATING TABLE A.6.1

```
PROGRAM   TABLE
00010 DIMENSION A(11),B(110),R(100),P(100),C(100)
00020 DIMENSIONT(100),E(100),Q(100),S(100)
00030 A(1)=1.58
00040 DO 20 L=1,11
00045 WRITE(6,10)
00046 10 FORMAT("--------------------",/////)
00050 A(L)=A(1)+L*0.02
00060 B(1)=0
00070 DO 20 I=1,10
00080 B(I)=B(1)+I*0.02
00090 R(1)=0.15
00100 DO 20 J=1,5
00110 R(J)=R(1)+J*0.05
00120 P(J)=R(J)/(1-B(I)+B(I)*R(J))
00130 T(J)=(R(J)**A(L))*(1-B(I)*P(J))
00140 C(J)=ALOG(B(I)*P(J)+T(J))/ALOG(P(J))
00150 E(J)=1/(P(J)**C(J))
00160 Q(J)=B(I)*P(J)
00170 S(J)=Q(J)/(P(J)-Q(J))
00180 WRITE(6,15) A(L),B(I),R(J),P(J),C(J)
00190   15FORMAT(8F10.5)
00200   20CONTINUE
00210 STOP
00220 END
READY.
```

m_0	f	ϕ_0	ϕ	m
1.50000	.02000	.20000	.20325	1.48973
1.50000	.02000	.30000	.30426	1.49216
1.50000	.02000	.35000	.35461	1.49308
1.50000	.02000	.40000	.40486	1.49390
1.50000	.02000	.45000	.45501	1.49462
1.50000	.06000	.20000	.21008	1.46991
1.50000	.06000	.30000	.31315	1.47683
1.50000	.06000	.35000	.36420	1.47951
1.50000	.06000	.40000	.41494	1.48188
1.50000	.06000	.45000	.46536	1.48400
1.50000	.08000	.20000	.21368	1.46033
1.50000	.08000	.30000	.31780	1.46933
1.50000	.08000	.35000	.36920	1.47285
1.50000	.08000	.40000	.42017	1.47596
1.50000	.08000	.45000	.47071	1.47876
1.50000	.10000	.20000	.21739	1.45095
1.50000	.10000	.30000	.32258	1.46194
1.50000	.10000	.35000	.37433	1.46627
1.50000	.10000	.40000	.42553	1.47010
1.50000	.10000	.45000	.47619	1.47356
1.50000	.12000	.20000	.22124	1.44177
1.50000	.12000	.30000	.32751	1.45466
1.50000	.12000	.35000	.37961	1.45976
1.50000	.12000	.40000	.43103	1.46429
1.50000	.12000	.45000	.48180	1.46840
1.50000	.14000	.20000	.22523	1.43277
1.50000	.14000	.30000	.33259	1.44747
1.50000	.14000	.35000	.38504	1.45332
1.50000	.14000	.40000	.43668	1.45854
1.50000	.14000	.45000	.48754	1.46328
1.50000	.16000	.20000	.22936	1.42395
1.50000	.16000	.30000	.33784	1.44038
1.50000	.16000	.35000	.39063	1.44696
1.50000	.16000	.40000	.44248	1.45285
1.50000	.16000	.45000	.49342	1.45820
1.50000	.18000	.20000	.23364	1.41530
1.50000	.18000	.30000	.34325	1.43338
1.50000	.18000	.35000	.39638	1.44067
1.50000	.18000	.40000	.44843	1.44720
1.50000	.18000	.45000	.49945	1.45316
1.50000	.20000	.20000	.23810	1.40681
1.50000	.20000	.30000	.34884	1.42647
1.50000	.20000	.35000	.40230	1.43444
1.50000	.20000	.40000	.45455	1.44161
1.50000	.20000	.45000	.50562	1.44816
1.50000	.22000	.20000	.24272	1.39847
1.50000	.22000	.30000	.35461	1.41965
1.50000	.22000	.35000	.40840	1.42828
1.50000	.22000	.40000	.46083	1.43607
1.50000	.22000	.45000	.51195	1.44320

1.52000	.02000	.20000	.20325	1.50904
1.52000	.02000	.30000	.30426	1.51166
1.52000	.02000	.35000	.35461	1.51266
1.52000	.02000	.40000	.40486	1.51352
1.52000	.02000	.45000	.45501	1.51430
1.52000	.06000	.20000	.21008	1.48793
1.52000	.06000	.30000	.31315	1.49538
1.52000	.06000	.35000	.36420	1.49826
1.52000	.06000	.40000	.41494	1.50078
1.52000	.06000	.45000	.46536	1.50305
1.52000	.08000	.20000	.21368	1.47774
1.52000	.08000	.30000	.31780	1.48743
1.52000	.08000	.35000	.36920	1.49120
1.52000	.08000	.40000	.42017	1.49452
1.52000	.08000	.45000	.47071	1.49750
1.52000	.10000	.20000	.21739	1.46779
1.52000	.10000	.30000	.32258	1.47960
1.52000	.10000	.35000	.37433	1.48422
1.52000	.10000	.40000	.42553	1.48831
1.52000	.10000	.45000	.47619	1.49200
1.52000	.12000	.20000	.22124	1.45806
1.52000	.12000	.30000	.32751	1.47189
1.52000	.12000	.35000	.37961	1.47734
1.52000	.12000	.40000	.43103	1.48218
1.52000	.12000	.45000	.48180	1.48655
1.52000	.14000	.20000	.22523	1.44853
1.52000	.14000	.30000	.33259	1.46429
1.52000	.14000	.35000	.38504	1.47054
1.52000	.14000	.40000	.43668	1.47610
1.52000	.14000	.45000	.48754	1.48114
1.52000	.16000	.20000	.22936	1.43921
1.52000	.16000	.30000	.33784	1.45679
1.52000	.16000	.35000	.39063	1.46381
1.52000	.16000	.40000	.44248	1.47008
1.52000	.16000	.45000	.49342	1.47578
1.52000	.18000	.20000	.23364	1.43007
1.52000	.18000	.30000	.34325	1.44940
1.52000	.18000	.35000	.39638	1.45717
1.52000	.18000	.40000	.44843	1.46413
1.52000	.18000	.45000	.49945	1.47046
1.52000	.20000	.20000	.23810	1.42111
1.52000	.20000	.30000	.34884	1.44211
1.52000	.20000	.35000	.40230	1.45060
1.52000	.20000	.40000	.45455	1.45822
1.52000	.20000	.45000	.50562	1.46518
1.52000	.22000	.20000	.24272	1.41233
1.52000	.22000	.30000	.35461	1.43492
1.52000	.22000	.35000	.40840	1.44410
1.52000	.22000	.40000	.46083	1.45238
1.52000	.22000	.45000	.51195	1.45995

1.54000	.02000	.20000	.20325	1.52832
1.54000	.02000	.30000	.30426	1.53114
1.54000	.02000	.35000	.35461	1.53221
1.54000	.02000	.40000	.40486	1.53314
1.54000	.02000	.45000	.45501	1.53397
1.54000	.06000	.20000	.21008	1.50587
1.54000	.06000	.30000	.31315	1.51388
1.54000	.06000	.35000	.36420	1.51696
1.54000	.06000	.40000	.41494	1.51966
1.54000	.06000	.45000	.46536	1.52207
1.54000	.08000	.20000	.21368	1.49507
1.54000	.08000	.30000	.31780	1.50547
1.54000	.08000	.35000	.36920	1.50949
1.54000	.08000	.40000	.42017	1.51303
1.54000	.08000	.45000	.47071	1.51621
1.54000	.10000	.20000	.21739	1.48452
1.54000	.10000	.30000	.32258	1.49719
1.54000	.10000	.35000	.37433	1.50212
1.54000	.10000	.40000	.42553	1.50648
1.54000	.10000	.45000	.47619	1.51040
1.54000	.12000	.20000	.22124	1.47422
1.54000	.12000	.30000	.32751	1.48903
1.54000	.12000	.35000	.37961	1.49485
1.54000	.12000	.40000	.43103	1.50000
1.54000	.12000	.45000	.48180	1.50465
1.54000	.14000	.20000	.22523	1.46416
1.54000	.14000	.30000	.33259	1.48101
1.54000	.14000	.35000	.38504	1.48767
1.54000	.14000	.40000	.43668	1.49359
1.54000	.14000	.45000	.48754	1.49895
1.54000	.16000	.20000	.22936	1.45432
1.54000	.16000	.30000	.33784	1.47310
1.54000	.16000	.35000	.39063	1.48058
1.54000	.16000	.40000	.44248	1.48725
1.54000	.16000	.45000	.49342	1.49329
1.54000	.18000	.20000	.23364	1.44468
1.54000	.18000	.30000	.34325	1.46531
1.54000	.18000	.35000	.39638	1.47358
1.54000	.18000	.40000	.44843	1.48097
1.54000	.18000	.45000	.49945	1.48769
1.54000	.20000	.20000	.23810	1.43525
1.54000	.20000	.30000	.34884	1.45763
1.54000	.20000	.35000	.40230	1.46666
1.54000	.20000	.40000	.45455	1.47475
1.54000	.20000	.45000	.50562	1.48213
1.54000	.22000	.20000	.24272	1.42601
1.54000	.22000	.30000	.35461	1.45006
1.54000	.22000	.35000	.40840	1.45982
1.54000	.22000	.40000	.46083	1.46860
1.54000	.22000	.45000	.51195	1.47662

1.56000	.02000	.20000	.20325	1.54757
1.56000	.02000	.30000	.30426	1.55061
1.56000	.02000	.35000	.35461	1.55175
1.56000	.02000	.40000	.40486	1.55274
1.56000	.02000	.45000	.45501	1.55362
1.56000	.06000	.20000	.21008	1.52374
1.56000	.06000	.30000	.31315	1.53234
1.56000	.06000	.35000	.36420	1.53563
1.56000	.06000	.40000	.41494	1.53850
1.56000	.06000	.45000	.46536	1.54107
1.56000	.08000	.20000	.21368	1.51229
1.56000	.08000	.30000	.31780	1.52344
1.56000	.08000	.35000	.36920	1.52774
1.56000	.08000	.40000	.42017	1.53151
1.56000	.08000	.45000	.47071	1.53489
1.56000	.10000	.20000	.21739	1.50114
1.56000	.10000	.30000	.32258	1.51470
1.56000	.10000	.35000	.37433	1.51996
1.56000	.10000	.40000	.42553	1.52460
1.56000	.10000	.45000	.47619	1.52876
1.56000	.12000	.20000	.22124	1.49026
1.56000	.12000	.30000	.32751	1.50610
1.56000	.12000	.35000	.37961	1.51229
1.56000	.12000	.40000	.43103	1.51777
1.56000	.12000	.45000	.48180	1.52270
1.56000	.14000	.20000	.22523	1.47964
1.56000	.14000	.30000	.33259	1.49763
1.56000	.14000	.35000	.38504	1.50472
1.56000	.14000	.40000	.43668	1.51101
1.56000	.14000	.45000	.48754	1.51669
1.56000	.16000	.20000	.22936	1.46927
1.56000	.16000	.30000	.33784	1.48931
1.56000	.16000	.35000	.39063	1.49726
1.56000	.16000	.40000	.44248	1.50433
1.56000	.16000	.45000	.49342	1.51074
1.56000	.18000	.20000	.23364	1.45913
1.56000	.18000	.30000	.34325	1.48111
1.56000	.18000	.35000	.39638	1.48989
1.56000	.18000	.40000	.44843	1.49773
1.56000	.18000	.45000	.49945	1.50485
1.56000	.20000	.20000	.23810	1.44922
1.56000	.20000	.30000	.34884	1.47303
1.56000	.20000	.35000	.40230	1.48261
1.56000	.20000	.40000	.45455	1.49119
1.56000	.20000	.45000	.50562	1.49900
1.56000	.22000	.20000	.24272	1.43951
1.56000	.22000	.30000	.35461	1.46507
1.56000	.22000	.35000	.40840	1.47542
1.56000	.22000	.40000	.46083	1.48472
1.56000	.22000	.45000	.51195	1.49321

1.58000	.02000	.20000	.20325	1.56679
1.58000	.02000	.30000	.30426	1.57006
1.58000	.02000	.35000	.35461	1.57128
1.58000	.02000	.40000	.40486	1.57234
1.58000	.02000	.45000	.45501	1.57327
1.58000	.06000	.20000	.21008	1.54153
1.58000	.06000	.30000	.31315	1.55074
1.58000	.06000	.35000	.36420	1.55425
1.58000	.06000	.40000	.41494	1.55731
1.58000	.06000	.45000	.46536	1.56004
1.58000	.08000	.20000	.21368	1.52942
1.58000	.08000	.30000	.31780	1.54135
1.58000	.08000	.35000	.36920	1.54593
1.58000	.08000	.40000	.42017	1.54994
1.58000	.08000	.45000	.47071	1.55353
1.58000	.10000	.20000	.21739	1.51764
1.58000	.10000	.30000	.32258	1.53213
1.58000	.10000	.35000	.37433	1.53774
1.58000	.10000	.40000	.42553	1.54266
1.58000	.10000	.45000	.47619	1.54708
1.58000	.12000	.20000	.22124	1.50617
1.58000	.12000	.30000	.32751	1.52307
1.58000	.12000	.35000	.37961	1.52966
1.58000	.12000	.40000	.43103	1.53547
1.58000	.12000	.45000	.48180	1.54070
1.58000	.14000	.20000	.22523	1.49499
1.58000	.14000	.30000	.33259	1.51416
1.58000	.14000	.35000	.38504	1.52170
1.58000	.14000	.40000	.43668	1.52837
1.58000	.14000	.45000	.48754	1.53438
1.58000	.16000	.20000	.22936	1.48408
1.58000	.16000	.30000	.33784	1.50540
1.58000	.16000	.35000	.39063	1.51385
1.58000	.16000	.40000	.44248	1.52135
1.58000	.16000	.45000	.49342	1.52813
1.58000	.18000	.20000	.23364	1.47342
1.58000	.18000	.30000	.34325	1.49679
1.58000	.18000	.35000	.39638	1.50610
1.58000	.18000	.40000	.44843	1.51441
1.58000	.18000	.45000	.49945	1.52194
1.58000	.20000	.20000	.23810	1.46302
1.58000	.20000	.30000	.34884	1.48831
1.58000	.20000	.35000	.40230	1.49846
1.58000	.20000	.40000	.45455	1.50754
1.58000	.20000	.45000	.50562	1.51580
1.58000	.22000	.20000	.24272	1.45284
1.58000	.22000	.30000	.35461	1.47996
1.58000	.22000	.35000	.40840	1.49092
1.58000	.22000	.40000	.46083	1.50076
1.58000	.22000	.45000	.51195	1.50972

1.60000	02000	.20000	.20325	1.58598
1.60000	.02000	.30000	.30426	1.58949
1.60000	.02000	.35000	.35461	1.59079
1.60000	.02000	.40000	.40486	1.59192
1.60000	.02000	.45000	.45501	1.59291
1.60000	.06000	.20000	.21008	1.55923
1.60000	.06000	.30000	.31315	1.56910
1.60000	.06000	.35000	.36420	1.57284
1.60000	.06000	.40000	.41494	1.57609
1.60000	.06000	.45000	.46536	1.57898
1.60000	.08000	.20000	.21368	1.54645
1.60000	.08000	.30000	.31780	1.55920
1.60000	.08000	.35000	.36920	1.56407
1.60000	.08000	.40000	.42017	1.56833
1.60000	.08000	.45000	.47071	1.57213
1.60000	.10000	.20000	.21739	1.53403
1.60000	.10000	.30000	.32258	1.54949
1.60000	.10000	.35000	.37433	1.55545
1.60000	.10000	.40000	.42553	1.56067
1.60000	.10000	.45000	.47619	1.56535
1.60000	.12000	.20000	.22124	1.52195
1.60000	.12000	.30000	.32751	1.53996
1.60000	.12000	.35000	.37961	1.54695
1.60000	.12000	.40000	.43103	1.55312
1.60000	.12000	.45000	.48180	1.55865
1.60000	.14000	.20000	.22523	1.51018
1.60000	.14000	.30000	.33259	1.53059
1.60000	.14000	.35000	.38504	1.53859
1.60000	.14000	.40000	.43668	1.54565
1.60000	.14000	.45000	.48754	1.55202
1.60000	.16000	.20000	.22936	1.49872
1.60000	.16000	.30000	.33784	1.52140
1.60000	.16000	.35000	.39063	1.53034
1.60000	.16000	.40000	.44248	1.53828
1.60000	.16000	.45000	.49342	1.54545
1.60000	.18000	.20000	.23364	1.48755
1.60000	.18000	.30000	.34325	1.51235
1.60000	.18000	.35000	.39638	1.52222
1.60000	.18000	.40000	.44843	1.53100
1.60000	.18000	.45000	.49945	1.53896
1.60000	.20000	.20000	.23810	1.47664
1.60000	.20000	.30000	.34884	1.50346
1.60000	.20000	.35000	.40230	1.51421
1.60000	.20000	.40000	.45455	1.52380
1.60000	.20000	.45000	.50562	1.53252
1.60000	.22000	.20000	.24272	1.46599
1.60000	.22000	.30000	.35461	1.49472
1.60000	.22000	.35000	.40840	1.50630
1.60000	.22000	.40000	.46083	1.51669
1.60000	.22000	.45000	.51195	1.52615

1.64000	.02000	.20000	.20325	1.62427
1.64000	.02000	.30000	.30426	1.62829
1.64000	.02000	.35000	.35461	1.62977
1.64000	.02000	.40000	.40486	1.63104
1.64000	.02000	.45000	.45501	1.63216
1.64000	.06000	.20000	.21008	1.59441
1.64000	.06000	.30000	.31315	1.60566
1.64000	.06000	.35000	.36420	1.60988
1.64000	.06000	.40000	.41494	1.61354
1.64000	.06000	.45000	.46536	1.61678
1.64000	.08000	.20000	.21368	1.58020
1.64000	.08000	.30000	.31780	1.59470
1.64000	.08000	.35000	.36920	1.60019
1.64000	.08000	.40000	.42017	1.60498
1.64000	.08000	.45000	.47071	1.60923
1.64000	.10000	.20000	.21739	1.56644
1.64000	.10000	.30000	.32258	1.58397
1.64000	.10000	.35000	.37433	1.59068
1.64000	.10000	.40000	.42553	1.59654
1.64000	.10000	.45000	.47619	1.60177
1.64000	.12000	.20000	.22124	1.55310
1.64000	.12000	.30000	.32751	1.57346
1.64000	.12000	.35000	.37961	1.58132
1.64000	.12000	.40000	.43103	1.58822
1.64000	.12000	.45000	.48180	1.59439
1.64000	.14000	.20000	.22523	1.54014
1.64000	.14000	.30000	.33259	1.56316
1.64000	.14000	.35000	.38504	1.57212
1.64000	.14000	.40000	.43668	1.58002
1.64000	.14000	.45000	.48754	1.58711
1.64000	.16000	.20000	.22936	1.52755
1.64000	.16000	.30000	.33784	1.55305
1.64000	.16000	.35000	.39063	1.56307
1.64000	.16000	.40000	.44248	1.57192
1.64000	.16000	.45000	.49342	1.57990
1.64000	.18000	.20000	.23364	1.51530
1.64000	.18000	.30000	.34325	1.54314
1.64000	.18000	.35000	.39638	1.55415
1.64000	.18000	.40000	.44843	1.56394
1.64000	.18000	.45000	.49945	1.57278
1.64000	.20000	.20000	.23810	1.50337
1.64000	.20000	.30000	.34884	1.53340
1.64000	.20000	.35000	.40230	1.54538
1.64000	.20000	.40000	.45455	1.55606
1.64000	.20000	.45000	.50562	1.56574
1.64000	.22000	.20000	.24272	1.49175
1.64000	.22000	.30000	.35461	1.52384
1.64000	.22000	.35000	.40840	1.53674
1.64000	.22000	.40000	.46083	1.54828
1.64000	.22000	.45000	.51195	1.55877

1.66000	.02000	.20000	.20325	1.64336
1.66000	.02000	.30000	.30426	1.64767
1.66000	.02000	.35000	.35461	1.64924
1.66000	.02000	.40000	.40486	1.65059
1.66000	.02000	.45000	.45501	1.65177
1.66000	.06000	.20000	.21008	1.61186
1.66000	.06000	.30000	.31315	1.62385
1.66000	.06000	.35000	.36420	1.62833
1.66000	.06000	.40000	.41494	1.63221
1.66000	.06000	.45000	.46536	1.63563
1.66000	.08000	.20000	.21368	1.59692
1.66000	.08000	.30000	.31780	1.61235
1.66000	.08000	.35000	.36920	1.61817
1.66000	.08000	.40000	.42017	1.62323
1.66000	.08000	.45000	.47071	1.62772
1.66000	.10000	.20000	.21739	1.58247
1.66000	.10000	.30000	.32258	1.60109
1.66000	.10000	.35000	.37433	1.60819
1.66000	.10000	.40000	.42553	1.61439
1.66000	.10000	.45000	.47619	1.61990
1.66000	.12000	.20000	.22124	1.56847
1.66000	.12000	.30000	.32751	1.59008
1.66000	.12000	.35000	.37961	1.59839
1.66000	.12000	.40000	.43103	1.60568
1.66000	.12000	.45000	.48180	1.61219
1.66000	.14000	.20000	.22523	1.55490
1.66000	.14000	.30000	.33259	1.57929
1.66000	.14000	.35000	.38504	1.58876
1.66000	.14000	.40000	.43668	1.59709
1.66000	.14000	.45000	.48754	1.60456
1.66000	.16000	.20000	.22936	1.54172
1.66000	.16000	.30000	.33784	1.56872
1.66000	.16000	.35000	.39063	1.57929
1.66000	.16000	.40000	.44248	1.58863
1.66000	.16000	.45000	.49342	1.59703
1.66000	.18000	.20000	.23364	1.52893
1.66000	.18000	.30000	.34325	1.55835
1.66000	.18000	.35000	.39638	1.56997
1.66000	.18000	.40000	.44843	1.58028
1.66000	.18000	.45000	.49945	1.58959
1.66000	.20000	.20000	.23810	1.51648
1.66000	.20000	.30000	.34884	1.54818
1.66000	.20000	.35000	.40230	1.56081
1.66000	.20000	.40000	.45455	1.57205
1.66000	.20000	.45000	.50562	1.58223
1.66000	.22000	.20000	.24272	1.50436
1.66000	.22000	.30000	.35461	1.53820
1.66000	.22000	.35000	.40840	1.55179
1.66000	.22000	.40000	.46083	1.56393
1.66000	.22000	.45000	.51195	1.57495

1.68000	.02000	.20000	.20325	1.66242
1.68000	.02000	.30000	.30426	1.66702
1.68000	.02000	.35000	.35461	1.66869
1.68000	.02000	.40000	.40486	1.67012
1.68000	.02000	.45000	.45501	1.67137
1.68000	.06000	.20000	.21008	1.62923
1.68000	.06000	.30000	.31315	1.64200
1.68000	.06000	.35000	.36420	1.64675
1.68000	.06000	.40000	.41494	1.65084
1.68000	.06000	.45000	.46536	1.65446
1.68000	.08000	.20000	.21368	1.61353
1.68000	.08000	.30000	.31780	1.62993
1.68000	.08000	.35000	.36920	1.63610
1.68000	.08000	.40000	.42017	1.64144
1.68000	.08000	.45000	.47071	1.64617
1.68000	.10000	.20000	.21739	1.59837
1.68000	.10000	.30000	.32258	1.61814
1.68000	.10000	.35000	.37433	1.62565
1.68000	.10000	.40000	.42553	1.63218
1.68000	.10000	.45000	.47619	1.63800
1.68000	.12000	.20000	.22124	1.58370
1.68000	.12000	.30000	.32751	1.60660
1.68000	.12000	.35000	.37961	1.61539
1.68000	.12000	.40000	.43103	1.62307
1.68000	.12000	.45000	.48180	1.62993
1.68000	.14000	.20000	.22523	1.56950
1.68000	.14000	.30000	.33259	1.59532
1.68000	.14000	.35000	.38504	1.60531
1.68000	.14000	.40000	.43668	1.61410
1.68000	.14000	.45000	.48754	1.62196
1.68000	.16000	.20000	.22936	1.55574
1.68000	.16000	.30000	.33784	1.58427
1.68000	.16000	.35000	.39063	1.59542
1.68000	.16000	.40000	.44248	1.60525
1.68000	.16000	.45000	.49342	1.61409
1.68000	.18000	.20000	.23364	1.54238
1.68000	.18000	.30000	.34325	1.57345
1.68000	.18000	.35000	.39638	1.58569
1.68000	.18000	.40000	.44843	1.59654
1.68000	.18000	.45000	.49945	1.60632
1.68000	.20000	.20000	.23810	1.52941
1.68000	.20000	.30000	.34884	1.56284
1.68000	.20000	.35000	.40230	1.57613
1.68000	.20000	.40000	.45455	1.58795
1.68000	.20000	.45000	.50562	1.59864
1.68000	.22000	.20000	.24272	1.51679
1.68000	.22000	.30000	.35461	1.55244
1.68000	.22000	.35000	.40840	1.56672
1.68000	.22000	.40000	.46083	1.57948
1.68000	.22000	.45000	.51195	1.59105

1.70000	.02000	.20000	.20325	1.68144
1.70000	.02000	.30000	.30426	1.68635
1.70000	.02000	.35000	.35461	1.68812
1.70000	.02000	.40000	.40486	1.68963
1.70000	.02000	.45000	.45501	1.69095
1.70000	.06000	.20000	.21008	1.64652
1.70000	.06000	.30000	.31315	1.66009
1.70000	.06000	.35000	.36420	1.66512
1.70000	.06000	.40000	.41494	1.66944
1.70000	.06000	.45000	.46536	1.67325
1.70000	.08000	.20000	.21368	1.63003
1.70000	.08000	.30000	.31780	1.64744
1.70000	.08000	.35000	.36920	1.65396
1.70000	.08000	.40000	.42017	1.65960
1.70000	.08000	.45000	.47071	1.66459
1.70000	.10000	.20000	.21739	1.61414
1.70000	.10000	.30000	.32258	1.63509
1.70000	.10000	.35000	.37433	1.64303
1.70000	.10000	.40000	.42553	1.64992
1.70000	.10000	.45000	.47619	1.65604
1.70000	.12000	.20000	.22124	1.59879
1.70000	.12000	.30000	.32751	1.62303
1.70000	.12000	.35000	.37961	1.63230
1.70000	.12000	.40000	.43103	1.64040
1.70000	.12000	.45000	.48180	1.64761
1.70000	.14000	.20000	.22523	1.58395
1.70000	.14000	.30000	.33259	1.61124
1.70000	.14000	.35000	.38504	1.62178
1.70000	.14000	.40000	.43668	1.63103
1.70000	.14000	.45000	.48754	1.63929
1.70000	.16000	.20000	.22936	1.56959
1.70000	.16000	.30000	.33784	1.59971
1.70000	.16000	.35000	.39063	1.61145
1.70000	.16000	.40000	.44248	1.62180
1.70000	.16000	.45000	.49342	1.63108
1.70000	.18000	.20000	.23364	1.55567
1.70000	.18000	.30000	.34325	1.58842
1.70000	.18000	.35000	.39638	1.60131
1.70000	.18000	.40000	.44843	1.61271
1.70000	.18000	.45000	.49945	1.62298
1.70000	.20000	.20000	.23810	1.54216
1.70000	.20000	.30000	.34884	1.57737
1.70000	.20000	.35000	.40230	1.59134
1.70000	.20000	.40000	.45455	1.60375
1.70000	.20000	.45000	.50562	1.61497
1.70000	.22000	.20000	.24272	1.52903
1.70000	.22000	.30000	.35461	1.56654
1.70000	.22000	.35000	.40840	1.58154
1.70000	.22000	.40000	.46083	1.59493
1.70000	.22000	.45000	.51195	1.60706

1.72000	.02000	.20000	.20325	1.70043
1.72000	.02000	.30000	.30426	1.70566
1.72000	.02000	.35000	.35461	1.70754
1.72000	.02000	.40000	.40486	1.70914
1.72000	.02000	.45000	.45501	1.71053
1.72000	.06000	.20000	.21008	1.66371
1.72000	.06000	.30000	.31315	1.67812
1.72000	.06000	.35000	.36420	1.68344
1.72000	.06000	.40000	.41494	1.68801
1.72000	.06000	.45000	.46536	1.69202
1.72000	.08000	.20000	.21368	1.64642
1.72000	.08000	.30000	.31780	1.66488
1.72000	.08000	.35000	.36920	1.67177
1.72000	.08000	.40000	.42017	1.67772
1.72000	.08000	.45000	.47071	1.68296
1.72000	.10000	.20000	.21739	1.62978
1.72000	.10000	.30000	.32258	1.65197
1.72000	.10000	.35000	.37433	1.66034
1.72000	.10000	.40000	.42553	1.66761
1.72000	.10000	.45000	.47619	1.67404
1.72000	.12000	.20000	.22124	1.61374
1.72000	.12000	.30000	.32751	1.63937
1.72000	.12000	.35000	.37961	1.64914
1.72000	.12000	.40000	.43103	1.65766
1.72000	.12000	.45000	.48180	1.66524
1.72000	.14000	.20000	.22523	1.59825
1.72000	.14000	.30000	.33259	1.62706
1.72000	.14000	.35000	.38504	1.63816
1.72000	.14000	.40000	.43668	1.64788
1.72000	.14000	.45000	.48754	1.65657
1.72000	.16000	.20000	.22936	1.58328
1.72000	.16000	.30000	.33784	1.61503
1.72000	.16000	.35000	.39063	1.62739
1.72000	.16000	.40000	.44248	1.63826
1.72000	.16000	.45000	.49342	1.64801
1.72000	.18000	.20000	.23364	1.56878
1.72000	.18000	.30000	.34325	1.60327
1.72000	.18000	.35000	.39638	1.61682
1.72000	.18000	.40000	.44843	1.62879
1.72000	.18000	.45000	.49945	1.63956
1.72000	.20000	.20000	.23810	1.55473
1.72000	.20000	.30000	.34884	1.59177
1.72000	.20000	.35000	.40230	1.60644
1.72000	.20000	.40000	.45455	1.61947
1.72000	.20000	.45000	.50562	1.63123
1.72000	.22000	.20000	.24272	1.54110
1.72000	.22000	.30000	.35461	1.58050
1.72000	.22000	.35000	.40840	1.59625
1.72000	.22000	.40000	.46083	1.61028
1.72000	.22000	.45000	.51195	1.62300

1.74000	.02000	.20000	.20325	1.71938
1.74000	.02000	.30000	.30426	1.72495
1.74000	.02000	.35000	.35461	1.72694
1.74000	.02000	.40000	.40486	1.72863
1.74000	.02000	.45000	.45501	1.73010
1.74000	.06000	.20000	.21008	1.68080
1.74000	.06000	.30000	.31315	1.69610
1.74000	.06000	.35000	.36420	1.70172
1.74000	.06000	.40000	.41494	1.70653
1.74000	.06000	.45000	.46536	1.71075
1.74000	.08000	.20000	.21368	1.66270
1.74000	.08000	.30000	.31780	1.68225
1.74000	.08000	.35000	.36920	1.68952
1.74000	.08000	.40000	.42017	1.69579
1.74000	.08000	.45000	.47071	1.70130
1.74000	.10000	.20000	.21739	1.64530
1.74000	.10000	.30000	.32258	1.66876
1.74000	.10000	.35000	.37433	1.67759
1.74000	.10000	.40000	.42553	1.68523
1.74000	.10000	.45000	.47619	1.69199
1.74000	.12000	.20000	.22124	1.62854
1.74000	.12000	.30000	.32751	1.65561
1.74000	.12000	.35000	.37961	1.66590
1.74000	.12000	.40000	.43103	1.67486
1.74000	.12000	.45000	.48180	1.68282
1.74000	.14000	.20000	.22523	1.61239
1.74000	.14000	.30000	.33259	1.64277
1.74000	.14000	.35000	.38504	1.65445
1.74000	.14000	.40000	.43668	1.66467
1.74000	.14000	.45000	.48754	1.67378
1.74000	.16000	.20000	.22936	1.59680
1.74000	.16000	.30000	.33784	1.63025
1.74000	.16000	.35000	.39063	1.64323
1.74000	.16000	.40000	.44248	1.65465
1.74000	.16000	.45000	.49342	1.66486
1.74000	.18000	.20000	.23364	1.58172
1.74000	.18000	.30000	.34325	1.61801
1.74000	.18000	.35000	.39638	1.63223
1.74000	.18000	.40000	.44843	1.64479
1.74000	.18000	.45000	.49945	1.65607
1.74000	.20000	.20000	.23810	1.56713
1.74000	.20000	.30000	.34884	1.60604
1.74000	.20000	.35000	.40230	1.62143
1.74000	.20000	.40000	.45455	1.63509
1.74000	.20000	.45000	.50562	1.64740
1.74000	.22000	.20000	.24272	1.55298
1.74000	.22000	.30000	.35461	1.59433
1.74000	.22000	.35000	.40840	1.61084
1.74000	.22000	.40000	.46083	1.62554
1.74000	.22000	.45000	.51195	1.63884

1.76000	.02000	.20000	.20325	1.73829
1.76000	.02000	.30000	.30426	1.74422
1.76000	.02000	.35000	.35461	1.74632
1.76000	.02000	.40000	.40486	1.74811
1.76000	.02000	.45000	.45501	1.74965
1.76000	.06000	.20000	.21008	1.69781
1.76000	.06000	.30000	.31315	1.71401
1.76000	.06000	.35000	.36420	1.71995
1.76000	.06000	.40000	.41494	1.72502
1.76000	.06000	.45000	.46536	1.72946
1.76000	.08000	.20000	.21368	1.67886
1.76000	.08000	.30000	.31780	1.69954
1.76000	.08000	.35000	.36920	1.70721
1.76000	.08000	.40000	.42017	1.71380
1.76000	.08000	.45000	.47071	1.71960
1.76000	.10000	.20000	.21739	1.66067
1.76000	.10000	.30000	.32258	1.68546
1.76000	.10000	.35000	.37433	1.69476
1.76000	.10000	.40000	.42553	1.70280
1.76000	.10000	.45000	.47619	1.70990
1.76000	.12000	.20000	.22124	1.64320
1.76000	.12000	.30000	.32751	1.67175
1.76000	.12000	.35000	.37961	1.68258
1.76000	.12000	.40000	.43103	1.69199
1.76000	.12000	.45000	.48180	1.70034
1.76000	.14000	.20000	.22523	1.62637
1.76000	.14000	.30000	.33259	1.65838
1.76000	.14000	.35000	.38504	1.67066
1.76000	.14000	.40000	.43668	1.68138
1.76000	.14000	.45000	.48754	1.69093
1.76000	.16000	.20000	.22936	1.61015
1.76000	.16000	.30000	.33784	1.64534
1.76000	.16000	.35000	.39063	1.65898
1.76000	.16000	.40000	.44248	1.67095
1.76000	.16000	.45000	.49342	1.68165
1.76000	.18000	.20000	.23364	1.59449
1.76000	.18000	.30000	.34325	1.63261
1.76000	.18000	.35000	.39638	1.64754
1.76000	.18000	.40000	.44843	1.66070
1.76000	.18000	.45000	.49945	1.67251
1.76000	.20000	.20000	.23810	1.57934
1.76000	.20000	.30000	.34884	1.62018
1.76000	.20000	.35000	.40230	1.63632
1.76000	.20000	.40000	.45455	1.65061
1.76000	.20000	.45000	.50562	1.66349
1.76000	.22000	.20000	.24272	1.56468
1.76000	.22000	.30000	.35461	1.60803
1.76000	.22000	.35000	.40840	1.62531
1.76000	.22000	.40000	.46083	1.64069
1.76000	.22000	.45000	.51195	1.65460

1.78000	.02000	.20000	.20325	1.75717
1.78000	.02000	.30000	.30426	1.76346
1.78000	.02000	.35000	.35461	1.76569
1.78000	.02000	.40000	.40486	1.76757
1.78000	.02000	.45000	.45501	1.76919
1.78000	.06000	.20000	.21008	1.71471
1.78000	.06000	.30000	.31315	1.73187
1.78000	.06000	.35000	.36420	1.73813
1.78000	.06000	.40000	.41494	1.74347
1.78000	.06000	.45000	.46536	1.74813
1.78000	.08000	.20000	.21368	1.69490
1.78000	.08000	.30000	.31780	1.71676
1.78000	.08000	.35000	.36920	1.72484
1.78000	.08000	.40000	.42017	1.73177
1.78000	.08000	.45000	.47071	1.73786
1.78000	.10000	.20000	.21739	1.67592
1.78000	.10000	.30000	.32258	1.70208
1.78000	.10000	.35000	.37433	1.71186
1.78000	.10000	.40000	.42553	1.72031
1.78000	.10000	.45000	.47619	1.72775
1.78000	.12000	.20000	.22124	1.65771
1.78000	.12000	.30000	.32751	1.68779
1.78000	.12000	.35000	.37961	1.69918
1.78000	.12000	.40000	.43103	1.70906
1.78000	.12000	.45000	.48180	1.71781
1.78000	.14000	.20000	.22523	1.64020
1.78000	.14000	.30000	.33259	1.67388
1.78000	.14000	.35000	.38504	1.68677
1.78000	.14000	.40000	.43668	1.69801
1.78000	.14000	.45000	.48754	1.70801
1.78000	.16000	.20000	.22936	1.62334
1.78000	.16000	.30000	.33784	1.66032
1.78000	.16000	.35000	.39063	1.67463
1.78000	.16000	.40000	.44248	1.68717
1.78000	.16000	.45000	.49342	1.69837
1.78000	.18000	.20000	.23364	1.60708
1.78000	.18000	.30000	.34325	1.64710
1.78000	.18000	.35000	.39638	1.66274
1.78000	.18000	.40000	.44843	1.67651
1.78000	.18000	.45000	.49945	1.68887
1.78000	.20000	.20000	.23810	1.59138
1.78000	.20000	.30000	.34884	1.63419
1.78000	.20000	.35000	.40230	1.65109
1.78000	.20000	.40000	.45455	1.66604
1.78000	.20000	.45000	.50562	1.67951
1.78000	.22000	.20000	.24272	1.57620
1.78000	.22000	.30000	.35461	1.62159
1.78000	.22000	.35000	.40840	1.63967
1.78000	.22000	.40000	.46083	1.65575
1.78000	.22000	.45000	.51195	1.67028

1.80000	.02000	.20000	.20325	1.77600
1.80000	.02000	.30000	.30426	1.78268
1.80000	.02000	.35000	.35461	1.78504
1.80000	.02000	.40000	.40486	1.78702
1.80000	.02000	.45000	.45501	1.78873
1.80000	.06000	.20000	.21008	1.73152
1.80000	.06000	.30000	.31315	1.74967
1.80000	.06000	.35000	.36420	1.75626
1.80000	.06000	.40000	.41494	1.76188
1.80000	.06000	.45000	.46536	1.76677
1.80000	.08000	.20000	.21368	1.71082
1.80000	.08000	.30000	.31780	1.73391
1.80000	.08000	.35000	.36920	1.74241
1.80000	.08000	.40000	.42017	1.74970
1.80000	.08000	.45000	.47071	1.75608
1.80000	.10000	.20000	.21739	1.69103
1.80000	.10000	.30000	.32258	1.71861
1.80000	.10000	.35000	.37433	1.72889
1.80000	.10000	.40000	.42553	1.73776
1.80000	.10000	.45000	.47619	1.74556
1.80000	.12000	.20000	.22124	1.67206
1.80000	.12000	.30000	.32751	1.70374
1.80000	.12000	.35000	.37961	1.71569
1.80000	.12000	.40000	.43103	1.72605
1.80000	.12000	.45000	.48180	1.73522
1.80000	.14000	.20000	.22523	1.65386
1.80000	.14000	.30000	.33259	1.68927
1.80000	.14000	.35000	.38504	1.70279
1.80000	.14000	.40000	.43668	1.71457
1.80000	.14000	.45000	.48754	1.72504
1.80000	.16000	.20000	.22936	1.63636
1.80000	.16000	.30000	.33784	1.67518
1.80000	.16000	.35000	.39063	1.69018
1.80000	.16000	.40000	.44248	1.70330
1.80000	.16000	.45000	.49342	1.71502
1.80000	.18000	.20000	.23364	1.61950
1.80000	.18000	.30000	.34325	1.66146
1.80000	.18000	.35000	.39638	1.67783
1.80000	.18000	.40000	.44843	1.69224
1.80000	.18000	.45000	.49945	1.70516
1.80000	.20000	.20000	.23810	1.60324
1.80000	.20000	.30000	.34884	1.64807
1.80000	.20000	.35000	.40230	1.66575
1.80000	.20000	.40000	.45455	1.68138
1.80000	.20000	.45000	.50562	1.69544
1.80000	.22000	.20000	.24272	1.58753
1.80000	.22000	.30000	.35461	1.63501
1.80000	.22000	.35000	.40840	1.65391
1.80000	.22000	.40000	.46083	1.67070
1.80000	.22000	.45000	.51195	1.68587

1.82000	.02000	.20000	.20325	1.79479
1.82000	.02000	.30000	.30426	1.80188
1.82000	.02000	.35000	.35461	1.80437
1.82000	.02000	.40000	.40486	1.80645
1.82000	.02000	.45000	.45501	1.80825
1.82000	.06000	.20000	.21008	1.74822
1.82000	.06000	.30000	.31315	1.76741
1.82000	.06000	.35000	.36420	1.77435
1.82000	.06000	.40000	.41494	1.78025
1.82000	.06000	.45000	.46536	1.78538
1.82000	.08000	.20000	.21368	1.72662
1.82000	.08000	.30000	.31780	1.75098
1.82000	.08000	.35000	.36920	1.75992
1.82000	.08000	.40000	.42017	1.76757
1.82000	.08000	.45000	.47071	1.77425
1.82000	.10000	.20000	.21739	1.70599
1.82000	.10000	.30000	.32258	1.73505
1.82000	.10000	.35000	.37433	1.74585
1.82000	.10000	.40000	.42553	1.75515
1.82000	.10000	.45000	.47619	1.76332
1.82000	.12000	.20000	.22124	1.68627
1.82000	.12000	.30000	.32751	1.71958
1.82000	.12000	.35000	.37961	1.73212
1.82000	.12000	.40000	.43103	1.74298
1.82000	.12000	.45000	.48180	1.75257
1.82000	.14000	.20000	.22523	1.66736
1.82000	.14000	.30000	.33259	1.70455
1.82000	.14000	.35000	.38504	1.71872
1.82000	.14000	.40000	.43668	1.73105
1.82000	.14000	.45000	.48754	1.74200
1.82000	.16000	.20000	.22936	1.64920
1.82000	.16000	.30000	.33784	1.68992
1.82000	.16000	.35000	.39063	1.70562
1.82000	.16000	.40000	.44248	1.71936
1.82000	.16000	.45000	.49342	1.73160
1.82000	.18000	.20000	.23364	1.63174
1.82000	.18000	.30000	.34325	1.67569
1.82000	.18000	.35000	.39638	1.69282
1.82000	.18000	.40000	.44843	1.70788
1.82000	.18000	.45000	.49945	1.72136
1.82000	.20000	.20000	.23810	1.61492
1.82000	.20000	.30000	.34884	1.66182
1.82000	.20000	.35000	.40230	1.68030
1.82000	.20000	.40000	.45455	1.69662
1.82000	.20000	.45000	.50562	1.71129
1.82000	.22000	.20000	.24272	1.59869
1.82000	.22000	.30000	.35461	1.64830
1.82000	.22000	.35000	.40840	1.66804
1.82000	.22000	.40000	.46083	1.68556
1.82000	.22000	.45000	.51195	1.70137

1.84000	.02000	.20000	.20325	1.81353
1.84000	.02000	.30000	.30426	1.82105
1.84000	.02000	.35000	.35461	1.82368
1.84000	.02000	.40000	.40486	1.82587
1.84000	.02000	.45000	.45501	1.82775
1.84000	.06000	.20000	.21008	1.76482
1.84000	.06000	.30000	.31315	1.78508
1.84000	.06000	.35000	.36420	1.79239
1.84000	.06000	.40000	.41494	1.79858
1.84000	.06000	.45000	.46536	1.80396
1.84000	.08000	.20000	.21368	1.74229
1.84000	.08000	.30000	.31780	1.76797
1.84000	.08000	.35000	.36920	1.77737
1.84000	.08000	.40000	.42017	1.78539
1.84000	.08000	.45000	.47071	1.79239
1.84000	.10000	.20000	.21739	1.72082
1.84000	.10000	.30000	.32258	1.75140
1.84000	.10000	.35000	.37433	1.76274
1.84000	.10000	.40000	.42553	1.77248
1.84000	.10000	.45000	.47619	1.78103
1.84000	.12000	.20000	.22124	1.70032
1.84000	.12000	.30000	.32751	1.73532
1.84000	.12000	.35000	.37961	1.74847
1.84000	.12000	.40000	.43103	1.75984
1.84000	.12000	.45000	.48180	1.76986
1.84000	.14000	.20000	.22523	1.68070
1.84000	.14000	.30000	.33259	1.71971
1.84000	.14000	.35000	.38504	1.73456
1.84000	.14000	.40000	.43668	1.74746
1.84000	.14000	.45000	.48754	1.75889
1.84000	.16000	.20000	.22936	1.66188
1.84000	.16000	.30000	.33784	1.70455
1.84000	.16000	.35000	.39063	1.72097
1.84000	.16000	.40000	.44248	1.73533
1.84000	.16000	.45000	.49342	1.74811
1.84000	.18000	.20000	.23364	1.64381
1.84000	.18000	.30000	.34325	1.68980
1.84000	.18000	.35000	.39638	1.70770
1.84000	.18000	.40000	.44843	1.72343
1.84000	.18000	.45000	.49945	1.73750
1.84000	.20000	.20000	.23810	1.62642
1.84000	.20000	.30000	.34884	1.67544
1.84000	.20000	.35000	.40230	1.69473
1.84000	.20000	.40000	.45455	1.71176
1.84000	.20000	.45000	.50562	1.72706
1.84000	.22000	.20000	.24272	1.60965
1.84000	.22000	.30000	.35461	1.66145
1.84000	.22000	.35000	.40840	1.68204
1.84000	.22000	.40000	.46083	1.70031
1.84000	.22000	.45000	.51195	1.71679

1.86000	.02000	.20000	.20325	1.83224
1.86000	.02000	.30000	.30426	1.84020
1.86000	.02000	.35000	.35461	1.84297
1.86000	.02000	.40000	.40486	1.84527
1.86000	.02000	.45000	.45501	1.84725
1.86000	.06000	.20000	.21008	1.78131
1.86000	.06000	.30000	.31315	1.80269
1.86000	.06000	.35000	.36420	1.81037
1.86000	.06000	.40000	.41494	1.81687
1.86000	.06000	.45000	.46536	1.82250
1.86000	.08000	.20000	.21368	1.75784
1.86000	.08000	.30000	.31780	1.78488
1.86000	.08000	.35000	.36920	1.79475
1.86000	.08000	.40000	.42017	1.80315
1.86000	.08000	.45000	.47071	1.81048
1.86000	.10000	.20000	.21739	1.73550
1.86000	.10000	.30000	.32258	1.76765
1.86000	.10000	.35000	.37433	1.77955
1.86000	.10000	.40000	.42553	1.78974
1.86000	.10000	.45000	.47619	1.79868
1.86000	.12000	.20000	.22124	1.71421
1.86000	.12000	.30000	.32751	1.75096
1.86000	.12000	.35000	.37961	1.76474
1.86000	.12000	.40000	.43103	1.77663
1.86000	.12000	.45000	.48180	1.78710
1.86000	.14000	.20000	.22523	1.69387
1.86000	.14000	.30000	.33259	1.73477
1.86000	.14000	.35000	.38504	1.75030
1.86000	.14000	.40000	.43668	1.76378
1.86000	.14000	.45000	.48754	1.77572
1.86000	.16000	.20000	.22936	1.67439
1.86000	.16000	.30000	.33784	1.71905
1.86000	.16000	.35000	.39063	1.73622
1.86000	.16000	.40000	.44248	1.75121
1.86000	.16000	.45000	.49342	1.76454
1.86000	.18000	.20000	.23364	1.65570
1.86000	.18000	.30000	.34325	1.70378
1.86000	.18000	.35000	.39638	1.72248
1.86000	.18000	.40000	.44843	1.73889
1.86000	.18000	.45000	.49945	1.75355
1.86000	.20000	.20000	.23810	1.63773
1.86000	.20000	.30000	.34884	1.68892
1.86000	.20000	.35000	.40230	1.70905
1.86000	.20000	.40000	.45455	1.72681
1.86000	.20000	.45000	.50562	1.74275
1.86000	.22000	.20000	.24272	1.62044
1.86000	.22000	.30000	.35461	1.67447
1.86000	.22000	.35000	.40840	1.69593
1.86000	.22000	.40000	.46083	1.71496
1.86000	.22000	.45000	.51195	1.73212

1.88000	.02000	.20000	.20325	1.85090
1.88000	.02000	.30000	.30426	1.85933
1.88000	.02000	.35000	.35461	1.86224
1.88000	.02000	.40000	.40486	1.86466
1.88000	.02000	.45000	.45501	1.86674
1.88000	.06000	.20000	.21008	1.79770
1.88000	.06000	.30000	.31315	1.82024
1.88000	.06000	.35000	.36420	1.82831
1.88000	.06000	.40000	.41494	1.83512
1.88000	.06000	.45000	.46536	1.84101
1.88000	.08000	.20000	.21368	1.77325
1.88000	.08000	.30000	.31780	1.80172
1.88000	.08000	.35000	.36920	1.81207
1.88000	.08000	.40000	.42017	1.82087
1.88000	.08000	.45000	.47071	1.82853
1.88000	.10000	.20000	.21739	1.75004
1.88000	.10000	.30000	.32258	1.78382
1.88000	.10000	.35000	.37433	1.79628
1.88000	.10000	.40000	.42553	1.80695
1.88000	.10000	.45000	.47619	1.81629
1.88000	.12000	.20000	.22124	1.72795
1.88000	.12000	.30000	.32751	1.76649
1.88000	.12000	.35000	.37961	1.78091
1.88000	.12000	.40000	.43103	1.79334
1.88000	.12000	.45000	.48180	1.80428
1.88000	.14000	.20000	.22523	1.70687
1.88000	.14000	.30000	.33259	1.74971
1.88000	.14000	.35000	.38504	1.76595
1.88000	.14000	.40000	.43668	1.78003
1.88000	.14000	.45000	.48754	1.79249
1.88000	.16000	.20000	.22936	1.68672
1.88000	.16000	.30000	.33784	1.73343
1.88000	.16000	.35000	.39063	1.75137
1.88000	.16000	.40000	.44248	1.76701
1.88000	.16000	.45000	.49342	1.78091
1.88000	.18000	.20000	.23364	1.66741
1.88000	.18000	.30000	.34325	1.71763
1.88000	.18000	.35000	.39638	1.73714
1.88000	.18000	.40000	.44843	1.75425
1.88000	.18000	.45000	.49945	1.76953
1.88000	.20000	.20000	.23810	1.64887
1.88000	.20000	.30000	.34884	1.70228
1.88000	.20000	.35000	.40230	1.72326
1.88000	.20000	.40000	.45455	1.74176
1.88000	.20000	.45000	.50562	1.75835
1.88000	.22000	.20000	.24272	1.63104
1.88000	.22000	.30000	.35461	1.68734
1.88000	.22000	.35000	.40840	1.70969
1.88000	.22000	.40000	.46083	1.72951
1.88000	.22000	.45000	.51195	1.74736

1.90000	.02000	.20000	.20325	1.86951
1.90000	.02000	.30000	.30426	1.87843
1.90000	.02000	.35000	.35461	1.88149
1.90000	.02000	.40000	.40486	1.88404
1.90000	.02000	.45000	.45501	1.88621
1.90000	.06000	.20000	.21008	1.81398
1.90000	.06000	.30000	.31315	1.83772
1.90000	.06000	.35000	.36420	1.84619
1.90000	.06000	.40000	.41494	1.85332
1.90000	.06000	.45000	.46536	1.85949
1.90000	.08000	.20000	.21368	1.78854
1.90000	.08000	.30000	.31780	1.81847
1.90000	.08000	.35000	.36920	1.82932
1.90000	.08000	.40000	.42017	1.83853
1.90000	.08000	.45000	.47071	1.84654
1.90000	.10000	.20000	.21739	1.76444
1.90000	.10000	.30000	.32258	1.79989
1.90000	.10000	.35000	.37433	1.81294
1.90000	.10000	.40000	.42553	1.82409
1.90000	.10000	.45000	.47619	1.83384
1.90000	.12000	.20000	.22124	1.74153
1.90000	.12000	.30000	.32751	1.78192
1.90000	.12000	.35000	.37961	1.79701
1.90000	.12000	.40000	.43103	1.80999
1.90000	.12000	.45000	.48180	1.82140
1.90000	.14000	.20000	.22523	1.71971
1.90000	.14000	.30000	.33259	1.76453
1.90000	.14000	.35000	.38504	1.78150
1.90000	.14000	.40000	.43668	1.79620
1.90000	.14000	.45000	.48754	1.80918
1.90000	.16000	.20000	.22936	1.69888
1.90000	.16000	.30000	.33784	1.74769
1.90000	.16000	.35000	.39063	1.76641
1.90000	.16000	.40000	.44248	1.78272
1.90000	.16000	.45000	.49342	1.79720
1.90000	.18000	.20000	.23364	1.67894
1.90000	.18000	.30000	.34325	1.73135
1.90000	.18000	.35000	.39638	1.75170
1.90000	.18000	.40000	.44843	1.76952
1.90000	.18000	.45000	.49945	1.78543
1.90000	.20000	.20000	.23810	1.65983
1.90000	.20000	.30000	.34884	1.71549
1.90000	.20000	.35000	.40230	1.73735
1.90000	.20000	.40000	.45455	1.75661
1.90000	.20000	.45000	.50562	1.77387
1.90000	.22000	.20000	.24272	1.64147
1.90000	.22000	.30000	.35461	1.70008
1.90000	.22000	.35000	.40840	1.72334
1.90000	.22000	.40000	.46083	1.74395
1.90000	.22000	.45000	.51195	1.76251

1.92000	.02000	.20000	.20325	1.88807
1.92000	.02000	.30000	.30426	1.89750
1.92000	.02000	.35000	.35461	1.90073
1.92000	.02000	.40000	.40486	1.90339
1.92000	.02000	.45000	.45501	1.90567
1.92000	.06000	.20000	.21008	1.83015
1.92000	.06000	.30000	.31315	1.85513
1.92000	.06000	.35000	.36420	1.86402
1.92000	.06000	.40000	.41494	1.87149
1.92000	.06000	.45000	.46536	1.87793
1.92000	.08000	.20000	.21368	1.80370
1.92000	.08000	.30000	.31780	1.83514
1.92000	.08000	.35000	.36920	1.84651
1.92000	.08000	.40000	.42017	1.85614
1.92000	.08000	.45000	.47071	1.86450
1.92000	.10000	.20000	.21739	1.77868
1.92000	.10000	.30000	.32258	1.81586
1.92000	.10000	.35000	.37433	1.82952
1.92000	.10000	.40000	.42553	1.84117
1.92000	.10000	.45000	.47619	1.85135
1.92000	.12000	.20000	.22124	1.75495
1.92000	.12000	.30000	.32751	1.79724
1.92000	.12000	.35000	.37961	1.81301
1.92000	.12000	.40000	.43103	1.82656
1.92000	.12000	.45000	.48180	1.83845
1.92000	.14000	.20000	.22523	1.73238
1.92000	.14000	.30000	.33259	1.77925
1.92000	.14000	.35000	.38504	1.79696
1.92000	.14000	.40000	.43668	1.81229
1.92000	.14000	.45000	.48754	1.82581
1.92000	.16000	.20000	.22936	1.71086
1.92000	.16000	.30000	.33784	1.76183
1.92000	.16000	.35000	.39063	1.78135
1.92000	.16000	.40000	.44248	1.79834
1.92000	.16000	.45000	.49342	1.81342
1.92000	.18000	.20000	.23364	1.69030
1.92000	.18000	.30000	.34325	1.74495
1.92000	.18000	.35000	.39638	1.76614
1.92000	.18000	.40000	.44843	1.78470
1.92000	.18000	.45000	.49945	1.80125
1.92000	.20000	.20000	.23810	1.67060
1.92000	.20000	.30000	.34884	1.72857
1.92000	.20000	.35000	.40230	1.75132
1.92000	.20000	.40000	.45455	1.77136
1.92000	.20000	.45000	.50562	1.78931
1.92000	.22000	.20000	.24272	1.65171
1.92000	.22000	.30000	.35461	1.71268
1.92000	.22000	.35000	.40840	1.73687
1.92000	.22000	.40000	.46083	1.75830
1.92000	.22000	.45000	.51195	1.77758

1.94000	.02000	.20000	.20325	1.90659
1.94000	.02000	.30000	.30426	1.91654
1.94000	.02000	.35000	.35461	1.91994
1.94000	.02000	.40000	.40486	1.92274
1.94000	.02000	.45000	.45501	1.92511
1.94000	.06000	.20000	.21008	1.84620
1.94000	.06000	.30000	.31315	1.87248
1.94000	.06000	.35000	.36420	1.88179
1.94000	.06000	.40000	.41494	1.88961
1.94000	.06000	.45000	.46536	1.89634
1.94000	.08000	.20000	.21368	1.81872
1.94000	.08000	.30000	.31780	1.85173
1.94000	.08000	.35000	.36920	1.86363
1.94000	.08000	.40000	.42017	1.87370
1.94000	.08000	.45000	.47071	1.88242
1.94000	.10000	.20000	.21739	1.79278
1.94000	.10000	.30000	.32258	1.83174
1.94000	.10000	.35000	.37433	1.84602
1.94000	.10000	.40000	.42553	1.85819
1.94000	.10000	.45000	.47619	1.86880
1.94000	.12000	.20000	.22124	1.76821
1.94000	.12000	.30000	.32751	1.81246
1.94000	.12000	.35000	.37961	1.82893
1.94000	.12000	.40000	.43103	1.84306
1.94000	.12000	.45000	.48180	1.85545
1.94000	.14000	.20000	.22523	1.74489
1.94000	.14000	.30000	.33259	1.79384
1.94000	.14000	.35000	.38504	1.81232
1.94000	.14000	.40000	.43668	1.82830
1.94000	.14000	.45000	.48754	1.84238
1.94000	.16000	.20000	.22936	1.72267
1.94000	.16000	.30000	.33784	1.77584
1.94000	.16000	.35000	.39063	1.79618
1.94000	.16000	.40000	.44248	1.81388
1.94000	.16000	.45000	.49342	1.82956
1.94000	.18000	.20000	.23364	1.70148
1.94000	.18000	.30000	.34325	1.75841
1.94000	.18000	.35000	.39638	1.78048
1.94000	.18000	.40000	.44843	1.79979
1.94000	.18000	.45000	.49945	1.81699
1.94000	.20000	.20000	.23810	1.68120
1.94000	.20000	.30000	.34884	1.74152
1.94000	.20000	.35000	.40230	1.76518
1.94000	.20000	.40000	.45455	1.78601
1.94000	.20000	.45000	.50562	1.80466
1.94000	.22000	.20000	.24272	1.66177
1.94000	.22000	.30000	.35461	1.72513
1.94000	.22000	.35000	.40840	1.75028
1.94000	.22000	.40000	.46083	1.77254
1.94000	.22000	.45000	.51195	1.79255

1.96000	.02000	.20000	.20325	1.92505
1.96000	.02000	.30000	.30426	1.93556
1.96000	.02000	.35000	.35461	1.93913
1.96000	.02000	.40000	.40486	1.94206
1.96000	.02000	.45000	.45501	1.94455
1.96000	.06000	.20000	.21008	1.86214
1.96000	.06000	.30000	.31315	1.88976
1.96000	.06000	.35000	.36420	1.89951
1.96000	.06000	.40000	.41494	1.90769
1.96000	.06000	.45000	.46536	1.91471
1.96000	.08000	.20000	.21368	1.83361
1.96000	.08000	.30000	.31780	1.86823
1.96000	.08000	.35000	.36920	1.88068
1.96000	.08000	.40000	.42017	1.89120
1.96000	.08000	.45000	.47071	1.90030
1.96000	.10000	.20000	.21739	1.80672
1.96000	.10000	.30000	.32258	1.84752
1.96000	.10000	.35000	.37433	1.86244
1.96000	.10000	.40000	.42553	1.87514
1.96000	.10000	.45000	.47619	1.88619
1.96000	.12000	.20000	.22124	1.78131
1.96000	.12000	.30000	.32751	1.82756
1.96000	.12000	.35000	.37961	1.84475
1.96000	.12000	.40000	.43103	1.85949
1.96000	.12000	.45000	.48180	1.87239
1.96000	.14000	.20000	.22523	1.75722
1.96000	.14000	.30000	.33259	1.80832
1.96000	.14000	.35000	.38504	1.82759
1.96000	.14000	.40000	.43668	1.84422
1.96000	.14000	.45000	.48754	1.85888
1.96000	.16000	.20000	.22936	1.73431
1.96000	.16000	.30000	.33784	1.78972
1.96000	.16000	.35000	.39063	1.81091
1.96000	.16000	.40000	.44248	1.82933
1.96000	.16000	.45000	.49342	1.84563
1.96000	.18000	.20000	.23364	1.71247
1.96000	.18000	.30000	.34325	1.77174
1.96000	.18000	.35000	.39638	1.79470
1.96000	.18000	.40000	.44843	1.81478
1.96000	.18000	.45000	.49945	1.83265
1.96000	.20000	.20000	.23810	1.69162
1.96000	.20000	.30000	.34884	1.75433
1.96000	.20000	.35000	.40230	1.77893
1.96000	.20000	.40000	.45455	1.80057
1.96000	.20000	.45000	.50562	1.81993
1.96000	.22000	.20000	.24272	1.67165
1.96000	.22000	.30000	.35461	1.73745
1.96000	.22000	.35000	.40840	1.76356
1.96000	.22000	.40000	.46083	1.78667
1.96000	.22000	.45000	.51195	1.80744

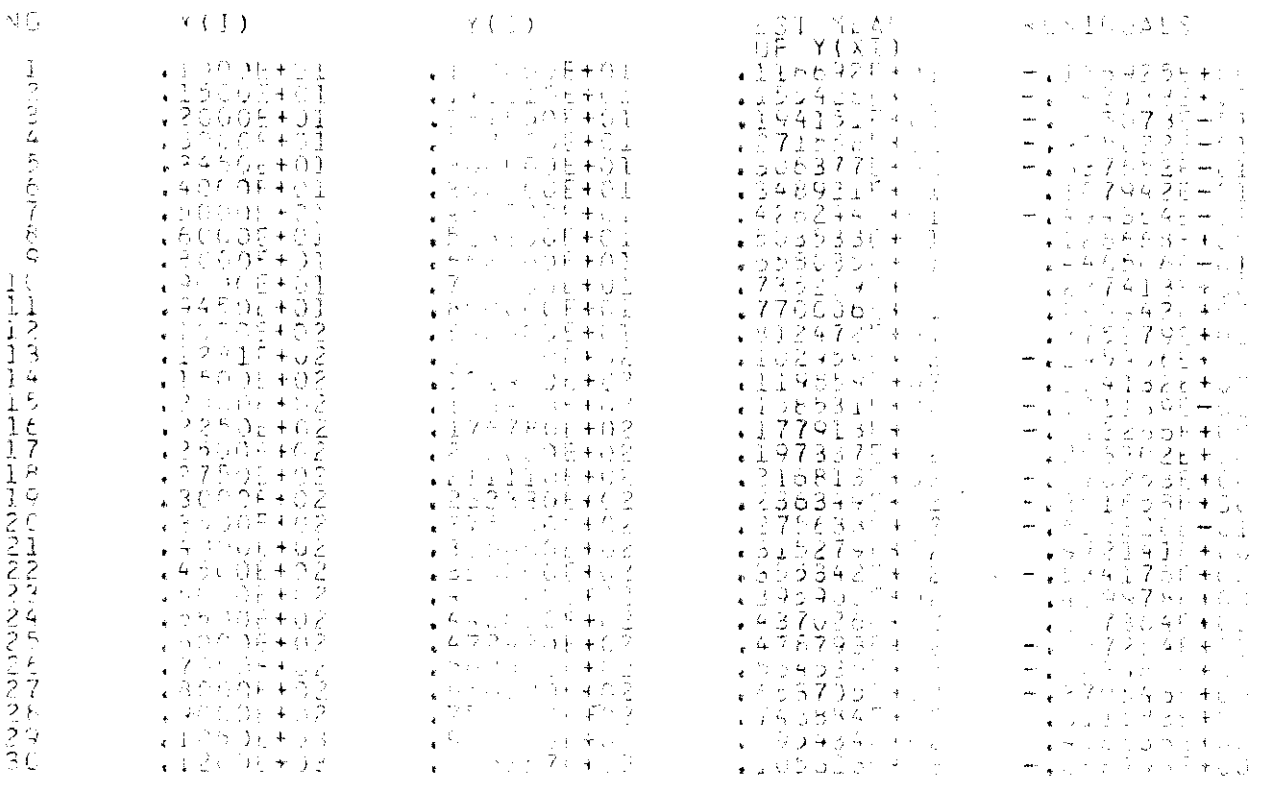
1.98000	.02000	.20000	.20325	1.94346
1.98000	.02000	.30000	.30426	1.95455
1.98000	.02000	.35000	.35461	1.95830
1.98000	.02000	.40000	.40486	1.96137
1.98000	.02000	.45000	.45501	1.96397
1.98000	.06000	.20000	.21008	1.87796
1.98000	.06000	.30000	.31315	1.90697
1.98000	.06000	.35000	.36420	1.91718
1.98000	.06000	.40000	.41494	1.92572
1.98000	.06000	.45000	.46536	1.93305
1.98000	.08000	.20000	.21368	1.84835
1.98000	.08000	.30000	.31780	1.88464
1.98000	.08000	.35000	.36920	1.89766
1.98000	.08000	.40000	.42017	1.90864
1.98000	.08000	.45000	.47071	1.91813
1.98000	.10000	.20000	.21739	1.82052
1.98000	.10000	.30000	.32258	1.86320
1.98000	.10000	.35000	.37433	1.87878
1.98000	.10000	.40000	.42553	1.89202
1.98000	.10000	.45000	.47619	1.90354
1.98000	.12000	.20000	.22124	1.79425
1.98000	.12000	.30000	.32751	1.84256
1.98000	.12000	.35000	.37961	1.86049
1.98000	.12000	.40000	.43103	1.87584
1.98000	.12000	.45000	.48180	1.88927
1.98000	.14000	.20000	.22523	1.76938
1.98000	.14000	.30000	.33259	1.82268
1.98000	.14000	.35000	.38504	1.84275
1.98000	.14000	.40000	.43668	1.86007
1.98000	.14000	.45000	.48754	1.87530
1.98000	.16000	.20000	.22936	1.74577
1.98000	.16000	.30000	.33784	1.80349
1.98000	.16000	.35000	.39063	1.82554
1.98000	.16000	.40000	.44248	1.84469
1.98000	.16000	.45000	.49342	1.86163
1.98000	.18000	.20000	.23364	1.72330
1.98000	.18000	.30000	.34325	1.78495
1.98000	.18000	.35000	.39638	1.80881
1.98000	.18000	.40000	.44843	1.82968
1.98000	.18000	.45000	.49945	1.84824
1.98000	.20000	.20000	.23810	1.70185
1.98000	.20000	.30000	.34884	1.76701
1.98000	.20000	.35000	.40230	1.79255
1.98000	.20000	.40000	.45455	1.81502
1.98000	.20000	.45000	.50562	1.83511
1.98000	.22000	.20000	.24272	1.68135
1.98000	.22000	.30000	.35461	1.74964
1.98000	.22000	.35000	.40840	1.77673
1.98000	.22000	.40000	.46083	1.80070
1.98000	.22000	.45000	.51195	1.82224

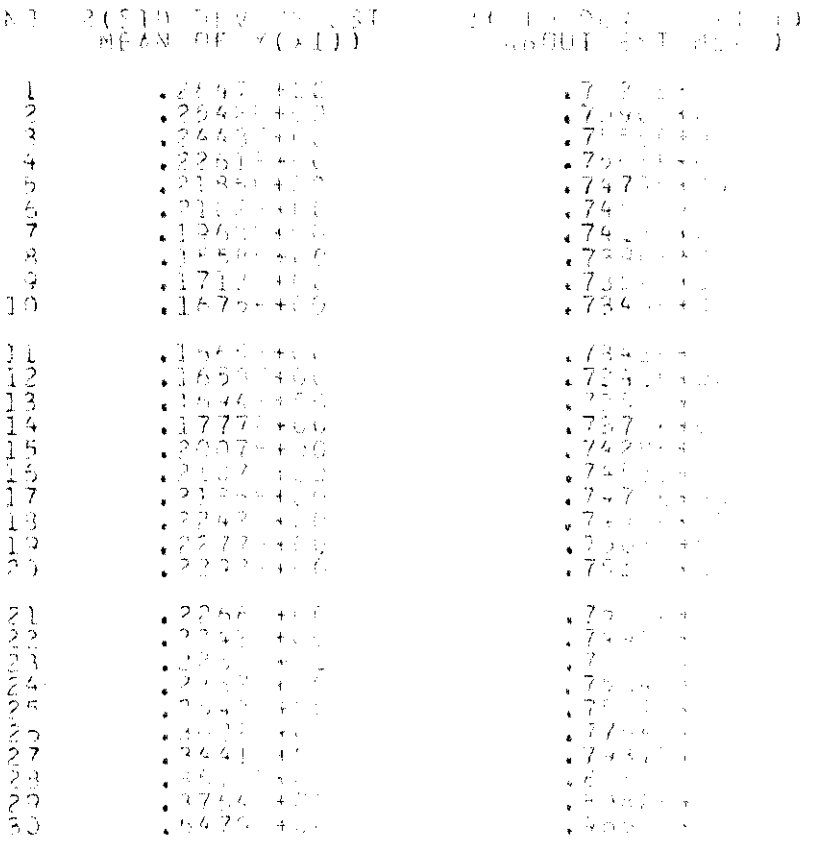
m_0	f	ϕ_0	ϕ	m
2.00000	.02000	.20000	.20325	1.96182
2.00000	.02000	.30000	.30426	1.97352
2.00000	.02000	.35000	.35461	1.97744
2.00000	.02000	.40000	.40486	1.98066
2.00000	.02000	.45000	.45501	1.98338
2.00000	.06000	.20000	.21008	1.89366
2.00000	.06000	.30000	.31315	1.92410
2.00000	.06000	.35000	.36420	1.93479
2.00000	.06000	.40000	.41494	1.94371
2.00000	.06000	.45000	.46536	1.95135
2.00000	.08000	.20000	.21368	1.86296
2.00000	.08000	.30000	.31780	1.90097
2.00000	.08000	.35000	.36920	1.91458
2.00000	.08000	.40000	.42017	1.92603
2.00000	.08000	.45000	.47071	1.93591
2.00000	.10000	.20000	.21739	1.83415
2.00000	.10000	.30000	.32258	1.87878
2.00000	.10000	.35000	.37433	1.89504
2.00000	.10000	.40000	.42553	1.90884
2.00000	.10000	.45000	.47619	1.92083
2.00000	.12000	.20000	.22124	1.80702
2.00000	.12000	.30000	.32751	1.85745
2.00000	.12000	.35000	.37961	1.87613
2.00000	.12000	.40000	.43103	1.89212
2.00000	.12000	.45000	.48180	1.90608
2.00000	.14000	.20000	.22523	1.78137
2.00000	.14000	.30000	.33259	1.83692
2.00000	.14000	.35000	.38504	1.85782
2.00000	.14000	.40000	.43668	1.87583
2.00000	.14000	.45000	.48754	1.89166
2.00000	.16000	.20000	.22936	1.75705
2.00000	.16000	.30000	.33784	1.81712
2.00000	.16000	.35000	.39063	1.84006
2.00000	.16000	.40000	.44248	1.85996
2.00000	.16000	.45000	.49342	1.87755
2.00000	.18000	.20000	.23364	1.73394
2.00000	.18000	.30000	.34325	1.79802
2.00000	.18000	.35000	.39638	1.82281
2.00000	.18000	.40000	.44843	1.84448
2.00000	.18000	.45000	.49945	1.86374
2.00000	.20000	.20000	.23810	1.71191
2.00000	.20000	.30000	.34884	1.77955
2.00000	.20000	.35000	.40230	1.80606
2.00000	.20000	.40000	.45455	1.82937
2.00000	.20000	.45000	.50562	1.85021
2.00000	.22000	.20000	.24272	1.69087
2.00000	.22000	.30000	.35461	1.76168
2.00000	.22000	.35000	.40840	1.78977
2.00000	.22000	.40000	.46083	1.81462
2.00000	.22000	.45000	.51195	1.83695

APPENDIX A.7

APPENDIX A.7

A.7.2 EVALUATION OF THE COEFFICIENTS OF EQ. 7.1 FOR A 150mm BOREHOLE





A.7.3. CURVE FITTING (POLYNOMIALS) (see Chapter VIII)

In the following paragraphs, the basic elements of the theory of curve fitting are presented. It has already been stated that it is important to be able to approximate the usual "correction Charts" used in the evaluation of normal resistivity devices. Since the same approach could be extended to a number of other "correction Charts", the author decided to include in the present thesis a least squares program, written in BASIC.

When fitting a polynomial to n data points (x_1,y_1), (x_2,y_2) ... (x_n,y_n) it is assumed that all the errors occur in the y values and that there are no errors in the x values. For each value of x_r there will be a calculated y value from the polynomial, and the difference between this and y_r will be the residual Δ_r. Thus

$$\Delta_r = y_r - (a + bx_r + cx_r^2 + dx_r^3 + \cdots) \qquad (A.7.3.1)$$

The principle underlying the fitting of the polynomial is to make the sum of the residuals squared as small as possible by choosing appropriate values of a,c,c,d ...

$$\text{Sum of residuals squared} = E = \sum_{r=1}^{r=n} \Delta_r^2 \qquad (A.7.3.2)$$

The 'best' polynomial of a given order is that which minimises E. The method for minimising E is to partially differentiate E with respect to each of the coefficients in turn, and equal each of the partial derivatives to zero. This will result in m + 1 simultaneous equations (m is the order of the polynomial) which are called the normal equations, and can be solved by the usual matrix inversion techniques.

In general if n data are selected from a "correction chart" and have to be fitted by a polynomial of order m, it is found that its coefficients may be obtained by the following matrix equation:

$$\begin{bmatrix} a \\ b \\ \vdots \end{bmatrix} = \begin{bmatrix} n & \Sigma x_r & \cdots & \Sigma x_r^m \\ \Sigma x_r & \Sigma x_r^2 & & \Sigma x_r^{m+1} \\ \vdots & \vdots & & \vdots \\ \Sigma x_r^m & \Sigma x_r^{m+1} & & \Sigma x_r^{2m} \end{bmatrix} \cdot \begin{bmatrix} \Sigma x_r \\ \Sigma x_r y_r \\ \vdots \\ \Sigma x_r^m y_r \end{bmatrix} \quad \text{(A.7.3.3)}$$

The use of portable microcomputers permits the above calculation to be performed very fast but, since a computer only carries a limited number of significant figures, there is a problem of defining the accuracy of the results obtained. The author found that even using double precision where the computer carries double the usual number of significant figures only allows reliable answers up to about an order of six on most portable computers. The major cause of inaccuracy is ill-conditioning of the solution of the normal equations with respect to the coefficients of the matrix. More simply a small change in the value of the terms in the matrix drastically changes the coefficients of the polynomial obtained as the solution. A second smaller source of inaccuracy is termed instability, and is caused by the accumulation of rounding errors in performing the calculations.

Having the above in mind the following suggestions are made:-

(a) The accuracy of the coefficients is likely to be improved by performing the calculations carrying a larger number of significant figures.

(b) Accuracy can be improved by scaling the data into a small range close to zero, before building and solving the matrix.

(c) The best results are obtained if a method is used to keep the off-diagonal terms small, and the ideal case is to have all off-diagnonal terms zero. A method of achieving this was devised by Forsythe (1957) and has revolutionized the whole subject of polynomial curve fitting. In this method, the value y is expressed in terms of a set of polynomials P_i, where P_i is an arbitrary polynomial of order i. Thus:

$$y = C_0 P_0(x) + C_1 P_1(x) + C_2 P_2(x) + \cdots + C_m P_m(x) \qquad \text{(A.7.3.4)}$$

and the simple normal equations given in Equation (A.7.2.3) are replaced by the following more complicated ones:-

$$\begin{bmatrix} c_0 \\ c_1 \\ c_2 \\ . \\ . \\ . \\ c_m \end{bmatrix} = \begin{bmatrix} \Sigma p_0(x_r)p_0(x_r) & \Sigma p_0(x_r)p_1(x_r) & \Sigma p_0(x_r)p_2(x_r) \ldots \\ \Sigma p_1(x_r)p_0(x_r) & \Sigma p_1(x_r)p_1(x_r) & \Sigma p_1(x_r)p_2(x_r) \ldots \\ \Sigma p_2(x_r)p_0(x_r) & \Sigma p_2(x_r)p_1(x_r) & \Sigma p_2(x_r)p_2(x_r) \ldots \\ . & & \\ . & & \\ . & & \\ \Sigma p_m(x_r)p_0(x_r) & \Sigma p_m(x_r)p_1(x_r) & \Sigma p_m(x_r)p_2(x_r) \ldots \end{bmatrix}^{-1} \begin{bmatrix} \Sigma p_0(x_r)y_r \\ \Sigma p_1(x_r)y_r \\ \Sigma p_2(x_r)y_r \\ . \\ . \\ . \\ \Sigma p_m(x_r)y_r \end{bmatrix}$$

The objective is to choose the polynomials P_i such that all terms which are off the leading diagonal in the matrix above will evaluate to zero. Forsythe showed that this was always possible if the polynomials were derived from the following formula:

$$P_{i+1}(x) = 2(x - \alpha_{i+1})P_i(x) - \beta_i P_{i-1}(x) \qquad \text{(A.7.3.5)}$$

$$\alpha_{i+1} = \frac{\sum_{r=1}^{r=n} x_r P_i^2(x_r)}{\sum_{r=1}^{r=n} P_i^2(x_r)} \qquad \text{(A.7.3.6)}$$

and

$$\beta_i = \frac{\sum_{r=1}^{r=n} P_i^2(x_r)}{\sum_{r=1}^{r=n} P_{i-1}^2(x_r)} \qquad \text{(A.7.3.7)}$$

The above procedure has been followed in the program presented below.

PROGRAM FOR LEAST SQUARE FIT

```
10 DIM P(100),R(100),T(100),U(100),V(100),W(100),X(100),Y(100),Z(100)
20 DIM A(10),B(10),C(10),D(11),F(10),G(10),L(10),Q(10),S(10)
30 DIM A$(2),I$(3),Q$(10)
40 REM ARRAY SIZES LIMIT PROGRAM TO A MAXIMUM OF 100 DATA POINTS.
50 REM THE NUMBER OF DATA POINTS SHOULD BE AT LEAST 2 GREATER THAN THE
60 REM MAXIMUM ORDER OF THE POLYNOMIAL.
70 PRINT "PROGRAM TO FIT A POLYNOMIAL TO A SET OF POINTS"
80 PRINT "======= == === = ========== == = === == ======"
90 PRINT
100 PRINT "WOULD YOU LIKE FULL INSTRUCTIONS.";
110 GOSUB 3600
120 LET I$ = Q$
130 IF I$ = "NO" THEN 160
140 PRINT "TYPE IN A PAIR OF X & Y VALUES & WEIGHT SEPARATED BY COMMAS"
150 PRINT "THEN PRESS RETURN, TYPE THE NEXT PAIR OF VALUES ETC"
160 PRINT "TERMINATE DATA WITH  999999, 999999, 999999"
170 PRINT
180 PRINT "STARTING DATA"
190 PRINT " X, Y, WEIGHT"
200 LET N = 0
210 FOR I = 1 TO 100
220   INPUT X(I), Y(I), W(I)
230   IF ABS(X(I) - 999999) + ABS(Y(I) - 999999) = 0 THEN 310
240   IF W(I) >= 0 THEN 270
250   PRINT "NEGATIVE WEIGHTS ARE IMPOSSIBLE - RETYPE LAST LINE"
260   GOTO 220
270   LET N = N + 1
280 NEXT I
290 PRINT "PROGRAM CAN ONLY HANDLE MAXIMUM OF 100 VALUES"
300 REM CHECK THAT THERE ARE AT LEAST 2 POINTS
310 IF N < 2 THEN 1070
320 PRINT
330 REM CALL SUBROUTINE TO CHECK THAT DATA ARE CORRECT
340 GOSUB 2770
350 PRINT
360 REM CALCULATE MAXIMUM ORDER BASED ON NUMBER OF DATA POINTS
370 LET N9 = 9
380 IF N - 2 >= 9 THEN 400
390 LET N9 = N - 2
400 IF I$ = "YES" THEN 430
410 PRINT "TYPE ORDER REQUIRED"
420 GOTO 480
430 PRINT "TYPE IN THE ORDER REQUIRED IN THE RANGE 1 -"; N9; " OF THE"
440 PRINT "ONE SPECIFIC POLYNOMIAL REQUIRED."
450 PRINT "OR TYPE 0 IF ALL THE POLYNOMIALS FROM ORDER 0 -";N9;"ARE TO"
460 PRINT "BE EXAMINED, AND THE ONE WHICH FITS BEST REPORTED,"
470 PRINT "THEN PRESS RETURN."
480 INPUT L
490 IF L <> INT(L) THEN 520
500 IF L < 0 THEN 520
510 IF L <= N9 THEN 550
520 PRINT "INCORRECT VALUE TYPED"
530 GOTO 430
```

```
540 REM SET THE MAXIMUM ORDER TO 9, IE M1 (MAXORDER+1) TO 10
550 LET M1 = 10
560 IF L <= 0 THEN 580
570 LET M1 = L + 1
580 LET I = N - 1
590 IF M1 <= I THEN 620
600 LET M1 = I
610 REM CALL SUBROUTINE TO FIT THE POLYNOMIAL
620 GOSUB 1180
630 LET M2 = M1 - 1
640 PRINT
650 IF L = 0 THEN 680
660 PRINT "ORDER OF POLYNOMIAL SPECIFIED ="; N2
670 GOTO 710
680 PRINT "MAXIMUM ORDER OF POLYNOMIAL TESTED FOR ="; M2
690 PRINT "ORDER OF BEST POLYNOMIAL FOUND ="; N2
700 PRINT
710 PRINT "POLYNOMIAL ORDER    GOODNESS OF FIT"
720 FOR I = 1 TO M1
730   PRINT I - 1; TAB(10); G(I)
740 NEXT I
750 PRINT
760 PRINT "COEFFICIENTS OF THE BEST OR SPECIFIED ORDER POLYNOMIAL"
770 PRINT "(Y = A + B*X + C*X^2 + D*X^3 +...)"
780 LET N3 = N2 + 1
790 FOR I = 1 TO N3
800   READ A$
810   PRINT A$; TAB(5); F(I)
820 NEXT I
830 DATA "A=", "B=", "C=", "D=", "E=", "F=", "G=", "H=", "I=", "J="
840 RESTORE
850 PRINT
860 PRINT "WOULD YOU LIKE A TABLE OF RESIDUALS"
870 GOSUB 3590
880 IF Q$ = "NO" THEN 980
890 PRINT "X              Y              Y(CALC)        DIFF"
900 LET R2 = 0
910 FOR I = 1 TO N
920   PRINT X(I), Y(I), Z(I), R(I)
930   LET R2 = R2 + R(I) ^ 2
940 NEXT I
950 PRINT
960 PRINT "SUM OF ERRORS SQUARED ="; R2
970 PRINT
980 PRINT "WOULD YOU LIKE ANOTHER RUN";
990 GOSUB 3590
1000 IF Q$ = "NO" THEN 1100
1010 LET I$ = "NO"
1020 PRINT "WOULD YOU LIKE TO TRY ANOTHER ORDER WITH THE SAME DATA"
1030 GOSUB 3590
1040 IF Q$ = "YES" THEN 310
1050 GOTO 160
1060 REM ENTER IF THERE ARE NOT ENOUGH POINTS
1070 PRINT "RUN TERMINATED - NOT ENOUGH DATA POINTS"
1080 GOTO 980
1090 REM TERMINATE JOB
1100 IF I$ = "NO" THEN 1140
1110 PRINT "REMEMBER THAT YOU MUST NOT EXTRAPOLATE BEYOND THE"
1120 PRINT "DATA POINTS, AND ALSO THAT INTERPOLATION BETWEEN"
1130 PRINT "POINTS IS DANGEROUS WITH HIGH ORDER POLYNOMIALS."
1140 PRINT "END OF JOB"
```

```
1150 STOP
1160 REM SUBROUTINE TO CALCULATE A WEIGHTED LEAST SQUARES POLYNOMIAL
1170 REM BY FORSYTHE"S METHOD USING ORTHOGONAL POLYNOMIALS.
1180 LET M3 = M1 - 1
1190 LET N2 = M3
1200 FOR I = 1 TO M1
1210   LET C(I) = 0
1220 NEXT I
1230 LET Q(1) = 0
1240 LET D(1) = 0
1250 LET D(2) = 0
1260 LET A(1) = 1
1270 LET D2 = 0
1280 LET P1 = 0
1290 LET S1 = 0
1300 LET G1 = 0
1310 LET I1 = 0
1320 LET S2 = W(1)
1330 REM FIND THE MAXIMUM AND MINIMUM X & Y
1340 LET X9 = X(1)
1350 LET X1 = X(1)
1360 LET Y9 = Y(1)
1370 LET Y1 = Y(1)
1380 FOR I = 2 TO N
1390   IF X(I) <= X9 THEN 1410
1400   LET X9 = X(I)
1410   IF X(I) >= X1 THEN 1430
1420   LET X1 = X(I)
1430   IF Y(I) <= Y9 THEN 1450
1440   LET Y9 = Y(I)
1450   IF Y(I) >= Y1 THEN 1470
1460   LET Y1 = Y(I)
1470   LET S2 = S2 + W(I)
1480 NEXT I
1490 REM CHECK THAT SUM OF WEIGHTS IS NOT ZERO
1500 IF S2 = 0 THEN 2740
1510 LET Y3 = (Y9 + Y1) / 2
1520 LET Y4 = (Y9 - Y1) / 2
1530 IF Y4 > 0 THEN 1580
1540 LET F(1) = Y(1)
1550 LET N2 = 0
1560 GOTO 2720
1570 REM SCALE Y TERMS INTO THE RANGE +1 TO -1
1580 FOR I = 1 TO N
1590   LET V(I) = (Y(I) - Y3) / Y4
1600   LET D2 = D2 + W(I) * V(I) ^ 2
1610   LET P(I) = 1
1620   LET T(I) = 0
1630   LET P1 = P1 + W(I) * V(I)
1640   LET S1 = S1 + W(I)
1650 NEXT I
1660 LET S(1) = P1 / S1
1670 LET C(1) = S(1)
1680 LET D2 = D2 - S(1) * P1
1690 LET G(1) = ABS(D2 / (N - 1))
1700 LET A1 = 4 / (X9 - X1)
1710 LET B1 = -2 - A1 * X1
1720 REM SCALE X TERMS INTO THE RANGE +2 TO -2
1730 FOR I = 1 TO N
1740   LET U(I) = A1 * X(I) + B1
1750 NEXT I
```

```
1760 REM START LOOP FOR EACH ORDER
1770 FOR I = 1 TO M3
1780   LET D1 = 0
1790   FOR J = 1 TO N
1800     LET D1 = D1 + W(J) * U(J) * P(J) ^ 2
1810   NEXT J
1820   REM L IS FORSYTHES ALPHA
1830   LET L(I + 1) = D1 / S1
1840   LET W2 = S1
1850   LET S1 = 0
1860   LET P1 = 0
1870   REM STORE VALUE OF CURRENT ORTHOGONAL POLYNOMIAL IN P( )
1880   REM AND OF PREVIOUS ORTHOGONAL POLYNOMIAL IN T( )
1890   FOR J = 1 TO N
1900     LET D1 = Q(I) * T(J)
1910     LET T(J) = P(J)
1920     LET P(J) = (U(J) - L(I + 1)) * P(J) - D1
1930     LET S1 = S1 + W(J) * P(J) ^ 2
1940     LET P1 = P1 + W(J) * V(J) * P(J)
1950   NEXT J
1960   REM Q IS FORSYTHES BETA
1970   LET Q(I + 1) = S1 / W2
1980   LET S(I + 1) = P1 / S1
1990   LET D2 = D2 - S(I + 1) * P1
2000   LET G(I + 1) = ABS(D2 / (N - I - 1))
2010   IF L > 0 THEN 2180
2020   REM ENTER IF PROGRAM HAS TO DECIDE ON BEST ORDER (L = 0)
2030   IF I1 = 1 THEN 2130
2040   IF G(I + 1) < G(I) THEN 2180
2050   REM ENTER IF A MINIMUM DETECTED
2060   LET N2 = I - 1
2070   LET I1 = 1
2080   LET G1 = G(I)
2090   FOR J = 1 TO M1
2100     LET B(J) = C(J)
2110   NEXT J
2120   GOTO 2180
2130   IF G(I + 1) >= 0.6 * G1 THEN 2180
2140   LET I1 = 0
2150   LET N2 = M3
2160   REM BUILD COEFFICIENTS OF J TH ORDER TERM IN A( ) & SUM TO FORM
2170   REM EXPLICIT POWER SERIES IN C( )
2180   FOR J = 1 TO I
2190     LET D1 = D(J + 1) * Q(I)
2200     LET D(J + 1) = A(J)
2210     LET A(J) = D(J) - L(I + 1) * A(J) - D1
2220     LET C(J) = C(J) + S(I + 1) * A(J)
2230   NEXT J
2240   LET C(I + 1) = S(I + 1)
2250   LET A(I + 1) = 1
2260   LET D(I + 2) = 0
2270   IF I1 = 0 THEN 2320
2280   IF I <> M3 THEN 2320
2290   FOR J = 1 TO M1
2300     LET C(J) = B(J)
2310   NEXT J
2320 NEXT I
2330 LET D(1) = 1
2340 LET B(1) = 1
2350 LET F(1) = C(1)
2360 FOR I = 2 TO M1
```

```
2370   LET D(I) = 1
2380   LET B(I) = B1 * B(I - 1)
2390   LET F(1) = F(1) + C(I) * B(I)
2400   REM WORK OUT EXPLICIT POWER SERIES IN UNSCALED X, & ADD
2410   REM INTO THE COEFFICIENTS F( ) THE RELEVANT CONTRIBUTIONS
2420 NEXT I
2430 FOR J = 2 TO M1
2440   LET D(1) = D(1) * A1
2450   LET F(J) = C(J) * D(1)
2460   LET K1 = 2
2470   LET J1 = J + 1
2480   IF J1 > M1 THEN 2560
2490   FOR I = J1 TO M1
2500     LET D(K1) = A1 * D(K1) + D(K1 - 1)
2510     LET F(J) = F(J) + C(I) * D(K1) * B(K1)
2520     LET K1 = K1 + 1
2530   NEXT I
2540 NEXT J
2550 REM CALCULATE YCALC & RESIDUAL FOR EACH POINT (ON ORIGINAL SCALE).
2560 FOR I = 1 TO N
2570   LET J = N2 + 1
2580   LET Y5 = F(J)
2590   IF N2 = 0 THEN 2630
2600   FOR K = 1 TO N2
2610     LET Y5 = F(J - 1) + (X(I) * Y5)
2620     LET J = J - 1
2630   NEXT K
2640   LET Z(I) = Y5 * Y4 + Y3
2650   LET R(I) = (V(I) - Y5) * Y4
2660 NEXT I
2670 REM CONVERT COEFF ARRAY F( ) BACK TO ORIGINAL SCALE
2680 LET F(1) = (F(1) * Y4) + Y3
2690 FOR I = 2 TO M1
2700   LET F(I) = F(I) * Y4
2710 NEXT I
2720 RETURN
2730 REM ENTER IF ERRORS DETECTED
2740 PRINT "JOB TERMINATED BY PROGRAM BECAUSE SUM OF WEIGHTS = 0"
2750 STOP
2760 REM SUBROUTINE TO CHECK THAT DATA ARE CORRECT & ALTER IF NECESSARY
2770 PRINT "ARE THE DATA VALUES ENTERED CORRECT?";
2780 REM A4 SHOULD BE SET TO THE NUMBER OF LINES ON THE VDU
2790 LET A4 = 20
2800 GOSUB 3590
2810 IF Q$ = "YES" THEN 3570
2820 PRINT "HERE IS A LIST OF THE CURRENT DATA"
2830 PRINT "LINE NUMBER", "X", "Y", "WEIGHT"
2840 FOR I = 1 TO N
2850   PRINT I, X(I), Y(I), W(I)
2860   IF INT(I / (A4 - 1)) * (A4 - 1) <> I THEN 2900
2870   PRINT "WOULD YOU LIKE TO CONTINUE LISTING";
2880   GOSUB 3590
2890   IF Q$ = "NO" THEN 2910
2900 NEXT I
2910 PRINT "TYPE R TO REPLACE";
2920 IF I$ = "NO" THEN 2940
2930 PRINT " AN EXISTING LINE OF DATA"
2940 IF N = 100 THEN 2990
2950 PRINT TAB(5); " A TO ADD";
2960 IF I$ = "NO" THEN 2980
2970 PRINT " AN EXTRA LINE"
```

```
2980 IF N = 1 THEN 3020
2990 PRINT TAB(5); " D TO DELETE";
3000 IF I$ = "NO" THEN 3020
3010 PRINT " AN EXISTING LINE"
3020 PRINT TAB(5); " L TO LIST";
3030 IF I$ = "NO" THEN 3050
3040 PRINT " THE DATA"
3050 PRINT "  OR C TO CONTINUE";
3060 IF I$ = "NO" THEN 3080
3070 PRINT " THE CALCULATION"
3080 INPUT Q$
3090 IF Q$ = "R" THEN 3190
3100 IF N = 100 THEN 3130
3110 IF Q$ = "A" THEN 3330
3120 IF N = 1 THEN 3140
3130 IF Q$ = "D" THEN 3430
3140 IF Q$ = "L" THEN 2820
3150 IF Q$ = "C" THEN 3570
3160 PRINT "REPLY '"; Q$; "' NOT UNDERSTOOD."
3170 GOTO 2910
3180 REM REPLACE LINE
3190 PRINT "TYPE THE LINENUMBER OF THE LINE TO BE REPLACED";
3200 INPUT I
3210 IF I <> INT(I) THEN 3230
3220 IF (I - 1) * (I - N) < = 0 THEN 3260
3230 PRINT "LINENUMBER MUST BE AN INTEGER IN THE RANGE 1 -"; N
3240 PRINT "RE-";
3250 GOTO 3190
3260 PRINT "TYPE THE CORRECT LINE TO REPLACE THE ONE WHICH IS WRONG:"
3270 PRINT "X, Y, WEIGHT"
3280 INPUT X(I), Y(I), W(I)
3290 IF W(I) >= 0 THEN 3400
3300 PRINT "NEGATIVE WEIGHTS ARE IMPOSSIBLE - LAST LINE REJECTED"
3310 GOTO 3260
3320 REM ADD A NEW LINE
3330 LET N = N + 1
3340 PRINT "TYPE THE ADDITIONAL LINE OF DATA AS SHOWN:"
3350 PRINT "X, Y, WEIGHT"
3360 INPUT X(N), Y(N), W(N)
3370 IF W(N) >= 0 THEN 3400
3380 PRINT "NEGATIVE WEIGHTS ARE IMPOSSIBLE - LAST LINE REJECTED"
3390 GOTO 3340
3400 PRINT "OK"
3410 GOTO 2910
3420 REM DELETE A LINE
3430 PRINT "TYPE THE LINENUMBER OF THE LINE TO BE DELETED"
3440 INPUT J
3450 IF (J - 1) * (J - N) >0 THEN 3470
3460 IF J = INT(J) THEN 3490
3470 PRINT "LINENUMBER MUST BE AN INTEGER IN THE RANGE 1 -"; N
3480 GOTO 3430
3490 FOR I = J + 1 TO N
3500   LET X(I - 1) = X(I)
3510   LET Y(I - 1) = Y(I)
3520 NEXT I
3530 LET N = N - 1
3540 PRINT "OK"
3550 IF J > N THEN 2910
3560 GOTO 2820
3570 RETURN
3580 REM SUBROUTINE TO CHECK REPLIES

3590 IF I$ = "NO" THEN 3610
3600 PRINT " TYPE YES OR NO & PRESS RETURN."
3610 PRINT
3620 INPUT Q$
3630 IF Q$ = "YES" THEN 3670
3640 IF Q$ = "NO" THEN 3670
3650 PRINT "REPLY '"; Q$; "' NOT UNDERSTOOD.";
3660 GOTO 3600
3670 RETURN
3680 END
```

A.7.4 PROGRAM "WINDOW"

The data to be processed are kept in an array (byte vector) starting at address #V. Since the first 100 bytes contain information about the log, the program processes the data from address #V + #64 onwards. Since B is the number of bytes used in the calculation of function C the parameter of W, which indicates the order of the data point from which the zonation starts, must satisfy the following condition:

$$W \geqslant \text{1st point} + B$$

```
 2P."ENTER NUMBER OF DATA"';IN.N
 10FDIM%QQ(100),%SS(N)
 14P."ENTER B"';IN.B;P."ENTER D"';FINPUT %D
 15P."START AT POINT"';IN.W
 20DIMFF(300)
 30V=#8464;C=#2900;Z=#93D0;U=#8C00
 60F.I=W   TO N
 70%A=0
 80F.J=1 TO B
 90%A=%A+FLT(V?(I+J-1)-V?(I-J))
100N.J
110%A=ABS(%A)/B-%D
120IF%A)0 GOTO140
130%A=0
140C?(I)=10*%A
150N.I
170E=W;FF(W)=E;G=0
180F.I=W TO N
190IFG=0GOTO260
200IFC?(I)-C?(I-1))0 GOTO 280
210E=E+1;FF(E)=I-1
220P.I
230P.FF(E);P."E";P.E'
240G=0
250GOTO280
260IFC?(I)-C?(I-1)(=0 GOTO 280
270G=1
280N.I
290L=0;K=0;H=0
300F.M=W   TO E-1
310L    =(FF(M+1)-FF(M))/3
320 K    =FF(M)  +L    ;H    =FF(M+1)- L    -1
330P."****************"'
340P.L    ;P." ";P.K    ;P." ";P.H'
350%SS(K-1)=0
360F.I=K TO H
370%SS(I)=%SS(I-1)+FLT(V?(I))
380N.I
390P."S(H(M)) IS"; FPRINT%SS(H)'
400%QQ(H)    =%SS(H)    /(ABS(H    -K    )+1)
410FPRINT%QQ(H)
420P." "'
430F.J=FF(M) TO FF(M+1)
440Z?(J)=%QQ(H)
450N.J
460N.M
470F.I=FF(W) TO FF(E-1);U?(I)=Z?(I);P.Z?(I)';N.I
480F.I=1 TO 35;P.$7;N.I
490P."ZONATION IS OVER"'
500P."THE ZONE BOUNDARIES ARE AT ARRAY FF"'
510P."YOU CAN ENTER P.$2 AT LINE 160 FOR PRINTING THE RESULTS"'
520P."IF YOU WANT THE RESULTS ON CASSETE TYPE 1"
530IN.Y
540IF Y()1 GOTO 590
550A=FOUT""
552M=N-2*W
556F.K=1 TO 20;WAIT;N.K
557F.I=1 TO M
580BPUT A,U?(I)
585F.J=1 TO 20;WAIT;N.J
587N.I
590END
```

A.7.5 PROGRAM "FILTER"

The program gets directly the data from the cassette and evaluates thedifference between 16-inches and 64-inches normal resistivity logs. It provides the facility of carrying out n-terms moving average filtering, where n is user-defined, Sheppard's five term, Spencer's twenty-one term and Spencer's-Sheppard's seven term moving average.

```
 5DIMBB(900)
 10N=#8664;M=#8A4C;Q=#8D00;S=#93D0
 15E=#80;F=#81;G=#82;H=#83;P=#84;R=#86;Z=#87;A=#88
 20P."ENTER NUMBER OF DATA";IN.K
 25 GOTO 135
 30P."ATTENTION ENTER THE 1ST"
 40A=FIN""
 50F.I=1 TO K
 60N?(I)=BGETA
 70N.I
 80F.I=1 TO 10:P.$7;N.I
 90P."ATTENTION ENTER THE 64N"
100B=FIN""
110F.I=1 TO K
120M?(I)=BGETB
130N.I
135WAIT
136P."DO YOU WANT THE DIFFERENCE OF THE BYTE VECTORS M,N";IN.$E
137IF$E="N" GOS.b
140F.I=1 TO 10:P.$7;N.I
150F.J=1 TO K
160C=N?(J)
170D=M?(J)
180P=C-D+100
190Q?(J)=P
200N.J
210bP."DO YOU WANT FILTERING";IN.$F
220IF $F="N" GOTO 550
290P."DO YOU WANT SHEPPARDS FIVE POINTS FILT.";IN.$P
300IF$P="N" GOTO 330
330P."DO YOU WANT SP-SH FILTERING";IN.$R
340IF$R="N" GOTO 400
344F.I=1 TO K
345%T=7*FLT(N?(I+3))+6*(FLT(N?(I+4))+FLT(N?(I+2)))
350%U=3*(FLT(N?(I+5))+FLT(N?(I+1)))
355%W=-2*(FLT(N?(I+6))+FLT(N?(I)))
360S?(I+3)=%((%T+%U+%W)/21)
365N.I
400P."DO YOU WANT TO USE SPENCERS FILTER";IN.$Z
410IF$Z="N" GOTO 470
415F.I=1 TO K
420 T=60*(N?(I+10))+57*(N?(I+11)+N?(I+9))
430 U=47*(N?(I+12)+N?(I+8))+33*(N?(I+13)+N?(I+7))
440 W=18*(N?(I+14)+N?(I+6))+6*(N?(I+15)+N?(I+5))
450 X=-2*(N?(I+16)+N?(I+4))-5*(N?(I+17)+N?(I+3))
460 Y=-5*(N?(I+18)+N?(I+2))-3*(N?(I+19)+N?(I+1))
465 S?(I+10)= (( T+ U+ W+ X+ Y+(N?(I+20)+N?(I)))/350)
467N.I
470P."DO YOU WANT L POINTS MOOVING AVERAGE";IN.$A
480IF$A="N" GOTO 550
490P."ENTER L";IN.L
500F.I=2 TO K
510BB(I-1)=0
515F.J=I TO I+L-1
520BB(J)=BB(J-1)+N?(J)
525N.J
530S?(I)=%(FLT(BB(J-1))/L)
540N.I
550END
```

A.7.6 PROGRAM "CORRECT"

This program uses, either the conductivity log or, a user defined value for average fluid conductivity, in order to correct the apparent normal resistivity values for the case of a 150 mm diameter borehole.

```
 5U=#80
10A=#3134;B=#4000;C=#8600
20P."ENTER NUMBER OF RES. DATA TOBE PROCESSED";IN.M
25P=FIN""
30F.I=1 TO M
40B?(I)=BGET P
50N.I
60P."INPUT DATA WERE:"'
65F.I=1 TO M;P.B?(I);N.I
66P."DO YOU WANT TO USE THE CONDUCTIVITY LOG"';IN.$U
67IF $U="N" GOTO 80
70P."LOAD"CONDUCTIVITY LOG AT LOCATION #3000"'
77GOTO 125
80P."ENTER VALUE FOR CONDUCTIVITY"'
90IN.K
100F.J=1 TO M
110A?(J)=K
120N.J
125WAIT
130%E=0.000009650894;%F=-0.00031229986;%G=0.77545259
135%H=0.39177459
140F.J=1 TO M
150%D=FLT(B?(J))*FLT(A?(J))/10000
160%R=%D*%D*%D*%D*%E+%D*%D*%F+%D*%G+%H
165C?(J)=%(%R*10000/FLT(A?(J)))
170N.J
180P."CORRECTED DATA ARE"';F.I=1 TO M;P.C?(I);N.I
190P."DO YOU WANT THE DATA ON TAPE";IN.$C
200IF $C="N" GOTO 260
210A=FOUT""
220F.I=1 TO M
230BPUT A,C?(I)
240F.J=1 TO 20;WAIT;N.J
250N.I
260END
```

A.7.7. PROGRAM "FORM"

```
  1GOTO40
 10P."ENTER @";IN.@
 20A=FIN""
 30P."No OF DATA IS:";P.@'
 40N=#30D0;B=#34B8;C=#4000;P=#43E8;L=#47D0
 45GOTO1:0
 50F.I=1 TO @
 60N?(I)=BGET A
 70N.I
 80F.I=1 TO 10;P.$7;N.I
 90P."DATA OK"
100F.I=1 TO @;P.N?(I);N.I
110P."ENTER INTERVAL FOR WHICH YOU WANT THE DISTRIBUTION"'
120P."EVERY HOW MANY BYTES:";IN.A
130Q=800;K=Q+A
135P.$2
150P."INTERVAL'S DATA ARE"'
160F.I=1 TO K-Q
170P.N?(I+Q)
180B?(I)=N?(I+Q)
200N.I
206 M=K-Q
209DO M=(M+2)/3
210F.H=M+1 TO K-Q
212F.J=H TO M+1 STEP -M
214IFB?(J))=B?(J-M) GOTOb
216T=B?(J);B?(J)=B?(J-M);B?(J-M)=T
218N.J
220bN.H
222UNTIL M=1
230P."SORTED DATA ARE:"'
240F.I=1 TO K-Q;P.B?(I);N.I
250S=Q
260I=0
270C?(0)=Q
280WAIT
290DO
300S=S+1
305IF S=K GOTO 320
310UNTIL (B?(S+1-Q)-B?(S-Q)))0
320I=I+1
330C?(I)=S
340P?(I)=B?(S-Q)
350P.S;P.P?(I)'
360IF S(K   GOTO 280
366P.$2
367P.$2
370P."RES. DISTRIB. FROM";FPRINT0.2*Q;P."TO"
380FPRINT 0.2*K;P."METERS"'
390P."-----------------------------------------------------------------------"'
400F.J=1 TO I
410L?(J)=C?(J)-C?(J-1)
420P.L?(J);P.P?(J)'
430N.J
```

```
440GOTO 470
450P."DO YOU WANT TO CALCULATE THE GEOELECTRIC PARAMETERS"
460P."IF YES ENTER 1";IN.D;IF D()1GOTO 670
470%F=0;%G=0;Y=0
480F.J=1 TO I
490%F=%F+ FLT(L?(J))*1.0*FLT(P?(J))
500%G=%G+FLT(L?(J))*1.0/FLT(P?(J))
510Y=Y+L?(J)
520N.J
530%V=%F/FLT(Y)
540%W=%G/FLT(Y)
550%X=SQR(%V*%W)
560%Z=1/%W
570P."***INTERVAL BETWEEN";FPRINT Q*0.2;P."METERS AND"
580FPRINT K*0.2;P."METERS***"'
590P."TRANSVERSE RESISTIVITY IS";FPRINT%V;P."Ω.m"'
600P."LONGITUDINAL RESISTIV.  IS";FPRINT %Z;P."Ω.m"'
610P."ANISOTROPY INDEX IS";FPRINT%X'
650F.I=1 TO 5;P." "'
6550=Q+A
657K=Q+A
660IF Q(@   GOTO 150
670END
```

APPENDIX A.8

A.8.1 COMPUTER PROGRAM FOR NORMAL RESISTIVITY LOG SIMULATION

```
 10FDIM%P(50)
 20DIMJJ(50)
 30P."INPUT WIDTH OF FISSURE ZONE IN M"
 40FINPUT%D
 50P."INPUT LOWER BOUNDARY OF FISSURE ZONE"
 60FINPUT%B
 70P."INPUT SPACING OF LOGGING TOOL IN M"
 80FINPUT%S
 90P."INPUT RESISTIVITY OF FISSURE ZONE"
100FINPUT%F
110P."INPUT RESISTIVITY OF SURROUNDING MEDIUM"
120FINPUT%C
130P."INPUT STARTING POINT OF LOG IN M"
140FINPUT%R
150P."INPUT LOGGING INTERVAL IN M"
160FINPUT%K
170P.$2
180%A=(%F-%C)/(%F+%C)
190%L=%S/%D
200%Z=%R
210M=0
220FIF%S(%D THEN GOTO a
23000
240%Z=%Z+%K
250%H=(%B-%Z)/%D
260%H=(%B-%Z)/%D
270%X=(2*(%H+1)-%L)
280GOSUBc
290%Q=%L*%C*(1/%L+%A/(2*%--%L)-(1-%A*%A)*%A*%B)
300%Q=%Q-%L*%C*(1-%A*%A)*%A/(2*(%H+1)-%L)
310FPRINT%Q;P."OHM.BED ";ICKN."
32060TOf
330aFIF%Z)%B+%D-%B THEN GOTO g
340%X=%L
350GOSUBc
360%U=%G
370%X=2*(%H+1)-%L
380GOSUBc
390%Q=%L*%C*(1+%A)*(1/%L-%L-%A/(2*(%H+1)-%L)-%A*%G)
400FPRINT%Q;P."OHM.BED ";ICKN"
41060TOf
420aFIF%Z)%B THEN GOTO h
430%Q=%L*%C*(1-%A*%A)*1/%L+%U)
440FPRINT%Q;P."OHM.BED ";ICKN"
45060TOf
460hFIF%Z)%B+%D THEN GOTO
470%X=%L-2*%-
480GOSUBc
490%Q=%L+%C*(1-%A)*(1/%L-%U-%A/(%L-2*%F)-%A*%Q)
500FPRINT%Q;P."OHM.BED ";ICKN"
51060TOf
520i%W=(%Z-%B-%D)/%D
530%X=(2*(%W+1)+%L)
54060SUBc
550%Q=%L*%C*(1/%L+%A/(2*%W+%L)-(1-%A*%A)*%A*%Q)
560%Q=%Q-%L*%C*(1-%A*%A)*%A/(2*(%W+1)+%L)
570FPRINT%Q;P."OHM.BED ";ICKN"
580fM=M+1
590%P(M)=%Q
```

```
600JJ(M)=M
610FUNTIL%Z)2*%B+%D-%R
620qWAIT
630DO
640%Z=%Z+%K
650%H=(%B-%Z)/%D
660FIF%Z)%B-%S THEN GOTO x
670%H=(%B-%Z)/%D
680%X=(2*(%H+1)-%L)
690GOSUBc
700%D=%L*%C*(1/%L+%A/(2*%H-%L)-(1-%A*%A)*%A*%D)
710%D=%D-%L*%C*(1-%A*%A)*%A/(2*(%H+1)-%L)
720FPRINT%D;P,"OHM.BED THICK\"
730GOTOp
740kFIF%Z)%B THEN GOTO i
750%X=%L
760GOSUBc
770%U=%D
780%X=2*(%H+1)-%L
790GOSUBc
800%D=%L*%E*(1+%A)*(1/%L-%L-%A/(2*(%H+1)-%L)-%A*%D)
810FPRINT%D;P,"OHM.BED THICK\"
920P,"B";FPRINT%Z'
830GOTOp
840IFIF%Z)%B+%D-%S THEN GOTO x
850%X=2*(%H+1)-%L
860GOSUBc
870%Y=%D
880%X=-%L
890GOSUBc
900%W=%D
910%X=%L-2*%H
920GOSUBc
930%D=%L*%F*(1/%L-%A/(%L-2*%H)-%A*%D+%U)
940%D=%D-%L*%F*(%A/(2*(%H+1)-%L)-%A*%Y+%A)
950FPRINT%D;P,"OHM.BED THICK\"
952P,"C";FPRINT%Z'
970GOTOp
980mFIF%Z)%B+%D THEN GOTO n
990%X=%L-2*%H
1000GOSUBc
1010%D=%L*%F*(1-%A)*(1/%L+%U-%A/(%L-2*%H)-%A*%D)
1020FPRINT%D;P,"OHM.BED THICK\"
1030P,"D";FPRINT%Z'
1040GOTOp
1050n%%=(%Z-%B-%D)/%D
1060%X=(2*(%H+1)+%L)
1070GOSUBc
1080%D=%L*%C*(1/%L+%A/(2*%H+%L)-(1-%A*%A)*%A*%D)
1090%D=%D-%L*%C*(1-%A*%A)*%A/(2*(%H+1)+%L)
1100FPRINT%D;P,"OHM.BED THICK\"
1110P,"E";FPRINT%Z'
1120pX=%+1
1130FUNTIL%Z)2*%B+%D-%R
1140END
1150c%D=-0.000254*%X*%X*%X+0.003683*%X*%X-0.0289*%X-0.05055
1160RETURN
```

APPENDIX A.9

A.9.1 INFORMATION RELATED TO THE BOREHOLES EXAMINED

No.	NAME	G.R.	DIA.	DEPTH	LINING	DATUM	DEPTH
1.	Victoria Gardens North	314044	200	250	20.5	11.26	4
2.	Findon No. 1	121082	200	152.4	34		
3.	Brick Kiln Farm	835124	200	100	11.26		22.18
4.	Park Bottom Barn Arundel	005079	200	120	10	17.84	14.02
5.	Kingstone Middle Rd.	234054	150	211	26	7.09	5
6.	St. Peter's Church	315049	200	250	17.06	13.56	5
7.	St. Catherines Hill, Winchester Well No. 3	483274	150	112			
8.	Madehurst	981101	550	130			
9.	Ludgershall (Sewage Works) Well No. 5	272496	200	70			
10.	Ludgershall (Sewage Works) Well No. 3	272496	200	70			
11.	Adcote (Shropshire)	422197	610	153			
12.	Houndean (near Lewes) Well No. 5		305	100	16		30.8

A.7.2 OUTPUT OF PROGRAM "FORM" FOR BOREHOLE NO.1

64 inches

```
...)***INTERVAL BETWEEN      0.0METERS AND4.00000000METERS***
     122      22     138     138     153     153     153     153     153     153
     153     153     153     153     153     153     153     154     154     154
SORTED DATA ARE:
      22     122     138     138     153     153     153     153     153     153
     153     153     153     153     153     153     153     154     154     154
RES. DISTRIB. FROM     0.0TO4.00000000METERS
-----------------------------------------------------
       1      22
       1     122
       2     138
      13     153
       3     154
TRANSVERSE RESISTIVITY IS143.5500000.m
LONGITUDINAL RESISTIV.   IS115.8803200.m
Rtr-R1:27.6696799 0.m
ANISOTROPY INDEX IS1.11300408

.
.
.
***INTERVAL BETWEEN4.00000000METERS AND8.00000000METERS***
     154     154     154     154     154     154     154     154     154     154
     154     154     154     154     154     154     154     154     154     154
SORTED DATA ARE:
     154     154     154     154     154     154     154     154     154     154
     154     154     154     154     154     154     154     154     154     154
RES. DISTRIB. FROM4.00000000TO8.00000000METERS
-----------------------------------------------------
      20     154
TRANSVERSE RESISTIVITY IS154.0000000.m
LONGITUDINAL RESISTIV.   IS154.0000000.m
Rtr-R1:      0.0 0.m
ANISOTROPY INDEX IS1.00000000


***INTERVAL BETWEEN8.00000000METERS AND12.0000000METERS***
     154     154     154     154     154     154     154     154     154     154
     154     154     149     149     149     149     149     149     149     149
SORTED DATA ARE:
     149     149     149     149     149     149     149     149     154     154
     154     154     154     154     154     154     154     154     154     154
RES. DISTRIB. FROM8.00000000TO12.0000000METERS
-----------------------------------------------------
       8     149
      12     154
TRANSVERSE RESISTIVITY IS152.0000000.m
LONGITUDINAL RESISTIV.   IS151.9602650.m
Rtr-R1:3.97350788E-2 0.m
ANISOTROPY INDEX IS1.00013073

.
.
.
***INTERVAL BETWEEN12.0000000METERS AND16.0000000METERS***
     149     149     149     149     149     149     149     149     149     149
     149     149     149     149     149     149     149     149     149     149
SORTED DATA ARE:
     149     149     149     149     149     149     149     149     149     149
     149     149     149     149     149     149     149     149     149     149
RES. DISTRIB. FROM12.0000000TO16.0000000METERS
-----------------------------------------------------
      20     149
TRANSVERSE RESISTIVITY IS149.0000000.m
LONGITUDINAL RESISTIV.   IS149.0000000.m
Rtr-R1:-5.96046448E-8 0.m
ANISOTROPY INDEX IS1.00000000

.
.
.
***INTERVAL BETWEEN16.0000000METERS AND20.0000000METERS***
     149     149     149     149     149     149     149     149     149     149
     149     149     149     149     149     149     149     155     155     155
SORTED DATA ARE:
     149     149     149     149     149     149     149     149     149     149
     149     149     149     149     149     149     149     155     155     155
RES. DISTRIB. FROM16.0000000TO20.0000000METERS
-----------------------------------------------------
      17     149
       3     155
TRANSVERSE RESISTIVITY IS149.9000000.m
LONGITUDINAL RESISTIV.   IS149.8702140.m
Rtr-R1:2.97058119E-2 0.m
ANISOTROPY INDEX IS1.00009937
```

```
.
***INTERVAL BETWEEN20.0000000METERS AND24.0000000METERS***
     155      155      155      155      155      155      155      155      155      155
     155      155      155      155      155      155      155      155      155      155
SORTED DATA ARE:
     155      155      155      155      155      155      155      155      155      155
     155      155      155      155      155      155      155      155      155      155
RES. DISTRIB. FROM20.0000000TO24.0000000METERS
----------------------------------------------------
      20      155
TRANSVERSE RESISTIVITY IS155.0000000.m
LONGITUDINAL RESISTIV.   IS155.0000000.m
Rtr-Rl:      0.0 0.m
ANISOTROPY INDEX IS1.00000000


.
***INTERVAL BETWEEN24.0000000METERS AND28.0000000METERS***
     155      155      155      155      172      172      172      172      172      172
     172      172      172      172      172      172      172      172      172      172
SORTED DATA ARE:
     155      155      155      155      172      172      172      172      172      172
     172      172      172      172      172      172      172      172      172      172
RES. DISTRIB. FROM24.0000000TO28.0000000METERS
----------------------------------------------------
       4      155
      16      172
TRANSVERSE RESISTIVITY IS168.6000000.m
LONGITUDINAL RESISTIV.   IS168.3080810.m
Rtr-Rl:2.91919231E-1 0.m
ANISOTROPY INDEX IS1.00086684

.
.
.
***INTERVAL BETWEEN28.0000000METERS AND32.0000000METERS***
     172      172      172      172      172      172      172      172      172      172
     172      172      172      172      172      172      172      172      172      172
SORTED DATA ARE:
     172      172      172      172      172      172      172      172      172      172
     172      172      172      172      172      172      172      172      172      172
RES. DISTRIB. FROM28.0000000TO32.0000000METERS
----------------------------------------------------
      20      172
TRANSVERSE RESISTIVITY IS172.0000000.m
LONGITUDINAL RESISTIV.   IS172.0000000.m
Rtr-Rl:      0.0 0.m
ANISOTROPY INDEX IS1.00000000

.
.
.
***INTERVAL BETWEEN32.0000000METERS AND36.0000000METERS***
     172      172      172      172      172      176      176      176      176      176
     176      176      177      177      177      177      177      177      177      177
SORTED DATA ARE:
     172      172      172      172      172      176      176      176      176      176
     176      176      177      177      177      177      177      177      177      177
RES. DISTRIB. FROM32.0000000TO36.0000000METERS
----------------------------------------------------
       5      172
       7      176
       8      177
TRANSVERSE RESISTIVITY IS175.4000000.m
LONGITUDINAL RESISTIV.   IS175.3766990.m
Rtr-Rl:2.33004589E-2 0.m
ANISOTROPY INDEX IS1.00006643

.
.
.
***INTERVAL BETWEEN36.0000000METERS AND40.0000000METERS***
     177      177      177      177      177      177      177      177      177      177
     177      177      177      177      177      182      182      182      182      189
SORTED DATA ARE:
     177      177      177      177      177      177      177      177      177      177
     177      177      177      177      177      182      182      182      182      189
RES. DISTRIB. FROM36.0000000TO40.0000000METERS
----------------------------------------------------
      15      177
       4      182
       1      189
TRANSVERSE RESISTIVITY IS178.6000000.m
LONGITUDINAL RESISTIV.   IS178.5478510.m
Rtr-Rl:5.21492958E-2 0.m
ANISOTROPY INDEX IS1.00014603
```

```
)***INTERVAL BETWEEN40.0000000METERS AND44.0000000METERS***
     189      189      189      189      189      189      189      189      189      189
     189      189      189      189      189      188      188      188      188      188
SORTED DATA ARE:
     188      188      188      188      188      189      189      189      189      189
     189      189      189      189      189      189      189      189      189      189
RES. DISTRIB. FROM40.0000000TO44.0000000METERS
----------------------------------------------------
       5      188
      15      189
TRANSVERSE RESISTIVITY IS188.7500000.m
LONGITUDINAL RESISTIV.  IS188.7490040.m
Rtr-Rl:9.96053219E-4 0.m
ANISOTROPY INDEX IS1.00000264

.
.
.
***INTERVAL BETWEEN44.0000000METERS AND48.0000000METERS***
     188      188      188      188      188      188      188      188      188      194
     194      194      194      194      194      194      194      194      194      194
SORTED DATA ARE:
     188      188      188      188      188      188      188      188      188      194
     194      194      194      194      194      194      194      194      194      194
RES. DISTRIB. FROM44.0000000TO48.0000000METERS
----------------------------------------------------
       9      188
      11      194
TRANSVERSE RESISTIVITY IS191.3000000.m
LONGITUDINAL RESISTIV.  IS191.2532770.m
Rtr-Rl:4.67225909E-2 0.m
ANISOTROPY INDEX IS1.00012214

.
.
.
***INTERVAL BETWEEN48.0000000METERS AND52.0000000METERS***
     194      194      194      194      194      194      194      194      194      194
     199      199      199      199      199      199      199      199      199      199
SORTED DATA ARE:
     194      194      194      194      194      194      194      194      194      194
     199      199      199      199      199      199      199      199      199      199
RES. DISTRIB. FROM48.0000000TO52.0000000METERS
----------------------------------------------------
      10      194
      10      199
TRANSVERSE RESISTIVITY IS196.5000000.m
LONGITUDINAL RESISTIV.  IS196.4681930.m
Rtr-Rl:3.18065882E-2 0.m
ANISOTROPY INDEX IS1.00008094

.
.
***INTERVAL BETWEEN52.0000000METERS AND56.0000000METERS***
     207      207      207      207      207      207      207      207      207      207
     207      207      207      207      213      213      213      213      213      213
SORTED DATA ARE:
     207      207      207      207      207      207      207      207      207      207
     207      207      207      207      213      213      213      213      213      213
RES. DISTRIB. FROM52.0000000TO56.0000000METERS
----------------------------------------------------
      14      207
       6      213
TRANSVERSE RESISTIVITY IS208.8000000.m
LONGITUDINAL RESISTIV.  IS208.7642040.m
Rtr-Rl:3.57953906E-2 0.m
ANISOTROPY INDEX IS1.00008573

.
.
.
***INTERVAL BETWEEN56.0000000METERS AND60.0000000METERS***
     213      209      209      209      209      209      209      218      218      218
     218      218      218      218      218      218      218      218      218      218
SORTED DATA ARE:
     209      209      209      209      209      209      213      218      218      218
     218      218      218      218      218      218      218      218      218      218
RES. DISTRIB. FROM56.0000000TO60.0000000METERS
----------------------------------------------------
       6      209
       1      213
      13      218
TRANSVERSE RESISTIVITY IS215.0500000.m
LONGITUDINAL RESISTIV.  IS214.9705550.m
Rtr-Rl:7.94445276E-2 0.m
ANISOTROPY INDEX IS1.00018476
```

```
***INTERVAL BETWEEN60.0000000METERS AND64.0000000METERS***
     218      218      218      218      218      218      218      218      218      218
     218      218      218      218      218      218      218      218      218      218
SORTED DATA ARE:
     218      218      218      218      218      218      218      218      218      218
     218      218      218      218      218      218      218      218      218      218
RES. DISTRIB. FROM60.0000000TO64.0000000METERS
----------------------------------------------------
      20      218
TRANSVERSE RESISTIVITY IS218.0000000.m
LONGITUDINAL RESISTIV.  IS218.0000000.m
Rtr-Rl:      0.0 0.m
ANISOTROPY INDEX IS1.00000000

.
.
.
***INTERVAL BETWEEN64.0000000METERS AND68.0000000METERS***
     204      204      204      204      204      223      223      223      223      223
     223      223      223      223      223      223      223      223      223      223
SORTED DATA ARE:
     204      204      204      204      204      223      223      223      223      223
     223      223      223      223      223      223      223      223      223      223
RES. DISTRIB. FROM64.0000000TO68.0000000METERS
----------------------------------------------------
       5      204
      15      223
TRANSVERSE RESISTIVITY IS218.2500030.m
LONGITUDINAL RESISTIV.  IS217.9257480.m
Rtr-Rl:3.24251473E-1 0.m
ANISOTROPY INDEX IS1.00074367

.
.
.
***INTERVAL BETWEEN68.0000000METERS AND72.0000000METERS***
     206      206      206      206      206      206      206      206      206      206
     206      206      206      195      195      195      195      195      195      195
SORTED DATA ARE:
     195      195      195      195      195      195      195      206      206      206
     206      206      206      206      206      206      206      206      206      206
RES. DISTRIB. FROM68.0000000TO72.0000000METERS
----------------------------------------------------
       7      195
      13      206
TRANSVERSE RESISTIVITY IS202.1500000.m
LONGITUDINAL RESISTIV.  IS202.0115680.m
Rtr-Rl:1.38433456E-1 0.m
ANISOTROPY INDEX IS1.00034258

.
.
.
***INTERVAL BETWEEN72.0000000METERS AND76.0000000METERS***
     195      195      195      195      195      195      195      195      195      195
     195      195      195      195      195      195      195      195      195      195
SORTED DATA ARE:
     195      195      195      195      195      195      195      195      195      195
     195      195      195      195      195      195      195      195      195      195
RES. DISTRIB. FROM72.0000000TO76.0000000METERS
----------------------------------------------------
      20      195
TRANSVERSE RESISTIVITY IS195.0000000.m
LONGITUDINAL RESISTIV.  IS195.0000000.m
Rtr-Rl:      0.0 0.m
ANISOTROPY INDEX IS1.00000000

.
.
.
***INTERVAL BETWEEN76.0000000METERS AND80.0000000METERS***
     195      195      195      204      204      204      204      204      217      217
     217      217      217      217      217      217      217      217      217      217
SORTED DATA ARE:
     195      195      195      204      204      204      204      204      217      217
     217      217      217      217      217      217      217      217      217      217
RES. DISTRIB. FROM76.0000000TO80.0000000METERS
----------------------------------------------------
       3      195
       5      204
      12      217
TRANSVERSE RESISTIVITY IS210.4500000.m
LONGITUDINAL RESISTIV.  IS210.0973670.m
Rtr-Rl:3.52633197E-1 0.m
ANISOTROPY INDEX IS1.00083886

***INTERVAL BETWEEN80.0000000METERS AND84.0000000METERS***
     217      217      217      217      217      207      207      207      207      207
     207      207      207      207      207      207      207      207      207      207
SORTED DATA ARE:
     207      207      207      207      207      207      207      207      207      207
     207      207      207      207      207      217      217      217      217      217
RES. DISTRIB. FROM80.0000000TO84.0000000METERS
----------------------------------------------------
      15      207
       5      217
TRANSVERSE RESISTIVITY IS209.5000000.m
LONGITUDINAL RESISTIV.  IS209.4175870.m
Rtr-Rl:8.74126553E-2 0.m
ANISOTROPY INDEX IS1.00020869
```

```
***INTERVAL BETWEEN84.0000000METERS AND88.0000000METERS***
     169      169      169      169      169      169      169      169      169      169
     169      169      169      169      169      189      189      189      189      189
SORTED DATA ARE:
     169      169      169      169      169      169      169      169      169      169
     169      169      169      169      169      189      189      189      189      189
RES. DISTRIB. FROM84.0000000TO88.0000000METERS
----------------------------------------------------------
      15      169
       5      189
TRANSVERSE RESISTIVITY IS174.0000000.m
LONGITUDINAL RESISTIV.   IS173.5923910.m
Rtr-R:4.07608688E-1 0.m
ANISOTROPY INDEX IS1.00117335

***INTERVAL BETWEEN88.0000000METERS AND92.0000000METERS***
     189      181      181      181      181      181      181      181      181      181
     175      175      175      175      147      147      147      147      147      147
SORTED DATA ARE:
     147      147      147      147      147      147      175      175      175      175
     181      181      181      181      181      181      181      181      181      189
RES. DISTRIB. FROM88.0000000TO92.0000000METERS
----------------------------------------------------------
       6      147
       4      175
       9      181
       1      189
TRANSVERSE RESISTIVITY IS170.0000000.m
LONGITUDINAL RESISTIV.   IS168.5087030.m
Rtr-R:1.49129671 0.m
ANISOTROPY INDEX IS1.00441524

.
.
.
***INTERVAL BETWEEN92.0000000METERS AND96.0000000METERS***
     147      147      147      147      147      119      119      119      119      119
     119      119      119      119      119      119      119      119      119      119
SORTED DATA ARE:
     119      119      119      119      119      119      119      119      119      119
     119      119      119      119      119      147      147      147      147      147
RES. DISTRIB. FROM92.0000000TO96.0000000METERS
----------------------------------------------------------
      15      119
       5      147
TRANSVERSE RESISTIVITY IS126.0000000.m
LONGITUDINAL RESISTIV.   IS124.9500000.m
Rtr-R:1.05000001 0.m
ANISOTROPY INDEX IS1.00419289

.
.
.
***INTERVAL BETWEEN96.0000000METERS AND100.000000METERS***
     119      133      133      133      133      133      133      133      133      133
      85       85       85       85       85       85       85       85       85       85
SORTED DATA ARE:
      85       85       85       85       85       85       85       85       85       85
     119      133      133      133      133      133      133      133      133      133
RES. DISTRIB. FROM96.0000000TO100.000000METERS
----------------------------------------------------------
      10       85
       1      119
       9      133
TRANSVERSE RESISTIVITY IS108.3000000.m
LONGITUDINAL RESISTIV.   IS103.2420090.m
Rtr-R:5.05799088 0.m
ANISOTROPY INDEX IS1.02420291

.
.
.
***INTERVAL BETWEEN100.000000METERS AND104.000000METERS***
      85       85       85       85       85       85      130      130      130
     130      130      130      130      130      130      130      130      130      130
SORTED DATA ARE:
      85       85       85       85       85       85      130      130      130      130
     130      130      130      130      130      130      130      130      130      130
RES. DISTRIB. FROM100.000000TO104.000000METERS
----------------------------------------------------------
       6       85
      14      130
TRANSVERSE RESISTIVITY IS116.5000000.m
LONGITUDINAL RESISTIV.   IS112.1827410.m
Rtr-R:4.31725892 0.m
ANISOTROPY INDEX IS1.01906043
```

```
.
.
***INTERVAL BETWEEN104.000000METERS AND108.000000METERS***
     127      127      127      109      109      109      109      109      109      109
     109      109      109      109      109      109      109      109      109      109
SORTED DATA ARE:
     109      109      109      109      109      109      109      109      109      109
     109      109      109      109      109      109      109      127      127      127
RES. DISTRIB. FROM104.000000TO108.000000METERS
----------------------------------------------------
      17      109
       3      127
TRANSVERSE RESISTIVITY IS111.7000000.m
LONGITUDINAL RESISTIV.   IS111.3676590.m
Rtr-Rl:3.32341134E-1 0.m
ANISOTROPY INDEX IS1.00149098

.
.
.
***INTERVAL BETWEEN108.000000METERS AND112.000000METERS***
     109      109      123      123      123      123      123      123      123      123
     123      123      123      123      123      109      109      109      109      109
SORTED DATA ARE:
     109      109      109      109      109      109      109      123      123      123
     123      123      123      123      123      123      123      123      123      123
RES. DISTRIB. FROM108.000000TO112.000000METERS
----------------------------------------------------
       7      109
      13      123
TRANSVERSE RESISTIVITY IS118.1000000.m
LONGITUDINAL RESISTIV.   IS117.7085160.m
Rtr-Rl:3.91483724E-1 0.m
ANISOTROPY INDEX IS1.00166156

.
.
.
***INTERVAL BETWEEN112.000000METERS AND116.000000METERS***
     105      105      105      105      105      105      105      105      114      114
     114      114      114      114      114      114      114      104      104      104
SORTED DATA ARE:
     104      104      104      105      105      105      105      105      105      105
     105      114      114      114      114      114      114      114      114      114
RES. DISTRIB. FROM112.000000TO116.000000METERS
----------------------------------------------------
       3      104
       8      105
       9      114
TRANSVERSE RESISTIVITY IS108.9000000.m
LONGITUDINAL RESISTIV.   IS108.7051060.m
Rtr-Rl:1.94894284E-1 0.m
ANISOTROPY INDEX IS1.00089603

.
.
.
***INTERVAL BETWEEN116.000000METERS AND120.000000METERS***
      95       95       95       95       95       95       95       95       95      100
     100      108      108      108      108      108      108      108      108      108
SORTED DATA ARE:
      95       95       95       95       95       95       95       95       95      100
     100      108      108      108      108      108      108      108      108      108
RES. DISTRIB. FROM116.000000TO120.000000METERS
----------------------------------------------------
       9       95
       2      100
       9      108
TRANSVERSE RESISTIVITY IS101.3500000.m
LONGITUDINAL RESISTIV.   IS100.9743130.m
Rtr-Rl:3.75686407E-1 0.m
ANISOTROPY INDEX IS1.00185858

.
.
.
***INTERVAL BETWEEN120.000000METERS AND124.000000METERS***
     108      108      108      108      108      108      108      108      108      108
     122      122      122      122      122      122      122      120      120      120

 ***INTERVAL BETWEEN120.000000METERS AND124.000000METERS***
     108      108      108      108      108      108      108      108      108      108
     122      122      122      122      122      122      122      120      120      120
SORTED DATA ARE:
     108      108      108      108      108      108      108      108      108      108
     120      120      120      122      122      122      122      122      122      122
RES. DISTRIB. FROM120.000000TO124.000000METERS
----------------------------------------------------
      10      108
       3      120
       7      122
TRANSVERSE RESISTIVITY IS114.7000000.m
LONGITUDINAL RESISTIV.   IS114.3055430.m
Rtr-Rl:3.94456506E-1 0.m
ANISOTROPY INDEX IS1.00172396
```

```
***INTERVAL BETWEEN112.000000METERS AND116.000000METERS***
     105      105      105      105      105      105      105      105      114      114
     114      114      114      114      114      114      114      104      104      104
SORTED DATA ARE:
     104      104      104      105      105      105      105      105      105      105
     105      114      114      114      114      114      114      114      114      114
RES. DISTRIB. FROM112.000000TO116.000000METERS
----------------------------------------------------------
       3      104
       8      105
       9      114
TRANSVERSE RESISTIVITY IS108.9000000.m
LONGITUDINAL RESISTIV.  IS108.7051060.m
Rtr-R|:1.94894284E-1 O.m
ANISOTROPY INDEX IS1.00089603

.
.
.
***INTERVAL BETWEEN116.000000METERS AND120.000000METERS***
      95       95       95       95       95       95       95       95       95      100
     100      108      108      108      108      108      108      108      108      108
SORTED DATA ARE:
      95       95       95       95       95       95       95       95       95      100
     100      108      108      108      108      108      109      108      108      108
RES. DISTRIB. FROM116.000000TO120.000000METERS
----------------------------------------------------------
       9       95
       2      100
       9      108
TRANSVERSE RESISTIVITY IS101.3500000.m
LONGITUDINAL RESISTIV.  IS100.9743130.m
Rtr-R|:3.75686407E-1 O.m
ANISOTROPY INDEX IS1.00185858

.
.
.
***INTERVAL BETWEEN120.000000METERS AND124.000000METERS***
     108      108      108      108      108      108      108      108      108      108
     122      122      122      122      122      122      122      120      120      120

 ***INTERVAL BETWEEN120.000000METERS AND124.000000METERS***
     108      108      108      108      108      108      108      108      108      108
     122      122      122      122      122      122      122      120      120      120
SORTED DATA ARE:
     108      108      108      108      108      108      108      108      108      108
     120      120      120      122      122      122      122      122      122      122
RES. DISTRIB. FROM120.000000TO124.000000METERS
----------------------------------------------------------
      10      108
       3      120
       7      122
TRANSVERSE RESISTIVITY IS114.7000000.m
LONGITUDINAL RESISTIV.  IS114.3055430.m
Rtr-R|:3.94456505E-1 O.m
ANISOTROPY INDEX IS1.00172396

.
.
.
***INTERVAL BETWEEN124.000000METERS AND128.000000METERS***
     120      120      120      120      124      124      124      124      124      114
     114      114      114      114      114      114      114      114      114      119
SORTED DATA ARE:
     114      114      114      114      114      114      114      114      114      114
     119      120      120      120      120      124      124      124      124      124
RES. DISTRIB. FROM124.000000TO128.000000METERS
----------------------------------------------------------
      10      114
       1      119
       4      120
       5      124
TRANSVERSE RESISTIVITY IS117.9500000.m
LONGITUDINAL RESISTIV.  IS117.8004950.m
Rtr-R|:1.49505049E-1 O.m
ANISOTROPY INDEX IS1.00063437

.
***INTERVAL BETWEEN128.000000METERS AND132.000000METERS***
     119      119      119      119      119      119      115      115      115      109
     109      109      109      109      109      109      109      109      109      109
SORTED DATA ARE:
     109      109      109      109      109      109      109      109      109      109
     109      115      115      115      119      119      119      119      119      119
RES. DISTRIB. FROM128.000000TO132.000000METERS
----------------------------------------------------------
      11      109
       3      115
       6      119
TRANSVERSE RESISTIVITY IS112.9000000.m
LONGITUDINAL RESISTIV.  IS112.7239680.m
Rtr-R|:1.76031738E-1 O.m
ANISOTROPY INDEX IS1.00078050

.
.
.
```

```
***INTERVAL BETWEEN132.000000METERS AND136.000000METERS***
     109      109      109      109      109      109      109      109      113      113
     113      119      119      119      119      119      119      119      119      119
SORTED DATA ARE:
     109      109      109      109      109      109      109      109      113      113
     113      119      119      119      119      119      119      119      119      119
RES. DISTRIB. FROM132.000000TO136.000000METERS
-----------------------------------------------------
       8      109
       3      113
       9      119
TRANSVERSE RESISTIVITY IS114.1000000.m
LONGITUDINAL RESISTIV.   IS113.9124590.m
Rtr-Rl:1.87541067E-1 0.m
ANISOTROPY INDEX IS1.00082284


.
***INTERVAL BETWEEN136.000000METERS AND140.000000METERS***
     119      119      119      119      119      119      119      119      119      119
     119      119      119      119      119      119      119      119      119      119
SORTED DATA ARE:
     119      119      119      119      119      119      119      119      119      119
     119      119      119      119      119      119      119      119      119      119
RES. DISTRIB. FROM136.000000TO140.000000METERS
-----------------------------------------------------
      20      119
TRANSVERSE RESISTIVITY IS119.0000000.m
LONGITUDINAL RESISTIV.   IS119.0000000.m
Rtr-Rl:2.98023224E-8 0.m
ANISOTROPY INDEX IS1.00000000

.
.
.
***INTERVAL BETWEEN140.000000METERS AND144.000000METERS***
     119      119      119      119      119      119      119      119      119      119
     119      119      119      119      119      119      119      119      119      119
SORTED DATA ARE:
     119      119      119      119      119      119      119      119      119      119
     119      119      119      119      119      119      119      119      119      119
RES. DISTRIB. FROM140.000000TO144.000000METERS
-----------------------------------------------------
      20      119
TRANSVERSE RESISTIVITY IS119.0000000.m
LONGITUDINAL RESISTIV.   IS119.0000000.m
Rtr-Rl:2.98023224E-8 0.m
ANISOTROPY INDEX IS1.00000000

.
.
.
***INTERVAL BETWEEN144.000000METERS AND148.000000METERS***
     119      119      119      134      134      134      142      142      142      142
     142      142      142      142      142      133      133      133      133      133
SORTED DATA ARE:
     119      119      119      133      133      133      133      133      134      134
     134      134      142      142      142      142      142      142      142      142
RES. DISTRIB. FROM144.000000TO148.000000METERS
-----------------------------------------------------
       3      119
       5      133
       4      134
       8      142
TRANSVERSE RESISTIVITY IS134.7000000.m
LONGITUDINAL RESISTIV.   IS134.2346350.m
Rtr-Rl:4.65364535E-1 0.m
ANISOTROPY INDEX IS1.00173190

.
.
.
***INTERVAL BETWEEN148.000000METERS AND152.000000METERS***
     133      133      133      133      133      133      133      133      133      133
     133      133      133      134      133      133      133      133      139      139
SORTED DATA ARE:
     129      129      133      133      133      133      133      133      133      133
     133      133      133      133      133      133      133      133      133      133
RES. DISTRIB. FROM148.000000TO152.000000METERS
-----------------------------------------------------
       2      129
      18      133
TRANSVERSE RESISTIVITY IS132.6000000.m
LONGITUDINAL RESISTIV.   IS132.5898720.m
Rtr-Rl:1.11283064E-2 0.m
ANISOTROPY INDEX IS1.00004196
```

```
.
***INTERVAL BETWEEN152.000000METERS AND156.000000METERS***
     129      129      129      129      129      129      129      129      129      129
     125      125      125      125      125      125      125      125      125      125
SORTED DATA ARE:
     125      125      125      125      125      125      125      125      125      125
     129      129      129      129      129      129      129      129      129      129
RES. DISTRIB. FROM152.000000TO156.000000METERS
----------------------------------------------------
      10      125
      10      129
TRANSVERSE RESISTIVITY IS127.0000000.m
LONGITUDINAL RESISTIV.  IS126.9685040.m
Rtr-R:3.14960182E-2 0.m
ANISOTROPY INDEX IS1.00012402

.
.
.
***INTERVAL BETWEEN156.000000METERS AND160.000000METERS***
     125      125      125      125      125      125      125      125      125      125
     125      125      125      125      125      125      125      125      125      125
SORTED DATA ARE:
     125      125      125      125      125      125      125      125      125      125
     125      125      125      125      125      125      125      125      125      125
RES. DISTRIB. FROM156.000000TO160.000000METERS
----------------------------------------------------
      20      125
TRANSVERSE RESISTIVITY IS125.0000000.m
LONGITUDINAL RESISTIV.  IS125.0000000.m
Rtr-R:-2.98023224E-8 0.m
ANISOTROPY INDEX IS1.00000000

.
.
.
***INTERVAL BETWEEN160.000000METERS AND164.000000METERS***
     134      134      134      134      134      134      134      115      115      115
     115      115      115       92       92       92       92       92       92       92
 ***INTERVAL BETWEEN160.000000METERS AND164.000000METERS***
     134      134      134      134      134      134      134      115      115      115
     115      115      115       92       92       92       92       92       92       92
SORTED DATA ARE:
      92       92       92       92       92       92       92      115      115      115
     115      115      115      134      134      134      134      134      134      134
RES. DISTRIB. FROM160.000000TO164.000000METERS
----------------------------------------------------
       7       92
       6      115
       7      134
TRANSVERSE RESISTIVITY IS113.6000000.m
LONGITUDINAL RESISTIV.  IS110.8035230.m
Rtr-R:2.79647672 0.m
ANISOTROPY INDEX IS1.01254045

.
.
.
***INTERVAL BETWEEN164.000000METERS AND168.000000METERS***
      92       92       70       70       70       70       70       70       51       51
      51       51       51       51       51       51       51       51       51       51
SORTED DATA ARE:
      51       51       51       51       51       51       51       51       51       51
      51       51       70       70       70       70       70       70       92       92
RES. DISTRIB. FROM164.000000TO168.000000METERS
----------------------------------------------------
      12       51
       6       70
       2       92
TRANSVERSE RESISTIVITY IS60.80000000.m
LONGITUDINAL RESISTIV.  IS58.35198800.m
Rtr-R:2.44801195 0.m
ANISOTROPY INDEX IS1.02076075

.
.
.
***INTERVAL BETWEEN168.000000METERS AND172.000000METERS***
      51       51       51       51       51       51       51       51       51       63
      63       63       63       63       70       70       70       70       70       79
SORTED DATA ARE:
      51       51       51       51       51       51       51       51       51       63
      63       63       63       63       70       70       70       70       70       79
RES. DISTRIB. FROM168.000000TO172.000000METERS
----------------------------------------------------
       9       51
       5       63
       5       70
       1       79
TRANSVERSE RESISTIVITY IS60.15000000.m
LONGITUDINAL RESISTIV.  IS58.83694650.m
Rtr-R:1.31305349 0.m
ANISOTROPY INDEX IS1.01109684
```

```
.
.
.
***INTERVAL BETWEEN172.000000METERS AND176.000000METERS***
      79       79       79       79       79       79       79       79       79       79
      79       79       79       79       79       79       79       79       79       79
SORTED DATA ARE:
      79       79       79       79       79       79       79       79       79       79
      79       79       79       79       79       79       79       79       79       79
RES. DISTRIB. FROM172.000000TO176.000000METERS
--------------------------------------------------
      20       79
TRANSVERSE RESISTIVITY IS79.00000000.m
LONGITUDINAL RESISTIV.   IS79.00000000.m
Rtr-Rl:      0.0 0.m
ANISOTROPY INDEX IS1.00000000

.
.
.
***INTERVAL BETWEEN176.000000METERS AND180.000000METERS***
      79       79       79       79       79       79       79       79       79       79
      79       79       79       79       79       79       79       79       79       79
SORTED DATA ARE:
      79       79       79       79       79       79       79       79       79       79
      79       79       79       79       79       79       79       79       79       79
RES. DISTRIB. FROM176.000000TO180.000000METERS
--------------------------------------------------
      20       79
TRANSVERSE RESISTIVITY IS79.00000000.m
LONGITUDINAL RESISTIV.   IS79.00000000.m
Rtr-Rl:      0.0 0.m
ANISOTROPY INDEX IS1.00000000
```

A.9.3 ANALOGUE TO DIGITAL AND DIGITAL TO ANALOGUE INTERFACE

The Analogue to Digital and Digital to Analogue interface which was used in the present work was based in a design by ACORN COMPUTERS Ltd. The electronic diagram of the device is shown in Fig. A.4. The printed circuit board was supplied by ACORN COMPUTERS and the author fitted all the necessary electronic components according to the electronic diagram. It was found that in order for the device to be compatible with the microcomputer used, transistor Q1 had to be replaced by two diodes in series.

The constructed device has 12 bits resolution and is designed to accept or produce analogue voltages in the range -5.12V to +5.12V. Thus there would be 4096 levels at 2.5mV steps between the above levels.

In order for the above unit to be linked to the microcomputer a 19-inches rack containing an appropriate socket was used.

Fig. A.4

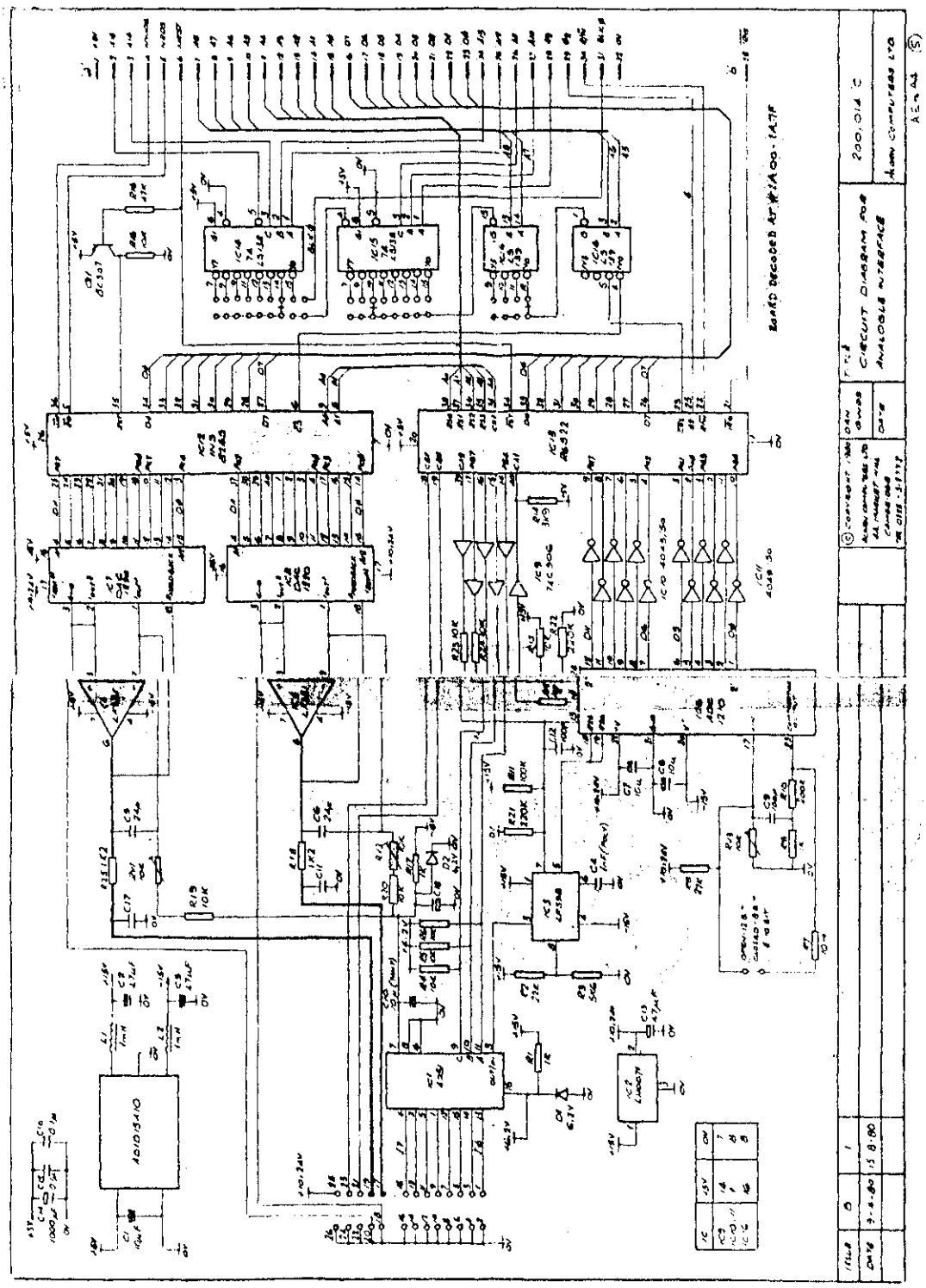


Fig. A.4 Electronic circuit of ADA interface

A.9.4 PERMANENT STORAGE OF SOFTWARE IN THE MICROCOMPUTER

The microcomputer used in the present research has a vacant expansion socket for a utility ROM which will accommodate up to a 4K by eight-bit device, such as the EPROM 2532. In order to transfer the necessary software in the EPROM an EP-ROM programmer had to be constructed, and the design published by J. Flower in the June issue of Practical Computing 1982 was used. Fig. A.5 represents the electronic circuit of the programmer.

Since more than one EPROMS were needed for storing all the necessary software, an 8-way ROM PAGER was fitted into the microcomputers single EPROM SOCKET, and provided the facility of accommodating up to 8 EPROMS (Fig. A.6).

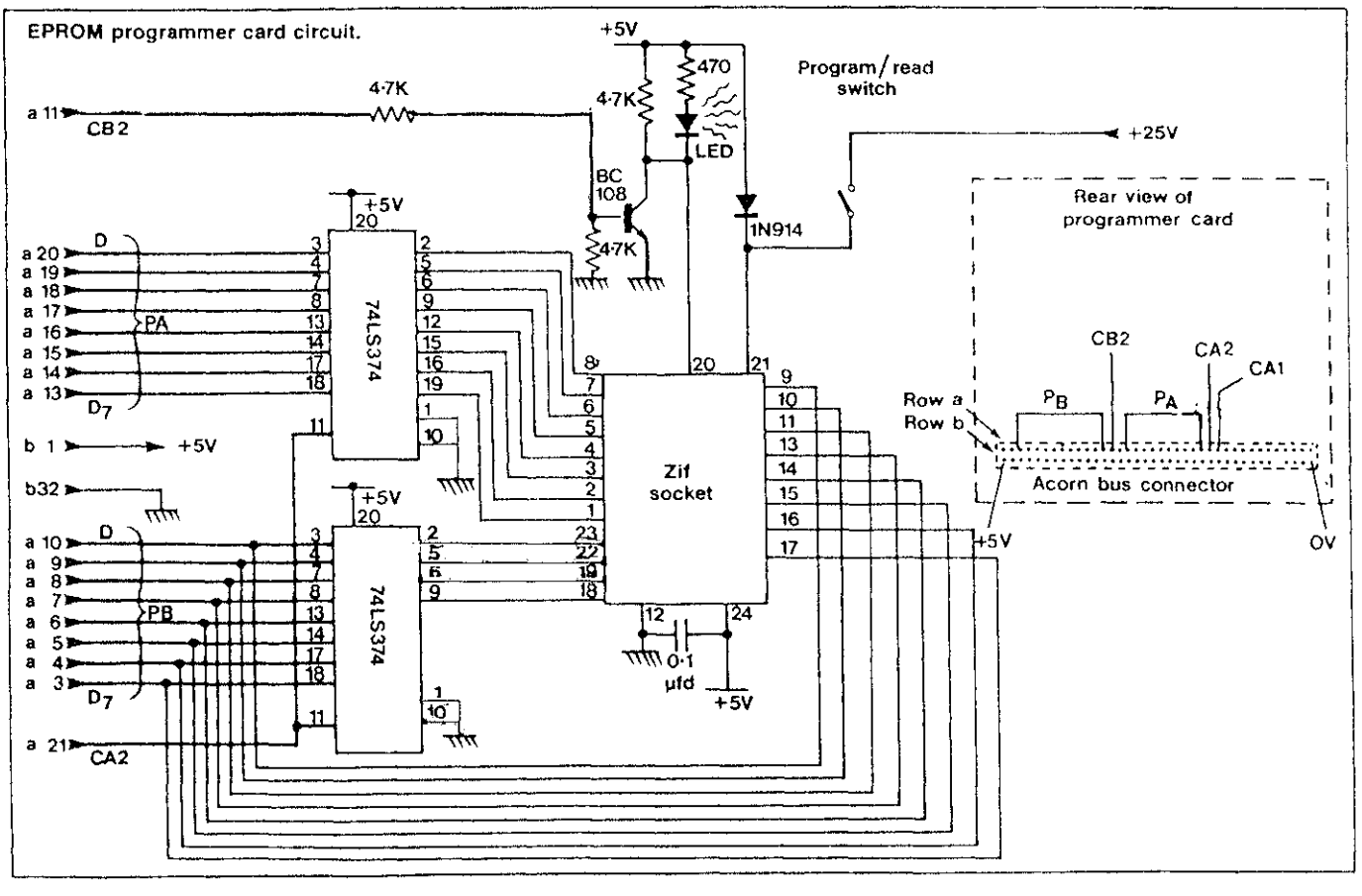


Fig. A.5 Electronic circuit of EPROM programmer

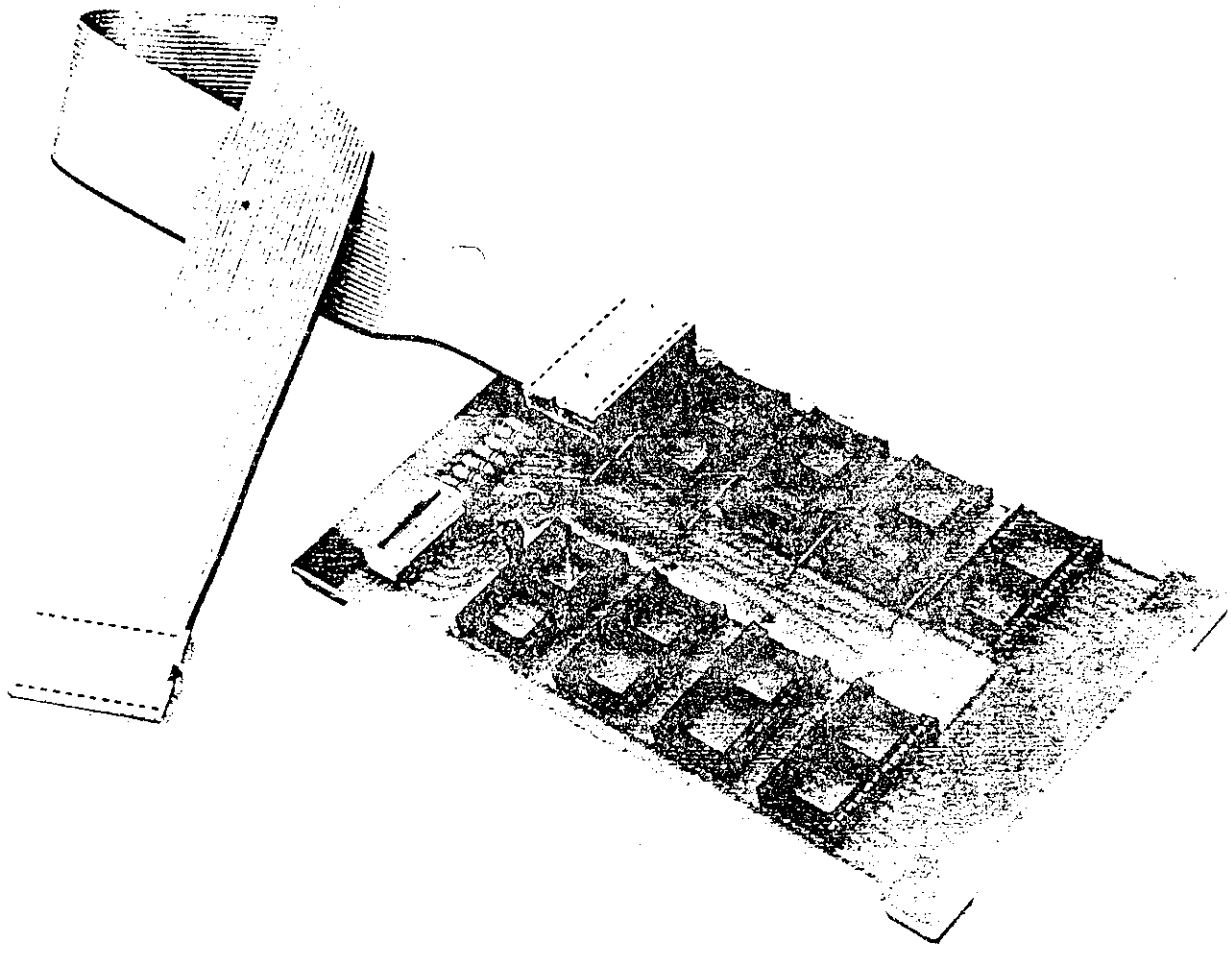
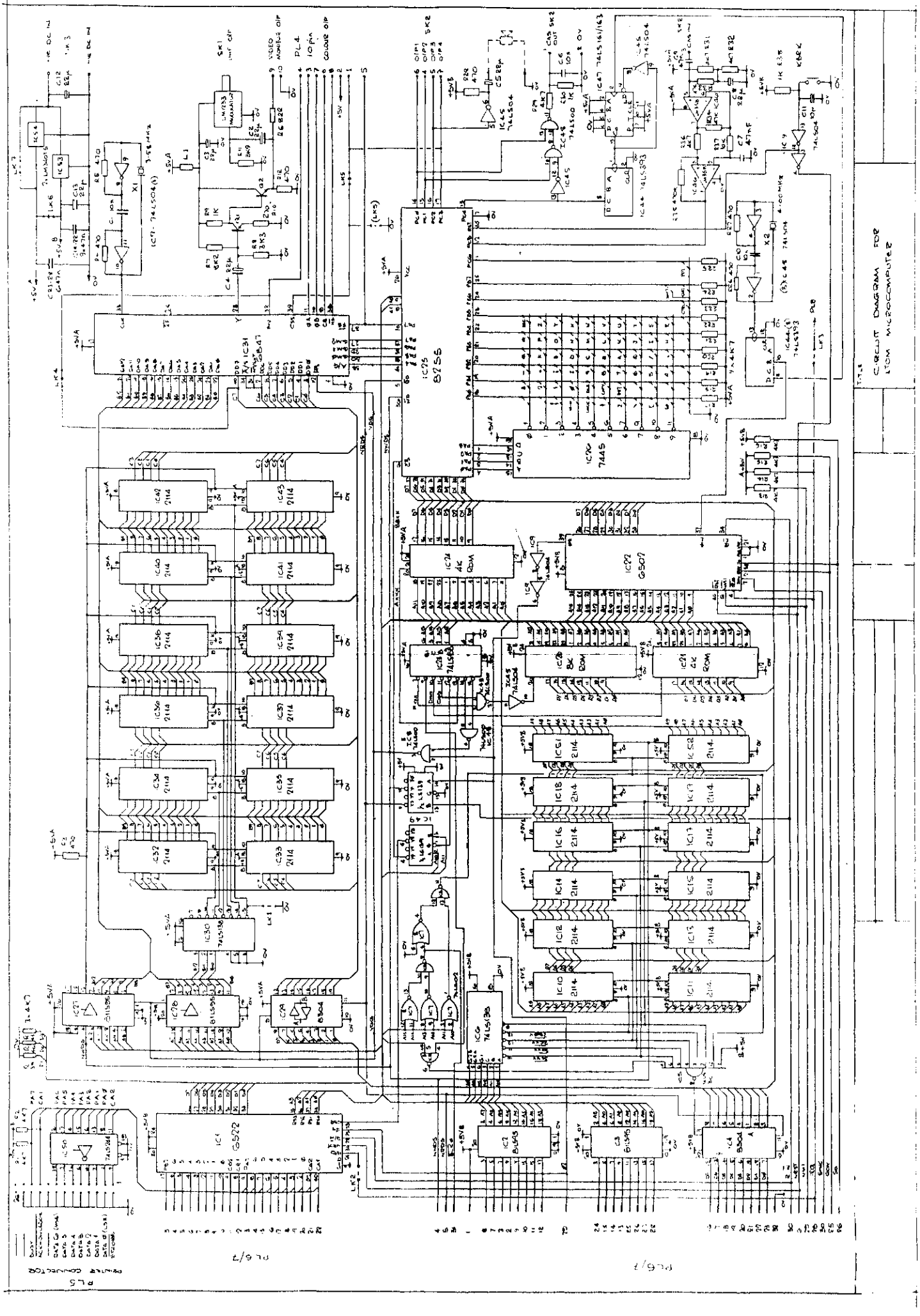


Fig. A.6 EPROM extension socket

A.9.5 ELECTRONIC CIRCUIT OF THE MICROCOMPUTER

Fig. A.7



A.9.6 TABLES CONTAINING THE CALCULATED GEOELECTRIC PARAMETERS OF THE BOREHOLES EXAMINED

Borehole No. 1: Geoelectric parameters calculated from 64-inches resistivity log

DEPTH INTERVAL (m)	Rtr (0.m)	Rl (0.m)	
4	143.55	115.88	1.1130
8	154.00	154.00	1
12	152.00	151.96	1.0001
16	149.00	149.00	1
20	149.90	149.87	1.0009
24	155.00	155.00	1
28	168.60	168.308	1.0008
32	172.00	172.00	1
36	175.40	175.38	1.0001
40	178.60	178.50	1.0001
44	188.75	188.75	1
48	191.30	191.25	1.0001
52	196.50	196.468	1.0000
56	208.80	208.76	1.0000
60	215.05	214.97	1.0002
64	218.00	218.00	1
68	218.25	217.93	1
72	202.15	202.01	1.00034
76	195.00	195.00	1
80	210.45	210.097	1.0008
84	209.50	209.41	1.0002
88	174.00	173.59	1.0012
92	170.00	168.50	1.0044
96	126.00	124.95	1.0042
100	108.30	103.24	1.0242
104	116.50	112.18	1.0190
108	111.70	111.36	1.0015
112	118.1	117.70	1.0017
116	108.90	108.705	1.00089
120	101.35	100.97	1.0018
124	114.7	114.35	1.0017
128	117.95	117.80	1.0006
132	112.9	112.72	1.0008
136	114.1	113.91	1.0008
140	119.0	119.0	1
144	119.0	119.0	1
148	134.7	134.23	1.0017
152	132.60	132.58	1.0004
156	127.00	126.97	1.0001
160	125	125	1
164	113.60	110.80	1.0125
168	60.80	58.35	1.0207
172	60.15	58.84	1.0111
176	79.00	79.00	1
180	79.00	79.00	1

Borehole No. 1: Geoelectric parameters calculated from 16-inches normal resistivity log

DEPTH INTERVAL (m)	Rtr (0.m)	R1 (0.m)	λ
4	115.90	98.56	1.0044
8	116.90	116.87	1.0001
12	121.10	120.95	1.0006
16	122.40	122.33	1.0003
20	118.40	118.40	1.0012
24	140.20	139.70	1.0018
28	157.60	157.59	1.0001
32	153.50	153.23	1.0009
36	165.15	165.04	1.0003
40	166.20	166.14	1.0001
44	178.80	178.63	1.0005
48	180.35	180.10	1.0007
52	185.75	185.39	1.0009
56	196.10	195.96	1.0004
60	192.70	192.32	1.0010
64	202.40	202.49	1.0003
68	206.90	206.73	1.0004
72	189.40	187.29	1.0043
76	180.20	179.89	1.0008
80	196.00	192.67	1.0086
84	207.05	206.85	1.0005
88	182.35	180.10	1.0006
92	185.80	181.30	1.0123
96	126.10	123.63	1.0099
100	119.25	106.98	1.0550
104	134.95	129.70	1.0197
108	114.40	107.76	1.0300
112	129.20	126.73	1.0096
116	115.45	113.57	1.0082
120	98.50	97.23	1.0065
124	118.70	118.23	1.0019
128	119.20	118.56	1.0027
132	113.70	112.89	1.0035
136	113.85	113.53	1.0011
140	116.45	116.31	1.0006
144	123.50	123.44	1.0023
148	143.95	143.86	1.0003
152	145.15	144.47	1.0023
156	132.50	130.53	1.0075
160	138.80	138.17	1.0022
164	134.15	133.16	1.0037
168	60.80	57.92	1.0246
172	63.75	59.24	1.0373
176	83.90	83.72	1.0010
180	85.40	85.32	1.0004
184	73.80	73.33	1.0031

Borehole No. 2: Geoelectric parameters calculated from 16-inches normal resistivity log

DEPTH INTERVAL (m)	Rtr (O.m)	Rl (O.m)	
52-56	64.00	64.00	1.0000
56-60	64.00	64.00	1.0000
60-64	64.00	64.00	1.0000
64-68	64.00	64.00	1.0000
68-72	64.00	64.00	1.0000
72-76	64.00	64.00	1.0000
76-80	64.00	64.00	1.0000
80-84	64.00	64.00	1.0000
84-88	64.00	64.00	1.0000
88-92	64.00	64.00	1.0000
92-96	65.80	65.67	1.0009
96-100	68.15	67.72	1.0031
100-104	62.00	61.76	1.0019
104-108	68.50	68.46	1.0002
108-112	54.05	53.94	1.0010
112-116	47.85	47.11	1.0078
116-120	52.00	51.48	1.0050
120-124	40.15	39.00	1.0145
124-128	43.00	43.00	1.0000
128-132	42.70	42.69	1.0000
132-136	42.00	42.00	1.0000
136-140	42.00	42.00	1.0000
140-144	42.00	42.00	1.0000

Borehole No. 3: Geoelectric parameters calculated from 16-inches normal resistivity log

DEPTH INTERVAL (m)	Rtr (O.m)	Rl (O.m)	λ
25-29	98.35	67.30	1.2089
29-33	107.30	107.24	1.0003
33-37	119.95	119.42	1.0022
37-41	125.85	125.83	1.0001
41-45	119.85	119.39	1.0019
45-49	116.25	115.60	1.0028
49-53	104.90	104.40	1.0024
53-57	99.45	98.44	1.0051
57-61	105.80	105.58	1.0010
61-65	104.25	103.48	1.0037
65-69	102.10	101.30	1.0039
69-73	98.00	97.95	1.0002
73-77	103.90	103.76	1.0007
77-81	102.05	101.99	1.0003
81-85	100.60	100.08	1.0026
85-89	103.80	103.67	1.0006
89-93	102.30	102.06	1.0012
93-97	106.85	106.81	1.0002

DEPTH INTERVAL (m)	Rtr (O.m)	Rl (O.m)	λ
25-29	45.40	41.39	1.0473
29-33	46.00	46.00	1.0000
33-37	53.55	53.08	1.0044
37-41	65.50	65.47	1.0003
41-45	66.05	66.03	1.0003
45-49	66.70	66.69	1.0001
49-53	64.75	64.67	1.0006
53-57	60.40	60.26	1.0012
57-61	67.90	67.84	1.0005
61-65	67.00	66.96	1.0003
65-69	65.65	65.60	1.0004
69-73	69.00	69.00	1.0000
73-77	69.00	69.00	1.0000
77-81	69.60	69.60	1.0000
81-85	66.60	66.53	1.0005
85-89	66.15	66.11	1.0003
89-93	67.00	67.00	1.0000
93-97	69.90	69.90	1.0000
97-101	70.40	70.38	1.0001

64″

Borehole No. 4: Geoelectric parameters calculated from 16-inches normal resistivity log

DEPTH INTERVAL (m)	Rtr (O.m)	R_1 (O.m)	λ
24-28	81.40	80.27	1.0070
28-32	84.10	84.10	1.0000
32-36	76.55	76.33	1.0015
36-40	78.60	78.45	1.0009
40-44	74.10	73.92	1.0012
44-48	76.05	74.67	1.0092
48-52	82.85	82.59	1.0016
52-56	85.00	85.00	1.0000
56-60	83.05	83.03	1.0001
60-64	83.20	83.19	1.0001
64-68	85.55	85.43	1.0007
68-72	81.10	81.04	1.0003
72-76	82.85	82.75	1.0006
76-80	87.50	87.30	1.0012
80-84	94.85	94.82	1.0001
84-88	93.20	93.14	1.0003
88-92	92.75	92.73	1.0001
92-96	102.75	102.46	1.0014
96-100	104.60	103.99	1.0029
100-104	90.90	90.80	1.0005
104-108	110.25	84.77	1.1403

DEPTH INTERVAL (m)	Rtr (O.m)	Rl (O.m)	λ
24-28	63.00	62.95	1.0004
28-32	66.00	66.00	1.0000
32-36	66.00	66.00	1.0000
36-40	66.00	66.00	1.0000
40-44	66.00	66.00	1.0000
44-48	67.20	67.12	1.0006
48-52	72.00	72.00	1.0000
52-56	73.50	73.49	1.0001
56-60	74.00	74.00	1.0000
60-64	74.00	74.00	1.0000
64-68	74.00	74.00	1.0000
68-72	74.00	74.00	1.0000
72-76	74.00	74.00	1.0000
76-80	74.00	74.00	1.0000
80-84	74.00	74.00	1.0000
84-88	74.00	74.00	1.0000
88-92	74.00	74.00	1.0000
92-96	74.85	74.77	1.0006
96-100	79.55	79.53	1.0001
100-104	83.75	83.74	1.0000

64"

Borehole No. 5: Geoelectric parameters calculated from 16-inches normal resistivity log

DEPTH INTERVAL (m)	Rtr (O.m)	Rl (O.m)	λ
24-28	120.15	117.88	1.0096
28-32	111.85	111.54	1.0014
32-36	97.75	97.69	1.00029
36-40	101.00	101.00	1.0000
40-44	106.00	103.58	1.0116
44-48	111.00	106.29	1.0219
48-52	111.00	106.29	1.0219
52-56	101.00	101.00	1.0000
56-60	113.70	111.21	1.0111
60-64	113.00	115.00	1.0000
64-68	122.00	121.82	1.0007
68-72	124.15	122.22	1.0078
72-76	139.95	138.98	1.0035
76-80	139.00	139.00	1.0000
80-84	139.00	139.00	1.0000
84-88	139.00	139.00	1.0000
88-92	139.00	139.00	1.0000
92-96	145.60	145.35	1.0008
96-100	151.00	151.00	1.0000
100-104	151.00	151.00	1.0000
104-108	151.00	151.00	1.0000
108-112	147.75	147.53	1.0008
112-116	132.50	131.19	1.0049
116-120	126.00	126.00	1.0000
120-124	126.00	126.00	1.0000
124-128	126.00	126.00	1.0000
128-132	136.80	136.73	1.0003
132-136	142.05	141.91	1.0005
136-140	152.90	151.33	1.0056
140-144	147.00	147.00	1.0000
144-148	167.90	167.74	1.0005
148-152	171.15	170.73	1.0012
152-156	168.60	168.59	1.0001

156-160	165.00	165.00	1.0000
160-164	164.15	164.06	1.0003
164-168	146.70	146.59	1.0004
168-172	141.85	140.16	1.0060
172-176	155.90	155.76	1.0004

Borehole No. 6: Geoelectric parameters calculated from 64-inches normal resistivity log

DEPTH INTERVAL (m)	Rtr (O.m)	Rl (O.m)	λ
24-28	136.40	136.38	1.0001
28-32	133.60	133.55	1.0002
32-36	132.85	132.80	1.0002
36-40	137.60	137.48	1.0004
40-44	133.85	133.72	1.0005
44-48	135.00	134.79	1.0008
48-52	142.90	142.84	1.0002
52-56	150.50	150.42	1.0003
56-60	166.30	166.25	1.0001
60-64	168.00	168.00	1.0000
64-68	168.00	168.00	1.0000
68-72	167.10	167.07	1.0001
72-76	158.00	158.00	1.0000
76-80	158.00	158.00	1.0000
80-84	159.00	158.98	1.0001
84-88	162.00	162.00	1.0000
88-92	167.00	166.85	1.0004
92-96	158.70	158.64	1.0002
96-100	134.60	134.53	1.0003
100-104	132.80	132.54	1.0010
104-108	103.10	102.72	1.0016
108-112	86.20	84.14	1.0122
112-116	90.00	89.06	1.0053
116-120	90.00	90.00	1.0000
120-124	94.20	93.86	1.0018
124-128	83.50	83.22	1.0017
128-132	87.45	86.10	1.0060
132-136	96.00	96.00	1.0000
136-140	96.00	96.00	1.0000
140-144	94.20	94.16	1.0002

144-148	99.00	98.50	1.0025
148-152	106.00	106.00	1.0000
152-156	109.50	109.30	1.0009
156-160	110.10	110.00	1.0004
160-164	109.00	108.84	1.0007
164-168	98.90	98.89	1.0001
168-172	104.65	104.63	1.0001
172-176	94.55	93.76	1.0042
176-180	55.05	53.30	1.0163
180-184	62.35	38.12	1.279

DEPTH INTERVAL	Rtr	Rtr	
24-28	120.80	120.79	1.0000
28-32	123.70	123.47	1.0009
32-36	131.00	131.00	1.0000
36-40	128.60	128.51	1.0003
40-44	155.45	154.87	1.0019
44-48	159.05	158.92	1.0004
48-52	165.95	165.79	1.0005
52-56	180.40	180.04	1.0010
56-60	196.60	196.59	1.0000
60-64	205.40	205.26	1.0003
64-68	198.00	197.83	1.0004
68-72	202.70	202.48	1.0005
72-76	195.40	195.17	1.0006
76-80	206.70	206.24	1.0009
80-84	183.95	183.75	1.0005
84-88	189.85	189.19	1.0017
88-92	219.40	217.98	1.0032
92-96	201.80	201.50	1.0007
96-100	184.30	182.80	1.0041

16"

100-104	191.65	191.59	1.0001
104-108	131.95	128.19	1.0146
108-112	126.95	115.21	1.0497
112-116	144.80	141.52	1.0115
116-120	112.20	106.74	1.0252
120-124	133.45	131.02	1.0092
124-128	122.05	116.10	1.0253
128-132	98.60	96.88	1.0088
132-136	117.50	115.95	1.0067
136-140	129.05	128.89	1.0006
140-144	128.25	127.64	1.0024
144-148	128.30	127.79	1.0020
148-152	140.80	140.44	1.0013
152-156	144.75	144.20	1.0019
156-160	149.85	147.68	1.0073
160-164	153.75	153.29	1.0015
164-168	132.00	130.75	1.0048
168-172	149.10	148.03	1.0036
172-176	141.55	140.30	1.0045
176-180	90.05	84.54	1.0320
180-184	52.95	49.09	1.0386
184-188	91.85	87.96	1.0219
188-192	80.60	80.58	1.0001
192-196	77.05	76.78	1.0017
196-200	82.80	78.39	1.0277

Borehole No. 7: Geoelectric parameters calculated from 16-inches normal resistivity log

DEPTH INTERVAL (m)	Rtr (O.m)	Rl (O.m)	
20-24	38.40	34.72	1.0516
24-28	48.10	47.97	1.0014
28-32	56.20	55.86	1.0031
32-36	56.50	56.22	1.0024
36-40	50.70	48.87	1.0185
40-44	29.10	27.74	1.0240
44-48	47.05	46.76	1.0030
48-52	45.80	45.64	1.0004
52-56	49.70	49.66	1.0003
56-60	42.20	41.92	1.0111
60-64	26.45	25.87	1.0111
64-68	19.20	19.08	1.0032
68-72	14.80	14.20	1.021

DEPTH INTERVAL (m)	Rtr (O.m)	Rl (O.m)	
50-54	72.85	61.18	1.0912
54-58	78.35	78.28	1.0004
58-62	82.00	82.00	1.0000
62-66	80.35	80.33	1.0001
66-70	83.00	83.00	1.0000
70-74	85.25	85.19	1.0004
74-78	78.10	78.02	1.0005
78-82	64.15	63.78	1.0029
82-86	50.85	50.81	1.0004
86-90	46.80	46.75	1.0005
90-94	44.00	43.96	1.0004
94-98	47.00	47.00	1.0000
98-102	45.80	45.74	1.0006
102-106	40.50	40.47	1.0003
106-110	32.75	32.58	1.0026
110-114	26.60	26.59	1.0002
114-118	23.20	23.17	1.0006
118-122	20.75	20.73	1.0004
122-126	20.00	20.00	1.0000
126-130	20.00	20.00	1.0000

Borehole No. 8: Geoelectric parameters calculated from 16-inches normal resistivity log

Borehole No. 9: Geoelectric parameters calculated from 16-inches normal resistivity log

DEPTH INTERVAL (m)	Rtr (O.m)	Rl (O.m)	λ
20-24	54.10	46.81	1.0750
24-28	58.00	58.00	1.0000
28-32	58.00	58.00	1.0000
32-36	59.95	59.64	1.0026
36-40	72.00	71.89	1.0008
40-44	74.05	73.70	1.0023
44-48	74.00	74.00	1.0000
48-52	74.00	74.00	1.0000
52-56	74.00	74.00	1.0000
56-60	74.00	74.00	1.0000
60-64	67.15	53.40	1.1214

DEPTH INTERVAL (m)	Rtr (O.m)	Rl (O.m)	λ
20-24	46.00	41.30	1.0554
24-28	48.00	48.00	1.0000
28-32	48.00	48.00	1.0000
32-36	48.00	48.00	1.0000
36-40	48.00	48.00	1.0000
40-44	48.00	48.00	1.0000
44-48	55.20	54.94	1.0024
48-52	57.00	57.00	1.0000
52-56	57.00	57.00	1.0000
56-60	57.00	57.00	1.0000
60-64	53.75	53-32	1.0041

64"

DEPTH INTERVAL (m)	Rtr (O.m)	Rl (O.m)	λ
25-29	59.95	51.60	1.0779
29-33	75.00	73.52	1.0100
33-37	87.45	87.32	1.0007
37-41	90.85	90.30	1.0031
41-45	82.75	82.51	1.0014
45-49	89.70	89.66	1.0002
49-53	97.50	97.49	1.0000
53-57	99.90	99.74	1.0008
57-61	96.65	96.48	1.0009

Borehole No. 10: Geoelectric parameters calculated from 16-inches normal resistivity log

Borehole No. 11: Geoelectric parameters calculated from 16-inches normal resistivity log

DEPTH INTERVAL (m)	Rtr (O.m)	Rl (O.m)	
20-24	66.65	56.46	1.0865
24-28	71.00	71.00	1.0000
28-32	71.80	71.73	1.0005
32-36	78.05	78.05	1.0000
36-40	76.00	75.92	1.0005
40-44	73.00	73.00	1.0000
44-48	73.00	73.00	1.0000
48-52	78.25	77.28	1.0063
52-56	82.10	81.69	1.0025
56-60	79.75	79.64	1.0007
60-64	97.65	97.57	1.0004
64-68	97.00	97.00	1.0000
68-72	78.25	76.96	1.0083
72-76	72.00	72.00	1.0000
76-80	72.00	72.00	1.0000
80-84	72.00	72.00	1.0000
84-88	72.00	72.00	1.0000
88-92	72.30	72.30	1.0000
92-96	72.30	72.30	1.0000
96-100	72.30	72.30	1.0000
100-104	72.30	72.30	1.0000
104-108	72.30	72.30	1.0000
108-112	72.30	72.30	1.0000
112-116	72.30	72.30	1.0000
116-120	72.30	72.30	1.0000

DEPTH INTERVAL (m)	Rtr (O.m)	Rl (O.m)	
20-24	86.90	68.95	1.1227
24-28	93.00	93.00	1.0000
28-32	91.80	91.78	1.0001
32-36	87.80	87.65	1.0008
36-40	90.00	90.00	1.0000
40-44	90.00	90.00	1.0000
44-48	98.35	98.03	1.0016
48-52	111.00	111.00	1.0000
52-56	111.00	111.00	1.0000
56-60	111.00	111.00	1.0000
60-64	101.00	100.01	1.0049
64-68	91.00	91.00	1.0000
68-72	91.00	91.00	1.0000
72-76	91.00	91.00	1.0000
76-80	91.00	91.00	1.0000
80-84	91.00	91.00	1.0000
84-88	91.00	91.00	1.0000
88-92	91.00	91.00	1.0000
92-96	91.00	91.00	1.0000
96-100	91.00	91.00	1.0000

64"

100-104	91.00	91.00	1.0000
104-108	91.00	91.00	1.0000
108-112	91.00	91.00	1.0000
112-116	94.75	94.64	1.0038
116-120	136.80	135.91	1.0033
120-124	142.00	142.00	1.0000

Journal of Hydrology, 58 (1982) 375—381
Elsevier Scientific Publishing Company, Amsterdam — Printed in The Netherlands

Technical Note

[2]

APPLICATION OF HOT-WIRE (-FILM) FLOWMETERS TO WATER VELOCITY MEASUREMENTS IN WELLS

AKIS TSELENTIS
Division of Engineering Geology, Imperial College, London SW7 2BP (Great Britain)
(Received December 15, 1981; revised and accepted February 5, 1982)

ABSTRACT

Tselentis, A., 1982. Application of hot-wire (-film) flowmeters to water velocity measurements in wells. J. Hydrol., 58: 375—381.

Hot wires have long been used for the measurement of air speeds, where they are particularly suitable for relatively small velocities. Unfortunately, it has not been possible to use them in water with the same precision and ease as in air. One of the main drawbacks of hot wires (films) when they are used in water measurements is that they become unstable because of the contamination of the wire (film) by dissolved gases, dirt and chemicals in the water, and they are very sensitive to ambient temperature fluctuations.

The present paper discusses the practical problems in using the hot-wire (-film) flowmeter for velocity measurements in water wells.

INTRODUCTION

Flowmeters are very useful in determining the magnitude of the velocity and direction of movement of water in a well at all depths.

From the flowmeter log we can identify and evaluate inflow levels, leaks in cased wells and aquifers tapped by cased wells having multiple screens. Hence, the use of flowmeters is essential in the solution of many hydrogeological problems.

Because the velocity regime under natural flow conditions is usually between 1 and 50 mm/s some useful results might be expected from the use of hot-wire flowmeters which are particularly well suited for very low velocities in air (Dring and Gebhart, 1969).

The first attempt to measure water velocities with hot wire known to us was published by Worthington and Malone (1917). They made some measurements on a vertical wire, 20 cm long and 0.025 cm in diameter, which they rotated in a tank of water. Their results were erratic at velocities below 60 mm/s as a result of the eddy currents set up by the wire and its holder.

0022-1694/82/0000—0000/$02.75 © 1982 Elsevier Scientific Publishing Company

Davis (1922) published the most comprehensive data yet taken with fine wires in liquids. Richardson and McQuivey (1968) mentioned the use of hot wires for the measurement of water velocities in open channels.

The development of hot-film probes to replace the wire has eliminated the instability which results from electrolysis of the wire and conductivity of the water. Recently, there has been a continual increase in the use of such sensors in various geotechnical problems (Harold and Thomas, 1972), but only recently attention has been focused on the special problems arising in water (Fabula, 1968; Shaukatullah and Gebhart, 1977; Castaldini et al., 1980).

THEORY

A brief discussion of the theory of hot-wire (-film) flowmeters will be given to facilitate a general understanding of the measuring principle. The hot-wire (-film) flowmeter is a resistance–temperature transducer. The wire (film) is heated above the temperature of the surrounding water by passing an electric current through it. Flow of the water over the heated sensor cools it by forced convection. The rate of cooling is a function of the velocity of the flow; temperature, density, viscosity and thermal conductivity of the water; and temperature, diameter and length of the sensor. If all but the velocity are kept constant then the hot wire (film) may be used to measure the flow velocity.

There are two methods of operating the hot-wire (-film) flowmeter; either by passing a constant current through it and measuring the fluctuation of the electrical resistance with velocity fluctuation, or by keeping the temperature of the sensor constant, by using an electrical feedback system, measuring the current fluctuation with fluctuating velocity. The constant-temperature method is easier and the following description is based upon the constant-temperature hot-wire flowmeter.

The theoretical analysis of the device was published by King (1914), who first derived an expression for the heat convected from a cylinder submerged into a moving fluid. For the case of continuous incompressible flow, the best experimental relation between mean heat loss and mean velocity is:

$$I^2 R_f^2 / R_a^2 (R_f - R_a) = A + BV^n \tag{1}$$

where

R_f = electrical resistance of wire at wire temperature
R_a = electrical resistance of wire at ambient temperature
I = electric current flowing through the wire (film)
A, B, n = constants
V = water velocity

Eq. 1 can be written as

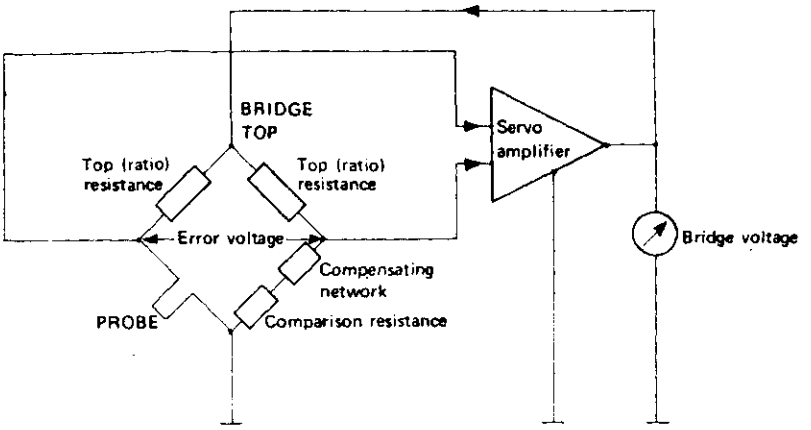


Fig. 1. Hot-film constant-temperature flowmeter bridge circuit.

$$\bar{E}^2 = R_a^2 K(K-1)(A+BV^n) \tag{2}$$

therefore

$$\bar{E}^2 = A' + B'V^n \tag{3}$$

where

$\bar{E}$ = mean bridge voltage (Fig. 1)
$K = R_f/R_a$, the overheat ratio

For $n = \frac{1}{2}$, one takes the original King's law form and for $n \neq \frac{1}{2}$, one can speak of a generalized King's law form. The value of n is of interest because bridge voltage linearizers produce a voltage proportional to V by, in effect, solving eq. 3 for V.

HOT FILMS — PROBE DESIGN

Hot-film sensors are more rugged and resistant to impact than hot-wire sensors; thus they are more amenable to the down-hole environment. Hot-film sensors are constructed by fusing a thin platinum film (or other suitable metal) on a ceramic or quartz substance. A thin coating of silica is deposited over the sensor to isolate it physically and electrically from the water. Typical sensors are shown in Fig. 2 and are known as conical, cylindrical or wedge-film sensors. Conical sensors tend to be self-cleaning and shed foreign particles.

PROBLEMS IN THE USE OF HOT-WIRE (-FILM) FLOWMETERS FOR WATER VELOCITY MEASUREMENTS IN WELLS

The high electrical conductivity of water, its low boiling point, its tem-

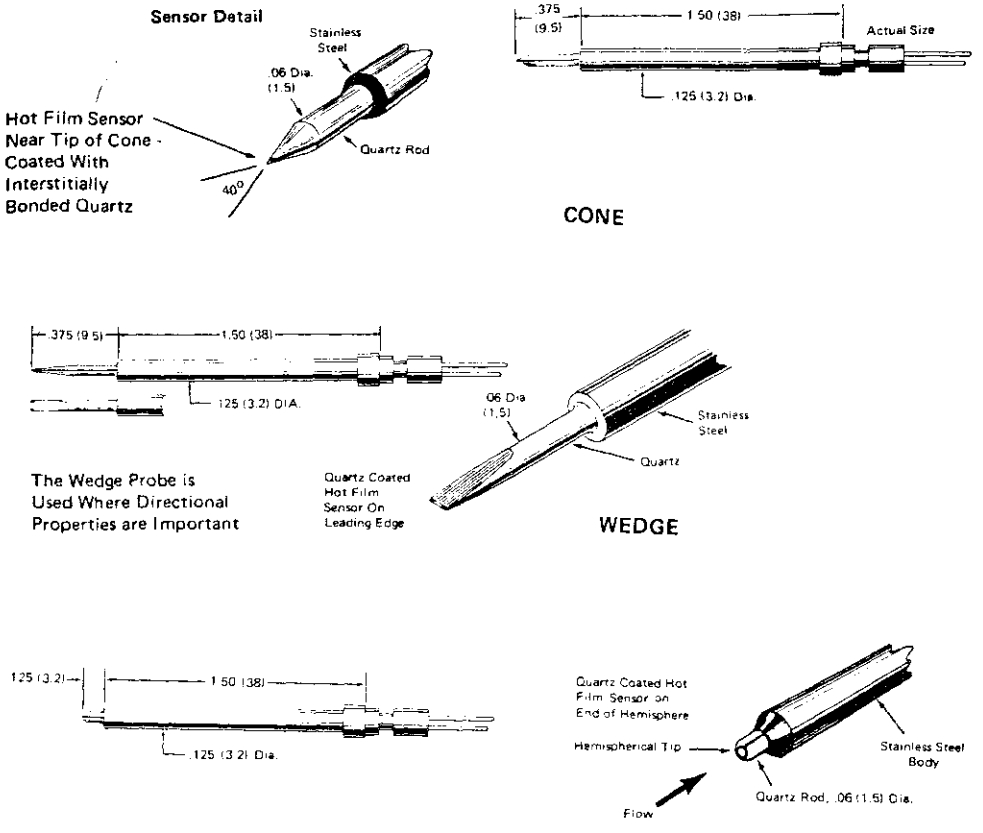


Fig. 2. Relative size and shape of hot-film sensors. (Dimensions in brackets are in millimetres, others are in inches.)

perature-dependent viscosity, and the large number of suspended particles found in well waters are some factors which make the behaviour in water of the hot-wire (-film) flowmeter very complicated. Our own experience in using the hot wire in water has not been very encouraging. It is essential when using a D.C. current to insulate the wire from the water, which is not easy, or to operate the instrument with less than ~1-V drop on the wire, in order to prevent electrolysis. Another problem is that since the wire (film) is hotter than the ambient water the solubility of air in the water is reduced near the wire. This means that bubbles of air form at the sensor and stick to it, thus changing the thermal conditions and considerably altering the calibration. The only means of eliminating these difficulties is to operate the

meter at very low temperature. Another major drawback of the hot-wire (-film) flowmeter in its use in water is the serious problem of contamination of the film surface by small solid particles in suspension in the water of the well.

Measurements in the dirty water of a well can cause large changes in the calibration of the device. Deposition of a layer of dirt on the wire (film) will alter its frequency response as well as the mean calibration. The smaller the sensing element, the sooner the thickness of the deposit will reach an appreciable fraction of its diameter. The deposit is usually confined to the upstream side of the sensor near the stagnation line; for this reason, it is preferable to use sensors in the form of wedges or cones.

Recently, a method was developed (Richardson and McQuivey, 1968), for using the hot-film flowmeter in extremely dirty water. Their method is based on a hypothesis that dirt and air bubbles accumulating on the sensor decrease the mean voltage for a given velocity, but in the domain of frequencies encountered in water, do not affect the frequency response of the sensor to velocity fluctuations. For a given sensor, there is a unique family of voltage—velocity relations which can be defined by calibration with different overheat ratios. Although this method is very useful for the measurement of turbulence in water, it is of little help if we want to make measurements of absolute flow velocity in water wells.

Another problem which affects the operation of the hot-film flowmeter in wells is that the water-temperature variations in the well may significantly alter the temperature difference between the hot film and water. Rose (1962) considered the response of a linearized hot wire in air to small ambient temperature fluctuations. Sandborn (1961) indicated that fluid-temperature fluctuations significantly affect results in many modes of operation. Resch and Coantic (1969) found it necessary to calibrate for fluid-temperature variations in water. Newman (1966) calibrated film probes in water at various temperature levels; his results show that fluid-temperature variations cause significant variation in the output of the device.

From the above, we can say that calibrating hot wires (films) over an adequately large range of ambient fluid temperatures and in the environment of a groundwater well is extremely inconvenient and difficult, especially when water temperature differs greatly from ambient laboratory conditions. Moreover, large temperature differences induce appreciable natural convection effects in the water.

An additional error which is induced by water-temperature fluctuations, arises from water property variations. It is known that variations of the viscosity and the density of the water can significantly vary the calibration results.

CONCLUSION

Hot-wire (-film) flowmeters are by no means a panacea for wellbore fluid-

flow measurements; but the device could be valuable if it could be made to work accurately in water. Its sensitivity increases with decreasing velocity, it could therefore be used to great advantage to measure those low velocities where an impeller flowmeter is not satisfactory. Unfortunately there are many problems to be solved and up to now thermal flowmeters can be considered to be of little practical value for water velocity measurements in wells.

Presently, a new device is under theoretical and experimental investigation in this laboratory, and has shown considerable promise in water velocity measurements as low as 1 mm/s. It uses the thermal wake of a heated wire, submerged in the water as a tracer. Important advantages of the heat-pulse method are its stability and repeatability over a wide dynamic range in a wide variety of conditions.

ACKNOWLEDGEMENTS

Thanks are due to M. De Freitas for his most helpful comments and criticisms.

REFERENCES

Bradshaw, P., 1970. An Introduction to Turbulence and Its Measurement. Pergamon, London, 218 pp.

Castaldini, M., Helland, K.N. and Malvestuto, V., 1980. Hot film anemometry in aqueous NaCl solutions. Int. J. Heat Mass Transfer, 24: 133—139.

Davis, A.H., 1922. The cooling power of a stream of viscous fluid. Philos. Mag., 6: 940—944.

Dring, R.P. and Gebhart, B., 1969. Hot wire anemometer calibration for measurements at very low velocity. Trans. A.S.M.E. (Am. Soc. Mech. Eng.), Pap. No. 69-HT-A.

Fabula, A.G., 1968. Operating characteristics of some hot film velocity sensors in water. In: W.L. Melnik and J.R. Weske (Editors), Advances in Hot Wire Anemometry. University of Maryland Press, College Park, Md., pp. 167—191.

Harold, E.T. and Thomas, E.S., 1972. Hot film flow logging as applied to in situ oil shale and mining experiments. Soc. Prof. Well Log Anal., 13: 1—14.

Hollasch, K. and Gebhart, B., 1972. Temperature hot wire anemometers at low velocities in water with variable fluid temperature. Trans. A.S.M.E. (Am. Soc. Mech. Eng.), Pap. No. 71-HT-9.

King, L.V., 1914. On the convection of heat from small cylinders in a stream of fluid — Determination of convection constants of small platinum wires with application to hot wire anemometry. Philos. Trans. R. Soc., London, Ser. A, 214: 373—432.

Ling, S.C., 1955. Ph.D. Thesis, University of Iowa, Iowa City, Iowa.

Newman, L., 1966. A survey of the literature on transition from laminar to turbulent flow in natural convection and forced flow. M.Sc. Thesis, Cornell University, Ithaca, N.Y.

Resch, F. and Coantic, M., 1969. Étude sur le fil chaud et le film chaud dans l'eau. Houille Blanche, No. 2, pp. 151—161.

Richardson, E.V. and McQuivey, R.S., 1968. Measurement of turbulence in water. J. Hydraul. Div., Proc. Am. Soc. Civ. Eng., 94(HY2): 411—429.

Rose, W.G., 1962. Some corrections to the linearized response of a constant temperature hot wire anemometer operated in low speed flow. J. Appl. Mech., 84: 554—558.

Sandborn, V.A., 1961. Hot wire anemometer measurements in large scale boundary layers. In: W.L. Melnik and J.R. Weske (Editors), Advances in Hot Wire Anemometry. University of Maryland Press, College Park, Md., pp. 102—119.

Shaukatullah, H. and Gebhart, B., 1977. Hot film anemometer calibration and use in fluids at varying background temperature. Lett. Heat Mass Transfer, 4: 309—317.

Worthington, H. and Malone, C.B., 1917. Measurements of velocities in water with hot wires. J. Franklin Inst., 184: 115—117.